HARD BUT HOPEFUL: THE CLINICAL AND TRANSLATIONAL RESEARCH PROGRESS IN PANCREATIC CANCER

EDITED BY: Taiping Zhang, Min Li, Bei Sun and Kuirong Jiang
PUBLISHED IN: Frontiers in Oncology

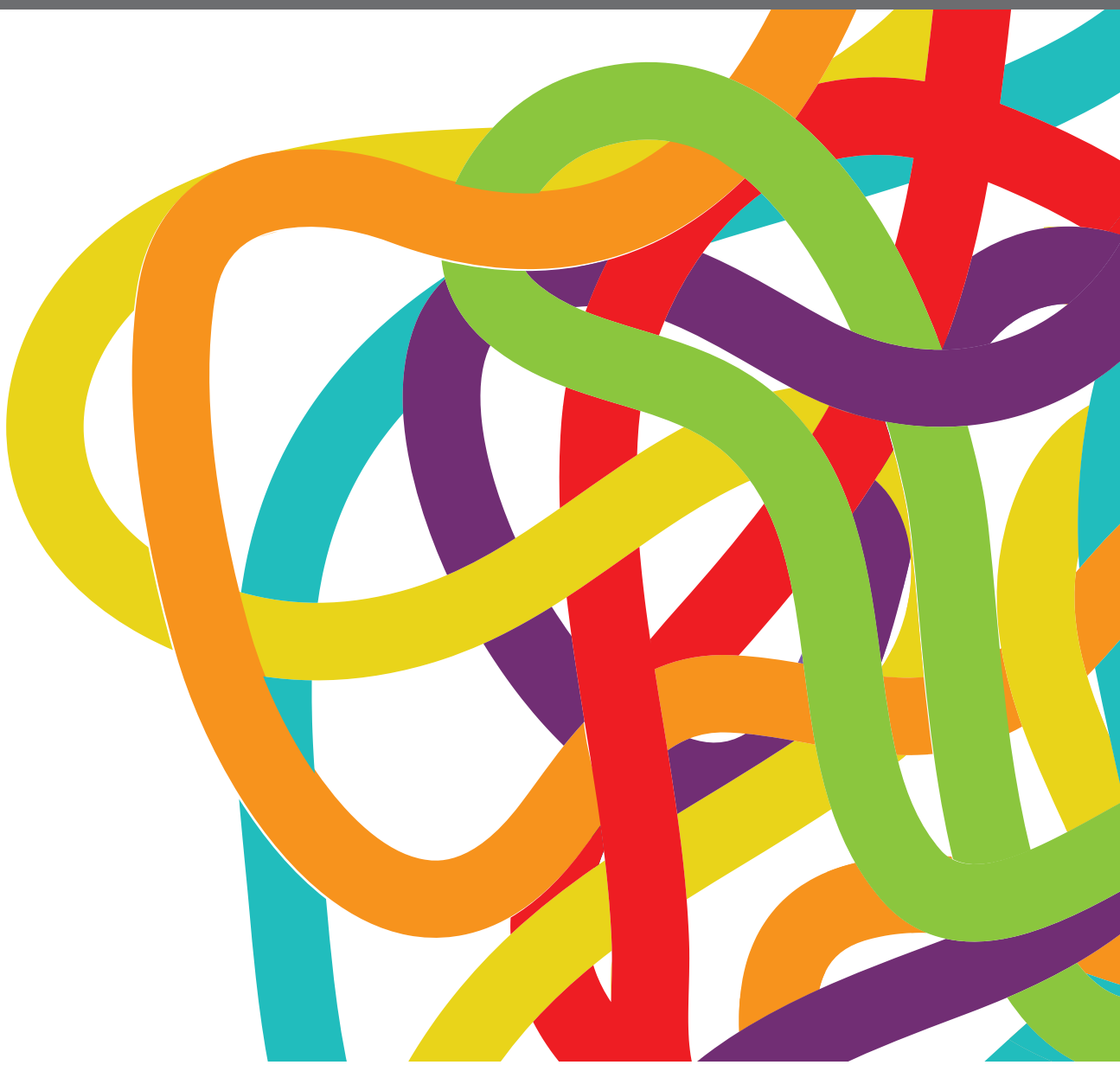

frontiers Research Topics

ISSN 1664-8714
ISBN 978-2-83250-387-4
DOI 10.3389/978-2-83250-387-4

About Frontiers

Frontiers is more than just an open-access publisher of scholarly articles: it is a pioneering approach to the world of academia, radically improving the way scholarly research is managed. The grand vision of Frontiers is a world where all people have an equal opportunity to seek, share and generate knowledge. Frontiers provides immediate and permanent online open access to all its publications, but this alone is not enough to realize our grand goals.

Frontiers Journal Series

The Frontiers Journal Series is a multi-tier and interdisciplinary set of open-access, online journals, promising a paradigm shift from the current review, selection and dissemination processes in academic publishing. All Frontiers journals are driven by researchers for researchers; therefore, they constitute a service to the scholarly community. At the same time, the Frontiers Journal Series operates on a revolutionary invention, the tiered publishing system, initially addressing specific communities of scholars, and gradually climbing up to broader public understanding, thus serving the interests of the lay society, too.

Dedication to Quality

Each Frontiers article is a landmark of the highest quality, thanks to genuinely collaborative interactions between authors and review editors, who include some of the world's best academicians. Research must be certified by peers before entering a stream of knowledge that may eventually reach the public - and shape society; therefore, Frontiers only applies the most rigorous and unbiased reviews.
Frontiers revolutionizes research publishing by freely delivering the most outstanding research, evaluated with no bias from both the academic and social point of view. By applying the most advanced information technologies, Frontiers is catapulting scholarly publishing into a new generation.

What are Frontiers Research Topics?

Frontiers Research Topics are very popular trademarks of the Frontiers Journals Series: they are collections of at least ten articles, all centered on a particular subject. With their unique mix of varied contributions from Original Research to Review Articles, Frontiers Research Topics unify the most influential researchers, the latest key findings and historical advances in a hot research area! Find out more on how to host your own Frontiers Research Topic or contribute to one as an author by contacting the Frontiers Editorial Office: frontiersin.org/about/contact

HARD BUT HOPEFUL: THE CLINICAL AND TRANSLATIONAL RESEARCH PROGRESS IN PANCREATIC CANCER

Topic Editors:
Taiping Zhang, Peking Union Medical College Hospital (CAMS), China
Min Li, University of Oklahoma Health Sciences Center, United States
Bei Sun, Harbin Medical University, China
Kuirong Jiang, Nanjing Medical University, China

Citation: Zhang, T., Li, M., Sun, B., Jiang, K., eds. (2022). Hard but Hopeful: The Clinical and Translational Research Progress in Pancreatic Cancer. Lausanne: Frontiers Media SA. doi: 10.3389/978-2-83250-387-4

Table of Contents

05 ***Type 2 Diabetes Mellitus Intersects With Pancreatic Cancer Diagnosis and Development***
Xiaoye Duan, Weihao Wang, Qi Pan and Lixin Guo

14 ***Plasma-Derived Exosome MiR-19b Acts as a Diagnostic Marker for Pancreatic Cancer***
Lei Wang, Jinxiang Wu, Naikuan Ye, Feng Li, Hanxiang Zhan, Shihong Chen and Jianwei Xu

21 ***Individualized Prediction of Survival Benefits of Pancreatectomy Plus Chemotherapy in Patients With Simultaneous Metastatic Pancreatic Cancer***
Duorui Nie, Guihua Lai, Guilin An, Zhuojun Wu, Shujun Lei, Jing Li and Jianxiong Cao

31 ***Prognostic Value of Preoperative NLR and Vascular Reconstructive Technology in Patients With Pancreatic Cancer of Portal System Invasion: A Real World Study***
Lin Zhou, Jing Wang, Xin-xue Zhang, Shao-cheng Lyu, Li-chao Pan, Guo-sheng Du, Ren Lang and Qiang He

44 ***AGIG Chemo-Immunotherapy in Patients With Advanced Pancreatic Cancer: A Single-Arm, Single-Center, Phase 2 Study***
Wangshu Dai, Xin Qiu, Changchang Lu, Zhengyun Zou, Huizi Sha, Weiwei Kong, Baorui Liu and Juan Du

53 ***Genomic Landscape in Neoplasm-Like Stroma Reveals Distinct Prognostic Subtypes of Pancreatic Ductal Adenocarcinoma***
Jiahong Jiang, Yaping Xu, Lianpeng Chang, Guoqing Ru, Xuefeng Xia, Ling Yang, Xin Yi, Zheling Chen, Dong-Sheng Huang and Liu Yang

65 ***Long Noncoding Competing Endogenous RNA Networks in Pancreatic Cancer***
Guangbing Xiong, Shutao Pan, Jikuan Jin, Xiaoxiang Wang, Ruizhi He, Feng Peng, Xu Li, Min Wang, Jianwei Zheng, Feng Zhu and Renyi Qin

89 ***Portal Venous Circulating Tumor Cells Undergoing Epithelial-Mesenchymal Transition Exhibit Distinct Clinical Significance in Pancreatic Ductal Adenocarcinoma***
Yujin Pan, Deyu Li, Jiuhui Yang, Ning Wang, Erwei Xiao, Lianyuan Tao, Xiangming Ding, Peichun Sun and Dongxiao Li

101 ***OXCT1 Enhances Gemcitabine Resistance Through NF-κB Pathway in Pancreatic Ductal Adenocarcinoma***
Jinsheng Ding, Hui Li, Yang Liu, Yongjie Xie, Jie Yu, Huizhi Sun, Di Xiao, Yizhang Zhou, Li Bao, Hongwei Wang and Chuntao Gao

114 ***Prediction of Pancreatic Neuroendocrine Tumor Grading Risk Based on Quantitative Radiomic Analysis of MR***
Wei Li, Chao Xu and Zhaoxiang Ye

121 ***Lipoxins and Resolvins in Patients With Pancreatic Cancer: A Preliminary Report***
Wojciech Blogowski, Katarzyna Dolegowska, Anna Deskur, Barbara Dolegowska and Teresa Starzynska

129 ***Pretherapeutic Assessment of Pancreatic Cancer: Comparison of FDG PET/CT Plus Delayed PET/MR and Contrast-Enhanced CT/MR***
Zaizhu Zhang, Nina Zhou, Xiaoyi Guo, Nan Li, Hua Zhu and Zhi Yang

138 ***Prognostic Effect of Age in Resected Pancreatic Cancer Patients: A Propensity Score Matching Analysis***
Yaolin Xu, Yueming Zhang, Siyang Han, Dayong Jin, Xuefeng Xu, Tiantao Kuang, Wenchuan Wu, Dansong Wang and Wenhui Lou

frontiers in Oncology

REVIEW
published: 16 August 2021
doi: 10.3389/fonc.2021.730038

Type 2 Diabetes Mellitus Intersects With Pancreatic Cancer Diagnosis and Development

Xiaoye Duan[1,2†], *Weihao Wang*[1†], *Qi Pan*[1] *and Lixin Guo*[1,2*]

[1] Department of Endocrinology, Beijing Hospital, National Center of Gerontology, Institute of Geriatric Medicine, Chinese Academy of Medical Sciences, Beijing, China, [2] Graduate School of Peking Union Medical College, Chinese Academy of Medical Sciences, Beijing, China

The relationship between type 2 diabetes mellitus (T2DM) and pancreatic cancer (PC) is complex. Diabetes is a known risk factor for PC, and new-onset diabetes (NOD) could be an early manifestation of PC that may be facilitate the early diagnosis of PC. Metformin offers a clear benefit of inhibiting PC, whereas insulin therapy may increase the risk of PC development. No evidence has shown that novel hypoglycemic drugs help or prevent PC. In this review, the effects of T2DM on PC development are summarized, and novel strategies for the prevention and treatment of T2DM and PC are discussed.

Keywords: type 2 diabetes mellitus, pancreatic cancer, hyperglycemia, insulin resistance, screening strategy, hypoglycemic therapy

OPEN ACCESS

Edited by:
Taiping Zhang,
Peking Union Medical College Hospital (CAMS), China

Reviewed by:
Bei Li,
Sichuan University, China
Yuxiu Li,
Peking Union Medical College Hospital (CAMS), China
Jianwei Xu,
Shandong University, China

****Correspondence:***
Lixin Guo
glx1218@163.com

†These authors have contributed equally to this work

Specialty section:
This article was submitted to Gastrointestinal Cancers, a section of the journal Frontiers in Oncology

Received: *24 June 2021*
Accepted: *30 July 2021*
Published: *16 August 2021*

Citation:
Duan X, Wang W, Pan Q and Guo L (2021) Type 2 Diabetes Mellitus Intersects With Pancreatic Cancer Diagnosis and Development. Front. Oncol. 11:730038. doi: 10.3389/fonc.2021.730038

INTRODUCTION

In recent years, the incidence of pancreatic cancer (PC) in the world has increased annually. PC has become the third leading cause of cancer-related death in the United States and the fourth in Japan (1). Despite considerable efforts in diagnosis and treatment, the 5-year survival rate has increased to only 10% (1). Because of nonspecific symptoms and a lack of screening recommendations, the vast majority of patients with PC are diagnosed at a late stage, and there is no opportunity for surgical intervention (2). According to data from Chinese Pancreatic Surgery Association, the 5-year overall survival rate of pancreatic cancer was is only 7.2% and the incidence of pancreatic cancer is expected to soar to the second place by 2030 in China (3). Unfortunately, early diagnosis rate of pancreatic cancer is only 5%. The proportion of estimated new cases of pancreatic cancer in China showed obvious regional characteristics, which is consistent with the result that the incidence and mortality increased from low to high urbanization areas in China, and the prevalence of diabetes increased from underdeveloped to developed region (4).

Type 2 diabetes mellitus (T2DM) is considered a risk factor for various malignant tumors, such as hepatocellular cancer, breast cancer, ovarian cancer, endometrial cancer, and gastrointestinal cancer. The incidence of cancer in patients with T2DM has increased by 10%, comparing the public population (5–7). Approximately 50% of patients with PC develop T2DM or impaired glucose tolerance at the very beginning (8). T2DM is a known risk factor for PC, and new-onset diabetes (NOD) may be an early manifestation of PC (9–11). Therefore, T2DM, especially NOD, may be a clue to early detection of PC and may improve the prognosis of this intractable malignant tumor.

However, the incidence of T2DM is too high to justify screening all patients with the condition for PC: the cost-benefit ratio does not justify such widespread use of medical resources. Additional

risk stratification is needed in patients with T2DM. In this review, we discuss the mechanism of the relationship between T2DM and PC, update the literature about risk factors and biomarkers of PC in patients with T2DM, and summarize PC prevention and treatment strategies.

MULTIPLE UNDERLYING MECHANISMS CONNECT T2DM AND PC

The mechanisms connecting T2DM with the formation and development of PC are multilayered and complex. Hyperglycemia, hyperinsulinemia, insulin resistance, chronic inflammation, and genetic factors all contribute to the association between these conditions (12).

Hyperglycemia and PC

In T2DM, hyperglycemia is caused by long-term excessive hepatic gluconeogenesis, decreased insulin activity, low peripheral glucose uptake, and changes in insulin signaling (13, 14). These events can cause cancer, especially PC (5–8) (**Figure 1**). In fact, patients can remain asymptomatic for many years, with undiscovered glucose intolerance and transient hyperglycemia. This time of prediabetes greatly increases the likelihood of developing PC (15, 16). One possible mechanism is the activation of the transforming growth factor-β1 (TGF-β1) pathway by glucose, which results in a decrease in the level of E-cadherin in pancreatic ductal cells and a significant mesenchymal phenotype that promotes tumor growth and metastasis (17). Hyperglycemia may also increase genetic instability and lead to *KRAS* mutations by activating O-GlcN acetylation and nucleotide deficiency (17, 18). Finally, the mTOR pathway controls protein synthesis and autophagy, and its deregulation is associated with diabetes and PC (19–23). Interestingly, inhibition of mTOR can reduce tumorigenesis in *KRAS*-dependent PC.

The tumor-promoting effect of N-carboxymethyllysine was found. N-carboxymethyllysine is a RAGE ligand and a major AGE in pancreatic cancer cell lines. The researchers found that PC was observed in eight (72.7%) of the 11 mice treated with N-carboxymethyllysine but in only one mouse (9.1%) in the control group (25). N-carboxymethyllysine upregulated the expression of RAGE in a concentration- and time-dependent manner, activated leukocyte cell adhesion molecule, and promoted the growth of PC cells (25). Reducing AGEs may be a good way to prevent PC.

Prospective cohort and case-control studies have shown that hyperglycemia is associated with increased free radical formation and may lead to the development of advanced glycosylation end product (AGEs), which may increase inflammation (24). The use of exogenous AGE in PC-susceptible mice can upregulate the expression of the AGE receptor (RAGE) in pancreatic intraepithelial neoplasia and greatly stimulate the development of invasive PC (25).

In 2018, Rahn et al. (17) explored the role of hyperglycemia in the malignant transformation of pancreatic ductal epithelial cell

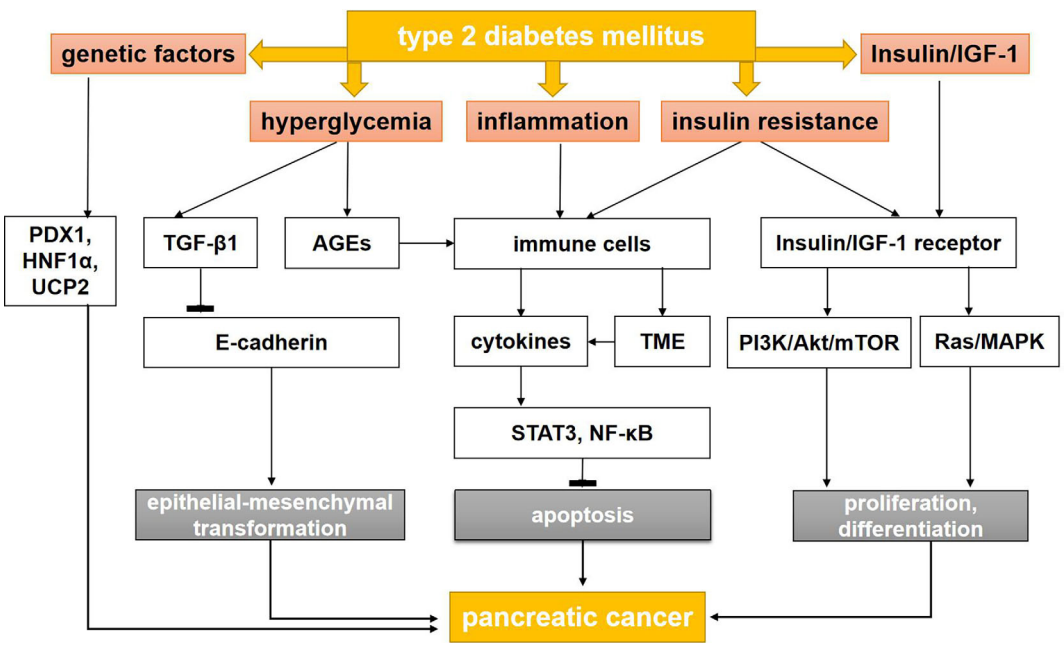

FIGURE 1 | The mechanisms between type 2 diabetes mellitus and pancreatic cancer. AGEs, advanced glycation end products; AMPK, adenosine monophosphate protein-activated kinase; IGF-1, insulin-like growth factor-1; LKB, liver kinase B; MAPK, mitogen-activated protein kinase; mTOR, mammalian target of rapamycin; NF-κB, nuclear factor kappa B; PI3K, phosphatidyl inositol-3 kinase; STAT3, signal transducer and activator of transcription 3; TGF-β1, transforming growth factor-β1; TME, tumor microenvironment; PDX1, pancreatic and duodenal homeobox-1; HNF1A, HNF1 Homeobox A; UCP2, uncoupling protein 2.

(PDEC), the occurrence and maintenance of cancer stem cells (CSCs), and the promotion of cancer-related epithelial-mesenchymal transformation (EMT). Hyperglycemia did not affect the mesenchymal phenotype of Panc-1 cells but did increase the characteristics of CSCs. In addition, in another study using H6c7-KRAS cells, high glucose stimulated the expression of a TGF-β1 signal and decreased the expression of E-cadherin, increased the expression of nestin, and increased the number of polyclonal cells in a TGF-β1–dependent manner (26). This study also found that decreased E-cadherin was detected in the pancreatic duct of hyperglycemic, but not normoglycemic, mice. These findings suggest that hyperglycemia promotes the acquisition of PDEC mesenchymal and vascular stem cell characteristics by activating TGF-β1 signaling, which may explain how T2DM promotes PC (**Figure 1**).

In addition, hyperglycemia also produce a large number of reactive oxygen species (ROS) (27–29) and reduce the activity of antioxidant enzymes (30, 31) to promote mitosis and stimulate cell proliferation. Luo et al. (28) found that the inactivation of the JNK pathway caused by the increase in ROS levels has a pivotal role on high glucose-induced cell proliferation. Their findings indicated that ROS stimulates proliferation of pancreatic cancer cells under high glucose conditions *via* inactivating the JNK pathway.

Hyperinsulinemia, Insulin Resistance, and PC

T2DM is characterized by insulin resistance (IR) with hyperinsulinemia and high levels of insulin-like growth factor (IGF)-1 (32–35). In patients with T2DM, IR can lead to hyperinsulinemia through serine phosphorylation of insulin receptor substrate proteins, thus activating protein kinase C and the mTOR complex/S6K and so participating in the downregulation of the insulin signal (36, 37). Insulin can reduce the production of IGF binding proteins 1 and 2 in the liver, both of which have high affinity for IGF-1 and IGF-2, thus increasing the levels of free IGF-1 in circulating blood (36–39).

Most cancer cells highly express insulin and IGF-1, because they are important members of the tyrosine kinase class of membrane receptors and are highly homologous to tyrosine kinase oncogenes (39–44). When insulin and IGF-1 bind to their receptors, they can mediate signal transduction, activate important intracellular signaling pathways—including Ras/Raf/MAPK and PI3K/Akt/mTOR pathways—and lead to the development of PC (45, 46).

Many studies have shown that IGF-1 has a stronger mitotic and anti-apoptotic effect than insulin (47–49). In addition, studies have indicated that cancer cell proliferation increases in a dose-dependent manner with increasing concentrations of IGF-1. Activation of the IGF-1 signal pathway leads to increased PC cell proliferation, invasion, and angiogenesis and to decreased apoptosis (50–53).

Inflammation and PC

Inflammation may increase the risk of PC in patients with T2DM. In patients with T2DM, insulin resistance and hyperinsulinemia often occur, accompanied by abundant adipocytes and a large amount of inflammatory cell infiltrating the pancreas tissue (54–56). The high glucose and fat diet may accelerate the inflammatory response by increasing oxidative stress and activating transcription factors, such as nuclear factor kappa B (NF-κB) and activator protein 1, which leads to the development of genomic aberration and carcinogenesis (57–59).

Inflammatory cytokines, ROS, and mediators of inflammatory pathways, such as cyclooxygenase-2 and NF-κB, are closely related to the STAT3 pathways. STAT3 and NF-κB signaling pathways are proven inhibitors of apoptosis and promoters of cell cycle progression. They also downregulate the expression of E-cadherin to induce EMT. During the inflammatory response, immune cells may directly promote the growth and progression of PC by releasing a large number of cytokines and growth factors into the microenvironment. The environment around the tumor is called as tumor microenvironment (TME), including Carcinoma-associated fibroblasts, endothelial cells and immune cells, which plays an significant role in growth, invasion and metastasis of pancreatic cancer. Inflammation change the TME and break balance of cancer cells in growth and apoptosis (60–63) (**Figure 1**).

Genetics Factors Driving DM and PC

A genome-wide association study has identified the relationship between diabetes and PC. Some pancreatic developmental genes, such as *NR5A2*, *PDX1*, and *HNF1A*, have been identified as susceptibility factors for PC in T2DM patients. Heterozygous mutations in some of these genes, such as *PDX1* and *HNF1A*, also lead to different types of monogenic diabetes in young people (types 4 and 5). Some variants in *PDX1* and *HNF1A* are also associated with an increased risk of T2DM (64, 65), obesity, or hyperglycemia (66).

The antioxidant mitochondrial uncoupling protein 2 (UCP2) controls pancreatic development and insulin secretion (67). UCP2 is overexpressed in PC tumors compared with normal adjacent tissues, indicating that its overexpression is a biomarker of poor prognosis. However, other recent studies using the PC cell line MiaPACA2 have shown that UCP2 can inhibit cancer cell proliferation and tumorigenesis (68). This effect is mediated by the retrograde mitochondrial signal on Warburg, which redirects mitochondrial function to oxidative phosphorylation rather than to glycolysis (69). Additional analysis is needed to clarify the differences between these two studies involving UCP2. Taken together, these data suggest a link between genes that control DM and PC.

SCREENING STRATEGIES FOR EARLY DIAGNOSIS OF PC IN PATIENTS WITH T2DM

NOD may be an early sign of PC, and a sudden increase in blood glucose in patients with previously well-controlled T2DM may also be a sign of PC (70). However, universal screening of PC in all elderly patients with NOD is difficult to achieve and not cost

effective. In recent years, many studies have proposed different strategies to stratify T2DM groups and facilitate targeted screening (71–74).

A prospective observation cohort study initiated by the Consortium for the Study of Chronic Pancreatitis, Diabetes, and Pancreatic Cancer proposed a new approach (define, enrich, find) to clarify the population at high risk of PC and to detect lesions in the high-risk groups (75). Patients older than age 50 years were divided into high-, medium-, and low-risk groups using the Enriched New-Onset Diabetes Score for Pancreatic Cancer (END-PAC). This scoring model provides a reference for early clinical screening of PC (76). Elderly patients with weight loss [low body mass index (BMI)] and rapidly rising blood glucose levels in a short period may be the target population for early screening of pancreatic cancer (77). Other indicators for screening PC in patients with T2DM include BMI; age of T2DM onset; hepatitis B virus infection; and total bilirubin, alanine aminotransferase, creatinine, apolipoprotein A1, and leukocyte (WBC) levels (78). Fatigue and depression caused by elevated interleukin-6, combined with severe weight loss (>10%) and NOD, may represent paraneoplastic syndrome and be early manifestations of PC (79).

In addition to contributing to risk stratification, the development of biomarkers to distinguish PC-associated DM is expected to be an important aspect of PC screening. Studies have shown that the numerous molecules, described in the following sections, may be effective biomarkers for an early diagnosis of PC (**Table 1**).

TABLE 1 | Risk factors, early signs, and biomarkers for pancreatic cancer in patients with type 2 diabetes mellitus.

Risk factor	NOD (≤2-year duration)
	Elderly onset (≥65 years)
Early sign	Body weight loss
	Rapid exacerbation of glycemic control
Biomarker	sTNF-αR2
	OPG
	VNN1
	IGF
	Circulating RNA

NOD, new-onset diabetes; sTNF-αR2, soluble receptor 2 of tumor necrosis factor-α; OPG, osteoprotegerin; VNN1, Vanin-1; IGF, Insulin-like growth factor.

Carbohydrate Antigen 19-9

The level of carbohydrate antigen 19-9 (CA19-9) secreted by cancer cells in patients with NOD may be a reliable indicator for predicting PC. However, CA19-9 has a high false-positive rate; any condition that causes inflammation of the pancreas increases the CA 19-9 level. One study has shown that the CA19-9 level is of little significance in screening PC in NOD, because the positive predictive value and sensitivity are zero, and the false-positive rate is 9% (80). However, the sample size of this study was small, so the conclusions cannot be applied to the entire population. Other studies have shown that, in the first 2 years of NOD, CA19-9 can be used as a cost-effective approach to detect small PC lesions that cannot be detected on imaging (81, 82).

Soluble Receptor 2 of Tumor Necrosis Factor-o

During the systemic inflammatory response to PC, C-reactive protein (CRP) levels can increase. Tumor necrosis factor-α (TNF-α) is the upstream regulator of CRP. Grote et al. (83) found that an increase in soluble TNF receptor 2 (sTNF-R2), significantly increases the risk of PC in patients with diabetes. In the diabetes arm of the study, the odds ratio of PC when the sTNF-R2 doubled was 4.76 (95% CI, 1.11–20.37); in the arm without diabetes, the odds ratio was only 1.12 (95% CI, 0.73–1.72) (83).

Osteoprotegerin

Osteoprotegerin (OPG) is a soluble decoy receptor of TNF-related apoptosis-inducing ligand, which belongs to the TNF receptor superfamily. Shi et al. (84) found that serum OPG was significantly increased in patients with PC-related DM. The sensitivity of serum OPG in identifying PC in patients with NOD was 68%; the specificity was 73.9%; and the area under the curve (AUC) was 73.7%.

Vanin-1

The enzyme vascular non-inflammatory molecule-1 (vanin-1) is highly expressed at gene and protein level in many organs. Recently, many researches have elucidated the role of vanin-1 under physiological conditions in relation to oxidative stress and inflammation, which is important in the pancreatic microenvironment (85). Huang et al. (86) identified vanin-1 (VNN1) as a potential biomarker for PC, using microarray analysis of the peripheral blood in patients with PC-associated DM compared with T2DM (84). Kang et al. (87) also explored the functional mechanism of VNN1 in PC-associated DM and found that overexpression of VNN1 in tumor tissues can decrease glutathione concentration and increase ROS, thus aggravating paraneoplastic islet dysfunction.

Circulating RNA

Recently, circulating RNAs have become research hotspots as noninvasive biomarkers for the early detection of PC (88). PC cells release a large amount of RNA into the bloodstream. These RNAs can effectively resist the RNA enzyme, thus increasing the expression level in the serum. Dai et al. (89) reported a microRNA panel (miR-483-5p, miR-19a, miR-29a, miR-20a, miR-24, miR-25) that distinguished PC-related DM from T2DM with an AUC of 0.887.

Although a number of studies have reported biomarkers for PC-related DM, most of them are case-control studies with limited sample sizes. Future studies must verify the role of these discussed biomarkers in distinguishing T2DM with PC *versus* without PC in larger samples.

EFFECTS OF ANTIDIABETIC THERAPY ON PC

Some antidiabetic medications may have an impact on PC development, progression, and outcome because of their direct effects on the key factors mediating the association between

T2DM and PC. The safety of antidiabetic medications with regard to PC risk is discussed in the following sections.

Insulin Therapy

Insulin therapy is usually necessary to treat T2DM in the long term. However, abundant research has shown that insulin therapy may increase the incidence of PC (90, 91).

To explore the risk relationship between insulin therapy and PC, Bosetti et al. (92) analyzed 15 case-control studies, which included 8,305 patient cases and 13,987 controls. Studies indicated that short-term insulin use (<5 years) was independently associated with a higher risk of PC (odds ratio [OR] = 5.6, 95% CI, 3.75–8.35), whereas long-term insulin use (≥15 years) was not (OR = 0.95, 95% CI, 0.53–1.70). At the same time, studies also showed that long-term oral antidiabetic use (≥15 years) in patients with T2DM might reduce the risk of PC (OR = 0.31, 95% CI, 0.14–0.69).

In 2018, Lee et al. (93) conducted a population-based study comparing PC risk in patients expose to antidiabetic drugs *versus* no drug exposure. The study concluded that, among several kinds of antidiabetic drugs, insulin alone was associated with an increased risk of PC (hazard ratio [HR] = 2.86, 95% CI, 1.43–5.74). The conclusion is similar with the research by Liu et al. (94), a case–control study using 12 years of data from Taiwan's National Health Insurance Research Database. The association between insulin use and high pancreatic cancer risk is significant.

Wang et al. (95) also found that insulin can promote the proliferation and glucose utilization of PC cells by activating ERK and PI3K and by increasing the expression of MMP-2. Insulin promotes migration and invasion in PC by activating the MMP-2 signal pathway. In addition, insulin induces phosphorylation of ERK and PI3K/Akt, which indicates that insulin can stimulate the Ras/Raf/MAPK and PI3K/Akt pathways and accelerate tumorigenesis and development (**Figure 1**). In summary, insulin use is associated with an increased risk of PC, so patients with T2DM who have a high risk of PC may not be candidates for insulin treatment. While insulin treatment was imperative for the patients with insulin secretion absolutely insufficient. For clinical physicians, we should pay attention to the risk of PC during long-term treatment with insulin and screen early PC in islet β-cell dysfunction patients with long-term treatment with insulin. We need more evidence for PC risk for patients with long-term treatment with insulin in the further research.

Metformin Therapy

Metformin is the cornerstone treatment of diabetes. Retrospective studies have shown that metformin can improve the survival of patients with T2DM and PC. During the past 5 years, numerous studies have suggested that metformin can reduce the risk of PC (96–99).

In the analysis of case-control studies by Bosetti et al. (100), long-term oral metformin use (≥15 years) reduced the risk of PC in patients with T2DM (OR = 0.31, 95% CI, 0.14–0.69). In 2018, Lee et al. (101) conducted a population-based study to assess the effects of T2DM and antidiabetic drugs on PC risk. That study identified metformin, among the antidiabetic drugs studied, as an independent risk factor for PC (HR = 0.86, 95% CI, 0.77–0.96). However, patients who received metformin combined with a thiazolidinedione or with dipeptidyl peptidase-4 inhibitors had lower risks of PC than patients receiving metformin alone. There are several clinical trials about metformin on PC treatment, such as metformin combined With Chemotherapy. Although addition of metformin does not improve outcome in patients with advanced PC treated with gemcitabine and erlotinib, future research should include studies of more potent biguanides, and should focus on patients with tumors showing markers of sensitivity to energetic stress, such as a lack of function of AMP kinase (102).

Currently, most scholars believe that metformin can reduce the risk of PC, because metformin can activate the liver kinase B1 (LKB1)–adenosine monophosphate protein-activated kinase (AMPK) pathway, which can not only promote cell energy production and inhibit liver glucose production but also inhibit the signal pathway of cancer cell proliferation (103). As a tumor suppressor, LKB1 can activate AMPK, which is a potent inhibitor of mTOR complex 1, and disrupt cross-talk between insulin/IGF-1 receptor and G protein–coupled receptors, thus regulating protein synthesis and replication. More importantly, metformin may play a role in the development of PC stem cells through the mTOR pathway (23, 104–107).

In a study evaluating the effect of metformin on PC, cancer stem cells (Alk4, nodal, activin, and Smad2) and pluripotency-related RNA proteins (Nanog, Oct4, and Sox2) changed significantly after metformin treatment. These changes may be due to the inhibition of nicotinamide-adenine dinucleotide dehydrogenase and the production of free ROS, which would directly increase the damage to PC stem cells (108). Ma M et al. found that metformin significantly inhibited proliferation and viability, induced apoptosis of pancreatic cancer cells, which was more pronounced in low-glucose than in high-glucose group, and metformin may play protective effect by suppressing glycolysis and inducing energy stress *via* up-regulation of miR-210-5p (109).

These studies have shown that metformin can reduce the risk of PC and activate the LKB1/AMPK pathway, thus inhibiting cell proliferation by mTOR. Therefore, metformin is expected to become part of the standard treatment for patients with PC.

Incretin-Based Medicines

The use of incretin-based medicines—glucagon-like peptide 1 receptor agonists (GLP1-RAs) and dipeptidyl peptidase-4 inhibitors (DPP4is)—is increasingly popular. Some studies in animal models have been speculated that the chronic overstimulation of GLP1 receptors in exocrine pancreatic cells may induce pancreatitis, ultimately increasing the risk of PC (110, 111). However, this hypothesis has not been supported by evidence from clinical trials (112, 113).

Monami et al. (112) analyzed 113 trials, and 15 studies that reported at least one event. Those 15 studies enrolled 14,866 and 12,849 patients in GLP1-RA and comparator groups, respectively, and the number of reported PCs was 24 for GLP1-RAs and was 23 for comparators (Mantel-Haenszel odds

ratio [MH-OR] for PC with GLP1-RA treatment = 0.94, 95% CI, 0.52–1.70, $P = 0.84$). Similar results were obtained in a post-hoc analysis excluding comparisons with DPP4is (MH-OR = 0.93, 95% CI, 0.51–1.69, $P = 0.80$).

In 2020, Nreu et al. (113) analyzed 43 randomized, controlled trials that met the following inclusion criteria: at least 52 weeks in duration, and comparison of a GLP1-RA *versus* any non–GLP1-RA treatment in patients with T2DM and PC. They found that GLP1-RA use showed no association with PC (MH-OR = 1.28, 95% CI, 0.87–1.89, $P = 0.20$) (107).

Currently, no clear evidence of risk for PC has been observed with the use of incretin-based medications. Data about the relationship between incretin-based medicines and PC may be too scarce to draw any conclusion.

Sodium-Glucose Cotransporter 2 Inhibitors

Sodium-glucose cotransporter 2 (SGLT2) inhibitors represent a novel class of oral antidiabetic drugs that help maintain glycemic control by decreasing the reabsorption of glucose and increasing the excretion of urinary glucose (114). In addition to substantial cardiovascular benefits, anti-tumor benefits or the safety of SGLT2 inhibitors have been considered by the public. Scafoglio et al. (115) found that SGLT2 was functionally expressed in pancreatic carcinomas and that SGLT2 inhibitors blocked glucose uptake and reduced tumor growth and survival in a xenograft model of PC. These findings suggest that SGLT2 inhibitors may be useful for cancer therapy.

In 2019, Tang et al. (116) undertook a study to systematically evaluate the association between SGLT2 inhibitors and pancreatic safety in patients with T2DM. Of the 35 trials, involving 44,912 patients with T2DM, 40 PC events (in 18 trials and 27,806 patients) were reported during a median follow-up of 52 weeks. SGLT2 inhibitors were not associated with PC (OR=1.34; 95% CI, 0.71–2.54; very-low-quality evidence) (116).

CONCLUSION

PC is highly aggressive and lethal malignancy, and T2DM is the most common metabolic disease. T2DM is a risk factor for PC. Conversely, NOD may be a sign and consequence of PC. Screening in patients with NOD combined with assessment of risk factors and biomarkers may be an important way to improve the early diagnosis of PC. The mechanisms that contribute to the relationship between PC and diabetes include insulin resistance, hyperinsulinemia, hyperglycemia, and chronic inflammation. Metformin, insulin, GLP1-RAs, DPP4is, and SGLT2 inhibitors are common drugs that treat T2DM. Studies have shown that metformin can reduce the risk of PC, whereas insulin therapy is associated with a higher risk of PC. Therefore, metformin may be used to prevent the development of malignant lesions and is expected to become an anticancer agent. T2DM-related studies will likely be crucial to improve the morbidity and mortality associated with PC.

AUTHOR CONTRIBUTIONS

XD consulted literatures and wrote the manuscript. LG designed the review. WW and QP assisted with writing and revised the manuscript. All authors contributed to the article and approved the submitted version.

FUNDING

This work was supported by the National Natural Science Foundation of China (grants 81670763 and 81471050).

ACKNOWLEDGMENTS

We sincerely thank editors at Charlesworth Author Services for editing the language of this article.

REFERENCES

1. Siegel RL, Miller KD, Fuchs HE, Jemal A. Cancer Statistics, 2021. *CA: A Cancer J Clin* (2021) 71(1):7–33. doi: 10.3322/caac.21654
2. Klein AP. Pancreatic Cancer Epidemiology: Understanding the Role of Lifestyle and Inherited Risk Factors. *Nat Rev Gastro Hepat* (2021) 18 (7):493–502. doi: 10.1038/s41575-021-00457-x
3. Chinese Pancreatic Surgery Association, Chinese Society of Surgery and Chinese Medical Association. Guidelines for the Diagnosis and Treatment of Pancreatic Cancer in China (2021). *Zhonghua wai ke za zhi [Chinese J Surgery]* (2021) 59(7):561–77. doi: 10.3760/cma.j.cn112139-20210416-00171
4. Zhao C, Gao F, Li Q, Liu Q, Lin X. The Distributional Characteristic and Growing Trend of Pancreatic Cancer in China. *Pancreas* (2019) 48(3):309–14. doi: 10.1097/MPA.0000000000001222
5. Cheng F, Carroll L, Joglekar MV, Januszewski AS, Wong KK, Hardikar AA, et al. Diabetes, Metabolic Disease, and Telomere Length. *Lancet Diabetes Endocrinol* (2021) 9(2):117–26. doi: 10.1016/S2213-8587(20)30365-X
6. Gallagher EJ, LeRoith D. Hyperinsulinaemia in Cancer. *Nat Rev Cancer* (2020) 20(11):629–44. doi: 10.1038/s41568-020-0295-5
7. Mizrahi JD, Surana R, Valle JW, Shroff RT. Pancreatic Cancer. *Lancet* (2020) 395(10242):2008–20. doi: 10.1016/S0140-6736(20)30974-0
8. Toledo FGS, Chari S, Yadav D. Understanding the Contribution of Insulin Resistance to the Risk of Pancreatic Cancer. *Am J Gastroenterol* (2021) 116 (4):669–70. doi: 10.14309/ajg.0000000000001104
9. Gallo M, Adinolfi V, Morviducci L, Acquati S, Tuveri E, Ferrari P, et al. Early Prediction of Pancreatic Cancer From New-Onset Diabetes: An Associazione Italiana Oncologia Medica (AIOM)/Associazione Medici Diabetologi (AMD)/Società Italiana Endocrinologia (SIE)/Società Italiana Farmacologia (SIF) Multidisciplinary Consensus Position Paper. *ESMO Open* (2021) 6(3):100155. doi: 10.1016/j.esmoop.2021.100155
10. Takikawa T, Kikuta K, Kume K, Hamada S, Miura S, Yoshida N, et al. New-Onset or Exacerbation of Diabetes Mellitus Is a Clue to the Early Diagnosis of Pancreatic Cancer. *Tohoku J Exp Med* (2020) 252(4):353–64. doi: 10.1620/tjem.252.353
11. Khan S, Safarudin RF, Kupec JT. Validation of the ENDPAC Model: Identifying New-Onset Diabetics at Risk of Pancreatic Cancer. *Pancreatology* (2021) 21(3):550–5. doi: 10.1016/j.pan.2021.02.001
12. Quoc Lam B, Shrivastava SK, Shrivastava A, Shankar S, Srivastava RK. The Impact of Obesity and Diabetes Mellitus on Pancreatic Cancer: Molecular Mechanisms and Clinical Perspectives. *J Cell Mol Med* (2020) 24(14):7706–16. doi: 10.1111/jcmm.15413
13. Perreault L, Skyler JS, Rosenstock J. Novel Therapies With Precision Mechanisms for Type 2 Diabetes Mellitus. *Nat Rev Endocrinol* (2021) 17 (6):364–77. doi: 10.1038/s41574-021-00489-y

14. Targher G, Corey KE, Byrne CD, Roden M. The Complex Link Between NAFLD and Type 2 Diabetes Mellitus - Mechanisms and Treatments. *Nat Rev Gastroenterol Hepatol* (2021) in press. doi: 10.1038/s41575-021-00448-y
15. Alpertunga I, Sadiq R, Pandya D, Lo T, Dulgher M, Evans S, et al. Glycemic Control as an Early Prognostic Marker in Advanced Pancreatic Cancer. *Front Oncol* (2021) 11:571855. doi: 10.3389/fonc.2021.571855
16. Yu Q, Zhang Z, Zhang H. Effect of Glucose Variability on Pancreatic Cancer Through Regulation of COL6A1. *Cancer Manag Res* (2021) 13:1291–8. doi: 10.2147/CMAR.S293473
17. Rahn S, Zimmermann V, Viol F, Knaack H, Stemmer K, Peters L, et al. Diabetes as Risk Factor for Pancreatic Cancer: Hyperglycemia Promotes Epithelial-Mesenchymal-Transition and Stem Cell Properties in Pancreatic Ductal Epithelial Cells. *Cancer Lett* (2018) 415:129–50. doi: 10.1016/j.canlet.2017.12.004
18. Sato K, Hikita H, Myojin Y, Fukumoto K, Murai K, Sakane S, et al. Hyperglycemia Enhances Pancreatic Cancer Progression Accompanied by Elevations in Phosphorylated STAT3 and MYC Levels. *PloS One* (2020) 15 (7):e235573. doi: 10.1371/journal.pone.0235573
19. Milton CK, Self AJ, Clarke PA, Banerji U, Piccioni F, Root DE, et al. A Genome-Scale CRISPR Screen Identifies the ERBB and mTOR Signaling Networks as Key Determinants of Response to PI3K Inhibition in Pancreatic Cancer. *Mol Cancer Ther* (2020) 19:1423–35. doi: 10.1158/1535-7163.MCT-19-1131
20. Javle MM, Shroff RT, Xiong H, Varadhachary GA, Fogelman D, Reddy SA, et al. Inhibition of the Mammalian Target of Rapamycin (mTOR) in Advanced Pancreatic Cancer: Results of Two Phase II Studies. *BMC Cancer* (2010) 10(1):368. doi: 10.1186/1471-2407-10-368
21. Wolpin BM, Hezel AF, Abrams T, Blaszkowsky LS, Meyerhardt JA, Chan JA, et al. Oral mTOR Inhibitor Everolimus in Patients With Gemcitabine-Refractory Metastatic Pancreatic Cancer. *J Clin Oncol* (2009) 27(2):193–8. doi: 10.1200/JCO.2008.18.9514
22. Kordes S, Klümpen HJ, Weterman MJ, Schellens JHM, Richel DJ, Wilmink JW. Phase II Study of Capecitabine and the Oral mTOR Inhibitor Everolimus in Patients With Advanced Pancreatic Cancer. *Cancer Chemoth Pharm* (2015) 75 (6):1135–41. doi: 10.1007/s00280-015-2730-y
23. Chen YH, Huang YC, Yang SF, Yen HH, Tsai HD, Hsieh MC, et al. Pitavastatin and Metformin Synergistically Activate Apoptosis and Autophagy in Pancreatic Cancer Cells. *Environ Toxicol* (2021) 36(8):1491–503. doi: 10.1002/tox.23146
24. Grote VA, Rohrmann S, Nieters A, Dossus L, Tjønneland A, Halkjær J, et al. Diabetes Mellitus, Glycated Haemoglobin and C-Peptide Levels in Relation to Pancreatic Cancer Risk: A Study Within the European Prospective Investigation Into Cancer and Nutrition (EPIC) Cohort. *Diabetologia* (2011) 54(12):3037–46. doi: 10.1007/s00125-011-2316-0
25. Menini S, Iacobini C, de Latouliere L, Manni I, Ionta V, Blasetti Fantauzzi C, et al. The Advanced Glycation End-Product N-Carboxymethyllysine Promotes Progression of Pancreatic Cancer: Implications for Diabetes-Associated Risk and Its Prevention. *J Pathol* (2018) 245(2):197–208. doi: 10.1002/path.5072
26. Kiss K, Baghy K, Spisák S, Szanyi S, Tulassay Z, Zalatnai A, et al. Chronic Hyperglycemia Induces Trans-Differentiation of Human Pancreatic Stellate Cells and Enhances the Malignant Molecular Communication With Human Pancreatic Cancer Cells. *PloS One* (2015) 10(5):e128059. doi: 10.1371/journal.pone.0128059
27. Martinez-Useros J, Li W, Cabeza-Morales M, Garcia-Foncillas J. Oxidative Stress: A New Target for Pancreatic Cancer Prognosis and Treatment. *J Clin Med* (2017) 6. doi: 10.3390/jcm6030029
28. Luo J, Xiang Y, Xu X, Fang D, Li D, Ni F, et al. High Glucose-Induced ROS Production Stimulates Proliferation of Pancreatic Cancer *via* Inactivating the JNK Pathway. *Oxid Med Cell Longev* (2018) 2018:1–10. doi: 10.1155/2018/6917206
29. Cao L, Chen X, Xiao X, Ma Q, Li W. Resveratrol Inhibits Hyperglycemia-Driven ROS-Induced Invasion and Migration of Pancreatic Cancer Cells *via* Suppression of the ERK and P38 MAPK Signaling Pathways. *Int J Oncol* (2016) 49(2):735–43. doi: 10.3892/ijo.2016.3559
30. Li W. Hyperglycemia as a Mechanism of Pancreatic Cancer Metastasis. *Front Biosci* (2012) 17(1):1761. doi: 10.2741/4017
31. Li W, Wu Z, Ma Q, Liu J, Xu Q, Han L, et al. Hyperglycemia Regulates TXNIP/TRX/ROS Axis *via* P38 MAPK and ERK Pathways in Pancreatic Cancer. *Curr Cancer Drug Tar* (2014) 14(4):348–56. doi: 10.2174/1568009614666140331231658
32. Shlomai G, Neel B, LeRoith D, Gallagher EJ. Type 2 Diabetes Mellitus and Cancer: The Role of Pharmacotherapy. *J Clin Oncol* (2016) 34(35):4261–9. doi: 10.1200/JCO.2016.67.4044
33. Gallagher EJ, LeRoith D. The Proliferating Role of Insulin and Insulin-Like Growth Factors in Cancer. *Trends Endocrinol Metab* (2010) 21(10):610–8. doi: 10.1016/j.tem.2010.06.007
34. Sathishkumar C, Prabu P, Balakumar M, Lenin R, Prabhu D, Anjana RM, et al. Augmentation of Histone Deacetylase 3 (HDAC3) Epigenetic Signature at the Interface of Proinflammation and Insulin Resistance in Patients With Type 2 Diabetes. *Clin Epigenet* (2016) 8(1):125. doi: 10.1186/s13148-016-0293-3
35. Sharma S, Taliyan R. Histone Deacetylase Inhibitors: Future Therapeutics for Insulin Resistance and Type 2 Diabetes. *Pharmacol Res* (2016) 113:320–6. doi: 10.1016/j.phrs.2016.09.009
36. Paneni F, Costantino S, Cosentino F. Insulin Resistance, Diabetes, and Cardiovascular Risk. *Curr Atheroscler Rep* (2014) 16(7):419. doi: 10.1007/s11883-014-0419-z
37. Ross JS, Russo SB, Chavis GC, Cowart LA. Sphingolipid Regulators of Cellular Dysfunction in Type 2 Diabetes Mellitus: A Systems Overview. *Clin Lipidol* (2014) 9(5):553–69. doi: 10.2217/clp.14.37
38. Rojas-Rodriguez R, Ziegler R, DeSouza T, Majid S, Madore AS, Amir N, et al. PAPPA-Mediated Adipose Tissue Remodeling Mitigates Insulin Resistance and Protects Against Gestational Diabetes in Mice and Humans. *Sci Transl Med* (2020) 12(571):y4145. doi: 10.1126/scitranslmed.aay4145
39. Thomas RJ, Kenfield SA, Jimenez A. Exercise-Induced Biochemical Changes and Their Potential Influence on Cancer: A Scientific Review. *Brit J Sport Med* (2017) 51(8):640–4. doi: 10.1136/bjsports-2016-096343
40. Belfiore A, Malaguarnera R, Vella V, Lawrence MC, Sciacca L, Frasca F, et al. Insulin Receptor Isoforms in Physiology and Disease: An Updated View. *Endocr Rev* (2017) 38(5):379–431. doi: 10.1210/er.2017-00073
41. Bassil F, Canron M, Vital A, Bezard E, Li Y, Greig NH, et al. Insulin Resistance and Exendin-4 Treatment for Multiple System Atrophy. *Brain* (2017) 140(5):1420–36. doi: 10.1093/brain/awx044
42. Matsushita M, Fujita K, Hayashi T, Kayama H, Motooka D, Hase H, et al. Gut Microbiota-Derived Short-Chain Fatty Acids Promote Prostate Cancer Growth *via* IGF-1 Signaling. *Cancer Res* (2021) 81(15):4014–26. doi: 10.1158/0008-5472.CAN-20-4090
43. Baxter RC. IGF Binding Proteins in Cancer: Mechanistic and Clinical Insights. *Nat Rev Cancer* (2014) 14(5):329–41. doi: 10.1038/nrc3720
44. Werner H, Sarfstein R, Laron Z. The Role of Nuclear Insulin and IGF1 Receptors in Metabolism and Cancer. *Biomolecules* (2021) 11:531. doi: 10.3390/biom11040531
45. Badarni M, Prasad M, Golden A, Bhattacharya B, Levin L, Yegodayev KM, et al. IGF2 Mediates Resistance to Isoform-Selective-Inhibitors of the PI3K in HPV Positive Head and Neck Cancer. *Cancers* (2021) 13:2250. doi: 10.3390/cancers13092250
46. Pollak M. The Insulin and Insulin-Like Growth Factor Receptor Family in Neoplasia: An Update. *Nat Rev Cancer* (2012) 12(3):159–69. doi: 10.1038/nrc3215
47. Hua H, Kong Q, Yin J, Zhang J, Jiang Y. Insulin-Like Growth Factor Receptor Signaling in Tumorigenesis and Drug Resistance: A Challenge for Cancer Therapy. *J Hematol Oncol* (2020) 13(1):64. doi: 10.1186/s13045-020-00904-3
48. LeRoith D, Holly JMP, Forbes BE. Insulin-Like Growth Factors: Ligands, Binding Proteins, and Receptors. *Mol Metab* (2021), in press. doi: 10.1016/j.molmet.2021.101245
49. Hua H, Kong Q, Zhang H, Wang J, Luo T, Jiang Y. Targeting mTOR for Cancer Therapy. *J Hematol Oncol* (2019) 12(1):71. doi: 10.1186/s13045-019-0754-1
50. Geleta B, Park KC, Jansson PJ, Sahni S, Maleki S, Xu Z, et al. Breaking the Cycle: Targeting of NDRG1 to Inhibit Bi-Directional Oncogenic Cross-Talk Between Pancreatic Cancer and Stroma. *FASEB J* (2021) 35(2):e21347. doi: 10.1096/fj.202002279R

51. Włodarczyk B, Borkowska A, Włodarczyk P, Małecka-Panas E, Gąsiorowska A. Insulin-Like Growth Factor 1 and Insulin-Like Growth Factor Binding Protein 2 Serum Levels as Potential Biomarkers in Differential Diagnosis Between Chronic Pancreatitis and Pancreatic Adenocarcinoma in Reference to Pancreatic Diabetes. *Gastroenterol Rev* (2021) 16(1):36–42. doi: 10.5114/pg.2020.95091
52. Zheng Y, Wu C, Yang J, Zhao Y, Jia H, Xue M, et al. Insulin-Like Growth Factor 1-Induced Enolase 2 Deacetylation by HDAC3 Promotes Metastasis of Pancreatic Cancer. *Signal Transduct Target Ther* (2020) 5(1):53. doi: 10.1038/s41392-020-0146-6
53. Wlodarczyk B, Gasiorowska A, Malecka-Panas E. The Role of Insulin-Like Growth Factor (IGF) Axis in Early Diagnosis of Pancreatic Adenocarcinoma (PDAC). *J Clin Gastroenterol* (2018) 52(7):569–72. doi: 10.1097/MCG.0000000000001073
54. Jin Q, Hart PA, Shi N, Joseph JJ, Donneyong M, Conwell DL, et al. Dietary Patterns of Insulinemia, Inflammation and Glycemia, and Pancreatic Cancer Risk: Findings From the Women's Health Initiative. *Cancer Epidem Biomar* (2021) 30(6):1229–40. doi: 10.1158/1055-9965.EPI-20-1478
55. Desai V, Patel K, Sheth R, Barlass U, Chan Y, Sclamberg J, et al. Pancreatic Fat Infiltration Is Associated With a Higher Risk of Pancreatic Ductal Adenocarcinoma. *Visceral Med* (2020) 36(3):220–6. doi: 10.1159/000507457
56. Liao WC, Chen PR, Huang CC, Chang YT, Huang BS, Chang CC, et al. Relationship Between Pancreatic Cancer-Associated Diabetes and Cachexia. *J Cachexia Sarcopenia Muscle* (2020) 11(4):899–908. doi: 10.1002/jcsm.12553
57. Spyrou N, Avgerinos KI, Mantzoros CS, Dalamaga M. Classic and Novel Adipocytokines at the Intersection of Obesity and Cancer: Diagnostic and Therapeutic Strategies. *Curr Obes Rep* (2018) 7(4):260–75. doi: 10.1007/s13679-018-0318-7
58. Mannelli M, Gamberi T, Magherini F, Fiaschi T. The Adipokines in Cancer Cachexia. *Int J Mol Sci* (2020) 21(14):4860. doi: 10.3390/ijms21144860
59. Garikapati KK, Ammu VVVR, Krishnamurthy PT, Chintamaneni PK, Pindiprolu SKSS. Type-II Endometrial Cancer: Role of Adipokines. *Arch Gynecol Obstet* (2019) 300(2):239–49. doi: 10.1007/s00404-019-05181-1
60. Takahashi M, Mutoh M, Ishigamori R, Fujii G, Imai T, Tanaka T, et al. Involvement of Inflammatory Factors in Pancreatic Carcinogenesis and Preventive Effects of Anti-Inflammatory Agents. *Semin Immunopathol* (2013) 35(2):203–27. doi: 10.1007/s00281-012-0340-x
61. Pothuraju R, Rachagani S, Junker WM, Chaudhary S, Saraswathi V, Kaur S, et al. Pancreatic Cancer Associated With Obesity and Diabetes: An Alternative Approach for Its Targeting. *J Exp Clin Canc Res* (2018) 37(1):319. doi: 10.1186/s13046-018-0963-4
62. Yadav RK, Gautam DK, Muj C, Madhubabu GB, Paddibhatla I. Methotrexate Negatively Acts on Inflammatory Responses Triggered in Drosophila Larva With Hyperactive JAK/STAT Pathway. *Dev Comp Immunol* (2021), in press. doi: 10.1016/j.dci.2021.104161
63. Paternoster S, Falasca M. The Intricate Relationship Between Diabetes, Obesity and Pancreatic Cancer. *Biochim Biophys Acta (BBA) - Rev Cancer* (2020) 1873(1):188326. doi: 10.1016/j.bbcan.2019.188326
64. Menini S, Iacobini C, de Latouliere L, Manni I, Vitale M, Pilozzi E, et al. Diabetes Promotes Invasive Pancreatic Cancer by Increasing Systemic and Tumour Carbonyl Stress in KrasG12D/+ Mice. *J Exp Clin Canc Res* (2020) 39(1):1–152. doi: 10.1186/s13046-020-01665-0
65. Tang Z, Chu Y, Tan Y, Li J, Gao S. Pancreatic and Duodenal Homeobox-1 in Pancreatic Ductal Adenocarcinoma and Diabetes Mellitus. *Chin Med J Peking* (2020) 133(3):344–50. doi: 10.1097/CM9.0000000000000628
66. Španinger E, Potočnik U, Bren U. Molecular Dynamics Simulations Predict That rSNP Located in the HNF-1α Gene Promotor Region Linked With MODY3 and Hepatocellular Carcinoma Promotes Stronger Binding of the HNF-4α Transcription Factor. *Biomolecules* (2020) 10(12):1700. doi: 10.3390/biom10121700
67. Broche B, Ben Fradj S, Aguilar E, Sancerni T, Bénard M, Makaci F, et al. Mitochondrial Protein UCP2 Controls Pancreas Development. *Diabetes* (2017) 67(1):78–84. doi: 10.2337/db17-0118
68. Esteves P, Pecqueur C, Ransy C, Esnous C, Lenoir V, Bouillaud F, et al. Mitochondrial Retrograde Signaling Mediated by UCP2 Inhibits Cancer Cell Proliferation and Tumorigenesis. *Cancer Res* (2014) 74(14):3971–82. doi: 10.1158/0008-5472.CAN-13-3383
69. Brandi J, Cecconi D, Cordani M, Torrens-Mas M, Pacchiana R, Dalla Pozza E, et al. The Antioxidant Uncoupling Protein 2 Stimulates Hnrnpa2/B1, GLUT1 and PKM2 Expression and Sensitizes Pancreas Cancer Cells to Glycolysis Inhibition. *Free Radical Bio Med* (2016) 101:305–16. doi: 10.1016/j.freeradbiomed.2016.10.499
70. Henrikson NB, Aiello Bowles EJ, Blasi PR, Morrison CC, Nguyen M, Pillarisetty VG, et al. Screening for Pancreatic Cancer. *JAMA* (2019) 322(5):445. doi: 10.1001/jama.2019.6190
71. Pereira SP, Oldfield L, Ney A, Hart PA, Keane MG, Pandol SJ, et al. Early Detection of Pancreatic Cancer. *Lancet Gastroenterol Hepatol* (2020) 5(7):698–710. doi: 10.1016/S2468-1253(19)30416-9
72. Singhi AD, Koay EJ, Chari ST, Maitra A. Early Detection of Pancreatic Cancer: Opportunities and Challenges. *Gastroenterology* (2019) 156(7):2024–40. doi: 10.1053/j.gastro.2019.01.259
73. Liao W, Huang B, Yu Y, Yang H, Chen P, Huang C, et al. Galectin-3 and S100A9: Novel Diabetogenic Factors Mediating Pancreatic Cancer–Associated Diabetes. *Diabetes Care* (2019) 42(9):1752–9. doi: 10.2337/dc19-0217
74. Petrusel L, Bilibou M, Drug V, Leucuta DC, Seicean R, Cainap C, et al. Risk Factors in Pancreatic Adenocarcinoma: The Interrelation With Familial History and Predictive Role on Survival. *J Gastrointest Liver Diseases: JGLD* (2020) 29:391–8. doi: 10.15403/jgld-2529
75. Maitra A, Sharma A, Brand RE, Van Den Eeden SK, Fisher WE, Hart PA, et al. A Prospective Study to Establish a New-Onset Diabetes Cohort. *Pancreas* (2018) 47(10):1244–8. doi: 10.1097/MPA.0000000000001169
76. Sharma A, Kandlakunta H, Nagpal SJS, Feng Z, Hoos W, Petersen GM, et al. Model to Determine Risk of Pancreatic Cancer in Patients With New-Onset Diabetes. *Gastroenterology* (2018) 155(3):730–9. doi: 10.1053/j.gastro.2018.05.023
77. Mueller AM, Meier CR, Jick SS, Schneider C. Weight Change and Blood Glucose Concentration as Markers for Pancreatic Cancer in Subjects With New-Onset Diabetes Mellitus: A Matched Case-Control Study. *Pancreatology* (2019) 19(4):578–86. doi: 10.1016/j.pan.2019.03.006
78. Dong X, Lou YB, Mu YC, Kang MX, Wu YL. Predictive Factors for Differentiating Pancreatic Cancer-Associated Diabetes Mellitus From Common Type 2 Diabetes Mellitus for the Early Detection of Pancreatic Cancer. *Digestion* (2018) 98(4):209–16. doi: 10.1159/000489169
79. Walter FM, Mills K, Mendonça SC, Abel GA, Basu B, Carroll N, et al. Symptoms and Patient Factors Associated With Diagnostic Intervals for Pancreatic Cancer (SYMPTOM Pancreatic Study): A Prospective Cohort Study. *Lancet Gastroenterol Hepatol* (2016) 1(4):298–306. doi: 10.1016/S2468-1253(16)30079-6
80. Illés D, Terzin V, Holzinger G, Kosár K, Róka R, Zsóri G, et al. New-Onset Type 2 Diabetes Mellitus – A High-Risk Group Suitable for the Screening of Pancreatic Cancer? *Pancreatology* (2016) 16(2):266–71. doi: 10.1016/j.pan.2015.12.005
81. Choe JW, Kim JS, Kim HJ, Hwang SY, Joo MK, Lee BJ, et al. Value of Early Check-Up of Carbohydrate Antigen 19-9 Levels for Pancreatic Cancer Screening in Asymptomatic New-Onset Diabetic Patients. *Pancreas* (2016) 45(5):730–4. doi: 10.1097/MPA.0000000000000538
82. Choe JW, Kim HJ, Kim JS, Cha J, Joo MK, Lee BJ, et al. Usefulness of CA 19–9 for Pancreatic Cancer Screening in Patients With New-Onset Diabetes. *Hepatob Pancreat Dis* (2018) 17(3):263–8. doi: 10.1016/j.hbpd.2018.04.001
83. Grote VA, Kaaks R, Nieters A, Tjønneland A, Halkjær J, Overvad K, et al. Inflammation Marker and Risk of Pancreatic Cancer: A Nested Case–Control Study Within the EPIC Cohort. *Brit J Cancer* (2012) 106(11):1866–74. doi: 10.1038/bjc.2012.172
84. Shi W, Qiu W, Wang W, Zhou X, Zhong X, Tian G, et al. Osteoprotegerin Is Up-Regulated in Pancreatic Cancers and Correlates With Cancer-Associated New-Onset Diabetes. *Biosci Trends* (2014) 8(6):322–6. doi: 10.5582/bst.2014.01092
85. Kang M, Qin W, Buya M, Dong X, Zheng W, Lu W, et al. VNN1, a Potential Biomarker for Pancreatic Cancer-Associated New-Onset Diabetes, Aggravates Paraneoplastic Islet Dysfunction by Increasing Oxidative Stress. *Cancer Lett* (2016) 373(2):241–50. doi: 10.1016/j.canlet.2015.12.031
86. Huang H, Dong X, Kang MX, Xu B, Chen Y, Zhang B, et al. Novel Blood Biomarkers of Pancreatic Cancer–Associated Diabetes Mellitus Identified by

Peripheral Blood–Based Gene Expression Profiles. *Am J Gastroenterol* (2010) 105(7):1661–9. doi: 10.1038/ajg.2010.32
87. Kang M, Qin W, Buya M, Dong X, Zheng W, Lu W, et al. VNN1, a Potential Biomarker for Pancreatic Cancer-Associated New-Onset Diabetes, Aggravates Paraneoplastic Islet Dysfunction by Increasing Oxidative Stress. *Cancer Lett* (2016) 373(2):241–50. doi: 10.1016/j.canlet.2015.12.031
88. Iovanna J. Implementing Biological Markers as a Tool to Guide Clinical Care of Patients With Pancreatic Cancer. *Transl Oncol* (2021) 14(1):100965. doi: 10.1016/j.tranon.2020.100965
89. Dai X, Pang W, Zhou Y, Yao W, Xia L, Wang C, et al. Altered Profile of Serum microRNAs in Pancreatic Cancer-Associated New-Onset Diabetes Mellitus. *J Diabetes* (2016) 8(3):422–33. doi: 10.1111/1753-0407.12313
90. Tan J, You Y, Guo F, Xu J, Dai H, Bie P. Association of Elevated Risk of Pancreatic Cancer in Diabetic Patients: A Systematic Review and Meta-Analysis. *Oncol Lett* (2017) 13(3):1247–55. doi: 10.3892/ol.2017.5586
91. Kautzky-Willer A, Thurner S, Klimek P. Use of Statins Offsets Insulin-Related Cancer Risk. *J Intern Med* (2017) 281(2):206–16. doi: 10.1111/joim.12567
92. Bosetti C, Rosato V, Li D, Silverman D, Petersen GM, Bracci PM, et al. Diabetes, Antidiabetic Medications, and Pancreatic Cancer Risk: An Analysis From the International Pancreatic Cancer Case-Control Consortium. *Ann Oncol* (2014) 25(10):2065–72. doi: 10.1093/annonc/mdu276
93. Lee DY, Yu JH, Park S, Han K, Kim NH, Yoo HJ, et al. The Influence of Diabetes and Antidiabetic Medications on the Risk of Pancreatic Cancer: A Nationwide Population-Based Study in Korea. *Sci Rep Uk* (2018) 8(1):9719. doi: 10.1038/s41598-018-27965-2
94. Liu YC, Nguyen PA, Humayun A, Chien SC, Yang HC, Asdary RN, et al. Does Long-Term Use of Antidiabetic Drugs Changes Cancer Risk? *Medicine* (2019) 98(40):e17461. doi: 10.1097/MD.0000000000017461
95. Wang G, Yin L, Peng Y, Gao Y, Gao H, Zhang J, et al. Insulin Promotes Invasion and Migration of KRASG12D Mutant HPNE Cells by Upregulating MMP-2 Gelatinolytic Activity *via* ERK- and PI3K-Dependent Signalling. *Cell Proliferat* (2019) 52(3):e12575. doi: 10.1111/cpr.12575
96. Cho J, Scragg R, Pandol SJ, Goodarzi MO, Petrov MS. Antidiabetic Medications and Mortality Risk in Individuals With Pancreatic Cancer–Related Diabetes and Postpancreatitis Diabetes: A Nationwide Cohort Study. *Diabetes Care* (2019) 42(9):1675–83. doi: 10.2337/dc19-0145
97. Wang C, Zhang T, Liao Q, Dai M, Guo J, Yang X, et al. Metformin Inhibits Pancreatic Cancer Metastasis Caused by SMAD4 Deficiency and Consequent HNF4G Upregulation. *Protein Cell* (2021) 12(2):128–44. doi: 10.1007/s13238-020-00760-4
98. Chen K, Qian W, Jiang Z, Cheng L, Li J, Sun L, et al. Metformin Suppresses Cancer Initiation and Progression in Genetic Mouse Models of Pancreatic Cancer. *Mol Cancer* (2017) 16(1):131. doi: 10.1186/s12943-017-0701-0
99. Han H, Hou Y, Chen X, Zhang P, Kang M, Jin Q, et al. Metformin-Induced Stromal Depletion to Enhance the Penetration of Gemcitabine-Loaded Magnetic Nanoparticles for Pancreatic Cancer Targeted Therapy. *J Am Chem Soc* (2020) 142(10):4944–54. doi: 10.1021/jacs.0c00650
100. Bosetti C, Rosato V, Li D, Silverman D, Petersen GM, Bracci PM, et al. Diabetes, Antidiabetic Medications, and Pancreatic Cancer Risk: An Analysis From the International Pancreatic Cancer Case-Control Consortium. *Ann Oncol* (2014) 25(10):2065–72. doi: 10.1093/annonc/mdu276
101. Lee DY, Yu JH, Park S, Han K, Kim NH, Yoo HJ, et al. The Influence of Diabetes and Antidiabetic Medications on the Risk of Pancreatic Cancer: A Nationwide Population-Based Study in Korea. *Sci Rep Uk* (2018) 8(1):9719. doi: 10.1038/s41598-018-27965-2
102. Kordes S, Pollak MN, Zwinderman AH, Mathôt RA, Weterman MJ, Beeker A, et al. Metformin in Patients With Advanced Pancreatic Cancer: A Double-Blind, Randomised, Placebo-Controlled Phase 2 Trial. *Lancet Oncol* (2015) 16:839–47. doi: 10.1016/S1470-2045(15)00027-3
103. De Souza A, Khawaja KI, Masud F, Saif MW. Metformin and Pancreatic Cancer: Is There a Role? *Cancer Chemoth Pharm* (2016) 77(2):235–42. doi: 10.1007/s00280-015-2948-8
104. Yoshida J, Ishikawa T, Endo Y, Matsumura S, Ota T, Mizushima K, et al. Metformin Inhibits TGF–β1–Induced Epithelial–Mesenchymal Transition and Liver Metastasis of Pancreatic Cancer Cells. *Oncol Rep* (2020) 44(1):371–81. doi: 10.3892/or.2020.7595
105. Zhao H, Zhou N, Jin F, Wang R, Zhao J. Metformin Reduces Pancreatic Cancer Cell Proliferation and Increases Apoptosis Through MTOR Signaling Pathway and its Dose-Effect Relationship. *Eur Rev Med Pharmaco* (2020) 24 (10):5336. doi: 10.26355/eurrev_202005_21316
106. Fitzgerald TL, Lertpiriyapong K, Cocco L, Martelli AM, Libra M, Candido S, et al. Roles of EGFR and KRAS and Their Downstream Signaling Pathways in Pancreatic Cancer and Pancreatic Cancer Stem Cells. *Adv Biol Regul* (2015) 59:65–81. doi: 10.1016/j.jbior.2015.06.003
107. Soliman GA, Shukla SK, Etekpo A, Gunda V, Steenson SM, Gautam N, et al. The Synergistic Effect of an ATP-Competitive Inhibitor of mTOR and Metformin on Pancreatic Tumor Growth. *Curr Developments Nutr* (2020) 4(9):a131. doi: 10.1093/cdn/nzaa131
108. Lonardo E, Cioffi M, Sancho P, Sanchez-Ripoll Y, Trabulo SM, Dorado J, et al. Metformin Targets the Metabolic Achilles Heel of Human Pancreatic Cancer Stem Cells. *PloS One* (2013) 8(10):e76518. doi: 10.1371/journal.pone.0076518
109. Ma M, Ma C, Li P, Ma C, Ping F, Li W, et al. Low Glucose Enhanced Metformin's Inhibitory Effect on Pancreatic Cancer Cells by Suppressing Glycolysis and Inducing Energy Stress *via* Up-Regulation of miR-210-5p. *Cell Cycle (Georgetown Tex)* (2020) 19(17):2168–81. doi: 10.1080/15384101.2020.1796036
110. Gale EAM. Response to Comment on: Butler Et al. A Critical Analysis of the Clinical Use of Incretin-Based Therapies: Are the GLP-1 Therapies Safe? *Diabetes Care* (2013) 36:2118–25. doi: 10.2337/dc13-1542
111. Gier B, Matveyenko AV, Kirakossian D, Dawson D, Dry SM, Butler PC. Chronic GLP-1 Receptor Activation by Exendin-4 Induces Expansion of Pancreatic Duct Glands in Rats and Accelerates Formation of Dysplastic Lesions and Chronic Pancreatitis in the KrasG12D Mouse Model. *Diabetes* (2012) 61(5):1250–62. doi: 10.2337/db11-1109
112. Monami M, Nreu B, Scatena A, Cresci B, Andreozzi F, Sesti G, et al. Safety Issues With Glucagon-Like Peptide-1 Receptor Agonists (Pancreatitis, Pancreatic Cancer and Cholelithiasis): Data From Randomized Controlled Trials. *Diabetes Obes Metab* (2017) 19(9):1233–41. doi: 10.1111/dom.12926
113. Nreu B, Dicembrini I, Tinti F, Mannucci E, Monami M. Pancreatitis and Pancreatic Cancer in Patients With Type 2 Diabetes Treated With Glucagon-Like Peptide-1 Receptor Agonists: An Updated Meta-Analysis of Randomized Controlled Trials. *Minerva Endocrinol* (2020) in press. doi: 10.23736/S0391-1977.20.03219-8
114. Ferrannini E, Solini A. SGLT2 Inhibition in Diabetes Mellitus: Rationale and Clinical Prospects. *Nat Rev Endocrinol* (2012) 8(8):495–502. doi: 10.1038/nrendo.2011.243
115. Scafoglio C, Hirayama BA, Kepe V, Liu J, Ghezzi C, Satyamurthy N, et al. Functional Expression of Sodium-Glucose Transporters in Cancer. *Proc Natl Acad Sci* (2015) 112(30):E4111–9. doi: 10.1073/pnas.1511698112
116. Tang H, Yang K, Li X, Song Y, Han J. Pancreatic Safety of Sodium-Glucose Cotransporter 2 Inhibitors in Patients With Type 2 Diabetes Mellitus: A Systematic Review and Meta-Analysis. *Pharmacoepidem Dr S* (2020) 29 (2):161–72. doi: 10.1002/pds.4943

Conflict of Interest: The authors declare that the research was conducted in the absence of any commercial or financial relationships that could be construed as a potential conflict of interest.

The handling editor and the reviewer (YL) declared a shared affiliation with the authors at time of review.

Publisher's Note: All claims expressed in this article are solely those of the authors and do not necessarily represent those of their affiliated organizations, or those of the publisher, the editors and the reviewers. Any product that may be evaluated in this article, or claim that may be made by its manufacturer, is not guaranteed or endorsed by the publisher.

frontiers in Oncology

ORIGINAL RESEARCH
published: 13 September 2021
doi: 10.3389/fonc.2021.739111

Plasma-Derived Exosome MiR-19b Acts as a Diagnostic Marker for Pancreatic Cancer

Lei Wang[1†], Jinxiang Wu[2†], Naikuan Ye[1,3], Feng Li[1], Hanxiang Zhan[1], Shihong Chen[1,3] and Jianwei Xu[1,4]*

[1] Department of Pancreatic Surgery, General Surgery, Qilu Hospital, Cheeloo College of Medicine, Shandong University, Jinan, China, [2] Department of Pulmonary and Critical Care Medicine, Qilu Hospital, Cheeloo College of Medicine, Shandong University, Jinan, China, [3] Cheeloo College of Medicine, Shandong University, Jinan, China, [4] School of Medicine, Cheeloo College of Medicine, Shandong University, Jinan, China

OPEN ACCESS

Edited by:
Taiping Zhang,
Peking Union Medical College Hospital (CAMS), China

Reviewed by:
Shanmiao Gou,
Huazhong University of Science and Technology, China
Gang Wang,
First Affiliated Hospital of Harbin Medical University, China

***Correspondence:**
Jianwei Xu
wdxujianwei@163.com
orcid.org/0000-0001-8487-6728

[†]These authors have contributed equally to this work

Specialty section:
This article was submitted to Gastrointestinal Cancers: Hepato Pancreatic Biliary Cancers, a section of the journal Frontiers in Oncology

Received: 10 July 2021
Accepted: 23 August 2021
Published: 13 September 2021

Citation:
Wang L, Wu J, Ye N, Li F, Zhan H, Chen S and Xu J (2021) Plasma-Derived Exosome MiR-19b Acts as a Diagnostic Marker for Pancreatic Cancer. Front. Oncol. 11:739111. doi: 10.3389/fonc.2021.739111

Background: Diagnosis of pancreatic cancer (Pca) is challenging. This study investigated the value of plasma-derived exosome miR-19b (Exo-miR-19b) in diagnosing patients with Pca.

Methods: Plasma was collected from 62 patients with Pca, 30 patients with other pancreatic tumor (OPT), 23 patients with chronic pancreatitis (CP), and 53 healthy volunteers. MiR-19b levels in plasma-derived exosomes were detected.

Results: Plasma-derived Exo-miR-19b levels normalized using miR-1228 were significantly lower in Pca patients than in patients with OPT, CP patients, and healthy volunteers. The diagnostic values of Exo-miR-19b normalized using miR-1228 were superior to those of serum cancer antigen 19-9 (CA19-9) in differentiating Pca patients from healthy volunteers (area under the curve (AUC): 0.942 *vs*. 0.813, p = 0.0054), potentially better than those of CA19-9 in differentiating Pca patients from CP patients (AUC: 0.898 *vs*. 0.792, p = 0.0720), and equivalent to those of CA19-9 in differentiating Pca patients from patients with OPT (AUC: 0.810 *vs*. 0.793, p = 0.8206). When normalized using *Caenorhabditis elegans* miR-39 (cel-miR-39), Exo-miR-19b levels in Pca patients were significantly higher than those in patients with OPT, CP patients, and healthy volunteers. The diagnostic values of Exo-miR-19b normalized using cel-miR-39 were equivalent to those of CA19-9 in differentiating Pca patients from healthy volunteers (AUC: 0.781 *vs*. 0.813, p = 0.6118) and CP patients (AUC: 0.672 *vs*. 0.792, p = 0.1235), while they were inferior to those of CA19-9 in differentiating Pca patients from patients with OPT (AUC: 0.631 *vs*. 0.793, p = 0.0353).

Conclusion: Plasma-derived Exo-miR-19b is a promising diagnostic marker for Pca. The diagnostic value of plasma-derived Exo-miR-19b normalized using miR-1228 is superior to that of serum CA19-9 in differentiating patients with Pca from healthy volunteers.

Keywords: pancreatic cancer, liquid biopsy, exosome, miRNA, biomarker, macrophages

INTRODUCTION

Pancreatic cancer (Pca) is a lethal disease with a 5-year survival rate of 10% and ranks as the fourth leading cause of cancer-related deaths in the United States (1). The difficulty in diagnosis of early stage diseases partly accounts for the poor prognosis of Pca. Several biomarkers for diagnosing Pca have been reported; however, most of these biomarkers have remained in the preclinical stage. Currently, only serum cancer antigen 19-9 (CA19-9) is proposed for the routine management of Pca. However, elevated CA19-9 is also observed in biliary infection or obstruction as well as other digestive cancers and inflammatory diseases and presents a moderate diagnostic value with a sensitivity and a specificity of 79% and 82%, respectively (2). Additionally, CA19-9 is not applicable for patients with negative expression of Lewis antigen, which is critical for CA19-9 biosynthesis, and the National Comprehensive Cancer Network guideline indicates that CA 19-9 is undetectable in Lewis (−) individuals (3). Notably, Luo et al. (4) reported that 8.4% of Pca patients (N = 1482) were Lewis (−). These results indicate that diagnosis of Pca based on CA19-9 will lead to missed diagnosis, and therefore, a more accurate circulating biomarker for Pca is urgently needed.

The application of liquid biopsy of circulating free DNA, tumor cells, or exosomes for cancer diagnosis has shown promise (5, 6), and among these markers, exosomes have been the subject of investigation. Exosomes are small (30–200 nm) vesicular structures that can carry pathogenic miRNAs, lncRNAs, mRNAs, DNA fragments, and proteins (7, 8). Several blood-derived exosome markers have been developed and show potential diagnostic value in Pca (5, 9). Circulating miRNAs serve as diagnostic biomarkers in multiple types of cancers, including biliary tract cancer (10), colorectal cancer (CRC) (11), Pca (5, 12), glioblastoma (13), prostate cancer (14), lung cancer (15), hepatocellular carcinoma (16), and other tumors (17). Unlike the multiple reports on circulating miRNAs, only a few studies have reported the diagnostic values of plasma- or serum-derived exosome miRNAs in Pca (18, 19).

Our previous study indicated that several plasma miRNAs were deregulated in Pca patients and presented diagnostic value[12]. Among the identified miRNAs, plasma miR-19b was significantly upregulated in patients with Pca and presented moderate diagnostic values in discriminating patients with Pca from those with chronic pancreatitis (CP) and pancreatic neuroendocrine tumor. Additionally, circulating exosomal miR-19b exhibited oncogenic functions in gastric cancer, lung adenocarcinoma, and esophageal squamous cell carcinoma (ESCC) (20–22).

In this study, we aimed to evaluate the potential diagnostic values of plasma-derived exosome miR-19b (Exo-miR-19b) in Pca. We investigated the expression levels and diagnostic values of Exo-miR-19b in patients with Pca, patients with CP, patients with other pancreatic tumor (OPT), and healthy volunteers.

MATERIALS AND METHODS

Ethics Statement

This study was approved by the Medical Ethics Committee of Qilu Hospital of Shandong University. Written informed consent was obtained from all subjects.

Diagnostic Criteria for Pancreatic Diseases

Pca was cytologically or pathologically diagnosed depending on the cytological or histological examinations. OPTs were pathologically diagnosed depending on histological examinations of the resected specimen, including pancreatic neuroendocrine tumor, solid pseudopapillary tumor, serous or mucinous cystadenomas, intraductal papillary mucinous neoplasms, and epithelial cysts. CP was diagnosed on the basis of clinical diagnostic criteria or histological examinations.

Sample Collection and Exosome RNA Isolation

The serum CA19-9 levels of all included subjects could be obtained from the medical records; if not, the subjects were excluded. Pca patients undergoing neoadjuvant therapy were excluded. Peripheral venous blood (5 ml) was collected in sterile ethylene diamine tetraacetic acid-treated anticoagulant tubes before clinical intervention or surgery. The blood samples were centrifuged at 3,000 revolutions per minute (rpm) for 10 min; then plasmas were collected and stored at −80°C for further isolation of exosome. Exosomes were isolated from plasma using exoRNeasy Serum/Plasma Midi Kit (the kit can directly purify total exosomes RNA from plasma without the intermediate isolation of exosomes, Exiqon QIAGEN, #77044) according to the manufacturer's instructions as reported by the previous study (23); then the RNA was harvested.

Quantitative Real-Time PCR for Detecting Plasma-Derived Exo-miR-19b

Synthetic *Caenorhabditis elegans* miR-39 (cel-miR-39, RiboBio, Guangzhou, China) at 30 nM was added to each exosome RNA sample for normalization before qRT-PCR. MiRNA was converted to cDNA using a TaqMan MicroRNA Reverse Transcription Kit (Applied Biosystems). The reverse transcription reactions were carried out at 16°C for 30 min,

at 42°C for 30 min, and at 85°C for 5 min and held at 4°C. cDNA was stored at −20°C until use. A total of 20 µl of amplification system containing 1.33 µl of cDNA, 10 µl of TaqMan 2× Universal PCR Master Mix with no AmpErase UNG (Applied Biosystems), 1 µl of miRNA-specific probe, and 7.67 µl of nuclease-free water was used for analyzing the expression of miRNA. qRT-PCR ran on a Stepone Plus real-time PCR system (Applied Biosystems) and the reaction mixtures were incubated at 95°C for 10 min, followed by 40 cycles at 95°C for 15 s, and 60°C for 1 min. The cycle threshold (CT) values were calculated with SDS software (Applied Biosystems). All reactions were performed in triplicate. The expression levels of miRNA were normalized using the endogenous control (miR-1228) (24) or the exogenous control (cel-miR-39). ΔCT was calculated by subtracting CT values of the miRNA from CT values of the control. The relative expression levels of miRNA were calculated with the equation $2^{-\Delta CT}$.

Statistical Analysis

All the statistical analyzes were performed by SPSS v.23.0 (IBM Corp., Armonk, NY). A two-sided $p < 0.05$ was considered as statistical significance. Continuous data were presented as the mean ± SD and analyzed using Student's *t*-tests. Receiver operating characteristic (ROC) curves were created; and the area under the curve (AUC), sensitivity, and specificity were calculated to evaluate the diagnostic values of plasma-derived Exo-miR-19b using MedCalc Statistical Software version 19.0.4 (MedCalc Software bvba; http://www.medcalc.org). AUCs of plasma-derived Exo-miR-19b (AUC1) and CA19-9 (AUC2) were compared using Z tests.

RESULTS

The Expression Levels of Plasma-Derived Exo-miR-19b in Patients With Pancreatic Cancer and Control Groups Normalized Using MiR-1228

Plasma samples were collected from 168 individuals, including 62 Pca patients, 30 patients with OPT, 23 CP patients, and 53 healthy volunteers. Exosomes RNA was extracted from the

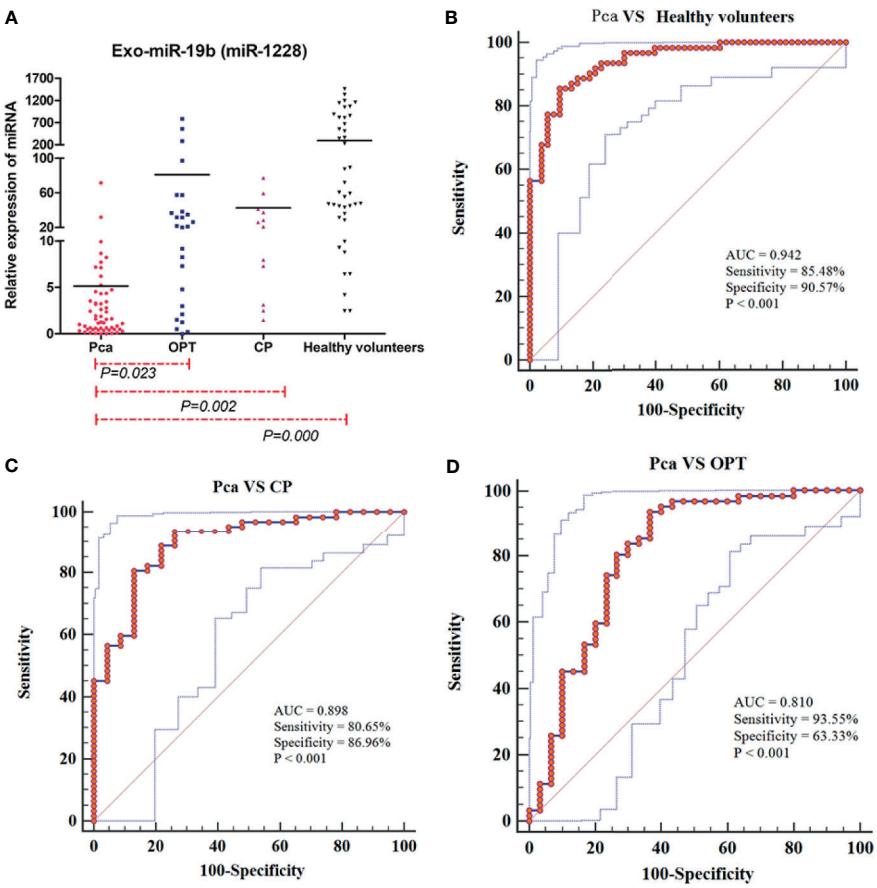

FIGURE 1 | Expression levels and diagnostic values of plasma-derived Exo-miR-19b normalized using miR-1228. **(A)** Exo-miR-19b levels were detected by qRT-PCR. **(B)** ROC for differentiating Pca patients from healthy volunteers. **(C)** ROC for differentiating Pca patients from CP patients. **(D)** ROC for differentiating Pca patients from patients with OPT. AUC, area under the curve; CP, chronic pancreatitis; OPT, other pancreatic tumor; Pca, pancreatic cancer; ROC, receiver operating characteristic.

plasma samples, and Exo-miR-19b levels were determined by qRT-PCR.

The levels of Exo-miR-19b in patients with Pca normalized using miR-1228 were significantly lower than the levels in patients with OPT, patients with CP, and healthy volunteers ($p < 0.05$, **Figure 1A**, **Supplementary Material 1**).

The Diagnostic Value of Plasma-Derived Exo-miR-19b Normalized Using MiR-1228

Levels of plasma-derived Exo-miR-19b normalized using miR-1228 displayed diagnostic value in differentiating patients with Pca from patients with OPT (AUC = 0.810), patients with CP (AUC = 0.898), and healthy volunteers (AUC = 0.942) (**Figures 1B–D**, **Supplementary Material 2**).

Exo-miR-19b was superior to serum CA19-9 in differentiating patients with Pca from healthy volunteers (AUC: 0.942 *vs.* 0.813, p = 0.0054), potentially better than CA19-9 in differentiating patients with Pca from CP (AUC: 0.898 *vs.* 0.792, p = 0.0720), and equivalent to CA19-9 in differentiating patients with Pca from patients with OPT (AUC: 0.810 *vs.* 0.793, p = 0.8206) (**Figure 2**, **Supplementary Material 3**).

The Diagnostic Value of Plasma-Derived Exo-miR-19b Normalized Using cel-miR-39

The levels of Exo-miR-19b normalized using cel-miR-39 were significantly higher in patients with Pca than in patients with OPT, patients with CP, and healthy volunteers ($p < 0.05$, **Figure 3A**, **Supplementary Material 1**).

Levels of plasma-derived Exo-miR-19b normalized using cel-miR-39 displayed diagnostic value in differentiating patients with Pca from patients with OPT (AUC = 0.631), patients with CP (AUC = 0.672), and healthy volunteers (AUC = 0.781) (**Figures 3B–D**, **Supplementary Material 2**).

Exo-miR-19b was equivalent to CA19-9 in differentiating patients with Pca from healthy volunteers (AUC: 0.781 vs. 0.813, p = 0.6118) and patients with CP (AUC: 0.672 *vs.* 0.792, p = 0.1235), while it was inferior to CA19-9 in differentiating patients with Pca from patients with OPT (AUC: 0.631 *vs.* 0.793, p = 0.0353) (**Figure 4**, **Supplementary Material 3**).

DISCUSSION

Although multiple studies are trying to find effective diagnostic markers for Pca, early diagnosis of Pca is still difficult (25). Several circulating exosomal miRNA biomarkers have been reported for the diagnosis of Pca[19], including miR-1226 (26), miR-196a/1246 (27), miR-191/21/451a (28), and miR-10b/21/30c/161a/let-7a (29). However, few studies have investigated the diagnostic value of Exo-miR-19b (20), and no reports have been performed in Pca. In this study, we showed that plasma-derived Exo-miR-19b level normalized using miR-1228 was superior to that using serum CA19-9 in differentiating patients with Pca from healthy volunteers, potentially better than that using CA19-9 in differentiating patients with Pca from patients with CP, and equivalent to that using CA19-9 in differentiating patients with Pca from patients with OPT.

The selection of an appropriate endogenous control for normalization of circulating miRNA expression is crucial for obtaining reliable data. Several miRNAs are commonly used as endogenous controls for quantifying circulating miRNAs, such as miR-16, miR-223, let-7a, and RNU6B (24, 30). However, none of the endogenous miRNAs have been widely accepted. Our study used endogenous miR-1228 as a control for the quantification of plasma-derived Exo-miR-19b. MiR-1228 is widely involved in metabolism-related signalling pathways and organ morphology and not influenced by hemolysis (30, 31), indicating the suitability of miR-1228 as a housekeeping miRNA. Hu et al. (24) examined a large cohort of 544 subjects to identify a stable endogenous control for the quantification of circulating miRNAs in cancer patients. The authors found that miR-1228 functioned as a housekeeping gene and was stable in plasma samples from different kinds of tumors, including hepatocellular cancer, CRC, lung cancer, ESCC, gastric cancer, renal cancer, prostate cancer, and breast cancer. Duran-Sanchon et al. (31)

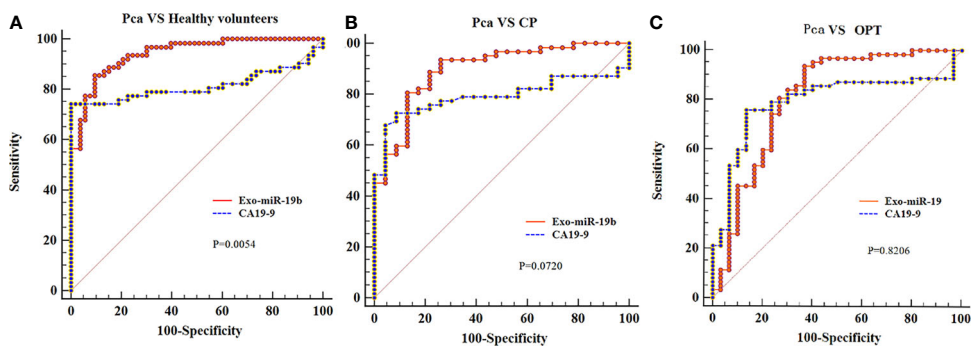

FIGURE 2 | Comparison of the areas under the curves of CA19-9 with plasma-derived Exo-miR-19b levels normalized using miR-1228. **(A)** AUCs of Exo-miR-19b and CA19-9 in discriminating patients with Pca from healthy volunteers. **(B)** AUCs of Exo-miR-19b and CA19-9 in discriminating patients with Pca from CP. **(C)** AUCs of Exo-miR-19b and CA19-9 in discriminating patients with Pca from OPT. AUC, area under the curve; CP, chronic pancreatitis; OPT, other pancreatic tumor; Pca, pancreatic cancer.

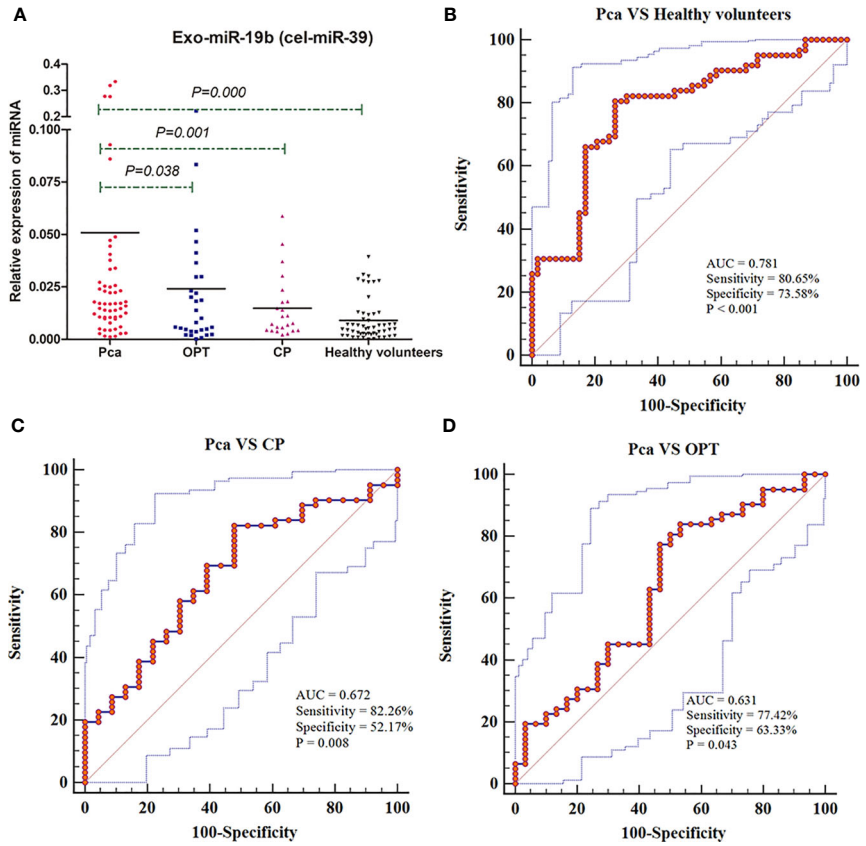

FIGURE 3 | Expression levels and diagnostic values of plasma-derived Exo-miR-19b normalized using cel-miR-39. **(A)** Exo-miR-19b levels were detected by qRT-PCR. **(B)** ROC for differentiating Pca patients from healthy volunteers. **(C)** ROC for differentiating Pca patients from CP patients. **(D)** ROC for differentiating Pca patients from patients with OPT. AUC, area under the curve; CP, chronic pancreatitis; OPT, other pancreatic tumor; Pca, pancreatic cancer; ROC, Receiver operating characteristic.

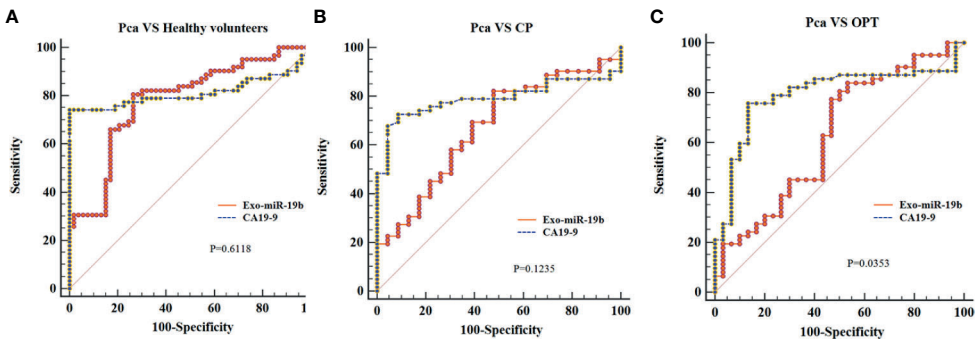

FIGURE 4 | Comparison of the areas under the curves of CA19-9 with plasma-derived Exo-miR-19b levels normalized using cel-miR-39. **(A)** AUCs of Exo-miR-19b and CA19-9 in discriminating patients with Pca from healthy volunteers. **(B)** AUCs of Exo-miR-19b and CA19-9 in discriminating patients with Pca from CP. **(C)** AUCs of Exo-miR-19b and CA19-9 in discriminating patients with Pca from OPT. AUC, area under the curve; CP, chronic pancreatitis; OPT, other pancreatic tumor; Pca, pancreatic cancer.

verified the housekeeping role of miR-1228 in CRC by a large sample study; the authors showed that miR-1228 was an adequate endogenous control for circulating miRNA analysis in CRC and demonstrated a variability and stability superior to that of miR-16. Danese et al. (30) reported the expression levels and stability of miR-1228; the study found that miR-1228 displayed median PCR-derived cycle threshold values and was sufficiently homogenous and stable in exosomes, plasma, and tissues from CRC patients and healthy controls.

Previous studies on miR-19b functions indicated its oncogenic role (32, 33), suggesting that plasma-derived Exo-miR-19b would be upregulated in Pca patients compared with controls. However, our study found conflicting results. While the plasma-derived Exo-miR-19b level in Pca patients was significantly lower than that in the control subjects when normalized using miR-1228, the plasma-derived Exo-miR-19b in Pca patients was significantly higher than that in controls when normalized using cel-miR-39, which was consistent with the literature (20, 21). While the mechanism and reason underlying the differences in these results are not yet clear, some potential explanations are possible. First, some studies reported miR-1228 as a functional miRNA (34, 35), which might influence its value as an internal control. The role of miR-1228 in Pca has not been investigated, and the housekeeping role and the value of normalization for plasma-derived exosome miRNA need further experimental verification. Second, the use of an exogenous control has limitations. Exogenous controls have shown utility for quality control for RNA extraction and PCR, but useless in quality control for exosome extraction. However, quality control during extraction is important for exosome studies. Because of the differences between the expression profiles of miRNAs in plasma, serum, and blood cells (36), quality control of exosome extraction is necessary to eliminate the influence of blood components. Finally, the source of plasma-derived Exo-miR-19b is unclear. Besides Pca cells, blood cells, bone marrow mesenchymal stem cells, endothelial cells, and other cells secrete Exo-miR-19b [4-6]. The function of miR-19b or Exo-miR-19b in Pca cells might be not equal to that of plasma-derived Exo-miR-19b in Pca patients. Further studies are necessary to investigate the biological functions of plasma-derived Exo-miR-19b in Pca patients.

This study has some limitations. The control diseases are not comprehensive; acute pancreatitis, obstructive jaundice caused by benign diseases, and other digestive cancers are no included. CP is diagnosed according to either the clinical criteria or histological examinations. However, CP has a potential of malignant transformation; diagnosis with clinical criteria might miss cases with focal cancerization. The sample size is moderate; there is no stratified analysis of Pca cases; influences of jaundice, and locations and stages of the tumors on the levels of plasma-derived Exo-miR-19b are unknown. A larger sample muticenter study is helpful to disclose the diagnostic value of plasma-derived Exo-miR-19b.

In conclusion, we reported the diagnostic value of plasma-derived Exo-miR-19b in Pca. Our results showed that plasma-derived Exo-miR-19b level normalized using miR-1228 was superior to serum CA19-9 in differentiating patients with Pca from healthy volunteers, potentially better than CA19-9 in differentiating patients with Pca from patients with CP, and equivalent to CA19-9 in differentiating patients with Pca from patients with OPT.

DATA AVAILABILITY STATEMENT

The original contributions presented in the study are included in the article/**Supplementary Material**. Further inquiries can be directed to the corresponding authors.

ETHICS STATEMENT

The studies involving human participants were reviewed and approved by the Medical Ethics Committee of Qilu Hospital of Shandong University. The patients/participants provided their written informed consent to participate in this study.

AUTHOR CONTRIBUTIONS

JX proposed and designed the study. LW and JW wrote the draft. LW, JW, NY, FL, HZ, and SC collected and analyzed the data. All authors contributed to the design and interpretation of the study and to further drafts. JX and FL revised the manuscript. All authors contributed to the article and approved the submitted version.

FUNDING

This study was supported by grants from the National Natural Science Foundation of China (81502051), the Shandong Provincial Natural Science Foundation, China (ZR2020MH256), Medical Health Science and Technology Project of Shandong Provincial Health Commission (2019WS386), Key Technology Research and Development Program of Shandong (2019GSF108065), and the China Postdoctoral Science Foundation (2018M632681).

ACKNOWLEDGMENTS

We thank Gabrielle White Wolf, PhD, from Liwen Bianji (Edanz) (www.liwenbianji.cn/), for editing the English text of a draft of this manuscript.

SUPPLEMENTARY MATERIAL

The Supplementary Material for this article can be found online at: https://www.frontiersin.org/articles/10.3389/fonc.2021.739111/full#supplementary-material

REFERENCES

1. Siegel RL, Miller KD, Fuchs HE, Jemal A. Cancer Statistic. *CA Cancer J Clin* (2021) 71(1):7–33. doi: 10.3322/caac.21654
2. Goonetilleke KS, Siriwardena AK. Systematic Review of Carbohydrate Antigen (CA 19-9) as a Biochemical Marker in the Diagnosis of Pancreatic Cancer. *Eur J Surg Oncol* (2007) 33(3):266–70. doi: 10.1016/j.ejso.2006.10.004
3. NCCN. *NCCN Clinical Practice Guidelines in Oncology: Pancreatic Adenocarcinoma (Version 1.2020)*. Available at: http://www.nccn.org.
4. Luo G, Fan Z, Cheng H, Jin K, Guo M, Lu Y, et al. New Observations on the Utility of CA19-9 as a Biomarker in Lewis Negative Patients With Pancreatic Cancer. *Pancreatology* (2018) 18(8):971–6. doi: 10.1016/j.pan.2018.08.003
5. Al-Shaheri FN, Alhamdani MSS, Bauer AS, Giese N, Büchler MW, Hackert T, et al. Blood Biomarkers for Differential Diagnosis and Early Detection of Pancreatic Cancer. *Cancer Treat Rev* (2021) 96:102193. doi: 10.1016/j.ctrv.2021.102193
6. Alix-Panabières C, Pantel K. Liquid Biopsy: From Discovery to Clinical Application. *Cancer Discov* (2021) 11(4):858–73. doi: 10.1158/2159-8290.cd-20-1311
7. Pegtel DM, Gould SJ. Exosomes. *Annu Rev Biochem* (2019) 88:487–514. doi: 10.1146/annurev-biochem-013118-111902
8. Gurung S, Perocheau D, Touramanidou L, Baruteau J. The Exosome Journey: From Biogenesis to Uptake and Intracellular Signalling. *Cell Commun Signal* (2021) 19(1):47. doi: 10.1186/s12964-021-00730-1
9. Zhou B, Xu JW, Cheng YG, Gao JY, Hu SY, Wang L, et al. Early Detection of Pancreatic Cancer: Where Are We Now and Where are We Going? *Int J Cancer* (2017a) 141(2):231–41. doi: 10.1002/ijc.30670
10. Ofoeyeno N, Ekpenyong E, Braconi C. Pathogenetic Role and Clinical Implications of Regulatory RNAs in Biliary Tract Cancer. *Cancers (Basel)* (2020) 13(1):12. doi: 10.3390/cancers13010012
11. Alves Dos Santos K, Clemente Dos Santos IC, Santos Silva C, Gomes Ribeiro H, de Farias Domingos I, Nogueira Silbiger V. Circulating Exosomal miRNAs as Biomarkers for the Diagnosis and Prognosis of Colorectal Cancer. *Int J Mol Sci* (2020) 22(1). doi: 10.3390/ijms22010346
12. Xu J, Cao Z, Liu W, You L, Zhou L, Wang C, et al. Plasma miRNAs Effectively Distinguish Patients With Pancreatic Cancer From Controls: A Multicenter Study. *Ann Surg* (2016) 263(6):1173–9. doi: 10.1097/sla.0000000000001345
13. Ahmed SP, Castresana JS, Shahi MH. Glioblastoma and MiRNAs. *Cancers (Basel)* (2021) 13(7):1581. doi: 10.3390/cancers13071581
14. Arrighetti N, Beretta GL. miRNAs as Therapeutic Tools and Biomarkers for Prostate Cancer. *Pharmaceutics* (2021) 13(3):380. doi: 10.3390/pharmaceutics13030380
15. Gayosso-Gómez LV, Ortiz-Quintero B. Circulating MicroRNAs in Blood and Other Body Fluids as Biomarkers for Diagnosis, Prognosis, and Therapy Response in Lung Cancer. *Diagnostics (Basel)* (2021) 11(3):421. doi: 10.3390/diagnostics11030421
16. Morishita A, Oura K, Tadokoro T, Fujita K, Tani J, Masaki T. MicroRNAs in the Pathogenesis of Hepatocellular Carcinoma: A Review. *Cancers (Basel)* (2021) 13(3):514. doi: 10.3390/cancers13030514
17. Galvão-Lima LJ, Morais AHF, Valentim RAM, Barreto E. miRNAs as Biomarkers for Early Cancer Detection and Their Application in the Development of New Diagnostic Tools. *BioMed Eng Online* (2021) 20(1):21. doi: 10.1186/s12938-021-00857-9
18. Gao Z, Jiang W, Zhang S, Li P. The State of the Art on Blood MicroRNAs in Pancreatic Ductal Adenocarcinoma. *Anal Cell Pathol (Amst)* (2019) 2019:9419072. doi: 10.1155/2019/9419072
19. Ariston Gabriel AN, Wang F, Jiao Q, Yvette U, Yang X, Al-Ameri SA, et al. The Involvement of Exosomes in the Diagnosis and Treatment of Pancreatic Cancer. *Mol Cancer* (2020) 19(1):132. doi: 10.1186/s12943-020-01245-y
20. Wang N, Wang L, Yang Y, Gong L, Xiao B, Liu X. A Serum Exosomal microRNA Panel as a Potential Biomarker Test for Gastric Cancer. *Biochem Biophys Res Commun* (2017) 493(3):1322–8. doi: 10.1016/j.bbrc.2017.10.003
21. Zhou X, Wen W, Shan X, Zhu W, Xu J, Guo R, et al. A six-microRNA Panel in Plasma Was Identified as a Potential Biomarker for Lung Adenocarcinoma Diagnosis. *Oncotarget* (2017b) 8(4):6513–25. doi: 10.18632/oncotarget.14311
22. Zeng Q, Zhu Z, Song L, He Z. Transferred by Exosomes-Derived MiR-19b-3p Targets PTEN to Regulate Esophageal Cancer Cell Apoptosis, Migration and Invasion. *Biosci Rep* (2020) 40(11):BSR20201858. doi: 10.1042/bsr20201858
23. Chen H, Zhou Y, Wang ZY, Yan BX, Zhou WF, Wang TT, et al. Exosomal microRNA Profiles From Serum and Cerebrospinal Fluid in Neurosyphilis. *Sex Transm Infect* (2019) 95(4):246–50. doi: 10.1136/sextrans-2018-053813
24. Hu J, Wang Z, Liao BY, Yu L, Gao X, Lu S, et al. Human miR-1228 as a Stable Endogenous Control for the Quantification of Circulating microRNAs in Cancer Patients. *Int J Cancer* (2014) 135(5):1187–94. doi: 10.1002/ijc.28757
25. Li C, Li S, Zhang F, Wu M, Liang H, Song J, et al. Endothelial Microparticles-Mediated Transfer of microRNA-19b Promotes Atherosclerosis via Activating Perivascular Adipose Tissue Inflammation in Apoe(-/-) Mice. *Biochem Biophys Res Commun* (2018) 495(2):1922–9. doi: 10.1016/j.bbrc.2017.11.195
26. Wang C, Wang J, Cui W, Liu Y, Zhou H, Wang Y, et al. Serum Exosomal miRNA-1226 as Potential Biomarker of Pancreatic Ductal Adenocarcinoma. *Onco Targets Ther* (2021) 14:1441–51. doi: 10.2147/ott.s296816
27. Xu YF, Hannafon BN, Zhao YD, Postier RG, Ding WQ. Plasma Exosome miR-196a and miR-1246 Are Potential Indicators of Localized Pancreatic Cancer. *Oncotarget* (2017) 8(44):77028–40. doi: 10.18632/oncotarget.20332
28. Goto T, Fujiya M, Konishi H, Sasajima J, Fujibayashi S, Hayashi A, et al. An Elevated Expression of Serum Exosomal microRNA-191, - 21, -451a of Pancreatic Neoplasm Is Considered to be Efficient Diagnostic Marker. *BMC Cancer* (2018) 18(1):116. doi: 10.1186/s12885-018-4006-5
29. Lai X, Wang M, McElyea SD, Sherman S, House M, Korc M. A microRNA Signature in Circulating Exosomes Is Superior to Exosomal Glypican-1 Levels for Diagnosing Pancreatic Cancer. *Cancer Lett* (2017) 393:86–93. doi: 10.1016/j.canlet.2017.02.019
30. Danese E, Minicozzi AM, Benati M, Paviati E, Lima-Oliveira G, Gusella M, et al. Reference miRNAs for Colorectal Cancer: Analysis and Verification of Current Data. *Sci Rep* (2017) 7(1):8413. doi: 10.1038/s41598-017-08784-3
31. Duran-Sanchon S, Vila-Navarro E, Marcuello M, Lozano JJ, Muñoz J, Cubiella J, et al. Validation of miR-1228-3p as Housekeeping for MicroRNA Analysis in Liquid Biopsies From Colorectal Cancer Patients. *Biomolecules* (2019) 10 (1):16. doi: 10.3390/biom10010016
32. Fuziwara CS, Kimura ET. Insights Into Regulation of the miR-17-92 Cluster of miRNAs in Cancer. *Front Med (Lausanne)* (2015) 2:64. doi: 10.3389/fmed.2015.00064
33. Fang LL, Wang XH, Sun BF, Zhang XD, Zhu XH, Yu ZJ, et al. Expression, Regulation and Mechanism of Action of the miR-17-92 Cluster in Tumor Cells (Review). *Int J Mol Med* (2017) 40(6):1624–30. doi: 10.3892/ijmm.2017.3164
34. Zhang Y, Dai J, Deng H, Wan H, Liu M, Wang J, et al. miR-1228 Promotes the Proliferation and Metastasis of Hepatoma Cells Through a P53 Forward Feedback Loop. *Br J Cancer* (2015) 112(2):365–74. doi: 10.1038/bjc.2014.593
35. Chang L, Gao H, Wang L, Wang N, Zhang S, Zhou X, et al. Exosomes Derived From miR-1228 Overexpressing Bone Marrow-Mesenchymal Stem Cells Promote Growth of Gastric Cancer Cells. *Aging (Albany NY)* (2021) 13. doi: 10.18632/aging.202878
36. Wang K, Yuan Y, Cho JH, McClarty S, Baxter D, Galas DJ. Comparing the MicroRNA Spectrum Between Serum and Plasma. *PloS One* (2012) 7(7): e41561. doi: 10.1371/journal.pone.0041561

Conflict of Interest: The authors declare that the research was conducted in the absence of any commercial or financial relationships that could be construed as a potential conflict of interest.

frontiers in Oncology

ORIGINAL RESEARCH
published: 16 September 2021
doi: 10.3389/fonc.2021.719253

Individualized Prediction of Survival Benefits of Pancreatectomy Plus Chemotherapy in Patients With Simultaneous Metastatic Pancreatic Cancer

Duorui Nie[1†], *Guihua Lai*[1†], *Guilin An*[2], *Zhuojun Wu*[1], *Shujun Lei*[1], *Jing Li*[3*] *and Jianxiong Cao*[4*]

[1] Graduate School, Hunan University of Chinese Medicine, Changsha, China, [2] School of Traditional Chinese Medicine, Ningxia Medical University, Yinchuan, China, [3] Department of Oncology, The First Hospital of Hunan University of Chinese Medicine, Changsha, China, [4] School of Continuing Education, Hunan University of Chinese Medicine, Changsha, China

OPEN ACCESS

Edited by:
Taiping Zhang,
Peking Union Medical College Hospital (CAMS), China

Reviewed by:
Antonio Giuliani,
University of L'Aquila, Italy
Ravindra Deshpande,
Wake Forest School of Medicine, United States

***Correspondence:**
Jianxiong Cao
003998@hnucm.edu.cn
Jing Li
lilee2711@sina.com

[†]These authors have contributed equally to this work

Specialty section:
This article was submitted to Gastrointestinal Cancers, a section of the journal Frontiers in Oncology

Received: 02 June 2021
Accepted: 23 August 2021
Published: 16 September 2021

Citation:
Nie D, Lai G, An G, Wu Z, Lei S, Li J and Cao J (2021) Individualized Prediction of Survival Benefits of Pancreatectomy Plus Chemotherapy in Patients With Simultaneous Metastatic Pancreatic Cancer. Front. Oncol. 11:719253. doi: 10.3389/fonc.2021.719253

Background: Metastatic pancreatic cancer (mPC) is a highly lethal malignancy with poorer survival. However, chemotherapy alone was unable to maintain long-term survival. This study aimed to evaluate the individualized survival benefits of pancreatectomy plus chemotherapy (PCT) for mPC.

Methods: A total of 4546 patients with mPC from 2004 to 2015 were retrieved from the Surveillance, Epidemiology, and End Results database. The survival curve was calculated using the Kaplan-Meier method and differences in survival curves were tested using log-rank tests. Cox proportional hazards regression analyses were performed to evaluate the prognostic value of involved variables. A new nomogram was constructed to predict overall survival based on independent prognosis factors. The performance of the nomogram was measured by concordance index, calibration plot, and area under the receiver operating characteristic curve.

Results: Compared to pancreatectomy or chemotherapy alone, PCT can significantly improve the prognosis of patients with mPC. In addition, patients with well/moderately differentiated tumors, age ≤66 years, tumor size ≤42 mm, or female patients were more likely to benefit from PCT. Multivariate analysis showed that age at diagnosis, sex, marital status, grade, tumor size, and treatment were independent prognostic factors. The established nomogram has a good ability to distinguish and calibrating.

Conclusion: PCT can prolong survival in some patients with mPC. Our nomogram can individualize predict OS of pancreatectomy combined with chemotherapy in patients with concurrent mPC.

Keywords: metastatic pancreatic cancer, surgery, chemotherapy, prognosis analysis, nomogram

BACKGROUND

Pancreatic cancer (PC) is a highly lethal malignancy, known as the "king of cancers". It was reported to cause 432,242 deaths worldwide in 2018, ranking fourth among cancer-related deaths (1). By 2030, it will be the second leading cause of cancer-related deaths (2). The poor prognosis for PC is associated with a later stage of diagnosis. It is reported that approximately 50% of patients are newly diagnosed with metastatic pancreatic cancer (mPC) (3). Moreover, the aggressive biological behavior of pancreatic cancer causes most patients who receive pancreatic cancer at an early stage to experience recurrence and metastasis (4). Therefore, the management of mPC deserves more attention. However, the treatment options for patients with mPC are limited, and systemic chemotherapy with Leucovorin, fluorouracil, irinotecan, and oxaliplatin or gemcitabine plus Nab-paclitaxel was recommended as the first-line treatment (5). Although significantly longer survival than gemcitabine monotherapy, the overall survival (OS) was only improved by a few months, and the clinical benefit was still limited (6, 7).

Surgery is the only cure for pancreatic cancer, but it is still underused in patients with early-stage pancreatic cancer because of concerns about its safety and complications (8). It is generally believed that metastatic disease is a contraindication to resection, but in the absence of effective treatment, the survival benefits of patients with mPC undergoing surgical resection are of concern (9–12). And with the advancement of surgical techniques and systemic chemotherapy, the perioperative mortality of patients with pancreatic cancer has dropped to 3%, and the 5-year survival rate has increased to about 30-40% (13). Pancreatectomy is considered to be a safe and effective treatment, but most patients who undergo surgery, even those who undergo radical resection, will eventually have a recurrence of the disease (14). Hence, the combination of chemotherapy seems to be a new combination therapy that offers hope for the treatment of pancreatic cancer. Highly selected patients with mPC may benefit from pancreatectomy and chemotherapy (15–17). But because they are small, single-center retrospective studies, we cannot draw reliable conclusions from these studies. Therefore, the exact role of pancreatectomy combined with chemotherapy deserves a more systematic evaluation.

Therefore, this study evaluated the prognostic effect of pancreatectomy combined with chemotherapy in patients with mPC. In addition, we have also explored the prognostic factors that affect mPC and established a nomogram to manage this type of patient.

METHODS

Patient Population

The Surveillance Epidemiology and End Results (SEER) database collects tumor clinicopathological information from 18 population-based cancer registries covering nearly 27.8% of the U.S. population, gathering information on patient demographics, primary tumor site, tumor type stage at diagnosis, the first course of treatment, and follow-up patients' vital status. The SEER database has limited access, and we have obtained SEER licenses (login number: 10952-Nov2019) to access the research data.

Patients with simultaneous metastatic pancreatic cancer were retrieved from 18 registries of the SEER Program (1975-2016), which was submitted in November 2018, by using SEER*Stat 8.38 software (18). Patients meeting the following criteria were included: (1) the patient was diagnosed with the International Classification of Diseases for Oncology, Third Edition (ICD-O-3, histology code: 8000/3: Neoplasm, malignant, 8010/3: Carcinoma, NOS, 8070/3: Squamous cell carcinoma, NOS, 8140/3: Adenocarcinoma, NOS, 8480/3: Mucinous adenocarcinoma, 8481/3: Mucin-producing adenocarcinoma, 8490/3: Signet ring cell carcinoma, 8500/3: Infiltrating duct carcinoma, NOS, 8560/3: Adenosquamous carcinoma; and the ICD-O-3 site code: C25.0-C25.9); (2) diagnosis was made between 2004 and 2015, (3) had 6th American Joint Committee on Cancer (AJCC) staging system M1 disease (4) age at diagnosis ≥18; (5) diagnosed with positive histology or cytology; (6) only one primary tumor; (7) with active follow-up time. And the following patients were excluded: (1) unknown clinical information, including T stage, N stage, race, grade, marital status, tumor size, surgery; (2) had radiotherapy. A detailed flow chart of patient screening is shown in **Figure 1**.

Covariates and Endpoint

The following variables were included in the study: gender, age at diagnosis, race, primary site, year of diagnosis, marital status at diagnosis, grade, tumor size, AJCC stage, radiotherapy, chemotherapy, primary site surgery, survival months, and vital status. For the purposes of statistical analysis, those patients whose marital status was widowed, separated, divorced, or single (a domestic partner, or never married) were classified as "unmarried". The tumor is located in "C25.3-Pancreatic Duct", "C25.7-Other specified parts of Pancreas", "C25.4-Islets of Langerhans", "C25.9-Pancreas, NOS" were classified as "Others". Consequently, the primary sites were categorized as "Head", "Body", "Tail", "Others", "Overlapping lesion". According to the code of surgery and chemotherapy, the treatment is divided into four categories: patients who did not receive pancreatectomy or chemotherapy (NPCT), patients who received chemotherapy merely (CT), patients receiving pancreatectomy only (PT), and patients who received pancreatectomy and chemotherapy (PCT). Since "tumor size" and "age at diagnosis" were quantifiable data, we converted them into categorical variables based on the median of the overall cohort. The endpoint event for this study is OS, which is defined as the time from the date of initial treatment to the patient's death of any cause or the most recent follow-up.

Statistical Analysis

Descriptive statistics were performed for patients' demographic and tumor characteristics. The comparison of the categorical variable among multiple groups were measured by Chi-square tests or Fisher's exact test, while continuous variable groups were tested for Kruskal - Wallis test. The survival curve was calculated using the Kaplan-Meier method and differences in survival curves were tested using log-rank tests. Cox proportional

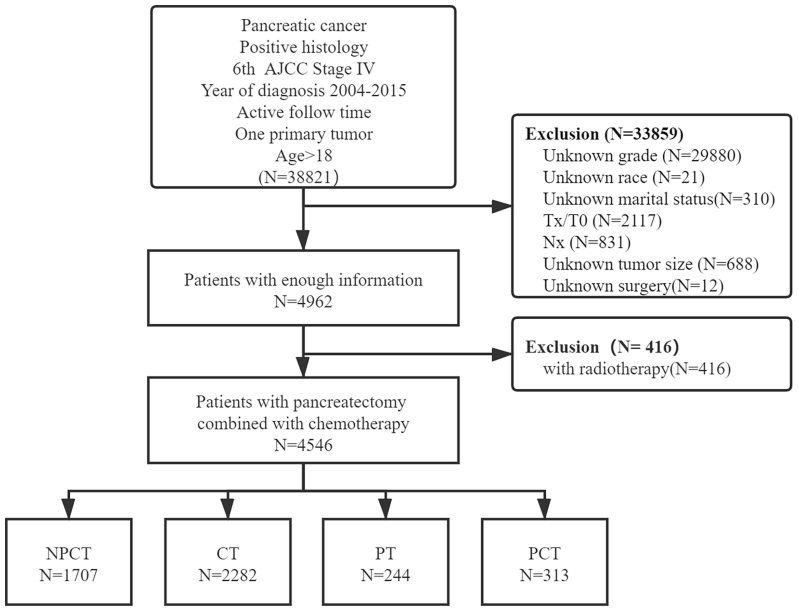

FIGURE 1 | Flowchart of patient selection for this study.

hazards models were used to evaluate variables that have independent predictive effects on the OS. Only variables that were significantly associated with OS in the univariate Cox analysis were included in the multivariate Cox analysis. Hazard ratios (HRs) and 95% confidence intervals (CIs) were also estimated using Cox proportional hazards models. All patients are used to form a training set to assess the prognostic role of surgery and chemotherapy, perform cox analysis and develop the nomogram.

Based on the results of the multivariate Cox proportional hazards model, the nomogram with 6-, 12- 18- month survival rates were plotted. We evaluated the performance of the nomogram by discrimination and calibration (19). Discrimination is the ability of the model to correctly distinguish between non-events and events, and is quantified by Harrell's consistency index (C-index) and time-dependent receiver operating characteristic (tROC) curve. Calibration compares the difference between the predicted probability and the actual survival rate and is represented by a calibration plot. The bootstrap analyses with 1000 resample were used to calculate C-indexes and generate calibration plots for internal validation of the model (20). All statistical tests were performed using SPSS Statistics 26.0 software (IBM SPSS, Inc., Chicago, IL, USA) and R 4.0.4 (http://www.r-project.org/). The statistical test was two-sided and P <0.05 was considered statistically significant.

RESULTS

Patient Characteristic

A total of 4,546 patients were enrolled in our study. Among them, 313 patients with "PCT", 244 patients with "PT", 2282 patients with "CT", 1707 patients with "NPCT". **Table 1** shows the patients' clinicopathological characteristics with different therapeutic modalities. The median age was 66 years (range 58-74), with 2466 (54.2%) males and 2080 (45.8%) females. Poorly differentiated was the most common grade for mPC (n=2415, 53.1%), followed by moderately differentiated (n=1649, 36.3%), well-differentiated (n=372, 8.2%) and undifferentiated (n=110, 2.4%). Chi-square test showed significant differences in some variables and treatment patterns, including age at diagnosis, year of diagnosis, race, tumor size, marital status, primary site, T stage, N stage ($P< 0.01$).

Prognosis Analysis

Due to poor prognosis, the median follow-up time was 4 months (range, 0-150 months). To investigate the prognostic role of pancreatectomy and chemotherapy in mPC, we performed survival analysis, and survival curves were shown in **Figure 2**. The results show that pancreatectomy combined with chemotherapy can significantly improve the prognosis of patients with mPC compared to pancreatectomy or chemotherapy alone ($P<0.001$). The median OS for patients with mPC receiving PCT was 12 months, while 6 months for CT, 4 months for PT, and 1 month for NPCT.

Subgroup Analysis

Although pancreatectomy combined with chemotherapy has a significant benefit in the overall population, it is not clear whether there is a benefit in the characteristic population, so we conducted exploratory stratification, such as age at diagnosis, sex, marital status, tumor size, and histological grade. We found that pancreatectomy combined with chemotherapy can

TABLE 1 | Clinicopathological Characteristics of mPC patients with PCT, PT, CT or with no treatment.

Variable	Level	Overall (N = 4546)	NPCT (N = 1707)	CT (N = 2282)	PT (N = 244)	PCT (N = 313)	P-value
Age at diagnosis (median [IQR])		66.0 [58.0, 74.0]	69.0 [60.0, 78.0]	65.0 [57.0, 72.0]	67.5 [58.8, 76.0]	63.0 [56.0, 70.0]	**<0.001**
Age at diagnosis (%)	≤66 years	2328 (51.2)	720 (42.2)	1293 (56.7)	119 (48.8)	196 (62.6)	**<0.001**
	>66 years	2218 (48.8)	987 (57.8)	989 (43.3)	125 (51.2)	117 (37.4)	
Sex (%)	Female	2080 (45.8)	792 (46.4)	1014 (44.4)	125 (51.2)	149 (47.6)	0.153
	Male	2466 (54.2)	915 (53.6)	1268 (55.6)	119 (48.8)	164 (52.4)	
Grade (%)	Well	372 (8.2)	116 (6.8)	204 (8.9)	24 (9.8)	28 (8.9)	**<0.001**
	Moderately	1649 (36.3)	558 (32.7)	835 (36.6)	112 (45.9)	144 (46.0)	
	Poorly	2415 (53.1)	993 (58.2)	1184 (51.9)	100 (41.0)	138 (44.1)	
	Undifferentiated	110 (2.4)	40 (2.3)	59 (2.6)	8 (3.3)	3 (1.0)	
Year of diagnosis (%)	2004-2009	1994 (43.9)	805 (47.2)	921 (40.4)	132 (54.1)	136 (43.5)	**<0.001**
	2010-2015	2552 (56.1)	902 (52.8)	1361 (59.6)	112 (45.9)	177 (56.5)	
Race (%)	Black	632 (13.9)	284 (16.6)	291 (12.8)	30 (12.3)	27 (8.6)	**<0.001**
	Other	362 (8.0)	134 (7.9)	177 (7.8)	19 (7.8)	32 (10.2)	
	White	3552 (78.1)	1289 (75.5)	1814 (79.5)	195 (79.9)	254 (81.2)	
Tumor size (median [IQR])		42.0 [31.0, 56.0]	43.0 [31.0, 58.0]	42.0 [32.0, 55.0]	40.0 [30.0, 60.0]	38.0 [28.0, 51.0]	**<0.001**
Tumor size (%)	≤42 mm	2309 (50.8)	835 (48.9)	1148 (50.3)	129 (52.9)	197 (62.9)	**<0.001**
	>42 mm	2237 (49.2)	872 (51.1)	1134 (49.7)	115 (47.1)	116 (37.1)	
Marital status at diagnosis (%)	Married	2750 (60.5)	878 (51.4)	1483 (65.0)	164 (67.2)	225 (71.9)	
	Unmarried	1796 (39.5)	829 (48.6)	799 (35.0)	80 (32.8)	88 (28.1)	
Primary Site (%)	Body	770 (16.9)	275 (16.1)	448 (19.6)	16 (6.6)	31 (9.9)	**<0.001**
	Head	2003 (44.1)	751 (44.0)	954 (41.8)	135 (55.3)	163 (52.1)	
	Others	368 (8.1)	167 (9.8)	169 (7.4)	15 (6.1)	17 (5.4)	
	Overlapping	480 (10.6)	170 (10.0)	263 (11.5)	20 (8.2)	27 (8.6)	
	Tail	925 (20.3)	344 (20.2)	448 (19.6)	58 (23.8)	75 (24.0)	**<0.001**
T stage (%)	T1	141 (3.1)	69 (4.0)	64 (2.8)	6 (2.5)	2 (0.6)	
	T2	1393 (30.6)	586 (34.3)	746 (32.7)	27 (11.1)	34 (10.9)	
	T3	1883 (41.4)	639 (37.4)	832 (36.5)	170 (69.7)	242 (77.3)	
	T4	1129 (24.8)	413 (24.2)	640 (28.0)	41 (16.8)	35 (11.2)	
N stage (%)	N0	2527 (55.6)	1034 (60.6)	1338 (58.6)	68 (27.9)	87 (27.8)	**<0.001**
	N1	2019 (44.4)	673 (39.4)	944 (41.4)	176 (72.1)	226 (72.2)	

Statistically significant inter-group comparisons of the four treatments are shown in bold (P < 0.05).

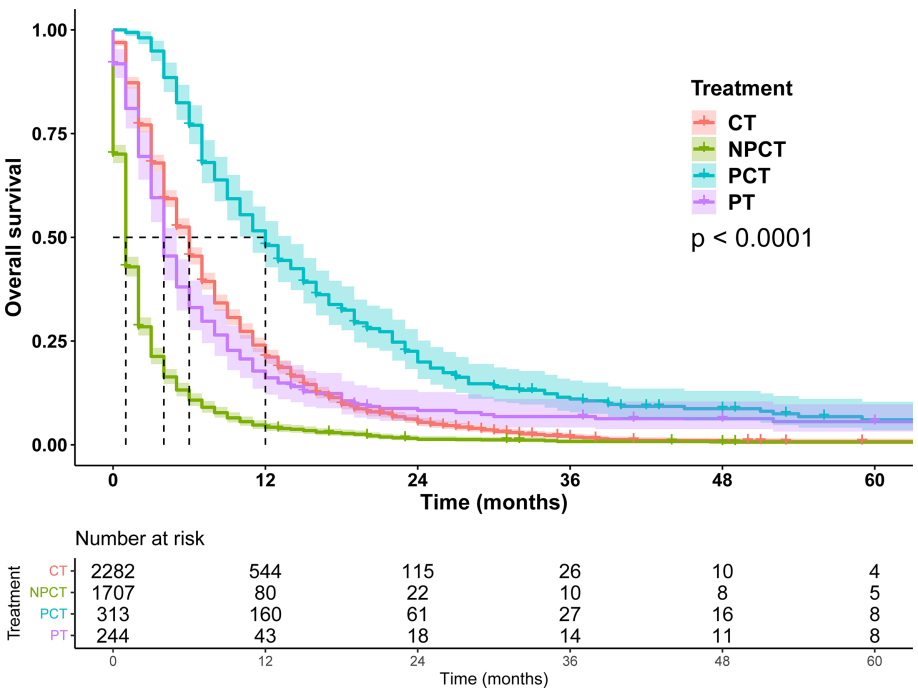

FIGURE 2 | Survival curves for patients with metastatic pancreatic cancer in different treatment modalities.

significantly prolonged OS time in patients with mPC, regardless of age at diagnosis, sex, marital status, tumor size, and histological grade (**Figures 3** and **4**).

It was further found that among patients with age ≤66 years and tumor ≤42 mm, patients receiving PCT had a more significant benefit, with a median OS of 13 months (95%CI: 11-15). Patients with well/moderately differentiated tumors or females also had a greater survival benefit, with a median OS of 14 months (95%CI: 11-16). We speculate that these may be favorable populations for surgery and chemotherapy

Construction and Validation of a Nomogram

To further investigate the risk factors for long-term survival of mPC, univariate and multivariate Cox regression analyses were used to identify independent prognostic factors (**Table 2**). Multivariate Cox regression results also indicated that PCT (HR = 0.250, 95% CI: 0.219-0.285, P<0.001) were a favorable prognostic factor for mPC. In addition, age at diagnosis, tumor size, marital status at diagnosis, sex, grade were also independent predictive factors (P< 0.001).

Based on the independent prognostic factors derived from multivariate Cox regression, we established a nomogram to predict 6-month, 12-month, 18-month OS probability for mPC (**Figure 5**). As shown in the nomogram, the treatment modality contributed the most to OS, followed by grade, tumor size, and age at diagnosis. The C index of our model was 0.717. After bootstrapping, it still had a good discriminative ability with a C-index of 0.716. When the tROC analysis was performed, the area under the ROC curve at 6-, 12- and 18-month was 0.772, 0.760, and 0.751, respectively (**Figure 6A**). These results all show that our model has a good discriminative ability. At the same time, the calibration analysis was performed. The calibration curve for predicting 6-, 12-, 18-month OS. was shown in **Figure 6B**, and

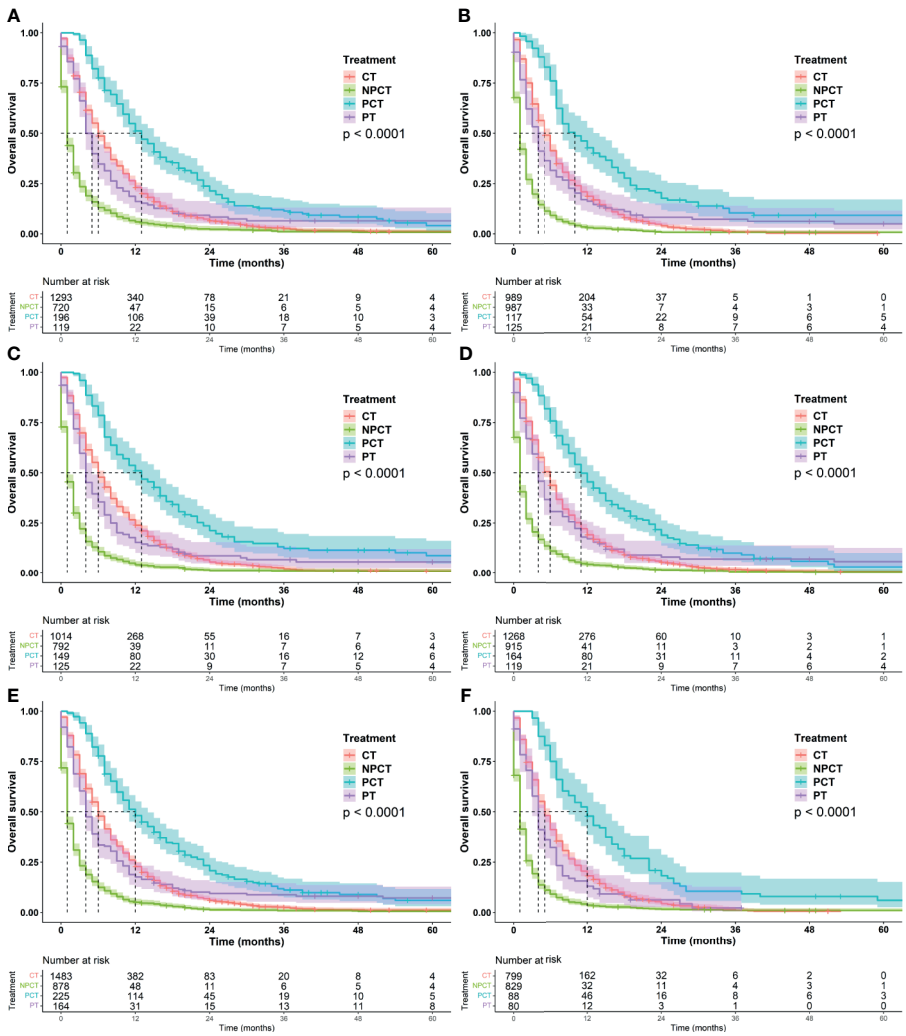

FIGURE 3 | Kaplan-Meier survival curves for subgroup analysis of patients with metastatic pancreatic cancer with different clinical characteristics. **(A)**: age ≤ 66 years, **(B)**: age>66 years, **(C)**: female, **(D)**: male, **(E)**: married, **(F)**: unmarried.

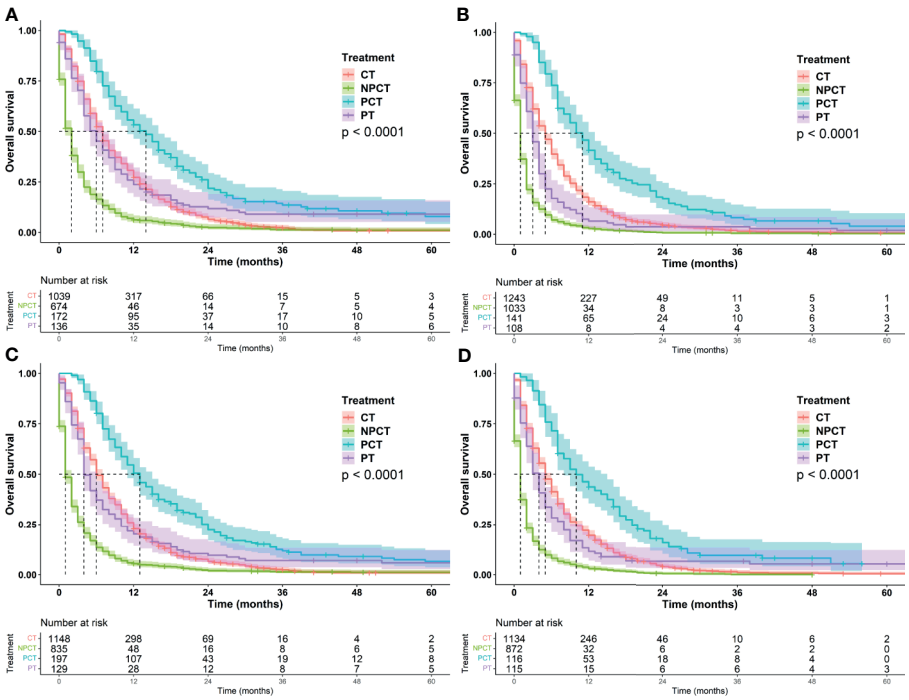

FIGURE 4 | Kaplan-Meier survival curves for subgroup analysis of patients with metastatic pancreatic cancer with different tumor characteristics. **(A)** grade: well/moderately differentiated **(B)** grade: Poor/Undifferentiated, **(C)**: tumor size ≤ 42mm, **(D)**: tumor size>42mm.

the bootstrapping calibration plots showed the good prediction accuracy of our nomogram.

DISCUSSION

In this study, we analyzed the treatment data of 4546 patients with mPC, revealing meaningful treatment modalities. We found that pancreatectomy combined with chemotherapy can significantly prolong the OS of patients with mPC compared to surgery or chemotherapy alone. In addition, we provide a nomogram to estimate the OS of mPC patients, which can be used to quantify the risk factors of patients and guide clinical treatment.

It is well known that patients with mPC are prone to pain, weight loss, obstruction, and other discomforts, which seriously affect their lives. Therefore, the treatment of metastatic pancreatic cancer usually takes chemotherapy as the main treatment to delay tumor progression and increase the survival time, and symptomatic treatment including oral opioid analgesics, ethanol ablation combined with celiac plexus neurolysis by endoscopic ultrasound, nutritional support, and endoscopic biliary and duodenal stent implantation to improve the quality of life (21, 22). But these non-surgical palliative treatments were not satisfactory. Surgery, as one of the main therapies for cancer treatment, seems to offer hope for patients with metastatic pancreatic cancer whose primary tumor is resectable. In particular, two new treatment regimens released in 2011 and beyond not only improved overall survival rates for pancreatic cancer but also showed good anti-tumor activity (6, 7). Therefore, some mPC patients received surgical treatment after conversion therapy, and the other part received adjuvant chemotherapy after surgical resection, and they may achieve long-term survival (23).

A multi-center phase II clinical study (24) revealed the prognostic analysis of 33 patients receiving an intravenous and intraperitoneal infusion of paclitaxel and combined with S-1 for the treatment of peritoneal metastasis of pancreatic cancer. Among them, the median OS of 8 patients who underwent conversion surgery after neoadjuvant chemotherapy was significantly higher than that of patients without surgery (27.8 vs 14.2 months, $P = 0.0062$). This is the highest level of evidence to date for the combination of surgery and chemotherapy, revealing the possibility of long-term survival after surgery in patients with partial loss of peritoneal metastases following neoadjuvant chemotherapy. In addition, liver metastasis is the most common mode of pancreatic cancer, and it usually indicates a worse prognosis than other sites (25). Of the 535 patients with hepatic metastases from pancreatic cancer who received neoadjuvant chemotherapy, 24 patients completed chemotherapy with radiographic findings indicating hepatic metastases disappeared, normal or significantly reduced cancer antigen 19-9 expression and received pancreatic resection. The overall group had OS and progression-free survival (PFS) of 56

TABLE 2 | Univariate and multivariate analysis for mPC patients.

Variable	Levels	Univariate		Multivariate	
		HR (95%CI)	P-value	HR (95%CI)	P-value
Age at diagnosis	≤66	Reference		Reference	
	>66	1.275 (1.202-1.354)	**<0.001**	1.218 (1.146-1.295)	**<0.001**
Gender	Female	Reference		Reference	
	Male	1.079 (1.016-1.145)	**0.013**	1.105 (1.039-1.176)	**0.001**
Race	Black	Reference		Reference	
	Other	0.863 (0.756-0.985)	**0.029**	0.961 (0.841-1.099)	0.565
	White	0.866 (0.794-0.944)	**0.001**	0.927 (0.848-1.013)	0.093
Material status at diagnosis	Married	Reference		Reference	
	Unmarried	1.267 (1.193-1.347)	**<0.001**	1.161 (1.089-1.237)	**<0.001**
Tumor size	≤42	Reference		Reference	
	>42	1.242 (1.17-1.318)	**<0.001**	1.238 (1.164-1.317)	**<0.001**
Location	Body	Reference			
	Head	0.936 (0.860-1.018)	0.123	–	
	Others	1.071 (0.944-1.216)	0.284		
	Overlapping	1.049 (0.934-1.177)	0.421		
	Tail	1.056 (0.958-1.163)	0.273		
Histological grade	Well differentiated	Reference			
	Moderately differentiated	1.184 (1.054-1.33)	**0.005**	1.261 (1.122-1.1417)	**<0.001**
	Poorly differentiated	1.597 (1.426-1.789)	**<0.001**	1.656 (1.477-1.4857)	**<0.001**
	Undifferentiated	1.452 (1.169-1.804)	**0.001**	1.372 (1.104-1.1706)	**0.004**
T stage	T1	Reference			
	T2	1.213 (1.016-1.448)	**0.033**	1.176 (0.983-1.408)	0.076
	T3	0.993 (0.834-1.183)	**0.940**	1.051 (0.879-1.258)	0.584
	T4	1.123 (0.939-1.343)	**0.203**	1.094 (0.911-1.313)	0.337
N stage	N0	Reference			
	N1	0.943 (0.889-1.001)	0.055		–
Treatment	NPCT	Reference			
	CT	0.409 (0.383-0.436)	**<0.001**	0.418 (0.391-0.447)	**<0.001**
	PT	0.432 (0.376-0.497)	**<0.001**	0.483 (0.419-0.557)	**<0.001**
	PCT	0.227 (0.199-0.258)	**<0.001**	0.250 (0.219-0.285)	**<0.001**

Statistically significant independent prognostic factors are shown in bold (P < 0.05).

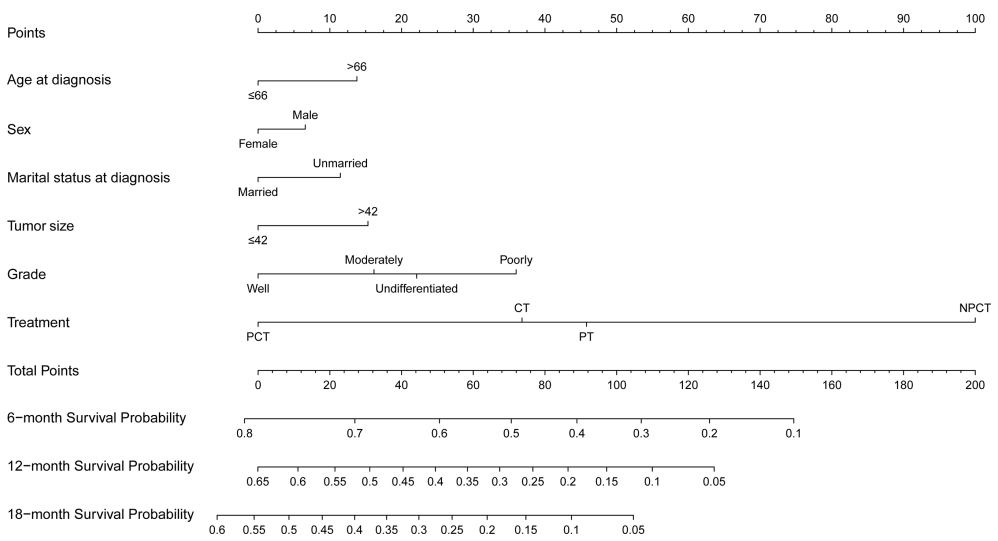

FIGURE 5 | Prognosis nomogram predicting 6-, 12-, and 18-month survival probability for patients with metastatic pancreatic cancer using six clinical characteristics.

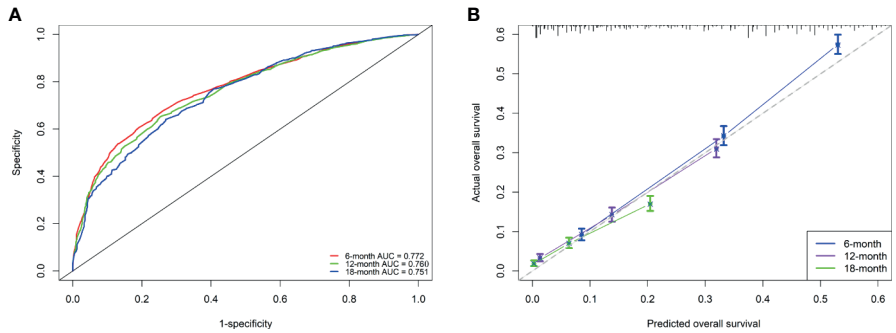

FIGURE 6 | Performance of the nomogram for metastatic pancreatic cancer patients **(A, B)**. **(A)** ROC curves and AUC at 6, 12, and 18 months were used to estimate discriminating power of the nomogram. the closer the area under the curve is to 1, the better the distinguishing ability is; **(B)** Calibration curves for predicting 6-, 12-, and 18-month OS were used to estimate the prediction accuracy of the nomogram. The *x*-axis indicates the predicted overall survival probability, and the *y*-axis indicates the actual survival probability. The 45-degree line (*gray line*) indicates that the prediction agrees with actuality.

and 27 months, respectively (26). Despite the lack of a control group, this treatment pattern has improved a lot compared to the previous reports of the mPC bad OS and PFS.

In our study, the median OS of pancreatectomy combined with chemotherapy was 12 months. The difference in survival between our study and other studies may be due to the difference in inclusion and exclusion criteria in the cohort. Our study included patients from 2004 to 2015, patients diagnosed with stage IV pancreatic cancer before 2011 were less likely to receive the new intensive treatment regimen. But pancreatectomy combined with chemotherapy still appears to be a favorable treatment. Kim (15) collected patients diagnosed with metastatic pancreatic cancer between 2000 and 2009, 35 of whom underwent surgical resection and matched 35 unresected patients with similar tumor size and peritoneal metastasis. The results showed that pancreatectomy for stage IV pancreatic duct adenocarcinoma can significantly improve the survival rate. Postoperative chemotherapy was statistically significant for survival (HR=0.44; 95% CI:1.03-3.15; P = 0.003).

Although prognostic factors for survival are not equal to predictors of treatment effectiveness, these results nevertheless remind us that these prognostic factors may be useful in further selecting specific subgroups that will benefit from pancreatectomy and chemotherapy. Therefore, we established a nomogram based on independent prognostic factors to select patients who might benefit from surgery and chemotherapy for survival. Those with smaller tumors, younger age, and better histological grades, women, married, undergoing surgery and chemotherapy, seem to have long-term survival. In addition, the subgroup analysis also showed that women, smaller tumors, younger age, and better histological grade appeared to benefit more from pancreatectomy and chemotherapy. These patients are the beneficiaries of pancreatectomy and chemotherapy, probably because they can tolerate the intense treatment and their tumors are more sensitive to chemotherapy and easier to remove. As for marital status, married patients may receive spiritual and financial support from their families compared with unmarried patients (27), and thus choose more intensive treatment and have a better prognosis. Similar to previous studies, our study also found a survival advantage for women over men in stage IV pancreatic cancer (28). In summary, the model has good discriminating and calibrating capabilities to select patients with stage IV pancreatic cancer who could potentially benefit from pancreatectomy and chemotherapy.

This study also has certain limitations. Firstly, because our study is a retrospective study and patients with unclear clinicopathological information were deleted, there is a possibility of selection bias. Secondly, there is no key information in the SEER database including physical status, nutritional status, details of the surgery, chemotherapy regimens, chemotherapy course, chemotherapy and surgery sequence, etc., and sarcopenia has recently been recognized as a risk factor for postoperative pancreatic cancer (29). Therefore, the inclusion of these important factors may make our model more accurate. Finally, although our model has good performance in internal validation, we still need to evaluate the accuracy of the model based on external verification of independent cohorts. Nevertheless, considering the scale of our study and the rigorous statistical calculations, the conclusions of the study are still credible.

CONCLUSION

In summary, this study used a large population-based SEER database to examine the influencing factors and the efficacy of surgery and chemotherapy in patients with mPC. We found that surgery and chemotherapy prolonged the overall survival of some mPC patients, and we established a nomogram to screen out those patients who might benefit. However, it is necessary to carefully evaluate the clinical effectiveness of pancreatectomy and chemotherapy in mPC. And further prospective studies are needed for verification.

DATA AVAILABILITY STATEMENT

Publicly available datasets were analyzed in this study. This data can be found here: https://seer.cancer.gov/.

AUTHOR CONTRIBUTIONS

JC, JL, and DN conceived and designed the study. DN and GL collected clinical data and performed the statistical analysis, GA, SL, and ZW prepared the figures and tables. All authors contributed to the article and approved the submitted version.

FUNDING

This work was supported by a grant from the Key Research and Development Projects in Hunan Province (No.2018SK2127).

ACKNOWLEDGMENTS

We would like to thank the staff of SEER Database for their contribution in collecting and collating the information.

REFERENCES

1. Bray F, Ferlay J, Soerjomataram I, Siegel RL, Torre LA, Jemal A. Global Cancer Statistics 2018: GLOBOCAN Estimates of Incidence and Mortality Worldwide for 36 Cancers in 185 Countries. *CA Cancer J Clin* (2018) 68 (6):394–424. doi: 10.3322/caac.21492
2. Rahib L, Smith BD, Aizenberg R, Rosenzweig AB, Fleshman JM, Matrisian LM. Projecting Cancer Incidence and Deaths to 2030: The Unexpected Burden of Thyroid, Liver, and Pancreas Cancers in the United States. *Cancer Res* (2014) 74(11):2913–21. doi: 10.1158/0008-5472.CAN-14-0155
3. Tempero MA, Malafa MP, Al-Hawary M, Behrman SW, Benson AB, Cardin DB, et al. Pancreatic Adenocarcinoma, Version 2.2021, NCCN Clinical Practice Guidelines in Oncology. *J Natl Compr Canc Netw* (2021) 19 (4):439–57. doi: 10.6004/jnccn.2021.0017
4. Nentwich MF, Bockhorn M, Konig A, Izbicki JR, Cataldegirmen G. Surgery for Advanced and Metastatic Pancreatic Cancer–Current State and Trends. *Anticancer Res* (2012) 32(5):1999–2002.
5. Tempero MA. NCCN Guidelines Updates: Pancreatic Cancer. *J Natl Compr Canc Netw* (2019) 17(5.5):603–5. doi: 10.6004/jnccn.2019.5007
6. Vaccaro V, Sperduti I, Milella M. FOLFIRINOX Versus Gemcitabine for Metastatic Pancreatic Cancer. *N Engl J Med* (2011) 365(8):768–769; author reply 769. doi: 10.1056/NEJMc1107627
7. Von Hoff DD, Ervin T, Arena FP, Chiorean EG, Infante J, Moore M, et al. Increased Survival in Pancreatic Cancer With Nab-Paclitaxel Plus Gemcitabine. *N Engl J Med* (2013) 369(18):1691–703. doi: 10.1056/NEJMoa1304369
8. Bilimoria KY, Bentrem DJ, Ko CY, Stewart AK, Winchester DP, Talamonti MS. National Failure to Operate on Early Stage Pancreatic Cancer. *Ann Surg* (2007) 246(2):173–80. doi: 10.1097/SLA.0b013e3180691579
9. Voss N, Izbicki JR, Nentwich MF. Oligometastases in Pancreatic Cancer (Synchronous Resections of Hepatic Oligometastatic Pancreatic Cancer: Disputing a Principle in a Time of Safe Pancreatic Operations in a Retrospective Multicenter Analysis). *Ann Gastroenterol Surg* (2019) 3 (4):373–7. doi: 10.1002/ags3.12255
10. Crippa S, Bittoni A, Sebastiani E, Partelli S, Zanon S, Lanese A, et al. Is There a Role for Surgical Resection in Patients With Pancreatic Cancer With Liver Metastases Responding to Chemotherapy? *Eur J Surg Oncol* (2016) 42 (10):1533–9. doi: 10.1016/j.ejso.2016.06.398
11. Hackert T, Niesen W, Hinz U, Tjaden C, Strobel O, Ulrich A, et al. Radical Surgery of Oligometastatic Pancreatic Cancer. *Eur J Surg Oncol* (2017) 43 (2):358–63. doi: 10.1016/j.ejso.2016.10.023
12. Shrikhande SV, Kleeff J, Reiser C, Weitz J, Hinz U, Esposito I, et al. Pancreatic Resection for M1 Pancreatic Ductal Adenocarcinoma. *Ann Surg Oncol* (2007) 14(1):118–27. doi: 10.1245/s10434-006-9131-8
13. Strobel O, Neoptolemos J, Jager D, Buchler MW. Optimizing the Outcomes of Pancreatic Cancer Surgery. *Nat Rev Clin Oncol* (2019) 16(1):11–26. doi: 10.1038/s41571-018-0112-1
14. Furuse J, Shibahara J, Sugiyama M. Development of Chemotherapy and Significance of Conversion Surgery After Chemotherapy in Unresectable Pancreatic Cancer. *J Hepatobiliary Pancreat Sci* (2018) 25(5):261–8. doi: 10.1002/jhbp.547
15. Kim Y, Kim SC, Song KB, Kim J, Kang DR, Lee JH, et al. Improved Survival After Palliative Resection of Unsuspected Stage IV Pancreatic Ductal Adenocarcinoma. *HPB (Oxford)* (2016) 18(4):325–31. doi: 10.1016/j.hpb.2015.10.014
16. Schneitler S, Kropil P, Riemer J, Antoch G, Knoefel WT, Haussinger D, et al. Metastasized Pancreatic Carcinoma With Neoadjuvant FOLFIRINOX Therapy and R0 Resection. *World J Gastroenterol* (2015) 21(20):6384–90. doi: 10.3748/wjg.v21.i20.6384
17. Neofytou K, Giakoustidis A, Smyth EC, Cunningham D, Mudan S. A Case of Metastatic Pancreatic Adenocarcinoma With Prolonged Survival After Combination of Neoadjuvant FOLFIRINOX Therapy and Synchronous Distal Pancreatectomy and Hepatectomy. *J Surg Oncol* (2015) 111(6):768–70. doi: 10.1002/jso.23867
18. Surveillance, Epidemiology, and End Results (SEER) Program. *SEER*Stat Database: Incidence - SEER 18 Regs Custom Data (With Additional Treatment Fields), Nov 2018 Sub (1975-2016 Varying) - Linked To County Attributes - Total U.S., 1969-2017 Counties, National Cancer Institute, DCCPS, Surveillance Research Program, Released April 2019, Based on the November 2018 Submission*. Available at: www.seer.cancer.gov.
19. Steyerberg EW, Vickers AJ, Cook NR, Gerds T, Gonen M, Obuchowski N, et al. Assessing the Performance of Prediction Models A Framework for Traditional and Novel Measures. *Epidemiology* (2010) 21(1):128–38. doi: 10.1097/EDE.0b013e3181c30fb2
20. Demler OV, Paynter NP, Cook NR. Tests of Calibration and Goodness-of-Fit in the Survival Setting. *Stat Med* (2015) 34(10):1659–80. doi: 10.1002/sim.6428
21. Facciorusso A, Di Maso M, Serviddio G, Larghi A, Costamagna G, Muscatiello N. Echoendoscopic Ethanol Ablation of Tumor Combined With Celiac Plexus Neurolysis in Patients With Pancreatic Adenocarcinoma. *J Gastroenterol Hepatol* (2017) 32(2):439–45. doi: 10.1111/jgh.13478
22. Perone JA, Riall TS, Olino K. Palliative Care for Pancreatic and Periampullary Cancer. *Surg Clin North Am* (2016) 96(6):1415–30. doi: 10.1016/j.suc.2016.07.012
23. Yoshitomi H, Takano S, Furukawa K, Takayashiki T, Kuboki S, Ohtsuka M. Conversion Surgery for Initially Unresectable Pancreatic Cancer: Current Status and Unresolved Issues. *Surg Today* (2019) 49(11):894–906. doi: 10.1007/s00595-019-01804-x
24. Satoi S, Fujii T, Yanagimoto H, Motoi F, Kurata M, Takahara N, et al. Multicenter Phase II Study of Intravenous and Intraperitoneal Paclitaxel With S-1 for Pancreatic Ductal Adenocarcinoma Patients With Peritoneal Metastasis. *Ann Surg* (2017) 265(2):397–401. doi: 10.1097/SLA.0000000000001705
25. Oweira H, Petrausch U, Helbling D, Schmidt J, Mannhart M, Mehrabi A, et al. Prognostic Value of Site-Specific Metastases in Pancreatic Adenocarcinoma: A Surveillance Epidemiology and End Results Database Analysis. *World J Gastroenterol* (2017) 23(10):1872–80. doi: 10.3748/wjg.v23.i10.1872
26. Frigerio I, Regi P, Giardino A, Scopelliti F, Girelli R, Bassi C, et al. Downstaging in Stage IV Pancreatic Cancer: A New Population Eligible for Surgery? *Ann Surg Oncol* (2017) 24(8):2397–403. doi: 10.1245/s10434-017-5885-4
27. Duorui N, Shi B, Zhang T, Chen C, Fang C, Yue Z, et al. The Contemporary Trend in Worsening Prognosis of Pancreatic Acinar Cell Carcinoma: A Population-Based Study. *PloS One* (2020) 15(12):e0243164. doi: 10.1371/journal.pone.0243164

28. Nipp R, Tramontano AC, Kong CY, Pandharipande P, Dowling EC, Schrag D, et al. Disparities in Cancer Outcomes Across Age, Sex, and Race/Ethnicity Among Patients With Pancreatic Cancer. *Cancer Med* (2018) 7(2):525–35. doi: 10.1002/cam4.1277
29. Pessia B, Giuliani A, Romano L, Bruno F, Carlei F, Vicentini V, et al. The Role of Sarcopenia in the Pancreatic Adenocarcinoma. *Eur Rev Med Pharmacol Sci* (2021) 25(10):3670–8. doi: 10.26355/eurrev_202105_25933

Conflict of Interest: The authors declare that the research was conducted in the absence of any commercial or financial relationships that could be construed as a potential conflict of interest.

Publisher's Note: All claims expressed in this article are solely those of the authors and do not necessarily represent those of their affiliated organizations, or those of the publisher, the editors and the reviewers. Any product that may be evaluated in this article, or claim that may be made by its manufacturer, is not guaranteed or endorsed by the publisher.

frontiers in Oncology

ORIGINAL RESEARCH
published: 17 September 2021
doi: 10.3389/fonc.2021.682928

Prognostic Value of Preoperative NLR and Vascular Reconstructive Technology in Patients With Pancreatic Cancer of Portal System Invasion: A Real World Study

Lin Zhou[1†], Jing Wang[1†], Xin-xue Zhang[1], Shao-cheng Lyu[1], Li-chao Pan[2], Guo-sheng Du[2], Ren Lang[1] and Qiang He[1*]*

[1] Department of Hepatobiliary and Pancreaticosplenic Surgery, Beijing ChaoYang Hospital, Capital Medical University, Beijing, China, [2] Faculty of Hepato-Pancreato-Biliary Surgery, Chinese People's Liberation Army (PLA) General Hospital, Beijing, China

The purpose was aimed to establish a simple computational model to predict tumor prognosis by combining neutrophil to lymphocyte Ratio (NLR) and biomarkers of oncological characteristics in patients undergoing vascular reconstructive radical resection of PDAC. The enrolled patients was divided into high or low NLR group with the cutoff value determined by the receiver operator characteristic (ROC) curve. Different vascular anastomoses were selected according to the Chaoyang classification of PDAC. Survival rates were calculated using the Kaplan-Meier and evaluated with the log-rank test. Cox risk regression model was used to analyze the independent risk factors for prognostic survival. The optimal cut-off value of NRL was correlated with the differentiation, tumor size, TNM stage and distant metastasis of advanced PDAC. A curative resection with vascular reconstructive of advanced PDAC according to Chaoyang classification can obviously improve the survival benefits. Cox proportional hazards demonstrated higher evaluated NLR, incisal margin R1 and lymphatic metastasis were the independent risk predictor for prognosis with the HR > 2, meanwhile, age beyond 55, TNM stage of III-IV or Tumor size > 4cm were also the obvious independent risk predictor for prognosis with the HR ≤ 2. The advanced PADC patients marked of RS group (3 < RS ≤ 6) showed no more than 24 months of survival time according to RS model based on the six independent risk predictors. Vascular reconstruction in radical resection of advanced PDAC improved survival, higher elevated NLR (>2.90) was a negative predictor of DFS and OS in those patients accompanying portal system invasion.

Keywords: neutrophil-lymphocyte ratio, pancreatic ductal cell carcinoma, vascular invasion, curative resection, real world study

Edited by:
Taiping Zhang, Peking Union Medical College Hospital (CAMS), China

Reviewed by:
Kimberly Washington, Texas Christian University, United States
Maoming Xiong, First Affiliated Hospital of Anhui Medical University, China

***Correspondence:**
Ren Lang
dr_langren@126.com
Qiang He
heqiang349@sina.com

†These authors have contributed equally to this work

Specialty section:
This article was submitted to Surgical Oncology, a section of the journal Frontiers in Oncology

Received: *19 March 2021*
Accepted: *30 August 2021*
Published: *17 September 2021*

Citation:
Zhou L, Wang J, Zhang X-x, Lyu S-c, Pan L-c, Du G-s, Lang R and He Q (2021) Prognostic Value of Preoperative NLR and Vascular Reconstructive Technology in Patients With Pancreatic Cancer of Portal System Invasion: A Real World Study. Front. Oncol. 11:682928. doi: 10.3389/fonc.2021.682928

INTRODUCTION

Pancreatic ductal adenocarcinoma (PDAC) accounts for more than 90% (1) of all pancreatic cancer which is fifth most common cancers around the world (2). Although pancreatectomy is considered the only approach of curative treatment of PDAC, which provides a chance of cure and longer survival (3), but the prognosis is generally poor with a reported 5-year overall survival (OS) ranged from 10 to 30% postoperative (4–6). Once diagnosed, there are only about 10% of patients localized, meanwhile 29% of patients spread to regional lymph nodes with a relative 5-years low survival of 11.5%, compared with 34.3% for localized disease (7). In addition, about 80% of patients with PDAC experience a recurrence despite adjuvant therapy after a radical resection (8). Therefore radical resection, including thorough lymph node dissection, is an effective means to improve prognosis and survival.

Some studies have asserted that about 17-32% of patients with pancreatic cancer showed portal system including portal vein (PV), superior mesenteric vein (SMV) and splenic vein (SV) invasion once diagnosed (9). Among them, SMV and PV are the most vulnerable and frequent to invasion because of the proximity of these vessels to the uncinate process and pancreatic head (10). These patients may have a rather low median survival of 8 months compared with there were no vascular invasion (11). Radical resection of pancreatic cancer combined with complete vascular resection and reconstruction of the PV-SMV venous axis in these patients is a possible approach. The feasibility and advantages of this approach was proved, which may provide survival results comparable to those obtained with standard pancreatectomy without venous resection (12–14). That approach may improve the worse survival benefit with a OS of 18.2 months when only palliative treatment was given (15). Although vascular invasion as a prognostic factor was carried out in several studies which mainly focus on whether there is an association between vascular invasion and poor prognosis, the types of vascular invasion, classification (location, depth and circumference) and anastomotic techniques of vascular reconstruction on the prognosis is not clear.

Except the radical excision, early diagnosis is of great significance for the prognosis of pancreatic cancer patients. Carbohydrate antigen 19-9 (CA19-9) which is the only authenticated marker for clinical application, lacks the specificity required for a differential diagnosis (16). Searching for novel biomarkers to detect and diagnose PDAC earlier maybe another approach to improve the poor prognosis. Literatures of inflammatory indices and immunologic ratios, including ratios comprised of intratumoral or circulating neutrophils, platelets, lymphocytes, and monocyte counts, have been proposed to be prognostic biomarkers for a wide range of malignancies (17, 18). There has studies showed that neutrophil to lymphocyte ratio (NLR), not platelet to lymphocyte (PLR), is predictive on survival benefits after resection of early-stage PDAC (19, 20). The prognostic value of lymphocyte to monocyte ratio (LMR) levels for PDAC patients remains to be determined (19, 20). The relationship between NLR and prognosis of advanced PDAC after resection with vascular reconstruction remains unclear. Meanwhile, there exist few studies on the prediction of inflammatory markers, biomarkers of tumor characteristics and surgical techniques for OS and DFS in advanced PDAC patients.

This presented paper was aimed to explore the effect of NLR, tumor marker such as CA19-9, vascular reconstruction methods, lymphatic metastasis and other surgical and pathologically related factors on the long-term prognosis of PDAC with portal system invasion. Therefore, establishing a predictive model based on the risk factor of Cox regression analysis to predict OS and disease-free survival (DFS) after radical resection with vascular reconstruction of advanced PDAC is necessary and promising.

MATERIALS AND METHODS

Patient Selection and Operative Techniques

Patient Selection

At the present study, we enrolled 241 patients who were diagnosed with pancreatic carcinoma from January 2011 to December 2019 and performed radical excision with strict criteria as follows. This study was approved by the Ethical Committee of Beijing Chao-Yang Hospital. All patients provided full written informed consent, which was obtained in accordance with the Declaration of Helsinki of the World Medical Association (Ethics approval and consent to participate: No.2020-D.-309-2). The authors are accountable for all aspects of the work in ensuring that questions related to the accuracy or integrity of any part of the work are appropriately investigated and resolved.

Included criteria: (1) Preoperative image indicated pancreatic malignancy. (2) Aged 20 to 85 years old. (3) En bloc resection of tumor during operation. (4) Postoperative pathology confirmed pancreatic ductal adenocarcinoma. (5) The mode of operation and treatment strategy obtained the informed consent of patients and their families.

Excluded criteria: (1) Unresectable condition or metastasis found during surgery. (2) Surgical rule violation. (3) Pathologic diagnosis other than conventional ductal adenocarcinoma. (4) Postoperative follow-up data were incomplete or lost to follow-up.

Operative Detections

Preoperative tumor evaluation was done by diagnostic imaging methods, including abdominal ultrasonography, computed tomography (CT) including lung and abdominal or abdominal magnetic resonance imaging (MRI). One should take a Positron Emission Tomography-Computed Tomography (PET-CT) or bone scan if distant metastasis is suspected. The laboratory measurement including liver function, tumor marker, hepatitis index, blood routine examination and thromboxane function.

Group and Operation

The patient compliance with the study criteria was admitted into the group. All the patients was divided into high NLR group and

low NLR group which criteria for grouping as determined by ROC curves for healthy people and all the patients.

At present, there existed no uniform clinical standard for the classification of vascular invasion in pancreatic cancer. The most commonly used clinical standard for vascular invasion is the Loyer classification and Shibata typing (21, 22). However, all of the above classifications have certain limitations. On the one hand, it is impossible to assess the site and scope of tumor invasion to portal vein system, on the other hand, it has no guiding value for the resection and reconstruction of the invaded portal vein system. In recent years, our center has carried out a beneficial attempt to optimize the above vascular invasion typing criteria in patients treated with radical surgery and proposed a new typing system named Chaoyang classification (23). There are four types: (I) Portal and/or superior mesenteric vein invasions of less than 1/4 circumference. In this type of patients, the lateral wall of the vein can be blocked without blocking the blood flow into the liver. The affected side wall can be partially excised and the vein can be sutured directly. After suturing, the vein can be guaranteed to have no obvious stenosis. (II) Portal vein and/or superior mesenteric vein were invaded to a range greater than 1/4 circumference, or the vein was clearly narrowed and occluded, without involving the splenic vein junction. In this type of patients, segmental resection of the involved vein is recommended, and end-to-end anastomosis or allograft or artificial vascular reconstruction is selected according to the tension of the upper and lower edges. (III) The tumor invaded the confluence of portal vein, splenic vein and superior mesenteric vein. In this type of patients, partial splenic vein resection can be performed in conjunction with the confluence part, and splenic vein reconstruction can be completed by using foreign blood vessels with branches. (IV) The tumor invaded a wide area, the portal vein, splenic vein and superior mesenteric vein are involved in the upper part, and the branch of superior mesenteric vein in the lower part is involved. In this type of patients, arterial approach is recommended to complete tumor dissociation and then resection of invaded vessels, for reconstruction, it is recommended that the superior mesenteric vein branch be shaped into an opening first, and then Allogeneic blood vessels with branches or other substitutes should be used to complete the reconstruction. Different methods of vascular resection and reconstruction are adopted according to the specific form of venous invasion. The technique of vascular reconstruction and the type of pancreatic, biliary, and enteric anastomoses depended on operating surgeon's choice.

According to the Chaoyang classification, about half of the patients included in this study are advanced PDAC with portal system invasion, with the standard of Chaoyang classification, we performed radical resection on the advanced pancreatic cancer, combined with vascular resection, reconstruction or allogeneic vascular replacement and lymph node dissection to meet the standard of R0 resection. Therefore, on the basis of NLR grouping, we used the operation mode, resection and reconstruction of invasive vessels in Chaoyang classification and the degree of tumor pathological differentiation (poorly differentiation, poorly-moderately differentiation, moderately differentiation and moderately-highly differentiation group) as subgroup criteria.

The follow up began when diagnosed and was in hospital, with whole data and records. The overall survival (OS) and disease-free survival (DFS) was the main index in measurement the survival benefits.

Sample Detection and Hematoxylin-Eosin Stain

The pancreatic and vascular specimens were obtained once the tumor excision from the patients, and fixed with 10% formaldehyde solution. The 10% formalin fixed tissues embedded in paraffin, then microtome section with 5μm, heated at 60°C on slides warmer for 30 min, undergo the steps of dewaxing, benzene removal, hematoxylin and eosin staining, then dehydration and fixation.

Statistical Analysis

Pathological results images were collected under optical microscopy for 40X, 100X and 200X visual fields. All data analysis was carried out by SPSS 22.0 software, each index was expressed by Means ± SD. Survival rates, including OS and DFS, were calculated using the Kaplan-Meier method and evaluated with the log-rank test. Cox proportional model was used to analyze the multivariate survival, and the independent risk factors affecting the survival time. Qualitative variables were compared using $\chi 2$ tests, and quantitative variables were compared using Wilcoxon tests (multi-group) or t test (two groups). Statistical significance was defined as $p < 0.05$.

RESULTS

NLR ROC Curve and Changes in Different Groups

According to the ROC curve, the optimal cutoff value of preoperative NLR that had a relatively high specificity was 2.9. The area under the ROC curves was 0.761 (P = 0.000) and 95% confidence interval (95% CI 0.716-0.805) (**Figure 1**). A cutoff value of 2.9 presented a sensitivity of 48.9% and a specificity of 95.6%.

The enrolled patients were divided into high NLR group and low NLR group according to the cutoff value. 118 patients (49%) identified as high NLR group had an elevated NLR (> 2.9), and 123 patients (51%) were identified as low NLR (≤ 2.9) group. There were significant differences among NLR with different degrees of differentiation (F = 2.826, P = 0.039), and also an obviously differences among neutrophil (NEUT) (F = 3.396, P = 0.019) but no differences among lymphocyte with different degrees of differentiation (F = 0.081, P = 0.462).

The Preoperative NLR in Patients With PDAC and Its Relationship With Clinical Pathologic Characteristics

The 241 enrolled patients who underwent radical excision between January 2011and December 2019 consisted of 136 males and 105 females. Their mean age was 62.838 ± 10.742

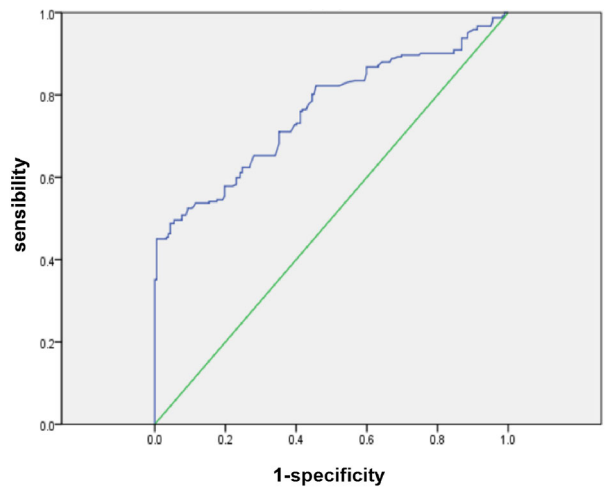

FIGURE 1 | ROC curves for NLR in patients with PDAC (NLR, neutrophil-to-lymphocyte ratio; PDAC, pancreatic ductal adenocarcinoma).

years (yrs) with male 62.394 ± 10.550 yrs and female 63.409 ± 11.010 yrs. The date of operation was the starting point of follow-up and ended to May 2020. The longest follow-up time was 82 months, the shortest was 1 months, and the median follow-up time was 15 months. No patients were lost or withdraw during the study preformed.

Pathological analysis showed that all patients were PDAC with 31/241 of low differentiation, 56/241 of moderate-low differentiation, 126/241 of moderate differentiation, 28/241 of high-moderate or high differentiation (**Figure 2**). The average size of tumors was 3.779 ± 1.644 cm and 97/241 with vascular invaders, the pathological results of different groups are shown in **Table 1**. The relationship between preoperative peripheral blood NLR and clinical pathologic characteristics was investigated. As listed above (**Table 1**), 118 patients (49%) identified as high NLR group had an elevated NLR (> 2.9), and 123 patients (51%) were identified as low NLR (≤ 2.9) group. An elevated preoperative NLR level was closely correlated with the tumor size (range, > 4cm) (χ^2 = 7.530; P=0.006), tumor differentiation (χ^2 = 8.287; P = 0.040), clinical TNM stage(range, > II b) (χ^2 = 12.770; P=0.000), distant metastasis (χ^2 = 7.858; P = 0.005), and bilirubin (TBIL *vs.*DBIL, *t* =-3.696 *vs.*-3.294, P = 0.000 *vs.*0.001). No obvious correlations with age, gender, CA-199, and other index (**Table 1**, P > 0.05).

Diagnosis Value of NLR in PDAC Comparison With CA-199

Although there has lower correlation between NLR ≤ 2.90 and CA19-9 (r = 0.2193,95%CI 0.03943~0.3854; P = 0.408), but the NLR and CA19-9 was no correlation for all the patients (P = 0.408) and high NLR (NLR > 2.90) (P = 0.841). The diagnostic value of NLR to PDAC was analyzed by using the statistical diagnostic experimental method based on the currently recognized diagnostic standard of CA19-9. There has proved that NLR was with a sensitivity of 0.496 and a specificity of 0.515 in the diagnosis of PDAC (OR = 1.38, 95%CI of OR 0.94~2.02) as well as with a positive predictive value of 0.576 and a positive likelihood ratio of 1.022.

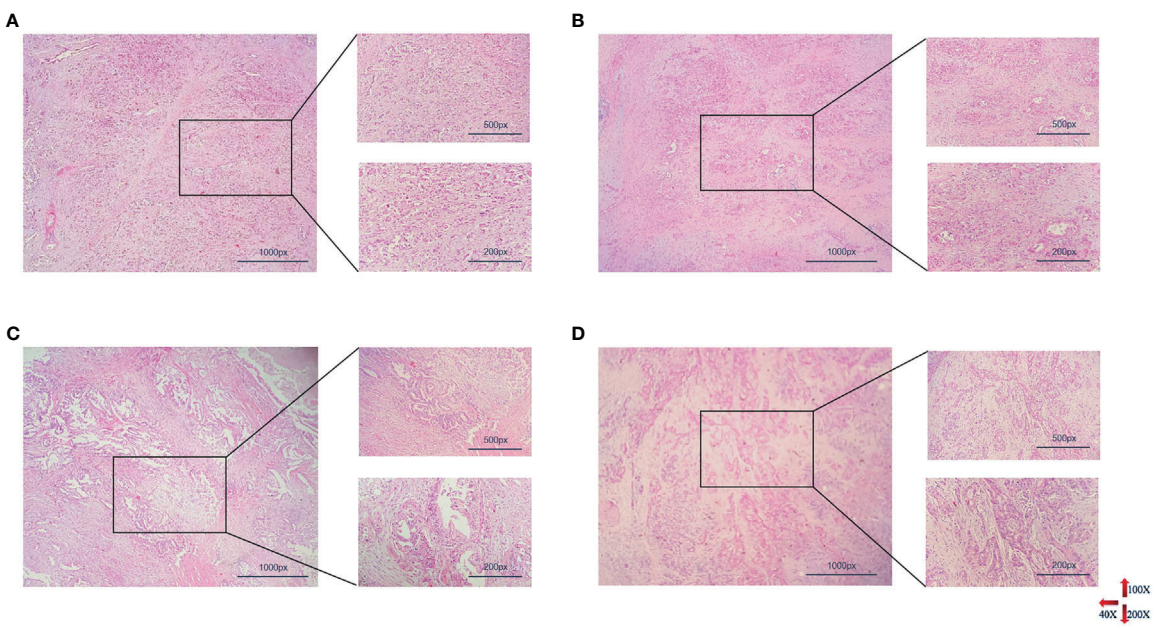

FIGURE 2 | Histopathological results of PDAC with different degrees of differentiation. From **(A–D)** represented poorly differentiation, moderately-poorly differentiation, moderately differentiation, highly-moderately differentiation respectively (PDAC, pancreatic ductal adenocarcinoma).

TABLE 1 | Background data preoperative and pathological results in various NLR groups.

Index	High NLR Group (n = 118)	Low NLR Group (n = 123)	*U*	*P*
Gender			2.719	0.099[a]
male	71	61		
female	47	62		
Age			3.751	0.053[a]
>55	100	85		
≤55	22	34		
Smoking (yes, %)	58 (49%)	51 (41%)	1.437	0.231[a]
Diabetes (yes, %)	50 (42%)	61 (50%)	1.264	0.261[a]
PBD (yes, %)	14 (12%)	9 (7%)	1.443	0.230[a]
NEUT	6.521 ± 3.079	3.129 ± 1.319	11.193	0.000[b]
Lymph	1.216 ± 0.820	1.804 ± 0.718	-5.925	0.000[b]
ALT (ng/ml)	(10-4583)	(10-336)	2.437	0.120[c]
TBIL	(3.6-552.8)	(5.5-275.4)	13.664	0.000[c]
DBIL	(2.1-505.5)	(0.79-219.5)	10.852	0.001[c]
Alb	37.079 ± 10.633	37.118 ± 4.715	-0.037	0.970[b]
CA199 (ng/ml)	42.89 (1.4-7000)	48.41 (2.6-7000)	1.324	0.251[c]
γ-GGT	6-1413	6-1957	1.055	0.305[c]
ALP	16-1398	47-1492	1.637	0.202[c]
Glu	7.308 ± 3.199	7.139 ± 2.708	0.439	0.661[b]
AMY	0.05-585	8-585	0.597	0.441[c]
Tumor site, n (%)			5.555	0.135[b]
uncinate process	79 (67%)	93 (76%)		
neck	6 (5%)	8 (7%)		
body and tail	33 (28%)	22 (18%)		
Tumor size, cm	4.057 ± 1.787	3.513 ± 1.543	2.597	0.010[b]
>4	45	27	7.530	0.006[b]
≤4	73	96		
Differentiation, n (%)			6.885	0.076[a]
poorly	21	10		
poorly-moderately	31	27		
moderately	54	68		
moderately-highly	12	18		
Vascular invasion, n (%)	45 (38%)	53 (43%)	8.874	0.096 [a]
LNs metastasis, n (%)	77 (65%)	81 (66%)	0.010	0.096 [a]
Nerve invasion, n (%)	108 (92%)	118 (96%)	0.010	0.096 [a]
Incisal Margin R0, n (%)	106 (90%)	121 (98%)	8.034	0.005[b]

[a]p-value from Chi-Squared Test or Fish's exact test; [b]p-value from Student' t test; [c]p-value from ANOVA; NLR, Neutrophil To Lymphocyte Ratio; PBD, preoperative biliary drainage; NEUT, neutrophil; ALT, Alanine transaminase; TBIL, total bilirubin; DBIL, direct bilirubin; Alb, albumin; CA19-9, carbohydrate antigen 199; γ-GGT, γ-gamma-glutamyl transpeptidase; ALP, A Lkaline Phosphatase; AMY, amylase; LN, lymph node.

Surgical Method and Vascular Anastomosis in Different NLR Group With PDAC

According to the results of preoperative imaging examination, 11 patients received palliative treatment (regarded as R1 resection), radical pancreaticoduodenectomy was performed in 160 cases, total pancreatectomy in 21 cases and distal pancreatectomy in 49 cases, of which 14 patients underwent R1 resection (2 patients in low NLR group, 1 patient in high NLR group) and the rest with R0 resection of a rate with 94.19%. There was no difference in the total number of lymph node dissection (19.789 ± 1.078, 19.297 ± 1.451, P = 0.785) and lymph node metastasis rate (2.252 ± 0.288, 3.297 ± 0.542, P = 0.087) between the two groups, nevertheless, there was significant difference in R0 resection rate (NLR ≤ 2.90 n = 2/123; NLR > 2.9 n = 12/118; $\chi^2 = 8.034$, P = 0.005). There was no significant difference in intraoperative blood loss (P = 0.699), blood transfusion (P = 0.753) and operation time (P = 0.687) between the two groups.

Patients undergoing pancreaticoduodenectomy and total pancreatectomy were divided into two categories based on whether portal system invasion exists. Different vascular anastomosis and replacement methods were selected according to Chaoyang classification, which including partially excised and sutured directly (**Figures 3A, E**), end-to-end anastomosis (**Figures 3B, F**) and allogeneic vascular replacement with type I: segmental vascular replacement (**Figures 3C, G**), or type II: branch vascular replacement (**Figures 3D, H**).

These results supported the original hypothesis that comparing with palliative treatment, vascular resection or reconstruction was able to significantly improve the survival time of patients with vascular invasion (OS *vs.* DFS 9.909 *vs.* 7.727), different anastomosis or reconstruction methods could improve the OS and DFS remarkably, (P < 0.01) (**Table 2**) among which end-to-end anastomosis was the best (OS *vs.* DFS 30.154 *vs.* 27.192). As for vascular invasion, the OS and DFS of patients with vascular wall invasion less than 1/4 circumference diameter (Chaoyang type I) (P = 0.007) were significantly longer than those with invasion range greater than 1/4 circumference diameter (Chaoyang type II-IV) (P = 0.012) (**Table 2**).

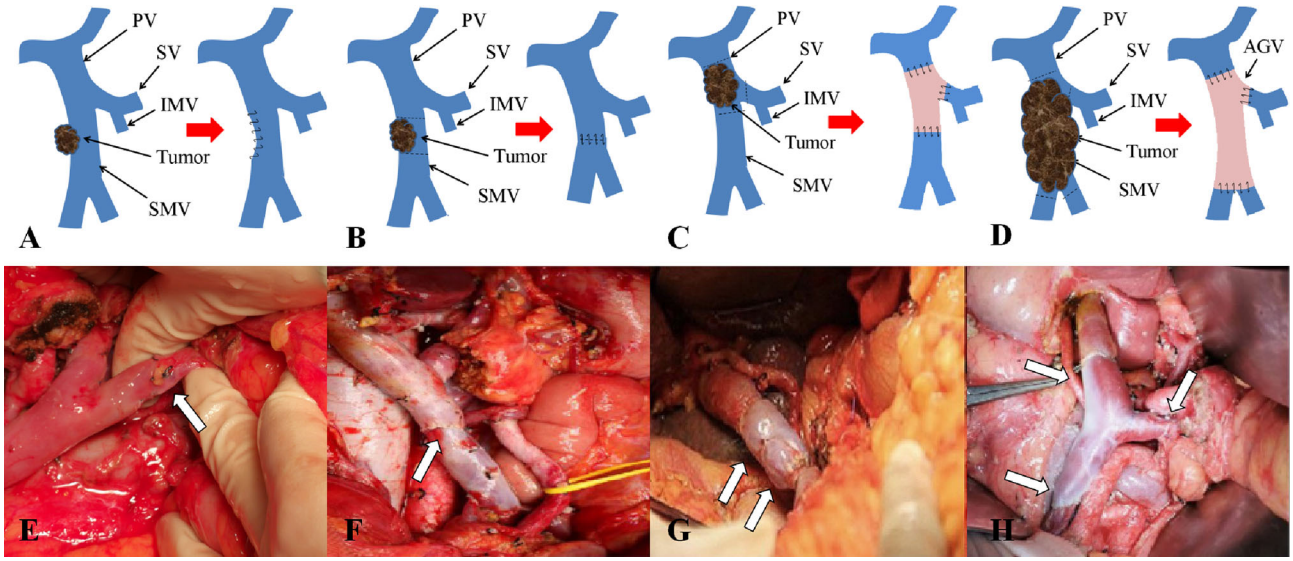

FIGURE 3 | Chaoyang classification and management of venous invasion of borderline resectable pancreatic cancer. **(A, E)** Tumor invades superior mesenteric vein with wedge anastomosis; **(B, F)** Tumor invades superior mesenteric vein with end-to-end anastomosis; **(C, G)** Tumor invades portal vein with segmental vascular replacement; **(D, H)** Tumor invades the confluence of portal vein with branch vascular replacement.

Preoperative NLR or Clinic-Pathologic Factors Associated With Postoperative DFS and OS

Kaplan-Meier survival analysis suggested that the OS (**Figure 4A**) and DFS (**Figure 4B**) of patients with NLR greater than 2.9 were shorter (all $P < 0.001$). Univariate analysis revealed that, clinical parameters of age, preoperative biliary drainage (PBD), CA19-9, TNM stage, tumor size, tumor differentiation, vascular anastomosis method, mode of operation, positive rate of incisal margin, lymph node metastasis, vascular invasion were all obvious associated both with DFS and OS (**Table 2**), however, gender, preoperative TB, DB, ALT, γGGT, ALP, Glu, amylase, history of smoking, history of diabetes and tumor location were not significantly correlated with OS and DFS ($P > 0.05$). Patients mean OS with NLR ≤ 2.90 and NLR > 2.9 was 36.574 (95% CI, 30.763-42.385) and 16.030 (95% CI, 12.149-19.912) months respectively ($P < 0.001$). Patients mean DFS with NLR ≤ 2.90 and NLR > 2.9 was 34.196 (95% CI, 27.989-40.402) and 14.116 (95% CI, 10.191-18.042) months respectively ($P < 0.001$). Moreover, the Age > 55, PBD, CA-199 > 37,TNM > II b, tumor size > 4cm, poorly differentiation, lymph node metastasis, incisal margin R1, vascular invasion were all associated with shorter OS and DFS (**Table 2**). Compared with palliative treatment, vascular resection/replacement could significantly improve the OS of patients, and there was significant difference among groups ($P = 0.042$), however, there was no significant difference in DFS among groups, which may be related to the short follow-up time.

As reported in previous literature, the cutoff value of NLR was selected as 3.0-5.0 (17, 18, 24–29) in different publications, so we also evaluated the patients with PDAC in this study using these cutoff values. Kaplan-Meier survival analysis showed that NLR > 3.0 (**Figures 4C, D**), 4.0 (**Figures 4E, F**) and 5.0 (**Figures 4G, H**) were associated with a relative shorter DFS and OS, but there are 86 (35.68%) cases with NLR > 4.0 (**Figures 4E, F**) and 77 (31.95%) cases with NLR > 5.0 (**Figures 4G, H**) in 241 patients with PDAC.

Comparison of Pathology Differentiation in NLR Group Between Postoperative DFS and OS

On the basis of the above results, we performed survival analysis on the patients in different groups of NLR with different pathological differentiation. Kaplan-Meier survival analysis suggested that PDAC patients of low, moderate-low, moderate, moderate-high and high differentiation, with an elevated NLR > 2.9 displayed a shorter OS (χ^2 = 8.718,15.291, 23.530, 61.760; P = 0.003, 0.000, 0.000, 0.000) and DFS (χ^2 = 8.992, 14.012, 20.640, 16.389; P = 0.003, 0.000, 0.000, 0.000) when compared with NLR ≤ 2.90. Meanwhile, we performed the survival analysis in grouped of NLR cutoff was 3,4,5 which all shown the lower survival benefits both in OS and DFS ($P < 0.001$).

Independent Predictors of DFS and OS in the Step Forward Multivariate Cox Proportional Hazards Model

In the presented study, the Cox proportional hazards model was used to evaluate the association between clinic and pathologic factors, surgical method and DFS/OS after surgical resection (**Table 3**). In addition to the correlation between vascular anastomosis method and OS, there remains six associated

TABLE 2 | Univariate Analysis of risk factors for tumor recurrence and long-term survival in patients with PDAC.

Index	Variables (Number)	OS (Moths)			Index	Variables (Number)	DFS (Moths)		
		Mean	95%CI	*P value (U)*			Mean	95%CI	*P value (U)*
NLR	>2.9 (118)	16.030	12.149-19.912	0.000	NLR	>2.9 (118)	14.116	10.191-18.042	0.000
	≤2.9 (123)	36.574	30.763-42.385	67.869		≤2.9 (123)	34.196	27.989-40.402	61.696
Age	>55 (185)	24.247	20.038-28.456	0.032	Age	>55 (185)	21.087	17.058-26.105	0.039
	≤55 (56)	33.689	24.385-42.992	4.662		≤55 (56)	32.156	22.300-42.013	4.257
PBD	Yes(23)	15.957	9.268-22.627	0.044	PBD	Yes(23)	13.304	6.566-20.053	0.041
	No (218)	27.088	22.919-31.258	4.064		No (218)	25.104	20.622-29.547	4.179
CA-199	>37 (137)	21.735	17.426-26.044	0.038	CA-199	>37 (137)	19.041	14.585-23.497	0.031
	≤37 (104)	32.587	25.769-39.404	4.291		≤37 (104)	31.050	23.895-38.205	4.639
TNM	>II b (91)	14.368	11.332-17.405	0.000	TNM	>II b (91)	12.248	9.007-15.488	0.000
	≤II b (150)	32.431	27.075-37.787	26.988		≤II b (150)	30.427	24.740-36.113	24.185
Tumor Size	>4 (72)	19.284	13.882-24.687	0.002	Tumor Size	>4 (72)	17.648	12.080-23.216	0.003
	≤4 (169)	28.526	23.927-33.126	9.627		≤4 (169)	26.286	21.418-31.153	8.600
Tumor differentiation	I (31)	15.782	9.902-21.663	0.012	Tumor differentiation	I (31)	13.660	7.416-119.905	0.015
	II (56)	21.715	14.656-28.775			II (56)	20.455	13.172-27.738	
	III (126)	28.928	23.525-34.342	10.883		III (126)	26.658	20.918-32.397	10.552
	VI (28)	25.982	16.998-34.966			VI (28)	23.969	14.171-33.767	
Vascular anastomosis	I (11)	9.909	4.403-15.415	0.042	Vascular anastomosis	I (11)	7.727	2.206-13.249	0.056
	II (146)	26.997	21.998-31.996			II (146)	24.984	19.658-30.310	
	III (26)	30.154	17.696-42.616	8.224		III (26)	27.192	14.788-39.596	7.549
	IV(58)	22.212	16.444-27.979			IV(58)	19.932	13.734-26.131	
Operation Methods	I (11)	9.909	4.403-15.415	0.001	Operation Methods	I (11)	7.727	2.206-13.249	0.004
	II (160)	28.484	23.566-33.402			II (160)	26.461	21.241-31.681	
	III (21)	11.333	8.608-14.059	17.073		III (21)	9.122	6.601-11.643	13.563
	IV (49)	26.952	18.133-35.772			IV (49)	25.142	15.821-34.463	
Incisal Margin	R0 (227)	27.153	23.111-31.195	0.000	Incisal Margin	R0 (227)	25.155	20.853-29.457	0.000
	R1(14)	8.929	4.460-13.397	14.909		R1(14)	6.857	2.395-11.319	12.684
Lymphatic metastasis	Negative (83)	37.618	29.653-45.582	0.000	Lymphatic metastasis	Negative (83)	36.558	28.178-44.937	0.000
	Positive (158)	19.878	16.454-23.301	14.786		Positive (158)	16.993	13.540-20.446	15.328
Vascular invasion	I (11)	9.909	4.403-15.415	0.007	Vascular invasion	I (11)	7.727	2.206-13.249	0.012
	II (146)	28.543	23.386-33.700	9.966		II (146)	26.260	20.744-31.745	8.852
	III (84)	21.510	16.696-26.325			III (84)	19.644	14.494-24.794	

NLR, Neutrophil To Lymphocyte Ratio; PBD, preoperative biliary drainage; Tumor differentiation I: poorly, II: poorly-moderately, III: moderately, VI: moderately-highly; Vascular anastomosis I: palliative operation, II: partially excised and sutured directly, III end-to-end anastomosis, VI allogeneic vascular replacement; Operation Methods I: palliative operation, II: radical pancreaticoduodenectomy, III: total pancreatectomy, VI: distal pancreatectomy; Vascular invasion I: palliative operation, II: Chaoyang type I, III: Beyond Chaoyang type I.

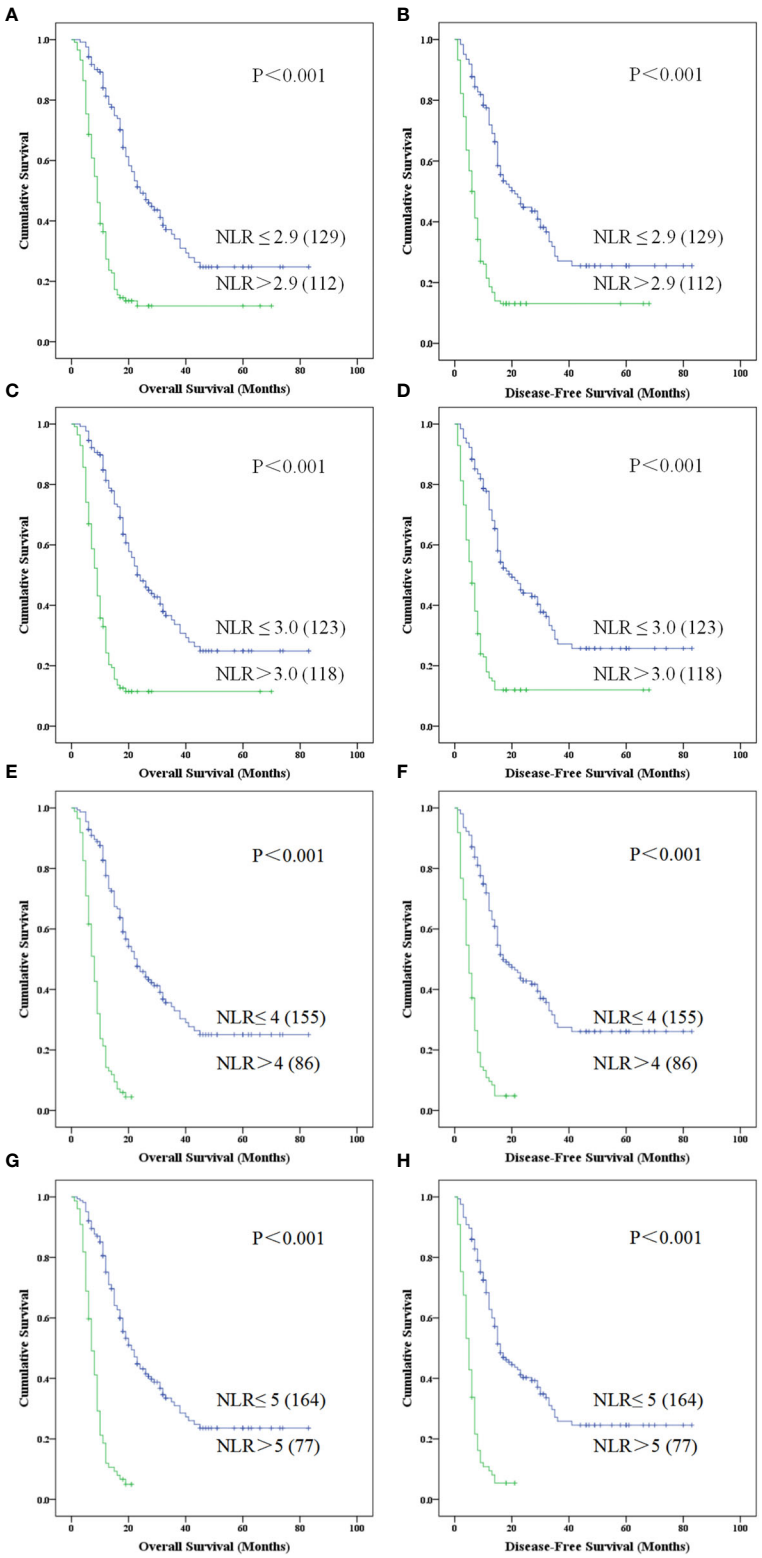

FIGURE 4 | Kaplan-Meier curve for overall survival and disease free survival of patients with advanced PDCA by high NLR *vs*. low NLR for different NLR divided standards. **(A–H)** represented patients with higher NLR is associated with poorer survival which was obviously in NLR > 5 (P < 0.001) (NLR, neutrophil-to-lymphocyte ratio; PDAC, pancreatic ductal adenocarcinoma).

factors which including high NLR, resection margin R1, lymphatic metastasis, age > 55years, TNM stage of III-IV and tumor size > 4cm, were analyzed for OS and DFS by applying the step forward (condition LR) multivariate Cox proportional hazards model. The hazard ratio (HR), 95%CI, and P values concluded by Cox proportional hazards as listed in **Table 3**, high NLR, resection margin R1 and lymphatic metastasis were the most obviously independent risk predictor for OS and DFS with the HR > 2, meanwhile, beyond 55 years old, at TNM stage of III-IV or Tumor size > 4cm which were also the obvious independent risk predictor for OS and DFS with the HR ≤ 2 (**Table 3**).

Grouped Kaplan-Meier Analysis of DFS and OS by Risk Scores of PDAC Patients Based on Multivariate Cox Proportional Hazards Model

Based on the above multivariate factor analysis results, we propose to establish a complex prognostic score calculating model by assigning value of multi-independent predictors (NLR, incisal margin, lymphatic metastasis, age, TNM stage, and tumor size). Each risk factor was allotted a score of 1 which all patients were grouped from risk scores (RS) 0 to 6 (RS = 0 reference without no any above factors as the control, and RS=6 reference with all of the above factors). Kaplan-Meier analysis of OS and DFS of the seven groups all indicated a significant survival difference (OS, χ^2 = 149.247, P = 0.000; DFS, χ^2 = 145.985, P = 0.000). There were only 5 cases in RS=0 group, and there was no difference in survival time between RS = 1 group and RS=0 group. In addition, the survival time of RS = 4, 5, 6 group were relatively short which were no more than two years (**Figures 5A, B**). Therefore, it was re-grouped into four groups: RS ≤ 1 (n = 46), = 2 (n = 74), = 3 (n = 55) and > 3 (n = 66). Survival analysis indicated that the survival time of RS ≤ 1, = 2 were more than 5 years, nevertheless, with the increase of RS factors, the survival time was gradually shortened (RS = 3). Once the RS > 3, patients with PDAC accounted for 27.38% of the total cases, meanwhile the survival time shortened rapidly, suggesting that the worse the prognosis (**Figures 5C, D**).

TABLE 3 | Cox multivariate proportional hazards of independent predictors on DFS and OS.

Variable	HR	95% CI	*P* Value
OS			
NLR (≤2.9 *vs.*>2.9)	3.138	2.234-4.410	0.000
Incisal margin (R0 *vs.*R1)	2.417	1.314-4.444	0.005
Lymphatic metastasis (yes *vs.*no)	2.019	1.427-2.858	0.000
Age,years (≤55 *vs.*>55)	1.611	1.089-2.385	0.017
TNM stage (I-II *vs.*III-IV)	1.506	1.087-2.087	0.014
Tumor size,cm (≤4 *vs.*>4)	1.441	1.025-2.026	0.035
DFS			
NLR (≤2.9 *vs.*>2.9)	2.970	2.121-4.158	0.000
Incisal margin (R0 *vs.*R1)	2.232	1.216-4.095	0.010
Lymphatic metastasis (yes *vs.*no)	2.072	1.463-2933	0.000
Age,years (≤55 *vs.*>55)	1.598	1.080-2.363	0.019
TNM stage (I-II *vs.*III-IV)	1.443	1.045-1.994	0.026
Tumor size,cm (≤4 *vs.*>4)	1.438	1.024-2.019	0.036

NLR, Neutrophil To Lymphocyte Ratio.

Moreover, we further combined RS=2 and 3 according to the results in Figures A, B above and regrouped patients with PDAC into four categories by their risk scores with RS=0, RS=1, 1 < RS ≤ 3, 3 < RS ≤ 6 which referred risk factors ranged from nonexistent to multiple effects on survival. Kaplan-Meier analysis also shown an obvious difference between different groups for OS and DFS (OS, χ2 = 74.051,P=0.000; DFS, χ2 = 68.721, P=0.000), but no difference between RS=1 and RS=0 both for OS and DFS (**Figures 5A, B**; P = 0.757 and P =0.771, respectively). Therefore, we combined these two groups as a new RS ≤ 1 group, redo survival analysis between the RS ≤ 1, 1 < RS ≤ 3, 3 < RS ≤ 6 respectively. That demonstrated that a distinguishable difference of OS (**Figure 5C**; RS ≤ 1 *vs.* 1 < RS ≤ 3, P = 0.002 and 1 < RS ≤ 3 *vs.* 3 < RS ≤ 6, P = 0.000) and DFS (**Figure 5D**; RS ≤ 1 *vs.* 1 < RS ≤ 3, P = 0.004 and 1 < RS ≤ 3 *vs.* 3 < RS ≤ 6, P = 0.000).

Surprisingly, the proportion of patients with PDAC with 3 < RS ≤ 6 was very high, occupying 27.38% (66/241) of total patients (**Figure 5**). The DFS and OS in the 66 patients with a score of 3 < RS ≤ 6 decreased sharply, and all these patients showed much shorter DFS and OS.

DISCUSSION

Pancreatic ductal adenocarcinoma (PDAC) accounts for more than 90% in pancreatic cancer, which is one of the most aggressive and lethal malignancies (1, 4, 5). Difficulties in early detection and diagnosis as well as R0 radical resection of PDAC contribute to the poor prognosis and high relapse to a great extent especially for advanced PDAC (3). Except CA19-9 as a marker for the diagnosis of pancreatic cancer, current studies on NLR in early pancreatic prognosis and diagnosis are deepening. Most studies believe that NLR can predict the prognosis of early pancreatic cancer, but there are few studies on advanced pancreatic cancer (17–20). Therefore, the enrolled PDAC patients of this study all met the criteria for Chaoyang classification of pancreatic cancer established by our center. In this presented study, evaluation of the prognostic predictive value of portal venous system resection and reconstruction in patients accepted radical surgical resection.

As pancreatectomy is considered the main treatment currently, all the enrolled patients were accepted curative excision with vascular resection and/or reconstruction according to the Chaoyang classification. The results showed improved survival benefits postoperative comparison with the palliative care patients with most obvious in those who have undergone pancreaticoduodenectomy. According to the Chaoyang classification and the actual intraoperative situation, the survival time of patients with the portal vein invasion was significantly prolonged after the resection of the vascular and end to end anastomosis. In addition to vascular invasion, lymph node metastasis was reported in 158 patients. All lymph nodes were biopsied intraoperatively until negative, but unfortunately, there were still 3 patients with positive lymph node biopsies.

Previous literature (30) asserted that vascular resection and reconstruction during the radical resection could improve the R0

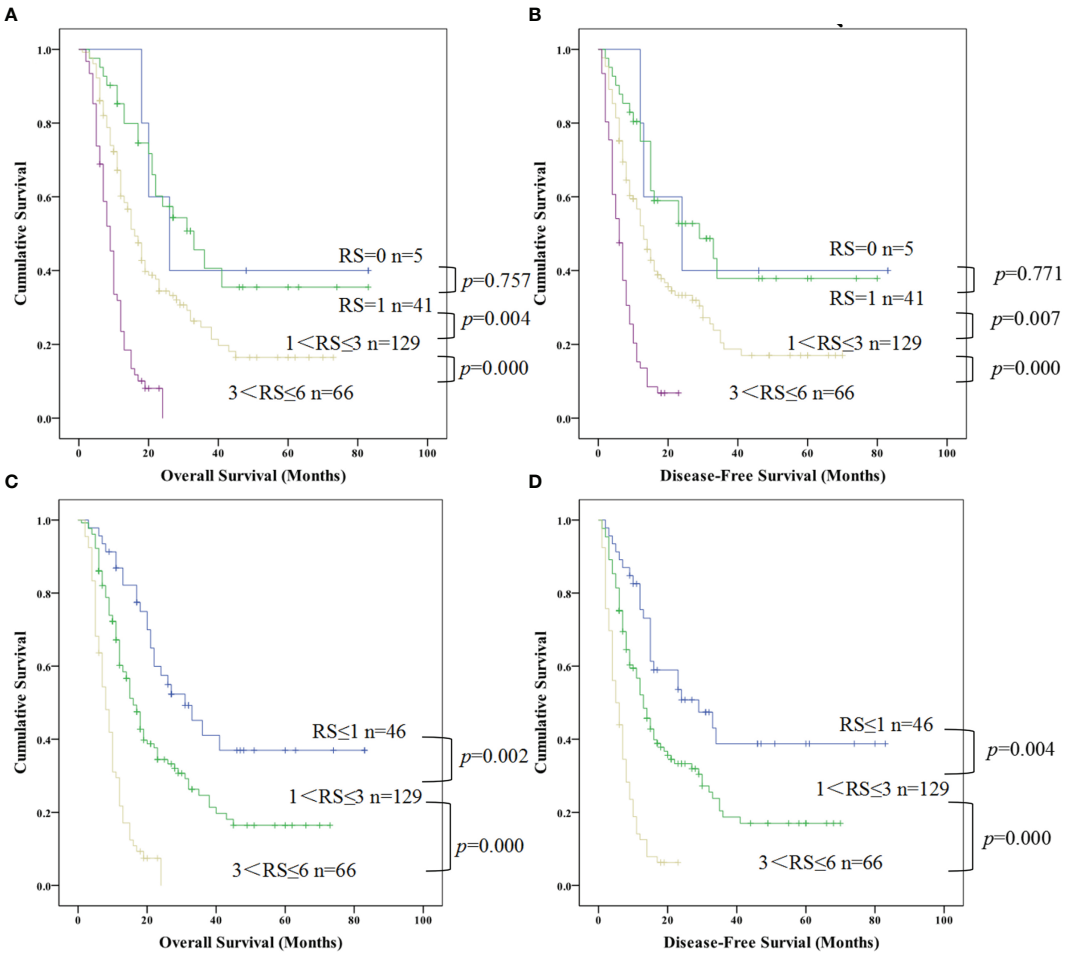

FIGURE 5 | Kaplan-Meier curve for overall survival and disease free survival of patients with advanced PDCA by risk scores (RS) based on multivariate cox proportional hazards model. **(A, B)** represented the survival difference from the low RS to high RS; **(C, D)** represented the survival difference in the re-grouped RS groups which combined RS=0 and RS=1 as a new group (PDAC, pancreatic ductal adenocarcinoma; RS, risk scores).

resection rate and long-term survival. The R0 resection rate and survival time in different centers were various. Among them, the mean R0 resection rate was 71.4%, ranged from 37% in England to 87% in Germany. Meanwhile, the mean median survival time was 15.4 months, ranged from 14 months in America to 17 months in Japan. In this presented study, it displayed a R0 resection rate of 94.17% and a median survival time of 15 months. This results may due to the regulation of vascular resection for different types of invasion and the application of radical vascular replacement technique by Chaoyang classification of pancreatic cancers. We may consider that a radical surgery combined with vascular reconstruction has an obvious improvement in the prognosis and R0 resection rate of patients with advanced pancreatic cancer.

Further, single-factor survival curve analysis suggested that surgical approach, vascular anastomosis, vascular invasion, lymph node metastasis, and R0 resection were all related to survival benefit of OS and DFS. We consider that radical resection and anastomosis, including biopsy of all lymph nodes for advanced PDAC with vascular invasion is clinically beneficial and recommended.

NLR derived from the ratio of neutrophils to lymphocyte which both from white blood cells with important role in inflammatory response and tumor immunity. Neutrophils promote angiogenesis, tumorigenesis, metastasis, and tumor cell proliferation and survival and can also protect tumor cells from immune mediated destruction (31–33) which may through recruit regulatory T-cells into tumors *via* secretion of CCL17 (32). As we known, the immune response of hosts to tumor is lymphocyte-dependent. High elevated NLR patients usually with a relative lymphocytopenia, this may lead to a worse lymphocyte-mediated immune response to tumor, resulting in a shorter survival and the high risk tumor relapse and metastases (34).

Based on the literature regarding NLR, the purpose was aimed to evaluate the potential value of NLR as a prognostic indicator in patients with PDAC undergoing vascular reconstructive, so as to establish a simple computational model to predict tumor prognosis by combining NLR and biomarkers of oncological characteristics.

Studies have suggested that systemic inflammation is an important factor which can affect the progression and long-term survival of cancer patients (35). NLR is a simple parameter easily obtained to reflect a systemic immune inflammatory response elicited by the tumor (36). Despite research on NLR has been reported more with different methods in different populations, there is no general value at present. Forget et al. have identified a normal NLR values of 1.65 range from 0.78 to 3.53 in an adult, non-geriatric, population in good health (37), so the NLR cutoff value of 2.9 identified by ROC curve in our study was considered credible.

Current literature is conflicting regarding the prognostic value of NLR, with some showing a prognostic significance, and others demonstrating no significance on survival (19, 20). From our study, it first found that NLR was clearly related to the pathological differentiation of PDAC, secondly, an elevated NLR and NEUT was significantly showed in low differentiation patients, but no changes of lymphocytes. The results presented here suggest that NLR > 2.9 is highly associated with a worse survival benefits for PDAC. Meanwhile, it also represents a relative specificity value in PDAC diagnosis when carried out diagnosis experiments comparison with CA19-9. Some studies asserted that the diagnostic role of NLR is distinct from that of CA19-9 because of high NLR expression was not associated with CA19-9 levels (24). The correlation concluded in this study was the same as the previous, but due to the existing experimental results, We believe that NLR may also play a credible role in the diagnosis of advanced pancreatic cancer, especially in combination with CA19-9. However, the diagnostic value of high NLR in patients with negative CA19-9 indicators still needs to be verified in a large sample.

These results demonstrated that high NLR has a worse survival for advanced PDAC after curative excision with vascular resection and (or) reconstruction. The NLR > 2.9 was identified as a risk factor for lower survival in patients with PDAC. Patients with high elevated NLR (> 2.9) showed a significantly shorter OS and DFS than those with low NLR (≤ 2.9). With no clearly defined cutpoint of NLR, a cutoff value ranging from 2 to 5 has been widely used to define high/low NLR, of which 5 is the most widely used (16–18, 25–29, 38), therefore, we chose to perform a continuous analysis from NLR value of 3 to 5 for the OS and DFS. There showed a rather lower survival rate and shorter time as the NLR cutoff value increases gradually, with a survival no longer exceed 24 months of patients with NLR=4 or 5. These results were all consistent with the above literature reports (16–18, 25–29, 38), NLR > 3.0, 4.0 and 5.0 were also showed a shorter OS and DFS, but there were 86 (35.68%) cases and 77 (31.95%) cases with NLR > 4.0 and 5.0 in 241 patients with PDAC respectively comparison with 118 (48.96%) cases and 112 (46.47%) cases with NLR > 2.9 and 3.0 in 241 patients with PDAC respectively. That may mean a higher NLR exclude more advanced PADC patients and a cutoff value of 2.9 shows a higher sensitivity in diagnosis. Therefore, we considered that preoperative NLR of 2.9 is worthy as an optimal index with PDAC in this presented study, but also for other prospective clinical trials. However, the diagnostic value of high NLR in patients with negative CA19-9 indicators still needs to be verified in a large sample.

High elevated NLR and poor prognosis regarding PDAC was studied rather clearly, but the trend of NLR changes in different cancers and their effects on tumor immunity need to be elucidated. Furthermore, tumor-infiltrating lymphocytes (and specifically T cells) are responsible for mounting the antitumor response within the microenvironment (39) which reflected a weaker lymphocytic infiltration in tumor may with worse prognosis (34). Notably, PDAC has proven to have a unique and complex immune dysfunction with immunosuppressive cell types, tumor-supportive immune cells and defective inflammatory cells (40). Therefore, the damage mechanism to host immunity of the changes of neutrophil and T cell subsets and that infiltrated in tumor tissue are the next research direction.

In addition to NLR, surgical methods and vascular anastomosis, we also found that age (> 55), PBD, CA19-9 (> 37ng/ml), tumor size (> 4cm), TNM stage (III-IV), tumor differentiation (poorly or poorly-moderate differentiated) were obviously related with shorter OS and DFS by univariate survival analysis. These are all consistent with several previous reports that tumor size, TMN, CA19-9 were significant risk factor of recurrence after radical resection (41–44). There are also studies indicating that CA19-9 is an independent prognostic factor in PDAC (44–46). Although univariate analysis in this study showed that operation methods, vascular anastomosis, vascular invasion, tumor differentiation, CA-199 and preoperative biliary drainage (PBD) were preoperative prognostic predictors of poor DFS and OS, none of these factors were identified as independent predictors by multivariate analysis. This did not indicate that these factors are not associated with recurrence and metastasis and are not potential prognostic factors for advanced PDAC after curative resection.

Taken together, vascular reconstruction in radical resection of advanced PDAC displayed a longer survival benefits, but not an independent risk factor. What's more, this study showed that high NLR (NLR > 2.90) was an independent predictor for DFS and OS of advanced PDAC undergoing vascular reconstruction.

Based on the Cox multivariate analysis, the results demonstrated that NLR, age, TNM stage, tumor size, lymphatic metastasis, and resection margin were independent prognostic factors for OS and DFS of the advanced PDAC. So, we have established a simple computational model of risk score (RS) with the above prognostic multiple-factor. In the RS model. In Cox multivariate analysis, NLR was the major component in predicting the survival and prognosis. According to the six predictors in the RS model, advanced PADC patients marked from 0 to 6 were grouped four RS groups (RS=0, RS=1, 1<RS ≤ 3, 3<RS ≤ 6). No matter which grouping method, the survival difference between groups was significantly with a no more than 24 months of survival time in group 3<RS ≤ 6.

It is worth noting that due to the limitations of the retrospective nature of this study and the small sample size of a single center, further multi-center, larger prospective studies are needed to verify this finding.

CONCLUSION

Vascular reconstructive in radical resection of advanced PDAC improve survival, a higher elevated NLR (>2.90) was a negative predictor of DFS and OS in those patients accompanying portal system invasion. This study suggested that NLR might be a novel prognostic biomarker in advanced PDAC after curative resection.

DATA AVAILABILITY STATEMENT

The original contributions presented in the study are included in the article/supplementary material. Further inquiries can be directed to the corresponding authors.

ETHICS STATEMENT

This study was approved by the Ethical Committee of Beijing Chao-Yang Hospital. All patients provided full written informed consent; written informed consent was obtained in accordance with the Declaration of Helsinki of the World Medical Association (Ethics approval and consent to participate: No.2020-D.-309-2).

AUTHOR CONTRIBUTIONS

(I) Conception and design: LZ, JW. (II) Administrative support: RL, QH. (III) Provision of study materials or patients: LZ, QH. (IV) Collection and assembly of data: JW, X-xZ and S-cL. (V) Data analysis and interpretation: LZ, L-cP and G-sD. All authors contributed to the article and approved the submitted version.

FUNDING

This study was supported by: Beijing Municipal Science & Technology Commission, PR China (Grant No. Z18110 0001718164); Capital's Funds for Health Improvement and Research, Beijing, PR China (CFH 2020-2-2036).

REFERENCES

1. Hidalgo M. Pancreatic Cancer. *N Engl J Med* (2010) 362:1605–17. doi: 10.1056/NEJMra0901557
2. Siegel RL, Miller KD, Jemal A. Cancer Statistics, 2019. *CA Cancer J Clin* (2019) 69(1):7–34. doi: 10.3322/caac.21551
3. Ryan DP, Hong TS, Bardeesy N. Pancreatic Adenocarcinoma. *N Engl J Med* (2014) 371(11):1039–49. doi: 10.1056/NEJMra1404198
4. Neoptolemos JP, Palmer DH, Ghaneh P, Psarelli EE, Valle JW, Halloran CM, et al. Comparison of Adjuvant Gemcitabine and Capecitabine With Gemcitabine Monotherapy in Patients With Resected Pancreatic Cancer (ESPAC-4): A Multicentre, Open-Label, Randomised, Phase 3 Trial. *Lancet* (2017) 389(10073):1011–24. doi: 10.1016/S0140-6736(16)32409-6
5. Richter A, Niedergethmann M, Sturm JW, Lorenz D, Post S, Trede M. Long-Term Results of Partial Pancreaticoduodenectomy for Ductal Adenocarcinoma of the Pancreatic Head: 25-Year Experience. *World J Surg* (2003) 27:324–9. doi: 10.1007/s00268-002-6659-z
6. Foucher ED, Ghigo C, Chouaib S, Galon J, Iovanna J, Olive D. Pancreatic Ductal Adenocarcinoma: A Strong Imbalance of Good and Bad Immunological Cops in the Tumor Microenvironment. *Front Immunol* (2018) 14(9):1044. doi: 10.3389/fimmu.2018.01044
7. Allen PJ, Kuk D, Castillo CF, Basturk O, Wolfgang CL, Cameron JL, et al. Multi-Institutional Validation Study of the American Joint Commission on Cancer (8th Edition) Changes for T and N Staging in Patients With Pancreatic Adenocarcinoma. *Ann Surg* (2017) 265:185–91. doi: 10.1097/SLA.0000000000001763
8. Kleeff J, Korc M, Apte M, La Vecchia C, Johnson CD, Biankin AV, et al. Pancreatic Cancer. *Nat Rev Dis Primers* (2016) 2:16022. doi: 10.1038/nrdp.2016.22
9. Egawa S, Toma H, Ohigashi H, Okusaka T, Nakao A, Hatori T, et al. Japan Pancreatic Cancer Registry; 30th Year Anniversary: Japan Pancreas Society. *Pancreas* (2012) 41(7):985–92. doi: 10.1097/MPA.0b013e318258055c
10. Tseng JF, Tamm EP, Lee JE, Pisters PW, Evans DB. Venous Resection in Pancreatic Cancer Surgery. *Best Pract Res Clin Gastroenterol* (2006) 20 (2):349–64. doi: 10.1016/j.bpg.2005.11.003
11. Masiak-Segit W, Rawicz-Pruszyński K, Skórzewska M, Polkowski WP. Surgical Treatment of Pancreatic Cancer. *Polish J Surg* (2018) 90(2):45–53. doi: 10.5604/01.3001.0011.7493
12. Fuhrman GM, Leach SD, Staley CA, Cusack JC, Charnsangavej C, Cleary KR, et al. Rationale for En Bloc Vein Resection in the Treatment of Pancreatic Adenocarcinoma Adherent to the Superior Mesenteric-Portal Vein Confluence. *Pancreatic Tumor Study Group Ann Surg* (1996) 223(2):154–62. doi: 10.1097/00000658-199602000-00007
13. Ramacciato G, Mercantini P, Petrucciani N, Giaccaglia V, Nigri G, Ravaioli M, et al. Does Portal-Superior Mesenteric Vein Invasion Still Indicate Irresectability for Pancreatic Carcinoma? *Ann Surg Oncol* (2009) 16(4):817–25. doi: 10.1245/s10434-008-0281-8
14. Zhou Y, Zhang Z, Liu Y, Li B, Xu D. Pancreatectomy Combined With Superior Mesenteric Vein-Portal Vein Resection for Pancreatic Cancer: A Meta-Analysis. *World J Surg* (2012) 36(4):884–91. doi: 10.1007/s00268-012-1461-z
15. Roch AM, House MG, Cioffi J, Ceppa EP, Zyromski NJ, Nakeeb A, et al. Significance of Portal Vein Invasion and Extent of Invasion in Patients Undergoing Pancreatoduodenectomy for Pancreatic Adenocarcinoma. *J Gastrointest Surg* (2016) 20(3):479–87. doi: 10.1007/s11605-015-3005-y
16. Winter JM, Yeo CJ. And Brody JR: Diagnostic, Prognostic, and Predictive Biomarkers in Pancreatic Cancer. *J Surg Oncol* (2013) 107:15–22. doi: 10.1002/jso.23192
17. Hong X, Cui B, Wang M, Yang Z, Wang L, Xu Q. Systemic Immuneinflammation Index, Based on Platelet Counts and Neutrophil-Lymphocyte Ratio, Is Useful for Predicting Prognosis in Small Cell Lung Cancer. *Tohoku J Exp Med* (2015) 236(4):297–304. doi: 10.1620/tjem.236.297
18. Templeton AJ, McNamara MG, Seruga B, Vera-Badillo FE, Aneja P, Ocaña A, et al. Prognostic Role of Neutrophilto-Lymphocyte Ratio in Solid Tumors: A Systematic Review and Meta-Analysis. *J Natl Cancer Inst* (2014) 106(6): dju124. doi: 10.1093/jnci/dju124
19. Pointer DT Jr, Roife D, Powers BD, Murimwa G, Elessawy S, Thompson ZJ, et al. Neutrophil to Lymphocyte Ratio, Not Platelet to Lymphocyte or Lymphocyte to Monocyte Ratio, Is Predictive of Patient Survival After Resection of Early-Stage Pancreatic Ductal Adenocarcinoma. *BMC Cancer* (2020) 20(1):750. doi: 10.1186/s12885-020-07182-9
20. Pu N, Yin H, Zhao G, Nuerxiati A, Wang D, Xu X, et al. Independent Effect of Postoperative Neutrophil-to-Lymphocyte Ratio on the Survival of Pancreatic Ductal Adenocarcinoma With Open Distal Pancreatosplenectomy and Its Nomogram-Based Predictio. *J Cancer* (2019) 10(24):5935–43. doi: 10.7150/jca.35856
21. Kahl S, Glasbrenner B, Zimmermann S, Malfertheiner P. Endoscopic Ultrasound in Pancreatic Diseases. *Dig Dis* (2002) 20(2):120–6. doi: 10.1159/000067481
22. Illuminati G, Carboni F, Lorusso R, D'Urso A, Ceccanei G, Papaspyropoulos V, et al. Results of a Pancreatectomy With a Limited Venous Resection for

Pancreatic Cancer. *Surg Today* (2008) 38(6):517–23. doi: 10.1007/s00595-007-3661-y
23. Zhu J, Li X, Kou J, Ma J, Li L, Fan H, et al. Proposed Chaoyang Vascular Classification for Superior Mesenteric-Portal Vein Invasion, Resection, and Reconstruction in Patients With Pancreatic Head Cancer During Pancreaticoduodenectomy - A Retrospective Cohort Study. *Int J Surg* (2018) 53:292–7. doi: 10.1016/j.ijsu.2018.04.011
24. Wang DS, Luo HY, Qiu MZ, Wang ZQ, Zhang DS, Wang FH, et al. Comparison of the Prognostic Values of Various Inflammation Based Factors in Patients With Pancreatic Cancer. *Med Oncol* (2012) 29(5):3092–100. doi: 10.1007/s12032-012-0226-8
25. Sierzega M, Lenart M, Rutkowska M, Surman M, Mytar B, Matyja A, et al. Preoperative Neutrophillymphocyte and Lymphocyte-Monocyte Ratios Reflect Immune Cell Population Rearrangement in Resectable Pancreatic Cancer. *Ann Surg Oncol* (2017) 24(3):808–15. doi: 10.1245/s10434-016-5634-0
26. Zhou Y, Wei Q, Fan J, Cheng S, Ding W, Hua Z. Prognostic Role of the Neutrophil-to-Lymphocyte Ratio in Pancreatic Cancer: A Meta-Analysis Containing 8252 Patients. *Clin Chim Acta* (2018) 479:181–9. doi: 10.1016/j.cca.2018.01.024
27. Sanjay P, de Figueiredo RS, Leaver H, Ogston S, Kulli C, Polignano FM, et al. Preoperative Serum C-Reactive Protein Levels and Post-Operative Lymph Node Ratio Are Important Predictors of Survival After Pancreaticoduodenectomy for Pancreatic Ductal Adenocarcinoma. *JOP* (2012) 13(2):199–204.
28. Garcea G, Ladwa N, Neal CP, Metcalfe MS, Dennison AR, Berry DP. Preoperative Neutrophil-to-Lymphocyte Ratio (NLR) Is Associated With Reduced Disease-Free Survival Following Curative Resection of Pancreatic Adenocarcinoma. *World J Surg* (2011) 35(4):868–72. doi: 10.1007/s00268-011-0984-z
29. Stotz M, Gerger A, Eisner F, Szkandera J, Loibner H, Ress AL, et al. Increased Neutrophil-Lymphocyte Ratio Is a Poor Prognostic Factor in Patients With Primary Operable and Inoperable Pancreatic Cancer. *Br J Cancer* (2013) 109 (2):416–21. doi: 10.1038/bjc.2013.332
30. Younan G, Tsai S, Evans DB, Christians KK. Techniques of Vascular Resection and Reconstruction in Pancreatic Cancer. *Surg Clin North Am* (2016) 96(6):1351–70. doi: 10.1016/j.suc.2016.07.005
31. Kim J, Bae JS. Tumor-Associated Macrophages and Neutrophils in Tumor Microenvironment. *Mediators Inflammation* (2016) 2016:6058147. doi: 10.1155/2016/6058147
32. Mishalian I, Bayuh R, Eruslanov E, Michaeli J, Levy L, Zolotarov L, et al. Neutrophils Recruit Regulatory T-Cells Into Tumors *via* Secretion of CCL17-A New Mechanism of Impaired Antitumor Immunity. *Int J Cancer* (2014) 135 (5):1178–86. doi: 10.1002/ijc.28770
33. Ding PR, An X, Zhang RX, Fang YJ, Li LR, Chen G, et al. Elevated Preoperative Neutrophil to Lymphocyte Ratio Predicts Risk of Recurrence Following Curative Resection for Stage IIA Colon Cancer. *Int J Colorectal Dis* (2010) 25:1427–33. doi: 10.1007/s00384-010-1052-0
34. Chew V, Tow C, Teo M, Wong HL, Chan J, Gehring A, et al. Inflammatory Tumour Microenvironment Is Associated With Superior Survival in Hepatocellular Carcinoma Patients. *J Hepatol* (2010) l52:370–9. doi: 10.1016/j.jhep.2009.07.013
35. Roxburgh CS, Salmond JM, Horgan PG, Oien KA, McMillan DC. The Relationship Between the Local and Systemic Inflammatory Responses and Survival in Patients Undergoing Curative Surgery for Colon and Rectal Cancers. *J Gastrointest Surg* (2009) 13:2011–8. doi: 10.1007/s11605-009-1034-0
36. Lee JM, Lee HS, Hyun JJ, Choi HS, Kim ES, Keum B, et al. Prognostic Value of Inflammation-Based Markers in Patients With Pancreatic Cancer Administered Gemcitabine and Erlotinib. *World J Gastrointest Oncol* (2016) 8:555–62. doi: 10.4251/wjgo.v8.i7.555
37. Forget P, Khalifa C, Defour J-P, Latinne D, MC VP, De Kock M. What Is the Normal Value of the Neutrophil-to-Lymphocyte Ratio? *BMC Res Notes* (2017) 10(1):12. doi: 10.1186/s13104-016-2335-5
38. Hamed MO, Roberts KJ, Smith AM, Morris Stiff G. Elevated Pre-Operative Neutrophil to Lymphocyte Ratio Predicts Disease Free Survival Following Pancreatic Resection for Periampullary Carcinomas. *Pancreatology* (2013) 13 (5):534–8. doi: 10.1016/j.pan.2013.07.283
39. Man YG, Stojadinovic A, Mason J, Avital I, Bilchik A, Bruecher B, et al. Tumor-Infiltrating Immune Cells Promoting Tumor Invasion and Metastasis: Existing Theories. *J Cancer* (2013) 4:84–95. doi: 10.7150/jca.5482
40. Inman KS, Francis AA, Murray NR. Complex Role for the Immune System in Initiation and Progression of Pancreatic Cancer. *World J Gastroenterol* (2014) 20:11160–81. doi: 10.3748/wjg.v20.i32.11160
41. Abe T, Amano H, Kobayashi T, Hanada K, Nakahara M, Ohdan H, et al. Preoperative Neutrophil-to-Lymphocyte Ratio as a Prognosticator in Early Stage Pancreatic Ductal Adenocarcinoma. *Eur J Surg Oncol* (2018) 44 (10):1573–9. doi: 10.1016/j.ejso.2018.04.022
42. Chawla A, Huang TL, Ibrahim AM, JM H, Siegel C, Ammori JB. Pretherapy Neutrophil to Lymphocyte Ratio and Platelet to Lymphocyte Ratio do Not Predict Survival in Resectable Pancreatic Cancer. *HPB (Oxford)* (2018) 20 (5):398–404. doi: 10.1016/j.hpb.2017.10.011
43. Recio-Boiles A, Nallagangula A, Veeravelli S, Vondrak J, Saboda K, Roe D, et al. Neutrophil-To-Lymphocyte and Platelet-to-Lymphocyte Ratios Inversely Correlate to Clinical and Pathologic Stage in Patients With Resectable Pancreatic Ductal Adenocarcinoma. *Ann Pancreat Cancer* (2019) 2:8. doi: 10.21037/apc.2019.06.01
44. Zhang L-X, Chen L, Xu A-M. A Simple Model Established by Blood Markers Predicting Overall Survival After Radical Resection of Pancreatic Ductal Adenocarcinoma. *Front Oncol* (2020) 10:583. doi: 10.3389/fonc.2020.00583
45. Arima K, Okabe H, Hashimoto D, Chikamoto A, Tsuji A, Yamamura K, et al. The Diagnostic Role of the Neutrophil-to-Lymphocyte Ratio in Predicting Pancreatic Ductal Adenocarcinoma in Patients With Pancreatic Diseases. *Int J Clin Oncol* (2016) 21(5):940–5. doi: 10.1007/s10147-016-0975-z
46. Tao L, Zhang L, Peng Y, Tao M, Li G, Xiu D, et al. Preoperative Neutrophil-to-Lymphocyte Ratio and Tumor-Related Factors to Predict Lymph Node Metastasis in Patients With Pancreatic Ductal Adenocarcinoma (PDAC). *Oncotarget* (2016) 7(45):74314–24. doi: 10.18632/oncotarget.11031

Conflict of Interest: The authors declare that the research was conducted in the absence of any commercial or financial relationships that could be construed as a potential conflict of interest.

frontiers in Oncology

ORIGINAL RESEARCH
published: 13 October 2021
doi: 10.3389/fonc.2021.693386

AGIG Chemo-Immunotherapy in Patients With Advanced Pancreatic Cancer: A Single-Arm, Single-Center, Phase 2 Study

Wangshu Dai[1,2†], Xin Qiu[3†], Changchang Lu[3†], Zhengyun Zou[1], Huizi Sha[1], Weiwei Kong[1], Baorui Liu[1] and Juan Du[1,3*]*

[1] The Comprehensive Cancer Center of Drum Tower Hospital, Medical School of Nanjing University & Clinical Cancer Institute of Nanjing University, Nanjing, China, [2] The Cadre Health Care Ward, Nanjing Drum Tower Hospital, The Affiliated Hospital of Nanjing University Medical School, Nanjing, China, [3] The Comprehensive Cancer Center of Drum Tower Hospital, Clinical College of Traditional Chinese and Western Medicine, Nanjing University of Chinese Medicine, Nanjing, China

OPEN ACCESS

Edited by:
Kuirong Jiang,
Nanjing Medical University, China

Reviewed by:
Xi Yang,
Fudan University, China
Pierpaolo Correale,
Azienda ospedaliera 'Bianchi-Melacrino-Morelli', Italy

***Correspondence:**
Juan Du
dujuanglyy@163.com
Baorui Liu
baoruiliu@nju.edu.cn

[†]These authors have contributed equally to this work

Specialty section:
This article was submitted to Gastrointestinal Cancers, a section of the journal Frontiers in Oncology

Received: *10 April 2021*
Accepted: *23 September 2021*
Published: *13 October 2021*

Citation:
Dai W, Qiu X, Lu C, Zou Z, Sha H, Kong W, Liu B and Du J (2021) AGIG Chemo-Immunotherapy in Patients With Advanced Pancreatic Cancer: A Single-Arm, Single-Center, Phase 2 Study. Front. Oncol. 11:693386. doi: 10.3389/fonc.2021.693386

Background: To date, chemotherapy remains the only effective treatment of unresectable pancreatic adenocarcinoma. In the past few years, the interest in immunological anticancer therapy rises sharply. AGIG is a novel chemo-immunotherapy regimen that combines nab-paclitaxel + gemcitabine chemotherapy with sequential recombinant interleukin-2 (IL-2) and granulocyte-macrophage colony stimulating factor (GM-CSF) therapy. We conducted a single-arm prospective phase II study to determine the efficacy and safety of the first-line treatment of advanced pancreatic cancer with AGIG regimen.

Methods: Nab-paclitaxel (125 mg/m^2) and gemcitabine (1000 mg/m^2) were administered intravenously to all patients on days 1 and 8 triweekly, interleukin-2 (1000000U) and GM-CSF (100 μg) were administered subcutaneously on days 3-5 after chemotherapy. The primary end point was ORR by the Response Evaluation Criteria in Solid Tumors, version 1.1. Secondary end points included safety profile, progression-free survival (PFS), overall survival (OS). Patients' conditions along with the efficacy and safety were assessed every two cycles.

Results: Between 11/2018 and 01/2020, sixty-four patients were enrolled. In the sixty-four evaluable patients, the disease control rate (DCR) and overall response rate (ORR) were 76.6% and 43.75%, respectively. The median follow-up time was 12.1 (range 7.1–22.4) months. The median PFS was 5.7 (range 1.63–15.8) months. The median OS was 14.2 (range 2.9–22.0) months. The most common adverse event was fever (75%). The incidence of III/IV grade neutropenia was 4.69%. In subgroup analyses, we found that

eosinophil count in the blood elevated three times higher than baseline level predicted a longer survival.

Conclusions: The AGIG chemo-immunotherapy regimen has presented favorable ORR, OS, and manageable toxicities as first-line therapeutic strategy of advanced pancreatic cancer treatment. This regimen may be a novel reliable therapeutic option for patients with preserved performance status. The improvement of treatment efficiency may be related to the activation of non-specific immune response.

Clinical Trial Registration: https://clinicaltrials.gov/. identifier NCT03768687.

Keywords: objective response rate, overall survival, advanced pancreatic adenocarcinoma, chemo-immunotherapy, nab-paclitaxel, gemcitabine

INTRODUCTION

Pancreatic cancer is one of the deadliest solid malignancies in the world. Despite decades of efforts, it remains the fourth leading cause of cancer-related death worldwide, with a five-year survival rate of less than 5% (1). Without treatment, the median survival time is consistently shorter than six months (2). Since 1997, gemcitabine had been the standard treatment for unresectable pancreatic adenocarcinoma (3). After decades of exploration, both FOLFIRINOX (fluorouracil, irinotecan, and oxaliplatin) and nab-paclitaxel with gemcitabine (AG) prolong overall survival (OS) compared with gemcitabine alone (4, 5). Till now, chemotherapy remains the only effective treatment of unresectable pancreatic adenocarcinoma (6).

As mentioned above, FOLFIRINOX is one of the standard treatment strategies for patients with advanced pancreatic cancer and has demonstrated good effectiveness in Europe and North America (7, 8). However, grade III/IV adverse events were commonly observed in the FOLFIRINOX treatment courses. To our knowledge, cancer drug tolerability is different between Asian and white populations. These differences may be related to genetic or environmental factor. Increased chemotherapy-induced myelosuppression was one of the most commonly observed adverse events in Asian patients (9, 10). Chinese patients were unendurable to FOLFIRINOX chemotherapy sometimes. The combination of nab-paclitaxel and gemcitabine is recommended as the first-line treatment regimen for patients with advanced pancreatic cancer by the National Comprehensive Cancer Network (NCCN) guidelines. A phase I/II study evaluated the AG chemotherapy regimen in Chinese patients with advanced pancreatic cancer (11). The study was carried out at a dose and schedule different from the classic MPACT study. The recommended administration schedule was described as follows, nab-paclitaxel (125 mg/m^2) along with gemcitabine (1000 mg/m^2) was administered on the first day and the eighth day, the treatment was repeated every three weeks (12). Although the trail did not meet its primary endpoint of identifying the maximum tolerated dose in Chinese pancreatic cancer sufferers, the study showed a manageable safety profile with a favorable antitumor effect in pancreatic cancer sufferers.

With the clinical development and application of PD-1/PD-L1 immune-checkpoint blockade, the interest in the exploration of immunological anticancer strategies rises sharply in these years. Immune-based regimens are showing promise where other approaches have failed when treating pancreatic cancer (13, 14). Immune checkpoint inhibitors along with therapeutic vaccines and combination immunotherapies are commonly used as immunotherapeutic strategies. Even though the antitumor effect and mechanism of the above-mentioned immunotherapeutic strategies remain unclear, these researches produced abundant data concerning the mechanisms of the efficient tumor-specific adaptive immune response triggered by immune-modulating agents (15).

It was reported that chemo-immunotherapy might represent as an innovative reliable therapy option for first-line treatment of metastatic colorectal cancer sufferers (16, 17). Interleukin-2 (IL-2) was used to promote the proliferation of cross-primed cytotoxic T lymphocyte clones, while granulocyte-macrophage colony stimulating factor (GM-CSF) was required to activate the antigen-presenting ability of the dendritic cells expressed in human peripheral blood mononuclear cells. GM-CSF is essential for the differentiation of dendritic cells, which are responsible for processing and presenting tumor antigens for the priming of antitumor cytotoxic T lymphocytes (18, 19). Some GM-CSF-based cancer immunotherapy strategies have been developed for in clinical practice (20). It was reported that IL-2 and GM-CSF were demonstrated as innovative and reliable adjuvants of chemotherapy for metastatic colorectal cancer (21, 22). These results offered the rationale to design a novel treatment chemo-immunotherapy regimen that combines traditional chemotherapy with IL-2 and GM-CSF.

AGIG is a novel chemo-immunotherapy regimen that combines AG chemotherapy with sequential recombinant IL-2 and GM-CSF therapy (nab-paclitaxel, gemcitabine, IL-2 and GM-CSF). In this study, we implemented a single-arm, single-center prospective phase II study to determine the efficacy and safety of the AGIG regimen as the first-line treatment of advanced pancreatic cancer in China.

MATERIALS AND METHOD

Patients

This was a prospective study involving pancreatic sufferers receiving AGIG Chemo-immunotherapy regimen from

November 2018 to January 2020 at the Comprehensive Cancer Centre of Drum Tower Hospital, Clinical Cancer Institute of Nanjing University. In all cases, a multidisciplinary team participated in the diagnosis of pancreatic adenocarcinoma followed by the NCCN guidelines. Patients with Eastern Cooperative Oncology Group (ECOG) performance score higher than 1, inadequate bone marrow, abnormal liver or renal functions, additional other malignancies, and patients older than eighty-five years were excluded. Patients enrolled in the trial were prescribed AGIG regimen.

Procedures

Patients enrolled in the trial received AGIG chemo-immunotherapy. Nab-paclitaxel (125 mg/m2) and gemcitabine (1000 mg/m2) were administered intravenously to all patients on the first day and the eighth day of the treatment cycle. IL-2 (10000000 U) and GM-CSF (100 μg) were administered subcutaneously on three to five days after chemotherapy. The treatment is repeated every three weeks. **Figure 1** showed the drug administration protocol of the AGIG regimen. We evaluate clinical and laboratory results at baseline and repeated every time before chemotherapy. Radiographic response evaluation was performed every six weeks. Subjects continued their treatment until disease progression, clinical judgment, occurrence of unacceptable toxicity, or withdrawal of consent. Supportive care was permitted during the treatment course. Second line therapy after disease progression was left to the discretion of the treating oncologist.

Assessment

All patients were evaluated every two cycles of AGIG chemo-immunotherapy using multislice computed tomography scans with contrast medium. Physical examination and laboratory tests including blood routine test, biochemical index and serum CA199 assays were performed every time before chemotherapy. We categorize tumor response into complete response (CR), partial response (PR), stable disease (SD), and progressive disease (PD) according to the Response Evaluation Criteria in Solid Tumors (version 1.1). With respect to the safety observation of the treatment, we graded adverse events according to the National Cancer Institute Common Terminology Criteria for Adverse Events (version 4.0). Overall survival (OS) was defined as the duration from the beginning of chemotherapy to the date of death of any cause. Progression free survival (PFS) was defined as the duration from the beginning of chemotherapy to the date of disease progression or death. Subjects without event were censored at the last follow-up date (August 1st, 2020). Characteristic files were collected at the moment of admission.

Statistical Analysis

All data were analyzed using Graphpad Prism 6 and SPSS software (version 21.0). Survival analyses were performed using the Kaplane-Meier method, Log-rank (Mantel-Cox) tests and Gehan-Breslow-Wilcoxon tests. Data were presented as median and range. A P value less than 0.05 was considered statistical significance.

RESULTS

Patient Characteristics

Between 11/2018 and 01/2020, a total of sixty-four patients were enrolled and evaluated in our trial. **Figure 2** showed the study flowchart of this trial. Patient characteristic files at baseline are summarized in **Table 1**. There were thirty-six (56.25%) males and twenty-eight (43.75%) females. The median age was 62 (range 33 - 81) years. All subjects were ECOG PS 0–1. Fifty-nine PC sufferers (92.19%) had elevated baseline CA199, with a median value of 1033 (range 27 - 30491) u/mL. In total, 51.56% (n = 33) of the tumors were located in the head and neck of the pancreas. 40.63% (n = 26) of the tumors were located in the body or tail of the pancreas. 49 patients were histologically diagnosed as adenocarcinoma including one case of cystadenocarcinoma and one case of mucinous adenocarcinoma. 4 patients were histologically diagnosed as adeno-squamous carcinoma, and none of the patients developed undifferentiated or undifferentiated neuroendocrine carcinoma. In addition, 11 patients' pathological types are still unknown due to the limited pathologic sampling ability of endoscopic ultrasonography. Nearly half of enrolled patients (n = 31, 48.44%) had metastases at the initial diagnosis. The majority of the cases had liver (n = 23, 74.19%) or peritoneal (n = 10, 32.26%) metastasis. Seven patients had undergone a prior resection.

Treatment Completion Rates

Seventy-four subjects were assessed for eligibility initially. Six patients were excluded because they did not meet inclusion criteria. Four patients had abnormal baseline laboratory results and two patients had immeasurable disease. Sixty-eight patients were allocated to intervention. Four patients did not receive allocated intervention, two for patient preference and two for unknown reason. A total of sixty-four patients proceeded to AGIG and were analyzed for toxic effects and efficacy. Forty-eight patients were observed disease progression throughout the follow up. Seven patients received surgical resection. Seven patients had been receiving maintenance therapy till the last follow-up date (August 1st, 2020). Two patients drop out the trial, 1 with obstructive jaundice and 1 with femoral head necrosis.

Radiographic Response Evaluation

Radiographic response was measured with RECIST 1.1 every two cycles of AGIG chemo-immunotherapy. With sixty-four patients evaluated, two patients discontinued chemotherapy early because of obstructive jaundice and femoral head necrosis. Twenty-eight patients (43.75%) had PR, twenty-one patients (32.81%) had SD, and fifteen patients (23.43%) had PD. **Table 2** summarized the detail information of best response. For all patients (n = 64), the overall response rate (ORR) and disease control rate (DCR) was 43.75% and 76.6% respectively. No significant difference in treatment response rate was observed between the two primary tumor sites.

Survival Analysis and Subgroup Analysis

At the last follow-up (1st August 2020), thirty-two patients (50%) had died. All sixty-four patients were included for

TABLE 1 | Baseline characteristics. (intention-to-treat population).

Characteristic	AGIG (N = 64)	No. (%)
Sex		
Male	36	56.25%
Female	28	43.75%
Age, median (range),y	62 (33-81)	
ECOG PS		
0	19	29.70%
1	45	70.30%
CA 19-9 level at baseline		
median (range), u/ml	1033 (27-30491)	
<37 × ULN Normal	28	43.75%
≥37 × ULN Normal	31	48.43%
Unknown	5	7.80%
Tumor site		
Head and neck	33	51.56%
Body and tail	26	40.63%
Unknown	5	7.81%
Histology		
Adenocarcinoma	49	76.56%
Adeno-squamous carcinoma	4	6.25%
Unclear	11	17.19%
Stage		
Resection	7	10.94%
locally advanced	26	40.63%
Metastatic	31	48.44%
Site of metastatic disease	N = 31	No.(%)
Liver	23	74.19%
Lung	4	12.90%
Peritoneum	10	32.26%
Bone	2	6.45%
No. of metastatic sites		
1	1	3.23%
2	5	16.13%
3	1	3.23%
>3	24	77.25%

survival analysis. The median follow-up time was 12.1 (range 7.1–22.4) months. For all patients, the median PFS was 5.7 (range 1.63–15.8) months (**Figure 3A**), the median OS was 14.2 (range 2.9–22.0) months (**Figure 3B**), and the one-year survival rate was 65%. We performed subgroup survival analyses in CA199 level (Figure 4A), eosinophil count variation (Figure 4B), NK cell count variation (**Figure 4C**) and CD3+CD4/CD3+CD8+ proportion (**Figure 4D**). We found that eosinophil count in the blood elevated three times higher than baseline level predicted a longer survival (P = 0.016) (**Figure 4B**).

Adverse Events

The therapy-related toxicities are summarized in **Table 3**. Generally, the incidence of adverse events was 79.69% (n=51), and fever was the most common side effect, with an incidence of 75%. For severe adverse events, thirty-eight patients (59.38%) were observed with grade III/IV toxicities, among which 84.21% (n = 32) was alopecia, 26.32% (n = 10) was peripheral sensory neuropathy, 7.89% (n = 3) was neutropenia, 13.16% (n = 5) was thrombocytopenia, 10.53% (n = 4) was anemia. Totally, three patients (4.69%) received granulocyte-colony stimulating factor treatment before or after chemotherapy. In addition, five patients (3.2%) were treated with thrombopoietin. No patients suffered adverse event leading to death.

DISCUSSION

Generally, advanced pancreatic ductal adenocarcinoma is considered an incurable presentation of PC. This trial was carried out to investigate the efficacy and safety of the AGIG regimen in Chinese patients with advanced PC. In the present study, the ORR was 43.75%, with a significantly higher ORR compared with MPACT study (22.96%, n=431) (p =0.0007) (12) and a slightly higher ORR compared with LAPACT study (33.64%, n=107) (23) and HALO 202 study (32.60% n=92) (3). Other efficacy endpoints (PFS, 5.7 months; OS, 14.2 months) were not inferior to the findings of the MPACT study (PFS, 5.5 months; OS, 8.5 months) (12) and the study of Karasic et al. (PFS, 6.4 months; OS, 12.1 months) (24). The PFS was a little shorter in this study than that in the study of Karasic et al. (5.7 months vs 5.5 months). We hypothesize that these discrepancies are attributed to differences in the radiographic response measuring frequency, with biweekly measurement in this study versus triweekly measurement in the study of Karasic et al. (24).

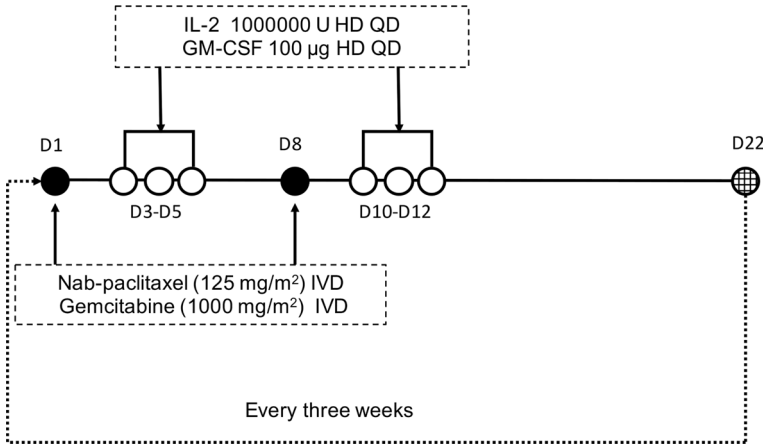

FIGURE 1 | Protocol of drug administration. Nab-paclitaxel (125 mg/m^2) and gemcitabine (1000 mg/m^2) were administered intravenously to all patients on days 1 and 8 triweekly. Interleukin-2 (10000000 U) and GM-CSF (100 μg) were administered subcutaneously on days 3-5 after chemotherapy.

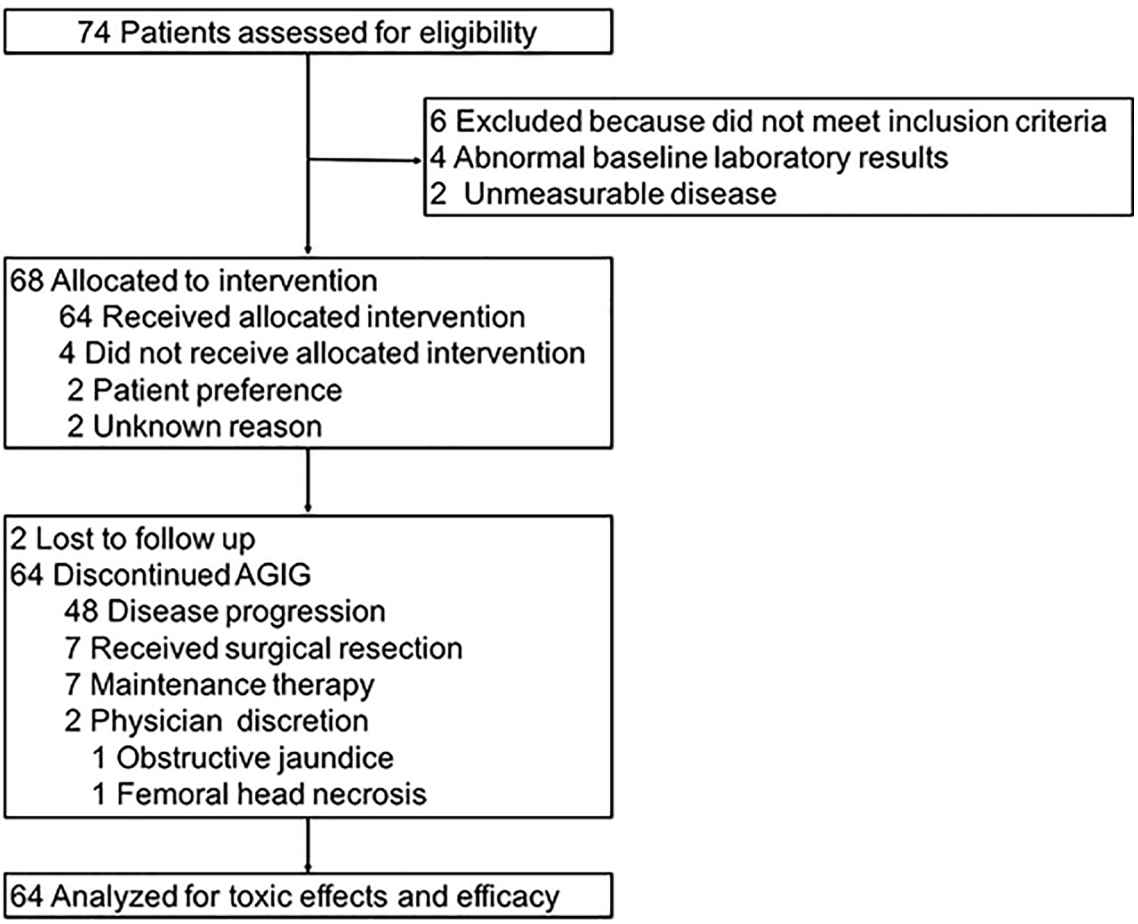

FIGURE 2 | Study flowchart.

TABLE 2 | Response rate by treatment group.

Best Response	Patients No. (%) Overall (n = 64)	Patients No. (%)		
		Head and neck	Body and tail	NA
Partial response	28 (43.75)	15 (45.45)	10 (38.46)	3 (6)
Stable disease	21 (32.81)	10 (30.30)	10 (38.46)	1 (20)
Progressive disease	15 (23.43)	8 (24.24)	6 (23.08)	1 (20)
Disease control rate	49 (76.56)	25 (75.76)	20 (76.92)	4 (80)

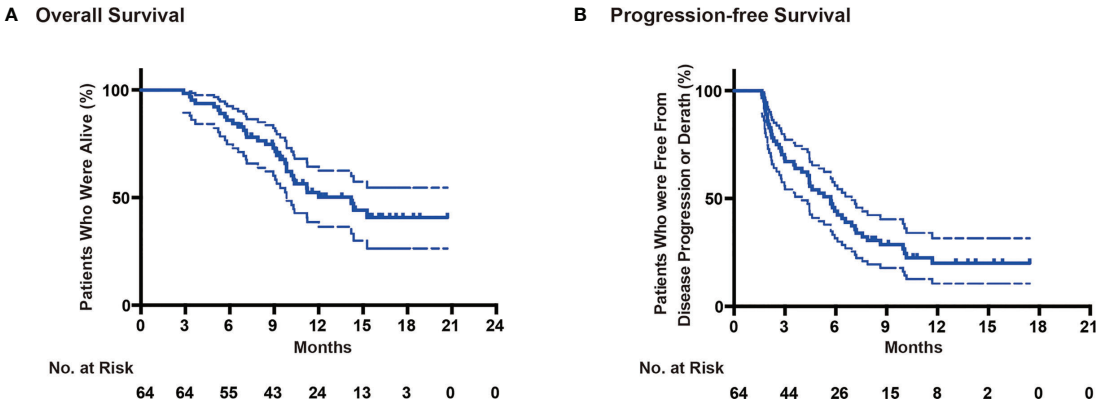

FIGURE 3 | Survival analysis. **(A)** Overall survival, **(B)** Progression-free survival.

TABLE 3 | Summary of adverse events.

Adverse event	Any grade (n = 64)	Grade 3-4 (n = 64)
White blood cell decreased	25 (39.06%)	3 (4.69%)
Anemia	33 (51.56%)	4 (6.25%)
Platelet count decreased	20 (31.25%)	5 (7.81%)
Neutrophil count decreased	32 (50%)	3 (4.69%)
Diarrhea	2 (3.13%)	0 (0%)
Rash maculopapular	22 (34.38%)	5 (7.81%)
Alopecia	52 (81.25%)	32 (50%)
Fatigue	28 (43.75%)	9 (14.06%)
Fever	48 (75%)	6 (9.38%)
Nausea	42 (65.63%)	12 (18.75%)
Vomiting	23 (35.94%)	15 (23.44%)
Dysgeusia	20 (31.25%)	0 (0%)
Anorexia	32 (50%)	8 (12.5%)
Peripheral sensory neuropathy	26 (40.6%)	10 (15.6%)
Adverse event leading to death	0 (0%)	

The effectiveness of the AGIG regimen was also favorable compared to other first-line treatment options presented by previous studies in patients with advanced PC (25–27). Accordingly, we consider the AGIG regimen to be not inferior to the traditional therapy regimen in Chinese patients with advanced PC.

The toxic effects of AGIG were modest. Two patients discontinued chemotherapy early because of obstructive jaundice and femoral head necrosis and none of the patients required discontinuation of AGIG because of toxicity. Exhilaratingly, we observed an obviously decrease in incidences of neutropenia and thrombocytopenia. Totally, only eight patients (12.5%) received granulocyte-colony stimulating factor (3/8) or thrombopoietin (5/8) treatment before or after chemotherapy. We attribute the results to the application of GM-CSF. GM-CSF is an important hematopoietic growth factor and immune modulator. It stimulates the proliferation of macrophage, granulocyte, erythroid, eosinophil, megakaryocyte and multipotent progenitors cells depending on its concentration (28). It also controls eosinophil function in some cases (29, 30). Fever was the most common adverse effect in sequential administration period of interleukin-2 and GM-CSF. Rash maculopapular, alopecia, fatigue, nausea, vomiting, peripheral

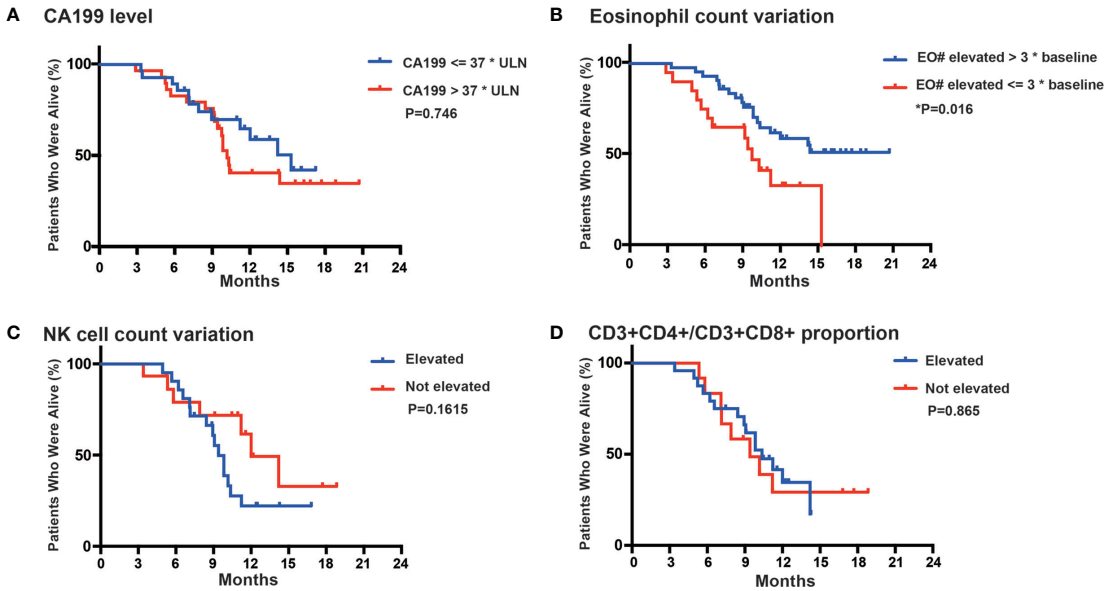

FIGURE 4 | Subgroup analysis in CA199 level **(A)**, Eosinophil count variation **(B)**, NK cell count variation **(C)** and CD3+CD4/CD3+CD8+ proportion **(D)**. *P < 0.05.

neuropathy, and neuropsychiatric symptoms were seen with AGIG regimen. However, these effects did not lead to decreased chemotherapy intensity or treatment discontinuation. These findings suggest that lower incidence of myelosuppression in AGIG regimen ensured full dose of drug administration and sufficient course of treatment, which may account for a survival benefit in the trial.

In previous researches, it was explained that the activity of chemo-immunotherapy is mainly depends on the presence of an efficient host's immune response. Cytotoxic drugs were able to induce immunogenic cell death, autophagy and antigen remodeling. In turn, immunological danger signals may empower an efficient tumor-specific immune response (31, 32). In subgroup analysis, we found that eosinophil count in the blood elevated three times higher than baseline level predicted a longer survival. But it is a pity that we did not investigate the underlying mechanisms due to the insufficient study design. The increase of eosinophils in cancer patients has been known for over decades (33). To our knowledge, tumor-infiltrating eosinophils was firstly described in human gastric cancers in the 1980s. The infiltrating of eosinophils suggests a good prognostic value for prolonged survival (30). Eosinophils exert anti-tumor effects *via* direct and indirect mechanisms (34). Eosinophils have been reported to infiltrate multiple tumors, either as an integral part of the tumor microenvironment or in response to various therapeutic strategies. An antitumor role for eosinophils has been demonstrated in various *in vitro* studies. Eosinophil recruitment, prolonged survival and degranulation have been demonstrated in both human and mouse models (35). The above literatures confirm the phenomenon we observed in this study. Lack of randomization restricts our ability to explore the implicated mechanisms, and further studies are needed.

This study has some limitations. Lack of randomization in a single-arm trial restricts our ability to assess the specific role of AGIG. Insufficient sample size limits the accuracy and authenticity of the results. The improvement of the benefit must be considered hypothesis generating. Given the favorable safety profile and the encouraging antitumor activity of the AGIG regimen, validation by a larger randomized trial is necessary.

In conclusion, the AGIG regimen appears more active and safe than the standard AG chemotherapy. To our knowledge, the study demonstrates the antitumor efficacy of a chemo-immunomodulatory strategy in treating advanced PC sufferers for the first time. These results open a new research area for the treatment of pancreatic cancer by combinatory approaches of cytotoxic chemotherapy and immune modulators. Further investigation is warranted.

CONCLUSION

The AGIG Chemo-immunotherapy has presented encouraging ORR, DCR, OS, and manageable toxicities as first-line treatment option for advanced PC sufferers. This regimen may be a reliable option for patients with preserved performance status. The improvement of treatment efficiency may result from the activation of non-specific immune response.

DATA AVAILABILITY STATEMENT

The original contributions presented in the study are included in the article/supplementary material. Further inquiries can be directed to the corresponding authors.

ETHICS STATEMENT

The studies involving human participants were reviewed and approved by the Ethics Committee of Drum Tower Hospital. The patients/participants provided their written informed consent to participate in this study. Written informed consent was obtained from the individual(s) for the publication of any potentially identifiable images or data included in this article.

AUTHOR CONTRIBUTIONS

WD has seen the original study data, reviewed the analysis of the data, approved the final manuscript, and is the author responsible for archiving the study files. XQ and CL helped analyzed the data. ZZ, HS, and WK reviewed the analysis of the data and approved the final manuscript. JD and BL helped design the study, analyze the data, and write the manuscript. All authors contributed to the article and approved the submitted version.

FUNDING

The study was supported by Chen Xiao-Ping Foundation for the Development of Science an Technology of Hubei Province (No. CXPJJH11900001-2019101). The Affiliated Nanjing Drum Tower Hospital of Nanjing University Medical School sponsored this study.

REFERENCES

1. Doherty GJ, Tempero M, Corrie PG. HALO-109-301: A Phase III Trial of PEGPH20 (With Gemcitabine and Nab-Paclitaxel) in Hyaluronic Acid-High Stage IV Pancreatic Cancer. *Future Oncol (London England)* (2018) 14(1):13–22. doi: 10.2217/fon-2017-0338
2. Hajatdoost L, Sedaghat K, Walker EJ, Thomas J, Kosari S. Chemotherapy in Pancreatic Cancer: A Systematic Review. *Medicina (Kaunas Lithuania)* (2018) 54(3):1–7. doi: 10.3390/medicina54030048
3. Hingorani SR, Zheng L, Bullock AJ, Seery TE, Harris WP, Sigal DS, et al. HALO 202: Randomized Phase II Study of PEGPH20 Plus Nab-Paclitaxel/Gemcitabine Versus Nab-Paclitaxel/Gemcitabine in Patients With Untreated, Metastatic Pancreatic Ductal Adenocarcinoma. *J Clin Oncol* (2018) 36 (4):359–66. doi: 10.1200/jco.2017.74.9564
4. Giordano G, Pancione M, Olivieri N, Parcesepe P, Velocci M, Di Raimo T, et al. Nano Albumin Bound-Paclitaxel in Pancreatic Cancer: Current Evidences and Future Directions. *World J Gastroenterol* (2017) 23 (32):5875–86. doi: 10.3748/wjg.v23.i32.5875
5. Goldstein D, El-Maraghi RH, Hammel P, Heinemann V, Kunzmann V, Sastre J, et al. Nab-Paclitaxel Plus Gemcitabine for Metastatic Pancreatic Cancer: Long-Term Survival From a Phase III Trial. *J Natl Cancer Inst* (2015) 107 (2):1–10. doi: 10.1093/jnci/dju413
6. Burki TK. AZD1775 Plus Chemoradiotherapy for Pancreatic Cancer. *Lancet Oncol* (2019) 20(9):e472. doi: 10.1016/s1470-2045(19)30537-6
7. Kang J, Hwang I, Yoo C, Kim KP, Jeong JH, Chang HM, et al. Nab-Paclitaxel Plus Gemcitabine Versus FOLFIRINOX as the First-Line Chemotherapy for Patients With Metastatic Pancreatic Cancer: Retrospective Analysis. *Invest New Drugs* (2018) 36(4):732–41. doi: 10.1007/s10637-018-0598-5
8. Velez-Velez LM, Hughes CL, Kasi PM. Clinical Value of Pharmacogenomic Testing in a Patient Receiving FOLFIRINOX for Pancreatic Adenocarcinoma. *Front Pharmacol* (2018) 9:1309. doi: 10.3389/fphar.2018.01309
9. Li X, Ma T, Zhang Q, Chen YG, Guo CX, Shen YN, et al. Modified-FOLFIRINOX in Metastatic Pancreatic Cancer: A Prospective Study in Chinese Population. *Cancer Lett* (2017) 406:22–6. doi: 10.1016/j.canlet.2017.07.012
10. Okusaka T, Ikeda M, Fukutomi A, Ioka T, Furuse J, Ohkawa S, et al. Phase II Study of FOLFIRINOX for Chemotherapy-Naïve Japanese Patients With Metastatic Pancreatic Cancer. *Cancer Sci* (2014) 105(10):1321–6. doi: 10.1111/cas.12501
11. Zhang DS, Wang DS, Wang ZQ, Wang FH, Luo HY, Qiu MZ, et al. Phase I/II Study of Albumin-Bound Nab-Paclitaxel Plus Gemcitabine Administered to Chinese Patients With Advanced Pancreatic Cancer. *Cancer Chemother Pharmacol* (2013) 71(4):1065–72. doi: 10.1007/s00280-013-2102-4
12. Von Hoff DD, Ervin T, Arena FP, Chiorean EG, Infante J, Moore M, et al. Increased Survival in Pancreatic Cancer With Nab-Paclitaxel Plus Gemcitabine. *N Engl J Med* (2013) 369(18):1691–703. doi: 10.1056/NEJMoa1304369
13. Jiang J, Zhou H, Ni C, Hu X, Mou Y, Huang D, et al. Immunotherapy in Pancreatic Cancer: New Hope or Mission Impossible? *Cancer Lett* (2019) 445:57–64. doi: 10.1016/j.canlet.2018.10.045
14. Akce M, Zaidi MY, Waller EK, El-Rayes BF, Lesinski GB. The Potential of CAR T Cell Therapy in Pancreatic Cancer. *Front Immunol* (2018) 9:2166. doi: 10.3389/fimmu.2018.02166
15. De Palma M, Biziato D, Petrova TV. Microenvironmental Regulation of Tumour Angiogenesis. *Nat Rev Cancer* (2017) 17(8):457–74. doi: 10.1038/nrc.2017.51
16. Caraglia M, Correale P, Giannicola R, Staropoli N, Botta C, Pastina P, et al. GOLFIG Chemo-Immunotherapy in Metastatic Colorectal Cancer Patients. A Critical Review on a Long-Lasting Follow-Up. *Front Oncol* (2019) 9:1102. doi: 10.3389/fonc.2019.01102
17. Correale P, Fioravanti A, Bertoldi I, Montagnani F, Miracco C, Francini G. Occurrence of Autoimmunity in a Long-Term Survivor With Metastatic Colon Carcinoma Treated With a New Chemo-Immunotherapy Regimen. *J Chemother (Florence Italy)* (2008) 20(2):278–81. doi: 10.1179/joc.2008.20.2.278
18. Dix SP, Gilmore CE. Cytokine Therapy After Bone Marrow Transplantation. *Pharmacotherapy* (1996) 16(4):593–608. doi: doi:10.1002/j.1875-9114.1996.tb03641.x
19. Yan WL, Shen KY, Tien CY, Chen YA, Liu SJ. Recent Progress in GM-CSF-Based Cancer Immunotherapy. *Immunotherapy* (2017) 9(4):347–60. doi: 10.2217/imt-2016-0141
20. Koehn TA, Trimble LL, Alderson KL, Erbe AK, McDowell KA, Grzywacz B, et al. Increasing the Clinical Efficacy of NK and Antibody-Mediated Cancer Immunotherapy: Potential Predictors of Successful Clinical Outcome Based on Observations in High-Risk Neuroblastoma. *Front Pharmacol* (2012) 3:91. doi: 10.3389/fphar.2012.00091
21. Correale P, Botta C, Rotundo MS, Guglielmo A, Conca R, Licchetta A, et al. Gemcitabine, Oxaliplatin, Levofolinate, 5-Fluorouracil, Granulocyte-Macrophage Colony-Stimulating Factor, and Interleukin-2 (GOLFIG) Versus FOLFOX Chemotherapy in Metastatic Colorectal Cancer Patients: The GOLFIG-2 Multicentric Open-Label Randomized Phase III Trial. *J Immunother (Hagerstown Md 1997)* (2014) 37(1):26–35. doi: 10.1097/cji.0000000000000004
22. Correale P, Tagliaferri P, Fioravanti A, Del Vecchio MT, Remondo C, Montagnani F, et al. Immunity Feedback and Clinical Outcome in Colon Cancer Patients Undergoing Chemoimmunotherapy With Gemcitabine + FOLFOX Followed by Subcutaneous Granulocyte Macrophage Colony-Stimulating Factor and Aldesleukin (GOLFIG-1 Trial). *Clin Cancer Res* (2008) 14(13):4192–9. doi: 10.1158/1078-0432.ccr-07-5278
23. Philip PA, Lacy J, Portales F, Sobrero A, Pazo-Cid R, Manzano Mozo JL, et al. Nab-Paclitaxel Plus Gemcitabine in Patients With Locally Advanced Pancreatic Cancer (LAPACT): A Multicentre, Open-Label Phase 2 Study. *Lancet Gastroenterol Hepatol* (2020) 5(3):285–94. doi: 10.1016/s2468-1253(19)30327-9
24. Karasic TB, O'Hara MH, Loaiza-Bonilla A, Reiss KA, Teitelbaum UR, Borazanci E, et al. Effect of Gemcitabine and Nab-Paclitaxel With or Without Hydroxychloroquine on Patients With Advanced Pancreatic Cancer: A Phase 2 Randomized Clinical Trial. *JAMA Oncol* (2019) 5 (7):993–8. doi: 10.1001/jamaoncol.2019.0684
25. Murphy JE, Wo JY, Ryan DP, Clark JW, Jiang W, Yeap BY, et al. Total Neoadjuvant Therapy With FOLFIRINOX in Combination With Losartan

Followed by Chemoradiotherapy for Locally Advanced Pancreatic Cancer: A Phase 2 Clinical Trial. *JAMA Oncol* (2019) 5(7):1020–7. doi: 10.1001/jamaoncol.2019.0892
26. Reni M, Zanon S, Peretti U, Chiaravalli M, Barone D, Pircher C, et al. Nab-Paclitaxel Plus Gemcitabine With or Without Capecitabine and Cisplatin in Metastatic Pancreatic Adenocarcinoma (PACT-19): A Randomised Phase 2 Trial. *Lancet Gastroenterol Hepatol* (2018) 3(10):691–7. doi: 10.1016/s2468-1253(18)30196-1
27. Xu R, Yu X, Hao J, Wang L, Pan H, Han G, et al. Efficacy and Safety of Weekly Nab-Paclitaxel Plus Gemcitabine in Chinese Patients With Metastatic Adenocarcinoma of the Pancreas: A Phase II Study. *BMC Cancer* (2017) 17 (1):885. doi: 10.1186/s12885-017-3887-z
28. Sugawara Y, Fisher SJ, Zasadny KR, Kison PV, Baker LH, Wahl RL. Preclinical and Clinical Studies of Bone Marrow Uptake of Fluorine-1-Fluorodeoxyglucose With or Without Granulocyte Colony-Stimulating Factor During Chemotherapy. *J Clin Oncol* (1998) 16(1):173–80. doi: 10.1200/jco.1998.16.1.173
29. Kitamura K. [GM-CSF.G-CSF]. *Gan To Kagaku Ryoho Cancer Chemother* (1995) 22(2):301–5.
30. Mattei F, Andreone S, Marone G, Gambardella AR, Loffredo S, Varricchi G, et al. Eosinophils in the Tumor Microenvironment. *Adv Exp Med Biol* (2020) 1273:1–28. doi: 10.1007/978-3-030-49270-0_1
31. Williams P, Galipeau J. GMCSF-Interleukin Fusion Cytokines Induce Novel Immune Effectors That Can Serve as Biopharmaceuticals for Treatment of Autoimmunity and Cancer. *J Internal Med* (2011) 269(1):74–84. doi: 10.1111/j.1365-2796.2010.02314.x
32. Kabacaoglu D, Ciecielski KJ, Ruess DA, Algül H. Immune Checkpoint Inhibition for Pancreatic Ductal Adenocarcinoma: Current Limitations and Future Options. *Front Immunol* (2018) 9:1878. doi: 10.3389/fimmu.2018.01878
33. Chusid MJ. Eosinophils: Friends or Foes? *J Allergy Clin Immunol Pract* (2018) 6(5):1439–44. doi: 10.1016/j.jaip.2018.04.031
34. Dennis KL, Wang Y, Blatner NR, Wang S, Saadalla A, Trudeau E, et al. Adenomatous Polyps are Driven by Microbe-Instigated Focal Inflammation and Are Controlled by IL-10-Producing T Cells. *Cancer Res* (2013) 73 (19):5905–13. doi: 10.1158/0008-5472.can-13-1511
35. Grisaru-Tal S, Itan M, Klion AD, Munitz A. A New Dawn for Eosinophils in the Tumour Microenvironment. *Nat Rev Cancer* (2020) 20(10):594–607. doi: 10.1038/s41568-020-0283-9

Conflict of Interest: The authors declare that the research was conducted in the absence of any commercial or financial relationships that could be construed as a potential conflict of interest.

Publisher's Note: All claims expressed in this article are solely those of the authors and do not necessarily represent those of their affiliated organizations, or those of the publisher, the editors and the reviewers. Any product that may be evaluated in this article, or claim that may be made by its manufacturer, is not guaranteed or endorsed by the publisher.

frontiers in Oncology

ORIGINAL RESEARCH
published: 18 October 2021
doi: 10.3389/fonc.2021.771247

Genomic Landscape in Neoplasm-Like Stroma Reveals Distinct Prognostic Subtypes of Pancreatic Ductal Adenocarcinoma

Jiahong Jiang[1,2†], Yaping Xu[3†], Lianpeng Chang[3†], Guoqing Ru[4], Xuefeng Xia[3], Ling Yang[3], Xin Yi[3], Zheling Chen[2], Dong-Sheng Huang[1] and Liu Yang[1,2†]*

[1] Key Laboratory of Tumor Molecular Diagnosis and Individualized Medicine of Zhejiang Province, Zhejiang Provincial People's Hospital, People's Hospital of Hangzhou Medical College, Hangzhou, China, [2] Department of Oncology, Zhejiang Provincial People's Hospital, People's Hospital of Hangzhou Medical College, Hangzhou, China, [3] Geneplus-Beijing Institute, Beijing, China, [4] Department of Pathology, Zhejiang Provincial People's Hospital, People's Hospital of Hangzhou Medical College, Hangzhou, China

OPEN ACCESS

Edited by:
Min Li,
University of Oklahoma Health Sciences Center, United States

Reviewed by:
Gang Jin,
Changhai Hospital, China
Yi Qin,
Fudan University, China

***Correspondence:**
Liu Yang
yangliu@hmc.edu.cn

†These authors have contributed equally to this work

Specialty section:
This article was submitted to Gastrointestinal Cancers: Hepato Pancreatic Biliary Cancers, a section of the journal Frontiers in Oncology

Received: *06 September 2021*
Accepted: *27 September 2021*
Published: *18 October 2021*

Citation:
Jiang J, Xu Y, Chang L, Ru G, Xia X, Yang L, Yi X, Chen Z, Huang D-S and Yang L (2021) Genomic Landscape in Neoplasm-Like Stroma Reveals Distinct Prognostic Subtypes of Pancreatic Ductal Adenocarcinoma. Front. Oncol. 11:771247. doi: 10.3389/fonc.2021.771247

As a main component of the tumor microenvironment, the stroma is critical in development, progression, and metastasis of pancreatic ductal adenocarcinoma (PDAC). The genomic status and its relationship of neoplastic and stromal components remain unclear in PDAC. We performed targeted sequencing for 1,021 cancer-suspected genes on parallel microdissected stromal and neoplastic components from 50 operable PDAC patients. Clonality analysis of mutations was conducted to reconstruct the evolutionary trajectory, and then molecular subtypes were established. Multi-lineage differentiation potential and mesenchymal transformation of *KRAS*-mutant cell line Panc1 were evaluated using RT-PCR and immunofluorescence staining. In this study, 39 (78.0%) were genomically altered in stroma, with *KRAS* (71.8%), *TP53* (61.5%), and *CDKN2A* (23.1%) as the most commonly mutated genes. The majority of stromal mutations (89.8%) were detected in matched neoplastic components. Patients with *KRAS/TP53*-mut stroma demonstrated a higher tumor cell fraction (TCF) than did those with wild-type (WT) stroma ($p = 0.0371$, $p = 0.0014$). In both components, mutants *KRAS* and *TP53* often occurred as clonal events, and the allele frequencies presented linear correlation in the same specimen. All neoplasm-like stroma (characterized with all or initial neoplastic clones and driver events in stroma) harbored *KRAS* or *TP53* mutations. Neoplasm-like and *KRAS*-mutant stroma was associated with shorter disease-free survival. It is a new finding for the existence of driver gene mutations in PDAC stroma. These data suggest that genomic features of stromal components may serve as prognostic biomarkers in resectable PDAC and might help to guide a more precise treatment paradigm in therapeutic options.

Keywords: pancreatic cancer, tumor microenvironment, stroma, *KRAS*, disease-free survival

BACKGROUND

Despite intense efforts over the last decade, pancreatic ductal adenocarcinoma (PDAC) is still considered one of the most aggressive and lethal solid tumors (1). Most patients who present with advanced PDAC will die within a year of diagnosis. Even with resectable PDAC, patients have a 5-year overall survival of only 15% to 25% after radical resection and adjuvant chemotherapy (2). Lack of effective markers for prognosis prediction and precision treatment is also attributed to the high morality. As the only monitoring marker permitted by the Food and Drug Administration (FDA), carbohydrate antigen 19-9 (CA19-9) is easily affected by biliary disease and is negative in Lewis (−) PDAC patients (3). Recent studies have proposed some biomarkers to predict prognosis of PDAC; however, none of them achieved satisfying results (4). In this condition, new biomarkers are urgently needed to guide precise treatment and predict prognosis for PDAC.

The tumor microenvironment (TME) is a complicated network that contains blood and lymphatic vessels, immune cells, stromal cells, and extracellular matrix (cytokines, growth factors, chemokines, and inflammatory factors). The dynamic communication between cancer cells and TME influences cancer proliferation, invasion, metastasis, drug resistance, and immune escape. Immune cells such as tumor-associated macrophages have critical functions in tumor development through manifold growth factor secretion and numerous immunosuppressive molecule production (5). As a critical component of the TME, the tumor stroma has a profound effect on many hallmarks of cancer (6). High stromal component in PDAC was confirmed as an independent prognostic factor through digitalized whole-mount histopathology, as well as the impact of tumor grade and perineural invasion (7). Therefore, exploring the characteristics of the stroma will help in addressing the progression and metastasis of PDAC.

Epithelial–mesenchymal transition (EMT) has been proposed as an important interactive way between tumor and stroma during malignant progression (8). Recent studies have reported that a mesenchymal or epithelial phenotype is not a stable property of cancer cells and is often defined by the gain of the mesenchymal marker vimentin and the loss of the epithelial marker E-cadherin. EMT is a process in which epithelial cells acquire mesenchymal features, with enhanced capacity of invasion and metastasis in cancer. Epithelially derived cells were observed to migrate into the stroma and transformed to mesenchymal phenotype using lineage tracing mouse model at early stage of PDAC (9). Based on this study, we guessed that epithelially derived cells might affect the genomic features of stroma *via* EMT. Whether genomic features of the stroma have prognostic value for PDAC is an issue of concern.

To identify genomic mutations in stroma components and to evaluate their prognostic value in patients with resectable PDAC, this prospective study collected surgical tissue samples from 50 patients with PDAC. We used laser capture microdissection (LCM) technique to separate stroma from neoplastic components, and then we performed next-generation sequencing (NGS) for both specimens. Clinical characteristics and clonality analysis of mutations were conducted to explore the role of stroma in PDAC, and *in vitro* experiments were performed to clarify this condition.

MATERIALS AND METHODS

Clinical Cohort

This single-center prospective study was conducted at Zhejiang Provincial People's Hospital. From May 2016 to November 2016, a total of 50 patients primarily diagnosed with PDAC and received surgery were enrolled in this study. The database was locked for follow-up and analyses on November 2018. Patients with a concurrent malignant neoplasm were excluded. The histopathological status was evaluated by at least two experienced pathologists. TNM staging was defined according to American Joint Committee on Cancer (AJCC) TNM staging system for pancreatic cancer (10). Radiographic assessment using the Response Evaluation Criteria in Solid Tumors (RECIST) version 1.1 was performed and based on standard of care clinical guidelines. We followed the Strengthening the Reporting of Observational Studies in Epidemiology reporting guideline statement to ensure the quality of data reported in this study (11). This study was approved by the ethical committee at Zhejiang Provincial People's Hospital (No. 2016KY129). All patients provided informed written consent before undergoing any study-related procedures. This study was performed in accordance with the Declaration of Helsinki.

Sample Collection

Surgical tumor tissue samples and blood lymphocytes were collected from each patient. Tissue samples were fixed by formalin-fixed paraffin-embedded (FFPE). H&E staining was performed for each section according to the manufacturer's instructions (Beyotime, Suzhou, China) before dissection. As a guide for stromal lesion, we performed immunohistochemistry staining for vimentin (Cat #5741 purchased from Cell Signaling Technology, Danvers, MA, USA) in the adjacent section. Ten to 15 sections of FFPE (thickness: 5–10 μm) were cut using a microtome (RM2265, Leica, Germany). LCM was performed to separate the neoplastic components, fibrotic stroma, and normal pancreatic tissue on a Leica LMD7000 microscope as previously described (12). The microdissection was performed by at least two senior pathologists, and any disagreement between these pathologists was resolved by discussion. All specimens were then stored in phosphate-buffered saline (PBS) before subsequent processing.

DNA Extraction

Genomic DNA was extracted from neoplastic, stromal, and normal components using a QIAamp DNA Mini Kit (Qiagen, Hilden, Germany). Germline DNA was extracted from blood lymphocytes using the DNeasy Blood & Tissue Kit (Qiagen, Hilden, Germany). DNA quality was estimated using a Qubit fluorometer and a Qubit dsDNA (BR) Assay Kit (Invitrogen, Carlsbad, CA, USA). Genomic DNA from normal tissues and germline DNA from blood lymphocytes were used as negative control to eliminate the interference of germline variants and contaminating cancer cells.

Sequencing Library Constructing

Extracted DNA was sheared into 200- to 250-bp fragments *via* a Covaris S2 instrument (Woburn, MA, USA). KAPA LTP Library Preparation Kit for Illumina (KAPA Biosystems, Boston, MA, USA) was used to prepare indexed NGS libraries. NEBNext FFPE DNA Repair Mix (Ipswich, UK) was used for FFPE DNA repair during library construction, and the detailed protocol can be obtained from https://international.neb.com/protocols/2015/01/16/protocol-for-use-with-nebnext-ffpe-dna-repair-mix-m6630-and-other-user-supplied-library-construction-reagents. Additional information regarding library preparation was described by Lv et al. (13).

Targeted Capture Sequencing

Libraries were hybridized to custom-designed biotinylated oligonucleotide probes (Integrated DNA Technologies, IA, USA). The captured genomic regions included the most common driver genes of solid tumors (14). We chose their entire exome regions to construct the basic panel. Next, genomic regions related relevant to the effects of chemotherapy, targeted drugs, and immunotherapy per available clinical and preclinical research were added to the panel. Finally, high-frequently mutant regions recorded in the Catalogue of Somatic Mutations in Cancer (COSMIC, http://cancer.sanger.ac.uk/cosmic) and The Cancer Genome Atlas (TCGA; https://cancergenome.nih.gov/) were involved. Overall, 1,021 genes were involved in this panel. Sequencing was carried out using Illumina 2 × 100-bp paired-end reads on an Illumina HiSeq 3000 instrument according to the manufacturer's recommendations using a TruSeq PE Cluster Generation Kit v3 and a TruSeq SBS Kit v3 (Illumina, San Diego, CA, USA). Additional detailed information regarding library preparation was described by Lv et al. (13). The median sequencing depth of stromal and neoplastic components was 941× (360× to 1,626×) and 1,045× (345× to 1728×), respectively.

Raw Data Processing

Terminal adaptor sequences and reads with more than 50% low-quality base reads, or those with more than 50% N bases, together with their mate pair were removed from raw reads. Subsequently, Burrows–Wheeler Aligner (BWA; version 0.7.12-r1039, http://bio-bwa.sourceforge.net/) tool was used to align clean reads to the reference human genome (hg19) with default parameters. Duplicate reads were identified and marked with Picard's Mark Duplicates tool (https://software.broadinstitute.org/gatk/documentation/tooldocs/4.0.3.0/picard_sam_markduplicates_MarkDuplicates.php). The Gene Analysis Toolkit (GATK, https://www.broadinstitute.org/gatk/) was used to perform local realignment and base quality recalibration.

Somatic Mutation Calling

Somatic single-nucleotide variations (SNVs) and insertions or deletions of small fragments (indels) were called using the MuTect2 algorithm (https://software.broadinstitute.org/gatk/documentation/tooldocs/3.8-0/org_broadinstitute_gatk_tools_walkers_cancer_m2_MuTect2.php). The filter criteria included 1) variants supported by fewer than five high-quality reads (base quality ≥30, mapping quality ≥30) were filtered; 2) variants were filtered as cross-contamination if present in >1% samples in custom single-nucleotide polymorphism (SNP) databases (dbsnp, https://www.ncbi.nlm.nih.gov/projects/SNP/; 1000G, https://www.1000genomes.org/; ESP6500, https://evs.gs.washington.edu/; ExAC, http://exac.broadinstitute.org/) and self-built SNP database; 3) synonymous mutations (also listed in **Table S1**) were removed; 4) variants with allele frequency less than 1% were removed; and 5) variants detected in matched blood lymphocytes and normal tissue were removed. The final candidate variants were all manually verified in the Integrative Genomics Viewer (IGV; https://igv.org/). Remaining mutations were considered validated somatic variants.

Determination of Driver Mutations

Two steps were performed to determine driver or passenger mutations. First, evidential driver genes of PDAC were determined according to Bailey et al. (15). Second, Polymorphism Phenotyping v2 (PolyPhen-2, http://genetics.bwh.harvard.edu/pph2/) and Sortig Intolerant From Tolerant (SIFT, http://sift.bii.a-star.edu.sg/) were used to predict whether the protein structural change derived by one mutation was harmful or not. Those with PolyPhen-2 Score >0.85 or SIFT Score <0.05 were defined as harmful mutations. Generally, harmful mutations in driver genes were defined as driver events, and the others, including harmless mutations in driver genes and all mutations in passenger genes, were defined as passenger events.

Clonality Analysis

PyClone algorithm was used to determine the clonal clusters (16). The essential parameters included the variant allele frequencies (VAFs) and copy numbers of non-synonymous mutations in both tumor and stromal components. Copy number was estimated by Contra algorithm (http://contra-cnv.sourceforge.net).

Cell Culture and Reagents

Human pancreatic cancer cell line Panc1 was purchased from American Type Culture Collection (Manassas, VA, USA), and it was grown in DMEM culture medium (Gibco, Carlsbad, CA, USA) supplemented with 10% fetal bovine serum (FBS) and 1% penicillin/streptomycin, in a humidified atmosphere at 37°C and 5% CO_2.

Reverse Transcriptase PCR

Total RNA was extracted from cells using TRIzol reagent (Invitrogen, California, USA) according to the manufacturer's instruction. cDNA was subsequently synthesized using PrimeScript™ RT Master Mix kit (Takara). RT-PCR was performed using SYBR Premix Ex Taq™ kit (Takara, Dalian, China). The primers are listed in **Table S2**.

Immunofluorescence Staining

Panc1 cells were seeded on coverslips and cultured under different glycemic conditions for 3 days. Then medium was removed, and vimentin was stained using the rabbit anti-human vimentin

antibody (Cat #5741) purchased from Cell Signaling Technology (Danvers, MA, USA). Evaluation was performed using confocal laser scanning microscope (Leica, Wetzlar, Germany).

Statistical Analysis

Descriptive statistics was performed using SPSS 22.0 (IBM, Armonk, NY, USA). Spearman's correlation analysis was performed using GraphPad Prism 7 (GraphPad Software, La Jolla, CA, USA) to assess the relevance of VAFs between mutants *KRAS* and *TP53*, as well as the correlation between tumor cell fraction (TCF) and maximal VAF in stromal or neoplastic component. The parameter comparison for different patient groups was performed using the Mann–Whitney U-test (two groups) or one-way ANOVA test (≥3 groups) (SPSS 22.0). The Kaplan–Meier survival analysis was used to compare disease-free survival (DFS) between different subgroups, and Cox regression was performed to determine the influence of multiple factors on DFS. Both analyses were conducted by SPSS 22.0. A two-tailed p-value <0.05 was considered statistically significant.

RESULTS

Clinical Characteristics

Clinical characteristics of patients are summarized in **Table 1**. All of 50 patients were diagnosed with primary PDAC. The median age at diagnosis was 65 years (ranged from 37 to 84 years). The number of male and female patients was 30 (60.0%) and 20 (40.0%), respectively. The majority of enrolled patients were stage I/II (n = 44, 88.0%). Histologically, 25 patient specimens (50.0%) were poorly differentiated in terms of cellular morphology, and the others were moderately differentiated. The maximal diameter of tumor *in situ* was >4 cm in seven patients (14.0%). Regional lymph nodes were involved in 19 patients (38.0%). The adjacent nerve and vasculature were invaded in 41 (82.0%) and 21 (42.0%) of patients, respectively.

Surgical resection was performed in all patients as the sole treatment for 20 patients (40.0%). Thirty (60.0%) received adjuvant chemotherapy after surgery. Eight (16.0%) patients had ≥2 lines of chemotherapy. At the time of last follow-up, 19 patients (38.0%) experienced local (two, 10.5%) or distant recurrences (17, 89.5%) postoperatively.

Mutant Prevalence of Stromal Components

Cellular morphology was determined *via* H&E staining, and the incisal margin of LCM was kept away from nests as much as possible to avoid the contamination of neoplastic cells. As a specific biomarker of stroma-derived cells, vimentin was enriched in stromal components isolated from the adjacent section (**Figure 1A**). We evaluated the mutant prevalence in the stromal components. In total, 127 somatic mutations (median = 3, ranged from 1 to 7) were detected in stromal components from 39 patients (**Table S1**). *KRAS* (n = 28, 71.8%),

TABLE 1 | Correlation between clinical characteristics and genomic status of stroma.

Characteristics	Any mutation (n = 50)			Mutant *KRAS* (n = 50)			Mutant *TP53* (n = 50)			Co-mutants *KRAS* and *TP53* (n = 50)		
	Positive (n = 39)	Negative (n = 11)	*p*	Positive (n = 28)	Negative (n = 22)	*p*	Positive (n = 24)	Negative (n = 26)	*p*	Positive (n = 21)	Negative (n = 29)	*p*
Age, years												
Median	66	65	0.3325	68	62.5	0.0036*	68.5	63.5	0.0101*	69	63	0.0029*
Gender, n (%)												
Male	23 (59)	7 (64)	0.9444	15 (54)	15 (68)	0.2952	13 (54)	17 (65)	0.4186	10 (48)	20 (69)	0.1283
Female	16 (41)	4 (36)		13 (46)	7 (32)		11 (46)	9 (35)		11 (52)	9 (31)	
Differentiation, n (%)												
Poor	19 (49)	6 (55)	0.7328	14 (50)	11 (50)	1.0000	13 (54)	12 (46)	0.5713	11 (52)	14 (48)	0.7745
Other	20 (51)	5 (45)		14 (50)	11 (50)		11 (46)	14 (54)		10 (48)	15 (52)	
Clinical stage, n (%)												
I	22 (56)	3 (27)	0.0878	15 (54)	10 (45)	0.5688	15 (63)	10 (38)	0.0894	12 (57)	13 (45)	0.3900
II-IV	17 (44)	8 (73)		13 (46)	12 (55)		9 (37)	16 (62)		9 (53)	16 (55)	
Tumor size, n (%)												
>4 cm	5 (13)	2 (18)	0.9686	4 (14)	3 (14)	0.7302	4 (17)	3 (12)	0.9091	4 (19)	3 (10)	0.6438
≤4 cm	34 (87)	9 (82)		24 (86)	19 (86)		20 (83)	23 (88)		17 (81)	26 (90)	
Lymph node, n (%)												
Positive	14 (36)	5 (45)	0.8219	11 (39)	8 (36)	0.8327	8 (33)	11 (42)	0.5137	7 (33)	12 (41)	0.5629
Negative	25 (64)	6 (55)		17 (61)	14 (64)		16 (67)	15 (58)		14 (67)	17 (59)	
Nerve invasion, n (%)												
Positive	32 (82)	9 (82)	0.6697	24 (86)	17 (77)	0.6888	21 (88)	20 (77)	0.5457	18 (86)	23 (79)	0.8346
Negative	7 (18)	2 (18)		4 (14)	5 (23)		3 (12)	6 (23)		3 (14)	6 (21)	
Vascular invasion, n (%)												
Positive	13 (33)	8 (73)	0.0464*	12 (43)	9 (41)	0.8898	9 (38)	12 (46)	0.5357	9 (53)	12 (41)	0.9168
Negative	26 (67)	3 (27)		16 (57)	13 (59)		15 (62)	14 (54)		12 (57)	17 (59)	

Statistical significance.

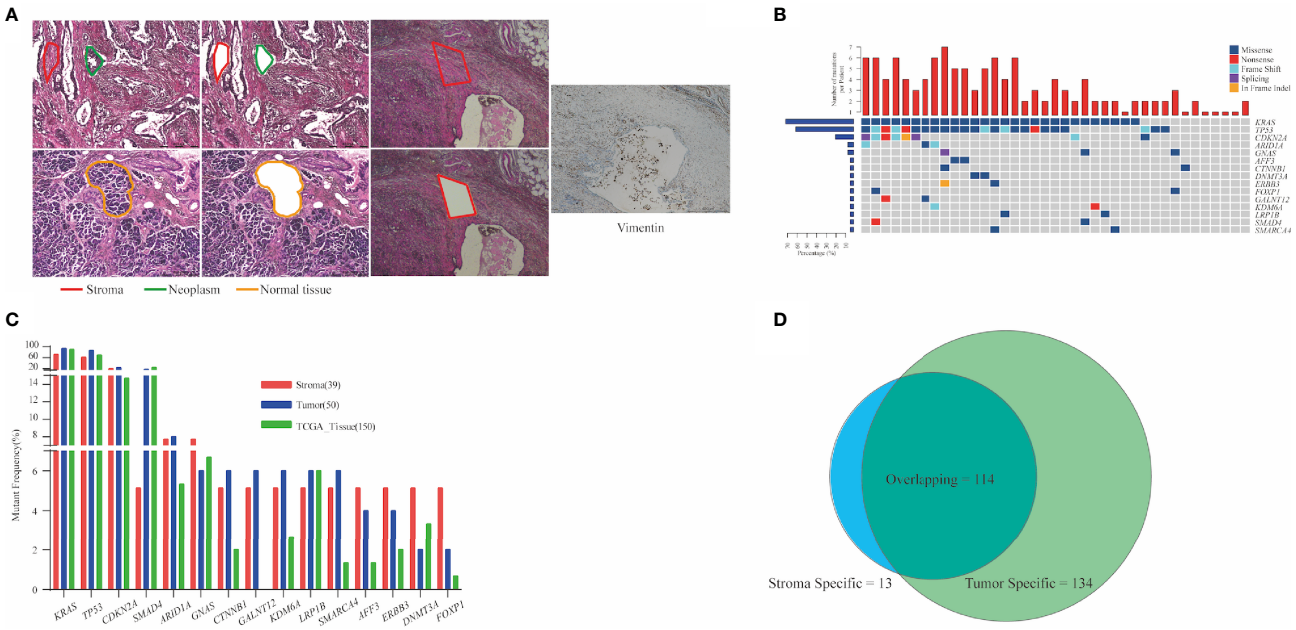

FIGURE 1 | Analysis of mutation detection in stromal components. **(A)** Representative schematic diagram showing the three components of PDAC: the neoplastic, stroma, and normal pancreatic components. Vimentin was enriched in stromal components. **(B)** Mutational prevalence of stromal components. Top 15 genes mutated in over two stroma specimens are shown. In total, 127 somatic mutations were detected in stromal components from 39 patients. *KRAS* (71.8%), *TP53* (61.5%), and *CDKN2A* (23.1%) were the most recurrent mutant genes. Top bars indicate the number of mutations. Left-hand bars represent the frequency of each gene. Hot plot shows the detailed mutations detected in each patient. **(C)** Comparison of mutant frequencies of top 15 genes in stroma, tumor, and public TCGA database. Altered *KRAS* and *TP53* were the most commonly altered genes and demonstrated concordance in three cohorts. **(D)** Common mutations in stromal and matched neoplastic components; 89.8% mutations in stroma also co-existed in matched neoplastic components. Thirteen stromal mutations were absent in matched neoplastic components, while 134 mutations were exclusive to the neoplastic components. PDAC, pancreatic ductal adenocarcinoma; TCGA, The Cancer Genome Atlas.

TP53 (n = 24, 61.5%), and *CDKN2A* (n = 9, 23.1%) were the most recurrent mutant genes (**Figure 1B**). All of *KRAS* mutations were located in the hot spot codons 12 and 61, including G12C (n = 1), G12D (n = 11), G12R (n = 2), G12V (n = 12), Q61H (n = 2), and Q61R (n = 1) (**Figure S1**). Two *KRAS* mutations (G12R and G12V) co-existed in P05. Twenty-one *TP53* mutations (87.5%) occurred in DNA-binding domain (**Figure S1**). As the top two prevalent mutant genes, *KRAS* and *TP53* were co-altered in 21 patients (**Figure 1B**).

Droplet digital PCR (ddPCR) was used to verify the credibility of stromal mutations, and the most common mutation site (*KRAS* G12D/V) from seven stromal specimens with different VAF range was selected. As the results, all of seven mutations were indeed repeated *via* ddPCR, and the VAFs estimated by ddPCR and NGS demonstrated strong consistency ($R^2 = 0.9067$, $p = 0.0009$, **Figure S2**).

Correlation between clinical characteristics and genomic alterations of the stroma was then explored. The stroma was more likely to be genomically altered in patients without vascular invasion than in those with vascular invasion ($p = 0.0464$, **Table 1**). Mutants *KRAS* ($p = 0.0036$) and *TP53* ($p = 0.0101$), as well as co-mutants *KRAS* and *TP53* ($p = 0.0029$), more likely occurred in older patients than in younger ones, although the distribution of age at diagnosis suggests no discrepancy between patients with and without stromal mutations (**Table 1**). Nevertheless, there was no significant correlation between other baseline characteristics and mutations in stroma (**Table 1**).

Mutational Overlap Between Stromal and Matched Neoplastic Components

Next, a total of 248 mutations were detected from 50 neoplastic specimens (median = 5, ranged from 1 to 11, **Table S1**). Commonly altered genes in neoplastic components included *KRAS* (n = 47, 94.0%), *TP53* (n = 43, 86.0%), *CDKN2A* (n = 12, 24.0%), and *SMAD4* (n = 9, 18.0%) (**Figure S3**). We validated the mutation prevalence of both stromal and neoplastic components using TCGA data. Altered *KRAS* and *TP53* were the most commonly altered genes and demonstrated concordance in three cohorts, with less prevalence in the stroma than in the other two cohorts (71.2% and 61.5% in stroma, 94.0% and 86.0% in tumor, and 90.7% and 69.3% in TCGA) (**Figure 1C**).

Stromal mutations were further verified in matched neoplastic components. Overall, 114 mutations co-existed in both components. Thirteen stromal mutations were absent in matched neoplastic components, while 134 mutations were exclusive to the neoplastic components (**Figures 1D**, **S3**). Critical driver gene analysis and function prediction showed 71 candidate driver events (62.3%, 71/114) that occurred in nine genes, including

KRAS, *TP53*, *CDKN2A*, *ARID1A*, *GNAS*, *KDM6A*, *RNF43*, *SMAD4*, and *TGFBR2* (**Figure S4**). All mutations of *KRAS* and *TP53* in stroma were also identified in matched neoplasm, except one *KRAS* mutation in P05, which harbored two different *KRAS* mutations in the stroma (**Figure S3**). Furthermore, *KRAS* mutations identified in the neoplastic components were absent in matched stroma for 19 patients (38.0%). The same *TP53* mutations were identified in matched neoplastic components of only 19 patients (38.0%) (**Figure S3**). For 13 stroma-specific mutations, there were only two driver events (15.4%, *KRAS* G12V for P05, *SMAD4* W302* for P43, **Table S1**), while 57 driver events (42.5%) were underlined in 134 neoplasm-specific mutations. We further performed pathway enrichment analysis for stroma-specific and neoplasm-specific mutations using Kyoto Encyclopedia of Genes and Genomes (KEGG) resource. As a result, a more intimate connection with tumorigenesis and development was highlighted for neoplasm-specific mutations compared with stroma-specific mutations (**Figure S5**). Those co-existed mutations in both components indicated that cancer cells affected the genomic features of stroma *via* EMT. On the other hand, those non-tumor-related mutations in stromal components demonstrated that genomic variants indeed occurred in TME, which might be attributed to clonal evolution.

Clonality Analysis of Mutations

The TCF could impact the analysis of clonality. The correlation between TCF estimated by microimaging and the mutational status of the neoplasm and stroma were evaluated (**Figure 2A**). The TCF in patients with mutant stroma was significantly higher than in those with normal stroma (p = 0.0019, **Figure 2B**). However, the VAFs in neither stroma (**Figure S6A**) nor neoplasm (**Figure S6B**) were correlated with the TCF. Patients with *KRAS/TP53*-mut stroma also demonstrated a higher TCF than did those with wild-type stroma (p = 0.0371, p = 0.0014, **Figures 2C, D**). Nevertheless, no discrepancy was seen for patients with or without *KRAS/TP53*-mut neoplasm (**Figure S7**), possibly due to the extremely high detection rate of *KRAS* and *TP53* mutation in neoplastic components.

To eliminate the frequency bias between neoplastic and stromal mutations, we normalized the VAFs of each mutation (absolute VAF/maximum VAF in the same specimen) in paired stromal and neoplastic components. Mutations with ≥50.0% normalized VAFs were more likely to be clonal events and occurred early during development of stroma or neoplasm than those with <50.0% normalized VAFs. For 114 mutations common in both components, 99 mutations (86.8%) were clonal events in stroma, among which 96 (84.2%) presented ≥50.0% normalized VAFs in both neoplasm and stroma (**Figure 3A**). However, for 134 neoplasm-specific mutations, only 72 (53.7%) were clonal in neoplastic components (**Figure 3A**), significantly lower than the proportion of common mutations (χ^2 $p < 0.0001$).

In neoplastic and stromal components, 95.8% (46/48) and 89.7% (26/29) of *KRAS* mutations were clonal, respectively (**Figure 3A**). For mutant *TP53*, 97.7% (42/43) in neoplasm and 87.5% (21/24) in stroma were clonal variants (**Figure 3A**). The VAFs of *KRAS* and *TP53* mutations in the same stroma presented statistically significant consistency (Spearman's r^2 = 0.7481, p < 0.0001, **Figure 3B**), indicating that mutants *KRAS* and *TP53* might have co-occurred around the same early period. Moreover, stroma with co-occurred *KRAS* and *TP53* tended to harbor more mutations in stroma than the others (p < 0.0001) (**Figure 3C**). Similarly in neoplastic components, *KRAS* and *TP53* often co-altered and showed significant consistency (Spearman's r^2 = 0.6841, p < 0.0001, **Figure 3D**). More mutations were detected

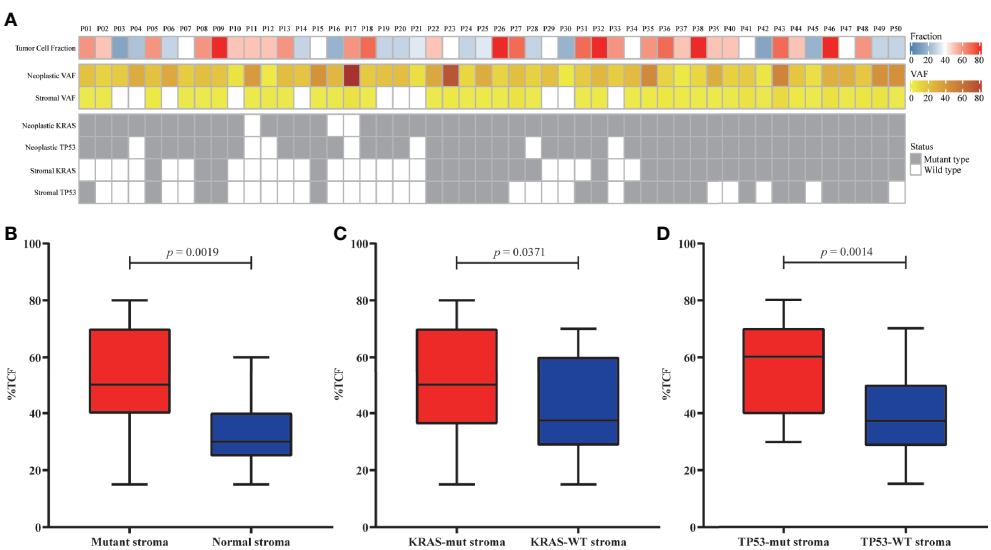

FIGURE 2 | Correlation between the tumor cell fraction (TCF) and genomic status. **(A)** Overview of the TCF, stroma/neoplastic VAF, and *KRAS/TP53* status for each patient. **(B–D)** Comparison of the TCF from patients with mutant or normal stroma **(B)**, with or without *KRAS* mutation **(C)**, and with or without *TP53* mutation **(D)**. VAF, variant allele frequency.

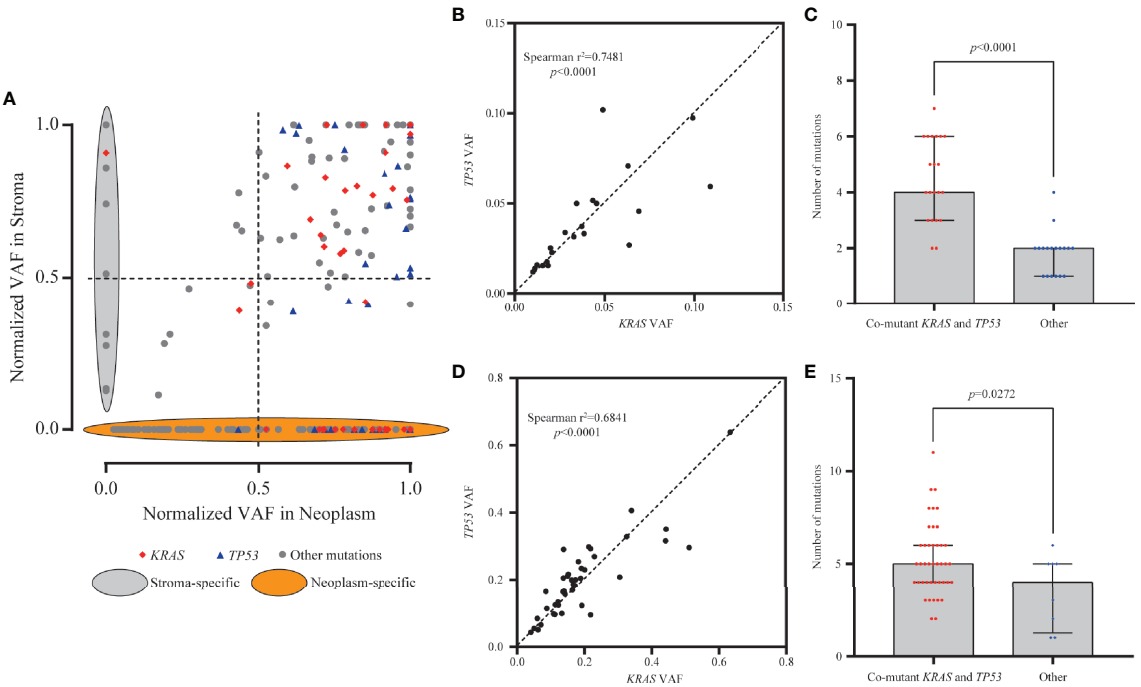

FIGURE 3 | Clonality and mutation burden analysis of *KRAS* in stromal and neoplastic components. **(A)** Variant allele frequencies (VAFs) of each mutation were normalized with maximum VAF in the same specimen to assess the clonality. Mutations with ≥50% normalized VAFs were more likely to be clonal events; 86.8% of common mutations were clonal events in stroma. **(B, D)** The VAFs of *KRAS* and *TP53* mutations showed statistically significant consistency in the stromal (Spearman's $r^2 = 0.7481$, $p < 0.0001$) and neoplastic (Spearman's $r^2 = 0.6841$, $p < 0.0001$) components, indicating that mutants *KRAS* and *TP53* might have co-occurred around the same early period. **(C, E)** Samples with co-mutants *KRAS* and *TP53* tended to harbor more mutations than the other mutant subtype samples, in both stromal ($p < 0.0001$) and neoplastic ($p = 0.0272$) components.

in neoplasm with co-mutations than those without co-mutations ($p = 0.0272$, **Figure 3E**). Altogether, these results indicated that the neoplasm and adjacent stroma were likely to share the similar clonal trunk events, especially for mutants *KRAS* and *TP53*, during the early tumorigenesis.

Subsequently, PyClone strategy was utilized to reconstruct the evolutionary trajectory for neoplastic components. Ultimately, four subtypes were clarified for patients according to the genetic and driver imprinting derived from neoplasm upon stroma. The first type (A) included 12 patients characterized by the overall genomic and evolutional concordance, indicating that all neoplastic clones and driver events could be identified in stroma (**Figures 4A**, **S8A**). The second type (B) included 20 patients, and all stroma harbored the neoplastic initial clones and driver events but lacked some of subsequent clones (**Figures 4B**, **S8B**). The third type (C) involving five patients demonstrated total absence of neoplastic mutations in stroma (**Figures 4C**, **S8C**). The fourth type (D) included only two patients. For the first patient, the initial clone was absent, but a driver mutation (*RNF43* K568Sfs*132) involved in a latter clone was identified in stroma (**Figure 4D**). For the second patient, the initial neoplastic clone indeed expressed in stroma, but no driver mutation was identified (**Figure S8D**). Of note, patients with mutants *KRAS* and *TP53* in stroma were either type A or B. There was no significant discrepancy of TCF among the four different subtypes (**Figure S9**). Overall, type A/B was defined as neoplasm-like stroma based on the similar genetic performance and evolutional entanglements between neoplastic and stromal components.

KRAS Mutation Promotes Mesenchymal Transformation of Epithelial Cancer Cell

Epithelial cancer cell were observed to migrate into the stroma and transformed to mesenchymal phenotype *via* EMT in a PanIN mouse model carried *KRAS* mutation (9). Based on this study and aforementioned findings, multi-lineage differentiation potential and mesenchymal transformation of *KRAS*-mutant cell line Panc1 were evaluated to validate this result. After 3 days of cell culture in DMEM with 5 and 25 μM of dextrose, five regulator markers of cell pluripotency involving OCT4, BMI1, NANOG, SOX2, and CD24 were detected by RT-PCR. These five markers exhibited significant increase in the 25 μM group compared with the 5 μM group (**Figure 5A**). Furthermore, the expression of E-cadherin was significantly decreased while β-catenin was significantly increased in a high-nutrient environment, indicating the progress of EMT and cell migration (**Figure 5A**). Subsequently, immunofluorescent staining revealed an enhanced expression of vimentin in the 25 μM dextrose group but absent in the 5 μM dextrose group (**Figure 5B**). Those findings indicated that a fraction of tumor cells harbor multi-lineage differentiation potential and that *KRAS* mutation might facilitate this process.

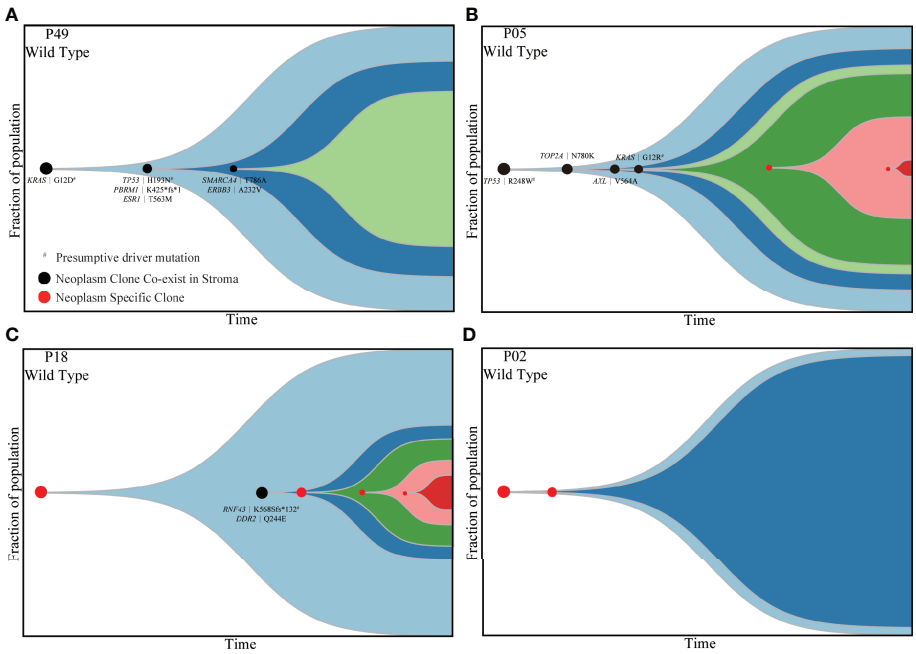

FIGURE 4 | Four types of patients demonstrating different evolutionary trajectories involving both stroma and neoplastic components. P49 **(A)**, P05 **(B)**, P18 **(C)** and P02 **(D)** presented four different subtypes of evolutionary trajectory. The black dots indicate clones shared by matched stroma and neoplasm. The red dots represent clones private to neoplastic components. The black characters indicate mutations shared by matched stromal and neoplastic components. The emergence and progression pattern of each clone are hypothesized according to the fraction of clonal population inferred from the average VAF of mutations involved in the same clone. VAF, variant allele frequency.

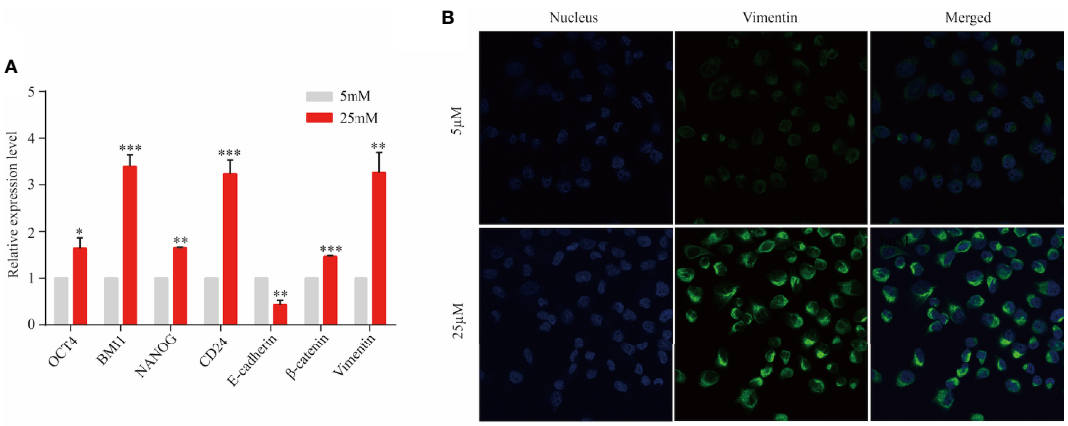

FIGURE 5 | *KRAS*-mutant tumor cells might transform into stem-like cells. Panc1 cells were cultured for 3 days in the presence of 5 or 25 μM of dextrose. **(A)** The expression level of OCT4, BMI1, NANOG, SOX2, CD24, E-cadherin, β-catenin, and vimentin was detected by RT-PCR. Data are presented as mean ± SEM of three independent experiments. **(B)** Vimentin expression was analyzed by immunofluorescent staining (blue, nucleus; green, vimentin). Original magnification ×600. $^{*}p < 0.05$, $^{**}p < 0.005$, $^{***}p < 0.0005$.

Genomic Status of Stroma Associated With the Postoperative Survival of Pancreatic Ductal Adenocarcinoma

The association between DFS and genomic status of stroma, as well as multiple clinicopathologic risk factors of PDAC, was analyzed for 32 patients who were followed up over 1 year after surgical operation. The Kaplan–Meier analysis showed that 32 patients with neoplasm-like stroma had a markedly reduced DFS time (median = 3.9 months) than had the other patients (median DFS unreached, hazard ratio = 3.079, 95% CI 1.126 to 7.215,

p = 0.0193, **Figure 6A**). We further evaluated whether stromal *KRAS* mutations were associated with postoperative survival. As the results, patients with *KRAS*-mutant stroma had a significantly poorer DFS time (median = 3.9 months) than those with *KRAS*-wild-type stroma (median DFS unreached, hazard ratio = 3.304, 95% CI 1.247 to 8.751, p = 0.0162, **Figure 6B**), which was also confirmed by multivariate analysis (hazard ratio = 2.962, 95% CI 1.174 to 7.471, p = 0.021, **Table 2**). Patients with *TP53*-mutant stroma also showed poorer DFS time (median = 3.8 months) than those with *TP53*-wild-type stroma (median DFS unreached, hazard ratio = 3.143, 95% CI 1.112 to 8.880, p = 0.0307). However, although exhibiting a certain trend in univariate analysis, all clinicopathologic risk factors of PDAC, including clinical stage, tumor size, histological differentiation, lymph node involvement, nerve, and vasculature invasion, showed no significant association with DFS in univariate and multivariate analyses (**Figure S10**, **Table 2**).

DISCUSSION

The tumor stroma has important roles in cancer development, progression, and metastasis (17). Although previous studies demonstrated the complex biophysical and transcriptional properties of stroma for patients with PDAC (18, 19), little evidence supports the clinical relevance of stroma genomic characteristics at present. In this study, we hypothesized that genomic mutations existed in stroma and might contribute to the clinical outcome of resectable PDAC. We identified 127 somatic mutations in stromal components separated by LCM methods and found *KRAS* mutations were highly prevalent and widely clonal in stroma. Subtyping based on genomic features, neoplasm-like, and *KRAS*-mutant stroma was associated with poor DFS.

As its first objective, our study initially reported the genomic alterations in the stroma and defined four subtypes according to

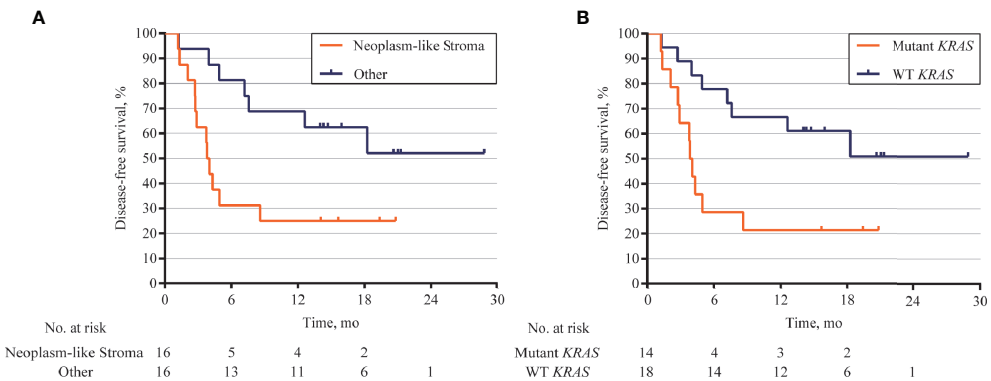

FIGURE 6 | Kaplan–Meier curves for disease-free survival (DFS) according to genomic status of stroma. **(A)** DFS analysis in 32 patients followed up over 1 year after surgical operation. Patients with neoplasm-like stroma had markedly short DFS (median = 3.9 months) than those without neoplasm-like stroma (median DFS unreached, hazard ratio = 3.079, 95% CI 1.126 to 7.215, p = 0.0193). **(B)** Patients with *KRAS*-mutant stroma also showed poor DFS (median = 3.9 months) than those with *KRAS*-wild-type stroma (median DFS unreached, hazard ratio = 3.304, 95% CI 1.247 to 8.751, p = 0.0162).

TABLE 2 | Univariate and multivariate Cox analyses for risk factors of relapse.

Variables	Univariate analysis		Multivariate analysis	
	HR (95% CI)	*p*	HR (95% CI)	*p*
Clinical stage, II/IV *vs*. I	0.73 (0.30–1.80)	0.492	–	–
Tumor size, >4 *vs*. ≤4 cm	0.53 (0.13–2.16)	0.378	–	–
Differentiation, poor *vs*. other	2.00 (0.80–4.87)	0.142	–	–
Lymph node metastasis, Positive *vs*. negative	2.05 (0.75–5.62)	0.164	–	–
Nerve invasion, positive *vs*. negative	2.43 (0.89–6.65)	0.085	–	–
Vascular invasion, positive *vs*. negative	1.93 (0.76–4.92)	0.169	–	–
Adjuvant chemotherapy, positive *vs*. negative	0.90 (0.36–2.28)	0.831	–	–
KRAS status in stroma, Mutant type *vs*. wild type	3.30 (1.25–8.75)	0.016*	2.96 (1.17–7.47)	0.021*,[a]

Statistical significance.

[a]*Multivariate analysis was performed using method Forward: LR.*

the genetic and driver imprinting derived from neoplasm upon stroma for patients with PDAC. In view of the substantial mutations shared by tumor and stroma and the clonal relationship of two components, the stromal cells with shared mutations derived from the common progenitor with neoplastic cells, supporting that tumor cells affected the genomic features of stroma *via* EMT. Interestingly, stromal and neoplastic cells also experienced divergent evolution because of the emerged private genetic variants in both components. Rhim et al. reported that tagged epithelial cells invaded stroma prior to tumor formation and transformed to mesenchymal phenotype at early stage of PDAC, which is consistent with our results (9). Although the cellular morphology persists as "normal stromal cells," the genetically and functionally neoplasm-like variants indicate the real status of stroma and distinguish different subtypes of PDAC for prognostic prediction. Activated stroma could promote the acquisition of more genetic and epigenetic changes in tumor cells and induce cancer development (20, 21). On the other side, autonomously genomic changes in the stroma were also suggested to induce tumorigenesis (22).

As a critical driver gene in early tumorigenesis (23), *KRAS* mutations were detected in stromal components from 28 PDAC (71.8%) cases, and 89.7% of these mutations were clonal events. Rhim et al. also reported that epithelial cancer cells can transform to mesenchymal phenotype and invade stroma in a PanIN mouse model that carried *KRAS* mutation (9). Based on these results, *KRAS*-mutant tumor cells might have more aggressive behavior on tumor progression and then affect the stroma genomic features *via* EMT; thus, we conducted some experiments to validate this condition *in vitro*. Results showed that *KRAS*-mutant tumor cells harbored higher multi-lineage differentiation potential and promote tumorigenesis *via* EMT, which was consistent with the above hypothesis. However, further mechanism needs to be explored by future fundamental researches, which can help in clarifying the underlying mechanisms and thus improving the therapeutic strategies for PDAC patients.

The outcome for resectable PDAC remains dismal despite improvements in surgical and oncological management strategies. In many cases, patients with similar clinicopathologic characteristics benefit variably in surgery outcome. Also, there is a lack of clear clinicopathologic evidence to guide clinicians to determine the therapeutic options before and after resection. Nowadays, resectability of PDAC has traditionally been assessed with geometric descriptions of the tumor–vessel interface (24). Despite recent therapeutic improvements, postoperative prognosis of PDAC remains very poor (25). Many clinicopathologic and serologic markers have been tested, but none is highly prognostic for PDAC patients (26). The genetic involvement between tumor and stroma seems associated with PDAC prognosis. In this study, we found that patients with *KRAS*-mutant stroma had a considerable risk of postoperative recurrence, and their survival was evidently worse than that of the other patients. If our results can be corroborated in a much larger prospective study, then analysis of driver mutation in PDAC stroma might help to guide a more precise treatment paradigm in adjuvant therapeutic options. For patients with neoplasm-like stroma, cutting off the crosstalk between neoplasm and stroma before conventional agents might improve their poor performance with PDAC. Furthermore, 94% patients harbor *KRAS* mutation in neoplasm, and prognosis of PDAC due to the extremely high mutant frequency failed to be predicted. Therefore, this stroma biomarker had evident advantage over conventional and tumor biomarkers, such as a more precise and accurate distinction of tumor prognosis.

Considering the complex immune environment in the stroma, another possible reason for worse prognosis is that such cancer-associated driver mutations in stroma may act to attenuate immune responses (27). Actually, it has been reported that mutations in the *KRAS* will activate the MAP kinase pathway and thus decrease the transcription of major histocompatibility complex class I molecules as well as the expression of other genes encoding molecules that are essential for peptide loading (28). In this case, cells harboring driver mutations might escape from immune response and act as the "bridgehead" to invade adjacent tissue and metastasize. These alterations might reduce inflammation in tumors and the killing of tumor cells by decreasing the density of T-cell ligands on tumor cells. The stiff extracellular matrix in stroma has a role as the bridge mediating the interactions between neoplasm and stroma, as well as the protector of tumor cells away from immune clearance and pharmacological effects (29). Therefore, several pro-fibrotic growth factors, such as TGF-β, PDGF, EGFR, and IGF-1, can be recruited as potential therapeutic targets to abolish such interactions and protections. Followed by these novel efforts, conventional chemoradiotherapy might achieve a much better effect for PDAC patients. Based on this finding, it may be useful to investigate the immune status of stroma for better understanding the prognostic effect of stromal *KRAS* mutations, which is in our plan.

Some limitations of this study persist. First, the follow-up time was short for some patients, and it still did not reach the median of overall survival, so the data were not efficiently utilized yet. Second, the limited morbidity of PDAC and the attribute of single-center study resulted in the relatively small sample size. To solve these problems, we have planned a multi-center study based on available results. Overall DFS and postoperative DFS are the primary and second endpoints, respectively. In order to further verify the results, we drew in this study. Third, to establish clinical utility of detecting mutations in stroma, the techniques applied here would also require improvement to satisfy feasibility for routine use. However, despite these limitations, this study can clearly indicate the genetic interaction between neoplastic and stromal components due to the normalized experimental and analytical procedures.

In this study, we performed parallel genotyping of stromal and neoplastic components and evaluated the prognostic ability of stromal markers for PDAC patients. We clarified the hereditary and evolutional connection between neoplasm and stroma, explored a novel prognostic marker based on stromal genomic status, and validated that *KRAS*-mutant stroma cells might derive from tumor cells with multi-lineage differentiation

potential and promote tumorigenesis *via* EMT. Although it is currently complex and beyond routine clinical use to obtain stroma by LCM technique, we hope these efforts will be helpful to improve clinical management for PDAC patients in the near future.

In conclusion, a considerable proportion of PDAC stroma exhibit cancer-associated driver mutations, and four molecular subtypes were clarified according to the evolutional connection between neoplasm and stroma. Stromal *KRAS* mutations may serve as prognostic biomarkers in resectable PDAC and might help to guide a more precise treatment paradigm in therapeutic options.

DATA AVAILABILITY STATEMENT

The datasets presented in this study can be found in online repositories. The names of the repository/repositories and accession number(s) can be found in https://www.ncbi.nlm.nih.gov/, PRJNA561217.

ETHICS STATEMENT

The studies involving human participants were reviewed and approved by Zhejiang Provincial People's Hospital (No. 2016KY129). The patients/participants provided their written informed consent to participate in this study.

AUTHOR CONTRIBUTIONS

JJ, YX, and LiuY contributed to conception and design of the study. JJ, XX and XY organized the database. JJ, GR, and LC performed the statistical analysis. JJ, YX, and LiuY wrote the first draft of the manuscript. JJ, YX, ZC, D-SH and LinY wrote sections of the manuscript. All authors contributed to manuscript revision and read and approved the submitted version.

FUNDING

This work was supported by the National Natural Science Foundation of China (Nos. 81772575, 81972455) and the Foundation of Science Technology Department of Zhejiang Province (No. 2017C33116).

ACKNOWLEDGMENTS

The authors would like to acknowledge all department colleagues for their constructive suggestions.

SUPPLEMENTARY MATERIAL

The Supplementary Material for this article can be found online at: https://www.frontiersin.org/articles/10.3389/fonc.2021.771247/full#supplementary-material

REFERENCES

1. Bray F, Ferlay J, Soerjomataram I, Siegel RL, Torre LA, Jemal A. Global Cancer Statistics 2018: GLOBOCAN Estimates of Incidence and Mortality Worldwide for 36 Cancers in 185 Countries. *CA: Cancer J Clin* (2018) 68 (6):394–424. doi: 10.3322/caac.21492
2. Ryan DP, Hong TS, Bardeesy N. Pancreatic Adenocarcinoma. *N Engl J Med* (2014) 371(11):1039–49. doi: 10.1056/NEJMra1404198
3. Sugiura T, Uesaka K, Kanemoto H, Mizuno T, Sasaki K, Furukawa H, et al. Serum CA19-9 Is a Significant Predictor Among Preoperative Parameters for Early Recurrence After Resection of Pancreatic Adenocarcinoma. *J Gastrointest Surg: Off J Soc Surg Alimentary Tract* (2012) 16(5):977–85. doi: 10.1007/s11605-012-1859-9
4. Osayi SN, Bloomston M, Schmidt CM, Ellison EC, Muscarella P. Biomarkers as Predictors of Recurrence Following Curative Resection for Pancreatic Ductal Adenocarcinoma: A Review. *BioMed Res Int* (2014) 2014:468959. doi: 10.1155/2014/468959
5. Grivennikov SI, Wang K, Mucida D, Stewart CA, Schnabl B, Jauch D, et al. Adenoma-Linked Barrier Defects and Microbial Products Drive IL-23/IL-17-Mediated Tumour Growth. *Nature* (2012) 491(7423):254–8. doi: 10.1038/nature11465
6. Bahrami A, Khazaei M, Bagherieh F, Ghayour-Mobarhan M, Maftouh M, Hassanian SM, et al. Targeting Stroma in Pancreatic Cancer: Promises and Failures of Targeted Therapies. *J Cell Physiol* (2017) 232(11):2931–7. doi: 10.1002/jcp.25798
7. Li B, Wang Y, Jiang H, Li B, Shi X, Gao S, et al. Pros and Cons: High Proportion of Stromal Component Indicates Better Prognosis in Patients With Pancreatic Ductal Adenocarcinoma-a Research Based on the Evaluation of Whole-Mount Histological Slides. *Front Oncol* (2020) 10:1472. doi: 10.3389/fonc.2020.01472
8. Polyak K, Weinberg RA. Transitions Between Epithelial and Mesenchymal States: Acquisition of Malignant and Stem Cell Traits. *Nat Rev Cancer* (2009) 9(4):265–73. doi: 10.1038/nrc2620
9. Rhim AD, Mirek ET, Aiello NM, Maitra A, Bailey JM, McAllister F, et al. EMT and Dissemination Precede Pancreatic Tumor Formation. *Cell* (2012) 148(1-2):349–61. doi: 10.1016/j.cell.2011.11.025
10. Adsay NV, Bagci P, Tajiri T, Oliva I, Ohike N, Balci S, et al. Pathologic Staging of Pancreatic, Ampullary, Biliary, and Gallbladder Cancers: Pitfalls and Practical Limitations of the Current AJCC/UICC TNM Staging System and Opportunities for Improvement. *Semin Diagn Pathol* (2012) 29(3):127–41. doi: 10.1053/j.semdp.2012.08.010
11. Vandenbroucke JP, von Elm E, Altman DG, Gotzsche PC, Mulrow CD, Pocock SJ, et al. Strengthening the Reporting of Observational Studies in Epidemiology (STROBE): Explanation and Elaboration. *Epidemiology* (2007) 18(6):805–35. doi: 10.1097/EDE.0b013e3181577511
12. Maurer C, Holmstrom SR, He J, Laise P, Su T, Ahmed A, et al. Experimental Microdissection Enables Functional Harmonisation of Pancreatic Cancer Subtypes. *Gut* (2019) 68(6):1034–43. doi: 10.1136/gutjnl-2018-317706
13. Lv X, Zhao M, Yi Y, Zhang L, Guan Y, Liu T, et al. Detection of Rare Mutations in Ctdna Using Next Generation Sequencing. *JoVE* (2017) 24 (126):56342. doi: 10.3791/56342
14. Kandoth C, McLellan MD, Vandin F, Ye K, Niu B, Lu C, et al. Mutational Landscape and Significance Across 12 Major Cancer Types. *Nature* (2013) 502 (7471):333–9. doi: 10.1038/nature12634
15. Bailey MH, Tokheim C, Porta-Pardo E, Sengupta S, Bertrand D, Weerasinghe A, et al. Comprehensive Characterization of Cancer Driver Genes and Mutations. *Cell* (2018) 173(2):371–85.e18. doi: 10.1016/j.cell.2018.02.060
16. Nobis M, Herrmann D, Warren SC, Kadir S, Leung W, Killen M, et al. A Rhoa-FRET Biosensor Mouse for Intravital Imaging in Normal Tissue

Homeostasis and Disease Contexts. *Cell Rep* (2017) 21(1):274–88. doi: 10.1016/j.celrep.2017.09.022
17. Neesse A, Algul H, Tuveson DA, Gress TM. Stromal Biology and Therapy in Pancreatic Cancer: A Changing Paradigm. *Gut* (2015) 64(9):1476–84. doi: 10.1136/gutjnl-2015-309304
18. Knudsen ES, Vail P, Balaji U, Ngo H, Botros IW, Makarov V, et al. Stratification of Pancreatic Ductal Adenocarcinoma: Combinatorial Genetic, Stromal, and Immunologic Markers. *Clin Cancer Res: an Off J Am Assoc Cancer Res* (2017) 23(15):4429–40. doi: 10.1158/1078-0432.CCR-17-0162
19. Tian H, Callahan CA, DuPree KJ, Darbonne WC, Ahn CP, Scales SJ, et al. Hedgehog Signaling Is Restricted to the Stromal Compartment During Pancreatic Carcinogenesis. *Proc Natl Acad Sci USA* (2009) 106(11):4254–9. doi: 10.1073/pnas.0813203106
20. Hanson JA, Gillespie JW, Grover A, Tangrea MA, Chuaqui RF, Emmert-Buck MR, et al. Gene Promoter Methylation in Prostate Tumor-Associated Stromal Cells. *J Natl Cancer Instit* (2006) 98(4):255–61. doi: 10.1093/jnci/djj051
21. Lin HJ, Zuo T, Lin CH, Kuo CT, Liyanarachchi S, Sun S, et al. Breast Cancer-Associated Fibroblasts Confer AKT1-Mediated Epigenetic Silencing of Cystatin M in Epithelial Cells. *Cancer Res* (2008) 68(24):10257–66. doi: 10.1158/0008-5472.CAN-08-0288
22. Campbell I, Qiu W, Haviv I. Genetic Changes in Tumour Microenvironments. *J Pathol* (2011) 223(4):450–8. doi: 10.1002/path.2842
23. Mueller S, Engleitner T, Maresch R, Zukowska M, Lange S, Kaltenbacher T, et al. Evolutionary Routes and KRAS Dosage Define Pancreatic Cancer Phenotypes. *Nature* (2018) 554(7690):62–8. doi: 10.1038/nature25459
24. Ferrone CR, Marchegiani G, Hong TS, Ryan DP, Deshpande V, McDonnell EI, et al. Radiological and Surgical Implications of Neoadjuvant Treatment With FOLFIRINOX for Locally Advanced and Borderline Resectable Pancreatic Cancer. *Ann Surg* (2015) 261(1):12–7. doi: 10.1097/SLA.0000000000000867
25. Neesse A, Bauer CA, Ohlund D, Lauth M, Buchholz M, Michl P, et al. Stromal Biology and Therapy in Pancreatic Cancer: Ready for Clinical Translation? *Gut* (2019) 68(1):159–71. doi: 10.1136/gutjnl-2018-316451
26. McGuigan A, Kelly P, Turkington RC, Jones C, Coleman HG, McCain RS. Pancreatic Cancer: A Review of Clinical Diagnosis, Epidemiology, Treatment and Outcomes. *World J Gastroenterol* (2018) 24(43):4846–61. doi: 10.3748/wjg.v24.i43.4846
27. Chen DS, Mellman I. Elements of Cancer Immunity and the Cancer-Immune Set Point. *Nature* (2017) 541(7637):321–30. doi: 10.1038/nature21349
28. Atkins D, Breuckmann A, Schmahl GE, Binner P, Ferrone S, Krummenauer F, et al. MHC Class I Antigen Processing Pathway Defects, Ras Mutations and Disease Stage in Colorectal Carcinoma. *Int J Cancer* (2004) 109(2):265–73. doi: 10.1002/ijc.11681
29. Weniger M, Honselmann KC, Liss AS. The Extracellular Matrix and Pancreatic Cancer: A Complex Relationship. *Cancers* (2018) 10(9):316. doi: 10.3390/cancers10090316

Conflict of Interest: Authors YX, LC, XX, LinY, XY were employed by company Geneplus-Beijing Institute.

The remaining authors declare that the research was conducted in the absence of any commercial or financial relationships that could be construed as a potential conflict of interest.

frontiers in Oncology

REVIEW
published: 25 October 2021
doi: 10.3389/fonc.2021.765216

Long Noncoding Competing Endogenous RNA Networks in Pancreatic Cancer

Guangbing Xiong†, Shutao Pan†, Jikuan Jin, Xiaoxiang Wang, Ruizhi He, Feng Peng, Xu Li, Min Wang, Jianwei Zheng, Feng Zhu* and Renyi Qin**

Department of Biliary-Pancreatic Surgery, Tongji Hospital, Tongji Medical College, Huazhong University of Science and Technology, Wuhan, China

OPEN ACCESS

Edited by:
Taiping Zhang,
Peking Union Medical College Hospital (CAMS), China

Reviewed by:
Gang Xu,
Sichuan University, China
Song Gao,
Tianjin Medical University Cancer Institute and Hospital, China

***Correspondence:**
Jianwei Zheng
54260192@qq.com
Feng Zhu
zfjch1977@163.com
Renyi Qin
ryqin@tjh.tjmu.edu.cn

†These authors have contributed equally to this work and share first authorship

Specialty section:
This article was submitted to Gastrointestinal Cancers: Hepato Pancreatic Biliary Cancers, a section of the journal Frontiers in Oncology

Received: *26 August 2021*
Accepted: *20 September 2021*
Published: *25 October 2021*

Citation:
Xiong G, Pan S, Jin J, Wang X, He R, Peng F, Li X, Wang M, Zheng J, Zhu F and Qin R (2021) Long Noncoding Competing Endogenous RNA Networks in Pancreatic Cancer. Front. Oncol. 11:765216. doi: 10.3389/fonc.2021.765216

Pancreatic cancer (PC) is a highly malignant disease characterized by insidious onset, rapid progress, and poor therapeutic effects. The molecular mechanisms associated with PC initiation and progression are largely insufficient, hampering the exploitation of novel diagnostic biomarkers and development of efficient therapeutic strategies. Emerging evidence recently reveals that noncoding RNAs (ncRNAs), including long ncRNAs (lncRNAs) and microRNAs (miRNAs), extensively participate in PC pathogenesis. Specifically, lncRNAs can function as competing endogenous RNAs (ceRNAs), competitively sequestering miRNAs, therefore modulating the expression levels of their downstream target genes. Such complex lncRNA/miRNA/mRNA networks, namely, ceRNA networks, play crucial roles in the biological processes of PC by regulating cell growth and survival, epithelial–mesenchymal transition and metastasis, cancer stem cell maintenance, metabolism, autophagy, chemoresistance, and angiogenesis. In this review, the emerging knowledge on the lncRNA-associated ceRNA networks involved in PC initiation and progression will be summarized, and the potentials of the competitive crosstalk as diagnostic, prognostic, and therapeutic targets will be comprehensively discussed.

Keywords: pancreatic cancer, long noncoding RNA, microRNA, competing endogenous RNA, network

INTRODUCTION

Pancreatic cancer (PC) is a highly aggressive malignancy with a dismal prognosis and limited treatment options worldwide (1). According to cancer statistics, it is the fourth leading cause of cancer-related deaths in the USA, with an overall 5-year survival rate of 8% and a median survival time of 6 months (2). Patients are often asymptomatic, and approximately 80%–85% of PC patients have unresectable or metastatic lesions at the time of initial diagnosis. Surgical resection remains the exclusive potential curative treatment. Owing to the aggressive nature of this neoplasm, early postoperative recurrence and occult metastasis also reduce the efficacy of surgical treatment, and only approximately 20% of patients treated with postoperative adjuvant chemotherapy can survive for 5 years (3). Systemic chemotherapy is indispensable in the treatment of advanced or metastatic PC. Despite many attempts to optimize the chemotherapeutic regimens for PC in clinical studies, such as FOLFIRINOX (fluorouracil, leucovorin, oxaliplatin, and irinotecan), gemcitabine/Nab-paclitaxel,

gemcitabine/erlotinib, gemcitabine/capecitabine, and capecitabine/oxaliplatin (XELOX), the increase in the overall survival rate is still poor. By contrast, there is little evidence to support the efficacy of radiotherapy in the treatment of PC (4). Thus, there is an urgent need for a better understanding of the molecular mechanisms of PC to improve patient prognosis.

Although several genes and pathways have been found to be involved in the occurrence and progression of PC, the underlying mechanisms remain unclear. According to previous studies, the mutations of the driver genes in the sentinel cell are the primary cause of tumor initiation (5, 6). These genetic alterations in the oncogene Kirsten RAt Sarcoma virus (*KRAS*) and tumor suppressor genes such as tumor protein 53 (*TP53*), cyclin-dependent kinase inhibitor 2A (*CDKN2A*), and Smad4 together lead to the occurrence of PC (7). *KRAS* mutations, which occur in more than 90% of PCs, are one of the most frequent oncogene changes associated with PC development (8, 9). Subsequently, at the later stage compared with the *KRAS* mutation, the inactivation of *TP53*, *CDKN2A*, and *Smad4* plays a key role in the pathogenesis and invasion of PC (10). Accumulating studies have revealed that the disorders of various signaling pathways mediate changes in the tumor stromal cells, and this process is closely associated with the occurrence and progression of PC (11, 12). Mutations in *KRAS* and epidermal growth factor receptor (EGFR) can activate different signaling pathways including renin-angiotensin system/ rapidly accelerated fibrosarcoma/Mitogen-activated protein kinase kinase/extracellular-signalregulated protein kinase (Ras/Raf/MEK/ ERK) and phosphatidylinositol-3-kinase (PI3K)/Akt (13, 14). In recent studies, targeting and regulating the key signaling molecules in these pathways have become a hot research topic for improving PC therapy (13). In addition, during the progression of PC, there are dysregulations of important signaling pathways such as EGFR/ mitogen-activated protein kinase (MAPK), tumor necrosis factor-related apoptosis-inducing ligand/ tumor necrosis factor receptor associated factor 2 (TRAIL/TRAF2), and Ikappa B kinase/nuclear factor-κ-gene binding (IKK/NF-κB), and in these signaling pathways, not only the apoptosis-inhibiting related proteins but also the expression of many other molecules including B-cell lymphoma-2 (Bcl-2), baculoviral IAP repeat containing 5/ (BIRC5), inhibitor of apoptosis protein 3 (IAP3), and cellular inhibitor of apoptosis protein (cIAP) has changed (15). At present, the research on PC-related pathways has become more attractive.

According to previous reports, most RNAs do not encode proteins (16). These noncoding RNAs (ncRNAs) can be divided into long noncoding RNAs (lncRNAs), circular RNAs (circRNAs), microRNA (miRNA), enhancer ncRNAs, etc., and are closely related to a variety of malignant tumors including PC (17, 18). With the support of innovative technologies such as high-throughput RNA sequencing, a large number of ncRNAs have been discovered and clearly classified (19). The ncRNAs play important roles in a variety of biological processes and have regulatory function in the process of transcription and posttranscriptional gene expression (20). The dysregulation of ncRNAs affects many cellular processes including signal transduction, posttranscriptional modifications, and chromatin remodeling, which is closely related to the occurrence and development of various cancers (21, 22). In addition to acting as tumor suppressors or oncogenic driver genes in a variety of malignant tumors, ncRNAs also regulate various molecules in the signaling pathways to exert effects (23, 24). The aberrant expression of ncRNAs participates in the regulation of drug resistance, cell invasion, metastasis, and other processes, which ultimately affects the development of PC (25–27). There are also interactions between different RNAs, and studying the interactions of RNAs may be helpful for the further understanding of PC pathogenesis (28, 29). In recent years, studies have reported the correlation between the aberrant expression levels of different ncRNAs in PC, including the interaction between mRNA and ncRNAs, basing on the competing endogenous RNAs (ceRNA) hypothesis (29, 30).

THE ceRNA HYPOTHESIS IN CANCERS

MiRNAs are short endogenous RNAs with a length of approximately 21–23 nt (31). The binding sites of miRNAs are called miRNA recognition elements (MREs), which are most commonly found in the 3′-untranslated regions (3′-UTRs) of RNA transcripts such as mRNA (32). In the traditional concept, miRNAs, as the regulatory molecules of the gene expression, bind to the MREs on the mRNAs and then guide the Argonaute protein to the target mRNA, leading to mRNA degradation or gene expression inhibition (33, 34). However, with the further in-depth research on RNA interaction, Franco-Zorrilla et al. (35) have discovered that ncRNAs could relieve the inhibitory effect of miR-399 on its target RNA in plants. Furthermore, Ebert et al. (36) found the similar molecular effects in the animal experiments. Studies indicate that miRNAs are regulated by other ncRNAs bearing MRE sequences in the process of regulating mRNA gene expression (37, 38). Different ncRNAs may possess the same MRE sequence, so multiple ncRNAs may competitively bind to the same miRNA (39). Initially, the phenomenon that ncRNAs compete with mRNAs to bind miRNAs through MREs is called "RNA sponge" (40). In 2011, Salmena et al. (41) formally proposed the ceRNA hypothesis, calling such ncRNAs that competitively bind miRNAs as ceRNAs.

It has been reported that miRNAs could be regulated by various RNA molecules such as lncRNA, circRNAs, and pseudogenes (37). There are over 500 miRNA genes in the human genome, and more than half of mRNA genes may carry MREs (42–44). Multiple miRNAs can regulate a single RNA with various MREs, while multiple RNAs may contain the same specific MRE (34). The different types of these RNA interactions together constitute ncRNA–miRNA–mRNA ceRNA regulatory networks. Current research indicates that the concentration of ceRNAs and miRNAs affects the competition efficiency of the ceRNA–miRNA network (45). In addition, RNA-binding proteins (RBPs), RNA 3′-UTRs, and the subcellular localization of ceRNAs all affect the activity of ceRNAs (36, 45). According to statistics, the potential targets of miRNAs account for more than 60% among the genes that encode human proteins (41, 46). Therefore, changes in the influencing factors of ceRNAs can lead to the imbalance of the ceRNA networks, which may further contribute to the occurrence or development of diseases, including cancer (47).

After the ceRNA hypothesis was put forward, more and more studies, supported by bioinformatics and other technologies, have confirmed the existence of ncRNA–miRNA–mRNA regulatory networks in cancer (29, 47). Researchers have discovered dense MREs in most cancer-related coding genes and lncRNAs in the human genome (32). In cancer cells, these aberrantly expressed lncRNAs interact and further affect the expression of miRNAs through the ceRNA network, which ultimately regulate related cancer genes (32). The lncRNA highly upregulated in liver cancer (HULC) was found to inhibit miR-372 as a ceRNA in liver cancer, thereby increasing the expression of cAMP-dependent protein kinase catalytic subunit beta (PRKACB) (48). In non-small cell lung cancer, LINC81507 acts as the sponge of miR-199b-5p and exerts effects through the Caveolin1/signal transducer and activator of transcription-3 (CAV1/STAT3) signaling pathway (49). In addition, the ceRNA network formed by lncRNA–miRNA–mRNA plays an important role in various cancers including PC. The lncRNA/miRNA/mRNA ceRNA networks in PC are shown in **Supplementary Table 1**.

LncRNA-MEDIATED CeRNA IN PANCREATIC CANCER PATHOGENESIS AND DEVELOPMENT

Recently, mounting evidence indicates that the identified lncRNAs could exert their oncogenic roles by acting as ceRNAs to regulate target gene expression (20, 50–53), thereby modulating cell proliferation (54), apoptosis (55), cell cycle (56), invasion and metastasis (57), epithelial–mesenchymal transition (EMT) (58), metabolism (59), autophagy (60), angiogenesis (61), stemness (62), as well as chemoresistance (63), thus involving in PC pathogenesis and progression (64–67). In this section, we will elucidate the functions of some lncRNA-mediated ceRNA regulatory networks in PC. Also, we highlight the ceRNA regulatory networks consisting of an lncRNA/miRNA/mRNA axis. We summarize the identified lncRNA/miRNA/mRNA networks in several hallmarks of PC in **Figure 1**.

LncRNAS AS ceRNAS REGULATING CELL GROWTH AND SURVIVAL

Cell growth and survival are complicated processes (68, 69) that are tightly regulated by tumor suppressor genes, oncogenes, along with other controlling mechanisms and associated with the hallmarks of sustaining proliferative signaling, evading growth suppression, enabling replicative immortality, and resisting cell death (65, 68, 70). Recent studies have uncovered the regulatory role of lncRNAs in cell growth and survival through multiple mechanisms in PC (20, 53, 65–67, 71). Apart from the oncogenic role of lncRNAs, growth and survival are also regulated by several lncRNA-mediated ceRNA networks in PC (67, 71). In this section, we will discuss some ceRNA networks and their role in PC cell growth and survival.

THAP9-AS1/miR-484/YAP

LncRNA THAP domain containing 9 antisense RNA 1 (THAP9-AS1), which is an antisense transcript of THAP9 and locates at chromosome 4q21.22, has been reported to act a key role in the tumorigenesis of gastric cancer (72) and esophageal squamous cell carcinoma (73, 74). A recent study by Li et al. (54) demonstrated that THAP9-AS1 promoted the cell growth of PC through the THAP9-AS1/miR-484/yes-associated protein (YAP) ceRNA pathway. Clinical evidence showed that THAP9-AS1 was overexpressed in PC tissues and significantly associated with poor prognosis of patients. THAP9-AS1 promoted PC cell growth both *in vitro* and *in vivo*. Ectopic THAP9-AS1 expression bound to miR-484 directly, and such competitive binding decreased the abundance of miR-484 and relieved its repression of the downstream target, YAP, an important downstream nuclear effector of the Hippo signaling pathway. Inversely, YAP overexpression or knockdown diminished the effects of THAP9-AS1 modulated in PC cells. Moreover, THAP9-AS1 bound to YAP protein and inhibited the phosphorylation-mediated inactivation of YAP by large tumor suppressor kinase 1 (LATS1). Reciprocally, YAP bound to THAP9-AS1 promoter *via* transcriptional enhanced associate domain 1 (TEAD1) and promoted THAP9-AS1 transcription to form a positive feedback regulatory loop in PC cells. Importantly, THAP9-AS1 level positively correlated with YAP expression in PC tissues. Thus, THAP9-AS1/miR-484/YAP axis might serve as a potential biomarker and therapeutic target for PC treatment.

MIR31HG/miR-193B

LncRNA miR-31 host gene (MIR31HG) is a recently identified 2,166-nt lncRNA and regulated by methylation of the promoter region in transcription level (75, 76). Accumulating studies have revealed that MIR31HG plays oncogenic or tumor-suppressive roles in cancer initiation and progression (75), and its overexpression can serve as a prognosis predictor for several malignancies, including oral cancer (77), hepatocellular carcinoma (78), and head and neck squamous cell carcinoma (79). Yang et al. (55) demonstrated that MIR31HG was markedly upregulated in PC tissues and cell lines. Knockdown of MIR31HG significantly suppressed PC cell growth, promoted apoptosis, and induced cell cycle G1/S arrest, whereas enhanced expression of MIR31HG exerted the opposite effects. Mechanistically, MIR31HG acted as an endogenous sponge by competing for miR-193b and regulated miR-193b targets, such as cyclin D1 (CCND1), myeloid cell leukemia sequence 1 (Mcl-1), ecto-5'-nucleotidase (NT5E), KRAS, u-plasminogen activator (uPA), and E-twenty six transcription factor 1(ETS1). Meanwhile, inhibition of miR-193b expression significantly upregulated the MIR31HG level, while overexpression of miR-193b suppressed MIR31HG's expression and function in PC cells. As a result, these results demonstrated that MIR31HG functioned as an oncogene to promote tumor progression, and MIR31HG/miR-193b axis served as a potential therapeutic target for PC (55).

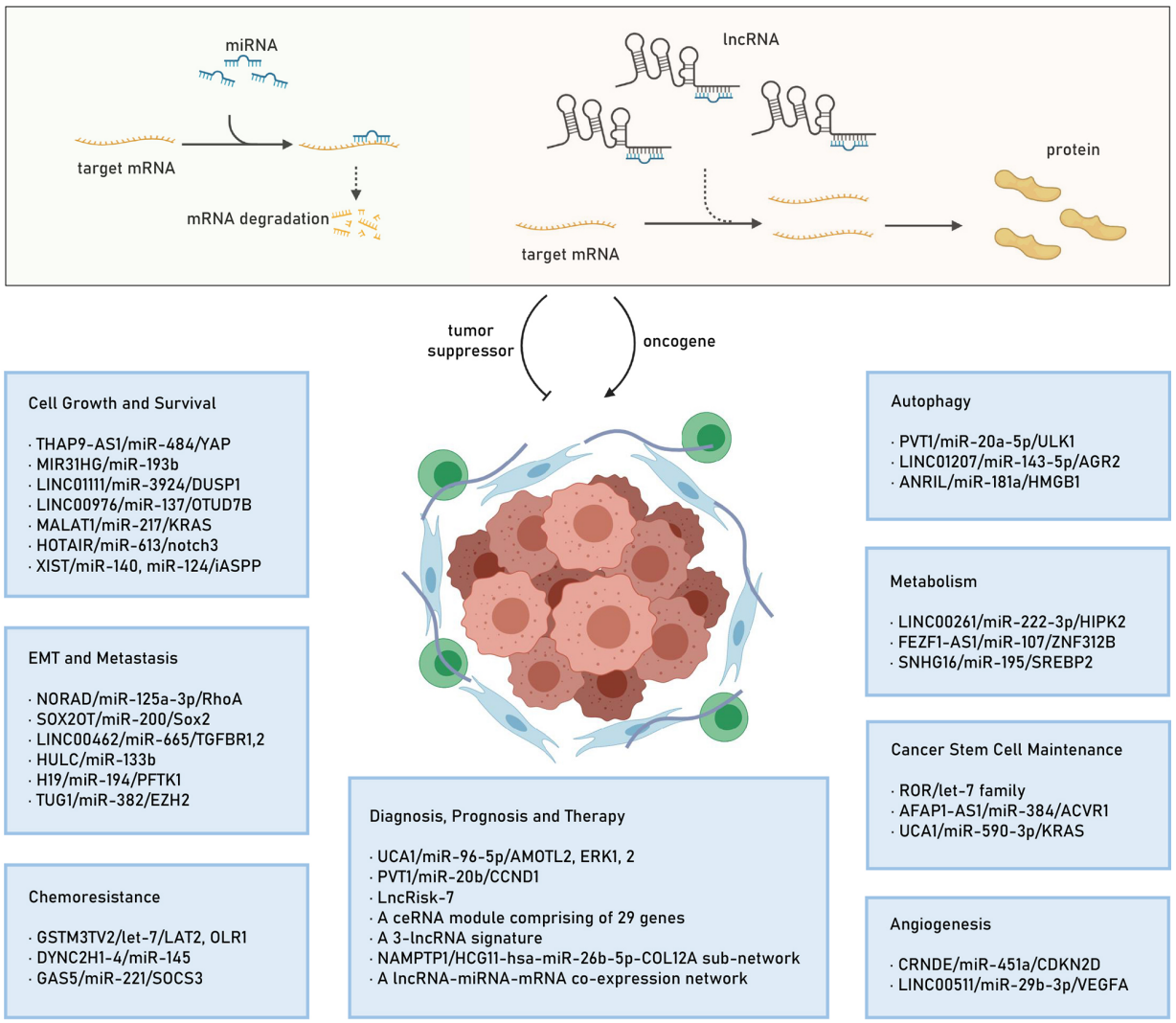

FIGURE 1 | The lncRNA mediated ceRNA mechanism and the identified lncRNA/miRNA/mRNA networks in several hallmarks of PC. lncRNA, long noncoding RNA; ceRNA, competitive endogenous RNA; miRNA, microRNA; mRNA: mRNA, messenger RNA; PC, pancreatic cancer; EMT, epithelial-mesenchymal transition.

LINC01111/miR-3924/DUSP1

LncRNA LINC01111 is a novel long intergenic ncRNA and located at chromosome 8q21.13 (80, 81). Pan et al. (81) found that LINC01111 expression was significantly downregulated in PC tissues and plasma and was positively associated with lymph node metastasis and tumor stage. Lower expression of LINC01111 was correlated with poor prognosis in PC patients. LINC01111 overexpression significantly inhibited cell proliferation and induced cell cycle G1/S arrest *in vitro*, as well as tumorigenesis *in vivo*. Conversely, LINC01111 knockdown enhanced cell proliferation and promoted cell cycle G1/S transition *in vitro*, as well as tumorigenesis *in vivo*. Meanwhile, the results also demonstrated that LINC01111 functioned as a molecular sponge for miR-3924 to upregulate dual-specificity protein phosphatase 1 (DUSP1) protein levels and then downregulate stress-activated protein kinase (SAPK) phosphorylation and the translocation of p-SAPK from the cytoplasm to the nucleus. Thus, the loss of LINC01111 in PC activated the SAPK/c-Jun N-terminal kinase (JNK) signaling pathway, resulting in the promotion of tumor growth. Moreover, LINC01111 also facilitated an important role in PC cell invasion and metastasis. Collectively, this study indicated that LINC01111/miR-3924/DUSP1 axis was a potential therapeutic target for treating PC (81).

LINC00976/miR-137/OTUD7B

LncRNA LINC00976, a novel long intergenic ncRNA, has been recently identified as an oncogenic lncRNA to promote the cell growth of PC through the LINC00976/miR-137/ovarian-tumour

family deubiquitinases domain-containing protein 7B (OTUD7B) (Cezanne) ceRNA pathway (82). The data showed that LINC00976 expression was overexpressed in PC tissues and cell lines and was positively associated with poorer survival in patients with PC. Function studies revealed that LINC00976 knockdown significantly suppressed cell proliferation, migration, and invasion *in vivo* and *in vitro*, whereas its overexpression reversed these effects. Furthermore, bioinformatics analysis, luciferase assays, and rescue experiments revealed that LINC00976/miR137/OTUD7B established a ceRNA network to modulate PC cell proliferation and tumor growth. Ultimately, OTUD7B mediated EGFR and MAPK signaling pathway, which suggested that LINC00976/miR-137/OTUD7B/EGFR axis might act as a potential biomarker and therapeutic target for PC (82).

MALAT1/miR-217/KRAS

LncRNA metastasis-associated lung adenocarcinoma transcript 1 (MALAT1), which is an evolutionarily highly conserved lncRNA and localized on chromosome 11q13, has been shown to be involved in the pathogenesis of multiple cancers by acting as an oncogene to promote cell growth, evade apoptosis, regulate cell cycle, maintain stemness, and enhance invasion and metastasis (83–85). Moreover, it is significantly overexpressed in many cancer types and may be related to tumor prognosis, indicating its potential use as a biomarker of cancers (83, 85). MALAT-1 played an important role in the carcinogenesis of PC by acting as a ceRNA. Liu et al. (86) demonstrated that MALAT1 functioned as a molecular sponge for miR-217 to upregulate the expression of KRAS for promoting tumor growth in PC. Knocking down MALAT1 reduced pancreatic tumor cell growth and proliferation both *in vitro* and *in vivo*. And MALAT1 knockdown also inhibited cell cycle progression and impaired tumor cell migration and invasion. However, MALAT1 knockdown attenuated the protein expression of KRAS not directly through inhibition of cellular miR-217 expression but decreased the miR-217 nucleus/cytoplasm ratio, which suggested that MALAT1 inhibited the translocation of miR-217 from the nucleus to the cytoplasm. Thus, MALAT1 acted as a tumor promoter at least in part by binding miR-217 and sequestering the molecule in the nucleus, thereby promoting oncogenic KRAS expression in PC (86). In contrast to the previous study by Liu et al., another study confirmed that the MALAT1 suppressed miR-200c-3p function *via* upregulating zinc finger E-box-binding homeobox 1 (ZEB1) expression to induce the capability of PC cell migration and invasion (87). Therefore, it can be proposed that MALAT1 could be a potential therapeutic target in PC.

HOTAIR/miR-613/notch3

LncRNA HOX transcript antisense RNA (HOTAIR), which is a well-characterized oncogenic lncRNA and dysregulated in variety of cancers, localizes in the HOXC locus of chromosome 12q13.13 that flanks between HOXC11 and HOXC12 loci (88–90). Notably, a growing body of evidence suggests that HOTAIR constitutes a critical contributor to various known or unknown mechanisms in the pathogenesis and progression of multiple cancers and is also an important negative prognostic factor for cancer patients, including PC (71, 88–90). Cai et al. (91) demonstrated that HOTAIR could act as a ceRNA *via* regulating miR-613/notch3 axis to promote cell growth and survival in PC. They revealed that HOTAIR was found to be upregulated in both PC tissues and cell lines, and HOTAIR was inversely correlated with miR-613 level in PC tissues. Knockdown of HOTAIR in PC cells suppressed the expression levels of miR-613 and tumor growth, suggesting that the oncogenic role of HOTAIR might be correlated with miR-613. Further investigation confirmed that HOTAIR suppressed miR-613 expression *via* sponging miR-613 in the PC cells. Thus, the HOTAIR/miR-613/notch3 axis might be a promising therapeutic target for PC (91). Meanwhile, Deng et al. (92) reported that HOTAIR sponged miR-34a to promote PC stem cell-like properties through activation of the JAK2/STAT3 pathway. Silencing of HOTAIR could inhibit the Wnt/β-catenin signaling pathway to alleviate EMT in PC (93).

XIST/miR-140, miR-124/iASPP

LncRNA X inactivation-specific transcript (XIST) is derived from XIST gene and is important for inactivation of X chromosome in the development of female mammals (94). It is reported that XIST is dysregulated in a variety of cancers and exerts its either tumor-suppressive or oncogenic role in tumorigenesis and progression of cancers, such as hepatocellular carcinoma, lung cancer, gastric cancer, and osteosarcoma (95–97). Recent studies indicated that XIST was overexpressed in PC and involved in regulating the cell proliferation, apoptosis, migration, and invasion (98). Liang et al. (56) demonstrated that XIST was specifically upregulated in PC tissues and related to the advanced TNM stage and larger tumor dimension. Patients with high XIST expression correlated to poorer survival compared with that low expression. Knockdown of XIST could induce PC cell cycle arrest at G0/G1 phase by regulating cell cycle arrest-related CDK1 and P21, and p53-independent apoptosis-related factor iASPP, which significantly leads to suppression of the cell viability and proliferation *in vivo* and *in vitro*. Mechanistically, XIST functioned as a ceRNA for interacting with miR-140 and miR-124 to upregulate the inhibitor for the apoptosis-stimulating protein of p53 (iASPP) expression. Meanwhile, iASPP could suppress p73 transcriptional activity to decrease the inhibitory effect of p73 on XIST expression without changing p73 protein levels. Moreover, XIST was inversely correlated with miR-140, miR-124, and p21, respectively, and positively correlated with iASPP and CDK1. Thus, these data all indicated that XIST played a key role in regulating PC cell proliferation and cell cycle and might provide a potential therapeutic strategy for PC (56). In addition, it has been proven that XIST/miR-133a/EGFR (99), XIST/miR-34a-5p (98), and XIST/miR-137/Notch1 (100) ceRNA axes also played important roles in PC cell growth and survival regulation,

while XIST/miR-429/ZEB1 (101) and XIST/miR-141-3p/TGF-β2 (102) ceRNA axes contributed to PC cell migration and invasion.

LncRNAs AS ceRNAs AFFECTING EPITHELIAL–MESENCHYMAL TRANSITION AND METASTASIS

EMT is a complex and developmental process in which polarized epithelial cells lose their characteristics instead of acquire mesenchymal properties with the capacity of migration and metastasis, playing a critical role in the progression of cancers (65, 68, 103–105). It has been shown that epithelial cells in this process that are induced by the transcriptional factors Snail, Twist, Slug, ZEB1, and ZEB2, would result in loss of E-cadherin expression and acquisition of mesenchymal markers, such as N-cadherin or vimentin (106–108). Recent studies have indicated that lncRNAs regulate PC EMT and metastasis (20, 53, 109, 110), and therefore, the mechanism underlying the role of lncRNAs should be addressed, knowing that some lncRNAs may serve as ceRNA for PC EMT and metastasis.

NORAD/miR-125A-3p/RhoA

LncRNA noncoding RNA activated by DNA damage (NORAD, also known as LINC00657) is a highly conserved, ubiquitously expressed cytoplasmic lncRNA and locates on chromosome 20q11.23, which is required for maintaining chromosomal stability and proper mitotic divisions in human cells (111, 112). Recent evidence indicates that NORAD is dysregulated in various human cancers and acts as an important regulator by interacting with different types of mechanisms to promote tumor progression, such as cell proliferation, invasion, metastasis, and apoptosis (113, 114). Chen et al. (58) revealed that NORAD could enhance the hypoxia-induced EMT to promote PC cell metastasis by acting as a ceRNA. Notably, they firstly revealed that NORAD expression was highly increased in PC tissues by using human microarray datasets GSE15471 and GSE16515 for analyzing its expression profile, and NORAD expression was significantly upregulated after hypoxic stimulation for 48 h. Knockdown of NORAD impaired PC cell migration and invasion *in vitro* and decreased the metastatic and disseminated ability in an orthotopic mouse metastatic model. Western blotting also showed that knockdown of NORAD significantly suppressed the expression levels of the mesenchymal cell markers N-cadherin, vimentin, and ZEB1 but increased the expression levels of the epithelial cell marker E-cadherin. Furthermore, they demonstrated that NORAD utilized its oncogenic role by directly binding to miR-125a-3p and inhibiting its expression in PC cells, thus leading to upregulation of RhoA expression. Meanwhile, treating with ras homolog gene family (RhoA) pathway specific inhibitor CCG-1423 could impede the flow of EMT and invasive behaviors induced by NORAD. Additionally, patients with higher NORAD expression had shorter overall survival and recurrence-free survival rates. Thus, NORAD/miR-125a-3p/RhoA axis might be a potential novel therapeutic target for the treatment of PC (115). Moreover, Bi et al. (116) also found that lncRNA LINC00657 (NORAD) enhanced PC cell proliferation, migration, and invasion but restricted the apoptosis by acting as a ceRNA on miR-433 to increase protein activated kinase 4 (PAK4) expression.

SOX2OT/miR-200/Sox2

LncRNA SOX2 overlapping transcript (SOX2OT), which is a highly expressed lncRNA in embryonic stem cells and maps to human the chromosome 3q26.3 locus, plays critical roles in embryogenesis, cell differentiation, and pluripotency maintenance (117). SOX2OT harbors SOX2 gene transcription in its intronic region and produces at least eight transcript variants to exploit its effect on various diseases, including cancer (117, 118). Recent studies have demonstrated that SOX2OT is overexpressed in many cancers and involved in tumor development and progression by acting as an oncogene to promote cell proliferation, invasion, migration, and growth and suppress cell apoptosis (118). Zhang et al. (119) demonstrated that SOX2OT was overexpressed in PC tissues and significantly correlated with TNM staging, acting as a potential prognosis marker for patient outcome. They found that the tumor suppressor YY1 bound to the promoter of SOX2OT and inhibited tumor growth *in vivo* and *in vitro* by suppressing SOX2OT and SOX2 expression in PC. Furthermore, they observed that SOX2OT could promote PC cell EMT by acting as a ceRNA (120). They found that plasma exosomal SOX2OT expression was high and correlated with TNM stage and overall survival rate of PC patients. Further research showed that SOX2OT or exosomal SOX2OT promoted PC cells metastasis and regulated EMT properties by increasing the expression levels of the mesenchymal cell markers N-cadherin and vimentin but suppressing the expression levels of the epithelial cell marker E-cadherin. Mechanistically, SOX2OT competitively bound to the miR-200 family to increase the expression of Sox2, thus promoting invasion and metastasis of PC *in vitro* and *in vivo*. Besides, they also found that SOX2OT/miR-200/Sox2 ceRNA axis could enhance stem cell-like properties of PC (120). Thus, SOX2OT/miR-200/Sox2 played important roles in tumor progression and might be a useful marker for PC prognosis.

LINC00462/miR-665/TGFBR1, TGFBR2

LncRNA LINC00462, which contains two exons with approximately 962 nucleotides in length and is located on chromosome 13 according to NONCODE 4.0, is found to promote tumor proliferation, migration, and invasion by regulating the AKT signaling pathway in multiple cancers, including hepatocellular carcinoma and renal cell carcinoma

(121, 122). Zhou et al. (123) demonstrated that LINC00462 promoted PC invasiveness through the miR-665/TGFBR1-TGFBR2/SMAD2/3 pathway. They found that the expression level of LINC00462 was significantly higher in tumor tissues and was correlated with large tumor size, poor tumor differentiation, TNM stage, and distant metastasis in PC patients. *In vitro*, LINC00462 promoted PC cell migration and invasion but inhibited cell adhesion. *In vivo*, LINC00462 enhanced PC cell metastasis to lung, liver, and spleen in a mouse xenograft model. LINC00462 also regulated PC cell EMT properties by increasing the expression of intracellular adhesion molecule (ICAM)-1, vimentin, Twist1, matrix metalloproteinase (MMP)2, and MMP9 but decreasing the expression of E-cadherin. Further study showed that LINC00462 acted as a ceRNA to promote the malignant phenotype of PC by sponging miR-665, thus upregulating the expression levels of transforming growth factor beta 1 (TGFBR1) and TGFBR2. Ectopic expression of miR-665 could reverse LINC00462 overexpression-mediated cell migration, invasion, and EMT in PC. In contrast, knockdown expression of miR-665 observed the opposite effects. While LINC00462-mediated cell malignant behavior promotion in PC was also rescued by loss of expression of TGFBR1 and TGFBR2. Furthermore, LINC00462 activated the SMAD2/SMAD3 signaling pathway by increasing the expression levels of p-SMAD2/3 and the nuclear distribution of SMAD2/3, which led to upregulating collagen 1, collagen 3, and fibronectin. Meanwhile, LINC00462 played important roles on cell proliferation and tumorigenesis in PC. Taken together, LINC00462/miR-665/TGFBR1/2 regulatory network might be a potential novel therapeutic target for the treatment of PC (123).

HULC/miR-133b

LncRNA is highly upregulated in liver cancer (HULC), which is originally identified as the most overexpressed lncRNA in hepatocellular carcinoma, and is located on chromosome 6p24.3 with approximately 500 nucleotides in length and contains two exons (124, 125). Increasing evidence demonstrates that HULC is also dysregulated in other types of cancer and plays essential roles in tumor initiation and progress by promoting different tumorigenic phenotypes, such as cell survival, proliferation, and invasion *in vitro*, as well as tumor growth and angiogenesis *in vivo* (124, 125). Peng et al. (126) found that HULC was overexpressed in PC tissues and associated with tumor size, lymph node metastasis, and vascular invasion. And multivariate analysis showed that HULC expression was an independent prognostic indicator for overall survival and time to recurrence of patients with PC. Knockdown of HULC significantly decreased PC cell ability of proliferation and induced cell cycle arrest at G1/S phase *in vitro*. Zheng et al. (127) further revealed that HULC promoted the proliferation and invasion of PC cells but inhibited apoptosis by being involved in the Wnt/β-catenin signaling pathway. Similarly, HULC downregulated the expression of miR-15a, then activated the PI3K/AKT pathway to enhance PC cell ability of migration and invasion (128). Meanwhile, exosomal HULC could function as ceRNA for contributing to PC cell invasion and migration by regulating EMT (129). Exosomal HULC expression was significantly increased in PC patients' serum compared to healthy individuals or intraductal papillary mucinous neoplasm patients. Further study showed that knockdown of HULC suppressed PC cell invasion and migration and inhibited the EMT by downregulating N-cadherin, vimentin, and Snail but upregulating E-cadherin *in vitro* and *in vivo*. Meanwhile, exosomal HULC derived from PC cells also promoted cancer cell invasion and migration by inducing EMT. Mechanistically, HULC interacted with miR-133b to alter PC cell invasion and migration, as well as EMT (129). Moreover, HULC and miR-622 *via* transfer by extracellular vesicle regulated PC cell invasion and migration (130). Thus, extracellular vesicle-encapsulated HULC could be a potential circulating biomarker and therapeutic target for PC.

H19/miR-194/PFTK1

LncRNA H19, which is firstly described as a fetal transcript in mice in 1984, is located on chromosome 11p15.5 and expressed exclusively from the maternal allele (131, 132). Recent studies indicate that H19 is dysregulated in various cancer types and serves as oncogene or tumor suppressor to affect the development and progression of cancer through various mechanisms. For example, H19 enhances invasion and metastasis in bladder cancer, glioma, breast cancer, non-small cell lung cancer, and gastric cancer but suppresses the aggressiveness of hepatocellular carcinoma and prostate cancer (131, 133). Further study demonstrated that H19 acted as a ceRNA to enhance invasion and metastasis by regulating Wnt/β-catenin signaling pathway in PC (134). Sun et al. (134) found that H19 was overexpressed and correlated with distant metastasis, advanced TNM stages, and poor survival in patients with PC. Multivariate analysis revealed that high H19 expression was an independent indicator of poor prognosis. H19 knockdown suppressed PC cell migration and invasion *in vitro*. Subsequently, they demonstrated that H19 promoted PC cell invasion and migration at least partially by increasing [cyclin-dependent kinase 14 (CDK14)] expression through antagonizing miR-194. H19 knockdown significantly reduced the expression of PFTK1, while miR-194 inhibition significantly increased the expression of PFTK1; the suppressive effect of H19 knockdown was partially attenuated by miR-194 inhibition and PFTK1 overexpression. Moreover, H19/miR-194 modulated Wnt/β-catenin signaling by upregulating p-LRP6, Snail but downregulating p-β-catenin to promote PC cell invasion and migration. The expression level of H19 and PFTK1 was positively correlated with each other, while miR-194 was negatively correlated with H19 and PFTK1 in tissue samples. Collectively, the H19/miR-194/PFTK1 ceRNA axis might be a potential novel therapeutic target for PC (134). In addition, the H19/let-7/HMGA2/EMT signaling axis also played important roles on PC metastasis and EMT (135). And H19 could maintain PC

cell EMT process and stemness by deriving miR-675-3p that directly targeted SOCS5 then activating the STAT3 pathway (136).

TUG1/miR-382/EZH2

LncRNA taurine upregulated gene 1 (TUG1), which is originally identified in the genomic screen of taurine-treated mouse retinal cells, is a nucleotide lncRNA sequence localized to chromosome 22q12.2 (137, 138). Recent studies have been indicated that TUG1 is dysregulated in numerous human cancers and acts as an unfavorable predictor of survival for patients with cancer, such as renal cell carcinoma, ovarian cancer, bladder urothelial carcinoma, oral squamous cell carcinoma, esophageal squamous cell carcinoma, hepatocellular carcinoma, and intrahepatic cholangiocarcinoma (137, 138). Zhao et al. (139) revealed that TUG1 was essential for the migration and EMT in PC by serving as a ceRNA. They firstly demonstrated that TUG1 was overexpressed in tumor tissues and correlated with large tumor size, poor tumor differentiation, TNM stage, vascular infiltration, distant metastasis, and overall survival of patients with PC, which indicated that upregulated TUG1 might contribute to the development of PC. Then, knockdown of TUG1 decreased the PC cell migration capacity and the formation of EMT by upregulating E-cadherin, β-catenin but downregulating N-cadherin, vimentin *in vitro*. In contrast, overexpression of TUG1 showed opposite effects. Further study confirmed that TUG1 exerted inhibitory effects on miR-382 expression through functioning as a ceRNA and therefore directly sponging miR-382 in PC. Overexpression of miR-382 could reverse the TUG1 effects on the promotion of PC cell migration and EMT formation. Additionally, TUG1 could positively regulate the expression of EZH2, a target of miR-382, by decreasing miR-382. Knockdown of EZH2 abolished PC cell migration and EMT formation, which was caused by TUG1 overexpression. Moreover, the expression level of TUG1 was negatively correlated with miR-382 and positively correlated with EZH2 in PC tissues. Collectively, these data indicated that TUG1/miR-382/EZH2 ceRNA regulatory signaling pathway enhanced PC cell migration capacity and EMT formation and might be a potential novel therapeutic target for PC (139). Otherwise, TUG1/miR-29c axis was also critical for promoting the growth and migratory ability of PC cells *in vitro* and *in vivo* (140). Inhibition of TUG1/miR-299-3p ceRNA axis suppressed PC cell malignant progression *via* deactivation of the Notch1 pathway (141).

LncRNAs AS CeRNAs RELATED TO CANCER STEM CELL MAINTENANCE

Cancer stem cells (CSCs) are a functional subpopulation of cells that exhibit high proliferation, self-renewal, and high tumorigenic, invasive, and metastatic capability, as well as chemoresistance, and their abundance is positively associated with the degree of PC malignancy (69, 142, 143). Studies have revealed that the cell surface proteins CD44, CD24, CD133, chemokine C-X-C-motif receptor 4 (CXCR4), aldehyde dehydrogenase 1 family, member A1 (ALDH1), Epithelial cell adhesion molecule (EPCAM), adenosine triphosphate binding box transporter G2 (ABCG2), and cellular-mesenchymal epithelial transition factor (c-MET) are identified as PC stem cell markers (69, 143, 144). Several lines of evidence have shown that oncogenic lncRNAs help sustain cancer stem cell traits by acting as ceRNAs in the initiation and progression of PC (20, 53, 145). Thus, the lncRNA-mediated ceRNA network may serve as a potential biomarker and therapeutic target for PC.

ROR/let-7 FAMILY

LncRNA regulator of reprogramming (ROR), which is highly expressed in induced pluripotent stem cells (iPSCs) and embryonic stem cells (ESCs), is located at 18q21.31 and can be regulated by pluripotency transcription factors, such as Sox2, Oct4, and Nanog (146, 147). It has been identified that ROR is an important regulator of reprogramming differentiated cells to iPSCs and maintenance of ESCs, which indicates that ROR plays critical roles in tumorigenesis and progression of human cancer (146, 147). Accumulating evidence has demonstrated that ROR is upregulated in multiple types of cancer and associated with tumor metastasis, EMT program, drug resistance, and stem cell-like characteristic promotion by various regulatory mechanisms in ovarian, lung, breast cancer, hepatocellular cancer, gastric cancer, and so on (146, 147). Meanwhile, recent studies also reveal that ROR acts as a ceRNA by sponging miR-145 (148), miR-205 (149), and miR-34a (151) to regulate gene transcription. Zhan et al. (150) demonstrated that ROR was overexpressed in PC tissues and enhanced PC cell metastasis, EMT promotion, and tumor growth by activation of ZEB1 pathway. Similarity, another study showed that ROR could modulate the expression of polypyrimidine tract-binding protein 1/pyruvate kinase isozymes M2 (PTBP1/PKM2) through sponging miR-124 to induce PC cell autophagy, which led to gemcitabine resistance for PC (152). Moreover, Fu et al. (153) revealed that ROR functioned as a ceRNA to promote stem cell-like phenotype in PC. They firstly found ROR was significantly upregulated and positively correlated with poor prognosis in patients with PC. Knockdown of the expression of ROR impaired cell proliferation, migration, and invasion ability, suppressed the EMT process, and induced cell cycle G1/S arrest in PC. Further study displayed that ROR was overexpressed in PC stem-like cells and promoted PC stem-like cell sphere formation capability *in vitro* and tumorigenicity *in vivo* by regulating the expression of Sox2 and Nanog. Mechanistically, ROR exerted its oncogenic effects by sponging several tumor suppressor miRNAs such as let-7 family (let-7i-5p, let-7b-5p, let-7e-5p, let-7e-3p, let-7b-3p, and let-7c-3p), miR-93-5p, miR-145-3p, miR-320a, and miR-320b to maintain the cancer stem cell properties of PC. Collectively, ROR was a potential therapeutic target for PC. In addition, Gao et al. (151) showed that ROR/miR-145/Nanog ceRNA axis also contributed to modulate PC cell stem-like properties.

AFAP1-AS1/miR-384/ACVR1

LncRNA actin filament-associated protein 1 antisense RNA 1 (AFAP1-AS1), which is transcribed from the AFAP1 gene in the antisense direction, is mapped to the 4p16.1 region of human chromosome with 6,810 bp in length (154, 155). AFAP1-AS1 contains several overlapping and complementary regions among the exons of AFAP1-AS1 and can affect the expression of AFAP1. Accumulated studies have shown that AFAP1-AS1 is aberrantly expressed and exerts a carcinogenic role in numerous types of tumors, including breast cancer, liver cancer, gastric cancer, non-small cell lung cancer, and colorectal cancer (154, 155). In PC, AFAP1-AS1 had also been reported to be aberrantly expressed and was able to function as a regulator of tumorigenesis by regulating cell proliferation, apoptosis, migration, invasion, stemness, and so on (156, 157). Wu et al. (62) revealed that AFAP1-AS1 functioned as a ceRNA to regulate the cancer stem cell properties of PC. They first found that AFAP1-AS1 was overexpressed in PC tissues and side population (SP) cells. While SP cells were rich with cancer stem cell markers Oct4, ABCG2, Nestin, CK19, and CD133, which indicated that AFAP1-AS1 was involved in maintaining stemness. Knockdown of AFAP1-AS1 exerted suppressive effects on PC cell sphere formation and clone formation, while overexpression of AFAP1-AS1 group showed the opposite trend. Moreover, AFAP1-AS1 positively regulated the expression of CSC markers Oct4, ABCG2, Nestin, CK19, and CD133 by gain or loss strategies in PC cells. Furthermore, their research identified that AFAP1-AS1 modulated PC cell stemness by upregulating activin receptor type-1 (ACVR1) through competitively binding to miR-384 (62). MiR-384 decreased PC cell ability of sphere formation and clone formation and inhibited the expression of Oct4, ABCG2, Nestin, CK19, and CD133. In contrast, ACVR1 enhanced PC cell stemness by increasing cell sphere formation and clone formation and upregulating of Oct4, ABCG2, Nestin, CK19, and CD133. Their study data also found that AFAP1-AS1-promoted PC cell tumorigenesis and stemness could be reversed by miR-384 *in vivo*. Therefore, these results suggested that AFAP1-AS1/miR-384/ACVR1 pathway might do duty for a potential therapeutic target for PC patients (62).

UCA1/miR-590-3p/KRAS

LncRNA urothelial cancer-associated 1 (UCA1), a member of the human endogenous retrovirus H family and firstly identified in bladder transitional cell carcinoma, is 1,442 bp in length and located on chromosome 19p13.12 with three exons and two introns (158–160). According to the tissue expression profiling, UCA1 is ubiquitously expressed at post-fertilization primary phase and not expressed in most normal tissues of adults. Further studies have shown that UCA1 is highly expressed and exerts oncogenic activity in numerous cancers, such as gastric cancer, colorectal cancer, liver cancer, breast cancer, cervical cancer, and prostate cancer (158–160). Several studies also indicate that highly expressed UCA1 is related to poor clinicopathological features and may serve as a prognostic marker for cancer patients (161). Meanwhile, an increasing number of studies showed that UCA1 played important roles in tumorigenesis of PC. Chen et al. (162) firstly demonstrated that UCA1 was significantly upregulated in PC and correlated with tumor size, depth of invasion, CA19-9 level, and tumor stage. UCA1 suppressed the expression of P27 to effectively inhibit PC cell proliferative activities, induce apoptotic rate, and cause cell cycle arrest. Zhang et al. (163) revealed that UCA1 promoted cell migration and invasion of PC cells through the Hippo signaling pathway *via* interacting with YAP. Moreover, recent studies have shown that UCA1 promoted progress and development of PC by serving as a ceRNA. Zhang et al. (164) elucidated that UCA1 enhanced PC cell growth, migration, and invasion ability by sponging miR-135a. And a study by Zhou et al. (165) reported that UCA1 could bind miR-96 to modulate the expression of forkhead box protein O3 (FOXO3) that promoted proliferation and metastasis while reduced apoptosis of PC cells. Additionally, Gong et al. (166) discovered that the regulatory network of UCA1/miR-107/ITGA2 regulated the migration and invasion of PC cells through focal adhesion pathway. Besides, Liu et al. (167) found that UCA1/miR-590-3p/KRAS axis was critical for stemness maintenance of PC. They revealed that UCA1 was overexpressed in PC and might be a negative prognostic factor for patients' overall survival. Knockdown of UCA1 decreased sphere formation capability of PC cells, as well as the expression of the stemness markers CD133, OCT4, NANOG, and SOX2. In contrast, overexpression of UCA1 resulted in the opposite effects. Mechanistically, UCA1 exerted its oncogenic role by enhancing the expression and activity of KRAS. UCA1 firstly could function as a molecular sponge by directly binding to miR-590-3p, which led to upregulating KRAS expression. Then, UCA1 promoted phospho-KRAS protein expression through interaction with hnRNPA2B1 to modulate oncogenic KRAS activity, which was subsequently necessary for tumorigenic activity in PC. Notably, KRAS also significantly promoted UCA1 expression, thus forming a positive feedback loop. Thus, these findings suggested that UCA1/miR-590-3p/KRAS regulatory network might be a target for new PC therapies (167). Meanwhile, Guo et al. (168) demonstrated that UCA1, which is derived from hypoxic PC exosomes, could promote angiogenesis and tumor growth through the miR-96-5p/AMOTL2/ERK1/2 ceRNA axis *in vitro* and *in vivo*.

LncRNAs AS CeRNAs CONTROLLING METABOLISM

Metabolism reprogramming has been regarded as a hallmark of cancer (169, 170). As a primary feature in carcinogenesis, metabolic reprogramming contributes to tumor cell proliferation, EMT, metastasis, immune escape, and resistance to chemotherapy (171–173). Meanwhile, reprogramming of cancer metabolism is composed of dysregulation of glucose and glutamine metabolism, alterations of lipid synthesis,

rewiring of mitochondrial function, etc. (171–173). Numerous genes have been shown to participate in the regulation of metabolic pathways, thus aberrant expression of these genes can be involved in the pathogenesis of PC (103, 170, 172, 174). The recent studies have revealed a significant attention toward the role of lncRNAs in the regulation of different aspects of cancer metabolism (20, 53, 175, 176). Here, we review lncRNAs as ceRNAs to modulate the processes of cancer metabolism in PC.

LINC00261/miR-222-3p/HIPK2

LncRNA LINC00261, firstly identified in hepatocellular carcinoma cells 9 years ago, is located on the 20th chromosome from site 22,560,552 to 22,578,642 (177). An increasing number of studies have indicated that LINC00261 is widely lowly expressed in a variety of cancers and acts as a tumor suppressor contributing to modulating cell proliferation, apoptosis, invasiveness, migration, chemoresistance, angiogenesis, and tumorigenesis *via* multiple molecular mechanisms (177). LINC00261 also plays vital roles in suppression of PC progression by acting as a ceRNA. Zhai et al. (59) demonstrated that overexpression of LINC00261 suppressed PC cell glycolysis *in vitro* and *in vivo*. They further confirmed that LINC00261 inhibited cell glucose metabolism by binding to miR-222-3p to induce homeodomain interacting protein kinase 2 (HIPK2) overexpression and then inactivated HIPK2-mediated ERK/c-Myc pathway, as well as c-Myc target genes [glucose transporter member 1 (GLUT1), hexokinase-2 (HK2), and L-lactate dehydrogenase A chain (LDHA)]. Functionally, miR-222-3p reversed the LINC00261 overexpression-induced decrease in cell glycolysis, similar to HIPK2 and miR-222-3p. Thus, these results revealed that LINC00261 suppressed glycolysis of PC *via* regulating miR-222-3p/HIPK2 ceRNA axis. Moreover, Zhai et al. (59) also found that LINC00261 could reduce c-Myc expression by sequestering Insulin-like growth factor 2 mRNA-binding protein 1 (IGF2BP1) to induce glycolysis suppression. In addition, Liu et al. (178) indicated that LINC00261 repressed c-Myc transcription by physically interacting and binding with the bromo domain of p300/cap binding protein (CBP), preventing the recruitment of p300/CBP to the promoter region of c-Myc. Furthermore, LINC00261 might interact with miR-23a-3p (179) or regulate the miR-552-5p/FOXO3 axis (180) to suppress the development of PC.

FEZF1-AS1/miR-107/ZNF312B

LncRNA FEZ finger zinc 1 antisense 1 (FEZF1-AS1), transcribed from the opposite strand of its cognate coding gene zinc finger protein 312B (ZNF312B), is a conserved RNA that is located on chromosome 7q31.32 with a length of 2,653 bp (181, 182). Recent research indicates that FEZF1-AS1 is significantly overexpressed and closely related to patient poor prognosis in a variety of malignancies, including nasopharyngeal carcinoma, hepatocellular carcinoma, cervical cancer, colorectal cancer, multiple myeloma, breast cancer, osteosarcoma, lung cancer, gastric cancer, and PC (181, 182). Li et al. (183) and Ye et al. (184) initially identified that FEZF1-AS1 was upregulated in PC tissues through lncRNA expression profile microarray analysis. Subsequently, they confirmed that FEZF1-AS1 and its sense-cognate ZNF312B were markedly expressed in PC tissues by using quantitative real-time PCR (qRT-PCR) and *in situ* hybridization (ISH) (184). FEZF1-AS1 and ZNF312B expression was positively related to advanced American Joint Committee on Cancer (AJCC) stages, nerve invasion, and patients' poor survival. And a nomogram, which incorporated the AJCC classification with significant prognostic factors neural invasion, ZNF312B expression, and FEZF1-AS1 expression, illustrated that FEZF1-AS1 and ZNF312B expression had important impacts on patient prognosis. Mechanistically, FEZF1-AS1 could act as an endogenous sponge by sequestering miR-107 and thus abolishing the miRNA-induced repressing effect on the ZNF312B expression. Functional experiments also confirmed that the FEZF1-AS1/miR-107/ZNF312B ceRNA axis played a key role in promoting PC cell proliferation, regulating cell cycle, enhancing migration and invasion, and inhibiting apoptosis. More importantly, the FEZF1-AS1/miR-107/ZNF312B pathway contributed to Warburg effect maintenance by promoting glycolytic process, glucose uptake, and lactate production, which met the demands for continuous energy and nutrients to support PC cell tumorigenesis and progression (184). Therefore, the ceRNA-mediated metabolic features of PC provided attractive therapeutic opportunities for treatments. Meanwhile, Ou et al. (185) demonstrated that FEZF1-AS1 could promote PC cell proliferation and invasion through miR-142/HIF-1α axis under hypoxic conditions and exert its oncogenic effect on PC cells through miR-133a/EGFR axis under normoxic conditions.

SNHG16/miR-195/SREBP2

LncRNA Small Nucleolar RNA Host Gene 16 (SNHG16), initially identified as an oncogene in neuroblastoma, is located on chromosome 17q25.1 and contains two splicing variants (186). Recent studies have shown that SNHG16 is upregulated in a variety of human cancers and significantly correlated with advanced pathological stage, lymph node metastasis, and poor prognosis in cancer patients (186, 187). Meanwhile, increasing evidence has suggested that SNHG16 functions as a tumor-promoting lncRNA that is involved in the regulation of numerous biological processes, including cell cycle, proliferation, apoptosis, migration, and invasion through a variety of potential mechanisms (186, 187). Yu et al. (188) found that SNHG16 accelerated the development of PC and promoted lipogenesis *via* directly regulating miR-195/SREBP2 axis. Knockdown of SNHG16 or Sterol regulatory element binding protein-2 (SREBP2) suppressed PC cell proliferation, migration, and invasion, as well as the lipogenesis that was

measured by decreasing the expression of fatty acid synthase (FASN), acetyl-CoA carboxylase 1 (ACACA), and stearoyl-CoA desaturase 1 (SCD1). While overexpression of miR-195 showed the same effect in PC cells. They further confirmed that SNHG16 directly sponged miR-195 from SREBP2 to modulate their expression. Meanwhile, miR-195 inhibitor upregulated the expression of SREBP2 and reversed the effects of shSNHG16 on progression and lipogenesis of PC. Thus, these results showed that SNHG16 promoted lipogenesis of PC *via* regulating miR-195/SREBP2 ceRNA axis. The lncRNA SNHG16/miR-195/SREBP2 axis might be developed as therapeutic targets for treating PC (188). Furthermore, Xu et al. (189) found that SNHG16 contributed to PC cell proliferation, migration, and invasion *via* the miR-302b-3p/SLC2A4 ceRNA axis.

LncRNAs AS CeRNAs INDUCING AUTOPHAGY

Autophagy is a highly conserved process in response to environmental stresses for ensuring cellular homeostasis through the removal of proteins or dysfunctional organelles (190–192). Existing studies indicate that autophagy plays a dynamic role in cancer initiation, progression, as well as drug resistance, by regulating interactions between the tumor and tumor microenvironment (190–193). There is increasing evidence that a large number of lncRNAs are obviously involved in PC autophagy (20, 53, 191, 194, 195). Identification of the mechanisms by which autophagy is activated in PC will help clarify PC pathogenesis (196). A number of research articles suggested that lncRNAs induce or suppress autophagy through ubiquitin-like modifier-activating enzyme (ATGs), and their signaling pathways may suppress or promote carcinogenesis of PC (192, 194, 195). Here, we describe the recently characterized lncRNAs that function as ceRNAs through inducing or inhibiting autophagy in PC.

PVT1/miR-20a-5p/ULK1

LncRNA plasmacytoma variant translocation 1 (PVT1), which originated from an intergenic region on chromosome 8, is an important oncogenic lncRNA highly expressed in human malignancies and correlated with patients' poor prognosis (197, 198). Compared to the majority of lncRNAs, the carcinogenic effect of PVT1 has been confirmed in various tumors. Numerous studies have revealed that PVT1 displays a crucial role to facilitate cancer progression by promoting growth and proliferation, enhancing migration and invasion, suppressing apoptosis, regulating metabolism, maintaining stemness, as well as inducing chemotherapy resistance (197–199). However, current research implies that the mechanisms underlying the carcinogenic role of PVT1 are rather complex. It has been proven that PVT1 can exert its varied oncogenic roles through overexpression and modulation of miRNA expression, protein interactions, targeting of regulatory genes, formation of fusion genes, functioning as a ceRNA, and interactions with myelocytomatosis oncogene (MYC), among many others molecular mechanisms (199, 200). Certainly, identifying the carcinogenic role and molecular mechanism of PVT1 has important implications for therapeutically targeting cancer. Huang et al. (60) demonstrated that PVT1 promoted the development of PC through the PVT1/miR-20a-5p/unc-51-like autophagy-activating kinase 1 (ULK1)/autophagy ceRNA pathway. They found that PVT1 was dramatically upregulated and positively associated with ULK1 protein expression in PC tissues and cells. And overexpression of PVT1 enhanced PC cells autophagy *in vitro* and *in vivo*, whereas knockdown of PVT1 showed the opposite trend. Meanwhile, PVT1 overexpression could promote cell proliferation and colony formation, suppress apoptosis, and increase S phase cells in PC cells; however, the attenuated effects were observed when treated with autophagy inhibitor 3-methyladenine. On the contrary, PVT1 knockdown with treatment of autophagy inducer rapamycin in PC cells would restore proliferation and colony formation, inhibit apoptosis, as well as ascend cell cycle S phase. These data suggested that PVT1 could induce cytoprotective autophagy in PC. Further studies revealed that PVT1 induced autophagy by upregulating ULK1 protein expression. Mechanistically, PVT1 modulated ULK1 expression by sponging miR-20a-5p. Moreover, the expression of PVT1 in high-grade (III + IV) PC tissues was higher than that in low-grade (I + II) tissues. And the overall survival time of patients with high PVT1 expression was significantly shorter than that of patients with low PVT1 expression. Thus, the study demonstrated that PVT1 acted as a sponge to regulate miR-20a-5p and subsequently affected ULK1 expression for inducing autophagy and promoting development of PC (60). Additionally, PVT1 could upregulate the expression of both Pygo2 and ATG14 and thus regulated Wnt/β-catenin signaling and autophagic activity to overcome gemcitabine resistance through sponging miR-619-5p in PC (201). And the ceRNA axes PVT1/miR-448/SERBP1 (202), PVT1/miR-519d-3p/HIF-1α (203), and PVT1/miR-143/HIF-1α (204) might also be potential biomarkers and therapeutic targets for PC.

LINC01207/miR-143-5p/AGR2

LncRNA LINC01207, located in the 4q32 genomic locus with three exons and two introns, has been reported to be upregulated in multiple types of cancer and associated with the prognosis of patients with poor survival (205–209). Recent studies have demonstrated that LINC01207 performs as an oncogenic lncRNA to promote cell growth, migration, invasion, and enhance apoptosis, as well as maintain stemness *via* ceRNA regulatory mechanism. Liu et al. (210) revealed that silencing of LINC01207 suppressed anterior gradient 2 (AGR2) expressions to facilitate autophagy and apoptosis of PC cells by sponging miR-143-5p. They first confirmed that LINC01207 and AGR2 were highly expressed, while miR-143-5p was poorly expressed in PC tissues when compared to the adjacent tissues. Further studies showed that LINC01207 could directly bind to

miR-143-5p, and AGR2 was a target gene of miR-143-5p. And knockdown of LINC01207 could decrease the expression of AGR2 by upregulating miR-143-5p, which indicated that LINC01207 functioned as a ceRNA to upregulate AGR2 expression by sponging miR-143-5p. Moreover, LINC01207 knockdown and miR-143-5p overexpression could inhibit PC cell proliferation, promote apoptosis, and induce autophagy by upregulating the expression of LC3II and beclin-1, while decreasing P62, AGR2, and the ratio of Bcl-2/Bax expression. Thus, LINC01207 silencing inhibited PC progression by inhibiting the mR-143-5p/AGR2 axis, providing a potential target for PC treatment (210).

ANRIL/miR-181a/HMGB1

LncRNA antisense noncoding RNA in the INK4 locus (ANRIL), initially identified in a kindred of familial melanoma-neural system tumor with a germ-line deletion of the entire CDKN2A/B locus in 2007, is located at the 9p21 region with 3.9 kb length and also named CDKN2B antisense RNA 1 (CDKN2B-AS) (211, 212). It has been proven that ANRIL is implicated in several malignant tumors, and high expression of ANRIL is associated with aggressive clinicopathologic features, such as high histological grade tumor size, advanced tumor–node–metastasis stage, and poor overall survival with the disease (211–213). Additionally, ANRIL participates in tumorigenesis by promoting cell proliferation, migration, invasion, and EMT but inhibiting cell apoptosis through a number of mechanisms (213, 214). Recent studies also show that ANRIL can act as an oncogenic ceRNA to facilitate tumor progression *via* miRNA regulation, including mechanisms involving let-7a (215) and miR-125a (216) in nasopharyngeal carcinoma, miR-99a (217) and miR-449a (218) in gastric cancer, miR-34a (219) in glioma, miR-122-5p (220), miR-191 (221), miR-144 (222), and miR-199a-5p (223) in hepatocellular carcinoma, miR-186 (224) in cervical cancer, let-7a in prostate cancer (225) and colorectal cancer (226), miR-125a-5p (227) in endometrial carcinoma, and miR-199a (228) in breast cancer. In PC, previous research demonstrated that ANRIL was overexpressed in cancer precursors known as intraductal papillary mucinous neoplasms (IPMNs) (229), and ANRIL could promote PC cell migration and invasion through modulation of EMT by activating ATM–E2F1 signaling pathway *in vivo* and *in vitro* (230). Whereas Wang et al. (231) have recently revealed that ANRIL aggravated PC cell gemcitabine chemoresistance by targeting inhibition of miR-181a and activating high-mobility group box-1 (HMGB1)-induced autophagy. They first demonstrated that ANRIL and HMGB1 were obviously higher in PC tissues and cell lines, while miR-181a was significantly lower in both PC tissues and cell lines. And knockdown of ANRIL could inhibit PC cell proliferation, invasion, and migration, as well as the expression of cell adhesion-related proteins. However, downregulation of miR-181a would reverse the inhibitory role of ANRIL knockdown on PC cell, which suggested that the oncogenic role of ANRIL on PC cells might be mediated by miR-181a. Meanwhile, ANRIL knockdown or miR-181a overexpression promoted the expression of LC3 II and Beclin1, while miR-181a inhibition could reverse the inhibition of autophagy by ANRIL knockdown, which indicated that ANRIL-modulated autophagy was mediated by miR-181a. Further studies revealed that miR-181a targeted HMGB1 to suppress PC cell proliferation, invasion, and migration, as well as stimulate autophagy. Mechanistically, ANRIL functioned as a ceRNA to regulate the expression of HMGB1 by inhibiting the activity of miR-181a in PC cells. And ANRIL could enhance PC cells to gemcitabine resistance *via* miR-181a/HMGB1 pathway, which provided new insights and potential targets for the therapy of PC. Moreover, the ANRIL/miR-181a axis also played important roles in laryngeal squamous cell carcinoma, colon cancer, and gastric cancer (232–234).

LncRNAs AS CeRNAs FACILITATING CHEMORESISTANCE

Chemotherapy resistance causes PC recurrence and failed clinical outcome (235). Cancers can exhibit either intrinsic or acquired chemoresistance to prevent the success of drug treatment (27, 236). It is clear that many factors and signaling pathways are involved in chemoresistance of PC, such as drug transport, metabolism, tumor microenvironment, EMT, DNA damage repair, mutation of drug targets, autophagy, epigenetics. and cancer stem cells (27, 237, 238). However, the molecular mechanisms of chemoresistance remain poorly understood, and the exploration of such mechanisms will help improve the current treatment of PC (238, 239). Since studies have indicated that lncRNAs play critical roles in initiation and progression of PC (20, 27, 53, 237, 240), it is increasingly speculated that the function and mechanism of lncRNA-mediated ceRNA network for chemoresistance regulation.

GSTM3TV2/let-7/LAT2, OLR1

LncRNA *Homo sapiens* glutathione S-transferase mu 3, transcript variant 2 and noncoding RNA (GSTM3TV2), a novel long intergenic ncRNA encoded from chromosome 1p13.3, has been recently identified as an oncogenic lncRNA to promote gemcitabine resistance through GSTM3TV2/let-7/L-type amino acid transporter 2 (LAT2), oxidized low-density lipoprotein receptor 1 (OLR1) ceRNA pathway in PC (63). The data showed that GSTM3TV2 expression was upregulated in PC tissues and gemcitabine-resistant cell lines and was positively associated with poorer survival in patients with PC. Function studies demonstrated that overexpression of GSTM3TV2 significantly decreased gemcitabine-induced cytotoxicity *in vivo* and *in vitro*, whereas its knockdown reversed these effects in PC. Furthermore, bioinformatics analysis, luciferase assays, and RNA immunoprecipitation assay revealed that GSTM3TV2 was physically associated with let-7 and functioned as ceRNA for let-7 to promote gemcitabine resistance. And let-7 directly targeted LAT2 and OLR1 and suppressed their expressions. LAT2, a transporter of neutral amino acids, activates mechanistic target of rapamycin (mTOR) kinase, thereby inhibiting apoptotic cell death in PC (241). OLR1 is also

known to increase HMGA2 transcription by upregulating c-Myc to promote the metastasis in PC (242). LAT2 and OLR1 were upregulated in gemcitabine-resistant cells, and that inhibiting their expression enhanced the chemosensitivity of PC cells to gemcitabine. Meanwhile, GSTM3TV2-mediated chemoresistance could be depressed by knocking down LAT2 and OLR1. Thus, GSTM3TV2 could upregulate the expression of LAT2, OLR1 through competitively sponging let-7 to enhance gemcitabine resistance of PC, which suggested that GSTM3TV2/let-7/LAT2, OLR1 axis might act as a potential biomarker and therapeutic target for PC (63).

DYNC2H1-4/miR-145

Linc-DYNC2H1-4, an intergenic ncRNA about 281 nt in length, has been originally discovered in human liver (237, 243). A recent study performed by Gao et al. (243) demonstrated that DYNC2H1-4 acted as a sponge of miR-145 to upregulate the expression of its targets, MMP3, Oct4, Lin28, Nanog, Sox2, and ZEB1, thereby promoting EMT progression and CSC formation, which led to chemoresistance in PC cells. They first found that DYNC2H1-4 was upregulated in PC tissues and BxPC-3 gemcitabine-resistant cell line with acquired gemcitabine resistance. Ectopic expression of DYNC2H1-4 promoted migration and invasion as well as pacreatosphere-forming ability in gemcitabine-sensitive PC cells. Knockdown of DYNC2H1-4 suppressed the acquisition of EMT phenotypes and CSC properties in gemcitabine-resistant cells. Mechanistically, DYNC2H1-4 competed with miR-145 to upregulate its targets' expression. MiR-145 was established as a tumor suppressor, targeting embryonic transcription factors including Lin28, Nanog, Sox2, and Oct4, and also inhibiting the EMT key regulator, ZEB1 expression. Overexpression of DYNC2H1-4 in parental BxPC-3 cells significantly elevated the Lin28, Nanog, Sox2, Oct4, and ZEB1 expressions, while knockdown of DYNC2H1-4 in BxPC-3 gemcitabine-resistant cells showed the opposite effects. Furthermore, upregulation of these miR-145 targets by DYNC2H1-4 was reverted by miR-145 overexpression. In addition, they also found that MMP3, a nearby gene of DYNC2H1-4, was expressed differentially in accordance with DYNC2H1-4 levels in gemcitabine-sensitive and -resistant cell lines. MiR-145 directly targeted MMP3. Overexpression of miR-145 decreased MMP3 expression in gemcitabine-resistant cell lines, and MMP3 upregulation induced by DYNC2H1-4 was downregulated by miR-145, which indicated that DYNC2H1-4/miR-145/MMP3 ceRNA axis was one of the mechanisms by which DYNC2H1-4 was involved in regulating chemoresistance of PC (243).

GAS5/miR-221/SOCS3

LncRNA growth arrest-specific transcript 5 (GAS5), which is located on chromosome 1q25 and originally found to accumulate in growth-arrested cells, acts as a decoy hormone response element for the glucocorticoid receptor (GR) (244, 245). It has been shown that GAS5 is downregulated and exerted a tumor-suppressive role in diverse cancers, including gastric cancer, non-small cell lung cancer, ovarian cancer, cervical cancer, gliomas, bladder cancer, renal cell carcinoma, and hepatocellular carcinoma (245, 246). The decreased expression of GAS5 has been correlated with poor tumor differentiation, metastasis to the lymph nodes, advanced pathological stages, adverse overall survival, resistance to chemotherapy, and so on (245, 246). Meanwhile, GAS5 interacts with the pathology of variety cancers by inhibiting cell proliferation, suppressing invasion and metastasis, stimulating apoptosis, as well as the induction of cell cycle arrest (237, 244). Recently, it has been reported that GAS5 is also involved in the therapy resistance of cancer by modulating the expression of various gene targets (237, 244). Previous studies have shown that GAS5 was involved in chemoresistance of PC by serving as a ceRNA for miRNA. Liu et al. (247) demonstrated that GAS5 functioned as a competing endogenous RNA for miR-221 to suppress gemcitabine resistance in PC by regulating the miR-221/SOCS3 pathway. They showed that the expression levels of GAS5 and suppressor of cytokine signalling-3 (SOCS3) were downregulated in both PC tissues and cell lines; however, the expression of miR-221 was increased. Upregulation of GAS5 promoted SOCS3 expression and suppressed cell growth, metastasis, and gemcitabine resistance by inhibiting the EMT and tumor stem cell accumulation both *in vivo* and *in vitro*. Mechanistically, GAS5 directly targeted and suppressed miR-221 expression and enhanced SOCS3 expression. Moreover, SOCS3 could reverse the development of miR-221-mediated EMT and stem cell-like phenotype by inhibiting cell proliferation, migration, and chemotherapy resistance. Thus, these results suggested that GAS5/miR-221/SOCS3 ceRNA axis might be a potential therapeutic strategy in PC (247). In addition, GAS5 could negatively regulate miR-181c-5p expression to antagonize gemcitabine and 5-fluorouracil (5-FU) resistance of PC through inactivation of the Hippo signaling (248).

LncRNAs AS CeRNAs MODULATING ANGIOGENESIS

Studies have shown that angiogenesis is of great importance in activating the proliferation, invasion, and metastasis of cancer cells, thus playing a crucial role in the initiation and development of solid tumors, including PC (68, 249–252). Many molecular pathways or angiogenic molecules are directly related to angiogenesis, such as VEGF, fibroblast growth factor (FGF), MMP-9, or the platelet-derived growth factor family. Similarly, accumulating studies have also reported that lncRNAs are associated with angiogenesis of cancers (20, 53, 253). In this section, we discuss the latest reports about lncRNAs as ceRNAs involved in angiogenesis of PC.

CRNDE/miR-451a/CDKN2D

LncRNA Colorectal neoplasia differentially expressed (CRNDE), originally identified to be specifically associated with colorectal

cancer, is located on chromosome 16 and is also highly expressed in other cancers, such as lung cancer, hepatocellular carcinoma, gastric cancer, breast cancer, and glioma (254–256). Meanwhile, increasing evidence suggests that CRNDE can function as a crucial tumor promoter to facilitate the progression of carcinogenesis in various cancers. It has been shown that overexpression of CRNDE promotes cell growth and proliferation, enhances migration and invasion, and modulates metabolism while suppressing apoptosis through multiple molecular regulatory networks (254–256). Zhu et al. (257) found that CRNDE promoted the progression and angiogenesis of PC *via* miR-451a/CDKN2D axis. They found that CRNDE was significantly upregulated in PC tissues as well as PC cell lines. And CRNDE overexpression enhanced the progression and angiogenesis of PC cells *in vitro* and *in vivo*. Further studies showed that CRNDE exerted its oncogenic role by sponging miR-451a to upregulate cyclin-dependent kinase inhibitor 2D (CDKN2D) expression. Furthermore, Pearson analysis showed that the expression of CRNDE and miR-451a was negatively correlated, and the expression of miR-451a and CDKN2D was also negatively correlated, while the expression of CRNDE and CDKN2D was positively correlated in PC tissues. Overexpression of miR-451a or CDKN2D knockdown significantly reversed CRNDE-mediated PC cell proliferation, migration, and angiogenesis. Consequently, the above data demonstrated that CRNDE/miR-451a/CDKN2D ceRNA axis might become a potential therapeutic target for PC treatment (257). In addition, Wang et al. (258) reported that CRNDE sponged miR-384 to promote PC cell proliferation and metastasis through upregulating insulin receptor substrate 1 (IRS1).

LINC00511/miR-29b-3p/VEGFA

LncRNA LINC00511 is transcribed from chromosome 17q24.3 region and upregulated in different malignancies, such as glioma, ovarian cancer, breast cancer, cervical cancer, lung cancer, hepatocellular carcinoma, gastric cancer, and renal cell cancer (259). It has been proven that aberrantly upregulated LINC00511 in malignant tumors is strongly associated with tumor size, clinical stage, lymph node metastasis, and unsatisfactory prognosis. Meanwhile, growing evidence reveals that LINC00511 can accelerate tumor progression by inhibiting malignant cell apoptosis and promoting tumor cell proliferation, migration, invasion, metastasis, chemotherapy resistance, and so on (259). Moreover, recent studies also displayed that LINC00511 played crucial roles in multiple malignant processes of carcinogenesis by serving as a ceRNA. For example, Lu et al. (260) revealed that LINC00511 acted as a ceRNA, which contributed to breast cancer tumorigenesis and stemness by inducing the miR-185-3p/E2F1/Nanog axis, whereas the LINC00511/miR-150/MMP13 ceRNA axis also promoted breast cancer proliferation, migration, and invasion (261). At the same time, LINC00511 facilitated lung squamous cell carcinoma progression *via* sequestering miR-150-5p and activating TADA1 by ceRNA mechanism (262). Additionally, LINC00511 could enhance glioblastoma tumorigenesis and EMT *via* LINC00511/miR-524-5p/YB1/ZEB1 positive feedback loop (263). In PC, Zhao et al. (264) demonstrated that LINC00511 functioned as a ceRNA to mediate the expression of VEGFA through competition for miR-29b-3p, hence serving as a tumor promoter for proliferation, migration, and angiogenesis. They found that LINC00511 was upregulated in PC samples compared with adjacent non-tumoral samples and significantly associated with lymph node metastasis, early recurrence, and poor patient survival. Knockdown of linc00511 impaired tumor proliferation *in vivo* and *in vitro*, concomitant with induction of cell apoptosis. Further studies showed that knockdown of linc00511 blocked PC cell migration, invasion, and angiogenesis *in vitro*. Mechanistically, LINC00511 promoted PC progression through sponging miR-29b-3p to upregulate VEGFA expression. VEGFA knockdown decreased the effect of LINC00511-mediated cell proliferation, invasion, and angiogenesis. In summary, LINC00511/miR-29b-3p/VEGFA axis played a critical role in the tumorigenesis and angiogenesis of PC. Simultaneously, Wang et al. (265) found that miR-29c-3p/LINC00511 may be utilized to indicate prognosis of PC based on ceRNA hypothesis through bioinformatics analysis.

LncRNAs AS CeRNA IN PANCREATIC CANCER DIAGNOSIS, PROGNOSIS, AND THERAPY

Diagnosis of diseases by detecting the differential expression of circulating RNA in plasma or serum has become a new technology in the field of noninvasive diagnostic applications (266). Recent studies have found that miRNA can be detected in human peripheral blood despite the large amount of endogenous ribonuclease in blood of cancer patients (267). In addition, a variety of plasma or serum lncRNAs have been characterized as potential tumor markers in human fluids. Ren et al. (268) found that in plasma of patients with prostate cancer, MALAT1 was significantly overexpressed and could significantly discriminate cancer patients from healthy controls. Plasma AA174084 levels were associated with invasion and lymphatic metastasis of gastric cancer and were found to drop markedly on day 15 after the patients received surgery (269). As reported, the aberrant expressions of other lncRNAs have potential to serve as diagnostic or prognostic biomarkers for the human colon, breast, liver, and lung malignancies (270–273). In this section, we discuss some ceRNA networks involved in the diagnosis, prognosis, and therapy of PC.

UCA1/miR-96-5p/AMOTL2, ERK1, ERK2

LncRNA UCA1 was found to be highly expressed in exosomes derived from hypoxic PC cells and could be transferred to human umbilical vein endothelial cells through the exosomes (168). Further detections revealed the elevated expression levels of

UCA1 in exosomes derived from serum of PC patients compared with healthy controls, which was associated with poor survival of PC patients. In addition, UCA1 could promote tumor growth and angiogenesis through the UCA1/miR-96-5p/AMOTL2, ERK1, ERK2 axis.

PVT1/miR-20b/CCND1

By searching The Cancer Genome Atlas (TCGA) and Genotype-Tissue Expression (GTEx) databases and performing functional enrichment analysis, Zu et al. (274) recognized that pathways in cancer was greatly associated with tumor formation and progression. To identify a meaningful ceRNA network, the stepwise prediction and validation from mRNA to lncRNA were applied according to the ceRNA rules. A total of 11 hub genes, four key miRNAs, and two key lncRNAs were found to be key factors in the ceRNA network, and the PVT1/miR-20b/CCND1 axis was identified as a promising pathway-related ceRNA axis in the progression of PC, which could be considered as encouraging a prognostic biomarker and therapeutic target for PC.

LncRISK-7

Zhou et al. (275) performed a genome-wide analysis to investigate potential lncRNA-mediated ceRNA interplay based on "ceRNA hypothesis" and uncovered seven novel lncRNAs as functional ceRNAs contributing to PC. Next, based on the expression data and the support vector machine (SVM) algorithm, a seven-lncRNA signature (termed LncRisk-7, including SH3BP5-AS1, STARD4-AS1, ARNTL2-AS1, AC002550.5, RP11-206L10.5, AC016738.4, and RP5-901A4.1) was developed as a novel diagnostic tool, which could significantly improve the early diagnosis of PC. The LncRisk-7 showed promising efficiency in distinguishing PC samples from non-malignant pancreas samples in the training cohort, and its high performance was further confirmed in two independent validation cohorts. Results of the functional experiments demonstrated that the seven lncRNA biomarkers were involved in the regulation of cell cycle, cell death, and cell adhesion of PC cells, mechanistically acting as ceRNAs. Results of this work improved our understanding of the lncRNA-mediated ceRNA regulatory mechanisms in the pathogenesis of PC and provided the LncRisk-7 as potential diagnostic biomarkers.

A ceRNA MODULE COMPRISING OF 29 GENES

Using the paired genome-wide expression profiles of lncRNA, miRNA, mRNA, and relationships between them, Zhao et al. (276) constructed a PC-specific hallmark gene-related ceRNA network (HceNet). The characteristics of HceNet was analyzed based on "ceRNA hypothesis," and a ceRNA module comprising of 12 lncRNAs, 2 miRNAs, and 15 mRNAs was identified as potential prognostic biomarkers associated with the overall survival of PC patients. The prognostic value of ceRNA module biomarkers was further validated to be statistically significant in all the training, the validation, and the entire cohorts. This study provided potential prognostic biomarkers for PC and provided novel insight into the ceRNA-related regulatory mechanism in PC progression.

A THREE-LncRNA SIGNATURE

To identify the specific lncRNAs and further analyze their function relating to PC, Shi et al. (277) constructed a global triple network based on the ceRNA theory and RNA-seq data from The Cancer Genome Atlas. Six lncRNAs in the lncRNA–miRNA–mRNA co-expression network were significantly associated with overall survival of PC patients, and a three-lncRNA (LINC00460, C9orf139, and MIR600HG) signature succeeded to predict survival of patients with PC. Protein–protein interaction network data uncovered the association of five genes with the overall survival of PC patients. The findings of this study deepened our understanding in the function of an lncRNA-associated ceRNA network involved in PC pathogenesis and identified the potential prognostic roles of the three-lncRNA signature in PC.

NAMPTP1/HCG11-hsa-miR-26b-5p-COL12A SUBNETWORK

By analyzing the expression and survival data of the aberrantly expressed genes in PC according to the systematic mRNA–miRNA–lncRNA/pseudogene network, Jing et al. (278) elucidated the new NAMPTP1/HCG11-hsa-miR-26b-5p-COL12A subnetwork in PC progression. Further validation indicated that the subnetwork might be a candidate diagnostic biomarker or potential therapeutic target for PC.

AN lncRNA–miRNA–mRNA CO-EXPRESSION NETWORK

To identify new prognostic markers and develop a multi-mRNAs-based classifier for survival prediction in patients with PC, Weng et al. (29) established an lncRNA–miRNA–mRNA co-expression network that consisted of 66 genes (60 lncRNAs, 3 miRNAs, and 3 mRNAs) relating to the prognosis of PC patients. In addition, a 14-mRNAs-based classifier was constructed based on a training dataset consisting of 178 PC patients. The area under the receiver operating characteristic (AUC) curves in the training dataset for prediction of 1-, 3-, and 5-year OS were 0.719, 0.806, and 0.794, respectively. In the independent validation dataset, the AUC of classifier was 0.604, 0.639, and 0.607, respectively, which showed the good prediction function of the network. The network was associated

with PC pathogenesis and might be used as a reference for future molecular biology research.

CONCLUSIONS

The ceRNA interplay is a universal posttranscriptional regulation involving miRNAs and various coding and noncoding RNAs through the functional interactions among them. Comprehensive investigations and understanding into the ceRNA network will greatly increase our knowledge in the underlying molecular mechanisms of cancer pathogenesis. As discussed in this review, the lncRNAs harboring the MREs can specifically sequester miRNAs and function as molecular decoys or sponges, competitively inhibiting the translation and function of their downstream target genes. The lncRNA–miRNA–mRNA ceRNA networks play important regulatory functions in PC progression, including almost all crucial biological processes. As important members of the ceRNA networks, lncRNAs are widely involved in the occurrence of PC, which suggests that plasma lncRNA can to be used as a novel and effective diagnostic biomarker. At the same time, lncRNAs have been found to be involved in the development of the advanced stages of PC, indicating the great potential of these lncRNAs as prognostic biomarkers. More importantly, overexpression or knockdown of related members in the ceRNA networks that are closely associated with the development of PC can significantly inhibit the malignant biological behavior of PC, which suggests them as candidate therapeutic targets for PC.

In recent decades, more and more studies have focused on in-depth explanations of the molecular mechanisms behind the malignant biological behavior of PC. However, the diagnosis and treatment measures related to PC are still limited, and the prognosis of PC has not been significantly improved. At present, the research and understanding of the novel lncRNA-related ceRNA networks are still in the early stage, and the exact mechanisms of their involvement in cancer progression remain largely unknown, which requires in-depth exploration in the molecular mechanisms to provide new advances in the treatment of PC.

AUTHOR CONTRIBUTIONS

GX and SP were responsible for gathering information of the related research and designing the review. JJ, XW, RH, FP, XL, and MW were responsible for language editing. JZ, FZ, and RQ have contributed to information interpretation and editing and critical revision of the article. All authors contributed to the article and approved the submitted version.

FUNDING

This study was supported by grants from the National Natural Science Foundation of China (No. 81902499, No. 81874205, and No. 81772950).

SUPPLEMENTARY MATERIAL

The Supplementary Material for this article can be found online at: https://www.frontiersin.org/articles/10.3389/fonc.2021.765216/full#supplementary-material

REFERENCES

1. Mizrahi JD, Surana R, Valle JW, Shroff RT. Pancreatic Cancer. *Lancet* (2020) 395(10242):2008–20. doi: 10.1016/S0140-6736(20)30974-0
2. Siegel RL, Miller KD, Jemal A. Cancer Statistics, 2020. *CA Cancer J Clin* (2020) 70(1):7–30. doi: 10.3322/caac.21590
3. Siegel RL, Miller KD, Jemal A. Cancer Statistics, 2019. *Ca Cancer J Clin* (2019) 69(1):7–34. doi: 10.3322/caac.21551
4. Grossberg AJ, Chu LC, Deig CR, Fishman EK, Hwang WL, Maitra A, et al. Multidisciplinary Standards of Care and Recent Progress in Pancreatic Ductal Adenocarcinoma. *CA Cancer J Clin* (2020) 70(5):375–403. doi: 10.3322/caac.21626
5. Aguirre AJ, Collisson EA. Advances in the Genetics and Biology of Pancreatic Cancer. *Cancer J* (2017) 23(6):315–20. doi: 10.1097/PPO.0000000000000286
6. Lotfi Z, Najjary S, Lotfi F, Amini M, Baghbanzadeh A, Rashid DJ, et al. Crosstalk Between MiRNAs and Signaling Pathways Involved in Pancreatic Cancer and Pancreatic Ductal Adenocarcinoma. *Eur J Pharmacol* (2021) 901:174006. doi: 10.1016/j.ejphar.2021.174006
7. Jones S, Zhang X, Parsons DW, Lin JC, Leary RJ, Angenendt P, et al. Core Signaling Pathways in Human Pancreatic Cancers Revealed by Global Genomic Analyses. *Science* (2008) 321(5897):1801–6. doi: 10.1126/science.1164368
8. Kamisawa T, Wood LD, Itoi T, Takaori K. Pancreatic Cancer. *Lancet* (2016) 388(10039):73–85. doi: 10.1016/S0140-6736(16)00141-0
9. Waddell N, Pajic M, Patch AM, Chang DK, Kassahn KS, Bailey P, et al. Whole Genomes Redefine the Mutational Landscape of Pancreatic Cancer. *Nature* (2015) 518(7540):495–501. doi: 10.1038/nature14169
10. Ryan DP, Hong TS, Bardeesy N. Pancreatic Adenocarcinoma. *N Engl J Med* (2014) 371(11):1039–49. doi: 10.1056/NEJMra1404198
11. Xiao G, Fu J. NF-κB and Cancer: A Paradigm of Yin-Yang. *Am J Cancer Res* (2011) 1(2):192–221.
12. Ying H, Dey P, Yao W, Kimmelman AC, Draetta GF, Maitra A, et al. Genetics and Biology of Pancreatic Ductal Adenocarcinoma. *Genes Dev* (2016) 30(4):355–85. doi: 10.1101/gad.275776.115
13. Chen RQ, Liu F, Qiu XY, Chen XQ. The Prognostic and Therapeutic Value of PD-L1 in Glioma. *Front Pharmacol* (2018) 9:1503. doi: 10.3389/fphar.2018.01503
14. Sato-Dahlman M, Wirth K, Yamamoto M. Role of Gene Therapy in Pancreatic Cancer-a Review. *Cancers (Basel)* (2018) 10(4). doi: 10.3390/cancers10040103
15. Koliopanos A, Avgerinos C, Paraskeva C, Touloumis Z, Kelgiorgi D, Dervenis C. Molecular Aspects of Carcinogenesis in Pancreatic Cancer. *Hepatobiliary Pancreat Dis Int* (2008) 7(4):345–56.
16. Hemberg M, Gray JM, Cloonan N, Kuersten S, Grimmond S, Greenberg ME, et al. Integrated Genome Analysis Suggests That Most Conserved Non-Coding Sequences Are Regulatory Factor Binding Sites. *Nucleic Acids Res* (2012) 40(16):7858–69. doi: 10.1093/nar/gks477
17. Pavet V, Portal MM, Moulin JC, Herbrecht R, Gronemeyer H. Towards Novel Paradigms for Cancer Therapy. *Oncogene* (2011) 30(1):1–20. doi: 10.1038/onc.2010.460
18. Yu J, Li A, Hong SM, Hruban RH, Goggins M. MicroRNA Alterations of Pancreatic Intraepithelial Neoplasias. *Clin Cancer Res* (2012) 18(4):981–92. doi: 10.1158/1078-0432.CCR-11-2347
19. Kung JT, Colognori D, Lee JT. Long Noncoding RNAs: Past, Present, and Future. *Genetics* (2013) 193(3):651–69. doi: 10.1534/genetics.112.146704

20. Goodall GJ, Wickramasinghe VO. RNA in Cancer. *Nat Rev Cancer* (2021) 21 (1):22–36. doi: 10.1038/s41568-020-00306-0
21. Anastasiadou E, Jacob LS, Slack FJ. Non-Coding RNA Networks in Cancer. *Nat Rev Cancer* (2018) 18(1):5–18. doi: 10.1038/nrc.2017.99
22. Chan JJ, Tay Y. Noncoding RNA:RNA Regulatory Networks in Cancer. *Int J Mol Sci* (2018) 19(5). doi: 10.3390/ijms19051310
23. Hejazi M, Baghbani E, Amini M, Rezaei T, Aghanejad A, Mosafer J, et al. MicroRNA-193a and Taxol Combination: A New Strategy for Treatment of Colorectal Cancer. *J Cell Biochem* (2020) 121(2):1388–99. doi: 10.1002/jcb.29374
24. Shirmohamadi M, Eghbali E, Najjary S, Mokhtarzadeh A, Kojabad AB, Hajiasgharzadeh K, et al. Regulatory Mechanisms of MicroRNAs in Colorectal Cancer and Colorectal Cancer Stem Cells. *J Cell Physiol* (2020) 235(2):776–89. doi: 10.1002/jcp.29042
25. Felix TF, Lopez Lapa RM, de Carvalho M, Bertoni N, Tokar T, Oliveira RA, et al. MicroRNA Modulated Networks of Adaptive and Innate Immune Response in Pancreatic Ductal Adenocarcinoma. *PloS One* (2019) 14(5): e0217421. doi: 10.1371/journal.pone.0217421
26. Ghasabi M, Mansoori B, Mohammadi A, Duijf PH, Shomali N, Shirafkan N, et al. MicroRNAs in Cancer Drug Resistance: Basic Evidence and Clinical Applications. *J Cell Physiol* (2019) 234(3):2152–68. doi: 10.1002/jcp.26810
27. Xiong G, Feng M, Yang G, Zheng S, Song X, Cao Z, et al. The Underlying Mechanisms of Non-Coding RNAs in the Chemoresistance of Pancreatic Cancer. *Cancer Lett* (2017) 397:94–102. doi: 10.1016/j.canlet.2017.02.020
28. Zhang Y, Li X, Zhou D, Zhi H, Wang P, Gao Y, et al. Inferences of Individual Drug Responses Across Diverse Cancer Types Using a Novel Competing Endogenous RNA Network. *Mol Oncol* (2018) 12(9):1429–46. doi: 10.1002/1878-0261.12181
29. Weng W, Zhang Z, Huang W, Xu X, Wu B, Ye T, et al. Identification of a Competing Endogenous RNA Network Associated With Prognosis of Pancreatic Adenocarcinoma. *Cancer Cell Int* (2020) 20:231. doi: 10.1186/s12935-020-01243-6
30. Mortoglou M, Tabin ZK, Arisan ED, Kocher HM, Uysal-Onganer P. Non-Coding RNAs in Pancreatic Ductal Adenocarcinoma: New Approaches for Better Diagnosis and Therapy. *Transl Oncol* (2021) 14(7):101090.
31. Pu M, Chen J, Tao Z, Miao L, Qi X, Wang Y, et al. Regulatory Network of MiRNA on Its Target: Coordination Between Transcriptional and Post-Transcriptional Regulation of Gene Expression. *Cell Mol Life Sci* (2019) 76 (3):441–51. doi: 10.1007/s00018-018-2940-7
32. Wang L, Cho KB, Li Y, Tao G, Xie Z, Guo B, et al. Long Noncoding RNA (LncRNA)-Mediated Competing Endogenous RNA Networks Provide Novel Potential Biomarkers and Therapeutic Targets for Colorectal Cancer. *Int J Mol Sci* (2019) 20(22). doi: 10.3390/ijms20225758
33. Meister G. Argonaute Proteins: Functional Insights and Emerging Roles. *Nat Rev Genet* (2013) 14(7):447–59. doi: 10.1038/nrg3462
34. Bartel DP. MicroRNAs: Target Recognition and Regulatory Functions. *Cell* (2009) 136(2):215–33. doi: 10.1016/j.cell.2009.01.002
35. Franco-Zorrilla JM, Valli A, Todesco M, Mateos I, Puga MI, Rubio-Somoza I, et al. Target Mimicry Provides a New Mechanism for Regulation of MicroRNA Activity. *Nat Genet* (2007) 39(8):1033–7. doi: 10.1038/ng2079
36. Ebert MS, Neilson JR, Sharp PA. MicroRNA Sponges: Competitive Inhibitors of Small RNAs in Mammalian Cells. *Nat Methods* (2007) 4 (9):721–6. doi: 10.1038/nmeth1079
37. Sen R, Ghosal S, Das S, Balti S, Chakrabarti J. Competing Endogenous RNA: The Key to Posttranscriptional Regulation. *ScientificWorldJournal* (2014) 2014:896206. doi: 10.1155/2014/896206
38. Yang C, Wu D, Gao L, Liu X, Jin Y, Wang D, et al. Competing Endogenous RNA Networks in Human Cancer: Hypothesis, Validation, and Perspectives. *Oncotarget* (2016) 7(12):13479–90. doi: 10.18632/oncotarget.7266
39. Sanchez-Mejias A, Tay Y. Competing Endogenous RNA Networks: Tying the Essential Knots for Cancer Biology and Therapeutics. *J Hematol Oncol* (2015) 8:30. doi: 10.1186/s13045-015-0129-1
40. Seitz H. Redefining MicroRNA Targets. *Curr Biol* (2009) 19(10):870–3. doi: 10.1016/j.cub.2009.03.059
41. Salmena L, Poliseno L, Tay Y, Kats L. A ceRNA Hypothesis: The Rosetta Stone of a Hidden RNA Language? *Cell* (2011) 146(3):353–8. doi: 10.1016/j.cell.2011.07.014
42. Jeyapalan Z, Deng Z, Shatseva T, Fang L, He C, Yang BB. Expression of CD44 3'-Untranslated Region Regulates Endogenous MicroRNA Functions in Tumorigenesis and Angiogenesis. *Nucleic Acids Res* (2011) 39(8):3026–41. doi: 10.1093/nar/gkq1003
43. Baek D, Villén J, Shin C, Camargo FD, Gygi SP, Bartel DP. The Impact of MicroRNAs on Protein Output. *Nature* (2008) 455(7209):64–71. doi: 10.1038/nature07242
44. Qi X, Zhang DH, Wu N, Xiao JH, Wang X, Ma W. CeRNA in Cancer: Possible Functions and Clinical Implications. *J Med Genet* (2015) 52 (10):710–8. doi: 10.1136/jmedgenet-2015-103334
45. Mukherji S, Ebert MS, Zheng GX, Tsang JS, Sharp PA, van Oudenaarden A. MicroRNAs can Generate Thresholds in Target Gene Expression. *Nat Genet* (2011) 43(9):854–9. doi: 10.1038/ng.905
46. Friedman RC, Farh KK, Burge CB, Bartel DP. Most Mammalian mRNAs Are Conserved Targets of MicroRNAs. *Genome Res* (2009) 19(1):92–105.
47. Zhao M, Feng J, Tang L. Competing Endogenous RNAs in Lung Cancer. *Cancer Biol Med* (2021) 18(1):1–20.
48. Wang J, Liu X, Wu H, Ni P, Gu Z, Qiao Y, et al. CREB Up-Regulates Long Non-Coding RNA, HULC Expression Through Interaction With microRNA-372 in Liver Cancer. *Nucleic Acids Res* (2010) 38(16):5366–83. doi: 10.1093/nar/gkq285
49. Peng W, He D, Shan B, Wang J, Shi W, Zhao W, et al. LINC81507 Act as a Competing Endogenous RNA of MiR-199b-5p to Facilitate NSCLC Proliferation and Metastasis *via* Regulating the CAV1/STAT3 Pathway. *Cell Death Dis* (2019) 10(7):533. doi: 10.1038/s41419-019-1740-9
50. Tay Y, Rinn J, Pandolfi PP. The Multilayered Complexity of CeRNA Crosstalk and Competition. *Nature* (2014) 505(7483):344–52. doi: 10.1038/nature12986
51. Statello L, Guo C, Chen L, Huarte M. Gene Regulation by Long Non-Coding RNAs and Its Biological Functions. *Nat Rev Mol Cell Biol* (2021) 22(2):96–118. doi: 10.1038/s41580-020-00315-9
52. Karreth FA, Pandolfi PP. ceRNA Cross-Talk in Cancer: When Ce-Bling Rivalries Go Awry. *Cancer Discov* (2013) 3(10):1113–21. doi: 10.1158/2159-8290.CD-13-0202
53. Schmitt A, Chang H. Long Noncoding RNAs in Cancer Pathways. *Cancer Cell* (2016) 29(4):452–63. doi: 10.1016/j.ccell.2016.03.010
54. Li N, Yang G, Luo L, Ling L, Wang X, Shi L, et al. LncRNA THAP9-AS1 Promotes Pancreatic Ductal Adenocarcinoma Growth and Leads to a Poor Clinical Outcome *via* Sponging MiR-484 and Interacting With YAP. *Clin Cancer Res* (2020) 26(7):1736–48. doi: 10.1158/1078-0432.CCR-19-0674
55. Yang H, Liu P, Zhang J, Peng X, Lu Z, Yu S, et al. Long Noncoding RNA MIR31HG Exhibits Oncogenic Property in Pancreatic Ductal Adenocarcinoma and Is Negatively Regulated by MiR-193b. *Oncogene* (2016) 35(28):3647–57. doi: 10.1038/onc.2015.430
56. Liang S, Gong X, Zhang G, Huang G, Lu Y, Li Y. The lncRNA XIST Interacts With MiR-140/MiR-124/iASPP Axis to Promote Pancreatic Carcinoma Growth. *Oncotarget* (2017) 8(69):113701–18. doi: 10.18632/oncotarget.22555
57. Wang J, He Z, Xu J, Chen P, Jiang J. Long Noncoding RNA LINC00941 Promotes Pancreatic Cancer Progression by Competitively Binding MiR-335-5p to Regulate ROCK1-Mediated LIMK1/Cofilin-1 Signaling. *Cell Death Dis* (2021) 12(1):36. doi: 10.1038/s41419-020-03316-w
58. Li H, Wang X, Wen C, Huo Z, Wang W, Zhan Q, et al. Long Noncoding RNA NORAD, a Novel Competing Endogenous RNA, Enhances the Hypoxia-Induced Epithelial-Mesenchymal Transition to Promote Metastasis in Pancreatic Cancer. *Mol Cancer* (2017) 16(1):169. doi: 10.1186/s12943-017-0738-0
59. Zhai S, Xu Z, Xie J, Zhang J, Wang X, Peng C, et al. Epigenetic Silencing of LncRNA LINC00261 Promotes C-Myc-Mediated Aerobic Glycolysis by Regulating miR-222-3p/HIPK2/ERK Axis and Sequestering IGF2BP1. *Oncogene* (2021) 40(2):277–91. doi: 10.1038/s41388-020-01525-3
60. Huang F, Chen W, Peng J, Li Y, Zhuang Y, Zhu Z, et al. LncRNA PVT1 Triggers Cyto-Protective Autophagy and Promotes Pancreatic Ductal Adenocarcinoma Development *via* the miR-20a-5p/ULK1 Axis. *Mol Cancer* (2018) 17(1):98. doi: 10.1186/s12943-018-0845-6
61. Han W, Sulidankazha Q, Nie X, Yilidan R, Len K. Pancreatic Cancer Cells-Derived Exosomal Long Non-Coding RNA CCAT1/MicroRNA-138-5p/

HMGA1 Axis Promotes Tumor Angiogenesis. *Life Sci* (2021) 278:119495. doi: 10.1016/j.lfs.2021.119495
62. Wu XB, Feng X, Chang QM, Zhang CW, Wang ZF, Liu J, et al. Cross-Talk Among AFAP1-AS1, ACVR1 and MicroRNA-384 Regulates the Stemness of Pancreatic Cancer Cells and Tumorigenicity in Nude Mice. *J Exp Clin Cancer Res* (2019) 38(1):107. doi: 10.1186/s13046-019-1051-0
63. Xiong G, Liu C, Yang G, Feng M, Xu J, Zhao F, et al. Long Noncoding RNA GSTM3TV2 Upregulates LAT2 and OLR1 by Competitively Sponging Let-7 to Promote Gemcitabine Resistance in Pancreatic Cancer. *J Hematol Oncol* (2019) 12(1):97. doi: 10.1186/s13045-019-0777-7
64. Huarte M. The Emerging Role of LncRNAs in Cancer. *Nat Med* (2015) 21 (11):1253–61. doi: 10.1038/nm.3981
65. Dragomir M, Kopetz S, Ajani J, Calin G. Non-Coding RNAs in GI Cancers: From Cancer Hallmarks to Clinical Utility. *Gut* (2020) 69(4):748–63. doi: 10.1136/gutjnl-2019-318279
66. Pandya G, Kirtonia A, Sethi G, Pandey A, Garg M. The Implication of Long Non-Coding RNAs in the Diagnosis, Pathogenesis and Drug Resistance of Pancreatic Ductal Adenocarcinoma and Their Possible Therapeutic Potential. *Biochim Biophys Acta Rev Cancer* (2020) 1874(2):188423. doi: 10.1016/j.bbcan.2020.188423
67. Sharma GG, Okada Y, Von Hoff D, Goel A. Non-Coding RNA Biomarkers in Pancreatic Ductal Adenocarcinoma. *Semin Cancer Biol* (2020). doi: 10.1016/j.semcancer.2020.10.001
68. Hanahan D, Weinberg RA. Hallmarks of Cancer: The Next Generation. *Cell* (2011) 144(5):646–74. doi: 10.1016/j.cell.2011.02.013
69. Crawford HC, Pasca di Magliano M, Banerjee S. Signaling Networks That Control Cellular Plasticity in Pancreatic Tumorigenesis, Progression, and Metastasis. *Gastroenterology* (2019) 156(7):2073–84. doi: 10.1053/j.gastro.2018.12.042
70. Venkat S, Alahmari AA, Feigin ME. Drivers of Gene Expression Dysregulation in Pancreatic Cancer. *Trends Cancer* (2021) 7(7):594–605. doi: 10.1016/j.trecan.2021.01.008
71. Gong R, Jiang Y. Non-Coding RNAs in Pancreatic Ductal Adenocarcinoma. *Front Oncol* (2020) 10:309. doi: 10.3389/fonc.2020.00309
72. Jia W, Zhang J, Ma F, Hao S, Li X, Guo R, et al. Long Noncoding RNA THAP9-AS1 Is Induced by Helicobacter Pylori and Promotes Cell Growth and Migration of Gastric Cancer. *Onco Targets Ther* (2019) 12:6653–63. doi: 10.2147/OTT.S201832
73. Cheng J, Ma H, Yan M, Xing W. THAP9-AS1/MiR-133b/SOX4 Positive Feedback Loop Facilitates the Progression of Esophageal Squamous Cell Carcinoma. *Cell Death Dis* (2021) 12(4):401.
74. Pan Q, Li B, Zhang J, Du X, Gu D. LncRNA THAP9-AS1 Accelerates Cell Growth of Esophageal Squamous Cell Carcinoma Through Sponging miR-335-5p to Regulate SGMS2. *Pathol Res Pract* (2021) 224:153526. doi: 10.1016/j.prp.2021.153526
75. Gupta SC, Awasthee N, Rai V, Chava S, Gunda V, Challagundla KB, et al. Long Non-Coding RNAs and Nuclear Factor-κb Crosstalk in Cancer and Other Human Diseases. *Biochim Biophys Acta Rev Cancer* (2020) 1873 (1):188316.
76. Montes M, Nielsen MM, Maglieri G, Jacobsen A, Højfeldt J, Agrawal-Singh S, et al. The LncRNA MIR31HG Regulates P16(INK4A) Expression to Modulate Senescence. *Nat Commun* (2015) 6:6967. doi: 10.1038/ncomms7967
77. Shih JW, Chiang WF, Wu ATH, Wu MH, Wang LY, Yu YL, et al. Long Noncoding RNA Lnchifcar/MIR31HG Is a HIF-1α Co-Activator Driving Oral Cancer Progression. *Nat Commun* (2017) 8:15874. doi: 10.1038/ncomms15874
78. Yan S, Tang Z, Chen K, Liu Y, Yu G, Chen Q, et al. Long Noncoding RNA MIR31HG Inhibits Hepatocellular Carcinoma Proliferation and Metastasis by Sponging MicroRNA-575 to Modulate ST7L Expression. *J Exp Clin Cancer Res* (2018) 37(1):214. doi: 10.1186/s13046-018-0853-9
79. Zhang L, Hou C, Xu Z, Wang L, Ling X, Xiu D. Laparoscopic Treatment for Suspected Gallbladder Cancer Confined to the Wall: A 10-Year Study From a Single Institution. *Chin J Cancer Res* (2018) 30(1):84–92. doi: 10.21147/j.issn.1000-9604.2018.01.09
80. Ramya Devi KT, Karthik D, Mahendran T, Jaganathan MK, Hemdev SP, et al. Long Noncoding RNAs: Role and Contribution in Pancreatic Cancer. *Transcription* (2021) 12(1):12–27. doi: 10.1080/21541264.2021.1922071
81. Pan S, Shen M, Zhou M, Shi X, He R, Yin T, et al. Long Noncoding RNA LINC01111 Suppresses Pancreatic Cancer Aggressiveness by Regulating DUSP1 Expression *via* MicroRNA-3924. *Cell Death Dis* (2019) 10(12):883. doi: 10.1038/s41419-019-2123-y
82. Lei S, He Z, Chen T, Guo X, Zeng Z, Shen Y, et al. Long Noncoding RNA 00976 Promotes Pancreatic Cancer Progression Through OTUD7B by Sponging MiR-137 Involving EGFR/MAPK Pathway. *J Exp Clin Cancer Res* (2019) 38(1):470. doi: 10.1186/s13046-019-1388-4
83. Amodio N, Raimondi L, Juli G, Stamato MA, Caracciolo D, Tagliaferri P, et al. MALAT1: A Druggable Long Non-Coding RNA for Targeted Anti-Cancer Approaches. *J Hematol Oncol* (2018) 11(1):63. doi: 10.1186/s13045-018-0606-4
84. Chen Q, Zhu C, Jin Y. The Oncogenic and Tumor Suppressive Functions of the Long Noncoding RNA MALAT1: An Emerging Controversy. *Front Genet* (2020) 11:93. doi: 10.3389/fgene.2020.00093
85. Goyal B, Yadav SRM, Awasthee N, Gupta S, Kunnumakkara AB, Gupta SC. Diagnostic, Prognostic, and Therapeutic Significance of Long Non-Coding RNA MALAT1 in Cancer. *Biochim Biophys Acta Rev Cancer* (2021) 1875 (2):188502.
86. Liu P, Yang H, Zhang J, Peng X, Lu Z, Tong W, et al. The LncRNA MALAT1 Acts as a Competing Endogenous RNA to Regulate KRAS Expression by Sponging MiR-217 in Pancreatic Ductal Adenocarcinoma. *Sci Rep* (2017) 7 (1):5186. doi: 10.1038/s41598-017-05274-4
87. Zhuo M, Yuan C, Han T, Cui J, Jiao F, Wang L. A Novel Feedback Loop Between High MALAT-1 and Low Mir-200c-3p Promotes Cell Migration and Invasion in Pancreatic Ductal Adenocarcinoma and Is Predictive of Poor Prognosis. *BMC Cancer* (2018) 18(1):1032. doi: 10.1186/s12885-018-4954-9
88. Loewen G, Jayawickramarajah J, Zhuo Y, Shan B. Functions of LncRNA HOTAIR in Lung Cancer. *J Hematol Oncol* (2014) 7:90. doi: 10.1186/s13045-014-0090-4
89. Cantile M, Di Bonito M, Tracey De Bellis M, Botti G. Functional Interaction Among LncRNA HOTAIR and MicroRNAs in Cancer and Other Human Diseases. *Cancers* (2021) 13(3). doi: 10.3390/cancers13030570
90. Qu X, Alsager S, Zhuo Y, Shan B. HOX Transcript Antisense RNA (HOTAIR) in Cancer. *Cancer Lett* (2019) 454:90–7. doi: 10.1016/j.canlet.2019.04.016
91. Cai H, Yao J, An Y, Chen X, Chen W, Wu D, et al. LncRNA HOTAIR Acts a Competing Endogenous RNA to Control the Expression of Notch3 *via* Sponging Mir-613 in Pancreatic Cancer. *Oncotarget* (2017) 8(20):32905–17. doi: 10.18632/oncotarget.16462
92. Deng S, Wang J, Zhang L, Li J, Jin Y. LncRNA HOTAIR Promotes Cancer Stem-Like Cells Properties by Sponging Mir-34a to Activate the JAK2/STAT3 Pathway in Pancreatic Ductal Adenocarcinoma. *Onco Targets Ther* (2021) 14:1883–93. doi: 10.2147/OTT.S286666
93. Tang Y, Song G, Liu H, Yang S, Yu X, Shi L. Silencing of Long Non-Coding RNA HOTAIR Alle*via*tes Epithelial-Mesenchymal Transition in Pancreatic Cancer *via* the Wnt/β-Catenin Signaling Pathway. *Cancer Manag Res* (2021) 13:3247–57. doi: 10.2147/CMAR.S265578
94. Sahakyan A, Yang Y, Plath K. The Role of Xist in X-Chromosome Dosage Compensation. *Trends Cell Biol* (2018) 28(12):999–1013. doi: 10.1016/j.tcb.2018.05.005
95. Ghafouri-Fard S, Dashti S, Farsi M, Taheri M, Mousavinejad S. X-Inactive-Specific Transcript: Review of Its Functions in the Carcinogenesis. *Front Cell Dev Biol* (2021) 9:690522. doi: 10.3389/fcell.2021.690522
96. Wang W, Min L, Qiu X, Wu X, Liu C, Ma J, et al. Biological Function of Long Non-Coding RNA (LncRNA) Xist. *Front Cell Dev Biol* (2021) 9:645647. doi: 10.3389/fcell.2021.645647
97. Mao H, Wang K, Feng Y, Zhang J, Pan L, Zhan Y, et al. Prognostic Role of Long Non-Coding RNA XIST Expression in Patients With Solid Tumors: A Meta-Analysis. *Cancer Cell Int* (2018) 18:34. doi: 10.1186/s12935-018-0535-x
98. Sun Z, Zhang B, Cui T. Long Non-Coding RNA XIST Exerts Oncogenic Functions in Pancreatic Cancer *via* Mir-34a-5p. *Oncol Rep* (2018) 39 (4):1591–600. doi: 10.3892/or.2018.6245
99. Wei W, Liu Y, Lu Y, Yang B, Tang L. LncRNA XIST Promotes Pancreatic Cancer Proliferation Through Mir-133a/EGFR. *J Cell Biochem* (2017) 118 (10):3349–58. doi: 10.1002/jcb.25988
100. Liu PJ, Pan YH, Wang DW, You D. Long Non−Coding RNA XIST Promotes Cell Proliferation of Pancreatic Cancer Through Mir−137 and Notch1 Pathway. *Eur Rev Med Pharmacol Sci* (2020) 24(23):12161–70.

101. Shen J, Hong L, Yu D, Cao T, Zhou Z, He S. LncRNA XIST Promotes Pancreatic Cancer Migration, Invasion and EMT by Sponging Mir-429 to Modulate ZEB1 Expression. *Int J Biochem Cell Biol* (2019) 113:17–26. doi: 10.1016/j.biocel.2019.05.021
102. Sun J, Zhang Y. LncRNA XIST Enhanced TGF-β2 Expression by Targeting Mir-141-3p to Promote Pancreatic Cancer Cells Invasion. *Biosci Rep* (2019) 39(7). doi: 10.1042/BSR20190332
103. Tao J, Yang G, Zhou W, Qiu J, Chen G, Luo W, et al. Targeting Hypoxic Tumor Microenvironment in Pancreatic Cancer. *J Hematol Oncol* (2021) 14 (1):14. doi: 10.1186/s13045-020-01030-w
104. Yang J, Antin P, Berx G, Blanpain C, Brabletz T, Bronner M, et al. Guidelines and Definitions for Research on Epithelial-Mesenchymal Transition. *Nat Rev Mol Cell Biol* (2020) 21(6):341–52. doi: 10.1038/s41580-020-0237-9
105. Williams E, Gao D, Redfern A, Thompson E. Controversies Around Epithelial-Mesenchymal Plasticity in Cancer Metastasis. *Nat Rev Cancer* (2019) 19(12):716–32. doi: 10.1038/s41568-019-0213-x
106. Dongre A, Weinberg R. New Insights Into the Mechanisms of Epithelial-Mesenchymal Transition and Implications for Cancer. *Nat Rev Mol Cell Biol* (2019) 20(2):69–84. doi: 10.1038/s41580-018-0080-4
107. Puisieux A, Brabletz T, Caramel J. Oncogenic Roles of EMT-Inducing Transcription Factors. *Nat Cell Biol* (2014) 16(6):488–94. doi: 10.1038/ncb2976
108. Lamouille S, Xu J, Derynck R. Molecular Mechanisms of Epithelial-Mesenchymal Transition. *Nat Rev Mol Cell Biol* (2014) 15(3):178–96. doi: 10.1038/nrm3758
109. Liu S, Dang H, Lim D, Feng F, Maher C. Long Noncoding RNAs in Cancer Metastasis. *Nat Rev Cancer* (2021) 21(7):446–60. doi: 10.1038/s41568-021-00353-1
110. Ming H, Li B, Zhou L, Goel A, Huang C. Long Non-Coding RNAs and Cancer Metastasis: Molecular Basis and Therapeutic Implications. *Biochim Biophys Acta Rev Cancer* (2021) 1875(2):188519.
111. Lee S, Kopp F, Chang TC, Sataluri A, Chen B, Sivakumar S, et al. Noncoding RNA NORAD Regulates Genomic Stability by Sequestering PUMILIO Proteins. *Cell* (2016) 164(1-2):69–80. doi: 10.1016/j.cell.2015.12.017
112. Elguindy MM, Mendell JT. NORAD-Induced Pumilio Phase Separation Is Required for Genome Stability. *Nature* (2021) 595(7866):303–8. doi: 10.1038/s41586-021-03633-w
113. Yang Z, Zhao Y, Lin G, Zhou X, Jiang X, Zhao H. Noncoding RNA Activated by DNA Damage (NORAD): Biologic Function and Mechanisms in Human Cancers. *Clin Chim Acta* (2019) 489:5–9. doi: 10.1016/j.cca.2018.11.025
114. Soghli N, Yousefi T, Abolghasemi M, Qujeq D. NORAD, A Critical Long Non-Coding RNA in Human Cancers. *Life Sci* (2021) 264:118665. doi: 10.1016/j.lfs.2020.118665
115. Chen D-L, Lu Y-x, Zhang J-x, Wei X-l, Wang F, Zeng Z-l, et al. Long Non-Coding RNA UICLM Promotes Colorectal Cancer Liver Metastasis by Acting as a CeRNA for MicroRNA-215 to Regulate ZEB2 Expression. *Theranostics* (2017) 7(19):4836–49. doi: 10.7150/thno.20942
116. Bi S, Wang Y, Feng H, Li Q. Long Noncoding RNA LINC00657 Enhances the Malignancy of Pancreatic Ductal Adenocarcinoma by Acting as a Competing Endogenous RNA on MicroRNA-433 to Increase PAK4 Expression. *Cell Cycle* (2020) 19(7):801–16. doi: 10.1080/15384101.2020.1731645
117. Shahryari A, Jazi M, Samaei N, Mowla S. Long Non-Coding RNA SOX2OT: Expression Signature, Splicing Patterns, and Emerging Roles in Pluripotency and Tumorigenesis. *Front Genet* (2015) 6:196. doi: 10.3389/fgene.2015.00196
118. Wang Y, Wu N, Luo X, Zhang X, Liao Q, Wang J. SOX2OT, A Novel Tumor-Related Long Non-Coding RNA. *BioMed Pharmacother* (2020) 123:109725. doi: 10.1016/j.biopha.2019.109725
119. Zhang JJ, Zhu Y, Zhang XF, Liu DF, Wang Y, Yang C, et al. Yin Yang-1 Suppresses Pancreatic Ductal Adenocarcinoma Cell Proliferation and Tumor Growth by Regulating SOX2OT-SOX2 Axis. *Cancer Lett* (2017) 408:144–54. doi: 10.1016/j.canlet.2017.08.032
120. Li Z, Jiang P, Li J, Peng M, Zhao X, Zhang X, et al. Tumor-Derived Exosomal lnc-Sox2ot Promotes EMT and Stemness by Acting as a CeRNA in Pancreatic Ductal Adenocarcinoma. *Oncogene* (2018) 37(28):3822–38. doi: 10.1038/s41388-018-0237-9
121. Wang R, Yan Y, Li C. LINC00462 Is Involved in High Glucose-Induced Apoptosis of Renal Tubular Epithelial Cells *via* AKT Pathway. *Cell Biol Int* (2019). doi: 10.1002/cbin.11231
122. Gong J, Qi X, Zhang Y, Yu Y, Lin X, Li H, et al. Long Noncoding RNA Linc00462 Promotes Hepatocellular Carcinoma Progression. *BioMed Pharmacother* (2017) 93:40–7. doi: 10.1016/j.biopha.2017.06.004
123. Zhou B, Guo W, Sun C, Zhang B, Zheng F. Linc00462 Promotes Pancreatic Cancer Invasiveness Through the MiR-665/TGFBR1-TGFBR2/SMAD2/3 Pathway. *Cell Death Dis* (2018) 9(6):706. doi: 10.1038/s41420-018-0072-3
124. Yu X, Zheng H, Chan MT, Wu WK. HULC: An Oncogenic Long Non-Coding RNA in Human Cancer. *J Cell Mol Med* (2017) 21(2):410–7. doi: 10.1111/jcmm.12956
125. Ghafouri-Fard S, Esmaeili M, Taheri M, Samsami M. Highly Upregulated in Liver Cancer (HULC): An Update on Its Role in Carcinogenesis. *J Cell Physiol* (2020) 235(12):9071–9. doi: 10.1002/jcp.29765
126. Peng W, Gao W, Feng J. Long Noncoding RNA HULC Is a Novel Biomarker of Poor Prognosis in Patients With Pancreatic Cancer. *Med Oncol* (2014) 31 (12):346. doi: 10.1007/s12032-014-0346-4
127. Ou ZL, Luo Z, Lu YB. Long Non-Coding RNA HULC as a Diagnostic and Prognostic Marker of Pancreatic Cancer. *World J Gastroenterol* (2019) 25 (46):6728–42. doi: 10.3748/wjg.v25.i46.6728
128. Feng H, Wei B, Zhang Y. Long Non-Coding RNA HULC Promotes Proliferation, Migration and Invasion of Pancreatic Cancer Cells by Down-Regulating MicroRNA-15a. *Int J Biol Macromol* (2019) 126:891–8. doi: 10.1016/j.ijbiomac.2018.12.238
129. Takahashi K, Ota Y, Kogure T, Suzuki Y, Iwamoto H, Yamakita K, et al. Circulating Extracellular Vesicle-Encapsulated HULC Is a Potential Biomarker for Human Pancreatic Cancer. *Cancer Sci* (2020) 111(1):98–111. doi: 10.1111/cas.14232
130. Takahashi K, Koyama K, Ota Y, Iwamoto H, Yamakita K, Fujii S, et al. The Interaction Between Long Non-Coding RNA HULC and MicroRNA-622 *via* Transfer by Extracellular Vesicles Regulates Cell Invasion and Migration in Human Pancreatic Cancer. *Front Oncol* (2020) 10:1013. doi: 10.3389/fonc.2020.01013
131. Raveh E, Matouk I, Gilon M, Hochberg A. The H19 Long Non-Coding RNA in Cancer Initiation, Progression and Metastasis - A Proposed Unifying Theory. *Mol Cancer* (2015) 14:184. doi: 10.1186/s12943-015-0458-2
132. Wang Y, Hylemon P, Zhou H. Long Non-Coding RNA H19: A Key Player in Liver Diseases. *Hepatology (Baltimore Md)* (2021). doi: 10.1002/hep.31765
133. Shermane Lim YW, Xiang X, Garg M, Le MT, Li-Ann Wong A, Wang L, et al. The Double-Edged Sword of H19 LncRNA: Insights Into Cancer Therapy. *Cancer Lett* (2021) 500:253–62. doi: 10.1016/j.canlet.2020.11.006
134. Sun Y, Zhu Q, Yang W, Shan Y, Yu Z, Zhang Q, et al. LncRNA H19/MiR-194/PFTK1 Axis Modulates the Cell Proliferation and Migration of Pancreatic Cancer. *J Cell Biochem* (2019) 120(3):3874–86. doi: 10.1002/jcb.27669
135. Ma C, Nong K, Zhu H, Wang W, Huang X, Yuan Z, et al. H19 Promotes Pancreatic Cancer Metastasis by Derepressing Let-7's Suppression on Its Target HMGA2-Mediated EMT. *Tumour Biol* (2014) 35(9):9163–9. doi: 10.1007/s13277-014-2185-5
136. Wang F, Rong L, Zhang Z, Li M, Ma L, Ma Y, et al. LncRNA H19-Derived MiR-675-3p Promotes Epithelial-Mesenchymal Transition and Stemness in Human Pancreatic Cancer Cells by Targeting the STAT3 Pathway. *J Cancer* (2020) 11(16):4771–82. doi: 10.7150/jca.44833
137. Ghaforui-Fard S, Vafaee R, Taheri M. Taurine-Upregulated Gene 1: A Functional Long Noncoding RNA in Tumorigenesis. *J Cell Physiol* (2019) 234(10):17100–12. doi: 10.1002/jcp.28464
138. Liang H, Cui Z, Song Q. TUG1 as a Therapy Target in Pancreatic Cancer. *Dig Dis Sci* (2020) 65(12):3756–7. doi: 10.1007/s10620-020-06636-1
139. Zhao L, Sun H, Kong H, Chen Z, Chen B, Zhou M. The Lncrna-TUG1/EZH2 Axis Promotes Pancreatic Cancer Cell Proliferation, Migration and EMT Phenotype Formation Through Sponging Mir-382. *Cell Physiol Biochem* (2017) 42(6):2145–58. doi: 10.1159/000479990
140. Lu Y, Tang L, Zhang Z, Li S, Liang S, Ji L, et al. Long Noncoding RNA TUG1/MiR-29c Axis Affects Cell Proliferation, Invasion, and Migration in Human Pancreatic Cancer. *Dis Markers* (2018) 2018:6857042. doi: 10.1155/2018/6857042
141. Xu K, Zhang L. Inhibition of TUG1/MiRNA-299-3p Axis Represses Pancreatic Cancer Malignant Progression *via* Suppression of the Notch1 Pathway. *Dig Dis Sci* (2020) 65(6):1748–60. doi: 10.1007/s10620-019-05911-0
142. Hermann PC, Sainz B Jr. Pancreatic Cancer Stem Cells: A State or an Entity? *Semin Cancer Biol* (2018) 53:223–31. doi: 10.1016/j.semcancer.2018.08.007

143. Sergeant G, Vankelecom H, Gremeaux L, Topal B. Role of Cancer Stem Cells in Pancreatic Ductal Adenocarcinoma. *Nat Rev Clin Oncol* (2009) 6(10):580–6. doi: 10.1038/nrclinonc.2009.127
144. Stoica AF, Chang CH, Pauklin S. Molecular Therapeutics of Pancreatic Ductal Adenocarcinoma: Targeted Pathways and the Role of Cancer Stem Cells. *Trends Pharmacol Sci* (2020) 41(12):977–93. doi: 10.1016/j.tips.2020.09.008
145. Melendez-Zajgla J, Maldonado V. The Role of LncRNAs in the Stem Phenotype of Pancreatic Ductal Adenocarcinoma. *Int J Mol Sci* (2021) 22 (12). doi: 10.3390/ijms22126374
146. Chen W, Yang J, Fang H, Li L, Sun J. Relevance Function of Linc-ROR in the Pathogenesis of Cancer. *Front Cell Dev Biol* (2020) 8:696. doi: 10.3389/fcell.2020.00696
147. Pan Y, Li C, Chen J, Zhang K, Chu X, Wang R, et al. The Emerging Roles of Long Noncoding RNA ROR (LincRNA-ROR) and Its Possible Mechanisms in Human Cancers. *Cell Physiol Biochem* (2016) 40:219–29. doi: 10.1159/000452539
148. Zhou X, Gao Q, Wang J, Zhang X, Liu K, Duan Z. Linc-RNA-Ror Acts as a "Sponge" Against Mediation of the Differentiation of Endometrial Cancer Stem Cells by MicroRNA-145. *Gynecol Oncol* (2014) 133(2):333–9. doi: 10.1016/j.ygyno.2014.02.033
149. Hou P, Zhao Y, Li Z, Yao R, Ma M, Gao Y, et al. LincRNA-ROR Induces Epithelial-to-Mesenchymal Transition and Contributes to Breast Cancer Tumorigenesis and Metastasis. *Cell Death Dis* (2014) 5(6):e1287. doi: 10.1038/cddis.2014.249
150. Zhan HX, Wang Y, Li C, Xu JW, Zhou B, Zhu JK, et al. LincRNA-ROR Promotes Invasion, Metastasis and Tumor Growth in Pancreatic Cancer Through Activating ZEB1 Pathway. *Cancer Lett* (2016) 374(2):261–71. doi: 10.1016/j.canlet.2016.02.018
151. Gao S, Wang P, Hua Y, Xi H, Meng Z, Liu T, et al. ROR Functions as a CeRNA to Regulate Nanog Expression by Sponging MiR-145 and Predicts Poor Prognosis in Pancreatic Cancer. *Oncotarget* (2016) 7(2):1608–18. doi: 10.18632/oncotarget.6450
152. Li C, Zhao Z, Zhou Z, Liu R. Linc-ROR Confers Gemcitabine Resistance to Pancreatic Cancer Cells *via* Inducing Autophagy and Modulating the MiR-124/PTBP1/PKM2 Axis. *Cancer Chemother Pharmacol* (2016) 78(6):1199–207. doi: 10.1007/s00280-016-3178-4
153. Fu Z, Li G, Li Z, Wang Y, Zhao Y, Zheng S, et al. Endogenous MiRNA Sponge LincRNA-ROR Promotes Proliferation, Invasion and Stem Cell-Like Phenotype of Pancreatic Cancer Cells. *Cell Death Discov* (2017) 3:17004. doi: 10.1038/cddiscovery.2017.4
154. Zhang F, Li J, Xiao H, Zou Y, Liu Y, Huang W. AFAP1-AS1: A Novel Oncogenic Long Non-Coding RNA in Human Cancers. *Cell Prolif* (2018) 51 (1). doi: 10.1111/cpr.12397
155. Xiong F, Zhu K, Deng S, Huang H, Yang L, Gong Z, et al. AFAP1-AS1: A Rising Star Among Oncogenic Long Non-Coding RNAs. *Sci China Life Sci* (2021). doi: 10.1007/s11427-020-1874-6
156. Müller S, Raulefs S, Bruns P, Afonso-Grunz F, Plötner A, Thermann R, et al. Next-Generation Sequencing Reveals Novel Differentially Regulated mRNAs, LncRNAs, MiRNAs, SdRNAs and a PiRNA in Pancreatic Cancer. *Mol Cancer* (2015) 14:94. doi: 10.1186/s12943-015-0358-5
157. Ye Y, Chen J, Zhou Y, Fu Z, Zhou Q, Wang Y, et al. High Expression of AFAP1-AS1 Is Associated With Poor Survival and Short-Term Recurrence in Pancreatic Ductal Adenocarcinoma. *J Transl Med* (2015) 13:137. doi: 10.1186/s12967-015-0490-4
158. Ramli S, Sim MS, Guad RM, Gopinath SCB, Subramaniyan V, Fuloria S, et al. Long Noncoding RNA UCA1 in Gastrointestinal Cancers: Molecular Regulatory Roles and Patterns, Mechanisms, and Interactions. *J Oncol* (2021) 2021:5519720. doi: 10.1155/2021/5519720
159. Ghafouri-Fard S, Taheri M. UCA1 Long Non-Coding RNA: An Update on Its Roles in Malignant Behavior of Cancers. *BioMed Pharmacother* (2019) 120:109459. doi: 10.1016/j.biopha.2019.109459
160. Xue M, Chen W, Li X. Urothelial Cancer Associated 1: A Long Noncoding RNA With a Crucial Role in Cancer. *J Cancer Res Clin Oncol* (2016) 142 (7):1407–19. doi: 10.1007/s00432-015-2042-y
161. Yao F, Wang Q, Wu Q. The Prognostic Value and Mechanisms of LncRNA UCA1 in Human Cancer. *Cancer Manag Res* (2019) 11:7685–96. doi: 10.2147/CMAR.S200436
162. Chen P, Wan D, Zheng D, Zheng Q, Wu F, Zhi Q. Long Non-Coding RNA UCA1 Promotes the Tumorigenesis in Pancreatic Cancer. *BioMed Pharmacother* (2016) 83:1220–6. doi: 10.1016/j.biopha.2016.08.041
163. Zhang M, Zhao Y, Zhang Y, Wang D, Gu S, Feng W, et al. LncRNA UCA1 Promotes Migration and Invasion in Pancreatic Cancer Cells *via* the Hippo Pathway. *Biochim Biophys Acta Mol Basis Dis* (2018) 1864(5 Pt A):1770–82. doi: 10.1016/j.bbadis.2018.03.005
164. Zhang X, Gao F, Zhou L, Wang H, Shi G, Tan X. UCA1 Regulates the Growth and Metastasis of Pancreatic Cancer by Sponging MiR-135a. *Oncol Res* (2017) 25(9):1529–41. doi: 10.3727/096504017X14888987683152
165. Zhou Y, Chen Y, Ding W, Hua Z, Wang L, Zhu Y, et al. LncRNA UCA1 Impacts Cell Proliferation, Invasion, and Migration of Pancreatic Cancer Through Regulating MiR-96/FOXO3. *IUBMB Life* (2018) 70(4):276–90. doi: 10.1002/iub.1699
166. Gong J, Lu X, Xu J, Xiong W, Zhang H, Yu X. Coexpression of UCA1 and ITGA2 in Pancreatic Cancer Cells Target the Expression of MiR-107 Through Focal Adhesion Pathway. *J Cell Physiol* (2019) 234(8):12884–96. doi: 10.1002/jcp.27953
167. Liu Y, Feng W, Gu S, Wang H, Zhang Y, Chen W, et al. The UCA1/KRAS Axis Promotes Human Pancreatic Ductal Adenocarcinoma Stem Cell Properties and Tumor Growth. *Am J Cancer Res* (2019) 9(3):496–510.
168. Guo Z, Wang X, Yang Y, Chen W, Zhang K, Teng B, et al. Hypoxic Tumor-Derived Exosomal Long Noncoding RNA UCA1 Promotes Angiogenesis *via* MiR-96-5p/AMOTL2 in Pancreatic Cancer. *Mol Ther Nucleic Acids* (2020) 22:179–95. doi: 10.1016/j.omtn.2020.08.021
169. Pavlova NN, Thompson CB. The Emerging Hallmarks of Cancer Metabolism. *Cell Metab* (2016) 23(1):27–47. doi: 10.1016/j.cmet.2015.12.006
170. Kerk SA, Papagiannakopoulos T, Shah YM, Lyssiotis CA. Metabolic Networks in Mutant KRAS-Driven Tumours: Tissue Specificities and the Microenvironment. *Nat Rev Cancer* (2021) 21(8):510–25. doi: 10.1038/s41568-021-00375-9
171. Cairns RA, Harris IS, Mak TW. Regulation of Cancer Cell Metabolism. *Nat Rev Cancer* (2011) 11(2):85–95. doi: 10.1038/nrc2981
172. Hirschey MD, DeBerardinis RJ, Diehl AME, Drew JE, Frezza C, Green MF, et al. Dysregulated Metabolism Contributes to Oncogenesis. *Semin Cancer Biol* (2015) (35Suppl):S129–50. doi: 10.1016/j.semcancer.2015.10.002
173. Vander Heiden MG. Targeting Cancer Metabolism: A Therapeutic Window Opens. *Nat Rev Drug Discov* (2011) 10(9):671–84. doi: 10.1038/nrd3504
174. Halbrook CJ, Lyssiotis CA. Employing Metabolism to Improve the Diagnosis and Treatment of Pancreatic Cancer. *Cancer Cell* (2017) 31(1):5–19. doi: 10.1016/j.ccell.2016.12.006
175. Sun H, Huang Z, Sheng W, Xu MD. Emerging Roles of Long Non-Coding RNAs in Tumor Metabolism. *J Hematol Oncol* (2018) 11(1):106. doi: 10.1186/s13045-018-0648-7
176. Fan C, Tang Y, Wang J, Xiong F, Guo C, Wang Y, et al. Role of Long Non-Coding RNAs in Glucose Metabolism in Cancer. *Mol Cancer* (2017) 16 (1):130. doi: 10.1186/s12943-017-0699-3
177. Zhang M, Gao F, Yu X, Zhang Q, Sun Z, He Y, et al. LINC00261: A Burgeoning Long Noncoding RNA Related to Cancer. *Cancer Cell Int* (2021) 21(1):274. doi: 10.1186/s12935-021-01988-8
178. Liu S, Zheng Y, Zhang Y, Zhang J, Xie F, Guo S, et al. Methylation-Mediated LINC00261 Suppresses Pancreatic Cancer Progression by Epigenetically Inhibiting C-Myc Transcription. *Theranostics* (2020) 10(23):10634–51. doi: 10.7150/thno.44278
179. Wang X, Gao X, Tian J, Zhang R, Qiao Y, Hua X, et al. LINC00261 Inhibits Progression of Pancreatic Cancer by Down-Regulating MiR-23a-3p. *Arch Biochem Biophys* (2020) 689:108469. doi: 10.1016/j.abb.2020.108469
180. Chen T, Lei S, Zeng Z, Zhang J, Xue Y, Sun Y, et al. Linc00261 Inhibits Metastasis and the WNT Signaling Pathway of Pancreatic Cancer by Regulating a Mir−552−5p/FOXO3 Axis. *Oncol Rep* (2020) 43(3):930–42. doi: 10.3892/or.2020.7480
181. Zhou Y, Xu S, Xia H, Gao Z, Huang R, Tang E, et al. Long Noncoding RNA FEZF1-AS1 in Human Cancers. *Clin Chim Acta* (2019) 497:20–6. doi: 10.1016/j.cca.2019.07.004
182. Shi C, Sun L, Song Y. FEZF1-AS1: A Novel Vital Oncogenic LncRNA in Multiple Human Malignancies. *Biosci Rep* (2019) 39(6). doi: 10.1042/BSR20191202

183. Li Z, Zhao X, Zhou Y, Liu Y, Zhou Q, Ye H, et al. The Long Non-Coding RNA HOTTIP Promotes Progression and Gemcitabine Resistance by Regulating HOXA13 in Pancreatic Cancer. *J Transl Med* (2015) 13:84. doi: 10.1186/s12967-015-0442-z
184. Ye H, Zhou Q, Zheng S, Li G, Lin Q, Ye L, et al. FEZF1-AS1/MiR-107/ZNF312B Axis Facilitates Progression and Warburg Effect in Pancreatic Ductal Adenocarcinoma. *Cell Death Dis* (2018) 9(2):34. doi: 10.1038/s41419-017-0052-1
185. Ou ZL, Zhang M, Ji LD, Luo Z, Han T, Lu YB, et al. Long Noncoding RNA FEZF1-AS1 Predicts Poor Prognosis and Modulates Pancreatic Cancer Cell Proliferation and Invasion Through MiR-142/HIF-1α and MiR-133a/EGFR Upon Hypoxia/Normoxia. *J Cell Physiol* (2019). doi: 10.1002/jcp.28188
186. Yang M, Wei W. SNHG16: A Novel Long-Non Coding RNA in Human Cancers. *Onco Targets Ther* (2019) 12:11679–90. doi: 10.2147/OTT.S231630
187. Gong CY, Tang R, Nan W, Zhou KS, Zhang HH. Role of SNHG16 in Human Cancer. *Clin Chim Acta* (2020) 503:175–80. doi: 10.1016/j.cca.2019.12.023
188. Yu Y, Dong JT, He B, Zou YF, Li XS, Xi CH, et al. LncRNA SNHG16 Induces the SREBP2 to Promote Lipogenesis and Enhance the Progression of Pancreatic Cancer. *Future Oncol* (2019) 15(33):3831–44. doi: 10.2217/fon-2019-0321
189. Xu H, Miao X, Li X, Chen H, Zhang B, Zhou W. LncRNA SNHG16 Contributes to Tumor Progression *via* the miR-302b-3p/SLC2A4 Axis in Pancreatic Adenocarcinoma. *Cancer Cell Int* (2021) 21(1):51.
190. Mizushima N, Levine B. Autophagy in Human Diseases. *N Engl J Med* (2020) 383(16):1564–76. doi: 10.1056/NEJMra2022774
191. Amaravadi R, Kimmelman A, Debnath J. Targeting Autophagy in Cancer: Recent Advances and Future Directions. *Cancer Discov* (2019) 9(9):1167–81. doi: 10.1158/2159-8290.CD-19-0292
192. Rybstein M, Bravo-San Pedro J, Kroemer G, Galluzzi L. The Autophagic Network and Cancer. *Nat Cell Biol* (2018) 20(3):243–51. doi: 10.1038/s41556-018-0042-2
193. Hessmann E, Buchholz SM, Demir IE, Singh SK, Gress TM, Ellenrieder V, et al. Microenvironmental Determinants of Pancreatic Cancer. *Physiol Rev* (2020) 100(4):1707–51. doi: 10.1152/physrev.00042.2019
194. Zhang J, Wang P, Wan L, Xu S, Pang D. The Emergence of Noncoding RNAs as Heracles in Autophagy. *Autophagy* (2017) 13(6):1004–24. doi: 10.1080/15548627.2017.1312041
195. Shafabakhsh R, Arianfar F, Vosough M, Mirzaei HR, Mahjoubin-Tehran M, Khanbabaei H, et al. Autophagy and Gastrointestinal Cancers: The Behind the Scenes Role of Long Non-Coding RNAs in Initiation, Progression, and Treatment Resistance. *Cancer Gene Ther* (2021). doi: 10.1038/s41417-020-00272-7
196. Chen X, Zeh H, Kang R, Kroemer G, Tang D. Cell Death in Pancreatic Cancer: From Pathogenesis to Therapy. *Nat Rev Gastroenterol Hepatol* (2021). doi: 10.1038/s41575-021-00486-6
197. Ghetti M, Vannini I, Storlazzi CT, Martinelli G, Simonetti G. Linear and Circular PVT1 in Hematological Malignancies and Immune Response: Two Faces of the Same Coin. *Mol Cancer* (2020) 19(1):69. doi: 10.1186/s12943-020-01187-5
198. Ghafouri-Fard S, Omrani MD, Taheri M. Long Noncoding RNA PVT1: A Highly Dysregulated Gene in Malignancy. *J Cell Physiol* (2020) 235(2):818–35. doi: 10.1002/jcp.29060
199. Onagoruwa OT, Pal G, Ochu C, Ogunwobi OO. Oncogenic Role of PVT1 and Therapeutic Implications. *Front Oncol* (2020) 10:17. doi: 10.3389/fonc.2020.00017
200. Wang W, Zhou R, Wu Y, Liu Y, Su W, Xiong W, et al. PVT1 Promotes Cancer Progression *via* MicroRNAs. *Front Oncol* (2019) 9:609. doi: 10.3389/fonc.2019.00609
201. Zhou C, Yi C, Yi Y, Qin W, Yan Y, Dong X, et al. LncRNA PVT1 Promotes Gemcitabine Resistance of Pancreatic Cancer *via* Activating Wnt/β-Catenin and Autophagy Pathway Through Modulating the MiR-619-5p/Pygo2 and MiR-619-5p/ATG14 Axes. *Mol Cancer* (2020) 19(1):118. doi: 10.1186/s12943-020-01237-y
202. Zhao L, Kong H, Sun H, Chen Z, Chen B, Zhou M. LncRNA-PVT1 Promotes Pancreatic Cancer Cells Proliferation and Migration Through Acting as a Molecular Sponge to Regulate MiR-448. *J Cell Physiol* (2018) 233(5):4044–55. doi: 10.1002/jcp.26072
203. Sun J, Zhang P, Yin T, Zhang F, Wang W. Upregulation of LncRNA PVT1 Facilitates Pancreatic Ductal Adenocarcinoma Cell Progression and Glycolysis by Regulating MiR-519d-3p and HIF-1A. *J Cancer* (2020) 11(9):2572–9. doi: 10.7150/jca.37959
204. Liu YF, Luo D, Li X, Li ZQ, Yu X, Zhu HW. PVT1 Knockdown Inhibits Autophagy and Improves Gemcitabine Sensitivity by Regulating the MiR-143/HIF-1α/VMP1 Axis in Pancreatic Cancer. *Pancreas* (2021) 50(2):227–34. doi: 10.1097/MPA.0000000000001747
205. Wang G, Chen H, Liu J. The Long Noncoding RNA LINC01207 Promotes Proliferation of Lung Adenocarcinoma. *Am J Cancer Res* (2015) 5(10):3162–73.
206. Chen C, Jiang L, Zhang Y, Zheng W. FOXA1-Induced LINC01207 Facilitates Head and Neck Squamous Cell Carcinoma *via* Up-Regulation of TNRC6B. *BioMed Pharmacother* (2020) 128:110220. doi: 10.1016/j.biopha.2020.110220
207. Liu R, Zhao W, Wang H, Wang J. Long Noncoding RNA LINC01207 Promotes Colon Cancer Cell Proliferation and Invasion by Regulating MiR-3125/TRIM22 Axis. *BioMed Res Int* (2020) 2020:1216325. doi: 10.1155/2020/1216325
208. Liu H, Liu X. LINC01207 Is Up-Regulated in Gastric Cancer Tissues and Promotes Disease Progression by Regulating MiR-671-5p/DDX5 Axis. *J Biochem* (2021) 170(3):337–47. doi: 10.1093/jb/mvab050
209. Wang S, Qiu J, Wang L, Wu Z, Zhang X, Li Q, et al. Long Non-Coding RNA LINC01207 Promotes Prostate Cancer Progression by Downregulating MicroRNA-1972 and Upregulating LIM and SH3 Protein 1. *IUBMB Life* (2020) 72(9):1960–75. doi: 10.1002/iub.2327
210. Liu C, Wang JO, Zhou WY, Chang XY, Zhang MM, Zhang Y, et al. Long Non-Coding RNA LINC01207 Silencing Suppresses AGR2 Expression to Facilitate Autophagy and Apoptosis of Pancreatic Cancer Cells by Sponging MiR-143-5p. *Mol Cell Endocrinol* (2019) 493:110424. doi: 10.1016/j.mce.2019.04.004
211. Aguilo F, Zhou MM, Walsh MJ. Long Noncoding RNA, Polycomb, and the Ghosts Haunting INK4b-ARF-INK4a Expression. *Cancer Res* (2011) 71(16):5365–9. doi: 10.1158/0008-5472.CAN-10-4379
212. Congrains A, Kamide K, Ohishi M, Rakugi H. ANRIL: Molecular Mechanisms and Implications in Human Health. *Int J Mol Sci* (2013) 14(1):1278–92. doi: 10.3390/ijms14011278
213. Kong Y, Hsieh CH, Alonso LC. ANRIL: A LncRNA at the CDKN2A/B Locus With Roles in Cancer and Metabolic Disease. *Front Endocrinol (Lausanne)* (2018) 9:405. doi: 10.3389/fendo.2018.00405
214. Aguilo F, Di Cecilia S, Walsh MJ. Long Non-Coding RNA ANRIL and Polycomb in Human Cancers and Cardiovascular Disease. *Curr Top Microbiol Immunol* (2016) 394:29–39. doi: 10.1007/82_2015_455
215. Wang Y, Cheng N, Luo J. Downregulation of LncRNA ANRIL Represses Tumorigenicity and Enhances Cisplatin-Induced Cytotoxicity *via* Regulating MicroRNA Let-7a in Nasopharyngeal Carcinoma. *J Biochem Mol Toxicol* (2017) 31(7). doi: 10.1002/jbt.21904
216. Hu X, Jiang H, Jiang X. Downregulation of LncRNA ANRIL Inhibits Proliferation, Induces Apoptosis, and Enhances Radiosensitivity in Nasopharyngeal Carcinoma Cells Through Regulating MiR-125a. *Cancer Biol Ther* (2017) 18(5):331–8. doi: 10.1080/15384047.2017.1310348
217. Liu P, Zhang M, Niu Q, Zhang F, Yang Y, Jiang X. Knockdown of Long Non-Coding RNA ANRIL Inhibits Tumorigenesis in Human Gastric Cancer Cells *via* MicroRNA-99a-Mediated Down-Regulation of BMI1. *Braz J Med Biol Res* (2018) 51(10):e6839. doi: 10.1590/1414-431x20186839
218. Zhang EB, Kong R, Yin DD, You LH, Sun M, Han L, et al. Long Noncoding RNA ANRIL Indicates a Poor Prognosis of Gastric Cancer and Promotes Tumor Growth by Epigenetically Silencing of MiR-99a/MiR-449a. *Oncotarget* (2014) 5(8):2276–92. doi: 10.18632/oncotarget.1902
219. Dong X, Jin Z, Chen Y, Xu H, Ma C, Hong X, et al. Knockdown of Long Non-Coding RNA ANRIL Inhibits Proliferation, Migration, and Invasion But Promotes Apoptosis of Human Glioma Cells by Upregulation of MiR-34a. *J Cell Biochem* (2018) 119(3):2708–18. doi: 10.1002/jcb.26437
220. Einama T, Kamachi H, Tsuruga Y, Sakata T, Shibuya K, Sakamoto Y, et al. Optimal Resection Area for Superior Mesenteric Artery Nerve Plexuses After Neoadjuvant Chemoradiotherapy for Locally Advanced Pancreatic Carcinoma. *Medicine (Baltimore)* (2018) 97(31):e11309. doi: 10.1097/MD.0000000000011309
221. Huang D, Bi C, Zhao Q, Ding X, Bian C, Wang H, et al. Knockdown Long Non-Coding RNA ANRIL Inhibits Proliferation, Migration and Invasion of

Hepg2 Cells by Down-Regulation of MiR-191. *BMC Cancer* (2018) 18 (1):919. doi: 10.1186/s12885-018-4831-6
222. Ma Y, Zhang H, Li G, Hu J, Liu X, Lin L. LncRNA ANRIL Promotes Cell Growth, Migration and Invasion of Hepatocellular Carcinoma Cells *via* Sponging MiR-144. *Anticancer Drugs* (2019) 30(10):1013–21. doi: 10.1097/CAD.0000000000000807
223. Li K, Zhao B, Wei D, Cui Y, Qian L, Wang W, et al. Long Non-Coding RNA ANRIL Enhances Mitochondrial Function of Hepatocellular Carcinoma by Regulating the MiR-199a-5p/ARL2 Axis. *Environ Toxicol* (2020) 35(3):313–21. doi: 10.1002/tox.22867
224. Zhang JJ, Wang DD, Du CX, Wang Y. Long Noncoding RNA ANRIL Promotes Cervical Cancer Development by Acting as a Sponge of MiR-186. *Oncol Res* (2018) 26(3):345–52. doi: 10.3727/096504017X14953948675449
225. Zhao B, Lu YL, Yang Y, Hu LB, Bai Y, Li RQ, et al. Overexpression of LncRNA ANRIL Promoted the Proliferation and Migration of Prostate Cancer Cells *via* Regulating Let-7a/TGF-β1/ Smad Signaling Pathway. *Cancer Biomark* (2018) 21(3):613–20. doi: 10.3233/CBM-170683
226. Zhang Z, Feng L, Liu P, Duan W. ANRIL Promotes Chemoresistance *via* Disturbing Expression of ABCC1 by Regulating the Expression of Let-7a in Colorectal Cancer. *Biosci Rep* (2018) 38(6). doi: 10.1042/BSR20180620
227. Shang C, Ao CN, Cheong CC, Meng L. Long Non-Coding RNA CDKN2B Antisense RNA 1 Gene Contributes to Paclitaxel Resistance in Endometrial Carcinoma. *Front Oncol* (2019) 9:27. doi: 10.3389/fonc.2019.00027
228. Xu ST, Xu JH, Zheng ZR, Zhao QQ, Zeng XS, Cheng SX, et al. Long Non-Coding RNA ANRIL Promotes Carcinogenesis *via* Sponging MiR-199a in Triple-Negative Breast Cancer. *BioMed Pharmacother* (2017) 96:14–21. doi: 10.1016/j.biopha.2017.09.107
229. Permuth JB, Chen DT, Yoder SJ, Li J, Smith AT, Choi JW, et al. Linc-Ing Circulating Long Non-Coding RNAs to the Diagnosis and Malignant Prediction of Intraductal Papillary Mucinous Neoplasms of the Pancreas. *Sci Rep* (2017) 7(1):10484. doi: 10.1038/s41598-017-09754-5
230. Chen S, Zhang JQ, Chen JZ, Chen HX, Qiu FN, Yan ML, et al. The Over Expression of Long Non-Coding RNA ANRIL Promotes Epithelial-Mesenchymal Transition by Activating the ATM-E2F1 Signaling Pathway in Pancreatic Cancer: An *In Vivo* and *In Vitro* Study. *Int J Biol Macromol* (2017) 102:718–28. doi: 10.1016/j.ijbiomac.2017.03.123
231. Wang L, Bi R, Li L, Zhou K, Yin H. LncRNA ANRIL Aggravates the Chemoresistance of Pancreatic Cancer Cells to Gemcitabine by Targeting Inhibition of MiR-181a and Targeting HMGB1-Induced Autophagy. *Aging (Albany NY)* (2021) 13(15):19272–81.
232. Hao YR, Zhang DJ, Fu ZM, Guo YY, Guan GF. Long Non-Coding RNA ANRIL Promotes Proliferation, Clonogenicity, Invasion and Migration of Laryngeal Squamous Cell Carcinoma by Regulating MiR-181a/Snai2 Axis. *Regener Ther* (2019) 11:282–9. doi: 10.1016/j.reth.2019.07.007
233. Sun C, Shen C, Zhang Y, Hu C. LncRNA ANRIL Negatively Regulated Chitooligosaccharide-Induced Radiosensitivity in Colon Cancer Cells by Sponging MiR-181a-5p. *Adv Clin Exp Med* (2021) 30(1):55–65. doi: 10.17219/acem/128370
234. Hu X, Lou T, Yuan C, Wang Y, Tu X, Wang Y, et al. Effects of LncRNA ANRIL-Knockdown on the Proliferation, Apoptosis and Cell Cycle of Gastric Cancer Cells. *Oncol Lett* (2021) 22(2):621.
235. Christenson ES, Jaffee E, Azad NS. Current and Emerging Therapies for Patients With Advanced Pancreatic Ductal Adenocarcinoma: A Bright Future. *Lancet Oncol* (2020) 21(3):e135–45. doi: 10.1016/S1470-2045(19)30795-8
236. Yu S, Zhang C, Xie KP. Therapeutic Resistance of Pancreatic Cancer: Roadmap to Its Reversal. *Biochim Biophys Acta Rev Cancer* (2021) 1875 (1):188461. doi: 10.1016/j.bbcan.2020.188461
237. Xie W, Chu M, Song G, Zuo Z, Han Z, Chen C, et al. Emerging Roles of Long Noncoding RNAs in Chemoresistance of Pancreatic Cancer. *Semin Cancer Biol* (2020). doi: 10.1016/j.semcancer.2020.11.004
238. Liu K, Gao L, Ma X, Huang JJ, Chen J, Zeng L, et al. Long Non-Coding RNAs Regulate Drug Resistance in Cancer. *Mol Cancer* (2020) 19(1):54. doi: 10.1186/s12943-020-01162-0
239. Coppola S, Carnevale I, Danen EHJ, Peters GJ, Schmidt T, Assaraf YG, et al. A Mechanopharmacology Approach to Overcome Chemoresistance in Pancreatic Cancer. *Drug Resist Updat* (2017) 31:43–51. doi: 10.1016/j.drup.2017.07.001
240. Chen Y, Li Z, Chen X, Zhang S. Long Non-Coding RNAs: From Disease Code to Drug Role. *Acta Pharm Sin B* (2021) 11(2):340–54. doi: 10.1016/j.apsb.2020.10.001
241. Feng M, Xiong G, Cao Z, Yang G, Zheng S, Qiu J, et al. LAT2 Regulates Glutamine-Dependent Mtor Activation to Promote Glycolysis and Chemoresistance in Pancreatic Cancer. *J Exp Clin Cancer Res* (2018) 37 (1):274. doi: 10.1186/s13046-018-0947-4
242. Yang G, Xiong G, Feng M, Zhao F, Qiu J, Liu Y, et al. OLR1 Promotes Pancreatic Cancer Metastasis *via* Increased C-Myc Expression and Transcription of HMGA2. *Mol Cancer Res* (2020) 18(5):685–97. doi: 10.1158/1541-7786.MCR-19-0718
243. Gao Y, Zhang Z, Li K, Gong L, Yang Q, Huang X, et al. Linc-DYNC2H1-4 Promotes EMT and CSC Phenotypes by Acting as a Sponge of MiR-145 in Pancreatic Cancer Cells. *Cell Death Dis* (2017) 8(7):e2924. doi: 10.1038/cddis.2017.311
244. Lambrou GI, Hatziagapiou K, Zaravinos A. The Non-Coding RNA GAS5 and Its Role in Tumor Therapy-Induced Resistance. *Int J Mol Sci* (2020) 21 (20):7633. doi: 10.3390/ijms21207633
245. Yang X, Xie Z, Lei X, Gan R. Long Non-Coding RNA GAS5 in Human Cancer. *Oncol Lett* (2020) 20(3):2587–94. doi: 10.3892/ol.2020.11809
246. Lu S, Su Z, Fu W, Cui Z, Jiang X, Tai S. Altered Expression of Long Non-Coding RNA GAS5 in Digestive Tumors. *Biosci Rep* (2019) 39(1). doi: 10.1042/BSR20180789
247. Liu B, Wu S, Ma J, Yan S, Xiao Z, Wan L, et al. LncRNA GAS5 Reverses EMT and Tumor Stem Cell-Mediated Gemcitabine Resistance and Metastasis by Targeting MiR-221/SOCS3 in Pancreatic Cancer. *Mol Ther Nucleic Acids* (2018) 13:472–82. doi: 10.1016/j.omtn.2018.09.026
248. Gao ZQ, Wang JF, Chen DH, Ma XS, Yang W, Zhe T, et al. Long Non-Coding RNA GAS5 Antagonizes the Chemoresistance of Pancreatic Cancer Cells Through Down-Regulation of MiR-181c-5p. *BioMed Pharmacother* (2018) 97:809–17. doi: 10.1016/j.biopha.2017.10.157
249. Oguntade A, Al-Amodi F, Alrumayh A, Alobaida M, Bwalya M. Anti-Angiogenesis in Cancer Therapeutics: The Magic Bullet. *J Egypt Natl Cancer Inst* (2021) 33(1):15. doi: 10.1186/s43046-021-00072-6
250. Jayson G, Kerbel R, Ellis L, Harris A. Antiangiogenic Therapy in Oncology: Current Status and Future Directions. *Lancet (London England)* (2016) 388 (10043):518–29. doi: 10.1016/S0140-6736(15)01088-0
251. Olejarz W, Kubiak-Tomaszewska G, Chrzanowska A, Lorenc T. Exosomes in Angiogenesis and Anti-Angiogenic Therapy in Cancers. *Int J Mol Sci* (2020) 21(16). doi: 10.3390/ijms21165840
252. Li S, Xu HX, Wu CT, Wang WQ, Jin W, Gao HL, et al. Angiogenesis in Pancreatic Cancer: Current Research Status and Clinical Implications. *Angiogenesis* (2019) 22(1):15–36. doi: 10.1007/s10456-018-9645-2
253. Zhao J, Wang ZX, Qin LX. Long Noncoding RNAs, Emerging and Versatile Regulators of Tumor-Induced Angiogenesis. *Am J Cancer Res* (2019) 9(7):1367–81.
254. Kim T, Croce CM. Long Noncoding RNAs: Undeciphered Cellular Codes Encrypting Keys of Colorectal Cancer Pathogenesis. *Cancer Lett* (2018) 417:89–95. doi: 10.1016/j.canlet.2017.12.033
255. Zhang J, Yin M, Peng G, Zhao Y. CRNDE: An Important Oncogenic Long Non-Coding RNA in Human Cancers. *Cell Prolif* (2018) 51(3):e12440. doi: 10.1111/cpr.12440
256. Lu Y, Sha H, Sun X, Zhang Y, Wu Y, Zhang J, et al. CRNDE: An Oncogenic Long Non-Coding RNA in Cancers. *Cancer Cell Int* (2020) 20:162. doi: 10.1186/s12935-020-01246-3
257. Zhu HY, Gao YJ, Wang Y, Liang C, Zhang ZX, Chen Y. LncRNA CRNDE Promotes the Progression and Angiogenesis of Pancreatic Cancer *via* MiR-451a/CDKN2D Axis. *Transl Oncol* (2021) 14(7):101088. doi: 10.1016/j.tranon.2021.101088
258. Wang G, Pan J, Zhang L, Wei Y, Wang C. Long Non-Coding RNA CRNDE Sponges MiR-384 to Promote Proliferation and Metastasis of Pancreatic Cancer Cells Through Upregulating IRS1. *Cell Prolif* (2017) 50(6). doi: 10.1111/cpr.12389
259. Ding J, Cao J, Chen Z, He Z. The Role of Long Intergenic Noncoding RNA 00511 in Malignant Tumors: A Meta-Analysis, Database Validation and Review. *Bioengineered* (2020) 11(1):812–23. doi: 10.1080/21655979.2020.1795384
260. Lu G, Li Y, Ma Y, Lu J, Chen Y, Jiang Q, et al. Long Noncoding RNA LINC00511 Contributes to Breast Cancer Tumourigenesis and Stemness by Inducing the MiR-185-3p/E2F1/Nanog Axis. *J Exp Clin Cancer Res* (2018) 37(1):289. doi: 10.1186/s13046-018-0945-6

261. Shi G, Cheng Y, Zhang Y, Guo R, Li S, Hong X. Long Non-Coding RNA LINC00511/MiR-150/MMP13 Axis Promotes Breast Cancer Proliferation, Migration and Invasion. *Biochim Biophys Acta Mol Basis Dis* (2021) 1867 (3):165957. doi: 10.1016/j.bbadis.2020.165957
262. Wu Y, Li L, Wang Q, Zhang L, He C, Wang X, et al. LINC00511 Promotes Lung Squamous Cell Carcinoma Proliferation and Migration *via* Inhibiting MiR-150-5p and Activating TADA1. *Transl Lung Cancer Res* (2020) 9 (4):1138–48. doi: 10.21037/tlcr-19-701
263. Du X, Tu Y, Liu S, Zhao P, Bao Z, Li C, et al. LINC00511 Contributes to Glioblastoma Tumorigenesis and Epithelial-Mesenchymal Transition *via* LINC00511/MiR-524-5p/YB1/ZEB1 Positive Feedback Loop. *J Cell Mol Med* (2020) 24(2):1474–87. doi: 10.1111/jcmm.14829
264. Zhao X, Liu Y, Li Z, Zheng S, Wang Z, Li W, et al. Linc00511 Acts as a Competing Endogenous RNA to Regulate VEGFA Expression Through Sponging Hsa-MiR-29b-3p in Pancreatic Ductal Adenocarcinoma. *J Cell Mol Med* (2018) 22(1):655–67. doi: 10.1111/jcmm.13351
265. Wang W, Lou W, Ding B, Yang B, Lu H, Kong Q, et al. A Novel mRNA-MiRNA-LncRNA Competing Endogenous RNA Triple Sub-Network Associated With Prognosis of Pancreatic Cancer. *Aging (Albany NY)* (2019) 11(9):2610–27. doi: 10.18632/aging.101933
266. Tsui NB, Ng EK, Lo YM. Stability of Endogenous and Added RNA in Blood Specimens, Serum, and Plasma. *Clin Chem* (2002) 48(10):1647–53. doi: 10.1093/clinchem/48.10.1647
267. Zanutto S, Pizzamiglio S, Ghilotti M, Bertan C, Ravagnani F, Perrone F, et al. Circulating MiR-378 in Plasma: A Reliable, Haemolysis-Independent Biomarker for Colorectal Cancer. *Br J Cancer* (2014) 110(4):1001–7. doi: 10.1038/bjc.2013.819
268. Ren S, Wang F, Shen J, Sun Y, Xu W, Lu J, et al. Long Non-Coding RNA Metastasis Associated in Lung Adenocarcinoma Transcript 1 Derived MiniRNA as a Novel Plasma-Based Biomarker for Diagnosing Prostate Cancer. *Eur J Cancer* (2013) 49(13):2949–59. doi: 10.1016/j.ejca.2013.04.026
269. Shao Y, Ye M, Jiang X, Sun W, Ding X, Liu Z, et al. Gastric Juice Long Noncoding RNA Used as a Tumor Marker for Screening Gastric Cancer. *Cancer* (2014) 120(21):3320–8. doi: 10.1002/cncr.28882
270. Redis RS, Sieuwerts AM, Look MP, Tudoran O, Ivan C, Spizzo R, et al. CCAT2, a Novel Long Non-Coding RNA in Breast Cancer: Expression Study and Clinical Correlations. *Oncotarget* (2013) 4(10):1748–62. doi: 10.18632/oncotarget.1292
271. Liu Q, Huang J, Zhou N, Zhang Z, Zhang A, Lu Z, et al. LncRNA Loc285194 Is a P53-Regulated Tumor Suppressor. *Nucleic Acids Res* (2013) 41(9):4976–87. doi: 10.1093/nar/gkt182
272. Gutschner T, Hämmerle M, Eissmann M, Hsu J, Kim Y, Hung G, et al. The Noncoding RNA MALAT1 Is a Critical Regulator of the Metastasis Phenotype of Lung Cancer Cells. *Cancer Res* (2013) 73(3):1180–9. doi: 10.1158/0008-5472.CAN-12-2850
273. Yuan SX, Yang F, Yang Y, Tao QF, Zhang J, Huang G, et al. Long Noncoding RNA Associated With Microvascular Invasion in Hepatocellular Carcinoma Promotes Angiogenesis and Serves as a Predictor for Hepatocellular Carcinoma Patients' Poor Recurrence-Free Survival After Hepatectomy. *Hepatology* (2012) 56(6):2231–41. doi: 10.1002/hep.25895
274. Zu F, Liu P, Wang H, Zhu T, Sun J, Sheng W, et al. Integrated Analysis Identifies a Pathway-Related Competing Endogenous RNA Network in the Progression of Pancreatic Cancer. *BMC Cancer* (2020) 20(1):958. doi: 10.1186/s12885-020-07470-4
275. Zhou M, Diao Z, Yue X, Chen Y, Zhao H, Cheng L, et al. Construction and Analysis of Dysregulated LncRNA-Associated CeRNA Network Identified Novel LncRNA Biomarkers for Early Diagnosis of Human Pancreatic Cancer. *Oncotarget* (2016) 7(35):56383–94. doi: 10.18632/oncotarget.10891
276. Zhao L, Liu B. Identification of Potential Prognostic CeRNA Module Biomarkers in Patients With Pancreatic Adenocarcinoma. *Oncotarget* (2017) 8(55):94493–504. doi: 10.18632/oncotarget.21783
277. Shi X, Zhao Y, He R, Zhou M, Pan S, Yu S, et al. Three-LncRNA Signature Is a Potential Prognostic Biomarker for Pancreatic Adenocarcinoma. *Oncotarget* (2018) 9(36):24248–59. doi: 10.18632/oncotarget.24443
278. Jing S, Tian J, Zhang Y, Chen X, Zheng S. Identification of a New Pseudogenes/LncRNAs-Hsa-MiR-26b-5p-COL12A1 Competing Endogenous RNA Network Associated With Prognosis of Pancreatic Cancer Using Bioinformatics Analysis. *Aging (Albany NY)* (2020) 12 (19):19107–28. doi: 10.18632/aging.103709

Conflict of Interest: The authors declare that the research was conducted in the absence of any commercial or financial relationships that could be construed as a potential conflict of interest.

Publisher's Note: All claims expressed in this article are solely those of the authors and do not necessarily represent those of their affiliated organizations, or those of the publisher, the editors and the reviewers. Any product that may be evaluated in this article, or claim that may be made by its manufacturer, is not guaranteed or endorsed by the publisher.

GLOSSARY

AFAP1-AS1	Actin filament-associated protein 1 antisense RNA 1
AGR2	Anterior gradient 2
ANRIL	Antisense noncoding RNA in the INK4 locus
CDKN2D	Cyclin-dependent kinase inhibitor 2D
ceRNAs	Competing endogenous RNAs
CRNDE	Colorectal neoplasia differentially expressed
CSC	Cancer stem cells
DUSP1	Dual-specificity protein phosphatase 1
EMT	Epithelial–mesenchymal transition
EZH2	Enhancer of zeste homolog 2
FEZF1-AS1	FEZ finger zinc 1 antisense 1
GAS5	Growth arrest–specific transcript 5
GSTM3TV2	Homo sapiens glutathione S-transferase mu 3, transcript variant 2 and noncoding RNA
HIF1A	Hypoxia-Inducible Factor 1A
HIPK2	Homeodomain-interacting protein kinase 2
HMGB1	High-mobility group box-1
HOTAIR	HOX transcript antisense RNA
HULC	Highly upregulated in liver cancer
iASPP	Inhibitor for the apoptosis-stimulating protein of p53
LAT2	L-type amino acid transporter 2
LncRNAs	Long noncoding RNAs
MALAT1	Metastasis-associated lung adenocarcinoma transcript 1
MAPK	Mitogen-activated protein kinase
MIR31HG	MiR-31 host gene
miRNA	MicroRNAs
MREs	MiRNA recognition elements
NORAD	noncoding RNA activated by DNA damage
OLR1	Oxidized low-density lipoprotein receptor 1
OTUD7B	Cezanne
PC	Pancreatic cancer
PRC2	Polycomb repressive complex 2
PVT1	Plasmacytoma variant translocation 1
ROR	Regulator of reprogramming
SNHG16	Small Nucleolar RNA Host Gene 16
SOCS3	Suppressor of cytokine signaling-3
SOX2OT	SOX2 overlapping transcript
SREBP2	Sterol regulatory element-binding protein-2
TGFBR1	Transforming growth factor beta 1
TGFBR2	Transforming growth factor beta 2
THAP9-AS1	THAP9 antisense RNA 1
TUG1	Taurine upregulated gene 1
UCA1	Urothelial cancer-associated 1
ULK1	Unc-51-like autophagy-activating kinase 1
XIST	X inactivation-specific transcript
YAP	Yes-associated protein

frontiers in Oncology

ORIGINAL RESEARCH
published: 28 October 2021
doi: 10.3389/fonc.2021.757307

Portal Venous Circulating Tumor Cells Undergoing Epithelial-Mesenchymal Transition Exhibit Distinct Clinical Significance in Pancreatic Ductal Adenocarcinoma

Yujin Pan[1,2,3†], *Deyu Li*[1,2,3†], *Jiuhui Yang*[1,2,3], *Ning Wang*[1,2,3], *Erwei Xiao*[1,2,3], *Lianyuan Tao*[1,2,3], *Xiangming Ding*[2,3,4], *Peichun Sun*[2,3,5*] *and Dongxiao Li*[2,3,4*]

[1] Department of Hepatobiliary Pancreatic Surgery, Henan Provincial People's Hospital, People's Hospital of Zhengzhou University, Zhengzhou, China, [2] Zhengzhou Key Laboratory of Minimally Invasive Treatment for Liver Cancer, Henan Provincial People's Hospital, Zhengzhou, China, [3] Henan Provincial Key Laboratory of Hepatobiliary and Pancreatic Diseases, Henan Provincial People's Hospital, Zhengzhou, China, [4] Department of Gastroenterology, Henan Provincial People's Hospital, People's Hospital of Zhengzhou University, Zhengzhou, China, [5] Department of Gastrointestinal Surgery, Henan Provincial People's Hospital Zhengzhou, People's Hospital of Zhengzhou University, Zhengzhou, China

Background: Much importance is attached to the clinical application value of circulating tumor cells (CTCs), meanwhile tumor-proximal CTCs detection has interested researchers for its unique advantage. This research mainly discusses the correlation of portal venous (PoV) CTCs counts in different epithelial-mesenchymal transition status with clinicopathologic parameters and postoperative prognosis in resectable pancreatic ductal adenocarcinoma patients (PDAC).

Methods: PDAC patients (n=60) who received radical resection were enrolled in this research. PoV samples from all patients and peripheral venous (PV) samples from 32 patients among them were collected to verify spatial heterogeneity of CTCs distribution, and explore their correlation with clinicopathologic parameters and clinical prognosis.

Results: CTCs detectable rate and each phenotype count of PoV were higher than those of PV. Patients with recurrence had higher PV and PoV epithelial CTCs (E-CTCs) counts than recurrence-free patients ($P<0.05$). Some unfavourable clinicopathologic parameters were closely related to higher PoV CTCs counts. Multivariate regression analysis demonstrated that PoV mesenchymal CTC (M-CTC)s≥1/5 ml was an independent risk factor for metastasis free survival (MFS) ($P=0.003$) and overall survival (OS) ($P=0.043$).

Conclusions: Our research demonstrated that portal venous was a preferable vessel for CTC test, and patients with PoV M-CTC≥1/5 ml had shorter MFS and OS time in resectable PDAC patients. PoV CTC phenotype detection has the potential to be a reliable and accurate tool to identify resectable PDAC patients with high tendency of postoperative metastasis for better stratified management.

Keywords: circulating tumor cell, pancreatic ductal adenocarcinoma, portal venous, prognosis, epithelial-mesenchymal transition

OPEN ACCESS

Edited by:
Taiping Zhang,
Peking Union Medical College Hospital (CAMS), China

Reviewed by:
Jianwei Xu,
Shandong University, China
Jikuan Jin,
Huazhong University of Science and Technology, China

***Correspondence:**
Dongxiao Li
651215540@qq.com
Peichun Sun
sunpeichun@126.com

[†]These authors have contributed equally to this work and share first authorship

Specialty section:
This article was submitted to Gastrointestinal Cancers: Hepato Pancreatic Biliary Cancers, a section of the journal Frontiers in Oncology

Received: *12 August 2021*
Accepted: *05 October 2021*
Published: *28 October 2021*

Citation:
Pan Y, Li D, Yang J, Wang N, Xiao E, Tao L, Ding X, Sun P and Li D (2021) Portal Venous Circulating Tumor Cells Undergoing Epithelial-Mesenchymal Transition Exhibit Distinct Clinical Significance in Pancreatic Ductal Adenocarcinoma. Front. Oncol. 11:757307. doi: 10.3389/fonc.2021.757307

INTRODUCTION

Pancreatic ductal adenocarcinoma (PDAC) remains one of the most aggressive malignancies with high metastatic tendency to distant organs (1), and it has been projected to be the second most lethal tumor by 2030 (2). A retrospective study pointed that nearly half of 957 PDAC patients had suffered tumor recurrence or metastasis within 1 year after surgery, including liver metastasis (33.8%) and lung metastasis (8.5%), though they had already received radical surgery (3). Cancer management strategy would benefit a lot from the accurate prognostic indicator in order to better stratify patients (4, 5). While the prognosis of PDAC is highly unpredictable, mainly due to the absence of precise and timely prognosis indicators (6).

Increasing evidence demonstrated that utilizing the circulating tumor cells (CTCs) count to early assess the postoperative prognosis can be considered as an efficient method in some solid tumors (5, 7–9). To date, research involving CTCs detection has mainly focused on peripheral blood samples with low detectable rates and detectable enumeration (7, 9). It is worth noting that researchers have utilized tumor-proximal liquid biopsy to overcome the mentioned limitations with the enhancement of detectable rates and the enumeration of CTCs (7, 9–11). In this research, we collected portal venous blood and peripheral venous blood for CTCs phenotypes detection to verify the value of tumor-proximal liquid biopsy.

Epithelial-mesenchymal transition (EMT) and its intermediate states have already been acknowledged as crucial drivers of tumor progression, though there is still far from a consensus on the significance of each EMT phenotype for prognosis (12, 13). Recently, exploring the correlation between CTCs in different EMT statuses and prognosis has attracted increasing attention (14–16). In this study, Canpatrol CTC detection technology was used to enrich and identify CTCs in different EMT statuses and then routinely classified them into three typical subgroups according to the expression of fluorescence signals: entirely epithelial-CTCs(E-CTCs), entirely mesenchymal-CTCs (M-CTCs), and hybrid phenotype CTCs (H-CTCs). Furthermore, we classified the H-CTC into E>M, E≈M, and E<M subtypes. The main aim of this study is to identify the correlation between the portal venous CTCs subtypes count with clinicopathological parameters and prognosis to verify the clinical application value of tumor-proximal liquid biopsy in resectable PDAC patients.

Abbreviations: AJCC, American Joint Committee on Cancer; AUC, Area under the curve; CA 19-9, Cancer antigen 19-9; CK8/18/19, cytokeratin8/18/19; CTC, Circulating tumor cell; DAPI, 4′,6-diamidino-2-phenylindole; E-CTC, Epithelial CTC; EDTA, Ethylenediaminetetraacetic acid; EMT, Epithelial-mesenchymal transition; EpCAM, Epithelial cell adhesion molecule; H-CTC, Hybrid CTC; HR, hazard ratio; IQR, Interquartile Range; ISET, Isolation by Size of Epithelial Tumor Cells, M-CTC, Mesenchymal CTC; MFS, metastasis free survival; OS, Overall survival; PDAC, Pancreatic ductal adenocarcinoma; PoV, Portal venous; PV, peripheral PV; RFS, Recurrence free survival; ROC, Receiver operating characteristic; SD, Standard deviation; T-CTC,Total CTC.

PATIENTS AND METHODS

Patients

This research was carried out at the Department of Hepatobiliary and Pancreatic Surgery, People's Hospital of Zhengzhou University (Zhengzhou, China). From August 2018 to September 2020, 60 PDAC patients receiving radical surgery were enrolled. The inclusion criteria were as follows: (a) radical resection confirmed by postoperative pathology; (b) PoV blood samples collecting was prior to specimen separation intraoperation; (c) definite pathological diagnosis of PDAC. The exclusion criteria were as follows: (a) previously treated with anticancer therapy before surgery, including radiotherapy, immunotherapy and chemotherapy; (b) patients with incomplete clinicopathological data; (c) patients with distant metastasis or others primary tumor. Ultimately, sixty patients met the inclusion criteria and were enrolled in this study. This study is consistent with the guidelines of the Declaration of Helsinki and approved by ethics committee of Henan Province People's hospital. Informed consent was obtained from each participant.

Portal Venous and Peripheral Venous Blood Samples

Portal venous (PoV) blood sample (5ml) collection was performed prior to specimen separation during surgery (**Figure 1A**). Peripheral blood (PV) samples (5ml) were obtained from the cubital vein before surgery (**Figure 1B**). Then, these blood samples were placed in ethylenediaminetetraacetic acid (EDTA) vacutainers for the CTC phenotype detection.

CTCs Enrichment and Identification

The Canpatrol™ CTCs detection platform (Sur Exam, Guangzhou, China) had been introduced by previous reports (5, 17, 18). Firstly, CTCs were isolated by a filtration system containing a membrane with 8-μm diameter pores (Sur Exam, Guangzhou, China). The nuclei were stained by4',6-diamidino-2-phenylindole (DAPI). RNA-*in situ* hybridization technology was used to identify the CTC phenotypes targeting different mRNA sequences that encode epithelial biomarkers (EpCAM, CK8/18/19), mesenchymal biomarkers (Vimentin and Twist), and the leukocyte biomarker CD45. CTCs phenotypes were analyzed with a fluorescent microscope, the epithelial CTCs (E-CTCs) were stained with red fluorescence, mesenchymal CTCs (M-CTCs) were stained with green fluorescence and hybrid CTCs (H-CTCs) were stained with both red and green fluorescence. Besides, leukocytes were stained with white fluorescence (**Figure 1C**).

Clinical and Pathologic Characteristic

Clinicopathological data from 60 PDAC patients were collected, including age, sex, hepatitis, diabetes, preoperative serum CA19-9 level and postoperative serum CA19-9 level (referring to the first postoperative review result), tumor location (head and neck *vs* body and tail), degree of tumor differentiation (medium and poorly differentiated *vs* well differentiated), TNM stage (referring AJCC cancer staging manual, 8th edition) (19), nerve invasion, tumor size, surgical method, PoV and PV CTCs subtype counts.

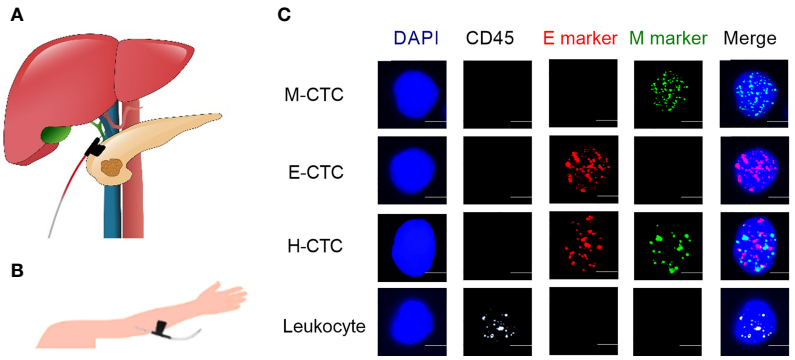

FIGURE 1 | Representative images of PoV, PV blood samples collection and typical multifluorescence signals of CTCs and leukocytes. **(A)** Collecting the portal venous blood sample. **(B)** Peripheral vessel blood sample was obtained by puncturing the cubital vein. **(C)** Based on mRNA sequence staining technology, the nuclei were stained with DAPI (blue), the epithelial markers (EpCAM and CK8/18/19) are indicated by red dots, the mesenchymal markers (Vimentin and Twist) are indicated by green dots, and the hybrid CTCs contain epithelial markers and mesenchymal markers are indicated by red and green dots. Leukocyte marker (CD45) is indicated by white dots. Scale bar = 5μm.

Follow Up

The postoperative follow-up mainly focuses on the disease progression, including recurrence, metastasis, death until to January 2021. According to the guidelines of PCCA, patients are recommended to undergo a comprehensive examination for status assessment every 3 months in the first year, every 3 to 6 months during the second to third years, and then every 6 months (20). The length of the recurrence free survival (RFS)/metastasis free survival (MFS)/overall survival (OS) was measured from the date of surgery until the date of recurrence/metastasis/death occurring.

Postoperative tumor progression was stratified into two mutually exclusive categories: local recurrence and distant metastasis and they were judged mainly by imaging examination. If a patient had diagnosed with both local recurrence and distant metastasis at a follow-up, then he was classified into the metastasis group for metastatic lesions can represent a more lethal progression.

Statistical Analysis

SPSS 21.0 and GraphPad Prism 8.0 software were used for data analysis. E-CTCs, M-CTCs, H-CTCs and T-CTC counts were used to investigate the prognosis assessment value and the correlation with clinicopathological parameters. Receiver operating characteristic curve (ROC) was used to determine the cut-off value of each CTCs subtype counts on different clinical outcomes. Then, we divided these patients with different CTC subtype count into different groups.

Continuous variables are presented as the median with inter-quartile range (IQR). CTCs count differences were compared by the nonparametric Mann–Whitney U test and/or the Kruskal-Wallis test. The Kaplan–Meier method with the log-rank test was used to assess the differences between the different groups. Univariate and multivariate factor analyses of prognosis-related factors were conducted using a Cox regression model to identify independent predictors. $P<0.05$ means statistically significant.

RESULTS

Patients Characteristics

Sixty patients were enrolled in this study, including 34 men and 26 women with a median age of 56.5 (range: 30–83 years old). The number of patients in I stage, II stage, and III stage of TNM stage were 16, 35, 9 respectively. In addition, PV blood samples were collected from 32 patients among them. Although it was an invasive operation to obtain portal venous blood, we had not observed immediate or delayed complications from portal vein draws including hematoma formation or gastrointestinal bleeding. With a median follow-up duration of 15 months (range: 3–29 months), 11 (18.3%) patients experienced local recurrence, and metastasis occurred in 30.0% (18/60), including 9 liver only metastases, 4 lung only metastases, 3 cases of multiple sites metastases, beside 3 patients had been diagnosed with both recurrence and metastatic. By the last follow-up, 17 patients had died due to tumor progression.

Spatial Heterogeneity of CTCs Distribution

Thirty-two patients were implemented both PoV and PV CTCs phenotype tests, and we found that the T-CTC detectable rate in PV was 87.5% (**Figure 2A**), while the PoV T-CTC detectable positive ratio was high to 96.9% (**Figure 2B**). Paired comparison of CTCs phenotype counts in different vessels of 32 patients, we found the count of T-CTC and three kinds of subtypes of CTC in PoV were all significantly higher than in PV (**Figure 2C**) ($P<0.05$).

To further investigate the correlation between the PoV and PV CTC counts, we performed a linear regression analysis and found that the counts of T-CTCs, H-CTCs, E-CTCs per 5ml of PoV were significantly correlated with the count of PV ($R^2 = 0.349$, $P < 0.001$; $R^2 = 0.335$, $P < 0.001$; $R^2 = 0.135$, $P = 0.039$; respectively) (**Supplementary Figures 1A–C**), while no significant association was observed in the count of M-CTCs per 5 mL of PoV and PV sample ($R^2 < 0.001$, $P = 0.973$) (**Supplementary Figure 1D**).

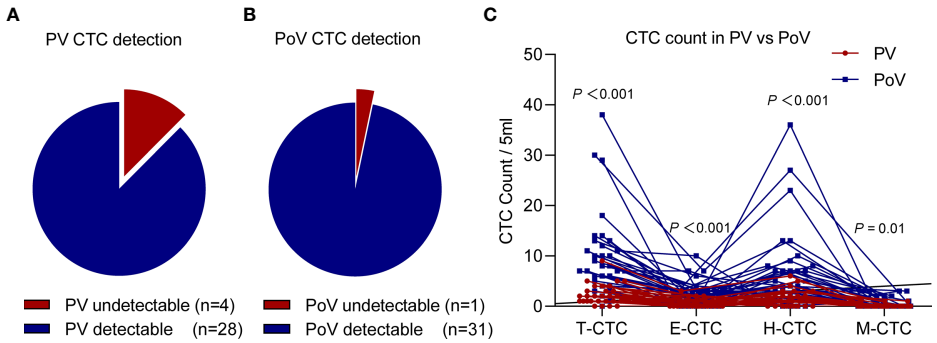

FIGURE 2 | The CTCs count paired comparison in PV and PoV samples (n=32). The detectable rate of T-CTCs in the PV sample **(A)** was lower than that of the PoV sample **(B)** (87.5% *vs* 96.9%). **(C)** Each CTCs phenotype (T-CTC, E-CTC, H-CTC, M-CTC) count of the PoV sample were higher than those of the PV sample.

PV CTCs Phenotype and Their Prognostic Significance

During the follow-up (median months=15, range 3 to 29), five patients (15.6%) suffered recurrence, eleven patients (34.5%) presented with tumor metastasis, and eleven patients (34.5%) died from tumor-related causes. The median counts of T-CTCs, E-CTCs, H-CTCs and M-CTCs were 2, 0.5, 1, and 0, respectively.

To evaluate the prognostic value of the PV CTC phenotype count in PDAC, we compared the count differences of T-CTC and CTCs subtype among patients with different outcomes including recurrence, metastasis, death. We had not noticed a correlation between PV CTCs subtype counts with survival and metastasis events (**Figures 3B, C**). However, we found that recurrent patients had higher E-CTC counts than recurrence-free patients (P<0.05) (**Figure 3A**). ROC curve analysis exhibited

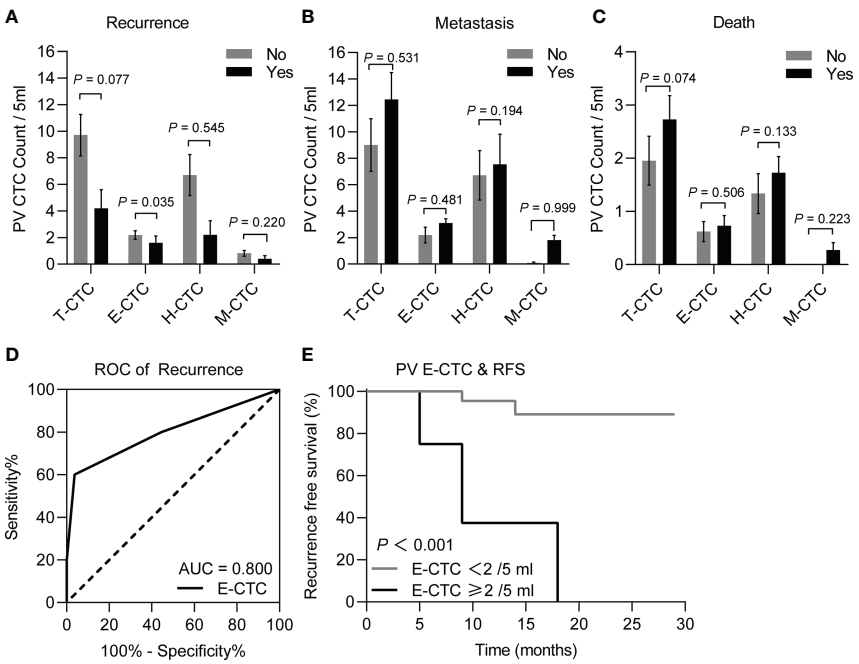

FIGURE 3 | Comparison of different CTC phenotype counts of peripheral blood samples between the PDAC patients (n=32) with different postoperative prognosis, including recurrence or recurrence-free **(A)**, metastasis or metastasis-free **(B)**, and death or survival **(C)**, through the Mann–Whitney U test, the results demonstrated that the recurrence patients (n=5) had significantly higher E-CTC counts than the recurrence-free patients (n=27) (P < 0.05). **(D)** ROC curves for PV E-CTC (cut-off = 2 CTCs/5 ml, AUC = 0.800 95% CI 0.621–0.920; P = 0.032) regarding on recurrence. **(E)** Kaplan-Meier RFS stratified with respect to the E-CTC cut-off value of 2/5 ml for PDAC patients, the curve showed patients with PV E-CTC ≥ 2/5ml had a significantly shorter RFS than patients with PV E-CTC < 2/5ml (P = 0.0002).

that E-CTC≥2/5 ml means a higher risk of tumor recurrence (*P*=0.02) (**Figure 3D**), and Kaplan–Meier curve analysis shown that patients with high PV E-CTC (E-CTC ≥ 2/5 ml) counts had significantly shorter RFS than patients with low E-CTC counts (*P*=0.002) (**Figure 3E**).

PV CTCs Count and Prognosis in Patients Received Adjuvant Chemotherapy

Peripheral blood CTCs of 18 unresectable advanced PDAC patients were also collected before and after the first cycle chemotherapy and chemotherapy mainly adopts gemcitabine -based monotherapy or combination regimens. Comparing the PV CTCs subtype count difference in resectable and unresectable PDAC patients before chemotherapy, we noticed that unresectable patients had significantly higher H-CTCs than resectable patients (*P*=0.035) (**Supplementary Figure 2A**). Besides, Kaplan-Meier analysis shown that there was no significantly difference on overall survival in patients with increased or non-increased T-CTCs/E-CTCs/H-CTCs/M-CTCs (**Supplementary Figures 2B–E**) (*P*=0.915, *P*=0.149, *P*=0.505, *P*=0.164, respectively).

TABLE 1 | Correlation between PoV CTC phenotype count and baseline characteristics.

Variables	n	T-CTC Median (IQR)	*P*	E-CTC Median (IQR)	*P*	H-CTC Median (IQR)	*P*	M-CTC Median (IQR)	*P*
Gender			0.487		0.142		0.742		0.061
Male	34	7.5 (4.75-13.25)		2 (1-4.25)		4 (1.75-8)		0 (0-1.25)	
Female	26	7 (3-13.25)		2 (0.75-3)		4.5 (2-9.5)		0 (0-0)	
Age (years)			0.470		0.234		0.829		0.452
≤65	38	7 (4-14)		2 (1-3.25)		4 (2-8.5)		0 (0-1)	
>65	22	7.5 (2-13)		1.5 (0-4.25)		5 (1.75-8.25)		0 (0-1)	
Diabetes			0.336		0.343		0.099		0.942
No	46	7 (3.75-13)		2 (1-5)		4 (1-7.5)		0 (0-1)	
Yes	14	9.5 (4.75-15)		2 (1-3)		7 (3-13)		0 (0-1.25)	
Hepatitis			0.959		0.925		0.795		0.902
No	51	7 (4-13)		2 (1-4)		5 (2-8)		0 (0-1)	
Yes	9	7 (3.5-13.5)		2 (1-3.5)		3 (2.5-9)		0 (0-2)	
Pre-op CA19-9 (u/ml)			0.087		0.853		0.038		0.335
≤37	23	6 (3-10)		2 (1-4)		3 (1-6)		0 (0-1)	
>37	37	8 (5-14)		2 (1-3.5)		6 (3-9.5)		0 (0-1.5)	
Post-op CA19-9 (u/ml)			**0.013***		**0.030***		**0.012***		0.339
≤37	40	6.5 (3-11)		2 (0.25-3)		3 (1-7)		0 (0-1)	
>37	20	11.5 (6.25-18.75)		3 (1.25-5.75)		7 (3.25-15.25)		0 (0-0.75)	
T stage			0.061		**0.006***		0.514		0.367
T1-T2	30	6.5 (3-10.5)		2 (0-2)		4 (2-7)		0 (0-1)	
T3	30	10 (4.75-17.25)		3 (1-5)		5.5 (1-11.5)		0 (0-2)	
Tumor location			0.242		0.099		0.859		0.349
Head、neck	29	9 (4-16)		3 (1-4.5)		5 (1-10.5)		0 (0-1.5)	
Body、tail	31	7 (3-13)		2 (1-3)		4 (2-8)		0 (0-0)	
Lymph node invasion			0.141		0.810		0.207		**0.014***
N0	30	6.5 (3-11.5)		2 (0.75-3.25)		3.5 (1.75-7.25)		0 (0-0)	
N1-N2	30	8.5 (4-14.75)		2 (1-4)		5.5 (2.75-10)		0 (0-2.25)	
TNM stage 8th AJCC			0.852		0.858		0.795		0.710
IA-IIB	51	7 (4-13)		2 (1-3)		4 (2-8)		0 (0-1)	
III	9	8 (3-21)		2 (0.5-4.5)		3 (1-15)		0 (0-1.5)	
Nerve invasion			0.064		0.128		0.240		0.225
No	34	7 (3-10)		2 (0-3)		4 (2-7)		0 (0-1)	
Yes	26	11 (4.75-17.25)		2.5 (1-4.25)		6.5 (1.75-13)		0 (0-2)	
Differentiation			0.125		0.201		0.375		**0.028***
High	36	7 (3-11.5)		2 (1-3)		3.5 (2-7)		0 (0-0)	
Middle and low	24	10.5 (4.5-14)		2.5 (1-5)		5 (2.25-10.75)		0.5 (0-2)	
Recurrence			**0.025***		**0.021***		0.067		0.309
No	49	7 (4-11.5)		2 (1-3)		4 (2-7)		0 (0-1)	
Yes	11	17 (6-23)		5 (1-7)		11 (3-18)		0 (0-0)	
Metastasis			0.068		0.075		0.616		**<0.001***
No	42	7 (3-11)		2 (1-3)		4 (2-8)		0 (0-0)	
Yes	18	12 (5.5-15)		3 (2-4.25)		5 (1.5-10)		2 (0.75-3)	
Death			0.278		0.070		0.439		**<0.001***
No	43	7 (3-13)		2 (1-3)		4 (2-9)		0 (0-0)	
Yes	17	12 (5-13.5)		3 (1.5-5)		4 (0.5-7.5)		1 (0-3)	

Pre-op, preoperative; post-op, postoperative.
Bold values indicate that the results were statistically significant.

PoV CTCs Count With Clinicopathologic Parameters and Prognosis

We obtained PoV blood samples for CTC phenotype test from 60 patients. Fifty-eight patients (96.7%) had detectable T-CTC in the PoV, and the median counts of T-CTCs, E-CTCs, H-CTCs and M-CTCs were 7, 2, 4, and 0, respectively. During the follow-up (median months=15, IQR 10.25 to 18), eleven patients (18.3%) presented with disease recurrence, eighteen patients (30%) presented with tumor metastasis, and seventeen patients (28.3%) died due to tumor-related causes.

The correlations between the clinicopathologic variables and the PoV CTC phenotype count of the 60 PDAC patients are listed in **Table 1**. The Mann-Whitney U test was used to compare the correlation between CTCs subtype counts and the clinicopathologic variables and outcomes. In this research, we noticed a correlation of the T-CTC count with an abnormal postoperative CA19-9 level and tumor recurrence; a correlation of the E-CTC count with a postoperative abnormal CA19-9 level, T stage and tumor recurrence; a correlation of the H-CTC count with a postoperative abnormal CA19-9; a correlation of the M-CTC count with lymph node invasion, tumor differentiation degree and tumor metastasis (P<0.05) (**Table 1**).

Based on the correlation between the clinical outcome and the CTC phenotype counts, ROC curves were used to determine the cut-off value of the CTC phenotype counts **Figures 4A–D**. The sensitivity, specificity and cut-off value are depicted in **Table 2**. According to tumor recurrence or recurrence-free, the cut-off values of the T-CTC and E-CTC

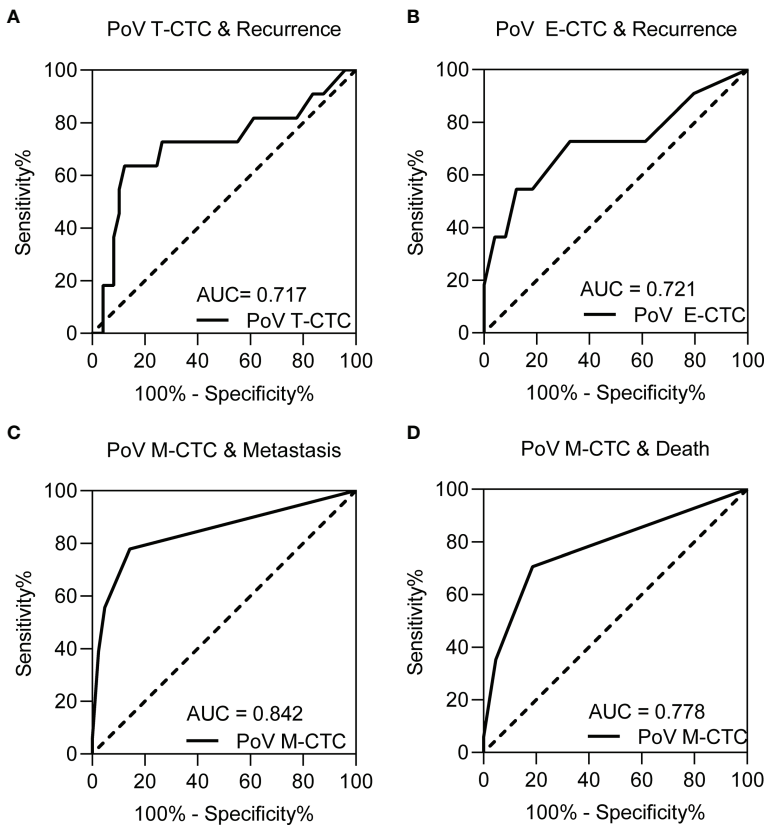

FIGURE 4 | The ROC curve for **(A)** PoV T-CTCs, **(B)** PoV E-CTCs on recurrence prediction, **(C)** PoV M-CTCs for metastasis prediction and **(D)** PoV M-CTCs for death prediction. The result of sensitivity, specificity and cut-off value of each ROC curve are depicted in **Table 2**.

TABLE 2 | ROC curves of PoV CTCs phenotype counts on postoperative progression.

Clinical outcome	CTC phenotype	Cut-off value	Sensitivity	Specificity	AUC	*P* value
Recurrence	T-CTC	14	63.6	87.8	0.717	**0.035***
Recurrence	E-CTC	5	54.55	87.76	0.721	**0.032***
Metastasis	M-CTC	1	77.78	85.71	0.842	**<0.001***
Death	M-CTC	1	70.60	81.40	0.778	**<0.001***

Bold values indicate that the results were statistically significant.

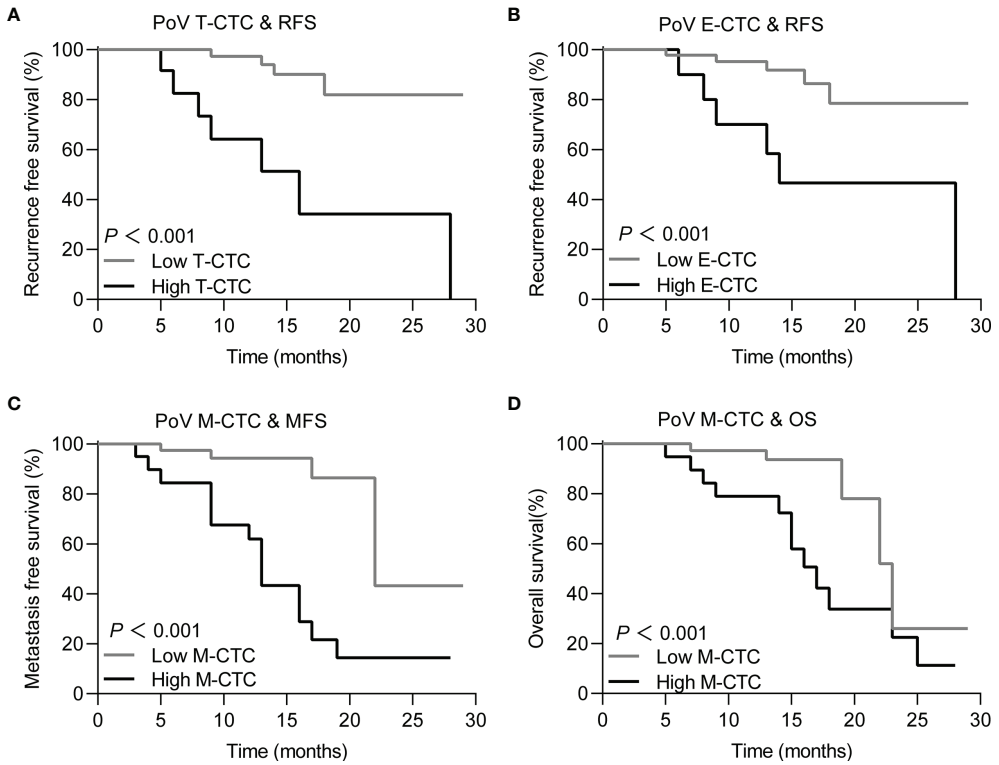

FIGURE 5 | Kaplan-Meier curves for PDAC patients with different prognosis in high/low CTC subtype count group for **(A)** T-CTC, for patients with high T-CTCs (≥ 14/5 ml) *vs* low T-CTC (<14/5 ml) and the mean RFS was 26.44 months (95%CI 24.07-28.83) *vs* 16.51 (95%CI 10.17 - 22.85). **(B)** E-CTC, for patients with high E-CTCs (≥ 5/5 ml) *vs* low E-CTC (<5/5 ml) and the mean RFS was 25.84 month (95%CI 23.268- 28.416) *vs* 18.51 (95%CI 12.106 - 24.927). **(C)** M-CTC, for patients with high M-CTCs (≥ 1/5 ml) *vs* low M-CTC (<1/5 ml) and the mean MFS was 14.19 month (95%CI 10.77 - 17.61) *vs* 23.78 (95%CI 19.207 - 28.368). **(D)** M-CTC, for patients with high M-CTCs (≥ 1/5 ml) *vs* low M-CTC (<1/5 ml) and the mean OS was 17.28 months (95% CI 13.91 to 20.65) *vs* 22.87 months (95% CI 19.51 - 26.22).

counts were 14/5 ml and 5/5 ml, respectively. The cut-off value of M-CTC to describe postoperative metastasis was 1/5 ml, and M-CTC≥1/5 ml was also an unfavourable factor of OS (**Figure 5**).

Based on the cut-off value, PoV CTC subtype counts were divided into high or low groups. Then, Kaplan–Meier analysis was used to compare the prognostic differences among the CTC counts in different groups. The Kaplan–Meier curves showed that PoV T-CTC≥14/5 ml predicts a shorter RFS (P<0.05), PoV E-CTC≥5/5 ml also predicts a shorter RFS (P<0.05), while PoV M-CTC≥1/5 ml predicts a shorter MFS (P<0.05), and a shorter OS (P<0.05)

PoV H-CTC Count to Predict the Postoperative Prognosis

A scholar had also adapted the Canpatrol™ CTC platform, then divided the CTCs into five phenotype with different plastic and reversible phenotypes (21), referring this division criteria, the H-CTCs were further classified into three subtypes as epithelial predominant (E>M), intermediate (E≈M), or mesenchymal predominant (E<M) according to the signal numbers of epithelial or mesenchymal biomarker (**Figure 6A**). H-CTCs are the main component of CTCs in both PV and PoV; interestingly, E ≈ M is also the most abundant subtype of H-CTCs (**Figure 6B**). We noticed a correlation between PoV E>M H-CTCs with postoperative recurrence, besides we had not found correlations between the other CTCs phenotypes with postoperative metastasis and survival (**Figures 6C–E**). The ROC curve results showed that the cut-off value of E> M H-CTC counts for recurrence assessment was 3/5 ml (**Figure 6F**). The Kaplan–Meier curves demonstrated that E>M H-CTC≥3/5 ml means a shorter RFS **(Figure 6G).**

Univariate and Multivariate Regression Analysis of Postoperative Prognosis

To identify the influence of baseline characteristics and particular PoV CTC phenotype count on the resectable PDAC postoperative prognosis. We noticed that postoperative CA19-9>37 U/ml, high T stage, PoV E>M H-CTC≥3/5 ml, PoV T-CTC≥14/5 ml, and PoV E-CTC≥5/5 ml were significantly associated with RFS (all P<0.05), while lymph node invasion and PoV M-CTC≥1/5 ml were significantly associated with MFS (all P<0.05) by univariate Cox regression. However, M-CTC≥1/5 ml and lymph node invasion were both associated with significantly shorter OS (all P<0.05) (**Table 3**). Next, the multivariable analysis revealed that postoperative CA19-9>37 U/ml was a significant independent predictor of RFS (95CI 1.237–40.908; P=0.028); lymph node invasion (95%CI 1.286–

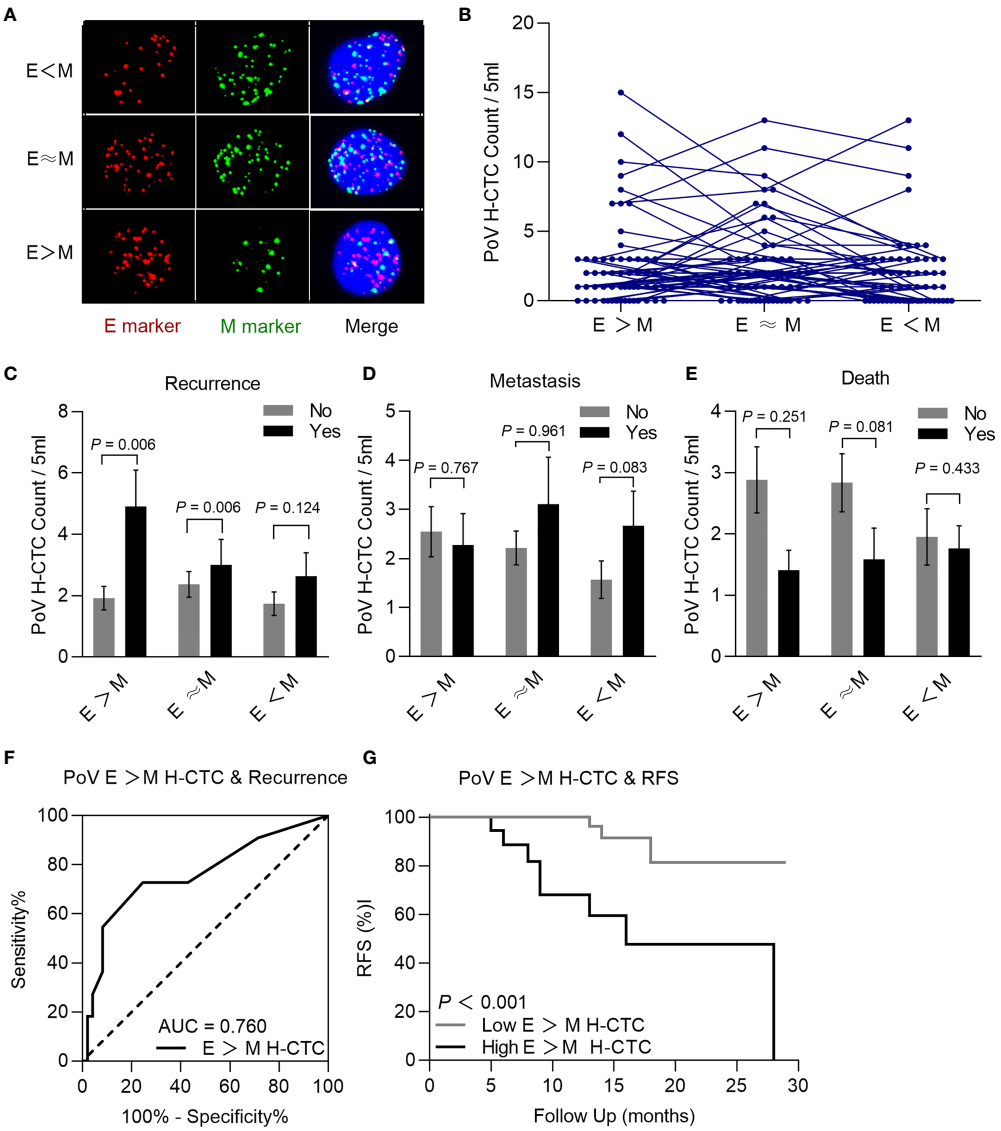

FIGURE 6 | Typical multi-fluorescence signals of hybrid CTCs subtypes and correlation with prognosis. **(A)** Epithelial predominant (E > M) hybrid CTC, intermediate (E≈ M) hybrid CTC, or mesenchymal predominant (E<M) hybrid CTC. **(B)** Each H-CTC subtype count in patients (n=60). Comparison of PoV H-CTC subtype counts with prognosis, recurrence **(C)**, metastasis **(D)**, and death **(E)**, the result demonstrated that recurrence patients had significantly higher E > M H-CTC counts than recurrence-free patients (P<0.05). **(F)** ROC curve was used to determine that the cut-off value of E > M H-CTC count was 3/5 ml (AUC = 0.760, sensitivity = 72.7%, specificity =75.5%, P=0.004). **(G)** Kaplan–Meier analysis showed that patients with E>M H-CTC ≥ 3/5ml had significantly shorter RFS than patients with E>M H-CTC<3/5ml (P < 0.001).

19.546; P=0.020) and PoV M-CTC≥1/5 ml (95%CI 1.893–24.396; P=0.003) were significantly associated with shorter MFS; and PoV M-CTC≥ 1/5 ml (95%CI 1.03–9.27; P=0.043) was significantly associated with shorter OS (**Table 4**).

DISCUSSION

In this study, 88.2% (15/17) of PDAC patients died due to postoperative metastasis with a median follow-up duration of 15 months. Tumor metastasis is an extremely aggressive characteristic of tumors and is the mainly cause of tumor related death of more than 90% of patients with malignant tumors (22). The most common metastasis organ of PDAC patients is the liver due to its unique anatomical features and microenvironment (1, 4, 7). Identifying patients with high tendency of postoperative metastasis or recurrence is of the utmost importance, and it could contribute to the development of novel treatment model and management strategies for PDAC patients (6, 7).

In EMT (epithelial–mesenchymal transition) process, tumor cells acquire some properties of mesenchymal cells which promote tumor cell migrate and invade (16, 23). However, whether EMT

TABLE 3 | Univariate Cox regression analysis for postoperative progression.

Variables	Recurrence Univariate Analysis		Metastasis Univariate Analysis		Death Univariate Analysis	
	HR (95% CI)	*p*	HR (95% CI)	*p*	HR (95% CI)	*p*
Gender: Male *vs* Female	1.347 (0.410-4.425)	0.623	0.779 (0.300-2.020)	0.607	0.533 (0.187-1.525)	0.241
Age (years): ≤65 *vs* >65	1.380 (0.419-4.549)	0.596	0.520 (0.171-1.586)	0.251	0.937 (0.326-2.689)	0.903
Diabetes: no *vs* yes	0.726 (0.153-3.442)	0.687	1.488 (0.547-4.048)	0.436	1.482 (0.533-4.115)	0.451
Hepatitis: no *vs* yes	1.978 (0.419-9.351)	0.389	1.135 (0.257-5.017)	0.867	2.762 (0.737-10.357)	0.132
Pre-op CA19-9 (u/ml): ≤37 *vs*>37	1.294 (0.377-4.439)	0.682	2.203 (0.722-6.728)	0.165	1.329 (0.461-3.827)	0.540
Post-op CA19-9 (u/ml):≤37 *vs*>37	9.432 (2.026-43.916)	**0.004***	0.423 (0.122-1.464)	0.175	0.540 (0.173-1.688)	0.396
T stage: T1-T2 *vs* T3	5.675 (1.222-26.355)	**0.027***	1.824 (.699-4.755)	0.219	1.464 (0.548-3.906)	0.447
Tumor location Head、neck *vs* Body、tail	1.081 (0.304-3.842)	0.904	0.439 (0.170-1.138)	0.090	0.615 (0.236-1.603)	0.320
Total laparoscopic: no *vs* yes	2.128 (0.564-8.037)	0.265	0.555 (0.216-1.423)	0.220	1.039 (0.390-2.771)	0.939
Lymph node invasion: N0 *vs* N1-N2	1.146 (0.347-3.785)	0.823	6.355 (1.829-22.086)	**0.004***	3.455 (1.112-10.733)	**0.032***
TNM stage: IA-IIB *vs* III	1.706 (0.362-8.049)	0.500	1.624 (0.528-4.998)	0.398	1.687 (0.537-5.295)	0.371
Nerve invasion: no *vs* yes	2.628 (0.731-9.446)	0.139	2.035 (0.769-5.380)	0.152	1.920 (0.706-5.225)	0.202
Differentiation: High *vs* Middle and low	2.940 (0.849-10.185)	0.089	3.253 (1.216-8.704)	**0.019***	2.070 (0.757-5.661)	0.156
PoV E>M H-CTC (per 5mL): <3 *vs* ≥ 3	6.867 (1.802-26.161)	**0.005***	1.318 (0.492-3.528)	0.583	0.935 (0.327-2.671)	0.900
PoV T-CTC (per 5mL): <14 *vs* ≥14	8.075 (2.308-28.248)	**0.001***	1.698 (0.596-4.837)	0.321	1.016 (0.325-3.183)	0.978
PoV E-CTC (per 5mL): <5 *vs* ≥ 5	4.989 (1.490-16.707)	**0.009***	1.253 (.410-3.828)	0.693	1.138 (0.385-3.365)	0.815
PoV M-CTC (per 5mL): <1 *vs* ≥ 1	0.485 (0.103-2.274)	0.358	7.704 (2.527-23.492)	**<0.001***	3.963 (1.371-11.455)	**0.011***

Variables which had a P value < 0.05 in univariable analysis was included in the multivariable analysis.
Bold values indicate that the results were statistically significant.

TABLE 4 | Multivariate Cox regression analysis for postoperative progression.

Variables	Recurrence multivariate analysis		Metastasis multivariate analysis		Death multivariate analysis	
	HR (95% CI)	*p*	HR (95% CI)	*p*	HR (95% CI)	*p*
Post-op CA19-9 (u/ml):≤ 37 *vs*>37	7.11 (1.23-40.90)	**0.028***	NA.		NA.	
T stage: T1-T2 vs T3	4.37 (0.75-25.55)	0.10	NA.		NA.	
Lymph node invasion: N0 *vs* N1-N2	NA.		5.01 (1.28-19.54)	**0.020***	2.531 (0.78-8.18)	0.12
Differentiation: High *vs* Middle and low	NA.		0.67 (0.20-2.27)	0.52	NA.	
PoV E>M H-CTC (per 5ml): <3 *vs* ≥ 3	1.22 (0.11-13.08)	0.870	NA.		NA.	
PoV T-CTC (per 5ml): <14 *vs* ≥ 14	3.84 (0.48-30.28)	0.202	NA.		NA.	
PoV E-CTC (per 5ml): <5 *vs* ≥ 5	0.58 (0.094-3.64)	0.56	NA.		NA.	
PoV M-CTC (per 5ml): <1 *vs* ≥ 1	NA.		6.795 (1.89-24.39)	**0.003***	3.100 (1.03-9.27)	**0.043***

NA, no application.
Bold values indicate that the results were statistically significant.

proceeds through intermediate states and, if so, how many intermediate steps exist in this transition, how plastic and reversible these intermediate states are, and what the implications of these different EMT status are for clinical applications (24). EMT and its different intermediate status have recently been noticed as crucial drivers of tumor progression and metastasis (16, 24, 25). In light of recent research demonstrated that the CTC count could be used as a prognostic biomarker, and a higher CTCs count may predict an unfavourable prognosis in malignant patients (26–30). In this research, we used the Canpatrol^{TM} CTC filtration platform to detect CTCs in different EMT statuses intend to explore their prognostic assessment value. The results of the PV CTC and PoV CTC subtype counts confirmed a correlation between high PV E-CTC, PoV E-CTC, and PoV E>M H-CTC counts with postoperative recurrence, but they were not significant independent risk factors of recurrence, while high M-CTC counts were significant independent risk factors for postoperative metastasis and death.

EMT is rather a binary process, and epithelial CTCs gradually lose polarity and intercellular adhesion, but gain increased migratory and invasive properties in this process (5, 30). CTCs have been reviewed as the seeds of tumor metastasis, and previous reports had noted that mesenchymal CTCs with an elongated shape were closely related to the tumor metastasis cascade (24, 31). Although we are far from reaching a consensus on the detailed mechanisms, some researchers have already demonstrated that M-CTCs play an essential role in tumor progression, especially the distant metastasis process (5, 30, 32, 33). In this research, we also noticed a correlation between PoV E>M H-CTC, PoV E-CTCs counts with RFS. The proliferation capability of E-CTCs and early hybrid CTCs may lead to tumor relapse may be due to their unique self-seeding effect (34).

The count of each PoV CTC subtype varied in patients with different clinicopathological factors. In our study, PoV M-CTCs counts were linked to lymph node invasion and tumor differentiation degree. Besides, PoV T-CTCs were closely related to the postoperative CA19-9 level, the E-CTCs count were closely related to the postoperative CA19-9 level and high T stage, meanwhile the H-CTC count was also related to the postoperative CA19-9 level. The above results demonstrated that

CTCs with different statuses might not be a separate indicator of tumor progression and they also had a closely association with the common clinical and pathological characteristics.

A previous study had reported that surgical operation could cause the increasing of PoV CTC count (35) and we total agree with this opinion, so we collected PoV sample prior to specimen separation during surgery. Paired analysis of the CTCs counts and detectable rate in the PV and PoV blood sample, we noticed that the CTCs detectable rate and CTCs count in PoV were both significantly higher than in PV and it is consistent with several previous reports that demonstrated the spatial heterogeneity of CTCs distribution (4, 7, 9). Besides, we also noticed a correlation between the PoV and PV CTCs counts in the count of T-CTC, H-CTC and M-CTC, and this phenomenon indirect the peculiar property of M-CTC.

Detecting CTCs in peripheral blood of PDAC was still challenging due to hepatic filtration and technical limitations which may limit its clinical application value (7, 36). Notably, abundant previous research had demonstrated that tumor-proximal liquid biopsy can enhance the diagnostic and prognosis assessment performance of CTCs in vessels closer to the tumor (4, 7, 9, 37). Portal veins are the main veins that drain blood from the pancreas to other organs, which may be related to the high frequency of liver metastasis from pancreatic cancer (38). portal venous as the main drain tube of pancreas with abundant CTCs and the promising clinical application value of portal venous CTCs test had been demonstrated by previous studies (4, 7, 9, 37). Recently, ultrasound-guided (9) and endoscopic ultrasound-guided (39, 40) fine-needle aspiration have gradually been used to obtain portal venous blood in advanced PDAC patients. However, portal vein puncture is an invasive approach with the possibility of bleeding、infection、thrombotic、tumor cell spread. besides it is also a challenge to recognize and obtain portal venous blood during surgery, especially in the vision of laparoscopic which may extend the operation duration.

Several reports had demonstrated that peripheral CTCs could be used to assess prognosis and the effect of chemotherapy in cancer patients (41–44). In addition, monitoring the dynamically change of peripheral CTC to assess the adjuvant therapy and neoadjuvant therapy effect could help to timely identify ineffective treatment and avoid unnecessary costs (45). In this research, we monitored the peripheral blood CTCs of 18 unresectable advanced PDAC patients before and after the first cycle chemotherapy, but we had not noticed the significantly difference on the overall survival time in patients with increased or non-increased CTCs regardless of the subtype which may related to the low counts of PV CTC and small research cohorts.

Some limitations exist in this research, including the small cohort size, short follow-up time, and single centre research. In addition, other unpredictable factors may also influence the final results. In this study, we used Canpatrol^{TM} technology to divide the EMT procedure into five stages, but the detailed procedure and property differences had not reached a consensus. Moreover, we should recognize that different detection methods for CTCs may lead to inconsistent results.

In conclusion, we have identified the spatial heterogeneity of the CTC distribution, and portal veins may be a better vessel for CTC phenotype testing to assess the PDAC prognosis than peripheral vessels. In addition, high PoV M-CTC counts are significant independent risk factors for postoperative metastasis and survival. Therefore, the PoV CTC phenotype test with the potential to be developed into an accurate and reliable biomarker to guide treatment decisions and patient stratified management.

DATA AVAILABILITY STATEMENT

The raw data supporting the conclusions of this article will be made available by the authors, without undue reservation.

ETHICS STATEMENT

The studies involving human participants were reviewed and approved by Henan Provincial People's Hospital. The patients/participants provided their written informed consent to participate in this study.

AUTHOR CONTRIBUTIONS

YP and DYL performed the literature search and manuscript drafting. JY, XD, and NW conducted data collection. YP, EX, and LT conducted statistical processing on the data. DXL, DYL, and PS supervised and revised the manuscript. All authors contributed to the article and approved the submitted version.

FUNDING

This research was supported by grants from the Key Projects of Medical Science and Technology in Henan Province, China No. 201602258, No. 212102310132.

ACKNOWLEDGMENTS

We would like to thank Dr. Fangyuan, Qin, and Dr. Yaping Zhai of Henan Eye Hospital, for valuable advice and assistance in CTCs test. We would also like to convey our gratitude to Ophthalmic Laboratory of Henan Province in Zhengzhou for their technical support.

SUPPLEMENTARY MATERIAL

The Supplementary Material for this article can be found online at: https://www.frontiersin.org/articles/10.3389/fonc.2021.757307/full#supplementary-material

Supplementary Figure 1 | Scatter plot showing the count of T-CTCs **(A)**, H-CTCs **(B)**, E-CTCs **(C)**, M-CTCs **(D)** per 5 ml in PoV and PV samples. Dashed line indicates linear fit.

Supplementary Figure 2 | PV CTCs counts in unresectable PDAC patients. Unresectable patients have significantly higher H-CTC count than resectable patients **(A)**. Kaplan-Meier analysis shown that there was no significant difference on overall survival time in patients with increased or non-increased T-CTCs **(B)**, E-CTCs **(C)**, H-CTCs **(D)**, M-CTCs **(E)**.

REFERENCES

1. Houg DS, Bijlsma MF. The Hepatic Pre-Metastatic Niche in Pancreatic Ductal Adenocarcinoma. *Mol Cancer* (2018) 17(1):95. doi: 10.1186/s12943-018-0842-9
2. Rahib L, Smith BD, Aizenberg R, Rosenzweig AB, Fleshman JM, Matrisian LM. Projecting Cancer Incidence and Deaths to 2030: The Unexpected Burden of Thyroid. *Liver Pancreas Cancers United States* (2014) 74 (11):2913–21. doi: 10.1158/0008-5472.CAN-14-0155%J Cancer Research
3. Groot VP, Gemenetzis G, Blair AB, Rivero-Soto RJ, Yu J, Javed AA, et al. Defining and Predicting Early Recurrence in 957 Patients With Resected Pancreatic Ductal Adenocarcinoma. *Ann Surg* (2019) 269(6):1154–62. doi: 10.1097/sla.0000000000002734
4. Tao L, Su L, Yuan C, Ma Z, Zhang L, Bo S, et al. Postoperative Metastasis Prediction Based on Portal Vein Circulating Tumor Cells Detected by Flow Cyt Ometry in Periampullary or Pancreatic Cancer. *Cancer Manag Res* (2019) 11:7405–25. doi: 10.2147/CMAR.S210332
5. Qi LN, Xiang BD, Wu FX, Ye JZ, Zhong JH, Wang YY, et al. Circulating Tumor Cells Undergoing EMT Provide a Metric for Diagnosis and Prognosis of Patients With Hepatocellular Carcinoma. *Cancer Res* (2018) 78(16):4731–44. doi: 10.1158/0008-5472.Can-17-2459
6. Zhou B, Xu JW, Cheng YG, Gao JY, Hu SY, Wang L, et al. Early Detection of Pancreatic Cancer: Where Are We Now and Where are We Going? *Int J Cancer* (2017) 141(2):231–41. doi: 10.1002/ijc.30670
7. Buscail E, Chiche L, Laurent C, Vendrely V, Denost Q, Denis J, et al. Tumor-Proximal Liquid Biopsy to Improve Diagnostic and Prognostic Performances of Circulating Tumor Cells. *Mol Oncol* (2019) 13(9):1811–26. doi: 10.1002/1878-0261.12534
8. Guo W, Sun YF, Shen MN, Ma XL, Wu J, Zhang CY, et al. Circulating Tumor Cells With Stem-Like Phenotypes for Diagnosis, Prognosis, and Therapeutic Response Evaluation in Hepatocellular Carcinoma. *Clin Cancer Res* (2018) 24 (9):2203–13. doi: 10.1158/1078-0432.CCR-17-1753
9. Liu X, Li C, Li J, Yu T, Zhou G, Cheng J, et al. Detection of CTCs in Portal Vein was Associated With Intrahepatic Metastases and Prognosis in Patients With Advanced Pancreatic Cancer. *J Cancer* (2018) 9(11):2038–45. doi: 10.7150/jca.23989
10. Tien YW, Kuo HC, Ho BI, Chang MC, Chang YT, Cheng MF, et al. A High Circulating Tumor Cell Count in Portal Vein Predicts Liver Metastasis From Periampullary or Pancreatic Cancer: A High Portal Venous CTC Count Predicts Liver Metastases (2016) 95(16)e3407. doi: 10.1097/md.0000000000003407
11. Reddy RM, Murlidhar V, Zhao L, Grabauskiene S, Zhang Z, Ramnath N, et al. Pulmonary Venous Blood Sampling Significantly Increases the Yield of Circulating Tumor Cells in Early-Stage Lung Cancer. *J Thorac Cardiovasc Surg* (2016) 151(3):852–8. doi: 10.1016/j.jtcvs.2015.09.126
12. Nieto MA, Huang RY, Jackson RA, Thiery JP. EMT: 2016. *Cell* (2016) 166(1) 21–45. doi: 10.1016/j.cell.2016.06.028
13. Pastushenko I, Brisebarre A, Sifrim A, Fioramonti M, Revenco T, Boumahdi S, et al. Identification of the Tumour Transition States Occurring During EMT. *Nature* (2018) 556(7702):463–8. doi: 10.1038/s41586-018-0040-3
14. Pastushenko I, Blanpain C. EMT Transition States During Tumor Progression and Metastasis. *Trends Cell Biol* (2019) 29(3):212–26. doi: 10.1016/j.tcb.2018.12.001
15. Chen J, Cao S, Situ B, Zhong J, Hu Y, Li S, et al. Metabolic Reprogramming-Based Characterization of Circulating Tumor Cells in Prostate Cancer. *J Exp Clin Cancer Res* (2018) 37(1):127. doi: 10.1186/s13046-018-0789-0
16. Genna A, Vanwynsberghe AM, Villard AV, Pottier C, Ancel J, Polette M, et al. EMT-Associated Heterogeneity in Circulating Tumor Cells: Sticky Friends on the Road to Metastasis. *Cancers (Basel)* 12(6). doi: 10.3390/cancers12061632
17. Liu YK, Hu BS, Li ZL, He X, Li Y, Lu LG. An Improved Strategy to Detect the Epithelial-Mesenchymal Transition Process in Circulating Tumor Cells in Hepatocellular Carcinoma Patients. *Hepatol Int* (2016) 10(4):640–6. doi: 10.1007/s12072-016-9732-7
18. Dong J, Zhu D, Tang X, Qiu X, Lu D, Li B, et al. Detection of Circulating Tumor Cell Molecular Subtype in Pulmonary Vein Predicting Prognosis of Stage I-III Non-Small Cell Lung Cancer Patients. *Front Oncol* (2019) 9:e1139. doi: 10.3389/fonc.2019.01139
19. Tempero MA, Malafa MP, Al-Hawary M, Behrman SW, Benson AB, Cardin DB, et al. Pancreatic Adenocarcinoma, Version 2.2021, NCCN Clinical Practice Guidelines in Oncology. *J Natl Compr Canc Netw* (2021) 19 (4):439–57. doi: 10.6004/jnccn.2021.0017
20. Comprehensive Guidelines for the Diagnosis and Treatment of Pancreatic Cancer (2018 Version). *Zhonghua Wai Ke Za Zhi* (2018) 56(7):481–94. doi: 10.3760/cma.j.issn.0529-5815.2018.07.001
21. Latil M, Nassar D, Beck B, Boumahdi S, Wang L, Brisebarre A, et al. Cell-Type-Specific Chromatin States Differentially Prime Squamous Cell Carcinoma Tumor-Initiating Cells for Epithelial to Mesenchymal Transition. *Cell Stem Cell* (2017) 20(2):191–204.e5. doi: 10.1016/j.stem.2016.10.018
22. Hong B, Zu Y. Detecting Circulating Tumor Cells: Current Challenges and New Trends. *Theranostics* (2013) 3(6):377–94.
23. Lamouille S, Xu J, Derynck R. Molecular Mechanisms of Epithelial-Mesenchymal Transition. *Nat Rev Mol Cell Biol* (2014) 15(3):178–96.
24. Pastushenko I, Brisebarre A, Sifrim A, Fioramonti M, Revenco T, Boumahdi S, et al. Identification of the Tumour Transition States Occurring During EMT. *Nature* (2018) 556(7702):463–8. doi: 10.1038/s41586-018-0040-3
25. Nieto MA, Huang RY, Jackson RA, Thiery JP. EMT: 2016. *Cell* (2016) 166 (1):21–45. doi: 10.1016/j.cell.2016.06.028
26. Sundling KE, Lowe AC. Circulating Tumor Cells: Overview and Opportunities in Cytology. *Adv Anat Pathol* (2019) 26(1):56–63. doi: 10.1097/pap.0000000000000217
27. Sun Y, Wu G, Cheng KS, Chen A, Neoh KH, Chen S, et al. CTC Phenotyping for a Preoperative Assessment of Tumor Metastasis and Overall Survival of Pancreatic Ductal Adenocarcinoma Patients. *EBioMedicine* (2019) 46:133–49. doi: 10.1016/j.ebiom.2019.07.044
28. Szczerba BM, Castro-Giner F, Vetter M, Krol I, Gkountela S, Landin J, et al. Neutrophils Escort Circulating Tumour Cells to Enable Cell Cycle Progression. *Nature* (2019) 566(7745):553–7. doi: 10.1038/s41586-019-0915-y
29. Mathias TJ, Chang KT, Martin SS, Vitolo MI. Gauging the Impact of Cancer Treatment Modalities on Circulating Tumor Cells (CTCs). *Cancers (Basel)* (2020) 12(3).
30. Yang YJ, Kong YY, Li GX, Wang Y, Ye DW, Dai B. Phenotypes of Circulating Tumour Cells Predict Time to Castration Resistance in Metastatic Castration-Sensitive Prostate Cancer. *BJU Int* (2019) 124(2):258–67. doi: 10.1111/bju.14642
31. Dong X, Ma Y, Zhao X, Tian X, Sun Y, Yang Y, et al. Spatial Heterogeneity in Epithelial to Mesenchymal Transition Properties of Circulating Tumor Cells Associated With Distant Recurrence in Pancreatic Cancer Patients. *2020* (2020) 8(11):676. doi: 10.21037/atm-20-782
32. Wei C, Yang C, Wang S, Shi D, Zhang C, Lin X, et al. Crosstalk Between Cancer Cells and Tumor Associated Macrophages Is Required for Mesenchymal Circulating Tumor Cell-Mediated Colorectal Cancer Metastasis. *Mol Cancer* (2019) 18(1):64. doi: 10.1186/s12943-019-0976-4
33. Li S, Chen Q, Li H, Wu Y, Feng J, Yan Y. Mesenchymal Circulating Tumor Cells (CTCs) and OCT4 mRNA Expression in CTCs for Prognosis Prediction in Patients With Non-Small-Cell Lung Cancer. *Clin Transl Oncol* (2017) 19 (9):1147–53. doi: 10.1007/s12094-017-1652-z
34. Kim M-Y, Oskarsson T, Acharyya S, Nguyen DX, Zhang XHF, Norton L, et al. Tumor Self-Seeding by Circulating Cancer Cells. *Cell* (2009) 139(7):1315–26. doi: 10.1016/j.cell.2009.11.025
35. White MG, Lee A, Vicente D, Hall C, Kim MP, Katz MHG, et al. Measurement of Portal Vein Blood Circulating Tumor Cells is Safe and May Correlate With Outcomes in Resected Pancreatic Ductal Adenocarcinoma. *Ann Surg Oncol* (2021) 28(8):4615–22. doi: 10.1245/s10434-020-09518-y
36. Denve E, Riethdorf S, Ramos J, Nocca D, Coffy A, Daurs JP, et al. Alix-Panabires: Capture of Viable Circulating Tumor Cells in the Liver of Colorectal Cancer Patients. *Clin Chem* (2013) 59(9):1384–92. doi: 10.1373/clinchem.2013.202846
37. Tien YW, Kuo HC, Ho BI, Chang MC, Chang YT, Cheng MF, et al. A High Circulating Tumor Cell Count in Portal Vein Predicts Liver Metastasis From Periampullary or Pancreatic Cancer: A High Portal Venous CTC Count Predicts Liver Metastases. *Med (Baltimore)* (2016) 95(16):e3407. doi: 10.1097/md.0000000000003407
38. Catenacci DV, Chapman CG, Xu P, Koons A, Konda VJ, Siddiqui UD, et al. Acquisition of Portal Venous Circulating Tumor Cells From Patients With Pancreaticobiliary Cancers by Endoscopic Ultrasound. *Gastroenterology* (2015) 149(7):1794–803.e4. doi: 10.1053/j.gastro.2015.08.050
39. Chapman CG, Ayoub F, Swei E, Llano EM, Li B, Siddiqui UD, et al. Endoscopic Ultrasound Acquired Portal Venous Circulating Tumor Cells Predict Progression

Free Survival and Overall Survival in Patients With Pancreaticobiliary Cancers. *Pancreatology* (2020) 20(8):1747–54. doi: 10.1016/j.pan.2020.10.039
40. Chapman CG, Waxman I. EUS-Guided Portal Venous Sampling of Circulating Tumor Cells. *Curr Gastroenterol Rep* (2019) 21(12):68. doi: 10.1007/s11894-019-0733-2
41. Tan K, Leong SM, Kee Z, Caramat PV, Teo J, Blanco MVM, et al. Longitudinal Monitoring Reveals Dynamic Changes in Circulating Tumor Cells (CTCs) and CTC-Associated miRNAs in Response to Chemotherapy in Metastatic Colorectal Cancer Patients. *Cancer Lett* (2018) 423:1–8. doi: 10.1016/j.canlet.2018.02.039
42. Zhang Z, Xiao Y, Zhao J, Chen M, Xu Y, Zhong W, et al. Relationship Between Circulating Tumour Cell Count and Prognosis Following Chemotherapy in Patients With Advanced Non-Small-Cell Lung Cancer. *Respirology* (2016) 21(3):519–25. doi: 10.1111/resp.12696
43. Xu Y, Qin T, Li J, Wang X, Gao C, Xu C, et al. Detection of Circulating Tumor Cells Using Negative Enrichment Immunofluorescence and an *In Situ* Hybridization System in Pancreatic Cancer. *Int J Mol Sci* (2017) 18(4). doi: 10.3390/ijms18040622
44. Bidard FC, Huguet F, Louvet C, Mineur L, Bouché O, Chibaudel B, et al. Circulating Tumor Cells in Locally Advanced Pancreatic Adenocarcinoma: The Ancillary CirCe 07 Study to the LAP 07 Trial. *Ann Oncol* (2013) 24(8):2057–61. doi: 10.1093/annonc/mdt176
45. Chong MH, Zhao Y, Wang J, Zha XM, Liu XA, Ling LJ, et al. The Dynamic Change of Circulating Tumour Cells in Patients With Operable Breast Cancer Before and After Chemotherapy Based on a Multimarker QPCR Platform. *Br J Cancer* (2012) 106(10):1605–10. doi: 10.1038/bjc.2012.157

Conflict of Interest: The authors declare that the research was conducted in the absence of any commercial or financial relationships that could be construed as a potential conflict of interest.

Publisher's Note: All claims expressed in this article are solely those of the authors and do not necessarily represent those of their affiliated organizations, or those of the publisher, the editors and the reviewers. Any product that may be evaluated in this article, or claim that may be made by its manufacturer, is not guaranteed or endorsed by the publisher.

frontiers in Oncology

ORIGINAL RESEARCH
published: 05 November 2021
doi: 10.3389/fonc.2021.698302

OXCT1 Enhances Gemcitabine Resistance Through NF-κB Pathway in Pancreatic Ductal Adenocarcinoma

Jinsheng Ding[1,2,3†], Hui Li[1,2†], Yang Liu[1,2†], Yongjie Xie[1,2], Jie Yu[1], Huizhi Sun[1,2], Di Xiao[1], Yizhang Zhou[1], Li Bao[3], Hongwei Wang[1*] and Chuntao Gao[1*]*

[1] Department of Pancreatic Cancer, Key Laboratory of Cancer Prevention and Therapy, Tianjin Medical University Cancer Institute and Hospital, National Clinical Research Center for Cancer, Tianjin's Clinical Research Center for Cancer, Tianjin, China, [2] The Graduate School, Tianjin Medical University, Tianjin, China, [3] Key Laboratory of Cancer Prevention and Therapy, Key Laboratory of Breast Cancer Prevention and Therapy, Tianjin Medical University Cancer Institute and Hospital, National Clinical Research Center for Cancer, Tianjin's Clinical Research Center for Cancer, Tianjin, China

OPEN ACCESS

Edited by:
Kuirong Jiang,
Nanjing Medical University, China

Reviewed by:
Suraj Kadunganattil,
Amala Cancer Research Centre, India
Chun Hei Antonio Cheung,
National Cheng Kung University, Taiwan

***Correspondence:**
Li Bao
chengdu1125@hotmail.com
Hongwei Wang
wanghongwei_tj@sina.com
Chuntao Gao
gaochuntao@tjmuch.com

[†]These authors have contributed equally to this work and share first authorship

Specialty section:
This article was submitted to Gastrointestinal Cancers, a section of the journal Frontiers in Oncology

Received: *21 April 2021*
Accepted: *18 October 2021*
Published: *05 November 2021*

Citation:
Ding J, Li H, Liu Y, Xie Y, Yu J, Sun H, Xiao D, Zhou Y, Bao L, Wang H and Gao C (2021) OXCT1 Enhances Gemcitabine Resistance Through NF-κB Pathway in Pancreatic Ductal Adenocarcinoma. Front. Oncol. 11:698302. doi: 10.3389/fonc.2021.698302

Background: Pancreatic ductal adenocarcinoma (PDAC) is a type of malignant tumor with a five-year survival rate of less than 10%. Gemcitabine (GEM) is the most commonly used drug for PDAC chemotherapy. However, a vast majority of patients with PDAC develop resistance after GEM treatment.

Methods: We screened for GEM resistance genes through bioinformatics analysis. We used immunohistochemistry to analyze 3-oxoacid CoA-transferase 1 (OXCT1) expression in PDAC tissues. The survival data were analyzed using the Kaplan–Meier curve. The expression levels of the genes related to OXCT1 and the NF-κB signaling pathway were quantified using real–time quantitative PCR and western blot analyses. We performed flow cytometry to detect the apoptosis rate. Colony formation assay was performed to measure the cell proliferation levels. The cytotoxicity assays of cells were conducted using RTCA. The downstream pathway of OXCT1 was identified *via* the Gene Set Enrichment Analysis. Tumor growth response to GEM *in vivo* was also determined in mouse models.

Results: Bioinformatics analysis revealed that OXCT1 is the key gene leading to GEM resistance. Patients with high OXCT1 expression exhibited short relapse-free survival under GEM treatment. OXCT1 overexpression in PDAC cell lines exerted inhibitory effect on apoptosis after GEM treatment. However, the down-regulation of OXCT1 showed the opposite effect. Blocking the NF-κB signaling pathway also reduced GEM resistance of PDAC cells. Tumor growth inhibition induced by GEM *in vivo* reduced after OXCT1 overexpression. Moreover, the effect of OXCT1 on GEM refractoriness in PDAC cell lines was reversed through using an NF-κB inhibitor.

Conclusion: OXCT1 promoted GEM resistance in PDAC *via* the NF-κB signaling pathway both *in vivo* and *in vitro*. Our results suggest that OXCT1 could be used as a potential therapeutic target for patients with PDAC.

Keywords: Pancreatic ductal adenocarcinoma, OXCT1, gemcitabine, chemoresistance, NF-κB

INTRODUCTION

Pancreatic ductal adenocarcinoma (PDAC) is the most common type of pancreatic cancer. It is a highly malignant tumor with poor prognosis and a five-year survival rate of only 10% (1). It is projected to be the second leading cause of cancer-related deaths in the western world by 2030 (2–5). In recent years, the incidence of pancreatic cancer has been increasing, whereas the progress in its treatment has been rather slow. In 2014, 46,420 patients were newly diagnosed with pancreatic cancer, and 39,590 patients died from pancreatic cancer in the United States. In China, the mortalities attributed to pancreatic cancer ranks fifth among all cancer mortalities. Surgical operation is the most effective treatment for pancreatic cancer, and radical resection has been shown to considerably improve the survival rate of patients (6). However, only 10–15% of patients with PDAC have a chance to receive radical surgery clinically because most patients with PDAC are already at an advanced stage during diagnosis given that the early symptoms of pancreatic cancer are not noticeable (7–10). Therefore, at present, chemotherapy is an important means for the treatment of advanced PDAC (11). However, considerable drug resistance against gemcitabine (GEM), which is used as the first-line treatment for PDAC (12), develops after a certain period of its use. This gives rise to great challenges for PDAC treatment.

GEM is a deoxycytidine analog with multiple modes of action inside cells (13). It has been used as a classic chemotherapy agent for nearly 20 years (14). During this period, GEM has become the standard first-line treatment for advanced PDAC. The poor efficacy of GEM in the treatment of PDAC may be due to the difficulty of drug penetration into the dense and vascularized stroma of tumors (15). Many different cellular pathways, transcription factors, and nucleotide metabolic enzymes have been found to be associated with GEM resistance and sensitivity (16–19). Although GEM is used relatively widely and commonly, the mechanisms associated with GEM resistance remain unclear. Elucidating the relevant mechanisms of GEM resistance in PDAC is necessary to ultimately improve the survival rate of patients with PDAC.

In response to stress, stimuli, and malnutrition, cancer cells dysregulate some metabolic pathways and activate certain signaling pathways (20–22). These changes may cause metabolic disorders, eventually leading to cell damage and even death. Cells resist these adverse conditions through a series of compensatory mechanisms to escape from apoptosis and death. In 2016, Huang et al. confirmed that when the energy supply of cancer cells is insufficient, ketone metabolism is significantly enhanced to maintain the cellular needs (23). 3-Oxoacid CoA-transferase 1 (OXCT1) is a key rate-limiting enzyme in ketone body metabolism. The product of OXCT1 is converted into acetyl-CoA, which finally participates in the tricarboxylic acid cycle for oxidation and ATP production (24).

In this study, we first screened out the relevant target gene OXCT1 through bioinformatic analysis to explore the drug resistance mechanism of PDAC against GEM. Based on this analysis, we found that OXCT1 was highly expressed in tumor tissues and that its expression level was significantly negatively correlated with relapse-free survival (RFS). Through experimental validation, we found that OXCT1 could enhance GEM resistance in PDAC. Next, we identified that the NF-κB signaling pathway was a potential downstream pathway of OXCT1 and tested our hypothesis by inhibiting NF-κB signaling pathway. Our study provides new theoretical and experimental support for GEM tolerance in PDAC and identify a new potential therapeutic target.

MATERIAL AND METHODS

Patients and Samples in Public Database

The gene expression profiles of GSE12945 and GSE80617 were downloaded from the Gene Expression Omnibus (GEO) database (http://www.ncbi.nlm.nih.gov/geo/). The mRNA profiles of pancreatic tumors and adjacent normal tissues were generated *via* high-throughput sequencing based on GPL11154 Illumina HiSeq2000 (*Homo sapiens*). Twenty samples were obtained from 20 patients, among which the samples were paired consisting of tumor/normal specimens from the same patients. The gene expression profiles of tumor specimens were compared with those of normal specimens to identify the differentially expressed genes (DEGs). The Venn diagram of the DEGs was generated using three datasets. From these three datasets, 18 common co-expressed genes were identified. OXCT1 was selected for further analysis among all the identified DEGs.

Identification of Differentially Expressed mRNAs

Log fold change (FC) and *P* value were used to filter the differentially expressed mRNAs among the three datasets. We selected the DEGs in accordance with the *P* value threshold and absolute value of FC. $P<0.05$ was considered to indicate statistically significant difference.

Mice, Cell Culture, and Reagents

Female nude BALB/c mice, 6–8 weeks old, were obtained from SiPeiFu, Beijing, China. BxPC-3, MIA PaCa-2, AsPC-1, CFPAC-1, PANC-1, Pan02, SW1990, HPDE6C7, and 293T cell lines were used in this study. These cell lines were obtained from the American Type Culture Collection. We used DMEM or RPMI-1640 (Gibco) medium supplemented with 10% fetal bovine serum (Gibco) to culture the cells in a humidified 5% CO_2 atmosphere at 37°C. GEM was purchased from Lily France, Fegersheim, France. Antibodies against NF-κB P65 (cat. no. 8242S), NF-κB p-P65 (ser536) (cat. no. 3033S), Caspase-3 (cat. no. 9662S), Cleaved Caspase-3 (cat. no. 9661S), γ-H2AX (cat. no. 9718S), IKKβ (cat. no. 9936T), p-IKKβ (cat. no. 9936T), Ikb-α (cat. no. 9936T), p-Ikb-α (cat. no. 9936T), and GAPDH (cat. no. 51332S) were purchased from Cell Signaling Technology, USA. Antibody against Histone H3 (cat. no. RM2005) was purchased from Beijing Ray Antibody Biotech, Beijing, China. Antibody against OXCT1 (cat. no. NBP1-82462) was purchased from Novus Biologicals, USA. Annexin V-APC and propidium iodide (PI) were purchased from BioLegend, San Diego, USA.

Stable Cell Lines

ShRNAs in the PLKO-Puro lentiviral vector against OXCT1 were purchased from Sangon Biotech, Shanghai, China. The coding sequence of OXCT1 was inserted into the pLV-Bsd lentiviral vector. The main plasmid and helper plasmid were packaged into the virus using 293T cells as the host. The target cell lines were then infected using the resulting virus.

Real–Time Quantitative PCR

RNAiso Plus (TaKaRa, Kusatsu, Japan) was used to extract the total RNA of cells. In accordance with the kit's instructions (Biomake, Houston, USA), total RNA was subjected to reverse transcription to obtain cDNA. Then, we used 2× SYBR Green qPCR Master Mix (Biomake, Houston, USA) to quantify the target genes. The primer sequences of GAPDH and OXCT1 are as follows:

GAPDH: forward primer: 5′-TGCACCACCAACTGCTTAGC-3′, reverse primer: 5′- GGCATGGACTGTGGTCATGAG-3′;
OXCT1: forward primer: 5′-GAGAGGAACTTCCCCGCGAT-3′, reverse primer: 5′-TCCACATAGCCCAAAACCACC-3′.

Immunohistochemistry

Tumor specimens were fixed in 10% formalin and subsequently embedded in paraffin. Tumor sections were prepared, blocked with 5% BSA for 2 h, and incubated overnight with the primary antibody. They were subsequently incubated for 30 min with the appropriate secondary antibody. Then, the DAB developer was added for further development. Finally, the slides were counterstained with hematoxylin and eosin, and examined under a light microscope (Olympus, Japan).

Western Blot Analysis

The cells were washed twice with PBS and lysed in RIPA buffer with a proteinase inhibitor cocktail to extract total protein. Nuclear and cytoplasmic components were separated using nuclear and cytoplasmic extraction reagents (Thermo Fisher Scientific, Waltham, USA) according to the manufacturer's protocol. A total of 20 μg of protein samples was separated on 10% polyacrylamide SDS gels and transferred to polyvinylidene difluoride membranes. The target proteins were detected using western blot analysis.

Colony Formation Assay

1000 cells were seeded into six-well plates and cultured at 37°C overnight. Then, 50 nM GEM (**Supplementary Figure 1**) was added into the wells. After 12 days, the cells were fixed with 4% paraformaldehyde and then stained with 0.1% crystal violet. Finally, the colonies were counted using a light microscope (Olympus, Japan).

Apoptosis Assay

The cells were seeded into six-well plates and cultured for 24 h. Then, 50 nM GEM or/and 20 μM BAY 11-7082 were added to the culture for 72 h. Thereafter, the cells were harvested and resuspended using binding buffer. Subsequently, the cells were supplemented with Annexin V-APC and PI. The mixture was incubated at room temperature for 15 min. Finally, the percentage of apoptotic cells was detected using FACSCanto II (BD, USA). All data were analyzed with FlowJo V.10.0.

Real-Time Cell Analysis

The cell cytotoxicity assay of PDAC cells was performed using an xCELLigence Real-Time Cell Analyzer-Multiple Plate system (Roche Applied Science). This platform was used to measure the viable adhesive target cells in real-time. The cells were resuspended and plated into each well at 37°C with 5% CO_2. When the normalized cell index reached 1 (about 24 h after plating), the cells were treated with the corresponding agents. The normalized cell index was automatically recorded every 15 min until the end of 72 h (i.e. 48 h after treatment), after which, the final statistical data was recorded. Cell index data for each group were represented as the mean value from three independent wells.

CCK-8 Assay

For the CCK-8 assay, PDAC cells were plated at the density of 3000 cells/well in the 96-wells plates. After 12 h of culturing, the cells were treated with the gradient concentration of GEM (0.1, 1, 10, 100, 1000, and 10000 nM). Then, the cells treated with GEM were incubated at 37°C in an incubator supplied with 5% CO_2 for 48 h. Finally, the cell viability was determined using the CCK-8 assay (Biomake, 10μL/well). The cytotoxic activities of PDAC cells were measured under the 450 nm using an immunosorbent instrument (BioTek Synergy H1).

GSEA

The data of 161 PDAC samples were downloaded from the TCGA database and divided into two groups based on OXCT1 expression level. Pancreatic cancer tissues were subjected to GSEA on the basis of the mRNA expression level of OXCT1 using KEGG gene sets. Then, we selected significantly differentially enriched pathways in accordance with the *P* value threshold and ES. Finally, the absolute value of $P < 0.05$ was considered to represent a statistically significant difference.

In Vivo Tumorigenesis Assay

PDAC cell line MIA PaCa-2 (pLV-vector and pLV-OXCT1) was subcutaneously injected into the BALB/c nude mice. Ten days later, the mice were intraperitoneally injected with saline, GEM (50 mg/kg/week), or a combination of GEM (50 mg/kg/week) and BAY 11-7082 (5 mg/kg/3 days). Tumor sizes were examined every 2 days. The mice were sacrificed after 34 days. All procedures were approved by the Institutional Animal Care and Use Committee of Tianjin Medical University Cancer Institute and Hospital.

Statistical Analysis

GraphPad Prism 8.0.1 was used for statistical analysis. Each experiment was conducted in triplicate and conducted three or more times. Data were presented as mean from all experiments (± standard error). The Kaplan–Meier method and log-rank test were applied to determine the difference in the survival of patients

with PDAC. Single-factor analysis of variance (one-way ANOVA) was used to compare multiple groups. Two-tailed independent-sample Student's t/t′ tests was used to compare the two groups. *P* value < 0.05 was considered to be statistically significant.

RESULTS

OXCT1 Was Screened as the Key Gene Associated With GEM Resistance in PDAC

First, the data on GEM-resistant and -sensitive PDAC groups in the TCGA public database were subjected to differential gene analysis, and the results were represented using a volcano plot (**Figure 1A**). A total of 2955 up-regulated and 471 down-regulated genes with a significant *P* value and FC were identified. Up-regulated genes were marked with red plots, and down-regulated genes with blue plots. The top 100 DEGs between GEM-resistant and -sensitive PDAC groups were presented as a heatmap based on log FC and *P* values (**Figure 1B**). Then, we analyzed multiple datasets containing information on patients with PDAC and differential sensitivity to GEM in TCGA, paired PDAC tumor and normal tissues, and cell lines resistant to GEM in GEO. Finally, 18 critical genes were identified as shown using the Venn diagram in **Figure 1C**.

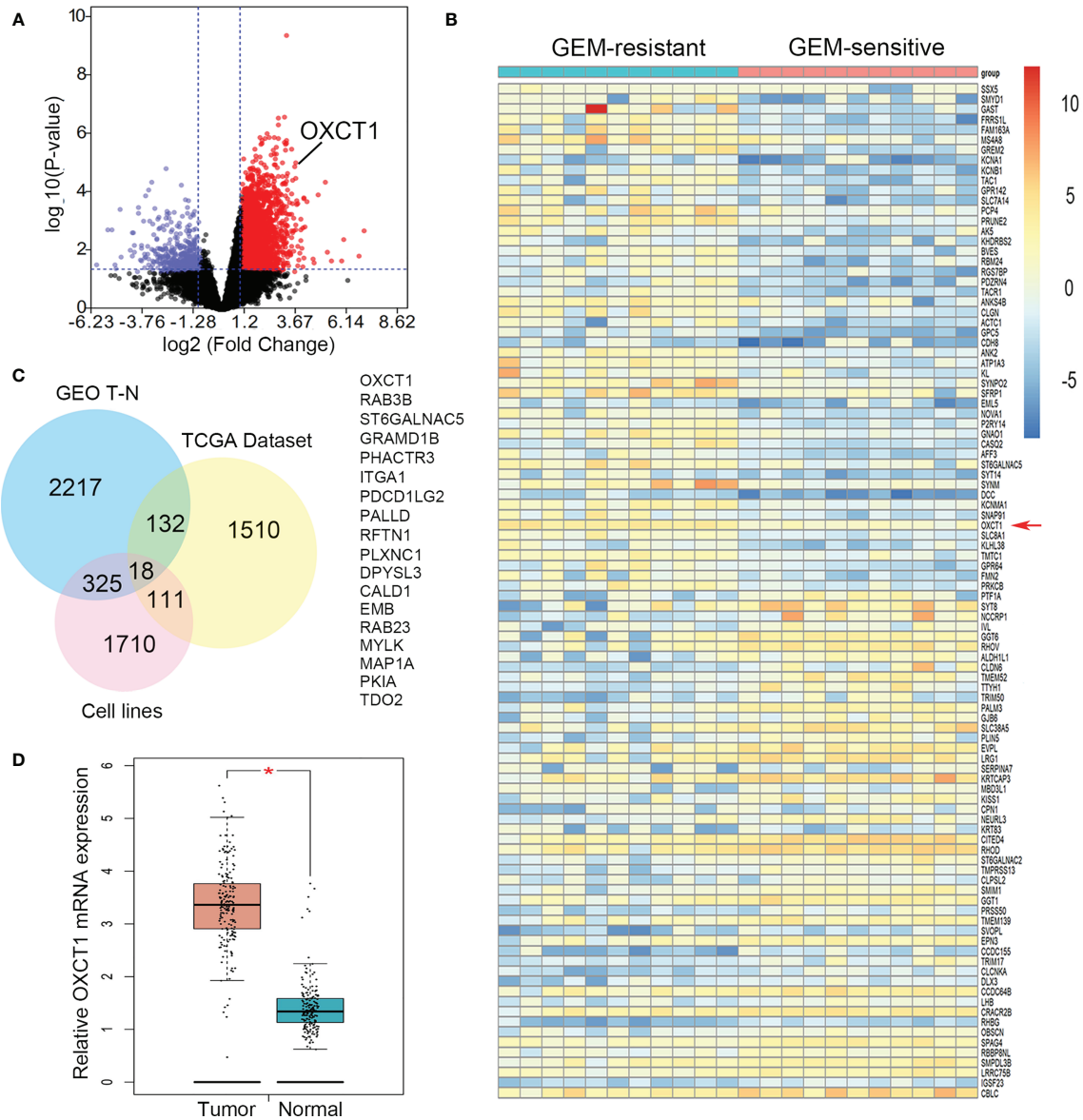

FIGURE 1 | Identification of OXCT1 through DEG analysis. **(A)** Volcano plot depicting the DEGs between GEM-resistant and -sensitive PDAC groups in the TCGA public database. **(B)** Heatmap showing the expression of the top DEGs. **(C)** Venn diagram in which OXCT1 was identified as one of the core intersections of DEGs in the GEO and TCGA datasets. **(D)** Boxplot showing the basic mRNA expression of OXCT1 in tumor and normal tissues in the combined TCGA and GTEx datasets. $^{**}P < 0.05$.

These genes included OXCT1, RAB3B, ST6GALNAC5, GRAMD1B, PHACTR3, ITGA1, PDCD1LG2, PALLD, RFTN1, PLXNC1, DPYSL3, CALD1, EMB, RAB23, MYLK, MAP1A, PKIA, and TDO2 (**Figure 1C**). Moreover, OXCT1 was identified as a valuable and critical gene on the basis of the combined summary rank of *P* values and log FC. Next, we selected all PDAC samples in the TCGA database and normal tissues in the GTEx database as the validated datasets for further validating differential mRNA levels between tumor and normal tissues. The mRNA expression of OXCT1 in tumor tissues was found to be significantly higher than that in normal tissues (**Figure 1D**).

OXCT1 Was Highly Expressed in PDAC

We performed western blot analysis to verify the expression level of OXCT1 in PDAC and transformed epithelial cell lines, primary tumor tissues, and paired adjacent normal pancreatic tissues. The protein level of OXCT1 in the other six pancreatic cancer cell lines, except for the BxPC-3 cell line, was found to be higher than that in 293T and HPDE6C7 cell lines (**Figure 2A**). Despite interindividual variations, we found that the expression of OXCT1 was significantly higher in cancer tissues than in para-cancerous tissues (**Figure 2B**).

OXCT1 Was Inversely Associated With RFS in Patients With PDAC Subjected to GEM Treatment

OXCT1 immunohistochemical staining was conducted on the surgical tissue samples of 195 patients with PDAC. The tissue samples were divided into two groups (low and high) based on their H-score (**Figure 2C**). Besides, we divided the patients into GEM-untreated and -treated groups based on the treatment

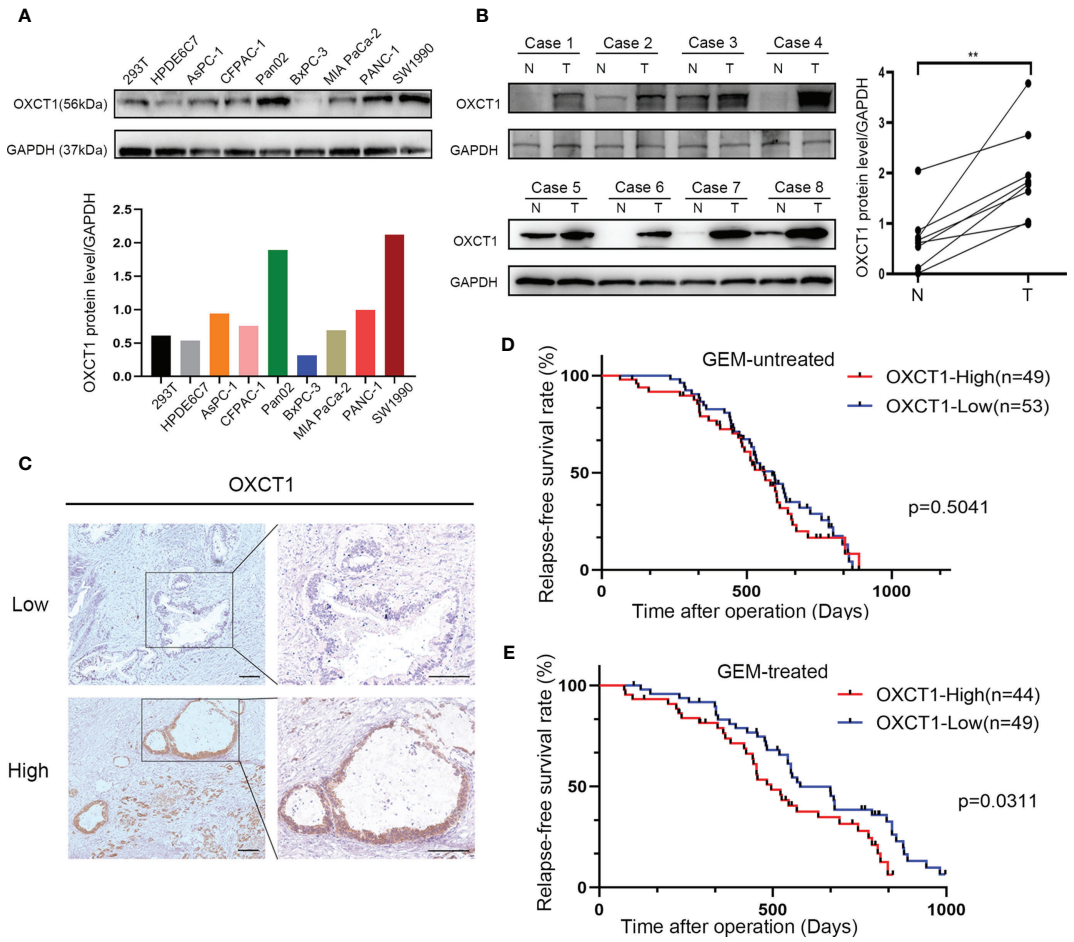

FIGURE 2 | High OXCT1 expression in patients with PDAC treated with GEM predicted poor RFS. **(A)** Basal expression levels of OXCT1 in seven classical pancreatic cancer cell lines, a human pancreatic ductal epithelial cell line (HPDE6C7), and 293T cell line were analyzed through western blot analysis. OXCT1/GAPDH protein expression level is depicted in the histogram. **(B)** Western blot analysis of OXCT1 levels in eight paired PDAC tumorous and adjacent normal pancreatic tissues (T, tumor tissues; N, normal tissues). The corresponding statistics are presented in the line chart. **(C)** Immunohistochemical analysis of OXCT1 protein expression in PDAC specimens. **(D)** Association between tumor OXCT1 expression levels and RFS in 102 patients with PDAC who were not treated with GEM ($P = 0.5041$ based on log-rank test). **(E)** Association between specimen OXCT1 expression levels and RFS in 93 patients with PDAC who were treated with GEM ($P = 0.0311$ based on log-rank test). $^{**}P < 0.01$.

modality. To determine the pathologic significance of OXCT1 expression regarding PDAC progression in GEM-treated group, we evaluated the correlation between OXCT1 expression and established PDAC prognostic factors (**Table 1**). We found that OXCT1 expression was positively correlated with lymph node metastasis and vessel invasion in PDAC specimens (**Table 1**). According to Kaplan–Meier analysis, the RFS of the two groups exhibited significant differences among 93 patients treated with GEM, whereas no significant difference was observed among 102 patients who were not treated with GEM (**Figures 2D, E**). In the GEM-treated group, the patients whose tumors expressed high level of OXCT1 exhibited a significantly shorter RFS than those whose tumors expressed no or low level of OXCT1 (median RFS: 495 days versus 579 days, P=0.0311). To elucidate the role of OXCT1 in PDAC progression, we also performed univariate and multivariate analyses of clinical follow-up data for our cohort of PDAC patients (**Table 2**). Consistently, OXCT1 expression was found to be negatively correlated with RFS in both analyses, that is, overexpressed OXCT1 predicted shorter RFS, supporting that OXCT1 could be used as a molecular marker to predict the survival prognosis of PDAC.

TABLE 1 | Correlation of OXCT1 expression to clinicopathologic features in PDAC.

Parameters	OXCT1(*n*)		χ^2	*P*
	Low	High		
Age, years			0.571	0.450
<60	24	25		
≥60	25	19		
Gender			0.610	0.435
Male	24	18		
Female	25	26		
Histologic grade			2.444	0.118
G1,G2	28	18		
G3	21	26		
Tumor size			2.521	0.112
T1	27	17		
T2	22	27		
LN metastasis			3.915	**0.048**[a]
N0	29	17		
N1	20	27		
Vessel invasion			5.631	**0.018**[a]
M0	31	17		
M1	18	27		

Statistical data on OXCT1 expression in relation to clinicohistopathologic features for surgical PDAC specimens. P values were calculated using the χ^2 test.
LN, lymph node.
[a]*Statistically significant (P < 0.05).*

Changes in OXCT1 Expression Level Affected GEM Resistance Capability of PDAC

We first constructed stable cell lines to detect GEM resistance capability of PDAC cells on the basis of the basic expression level of OXCT1. We transfected pLV-OXCT1 lentivirus into BxPC-3 and MIA PaCa-2 cell lines to increase OXCT1 expression and constructed sequence-specific shRNA target OXCT1 to silence the expression of OXCT1 in the MIA PaCa-2 and SW1990 cell lines. The expression levels of OXCT1 protein and mRNA in the pLV-OXCT1 group were significantly higher than those in the pLV-vector group. Correspondingly, the expression levels of OXCT1 protein and mRNA in the shRNA-OXCT1 group were significantly lower than those in the scramble group (**Figures 3A, B**). Antiapoptosis is one of the main mechanisms of GEM resistance. First, to investigate a suitable GEM concentration for the following experiments, we observed the GEM cytotoxic effect in 3 PDAC cell lines, including BxPC-3, MIA PaCa-2, SW1990 cells (**Supplementary Figure 1**). Based on the 3 PDAC cells' IC50 value, we confirmed that 50 nM was the most suitable concentration for cell lines treatment. Next, we assessed the cytotoxic potential of GEM (50 nM) using real-time cell index (xCELLigence) measurements. In contrast to OXCT1 silencing, OXCT1 overexpression could significantly improve the capability of PDAC to tolerate GEM cytotoxicity (**Figure 3C**). Additionally, under GEM treatment (50 nM), OXCT1-overexpressing cells formed more colonies than OXCT1-silenced cells (**Figure 3D**). Moreover, apoptosis flow cytometry assays suggested that the upregulation of OXCT1 decreased the apoptosis rate of PDAC cells induced by GEM (50 nM). However, the downregulation of OXCT1 showed the opposite effect (**Figure 3E**). Overall, our data suggested that OXCT1 could significantly improve the resistance of PDAC cells to GEM.

Further, we confirmed the effect of OXCT1-induced chemoresistance of GEM. Cleaved-caspase3 and γ-H2AX were

TABLE 2 | Univariate and multivariate analysis of clinicopathologic factors for RFS.

Characteristics	Univariate Cox			Multivariate Cox		
	Hazard ratio	95% CI	*P*	Hazard ratio	95% CI	*P*
Age (<60 vs. ≥60)	0.785	(0.491, 1.254)	0.311			
Gender (Male vs. Female)	0.979	(0.608, 1.575)	0.929			
Tumor size (T1 vs. T2)	1.491	(0.926, 2.401)	0.100			
Histologic grade (G1,2 vs. G3)	1.662	(1.034, 2.670)	**0.036**[a]	1.653	(1.028, 2.659)	**0.038**[a]
LN metastasis (N0 vs. N1)	1.435	(0.895, 2.300)	0.133			
Vessel invasion (No vs. Yes)	1.081	(0.674, 1.734)	0.746			
OXCT1(Low vs. High)	1.711	(1.043, 2.807)	**0.034**[a]	1.703	(1.035, 2.802)	**0.036**[a]

Univariate analysis: log rank; multivariate Cox proportional hazards analysis.
LN, lymph node.
[a]*Statistically significant (P < 0.05).*

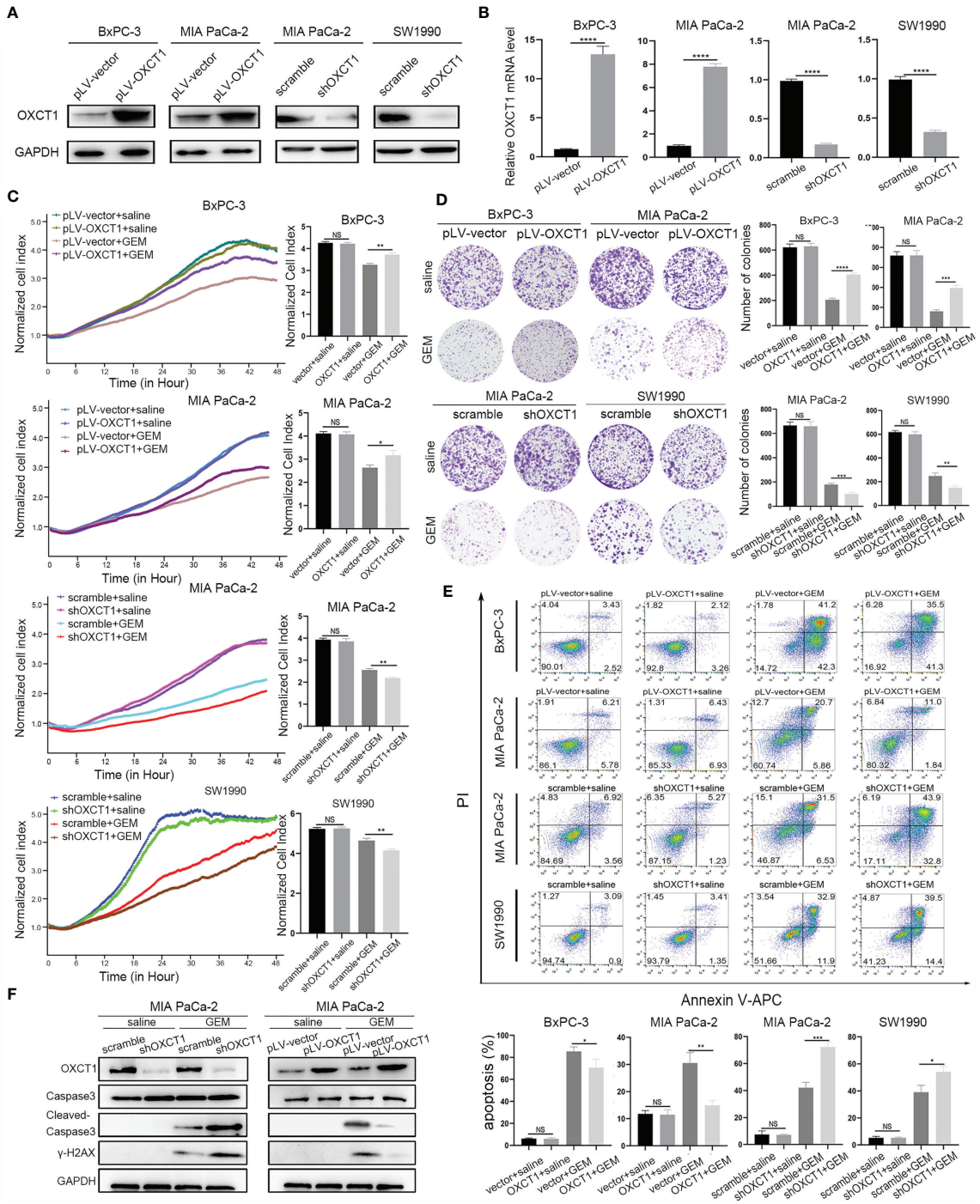

FIGURE 3 | Effect of OXCT1 on GEM resistance in PDAC cells. **(A)** Western blot analysis of proteins extracted from the two OXCT1-overexpressing stable cell lines (BxPC-3 and MIA PaCa-2) and two OXCT1-knockdown cell lines (MIA PaCa-2 and SW1990). **(B)** Real–time quantitative PCR analysis of OXCT1 expression levels in PDAC stable cell line included in **(A)**. **(C)** OXCT1-overexpressing stable cell lines (BxPC-3 and MIA PaCa-2) and OXCT1-knockdown cell lines (MIA PaCa-2 and SW1990) were treated with either 50 nM GEM or saline before conducting the cytotoxicity assay. Real-time cell index measurements (xCELLigence) of the live target cells cultured with GEM or saline are shown in **(C)**. The corresponding 72 h normalized cell index is shown as the histogram**. (D)** Representative images and quantification using the colony formation assay of the indicated cell lines that were treated for 72 h with GEM or saline. **(E)** Flow cytometry was performed to measure the apoptosis rates of the indicated cell lines treated with 50 nM GEM or saline for 72 h The corresponding statistics are presented in the histogram. **(F)** Detection of cleaved-caspas3 and γ-H2AX in OXCT1 overexpression and knockdown MIA PaCa-2 cell lines. The data are expressed as mean ± SEM from three independent experiments. *$P < 0.05$; **$P < 0.01$; ***$P < 0.001$; ****$P < 0.0001$ (one-way ANOVA). NS, not significant.

tested using western blot analysis (**Figure 3F**). Compared with the control group, cleaved-caspase3 expression was found to be increased in the sh-OXCT1 group, and decreased in the pLV-OXCT1 group when treated with 50 nM GEM. Similarly, γ-H2AX expression exhibited the same trend. These results reflect that OXCT1 overexpression increases the PDAC cells' refractory capability to DNA damaging effect induced by GEM and OXCT1 knockdown enhances the PDAC cells' sensitivity to this chemotherapy.

OXCT1 Induced GEM Resistance Through NF-κB Signaling Pathway

We validated the phenotype of OXCT1 through the above experiments. GSEA was conducted on the basis of PDAC samples in the TCGA database to identify the concrete downstream mechanism of OXCT1's phenotypic effect. We found that the NF-κB signaling pathway was remarkably positively correlated with OXCT1 expression with a statistically significant *P* value and fold change ($P<0.05$, FDR<0.25) in accordance with the mRNA expression of OXCT1 (**Figure 4A**). To determine the key role of the NF-κB signaling pathway in the OXCT1-induced chemoresistance, we tested the expression of IKKβ, Ikb-α, and P65 and their phosphorylation levels in the NF-κB signaling pathway. As is shown in the western blot analysis (**Figure 4B** and **Supplementary Figure 3**), upregulation of OXCT1 led to an increase in the phosphorylation levels of IKKβ, Ikb-α, and P65. Conversely, the knockdown of OXCT1 decreased the levels of phosphorylation of IKKβ, Ikb-α, and P65. The above results indicate that OXCT1 promotes the activation of the NF-κB signaling pathway. Besides, in this study, NF-κB activation was caused by OXCT1 upregulation, and not by GEM action. We also examined the nuclear localization of P65 protein by subjecting fractionated proteins from PDAC cell lines with or without OXCT1 overexpression to western blot analysis to validate GSEA results. The levels of the activated nuclear-form p-P65 were significantly higher in pLV-OXCT1 cells than in pLV-vector cells (**Figure 4C**). BAY 11-7082, an inhibitor of the NF-κB signaling pathway, was used to explore the effects of NF-κB inhibition in the OXCT1-mediated GEM refractoriness. First, we utilized BAY 11-7082 individually to treat BxPC-3 and MIA PaCa-2 cell lines. After 48 h of treatment, we did not observe any difference between the vector and OXCT1-overexpression groups (**Supplementary Figure 4**). Next, as shown in **Figures 4D–F**, we conducted real-time cell cytotoxicity, colony, and apoptosis assays with GEM and/or BAY 11-7082 to further validate whether OXCT1 induced chemotherapy resistance in PDAC is *via* the NF-κB signaling pathway. Remarkably, the effect induced by OXCT1 could be mostly abrogated by BAY 11-7082, indicating that the induction of GEM resistance by OXCT1 was dependent on the NF-κB signaling pathway.

Targeting NF-κB Signaling Pathway Reversed OXCT1-Induced PDAC Resistance to GEM in the Mouse Model

Given that OXCT1 plays an important role in PDAC resistance to GEM *via* the NF-κB signaling pathway, NF-κB targeted therapy may contribute to the effect of chemotherapy on PDAC with high OXCT1 expression. Therefore, subcutaneous mouse xenograft models were used to assess whether the NF-κB signaling pathway inhibitor could enhance the chemotherapy effect upon OXCT1 overexpression. MIA PaCa-2-vector cells and MIA PaCa2-OXCT1 cells were injected into nude mice. BAY 11-7082 was used to block NF-κB pathway in tumor cells. The mice were treated with saline, GEM, or a combination of GEM and BAY 11-7082 to compare the efficacy of GEM with or without targeted NF-κB therapy in MIA PaCa2-vector and MIA PaCa-2-OXCT1 tumors. Compared with that under GEM monotherapy, tumor growth in MIA PaCa-2-OXCT1 tumors was significantly inhibited under GEM + BAY 11-7082 therapy. However, no significant difference was observed in the GEM + BAY 11-7082 group (**Figures 5A, B**). Furthermore, tumor weight demonstrated the same effect (**Figure 5C**). Our data suggest that targeting the NF-κB signaling pathway might be a potential treatment strategy for inhibiting OXCT1-induced PDAC resistance to GEM. Moreover, NF-κB targeted therapy, as a complement to GEM chemotherapy, might offer an alternate option for treating PDAC with high OXCT1 levels.

DISCUSSION

GEM has been used as the front-line treatment option for PDAC for nearly 24 years (25) despite its extremely limited effects on the survival of patients. The new first-line treatment options including GEM+nab-paclitaxel and FOLFIRINOX (5-FU, leucovorin, irinotecan, and oxaliplatin) have been established during the last few years (13, 16, 26, 27). However, the side effects of FOLFIRINOX limit their effectiveness (28, 29). Therefore, GEM remains an important chemotherapeutic agent in PDAC therapy. PDAC is the most malignant tumor with limited therapeutic options for patients who often present resistance to GEM (15, 30). Therefore, finding an efficient therapeutic target to inhibit GEM resistance remains a great challenge, but it is essential to improve the survival of patients. Elucidating the molecular mechanisms underlying the chemoresistance to GEM is extremely valuable.

In this study, we used public databases to analyze PDAC chemoresistance, and then, selected the screened intersection gene OXCT1 as the target for inhibiting PDAC resistance to GEM. Ketolysis is an avenue for cells to obtain energy when hungry or stressed (31). OXCT1 is a key enzyme in ketone body metabolism that catalyzes the first and rate-determining step of ketolysis (12, 24, 32–34). It promotes ketone metabolism, thereby increasing ATP production.

PDAC tumor tissue fibrosis is a serious complication, and the tumor microenvironment of PDAC is characterized by the lack of oxygen and blood supply, which further promotes malnutrition (19, 35–37). Therefore, in PDAC, the metabolic model may change to a certain extent, and ketolysis is enhanced (35, 38, 39). In 2016, De Huang et al. found that OXCT1 is activated in liver cancer cells and facilitates ketone body utilization as an energy source for cell survival and growth under malnutrition (23). Their findings provided a new method for treating patients with HCC through regulating

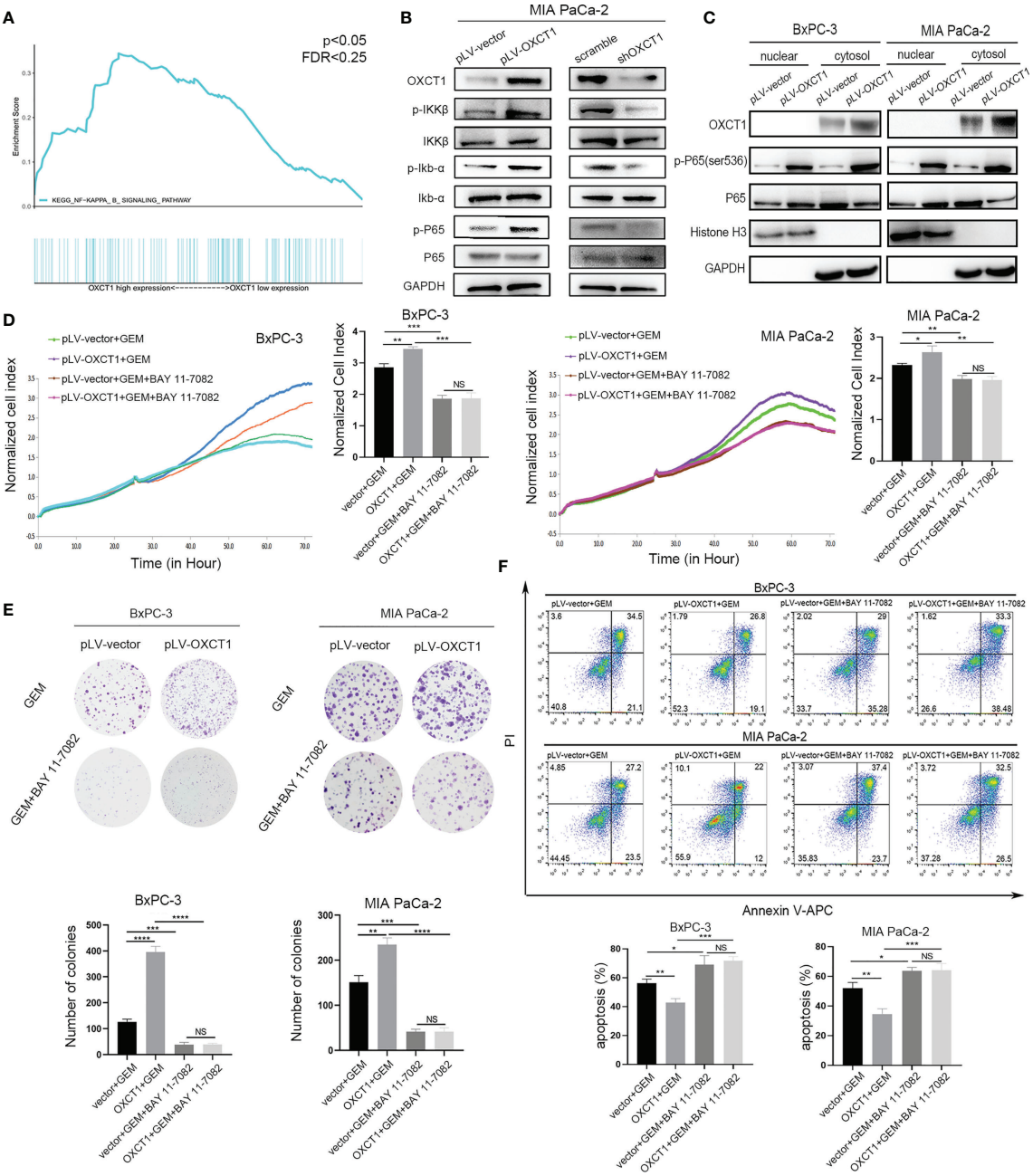

FIGURE 4 | OXCT1 promoted GEM resistance through the NF-κB signaling pathway. **(A)** The TCGA dataset was subjected to GSEA on the basis of OXCT1 expression. **(B)** The expression levels of p-IKKβ, p-Ikb-α, and p-P65 in MIA PaCa-2 cell lines with OXCT1 overexpression and knockdown were detected using western blot analysis. **(C)** Western blot analysis of the fractionated BxPC-3 and MIA PaCa-2 cells stably transfected with the empty vector or OXCT1. **(D–F)** BxPC-3 and MIA PaCa-2 cell lines with or without OXCT1 overexpression were treated with GEM or the combination of GEM and BAY 11-7082. Cell cytotoxicity was analyzed using RTCA **(D)**. Cell cloning capability was analyzed using the colony formation assay **(E)**. Apoptosis was detected *via* flow cytometry **(F)**. The data are expressed as mean ± SEM from three independent experiments. *$P < 0.05$; **$P < 0.01$; ***$P < 0.001$; ****$P < 0.0001$ (one-way ANOVA). NS, not significant.

OXCT1, a key enzyme of ketolysis. Recently, Ozsvari et al. demonstrated that a ketone shuttle is present in tumors (40). They found that some cancer-associated fibroblasts can produce ketone bodies, which are then taken up and utilized by the surrounding tumor cells. These evidences (41–45) prove that OXCT1 can help drive tumor progression and metastasis, and also confirm the reliability of our screening results.

In our study, we first evaluated the association between OXCT1 expression and RFS in patients with PDAC who were treated with GEM and found a significant negative correlation between high

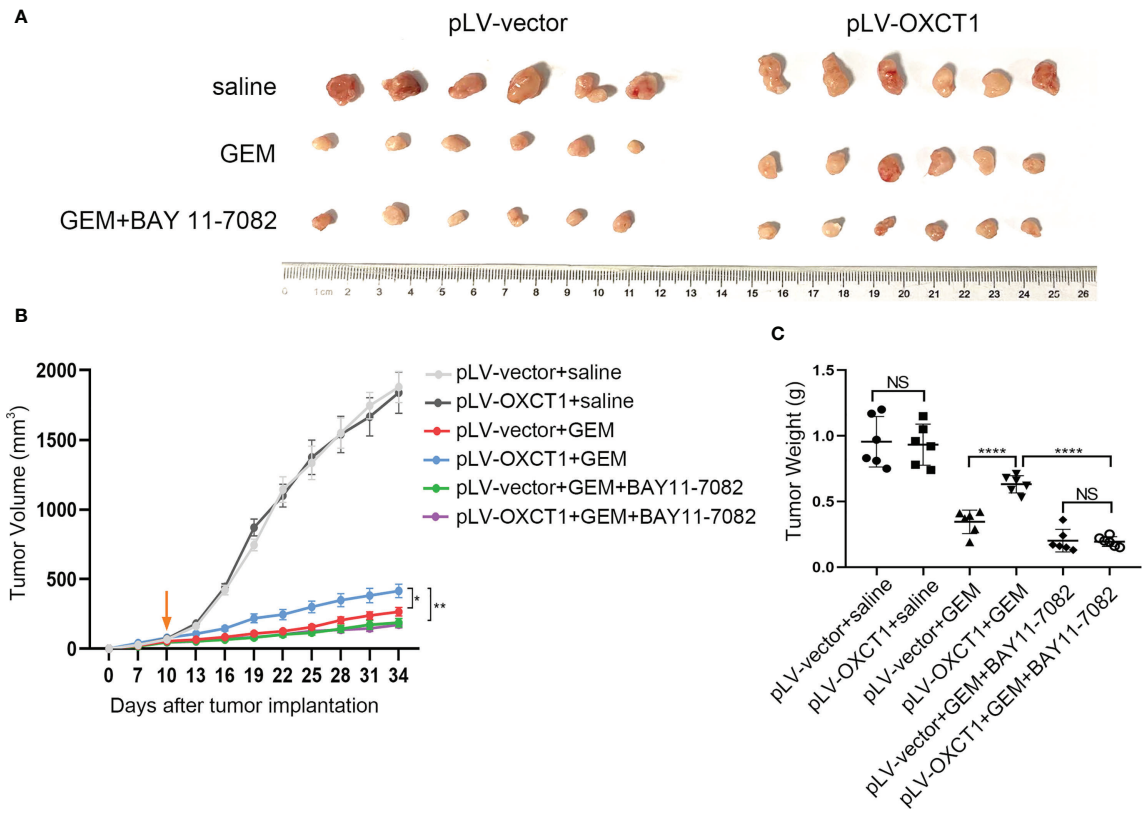

FIGURE 5 | NF-κB inhibitor reversed OXCT1-induced PDAC resistance to GEM in mouse models. **(A–C)** The indicated tumor cells were subcutaneously transplanted into the nude mouse model to develop tumors (n=6 for each group). Ten days later, the mice were treated with saline, GEM, or the combination of GEM and BAY 11-7082. Tumor volumes were measured every 3 days using the calipers. Then, the mice were sacrificed, and tumors were excised. The representative images of the tumors are depicted **(A)**. Repeated measure two-way ANOVA (time × tumor volume) analysis was performed to compare the tumor growth curve among the six groups **(B)**. Tumor weights at the end of the experiment are also shown and were analyzed **(C)**. Data are presented as mean ± SD; $^{*}P < 0.05$; $^{**}P < 0.01$; $^{****}P < 0.0001$. NS, not significant.

OXCT1 expression and the patients' RFS (**Figure 2E**). Subsequently, the validation was performed at the cell-line level *via* the overexpression and knockdown of OXCT1 in PDAC cell lines (BxPC-3, MIA PaCa-2, and SW1990). We found that GEM-treated cell lines significantly outperformed the cell line in the control group in terms of antiapoptotic effect following OXCT1 overexpression (**Figures 3C–F** and **Supplementary Figures 2A–C**). Conversely, the antiapoptotic capability of cell lines were significantly reduced after OXCT1 knockdown under the same treatment conditions. OXCT1 was identified as a bona fide metabolic oncogene, which promotes the occurrence and development of tumors in 2012 (44, 46). Our conclusion is consistent with theirs. Next, we questioned how OXCT1 caused GEM chemoresistance in PDAC cells.

Through GSEA, we discovered that the NF-κB signaling pathway was significantly positively correlated with OXCT1 expression. Therefore, we postulated that the NF-κB signaling pathway might be downstream of OXCT1 (**Figure 4A**). NF-κB is a transcription factor that is regulated by many stimuli, including chemotherapeutic drugs, hypoxia, and malnutrition, and some cytokines have recently emerged as popular targets for cancer research (47). In BxPC-3 and MIA PaCa-2 cell lines, the activated nuclear form p-P65 was found to be significantly elevated when OXCT1 was overexpressed (**Figure 4C**). Previous research revealed that when NF-κB is activated, it translocates into the nucleus where it binds to the cognate sequences in the promoter region of multiple genes that encode factors in tumor promotion and proliferation, cytokines, antiapoptotic proteins, and genes related to chemoresistance (48–50). The results of our study demonstrated that the resistance to GEM induced by OXCT1 overexpression was significantly inhibited upon blocking the NF-κB signaling pathway using an inhibitor (**Figures 4D–F**). Additionally, we reached the same conclusion through *in vivo* validation through conducting a tumor formation assay in nude mice. The above evidence suggested that OXCT1 promotes PDAC resistance to GEM *via* the NF-κB signaling pathway.

Upon validation using cell lines and mouse model (**Figure 5**) experiments, we confirmed that OXCT1 significantly promotes the resistance of PDAC cells to the cytotoxic effect of GEM *via* the NF-κB signaling pathway (**Figure 6**). Our results indicate that OXCT1 is a potential chemoresistance target and a crucial biomarker for assessing the prognosis and determining the

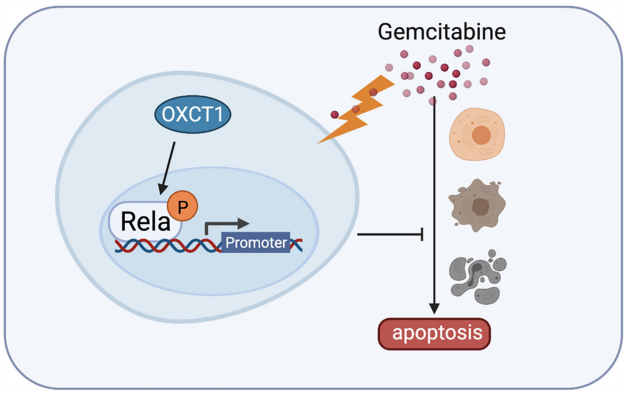

FIGURE 6 | Detailed mechanism of gemcitabine resistance in PDAC induced by OXCT1. Schematic diagram shows that OXCT1 can significantly enhance the resistance to gemcitabine by activating the NF-κB signaling pathway in PDAC cells, thereby inhibit cell apoptosis, and finally promote the occurrence and progression of PDAC.

optimal chemotherapy strategies for patients with PDAC. Through our study, we identified OXCT1 as a new research target, thereby providing a useful reference for PDAC precision therapy.

DATA AVAILABILITY STATEMENT

The datasets presented in this study can be found in online repositories. The names of the repository/repositories and accession number(s) can be found in the article/**Supplementary Material**.

ETHICS STATEMENT

The studies involving human participants were reviewed and approved by Ethics Committee of Tianjin Medical University in Tianjin Medical University Cancer Institute and Hospital. The patients/participants provided their written informed consent to participate in this study. The animal study was reviewed and approved by Ethics Committee of Tianjin Medical University in Tianjin Medical University Cancer Institute and Hospital. Written informed consent was obtained from the individual(s) for the publication of any potentially identifiable images or data included in this article.

AUTHOR CONTRIBUTIONS

JD, HL, YL, LB, HW, and CG: design and initiation of the study, quality control of data, data analysis and interpretation, and manuscript preparation and editing. YX: perform the bioinformatics data analysis. JY, HS, DX, and YZ: data acquisition. All authors contributed to the article and approved the submitted version.

FUNDING

This work was supported by the National Natural Science Foundation of China (grants 82030092, 81720108028, 82072657, 81802432, 82072716, 81802433, 82072659, 81871968, and 81871978), Key Program of Prevention and Treatment of Chronic Diseases of Tianjin (17ZXMFSY00010), the programs of Tianjin Prominent Talents, Tianjin Eminent Scholars, Tianjin Natural Science Foundation (18JCJQJC47800, 19JCJQJC63100, 19JCYBJC26200, and 20JCQNJC01330), Tianjin Postgraduate Research and Innovation Project (2019YJSB104), and Tianjin Research Innovation Project for Postgraduate Students(2019YJSB104).

ACKNOWLEDGMENTS

The authors would like to acknowledge the helpful suggestions concerning this study received from their colleagues.

SUPPLEMENTARY MATERIAL

The Supplementary Material for this article can be found online at: https://www.frontiersin.org/articles/10.3389/fonc.2021.698302/full#supplementary-material

Supplementary Figure 1 | Determination of gemcitabine IC50 in the *in vitro* study. CCK-8 (cell counting kit-8) was used to analysis IC50 of BxPC-3, MIA PaCa-2 and SW1990 cell lines. The data are expressed as mean ± SEM from three independent experiments.

Supplementary Figure 2 | OXCT1-knockdown BxPC-3 stable cell line and OXCT1-overexpressing SW1990 stable cell line construction and functional verification. **(A)** Western blot analysis of proteins extracted from OXCT1-knockdown cell line (BxPC-3) and OXCT1-overexpressing cell line (SW1990). **(B)** Representative images and quantification using the colony formation assay of the indicated cell lines that were treated for 72 h with 50 nM GEM or saline. **(C)** Flow cytometry was performed to measure the apoptosis rates of the indicated cell lines treated with 50 nM GEM or saline for 72 h. The corresponding statistics are presented in the histogram. The data are expressed as mean ± SEM from three independent experiments. $^{*}P < 0.05$; $^{**}P < 0.01$; $^{***}P < 0.001$; $^{****}P < 0.0001$ (one-way ANOVA).

Supplementary Figure 3 | Effect of OXCT1 on NF-κB signaling pathway. Western blot analysis was used to detect the expression levels of p-IKKβ, p-Ikb-α and p-P65 in OXCT1-overexpressing and OXCT1-knockdown MIA PaCa-2 cell lines treated with 50 nM gemcitabine.

Supplementary Figure 4 | Effect of NF-κB signaling pathway inhibitor BAY 11-7082 on cell lines apoptosis. **(A)** Flow cytometry was performed to measure the apoptosis rates of OXCT1-overexpressing cell lines (BxPC-3 and MIA PaCa-2) treated with 50 nM GEM or saline for 72 h. The corresponding statistics are presented in the histogram. **(B)** Flow cytometry was performed to measure the apoptosis rates of OXCT1-knockdown cell lines (SW1990 and MIA PaCa-2) treated with 50 nM GEM or saline for 72 h. The corresponding statistics are presented in the histogram. The data are expressed as the means ± SEM from three independent experiments. $^{*}P < 0.05$; $^{**}P < 0.01$; $^{***}P < 0.001$; $^{****}P < 0.0001$ (one-way ANOVA).

REFERENCES

1. Siegel R, Miller K, Fuchs H, Jemal A. Cancer Statistics, 2021. *CA: Cancer J Clin* (2021) 71(1):7–33. doi: 10.3322/caac.21654
2. Kamisawa T, Wood LD, Itoi T, Takaori K. Pancreatic Cancer. *Lancet* (2016) 388(10039):73–85. doi: 10.1016/S0140-6736(16)00141-0
3. Neoptolemos JP, Kleeff J, Michl P, Costello E, Greenhalf W, Palmer DH. Therapeutic Developments in Pancreatic Cancer: Current and Future Perspectives. *Nat Rev Gastroenterol Hepatol* (2018) 15(6):333–48. doi: 10.1038/s41575-018-0005-x
4. Henley S, Ward E, Scott S, Ma J, Anderson R, Firth A, et al. Annual Report to the Nation on the Status of Cancer, Part I: National Cancer Statistics. *Cancer* (2020) 126(10):2225–49. doi: 10.1002/cncr.32802
5. Siegel R, Miller K, Jemal A. Cancer Statistics, 2020. *CA: Cancer J Clin* (2020) 70(1):7–30. doi: 10.3322/caac.21590
6. Clancy TE. Surgery for Pancreatic Cancer. *Hematol Oncol Clin North Am* (2015) 29(4):701–16. doi: 10.1016/j.hoc.2015.04.001
7. Bramhall S, Allum W, Jones A, Allwood A, Cummins C, Neoptolemos J. Treatment and Survival in 13,560 Patients With Pancreatic Cancer, and Incidence of the Disease, in the West Midlands: An Epidemiological Study. *Br J Surg* (1995) 82(1):111–5. doi: 10.1002/bjs.1800820137
8. Stathis A, Moore MJ. Advanced Pancreatic Carcinoma: Current Treatment and Future Challenges. *Nat Rev Clin Oncol* (2010) 7(3):163–72. doi: 10.1038/nrclinonc.2009.236
9. Wolfgang CL, Herman JM, Laheru DA, Klein AP, Erdek MA, Fishman EK, et al. Recent Progress in Pancreatic Cancer. *CA Cancer J Clin* (2013) 63 (5):318–48. doi: 10.3322/caac.21190
10. He XY, Yuan YZ. Advances in Pancreatic Cancer Research: Moving Towards Early Detection. *World J Gastroenterol* (2014) 20(32):11241–8. doi: 10.3748/wjg.v20.i32.11241
11. Springfeld C, Jäger D, Büchler MW, Strobel O, Hackert T, Palmer DH, et al. Chemotherapy for Pancreatic Cancer. *Presse Med 48(3 Pt* (2019) 2):e159–74. doi: 10.1016/j.lpm.2019.02.025
12. Kokkali S, Tripodaki ES, Drizou M, Stefanou D, Magou E, Zylis D, et al. Biweekly Gemcitabine/Nab-Paclitaxel as First-Line Treatment for Advanced Pancreatic Cancer. *In Vivo* (2018) 32(3):653–7. doi: 10.21873/invivo.11289
13. Mini E, Nobili S, Caciagli B, Landini I, Mazzei T. Cellular Pharmacology of Gemcitabine. *Ann Oncol* (2006) 17 Suppl 5:v7–12. doi: 10.1093/annonc/mdj941
14. Sarvepalli D, Rashid MU, Rahman AU, Ullah W, Hussain I, Hasan B, et al. Gemcitabine: A Review of Chemoresistance in Pancreatic Cancer. *Crit Rev Oncog* (2019) 24(2):199–212. doi: 10.1615/CritRevOncog.2019031641
15. Neesse A, Michl P, Frese KK, Feig C, Cook N, Jacobetz MA, et al. Stromal Biology and Therapy in Pancreatic Cancer. *Gut* (2011) 60(6):861–8. doi: 10.1136/gut.2010.226092
16. de Sousa Cavalcante L, Monteiro G. Gemcitabine: Metabolism and Molecular Mechanisms of Action, Sensitivity and Chemoresistance in Pancreatic Cancer. *Eur J Pharmacol* (2014) 741:8–16. doi: 10.1016/j.ejphar.2014.07.041
17. Binenbaum Y, Na'ara S, Gil Z. Gemcitabine Resistance in Pancreatic Ductal Adenocarcinoma. *Drug Resist Update* (2015) 23:55–68. doi: 10.1016/j.drup.2015.10.002
18. Shukla SK, Purohit V, Mehla K, Gunda V, Chaika NV, Vernucci E, et al. MUC1 and HIF-1alpha Signaling Crosstalk Induces Anabolic Glucose Metabolism to Impart Gemcitabine Resistance to Pancreatic Cancer. *Cancer Cell* (2017) 32(1):71–87.e7. doi: 10.1016/j.ccell.2017.06.004
19. Tadros S, Shukla SK, King RJ, Gunda V, Vernucci E, Abrego J, et al. *De Novo* Lipid Synthesis Facilitates Gemcitabine Resistance Through Endoplasmic Reticulum Stress in Pancreatic Cancer. *Cancer Res* (2017) 77(20):5503–17. doi: 10.1158/0008-5472.Can-16-3062
20. Wang YP, Lei QY. Perspectives of Reprogramming Breast Cancer Metabolism. *Adv Exp Med Biol* (2017) 1026:217–32. doi: 10.1007/978-981-10-6020-5_10
21. Li X, Wenes M, Romero P, Huang SC, Fendt SM, Ho PC. Navigating Metabolic Pathways to Enhance Antitumour Immunity and Immunotherapy. *Nat Rev Clin Oncol* (2019) 16(7):425–41. doi: 10.1038/s41571-019-0203-7
22. Recalcati S, Gammella E, Cairo G. Dysregulation of Iron Metabolism in Cancer Stem Cells. *Free Radic Biol Med* (2019) 133:216–20. doi: 10.1016/j.freeradbiomed.2018.07.015
23. Huang T, Wang L, Zhang L, Yan R, Li K, Xing S, et al. Zhang: Hepatocellular Carcinoma Redirects to Ketolysis for Progression Under Nutrition Deprivation Stress. *Cell Res* (2016) 26(10):1112–30. doi: 10.1038/cr.2016.109
24. Zhang S, Xie C. The Role of OXCT1 in the Pathogenesis of Cancer as a Rate-Limiting Enzyme of Ketone Body Metabolism. *Life Sci* (2017) 183:110–5. doi: 10.1016/j.lfs.2017.07.003
25. Burris H, Moore M, Andersen J, Green M, Rothenberg M, Modiano M, et al. Improvements in Survival and Clinical Benefit With Gemcitabine as First-Line Therapy for Patients With Advanced Pancreas Cancer: A Randomized Trial. *J Clin Oncol Off J Am Soc Clin Oncol* (1997) 15(6):2403–13. doi: 10.1200/jco.1997.15.6.2403
26. Conroy T, Desseigne F, Ychou M, Bouché O, Guimbaud R, Bécouarn Y, et al. FOLFIRINOX Versus Gemcitabine for Metastatic Pancreatic Cancer. *N Engl J Med* (2011) 364(19):1817–25. doi: 10.1056/NEJMoa1011923
27. Von Hoff DD, Ervin T, Arena FP, Chiorean EG, Infante J, Moore M, et al. Increased Survival in Pancreatic Cancer With Nab-Paclitaxel Plus Gemcitabine. *N Engl J Med* (2013) 369(18):1691–703. doi: 10.1056/NEJMoa1304369
28. Hoshi N, Kofunato Y, Yashima R, Shimura T, Takenoshita S. [Treating Side Effects of FOLFIRINOX–A Study of the Effect of Hange-Shashin-To on Preventing Diarrhea]. *Gan To Kagaku Ryoho* (2015) 42(12):2364–6.
29. de Jesus VHF, Camandaroba MPG, Donadio MDS, Cabral A, Muniz TP, de Moura Leite L, et al. Retrospective Comparison of the Efficacy and the Toxicity of Standard and Modified FOLFIRINOX Regimens in Patients With Metastatic Pancreatic Adenocarcinoma. *J Gastrointest Oncol* (2018) 9 (4):694–707. doi: 10.21037/jgo.2018.04.02
30. Amrutkar M, Gladhaug I. Pancreatic Cancer Chemoresistance to Gemcitabine. *Cancers* (2017) 9(11):157. doi: 10.3390/cancers9110157
31. Fukao T, Lopaschuk GD, Mitchell GA. Pathways and Control of Ketone Body Metabolism: On the Fringe of Lipid Biochemistry. *Prostaglandins Leukot Essent Fatty Acids* (2004) 70(3):243–51. doi: 10.1016/j.plefa.2003.11.001
32. Fukao T, Ishii T, Amano N, Kursula P, Takayanagi M, Murase K, et al. A Neonatal-Onset Succinyl-CoA:3-Ketoacid CoA Transferase (SCOT)-Deficient Patient With T435N and C.658-666dupaacgtgatt P.N220_I222dup Mutations in the OXCT1 Gene. *J Inherit Metab Dis* (2010) 33 Suppl:3, S307–13. doi: 10.1007/s10545-010-9168-5
33. Cotter DG, Ercal B, d'Avignon DA, Dietzen DJ, Crawford PA. Impact of Peripheral Ketolytic Deficiency on Hepatic Ketogenesis and Gluconeogenesis During the Transition to Birth. *J Biol Chem* (2013) 288(27):19739–49. doi: 10.1074/jbc.M113.454868
34. Zeng J, Zhou SW, Zhao J, Jin MH, Kang DJ, Yang YX, et al. Role of OXCT1 in Ovine Adipose and Preadipocyte Differentiation. *Biochem Biophys Res Commun* (2019) 512(4):779–85. doi: 10.1016/j.bbrc.2019.03.128
35. Locasale JW. Serine, Glycine and One-Carbon Units: Cancer Metabolism in Full Circle. *Nat Rev Cancer* (2013) 13(8):572–83. doi: 10.1038/nrc3557
36. Tandon M, Coudriet GM, Criscimanna A, Socorro M, Eliliwi M, Singhi AD, et al. Prolactin Promotes Fibrosis and Pancreatic Cancer Progression. *Cancer Res* (2019) 79(20):5316–27. doi: 10.1158/0008-5472.Can-18-3064
37. Thomas D, Radhakrishnan P. Tumor-Stromal Crosstalk in Pancreatic Cancer and Tissue Fibrosis. *Mol Cancer* (2019) 18(1):14. doi: 10.1186/s12943-018-0927-5
38. Peiris-Pagès M, Martinez-Outschoorn UE, Pestell RG, Sotgia F, Lisanti MP. Cancer Stem Cell Metabolism. *Breast Cancer Res* (2016) 18(1):55. doi: 10.1186/s13058-016-0712-6
39. Martinez-Outschoorn UE, Peiris-Pagés M, Pestell RG, Sotgia F, Lisanti MP. Cancer Metabolism: A Therapeutic Perspective. *Nat Rev Clin Oncol* (2017) 14 (1):11–31. doi: 10.1038/nrclinonc.2016.60
40. Ozsvari B, Sotgia F, Simmons K, Trowbridge R, Foster R, Lisanti MP. Mitoketoscins: Novel Mitochondrial Inhibitors for Targeting Ketone Metabolism in Cancer Stem Cells (CSCs). *Oncotarget* (2017) 8(45):78340–50. doi: 10.18632/oncotarget.21259
41. Mitchell GA, Kassovska-Bratinova S, Boukaftane Y, Robert MF, Wang SP, Ashmarina L, et al. Medical Aspects of Ketone Body Metabolism. *Clin Invest Med* (1995) 18(3):193–216.
42. Capparelli C, Guido C, Whitaker-Menezes D, Bonuccelli G, Balliet R, Pestell TG, et al. Autophagy and Senescence in Cancer-Associated Fibroblasts Metabolically Supports Tumor Growth and Metastasis *via* Glycolysis and Ketone Production. *Cell Cycle* (2012) 11(12):2285–302. doi: 10.4161/cc.20718

43. Martinez-Outschoorn UE, Lin Z, Whitaker-Menezes D, Howell A, Lisanti MP, Sotgia F. Ketone Bodies and Two-Compartment Tumor Metabolism: Stromal Ketone Production Fuels Mitochondrial Biogenesis in Epithelial Cancer Cells. *Cell Cycle* (2012) 11(21):3956–63. doi: 10.4161/cc.22136
44. Martinez-Outschoorn UE, Lin Z, Whitaker-Menezes D, Howell A, Sotgia F, Lisanti MP. Ketone Body Utilization Drives Tumor Growth and Metastasis. *Cell Cycle* (2012) 11(21):3964–71. doi: 10.4161/cc.22137
45. Puchalska P, Crawford PA. Multi-Dimensional Roles of Ketone Bodies in Fuel Metabolism, Signaling, and Therapeutics. *Cell Metab* (2017) 25(2):262–84. doi: 10.1016/j.cmet.2016.12.022
46. Martinez-Outschoorn UE, Prisco M, Ertel A, Tsirigos A, Lin Z, Pavlides S, et al. Ketones and Lactate Increase Cancer Cell "Stemness," Driving Recurrence, Metastasis and Poor Clinical Outcome in Breast Cancer: Achieving Personalized Medicine *via* Metabolo-Genomics. *Cell Cycle* (2011) 10(8):1271–86. doi: 10.4161/cc.10.8.15330
47. Bentires-Alj M, Barbu V, Fillet M, Chariot A, Relic B, Jacobs N, et al. NF-kappaB Transcription Factor Induces Drug Resistance Through MDR1 Expression in Cancer Cells. *Oncogene* (2003) 22(1):90–7. doi: 10.1038/sj.onc.1206056
48. Xiong HQ, Abbruzzese JL, Lin E, Wang L, Zheng L, Xie K. NF-kappaB Activity Blockade Impairs the Angiogenic Potential of Human Pancreatic Cancer Cells. *Int J Cancer* (2004) 108(2):181–8. doi: 10.1002/ijc.11562
49. Pan X, Arumugam T, Yamamoto T, Levin PA, Ramachandran V, Ji B, et al. Nuclear factor-kappaB P65/relA Silencing Induces Apoptosis and Increases Gemcitabine Effectiveness in a Subset of Pancreatic Cancer Cells. *Clin Cancer Res* (2008) 14(24):8143–51. doi: 10.1158/1078-0432.Ccr-08-1539
50. Kong R, Sun B, Jiang H, Pan S, Chen H, Wang S, et al. Downregulation of Nuclear factor-kappaB P65 Subunit by Small Interfering RNA Synergizes With Gemcitabine to Inhibit the Growth of Pancreatic Cancer. *Cancer Lett* (2010) 291(1):90–8. doi: 10.1016/j.canlet.2009.10.001

Conflict of Interest: The authors declare that the research was conducted in the absence of any commercial or financial relationships that could be construed as a potential conflict of interest.

Publisher's Note: All claims expressed in this article are solely those of the authors and do not necessarily represent those of their affiliated organizations, or those of the publisher, the editors and the reviewers. Any product that may be evaluated in this article, or claim that may be made by its manufacturer, is not guaranteed or endorsed by the publisher.

frontiers in Oncology

ORIGINAL RESEARCH
published: 17 November 2021
doi: 10.3389/fonc.2021.758062

Prediction of Pancreatic Neuroendocrine Tumor Grading Risk Based on Quantitative Radiomic Analysis of MR

Wei Li[1], *Chao Xu*[2] *and Zhaoxiang Ye*[1]*

[1] *Department of Radiology, Tianjin Medical University Cancer Institute and Hospital, National Clinical Research Center for Cancer, Key Laboratory of Cancer Prevention and Therapy, Tianjin's Clinical Research Center for Cancer, Tianjin, China,* [2] *Department of Pancreatic Cancer, Tianjin Medical University Cancer Institute and Hospital, National Clinical Research Center for Cancer, Key Laboratory of Cancer Prevention and Therapy, Tianjin's Clinical Research Center for Cancer, Tianjin, China*

OPEN ACCESS

Edited by:
Kuirong Jiang,
Nanjing Medical University, China

Reviewed by:
Andrea Liostti,
Local Health Authority of Imola, Italy
Stefano Francesco Crinò,
University of Verona, Italy

****Correspondence:***
Zhaoxiang Ye
yezhaoxiang@163.com

Specialty section:
This article was submitted to Gastrointestinal Cancers: Hepato Pancreatic Biliary Cancers, a section of the journal Frontiers in Oncology

Received: *13 August 2021*
Accepted: *26 October 2021*
Published: *17 November 2021*

Citation:
Li W, Xu C and Ye Z (2021) Prediction of Pancreatic Neuroendocrine Tumor Grading Risk Based on Quantitative Radiomic Analysis of MR. Front. Oncol. 11:758062. doi: 10.3389/fonc.2021.758062

Background: Pancreatic neuroendocrine tumors (PNETs) grade is very important for treatment strategy of PNETs. The present study aimed to find the quantitative radiomic features for predicting grades of PNETs in MR images.

Materials and Methods: Totally 48 patients but 51 lesions with a pathological tumor grade were subdivided into low grade (G1) group and intermediate grade (G2) group. The ROI was manually segmented slice by slice in 3D-T1 weighted sequence with and without enhancement. Statistical differences of radiomic features between G1 and G2 groups were analyzed using the independent sample *t*-test. Logistic regression analysis was conducted to find better predictors in distinguishing G1 and G2 groups. Finally, receiver operating characteristic (ROC) was constructed to assess diagnostic performance of each model.

Results: No significant difference between G1 and G2 groups ($P > 0.05$) in non-enhanced 3D-T1 images was found. Significant differences in the arterial phase analysis between the G1 and the G2 groups appeared as follows: the maximum intensity feature ($P = 0.021$); the range feature ($P = 0.039$). Multiple logistic regression analysis based on univariable model showed the maximum intensity feature (P=0.023, OR = 0.621, 95% CI: 0.433–0.858) was an independent predictor of G1 compared with G2 group, and the area under the curve (AUC) was 0.695.

Conclusions: The maximum intensity feature of radiomic features in MR images can help to predict PNETs grade risk.

Keywords: grade risk, radiomic features, MR, prediction, PNETs

INTRODUCTION

Pancreatic neuroendocrine tumors (PNETs), as the second most common epithelial neoplasm of the pancreas (1, 2), have increased significantly over the last decade (3). Based on histological differentiation (including mitoses and Ki-67 proliferation index), the WHO 2017 classification (4) has separated well-differentiated PNETs into three groups: low grade (G1), intermediate grade (G2), and high grade (G3). PNETs often cause severe morbidity due to excessive secretion of hormones (such as serotonin) and/or overall tumor mass, but in the clinic, lack of specific biomarkers inhibits early diagnosis (5). It was reported (6) that the PNETs grading was useful for therapeutic decisions and had a great impact on survival for PNETs (7). According to the different grades risk of PNETs, surgical resection or medical therapies should be performed for different patients (2). As the biological behavior of PNETs is relatively variable, pretreatment predictive aggressiveness of individual tumors is therefore very important in determining an efficient treatment strategy for patients to minimize harm from possible over- or undertreatment, especially for those with more advanced disease that cannot be resected (8).

MR imaging methods may help define the more appropriate treatment strategy for PNETs in a non-invasive way (2). In fact, previous studies have identified several traditional MR imaging features that could be potentially valuable for discrimination of tumor grades in PNETs (9–14), such as tumor sizes (15), irregular margins, and enhancement pattern (9, 16, 17); moreover, some authors reported that diffusion weighted imaging (DWI) in MR imaging might have the capability of roughly distinguishing high-grade PNETs from G1 tumors (16, 18–25).

However, now, except for these traditional MR features, especially in DWI that suggested the discrimination of tumor grades in PNETs, there are still no generally accepted quantitative guidelines to predict the PNETs grading. Radiomic analysis, as a more systematic approach, may provide more quantitative information regarding the discrimination of different biological behavior of PNETs (26), as it is able to identify voxel-level changes within PNETs. Several studies had focused on predictors of PNETs grades based on radiomic analysis just only in CT imaging (27, 28). There were few studies that focused on MR imaging based on radiomic analysis. Thus, our study presents the hypothesis that there may be some radiomic features in MR that can help to predict grades of PNETs. The present study aims to find the quantitative radiomic features for predicting grades of PNETs in MR images with pathological diagnoses using radiomic analysis.

MATERIALS AND METHODS

MRI Examinations

All the MR examinations were performed using a 1.5T GE MRI scanner (SignaExcite HD, GE Healthcare, Milwaukee, WI, USA) equipped with eight channel phased-array coils, and the scanning parameters were as follows: T2-weighted MR images with respiratory-triggered fat-saturated fast spin-echo sequences for identifying the lesion's location [TR/TE =7,500/86 ms; slice thickness = 7 mm; space gap = 1 mm; field of view (FOV) = 40×34 cm; matrix = 128 × 128 or 320×160]. An axial breath-hold T1-weighted 3D fat suppressed spoiled gradient-echo (GRE) sequence (liver acquisition with volume acceleration, LAVA) before contrast agent injection was used for dynamic contrast-enhanced imaging (TR/TE = 6.2/3.1 ms; flipangle = 12; FOV = 315×360; matrix = 256×256; section thickness = 4 mm). Contrast images were acquired during the arterial (20 s delay), portal venous (60 s delay), and equilibrium phases (180 s delay), and the contrast agent was applied with a bolus injection of 0.1 mmol/kg body weight of gadopentetate dimeglumine (Magnevist, Bayer Schering, Berlin, Germany).

Delineation of ROI

The ROI in the present study was manually delineated and segmented on the MR images. The lesions were manually delineated and segmented slice by slice on the non-enhanced and the enhancement T1 images for ROIs of the radiomic analysis.

Finally, the seed ROIs were checked in each lesion of each patient by another radiologist to ensure that the ROI in each patient satisfied the lesion boundary definition.

Computerized Radiomic Analysis Based on the ROI

The radiomic analysis was performed using the 3D slicer software (Version 4.6.2; Surgical Planning Laboratory, Brigham and Women's Hospital, Harvard Medical School, Boston, MA, USA) (http://www.slicer.org) (29). Then, the radiomic features were calculated and extracted automatically using the module called "Heterogeneity CAD". The radiomic features (a total of 44 features, shown in **Table S1** of the **Supplementary Materials**) were divided into three categories, including the following (1): first-order and distribution statistics (2), shape and morphology metrics (3), the gray-level co-occurrence matrix (GLCM).

The overall procedure of this analytical scheme was performed by two radiologists (with 9 and 6 years' experience in abdominal MR imaging, respectively). Finally, we computed the means of each of the MR radiomic feature values measured by the two independent observers. The interobserver agreement regarding the radiomic features of the ROIs was calculated using the interclass correlation coefficient analysis (ICC) using the SPSS software.

Radiomic Statistical Analysis

All statistical analyses were conducted with the Statistical Package for the Social Sciences version 19.0 (IBM Corp. IBM SPSS Statistics for Windows). Interobserver agreement was assessed using the interclass correlation coefficient analysis (ICC). ICC value of ≤0.4 indicated poor agreement; 0.41–0.6, moderate agreement; 0.61–0.80, substantial agreement; 0.81–1.00, excellent agreement. Continuous variables were expressed as mean ± SD, and statistical differences between G1 group and G2 group were analyzed using the independent sample *t*-test for

differences in the radiomic features. The data was corrected by Bonferroni's approach (P < 0.05) with two-sided to control for the type 1 errors.

Logistic regression analysis was conducted to find better predictors in distinguishing G1 group and G2 group. Features with *p* value of <0.05 in univariable model were entered into the multiple logistic regression analysis. The stepwise model selection using forward.LR (likelihood ratio test) methods was used to select the final predictive model. Receiver operating characteristic (ROC) curves for each model were constructed. The area under the curve (AUC) and its 95% confidence interval estimated using DeLong's method were calculated to evaluate the performances of the regressive models. A *p* value of <0.05 was considered a significant difference.

RESULTS

Patients Population

The study was approved by the Medical Research Ethics Committee and the Institutional Review Board. The patients in our study underwent preoperative upper abdominal MRI at our institution between January 2011 and January 2018. The inclusion criteria for the PNETs patients in our study were as follows: (1) patients with a surgery and pathological diagnosis of pancreas tumor, and graded by the European Neuroendocrine Tumor Society (ENETS), WHO 2017, based on mitotic count and Ki-67 index; (2) diagnostic MRI scans before surgery; (3) MRI images with a slice thickness of 5 mm or less.

Ultimately, there were 48 patients with 51 lesions (mean age, 50.4 years; age range, 16–74 years) who enrolled in our study. Based on systems of grading for PNETs, in our study, the lesions were subdivided into low grade (G1) group and intermediate grade (G2) group. Twenty-six of the patients (51.0%) had G1 lesions, and 25 (49.0%) had G2 lesions. The patients' basic clinical characteristics and the MRI features of the PNETs are shown in **Table 1**.

The interobserver agreement regarding the radiomic features of the PNETs ROI was generally acceptable (the value ranged from 0.717 to 0.986).

Significant Radiomic Features Differences of Tumor Grades

In the comparison of the radiomic analyses in non-enhanced T1 images, there was no significant difference between G1 group and G2 group ($P > 0.05$). However, significant differences only in the arterial phase analysis of enhanced images between the G1 group and the G2 group appeared in the radiomic features as follows: maximum intensity ($P = 0.021$, ICC = 0.807); range ($P = 0.039$, ICC = 0.908) (**Table 2**).

Logistic Regression Analysis and ROC Analysis for the Prediction of Tumor Grades

We used the maximum intensity feature and the range feature above as input variables for multiple logistic regression analysis. Logistic regression analysis revealed that the maximum intensity feature ($P = 0.023$, OR = 0.621, 95% CI: 0.433–0.858) was an independent predictor of G1 group compared with G2 groups (**Table 3**). The area under the curve (AUC) was 0.695 (95% CI: 0.543–0.846; P = 0.017) with a sensitivity and specificity of 50.0 and 92.0%, respectively (**Figure 1**).

TABLE 1 | The basic clinical characteristics of patients and the MRI features with WHO tumor grade of pancreatic neuroendocrine tumors. .

Features	Tumor grade	
	G1 (n = 26)	G2 (n = 25)
Female	18 (69.2%)	15 (60.0%)
Male	8 (30.8%)	10 (40.0%)
Age (years)		
Mean	53.34	49.1
Range	16–67	26–74
Standard deviation	11.8	11.7
Tumor location		
Pancreas head	8 (30.8%)	6 (24.0%)
Pancreas body	12 (46.2%)	12 (48.0%)
Pancreas tail	6 (23.0%)	7 (28.0%)
Tumor sizes (cm)		
Mean ± SD	3.4 ± 2.1	3.6 ± 2.5
Range	1.0–10.3	1.0–10.5
Lesions (<2 cm)	9	6
Tumor pattern		
Pancreatic duct dilatation	7	6
Chronic atrophic pancreatitis	3	5
Vascular involvement	6	12
Fibrosis on the surrounding pancreatic parenchyma	0	2
Ki-67 index (%)	<2	3–10
Lymphadenopathy	0	4
Synchronous liver metastases	3	3

TABLE 2 | Significant differences in the radiomic features between PNETs G1 group and PNETs G2 group.

Texture features	*G1 group (n=26)*	*G2 group (n=25)*	*P value**
Maximum intensity	1,868.73 ± 489.34	1,595.80 ± 298.50	0.021
Range	1,284.88 ± 577.693	997.68 ± 358.45	0.039

Data are mean ± standard deviation
**Independent sample t test.*
PNETs, pancreatic neuroendocrine tumors.

DISCUSSION

PNETs grades were significant for tumor treatment. The present study used MR imaging to predict the grades based on radiomic analysis, and it showed that the maximum intensity feature in the arterial phase T1 weight images of MR could be an independent predictor of G1lesions compared with G2 lesions of PNETs.

Radiomic analysis has been suggested a useful tool for the quantitative assessment of tumor heterogeneity (30, 31). The heterogeneity within tumors is associated with histopathologic grade and prognosis of tumors, which can reflect the intrinsic biologic aggressiveness of tumors (32–34). Several previous (35) studies have shown that the assessment of tumor heterogeneity had an important value for diagnosis, grading, prognosis, and treatment monitoring. MR imaging of tumor may provide a non-invasive assessment of tumor heterogeneity and may represent a valuable non-invasive tool in predicting the grading of PNETs and help for aggressiveness and prognosis of PNETs.

There have been several studies that investigated the CT radiomic characteristics, which can predict the grades of PNETs (27, 28). It was shown that the sphericity feature of radiomic variables on arterial 2D analysis of CT could be significant predictors between grade 2/3 and grade 1 (28). And also, the entropy feature of radiomic features in CT images was found as an independent predictor of PNETs grade (27).

However, there were few studies focused on radiomic analysis in MR images, although MR scanning can provide more sensitivity for structural investigation and higher soft tissue contrast resolution that makes it superior to CT in detecting PNETs, especially small tumors. Several studies (36, 37) about MR data applied to PNETs focused on ADC map, and it was found that the entropy and the kutosis features of histogram analysis, which was a part of radiomic analysis in ADC images of MR, could predict the G1 compared with the G2 of PNETs (36). Besides the most studies about MR features in ADC map associated with PNETs grades, radiomic analysis of PNETs in T1 weight images of MR were scarce, which could provide some more different information of MR images than ADC map. In a recent study it suggested that MRI radiomic score showed a significant association with the grades of PNETs (38), and another study showed the developed radiomics model using non-contrast MRI could help differentiate G1 and G2/3 tumors (39); both of that suggested radiomic MRI may be used as a valuable non-invasive tool for differential PNET grading.

In our study, we found that the maximum intensity feature of radiomic features was an independent predictor of G1 lesions compared with G2 lesions in the arterial phase T1 weight images of MR, although statistical significance was not found in the non-enhanced T1 images of MR. The results in our study showed G1 PNETs had significant differences on the maximum intensity feature of radiomic features after enhancement compared with higher grade tumors. It also coordinated with the previous report, which demonstrated that G1 PNETs were enhanced more prominently than higher-grade tumors in MR imaging (1). The lower-grade PNETs showed significantly increased tumor blood flow than higher-grade lesions (40). In the present study, the maximum intensity feature means the value of the voxels in the image ROI with the greatest value, which is thought to reflect tissue heterogeneity quantitatively by images. The maximum intensity feature of radiomic features may reflect the differences of blood flow within the tumor by different values in the image, and also reflect the tumor heterogeneity.

The results of our study may contribute to the development of predicting models that combine quantitative and qualitative radiomic features of imaging and traditional MR image feature predictors.

In the last couple of decades, the introduction and development of the endoscopic ultrasonography (EUS) opened a new era of diagnosis and treatment of PNETs, which had become a very useful imaging modality to evaluate pancreatic lesions. Contrast-enhanced EUS is helpful in categorizing small hypervascular PNETs (41), and studies showed that EUS was superior for the detection of PNETs lesions smaller than 2 cm (42–47). Its sensitivity was equal to MRI for the detection of PNETs. Other befits of EUS include the detection of lymph node involvement and vascular invasion. In the last few years, as the development of properly designed needles for EUS-guided fine-needle biopsy (EUS-FNB), the EUS-FNB was more important in the evaluation of suspected PNETs, especially in small (with a diameter smaller than 2 cm), non-functioning PNETs (45–47), which showed stronger and more accurate correlation for Ki-67 values with surgical specimens. MRI may not provide more accurate cytological information inside the tumor than EUS-FNB; however, it is a non-invasive technology compared with EUS-FNB, which can quantitatively assess tumor heterogeneity. Also, each imaging method is not perfect and needs to be combined in future applications.

TABLE 3 | Logistic regression analysis of the radiomic features between grade G1 and G2 group of PNETs.

Feature	Regression coefficients	P value	OR	95% CI
Maximum intensity	–0.103	0.023	0.621	0.433~0.858

PNETs, pancreatic neuroendocrine tumors.

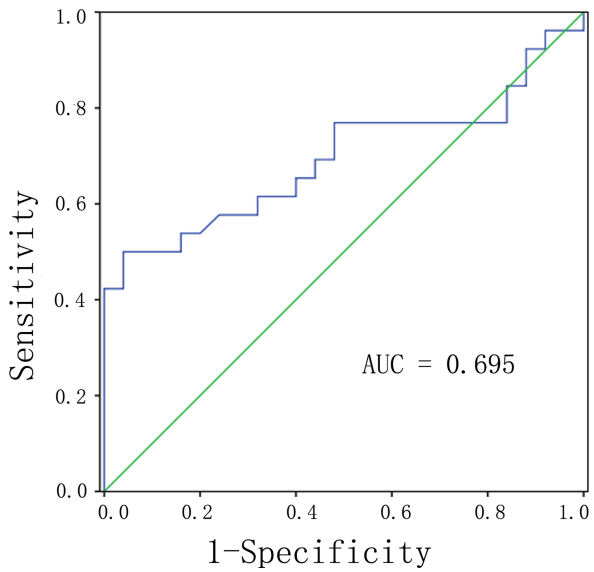

FIGURE 1 | ROC analysis of the significant differences of radiomic analysis between G1 and G2 of PNETs. Abbreviations: PNETs, pancreatic neuroendocrine tumors.

Our study had several limitations. First, as it was of retrospective design and PNETs are rare tumors. The patients in our study included only 48 patients with 51 lesions with G1or G2 PNETs. Second, in our study, tumor segmentation was manually performed and which may be influenced by some manual errors, as well as affecting the radiomic analysis results. So robust automatic boundary extraction method should be further developed for accurate ROI lesions. Nevertheless, additional long-term studies are needed to validate the results in larger population and in other sequences of MR images.

CONCLUSIONS

In conclusion, radiomic analysis of MR is helpful for the prediction of PNETs grade. The maximum intensity feature can help to identify the G1 PNETs from G2 PNETs on the arterial phase images of MR, which may be also applied to early recurrence or progression after surgical resection of PNETs in the further study.

DATA AVAILABILITY STATEMENT

The original contributions presented in the study are included in the article/**Supplementary Material**. Further inquiries can be directed to the corresponding author.

ETHICS STATEMENT

The studies involving human participants were reviewed and approved by the Medical Research Ethics Committee and the Institutional Review Board of Tianjin Medical University Cancer Institute and Hospital. Written informed consent for participation was not required for this study in accordance with the national legislation and the institutional requirements.

AUTHOR CONTRIBUTIONS

WL made contributions to study concepts and design, literature research, statistical analysis, manuscript preparation, and manuscript editing. CX made contributions to clinical studies. ZY contributed as guarantor of the integrity of the entire study. All authors contributed to the article and approved the submitted version.

SUPPLEMENTARY MATERIAL

The Supplementary Material for this article can be found online at: https://www.frontiersin.org/articles/10.3389/fonc.2021.758062/full#supplementary-material

REFERENCES

1. Kim JH, Eun HW, Kim YJ, Han JK, Choi BI. Staging Accuracy of MR for Pancreatic Neuroendocrine Tumor and Imaging Findings According to the Tumor Grade. *Abdominal Imaging* (2013) 38:1106–14. doi: 10.1007/s00261-013-0011-y
2. Falconi M, Eriksson B, Kaltsas G, Bartsch DK, Capdevila J, Caplin M, et al. ENETS Consensus Guidelines Update for the Management of Patients With Functional Pancreatic Neuroendocrine Tumors and Non-Functional

Pancreatic Neuroendocrine Tumors. *Neuroendocrinology* (2016) 103(2):153–71. doi: 10.1159/000443171
3. Halfdanarson TR, Rabe KG, Rubin J, Petersen GM. Pancreatic Neuroendocrine Tumors (PNETs): Incidence, Prognosis and Recent Trend Toward Improved Survival. *Ann Oncol: Off J Eur Soc Med Oncol/ESMO* (2008) 19(10):1727–33. doi: 10.1093/annonc/mdn351
4. Lloyd RV, Osamura RY, Klöppel G, Rosai J. *WHO Classification of Tumours of Endocrine Organs*. Lyon: International Agency for Research on Cancer (IARC) (2017).
5. Mpilla GB, Philip PA, B. El-Rayes and AS. Pancreatic Neuroendocrine Tumors: Therapeutic Challenges and Research Limitations. *World J Gastroenterol* (2020) 26(28):4036–54. doi: 10.3748/wjg.v26.i28.4036
6. Butturini G, Bettini R, Missiaglia E, Mantovani W, Dalai I, Capelli P, et al. Predictive Factors of Efficacy of the Somatostatin Analogue Octreotide as First Line Therapy for Advanced Pancreatic Endocrine Carcinoma. *Endocrine-Related Cancer* (2006) 13(4):1213–21. doi: 10.1677/erc.1.01200
7. Pezzilli R, Partelli S, Cannizzaro R, Pagano N, Crippa S, Pagnanelli M, et al. Ki-67 Prognostic and Therapeutic Decision Driven Marker for Pancreatic Neuroendocrine Neoplasms (PNENs): A Systematic Review. *Adv Med Sci* (2016) 61(1):147–53. doi: 10.1016/j.advms.2015.10.001
8. Scarpa A, Mantovani W, Capelli P, Beghelli S, Boninsegna L, Bettini R, et al. Pancreatic Endocrine Tumors: Improved TNM Staging and Histopathological Grading Permit a Clinically Efficient Prognostic Stratification of Patients. *Modern Pathol: An Off J United States Can Acad Pathol* (2010) 23(6):824–33. doi: 10.1038/modpathol.2010.58
9. De Robertis R, Cingarlini S, Tinazzi Martini P, Ortolani S, Butturini G, Landoni L, et al. Pancreatic Neuroendocrine Neoplasms: Magnetic Resonance Imaging Features According to Grade and Stage. *World J Gastroenterol* (2017) 23(2):275–85. doi: 10.3748/wjg.v23.i2.275
10. Jeon SK, Lee JM, Joo I, Lee ES, Park HJ, Jang JY, et al. Nonhypervascular Pancreatic Neuroendocrine Tumors: Differential Diagnosis From Pancreatic Ductal Adenocarcinomas at MR Imaging-Retrospective Cross-Sectional Study. *Radiology;* (2017) 284(1):77–87. doi: 10.1148/radiol.2016160586
11. Yamamoto Y, Okamura Y, Uemura S, Sugiura T, Ito T, Ashida R, et al. Vascularity and Tumor Size Are Significant Predictors for Recurrence After Resection of a Pancreatic Neuroendocrine Tumor. *Ann Surg Oncol* (2017) 24 (8):2363–70. doi: 10.1245/s10434-017-5823-5
12. Manfredi R, Bonatti M, Mantovani W, Graziani R, Segala D, Capelli P, et al. Non-Hyperfunctioning Neuroendocrine Tumours of the Pancreas: MR Imaging Appearance and Correlation With Their Biological Behaviour. *Eur Radiol* (2013) 23(11):3029–39. doi: 10.1007/s00330-013-2929-4
13. Guo C, Chen X, Xiao W, Wang Q, Sun K, Wang Z. Pancreatic Neuroendocrine Neoplasms at Magnetic Resonance Imaging: Comparison Between Grade 3 and Grade 1/2 Tumors. *OncoTargets Ther* (2017) 10:1465–74. doi: 10.2147/OTT.S127803
14. Kartalis N, Mucelli RM, Sundin A. Recent Developments in Imaging of Pancreatic Neuroendocrine Tumors. *Ann Gastroenterol* (2015) 28(2):193–202.
15. Bettini R, Partelli S, Boninsegna L, Capelli P, Crippa S, Pederzoli P, et al. Tumor Size Correlates With Malignancy in Nonfunctioning Pancreatic Endocrine Tumor. *Surgery* (2011) 150(1):75–82. doi: 10.1016/j.surg.2011.02.022
16. Lotfalizadeh E, Ronot M, Wagner M, Cros J, Couvelard A, Vullierme MP, et al. Prediction of Pancreatic Neuroendocrine Tumour Grade With MR Imaging Features: Added Value of Diffusion-Weighted Imaging. *Eur Radiol* (2017) 27(4):1748–59. doi: 10.1007/s00330-016-4539-4
17. Kim DW, Kim HJ, Kim KW, Byun JH, Song KB, Kim JH, et al. Neuroendocrine Neoplasms of the Pancreas at Dynamic Enhanced CT: Comparison Between Grade 3 Neuroendocrine Carcinoma and Grade 1/2 Neuroendocrine Tumour. *Eur Radiol* (2015) 25(5):1375–83. doi: 10.1007/s00330-014-3532-z
18. Jang KM, Kim SH, Lee SJ, Choi D. The Value of Gadoxetic Acid-Enhanced and Diffusion-Weighted MRI for Prediction of Grading of Pancreatic Neuroendocrine Tumors. *Acta Radiol* (2014) 55(2):140–8. doi: 10.1177/0284185113494982
19. Hwang EJ, Lee JM, Yoon JH, Kim JH, Han JK, Choi BI, et al. Intravoxel Incoherent Motion Diffusion-Weighted Imaging of Pancreatic Neuroendocrine Tumors: Prediction of the Histologic Grade Using Pure Diffusion Coefficient and Tumor Size. *Invest Radiol* (2014) 49(6):396–402. doi: 10.1097/RLI.0000000000000028
20. De Robertis R, D'Onofrio M, Zamboni G, Tinazzi Martini P, Gobbo S, Capelli P, et al. Pancreatic Neuroendocrine Neoplasms: Clinical Value of Diffusion-Weighted Imaging. *Neuroendocrinology* (2016) 103(6):758–70. doi: 10.1159/000442984
21. Dromain C, Deandreis D, Scoazec JY, Goere D, Ducreux M, Baudin E, et al. Imaging of Neuroendocrine Tumors of the Pancreas. *Diagn Interventional Imag* (2016) 97(12):1241–57. doi: 10.1016/j.diii.2016.07.012
22. Kang KM, Lee JM, Yoon JH, Kiefer B, Han JK, Choi BI. Intravoxel Incoherent Motion Diffusion-Weighted MR Imaging for Characterization of Focal Pancreatic Lesions. *Radiology* (2014) 270(2):444–53. doi: 10.1148/radiol.13122712
23. Wang Y, Chen ZE, Yaghmai V, Nikolaidis P, McCarthy RJ, Merrick L, et al. Diffusion-Weighted MR Imaging in Pancreatic Endocrine Tumors Correlated With Histopathologic Characteristics. *J Magnetic Resonance Imaging: JMRI* (2011) 33(5):1071–9. doi: 10.1002/jmri.22541
24. Pereira JA, Rosado E, Bali M, Metens T, Chao SL. Pancreatic Neuroendocrine Tumors: Correlation Between Histogram Analysis of Apparent Diffusion Coefficient Maps and Tumor Grade. *Abdom Imaging* (2015) 40(8):3122–8. doi: 10.1007/s00261-015-0524-7
25. Kulali F, Semiz-Oysu A, Demir M, Segmen-Yilmaz M, Bukte Y. Role of Diffusion-Weighted MR Imaging in Predicting the Grade of Nonfunctional Pancreatic Neuroendocrine Tumors. *Diagn Interventional Imag* (2018) 99 (5):301–9. doi: 10.1016/j.diii.2017.10.012
26. Saleh M, Bhosale PR, Yano M, Itani M, Elsayes AK, Halperin D, et al. New Frontiers in Imaging Including Radiomics Updates for Pancreatic Neuroendocrine Neoplasms. *Abdom Radiol (NY)* (2020). doi: 10.1007/s00261-020-02833-8
27. Canellas R, Burk KS, Parakh A, Sahani DV. Prediction of Pancreatic Neuroendocrine Tumor Grade Based on CT Features and Radiomic Analysis. *AJR Am J Roentgenol* (2018) 210(2):341–6. doi: 10.1007/s00330-019-06176-x
28. Choi TW, Kim JH, Yu MH, Park SJ, Han JK. Pancreatic Neuroendocrine Tumor: Prediction of the Tumor Grade Using CT Findings and Computerized Radiomic Analysis. *Acta Radiol* (2018) 59(4):383–92. doi: 10.1177/0284185117725367
29. Fedorov A, Beichel R, Kalpathy-Cramer J, Finet J, Fillion-Robin JC, Pujol S, et al. 3d Slicer as an Image Computing Platform for the Quantitative Imaging Network. *Magnetic Resonance Imaging* (2012) 30(9):1323–41. doi: 10.1016/j.mri.2012.05.001
30. Ganeshan B, Miles KA. Quantifying Tumour Heterogeneity With CT. *Cancer Imaging: Off Publ Int Cancer Imaging Soc* (2013) 13:140–9. doi: 10.1102/1470-7330.2013.0015
31. Bartoli M, Barat M, Dohan A, Gaujoux S, Coriat R, Hoeffel C, et al. CT and MRI of Pancreatic Tumors: An Update in the Era of Radiomics. *Jpn J Radiol 38* (2020) 12:1111–24. doi: 10.1007/s11604-020-01057-6
32. Davnall F, Yip CS, Ljungqvist G, Selmi M, Ng F, Sanghera B, et al. Assessment of Tumor Heterogeneity: An Emerging Imaging Tool for Clinical Practice? *Insights Into Imag* (2012) 3(6):573–89. doi: 10.1102/1470-7330.2013.0015
33. Ryu YJ, Choi SH, Park SJ, Yun TJ, Kim JH, Sohn CH. Glioma: Application of Whole-Tumor Radiomic Analysis of Diffusion-Weighted Imaging for the Evaluation of Tumor Heterogeneity. *PloS One* (2014) 9(9):e108335. doi: 10.1371/journal.pone.0108335
34. Skogen K, Ganeshan B, Good C, Critchley G, Miles K. Measurements of Heterogeneity in Gliomas on Computed Tomography Relationship to Tumour Grade. *J Neuro-Oncol* (2013) 111(2):213–9. doi: 10.1007/s11060-012-1010-5
35. Nguyen HT, Shah ZK, Mortazavi A, Pohar KS, Wei L, Jia G, et al. Non-Invasive Quantification of Tumour Heterogeneity in Water Diffusivity to Differentiate Malignant From Benign Tissues of Urinary Bladder: A Phase I Study. *Eur Radiol* (2017) 27(5):2146–52. doi: 10.1007/s00330-016-4549-2
36. De Robertis R, Maris B, Cardobi N, Tinazzi Martini P, Gobbo S, Capelli P, et al. Can Histogram Analysis of MR Images Predict Aggressiveness in Pancreatic Neuroendocrine Tumors? *Eur Radiol* (2018) 28(6):2582–91. doi: 10.1007/s00330-017-5236-7
37. Hu Y, Rao S, Xu X, Tang Y, Zeng M. Grade 2 Pancreatic Neuroendocrine Tumors: Overbroad Scope of Ki-67 Index According to MRI Features. *Abdom Radiol (NY)* (2018) 43(11):3016–24. doi: 10.1007/s00261-018-1573-5

38. Bian Y, Li J, Cao K, Fang X, Jiang H, Ma C, et al. Magnetic Resonance Imaging Radiomic Analysis Can Preoperatively Predict G1 and G2/3 Grades in Patients With NF-pNETs. *Abdom Radiol (NY)* (2021) 46(2):667–80. doi: 10.1007/s00261-020-02706-0
39. Bian Y, Zhao Z, Jiang H, Fang X, Li J, Cao K, et al. Noncontrast Radiomics Approach for Predicting Grades of Nonfunctional Pancreatic Neuroendocrine Tumors. *J Magn Reson Imaging* (2020) 52(4):1124–36. doi: 10.1002/jmri.27176
40. d'Assignies G, Couvelard A, Bahrami S, Vullierme MP, Hammel P, Hentic O, et al. Pancreatic Endocrine Tumors: Tumor Blood Flow Assessed With Perfusion CT Reflects Angiogenesis and Correlates With Prognostic Factors. *Radiology* (2009) 250(2):407–16. doi: 10.1148/radiol.2501080291
41. Braden B, Jenssen C, D'Onofrio M, Hocke M, Will U, Moller K, et al. B-Mode and Contrast-Enhancement Characteristics of Small Nonincidental Neuroendocrine Pancreatic Tumors. *Endoscopic Ultrasound* (2017) 6(1):49–54. doi: 10.4103/2303-9027.200213
42. Khashab MA, Yong E, Lennon AM, Shin EJ, Amateau S, Hruban RH, et al. EUS Is Still Superior to Multidetector Computerized Tomography for Detection of Pancreatic Neuroendocrine Tumors. *Gastrointestinal Endoscopy* (2011) 73(4):691–6. doi: 10.1016/j.gie.2010.08.030
43. James PD, Tsolakis AV, Zhang M, Belletrutti PJ, Mohamed R, Roberts DJ, et al. Incremental Benefit of Preoperative EUS for the Detection of Pancreatic Neuroendocrine Tumors: A Meta-Analysis. *Gastrointestinal Endoscopy* (2015) 81(4):848–56.e1. doi: 10.1016/j.gie.2014.12.031
44. Ishii T, Katanuma A, Toyonaga H, Chikugo K, Nasuno H, Kin T, et al. Role of Endoscopic Ultrasound in the Diagnosis of Pancreatic Neuroendocrine Neoplasms. *Diagnostics* (2021) 11(2):316. doi: 10.3390/diagnostics11020316
45. Crino SF, Ammendola S, Meneghetti A, Bernardoni L, MC CB, Gabbrielli A, et al. Comparison Between EUS-Guided Fine-Needle Aspiration Cytology and EUS-Guided Fine-Needle Biopsy Histology for the Evaluation of Pancreatic Neuroendocrine Tumors. *Pancreatol: Off J Int Assoc Pancreatol* (2021) 21 (2):443–50. doi: 10.1016/j.pan.2020.12.015
46. Crino SF, Di Mitri R, Nguyen NQ, Tarantino I, de Nucci G, Deprez PH, et al. Endoscopic Ultrasound-Guided Fine-Needle Biopsy With or Without Rapid On-Site Evaluation for Diagnosis of Solid Pancreatic Lesions: A Randomized Controlled Non-Inferiority Trial. *Gastroenterology* (2021) 161(3):899–909.e5. doi: 10.1053/j.gastro.2021.06.005
47. Paiella S, Landoni L, Rota R, Valenti M, Elio G, Crino SF, et al. Endoscopic Ultrasound-Guided Fine-Needle Aspiration for the Diagnosis and Grading of Pancreatic Neuroendocrine Tumors: A Retrospective Analysis of 110 Cases. *Endoscopy* (2020) 52(11) 988–94. doi: 10.1055/a-1180-8614

Conflict of Interest: The authors declare that the research was conducted in the absence of any commercial or financial relationships that could be construed as a potential conflict of interest.

Publisher's Note: All claims expressed in this article are solely those of the authors and do not necessarily represent those of their affiliated organizations, or those of the publisher, the editors and the reviewers. Any product that may be evaluated in this article, or claim that may be made by its manufacturer, is not guaranteed or endorsed by the publisher.

frontiers in Oncology

ORIGINAL RESEARCH
published: 11 January 2022
doi: 10.3389/fonc.2021.757073

Lipoxins and Resolvins in Patients With Pancreatic Cancer: A Preliminary Report

Wojciech Blogowski[1]*, *Katarzyna Dolegowska*[2], *Anna Deskur*[3], *Barbara Dolegowska*[2] *and Teresa Starzynska*[3]

[1] Institute of Medical Sciences, University of Zielona Gora, Zielona Gora, Poland, [2] Department of Microbiology, Immunology and Laboratory Medicine, Pomeranian Medical University, Szczecin, Poland, [3] Department of Gastroenterology, Pomeranian Medical University, Szczecin, Poland

OPEN ACCESS

Edited by:
Min Li,
University of Oklahoma Health Sciences Center, United States

Reviewed by:
Andrea Liostti,
Local Health Authority of Imola, Italy
Alessandro Boscarelli,
Institute for Maternal and Child Health Burlo Garofolo (IRCCS), Italy

***Correspondence:**
Wojciech Blogowski
drannab@wp.pl

Specialty section:
This article was submitted to Gastrointestinal Cancers: Hepato Pancreatic Biliary Cancers, a section of the journal Frontiers in Oncology

Received: 11 August 2021
Accepted: 30 November 2021
Published: 11 January 2022

Citation:
Blogowski W, Dolegowska K, Deskur A, Dolegowska B and Starzynska T (2022) Lipoxins and Resolvins in Patients With Pancreatic Cancer: A Preliminary Report. Front. Oncol. 11:757073. doi: 10.3389/fonc.2021.757073

Eicosanoids are bioactive lipids derived from arachidonic acid, which have emerged as key regulators of a wide variety of pathophysiological processes in recent times and are implicated as mediators of gastrointestinal cancer. In this study, we investigated the systemic levels of lipoxygenase (LOX)-derived lipoxin A4 and B4, together with resolvin D1 and D2 in patients with pancreatic adenocarcinoma (n = 68), as well as in healthy individuals (n = 32). Systemic concentrations of the aforementioned immunoresolvents were measured using an enzyme-linked immunosorbent assay (ELISA). In this study, we observed that compared with concentrations in healthy individuals, the peripheral concentrations of the aforementioned eicosanoids were significantly elevated (2- to 10-fold) in patients with pancreatic cancer (in all cases $p<0.00001$). No significant association was observed between eicosanoid levels and the TNM clinical staging. Furthermore, we observed no significant differences in concentrations of the analyzed bioactive lipids between patients diagnosed with early-stage (TNM stage I-II) and more advanced disease (TNM stage III-IV). Receiver operating characteristic (ROC) curve analysis of each aforementioned immunoresolvent showed area under the curve values ranging between 0.79 and 1.00. Sensitivity, specificity, as well as positive and negative predictive values of the eicosanoids involved in the detection/differentiation of pancreatic adenocarcinoma ranged between 56.8% and 100%. In summary, our research is the first study that provides clinical evidence to support a systemic imbalance in LOX-derived lipoxins and resolvins as the mechanism underlying the pathogenesis of pancreatic adenocarcinoma. This phenomenon occurs regardless of

the clinical TNM stage of the disease. Furthermore, our study is the first to preliminarily highlight the role of peripheral levels of immunoresolvents, particularly resolvin D1, as potential novel biomarkers of pancreatic cancer in humans.

Keywords: immunoresolvents, lipoxygenase, lipoxin, pancreatic cancer, resolvin

INTRODUCTION

Pancreatic adenocarcinoma is an extremely aggressive and invariably fatal malignancy in humans. Approximately 60,000 individuals are diagnosed with this malignancy that is known to cause 50,000 deaths annually in the United States. Multiple risk factors including age, certain genetic syndromes, smoking, diabetes, alcohol abuse, and obesity are implicated as etiopathogenetic contributors to pancreatic adenocarcinoma, and several molecular pathways associated with pancreatic cancer have been identified (1, 2). However, the exact mechanisms underlying this disease remain unclear. Therefore, prevention, early detection, and prompt treatment are clinically challenging.

Bioactive lipids derived from arachidonic acid (AA), referred to as eicosanoids are implicated as key factors in carcinogenesis, in recent times. These AA derivatives represent a large family of substances that affect multiorgan function, including gastrointestinal physiology and regulate several pathophysiological processes in the body, such as vascular flow, angiogenesis, cellular proliferation, inflammation, and metabolism (3–6). From the biochemical viewpoint, AA-derived eicosanoids are produced *via* the CYP450, cyclo-oxygenase (COX), or lipoxygenase (LOX) enzymatic pathways (7, 8). Among the various eicosanoids generated *via* the aforementioned enzymatic pathways, bioactive lipids such as leukotrienes, hydroxyeicosatetraenoic acids, lipoxins, and resolvins have gained much attention as significant contributors to malignancies. This effect is mainly associated with their actions on immune cell function and modulation of both initiation (leukotrienes) and resolution (lipoxins, resolvins) of inflammatory processes (9–12). Although acute inflammation is usually a physiological response that protects the body from temporary microbial infections or injurious stimuli, uncontrolled chronic inflammation predisposes to carcinogenesis *via* DNA injury, epigenetic dysregulation, genomic instability, and/or changes in intracellular signaling. LOX-derived lipoxins and resolvins participate in resolution of inflammation; several experimental studies have shown their benefits in suppression of chronic inflammation-induced tumorigenesis (13, 14). These results support the potential application of these immunoresolvents as promising preventive or anti-cancer agents (15–18); however, limited information is available regarding their role in the development of pancreatic adenocarcinoma in humans.

In this study, we preliminarily investigated the systemic concentrations of lipoxins (A4 and B4) and resolvins (D1 and D2) in patients with pancreatic cancer and compared these values with those observed in healthy individuals. Moreover, we investigated the association between clinical TNM staging of pancreatic adenocarcinoma and immunoresolvents' levels in patients with cancer. We additionally investigated whether systemic concentrations of lipoxins and resolvins show any significant diagnostic value for detection/differentiation of pancreatic cancer.

MATERIAL AND METHODS

Study Participants and Clinical Protocols

We recruited 100 individuals in this study. All participants were evaluated (in an outpatient or inpatient setting) at our Department and were confirmed to be stable with good general health. Exclusion criteria were as follows: an active infectious/inflammatory disease, a history of any malignancy, administration of medications that could potentially interfere with AA metabolism (such as COX inhibitors), a history of blood transfusions within 6 months prior to study enrollment, active supplementation of lipid derivatives (omega-3 fatty acids), and/or refusal to participate in the study.

Among the 100 patients recruited for the study, 68 were diagnosed with pancreatic adenocarcinoma and were categorized into the "cancer" group. Similar to previous studies performed by our group (19–21), diagnosis of pancreatic cancer was based on evaluation of biopsy specimens obtained *via* endoscopic ultrasound, paracentesis (in patients with neoplastic ascites), or liver biopsy (in patients with metastatic disease). All patients underwent laboratory tests and imaging (abdominal/chest computed tomography and/or abdominal ultrasonography), and these results were subsequently used for TNM staging of the cancer. In this study, stage I and II pancreatic adenocarcinoma was diagnosed in 5 and 17 patients, respectively. Advanced-stage disease (stage III) occurred in 11 patients and metastatic disease (stage IV) in 35 patients. All patients had a recent diagnosis of pancreatic cancer at the time of study inclusion; therefore, no patient received any chemotherapy or any cytotoxic therapy within a year preceding the diagnosis, and no active acute infection or disease was observed in any patient.

The control group in our study included 32 volunteers in an overall good state of health.

Blood Sample Collection and Systemic Immunoresolvent Level Measurements

Peripheral blood samples (8–10 mL) were obtained from all individuals enrolled in this study. The samples were immediately processed based on standard laboratory protocols; plasma was separated, frozen, and stored at –80°C until further tests were performed. The systemic concentrations of analyzed immunoresolvents (lipoxin A4 and B4 and resolvin D1 and D2) were measured using commercially available, high-sensitivity enzyme-linked immunosorbent assay kits (*Wuhan*

EIAab Science Co, Ltd., China and *Cayman Chemicals*, MI, USA) based on the manufacturers' instructions.

Statistical Analysis

Similarly to our previous studies (22, 23) all of the received results were subjected to a comprehensive analysis with use of statistical software. Specifically, normality of distribution of the variables was tested using the Shapiro–Wilk test. Continuous variables that were abnormally distributed were subjected to log transformation. Subsequently, if normality of the distribution was obtained then Student's t-test was used to compare mean values of examined parameters between appropriate groups. Otherwise a Mann–Whitney U-test for non-parametric variables was used. In order to calculate the correlations between parametric and non-parametric variables we used Pearson's or Spearman's correlation rank tests (respectively). In addition, a multivariate regression analyses were performed with use of a stepwise selection method. In order to exclude eventual presence of any residual confounding we entered individually the variables that initially were excluded from the constructed model. Finally, we constructed the receiver operating characteristics (ROC) curves and calculated the area under curve (AUC) values for all tested immunoresolvents as eventual diagnostic substances for pancreatic cancer in humans. All of these statistical analyses were performed with use of the SPSS software and $p<0.05$ values were considered as significant.

RESULTS

Baseline Characteristics of Study Participants

Table 1 summarizes baseline characteristics of the study participants. No statistically significant differences were observed in age and sex distribution, body mass index (BMI), smoking and alcohol consumption habits, and medication history. However, statistical analysis showed significantly higher levels of carbohydrate antigen 19-9 (CA19.9 - pancreatic cancer marker) in patients with pancreatic adenocarcinoma than in healthy controls. Similarly, C-reactive protein levels were significantly higher in the cancer group (**Table 1**).

Peripheral Concentrations of Immunoresolvents in Patients With Pancreatic Cancer vs. Healthy Volunteers

Figure 1 shows the mean values of systemic levels of immunoresolvents. We observed that peripheral levels of lipoxin A4 and B4 were significantly higher in patients with pancreatic adenocarcinoma than in healthy individuals (in both cases $p<0.00001$). Similar findings were observed with regard to resolvin D1 and D2 concentrations. Specifically, the mean peripheral levels of resolvin D1 and D2 were significantly higher (in both cases $p<0.00001$) in the cancer group than in the control group (**Figure 1**).

Clinical Association Between Systemic Levels of Immunoresolvents and TNM Staging of Pancreatic Cancer

We investigated the association, if any, between significant changes in systemic levels of immunoresolvents and the clinical staging of pancreatic adenocarcinoma. Correlation analysis showed no significant association between the TNM stage and lipoxin A4 ($r=0.08$), lipoxin B4 ($r=0.13$), resolvin D1 ($r=0.03$), and resolvin D2 ($r=0.01$) levels ($p>0.28$ in all cases). Multivariate regression analysis showed similar results (**Table 2**). Additionally, we subcategorized patients from the "cancer" group into two separate subgroups (TNM I–II and TNM III–IV) based on the clinical TNM staging and performed an intergroup comparison of the mean peripheral concentrations of lipoxins and resolvins. Analysis showed no significant differences in mean systemic immunoresolvent levels between patients diagnosed with TNM

TABLE 1 | General characteristics of analyzed patients and healthy individuals enrolled in the study [data presented as means ± SD or median (interquartile range)].

Parameters	Control	Cancer
Age (years)	61 ± 7	63 ± 11
Gender (M-men/W-women)	14-M/18-W	29-M/39-W
BMI (kg/m^2)	26.1 ± 4.3	24.0 ± 4.9
Smoking (Y-yes/N-no)	5-Y/27-N	8-Y/60-N
Alcohol (drinks/week)[#]	3.3 ± 1.9	3.4 ± 1.6
Medications (Y-yes/N-no):	25-Y/7-N	55-Y/13-N
Hypertension	25	55
Diabetes	0	0
Lipid lowering (statins)	8	14
Other	1	1
RBC (x10^{12} cells/L)	4.75 ± 0.55	4.31 ± 0.63
Hb (g/dL)	14 ± 1.7	13 ± 1.8
Platelets count (x10^9 cells/L)	228 ± 60	268 ± 121
WBC count (x10^9 cells/L)	6.15 ± 1.7	8.6 ± 3.3
CRP (mg/L)	3.0 ± 1.7	27.6 [4.8; 73.1]*
CA19.9 (U/mL)	11.0 ± 5.6	470 [87; 1700]*

BMI, body mass index; RBC, red blood cells; Hb, hemoglobin.

*WBC, white blood cells; CRP, C-reactive protein; *P<0.01 (vs "control" group).*

[#]a drink was defined as a single consumption of about 8 grams of pure ethanol (equal to for example a glass of wine or a single measure of spirits).

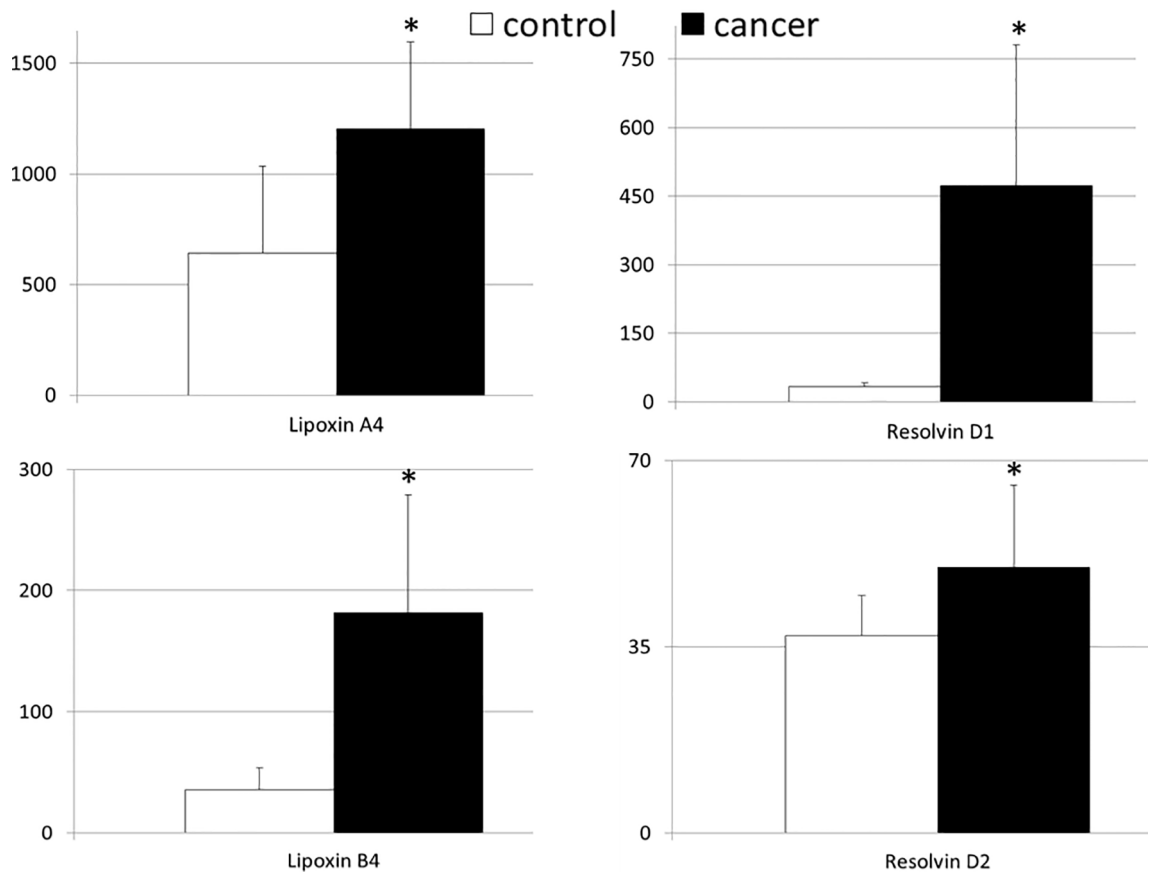

FIGURE 1 | Mean values of the systemic levels of examined immunoresolvents in patients with pancreatic cancer and control individuals together with their statistical comparison (values presented as means ± standard deviation in pg/mL). *p < 0.00001 (vs "control" group).

stage I–II pancreatic cancer and those with more advanced disease (stage III or IV) (p at least >0.21 in all cases) (**Figure 2**).

Immunoresolvents as Potential Markers of Pancreatic Adenocarcinoma

In view of the significant differences in the mean concentrations of all immunoresolvents between healthy individuals and patients with pancreatic adenocarcinoma, we performed preliminary analysis to determine whether systemic levels of these substances are of diagnostic value for the detection and/or differentiation of pancreatic cancer in humans. Therefore, we constructed ROC curves for each eicosanoid and calculated the AUC values. Preliminary analysis revealed that systemic levels of all immunoresolvents investigated in this study showed strong diagnostic potential as promising biomarkers of pancreatic adenocarcinoma. AUC values ranged between 0.79 and 1.00 (**Figure 3**). Based on these results, we attempted to determine potential diagnostic cut-off values for levels of the aforementioned immunoresolvents and preliminarily characterized their estimated sensitivity, specificity, and positive and negative predictive values (**Table 3**). We observed that resolvin D1 concentrations showed the most promising results with regard to diagnostic potential (up

TABLE 2 | Results of statistical analysis of associations between systemic concentrations of examined immunoresolvents and clinical staging of pancreatic cancer in patients (modelling using multivariate regression analysis).

Dependent variable	Independent variable	β	P of the variable	R^2	P of the model
*TNM Staging**	Lipoxin A4	0.08	0.51	0.01	0.51
	Lipoxin B4	0.13	0.28	0.02	0.28
	Resolvin D1	0.03	0.81	0.001	0.81
	Resolvin D2	0.001	0.99	0.001	0.99

β – standardized coefficient in the regression equation; p – level of significance.

**Variable was created by assigning 1, 2, 3 or 4 value to appropriate TNM stage that was present in patients with pancreatic cancer.*

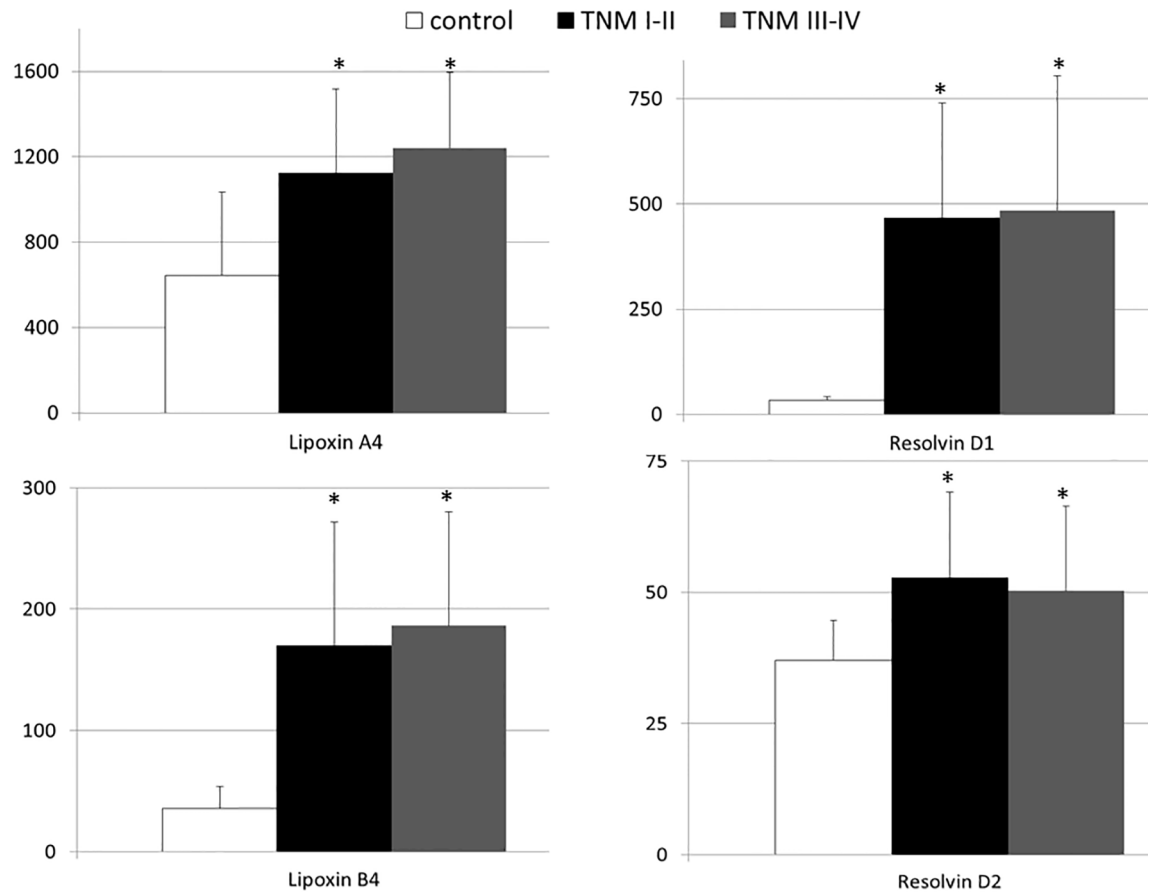

FIGURE 2 | Mean systemic levels of examined immunoresolvents in subgroups of pancreatic cancer patients divided according to the TNM staging and healthy individuals together with their statistical comparison (values presented as means ± standard deviation in pg/mL). *$p < 0.003$ (vs "control" group).

to 100%). Other newly proposed biomarkers showed approximately 75%–94.1% sensitivity, 65.6%–87.5% specificity, and 82.5%–94.1% and 56.8%–87.5% positive and negative predictive values, respectively.

DISCUSSION

LOX-derived lipoxins and resolvins represent a family of substances that play a major role in successful resolution of inflammation. Therefore, they are also expected to be significant mediators of carcinogenesis, because uncontrolled chronic inflammation is known to be associated with the development of solid malignancies (24–27). However, limited data are available regarding the significance of immunoresolvents in the development of pancreatic adenocarcinoma; few clinical studies have discussed these bioactive lipids in patients with this malignancy. In this study, we investigated a broad panel of immunoresolvents in patients with pancreatic cancer and attempted to determine the clinical associations and diagnostic value, if any, of these substances.

We observed that patients with pancreatic adenocarcinoma showed significantly elevated levels of immunoresolvents, such as lipoxins and resolvins. Our results are consistent with those reported by previous studies, which show significant genetic expression of LOX enzymes in the ductal cells of pancreatic adenocarcinoma and in resected tissue specimens (28–30). Previous studies have reported that only sporadic LOX expression was detected in pancreatic ductal cells in normal human pancreas. In our study, compared with levels in healthy individuals, we observed an approximate 2-fold mean increase in systemic lipoxin levels and specifically a 10-fold or higher increase in systemic resolvin D1 levels in patients with pancreatic cancer. Interestingly, such significant elevations in lipoxin and resolvin levels were observed regardless of the clinical staging of the pancreatic cancer based on the international TNM classification. The mean (elevated) immunoresolvent levels were similar between patients with both early- and advanced (metastatic)-stage disease. Unfortunately, currently, the exact etiology of elevated immunoresolvent levels and the exact molecular consequences of this phenomenon in patients with pancreatic cancer remain unclear. Several experimental studies that have investigated this

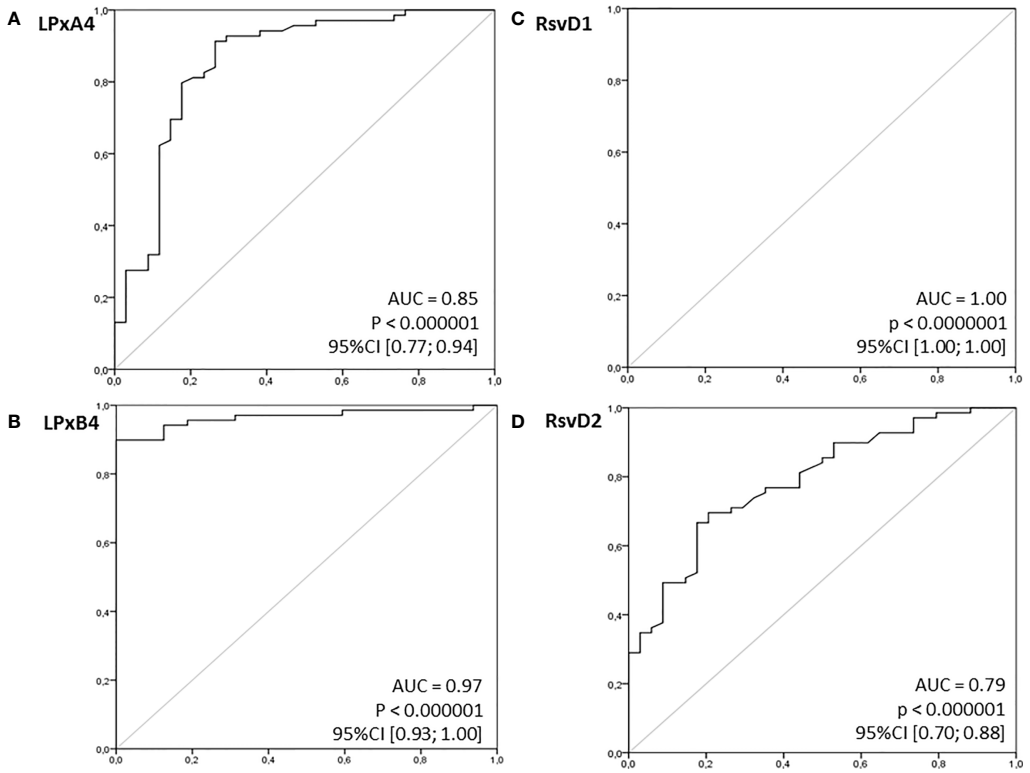

FIGURE 3 | Receiver operating characteristics (ROC) curves for examined immunoresolvents as potential (bio)markers of pancreatic cancer. Calculated sensitivity (y-axis) is plotted against 1-specificity formula (x-axis) for examined immunoresolvents: **(A)** lipoxin A4 (LPxA4), **(B)** lipoxin B4 (LPxB4), **(C)** resolvin D1 (RsvD1) and **(D)** resolvin D2 (RsvD2) as potential indicators of pancreatic cancer. AUC, area under ROC curve; p, level of significance.

TABLE 3 | Diagnostic value of examined immunoresolvents to discriminate presence of pancreatic adenocarcinoma in our patients.

Parameter	Lipoxin A4	Lipoxin B4	Resolvin D1	Resolvin D2
Suggested cut-off value	≥ 893.5 [pg/mL]	≥ 56.4 [pg/mL]	≥ 74.5 [pg/mL]	≥ 39.5 [pg/mL]
Sensitivity [%]	91.2	94.1	100.0	76.5
Specificity [%]	75.0	87.5	100.0	65.6
Positive predictive value [%]	88.5	94.1	100.0	82.5
Negative predictive value [%]	80.0	87.5	100.0	56.8

subject at the molecular level show that immunoresolvents may inhibit pancreatic cancer progression and dissemination. Specifically, research has shown that immunoresolvents may inhibit differentiation of pancreatic stellate cells into cancer-induced fibroblast-like myofibroblasts and "re-program" the tumor stroma, reverse mesenchymal phenotypes of pancreatic cancer cells, and attenuate their invasion and metastasis *via* inhibition of (i) autocrine transforming growth factor β1 signaling, (ii) reactive oxygen species production and, (iii) activity of the extracellular signal regulated kinases that downregulate matrix metalloproteinases (31–33). Based on the findings of these studies, the extent of the spontaneous eicosanoid response in patients with pancreatic cancer remains unclear, and the reason for the lack of a sustained increase in systemic generation of lipoxins and resolvins in advanced-stage pancreatic malignancy remains unexplained. Considering the conclusions drawn from all aforementioned molecular studies, it is reasonable to infer that significantly elevated lipoxin and resolvin levels most likely represent a natural response to pancreatic carcinogenesis in humans, to inhibit uncontrolled inflammation that is a hallmark of pancreatic cancer and additionally accelerates the progression of malignancy. However, further molecular and translational studies are warranted to accurately characterize this phenomenon, particularly focused on the exact mechanisms underlying this process and to verify whether modulation (particularly intensification) of the eicosanoid response could not offer clinical benefit in patients with pancreatic cancer.

In view of the significant differences in peripheral levels of lipoxins and resolvins observed in this study, we preliminarily

investigated the diagnostic potential of these eicosanoids as biomarkers of pancreatic adenocarcinoma in humans. ROC curve analysis showed significantly high clinical diagnostic potential of the aforementioned immunoresolvents, particularly of resolvin D1. Therefore, our results support the hypotheses presented by previous studies, which suggest that genetic expression of LOX and/or LOX-derived eicosanoids may be significantly associated with carcinogenesis in addition to being promising biomarkers of various types of solid malignancies (34, 35). We emphasize that our results are preliminary considering the small sample size of our study; further large-scale clinical studies are warranted to validate and characterize the diagnostic potential of the aforementioned immunoresolvents in patients with pancreatic cancer.

In summary, our study highlights the significant alterations in the systemic balance of immunoresolvents, such as lipoxins and resolvins in patients with pancreatic adenocarcinoma and that this finding is unaffected by the clinical TNM stage of the disease. Furthermore, our study is the first to preliminarily measure peripheral levels of lipoxins and resolvins, (particularly resolvin D1), which may potentially serve as novel biomarkers of pancreatic adenocarcinoma in humans.

DATA AVAILABILITY STATEMENT

The datasets presented in this article are not readily available because data set includes multiple clinical information. Requests to access the datasets should be directed to drannab@wp.pl.

ETHICS STATEMENT

The studies involving human participants were reviewed and approved by the (Bio)Ethics Committee of the Pomeranian Medical University, and study participants provided written informed consent for participation in the study.

AUTHOR CONTRIBUTIONS

WB, AD and TS developed and performed the clinical study protocols, as well as evaluated the clinical data. KD and BD developed the laboratory protocols and performed biochemical analyses. WB interpreted results, wrote and revised the article. All authors contributed to the article and approved its final version.

REFERENCES

1. Rawla P, Sunkara T, Gaduputi V. Epidemiology of Pancreatic Cancer: Global Trends, Etiology and Risk Factors. *World J Oncol* (2019) 10:10–27. doi: 10.14740/wjon1166
2. Ilic M, Ilic I. Epidemiology of Pancreatic Cancer. *World J Gastroenterol* (2016) 22:9694–705. doi: 10.3748/wjg.v22.i44.9694
3. Johnson AM, Kleczko EK, Nemenoff RA. Eicosanoids in Cancer: New Roles in Immunoregulation. *Front Pharmacol* (2020) 11:595498. doi: 10.3389/fphar.2020.595498
4. Das UN. "Cell Membrane Theory of Senescence" and the Role of Bioactive Lipids in Aging, and Aging Associated Diseases and Their Therapeutic Implications. *Biomolecules* (2021) 112:241. doi: 10.3390/biom11020241
5. Hisano Y, Hla T. Bioactive Lysolipids in Cancer and Angiogenesis. *Pharmacol Ther* (2019) 193:91–8. doi: 10.1016/j.pharmthera.2018.07.006
6. Verma G, Marella A, Shaquiquzzaman M, Alam M. Immunoinflammatory Responses in Gastrointestinal Tract Injury and Recovery. *Acta Biochim Pol* (2013) 60:143–9. doi: 10.18388/abp.2013_1964
7. Wang B, Wu L, Chen J, Dong L, Chen C, Wen Z, et al. Metabolism Pathways of Arachidonic Acids: Mechanisms and Potential Therapeutic Targets. *Signal Transduct Target Ther* (2021) 6:94. doi: 10.1038/s41392-020-00443-w
8. Calder P. Eicosanoids. *Essays Biochem* (2020) 64:423–41. doi: 10.1042/EBC20190083
9. Panigrahy D, Gilligan MM, Serhan CN, Kashfi K. Resolution of Inflammation: An Organizing Principle in Biology and Medicine. *Pharmacol Ther* (2021) 107879. doi: 10.1016/j.pharmthera.2021.107879
10. Serhan CN, Levy BD. Resolvins in Inflammation: Emergence of the Pro-Resolving Superfamily of Mediators. *J Clin Invest* (2018) 128:2657–69. doi: 10.1172/JCI97943
11. Chandrasekharan JA, Sharma-Walia N. Lipoxins: Nature's Way to Resolve Inflammation. *J Inflammation Res* (2015) 8:181–92. doi: 10.2147/JIR.S90380
12. Greene ER, Huang S, Serhan CN, Panigrahy D. Regulation of Inflammation in Cancer by Eicosanoids. *Prostaglandins Other Lipid Mediat* (2011) 96:27–36. doi: 10.1016/j.prostaglandins.2011.08.004
13. Lee HN, Na HK, Surh YS. Resolution of Inflammation as a Novel Chemopreventive Strategy. *Semin Immunopathol* (2013) 35:151–61. doi: 10.1007/s00281-013-0363-y
14. Fishbein A, Hammock BD, Serhan CN, Panigrahy D. Carcinogenesis: Failure of Resolution of Inflammation? *Pharmacol Ther* (2021) 218:107670. doi: 10.1016/j.pharmthera.2020.107670
15. de-Brito NM, da-Costa HC, Simoes RL, Barja-Fidalgo C. Lipoxin-Induced Phenotypic Changes in CD115 + LY6C Hi Monocytes TAM Precursors Inhibits Tumor Development. *Front Oncol* (2019) 9:540. doi: 10.3389/fonc.2019.00540
16. Khophai S, Thanee M, Techasen A, Namwat N, Klanrit P, Titapun A, et al. Zileuton Suppresses Cholangiocarcinoma Cell Proliferation and Migration Through Inhibition of the Akt Signaling Pathway. *Onco Targets Ther* (2018) 11:7019–29. doi: 10.2147/OTT.S178942
17. Claria J, Lee MH, Serhan CN. Aspirin-Triggered Lipoxins (15-Epi-LX) Are Generated by the Human Lung Adenocarcinoma Cell Line (A549)-Neutrophil Interactions and Are Potent Inhibitors of Cell Proliferation. *Mol Med* (1996) 2:583–96. doi: 10.1007/BF03401642
18. Gilligan MM, Gartung AA, Sulciner ML, Norris PC, Sukhatme VP, Bielenberg DR, et al. Aspirin-Triggered Proresolving Mediators Stimulate Resolution in Cancer. *Proc Natl Acad Sci USA* (2019) 116:6292–7. doi: 10.1073/pnas.1804000116
19. Deskur A, Salata D, Budkowska M, Dolegowska B, Starzynska T, Blogowski W. Selected Hemostatic Parameters in Patients With Pancreatic Tumors. *Am J Transl Res* (2014) 6:768–76.
20. Blogowski W, Dolegowska K, Deskur A, Dolegowska B, Starzynska T. An Attempt to Evaluate Selected Aspects of "Bone-Fat Axis" Function in Healthy Individuals and Patients With Pancreatic Cancer. *Medicine* (2015) 94:e1303. doi: 10.1097/MD.0000000000001303
21. Bodnarczuk T, Deskur A, Dolegowska K, Dolegowska B, Starzynska T, Blogowski W. Hydroxyeicosatetraenoic Acids in Patients With Pancreatic Cancer: A Preliminary Report. *Am J Cancer Res* (2018) 8:1865–72.
22. Madej-Michniewicz A, Budkowska M, Salata D, Dolegowska B, Starzynska T, Blogowski W. Evaluation of Selected Interleukins in Patients With Different Gastric Neoplasms: A Preliminary Report. *Sci Rep* (2015) 5:14382. doi: 10.1038/srep14382
23. Blogowski W, Madej-Michniewicz A, Marczuk N, Dolegowska B, Starzynska T. Interleukins 17 and 23 in Patients With Gastric Neoplasms. *Sci Rep* (2016) 6:37451. doi: 10.1038/srep37451
24. Zhang Q, Zhu B, Li Y. Resolution of Cancer-Promoting Inflammation: A New Approach for Anticancer Therapy. *Front Immunol* (2017) 8:71. doi: 10.3389/fimmu.2017.00071
25. Zhang T, Hao H, Zhou XY. The Role of Lipoxin in Regulating Tumor Immune Microenvironments. *Prostaglandins Other Lipid Mediat* (2019) 144:106341. doi: 10.1016/j.prostaglandins.2019.106341
26. Tian R, Zuo X, Jaoude J, Mao F, Colby J, Shureiqi I. ALOX15 as a Suppressor of Inflammation and Cancer: Lost in the Link. *Prostaglandins*

Other Lipid Mediat (2017) 132:77–83. doi: 10.1016/j.prostaglandins.2017.01.002
27. Janakiram NB, Rao CV. Role of Lipoxins and Resolvins as Anti-Inflammatory and Proresolving Mediators in Colon Cancer. *Curr Mol Med* (2009) 9:565–79. doi: 10.2174/156652409788488748
28. Knab LM, Grippo PJ, Bentrem DJ. Involvement of Eicosanoids in the Pathogenesis of Pancreatic Cancer: The Roles of Cyclooxygenase-2 and 5-Lipoxygenase. *World J Gastroenterol* (2014) 20:10729–39. doi: 10.3748/wjg.v20.i31.10729
29. Zhou GX, Ding XL, Wu SB, Zhang HF, Cao W, Qu LS, et al. Inhibition of 5-Lipoxygenase Triggers Apoptosis in Pancreatic Cancer Cells. *Oncol Rep* (2015) 33:661–8. doi: 10.3892/or.2014.3650
30. Hennig R, Ding XZ, Tong WG, Schneider MB, Standop J, Friess H, et al. 5-Lipoxygenase and Leukotriene B(4) Receptor Are Expressed in Human Pancreatic Cancers But Not in Pancreatic Ducts in Normal Tissue. *Am J Pathol* (2002) 161:421–8. doi: 10.1016/S0002-9440(10)64198-3
31. Schnittert J, Heinrich MA, Kuninty PR, Storm G, Prakash J. Reprogramming Tumor Stroma Using an Endogenous Lipid Lipoxin A4 to Treat Pancreatic Cancer. *Cancer Lett* (2018) 420:247–58. doi: 10.1016/j.canlet.2018.01.072
32. Zong L, Chen K, Jiang Z, Chen X, Sun L, Ma J, et al. Lipoxin A4 Reverses Mesenchymal Phenotypes to Attenuate Invasion and Metastasis *via* the Inhibition of Autocrine TGF-β1 Signaling in Pancreatic Cancer. *J Exp Clin Cancer Res* (2017) 36:181. doi: 10.1186/s13046-017-0655-5
33. Zong L, Li J, Chen X, Chen K, Li W, Li X, et al. Lipoxin A4 Attenuates Cell Invasion by Inhibiting ROS/ERK/MMP Pathway in Pancreatic Cancer. *Oxid Med Cell Longev* (2016) 2016:6815727. doi: 10.1155/2016/6815727
34. Chen A, Zhang Y, Sun D, Xu S, Guo Y, Wang X. Investigation of the Content Differences of Arachidonic Acid Metabolites in a Mouse Model of Breast Cancer by Using LC-MS/MS. *J Pharm BioMed Anal* (2021) 194:113763. doi: 10.1016/j.jpba.2020.113763
35. Ruan GT, Gong YZ, Zhu LC, Gao F, Liao XW, Wang XK, et al. The Perspective of Diagnostic and Prognostic Values of Lipoxygenases mRNA Expression in Colon Adenocarcinoma. *Onco Targets Ther* (2020) 13:9389–405. doi: 10.2147/OTT.S251965

Conflict of Interest: The authors declare that the research was conducted in the absence of any commercial or financial relationships that could be construed as a potential conflict of interest.

Publisher's Note: All claims expressed in this article are solely those of the authors and do not necessarily represent those of their affiliated organizations, or those of the publisher, the editors and the reviewers. Any product that may be evaluated in this article, or claim that may be made by its manufacturer, is not guaranteed or endorsed by the publisher.

frontiers in Oncology

ORIGINAL RESEARCH
published: 14 January 2022
doi: 10.3389/fonc.2021.790462

Pretherapeutic Assessment of Pancreatic Cancer: Comparison of FDG PET/CT Plus Delayed PET/MR and Contrast-Enhanced CT/MR

Zaizhu Zhang†, *Nina Zhou*†, *Xiaoyi Guo*, *Nan Li*, *Hua Zhu* and *Zhi Yang**

Key Laboratory of Carcinogenesis and Translational Research (Ministry of Education/Beijing), NMPA Key Laboratory for Research and Evaluation of Radiopharmaceuticals (National Medical Products Administration), Department of Nuclear Medicine; Peking University Cancer Hospital & Institute, Beijing, China

OPEN ACCESS

Edited by:
Min Li,
University of Oklahoma Health Sciences Center, United States

Reviewed by:
Fang Xie,
Fudan University, China
Tsukasa Ikeura,
Kansai Medical University, Japan

***Correspondence:**
Zhi Yang
pekyz@163.com

†*These authors have contributed equally to this work and share first authorship*

Specialty section:
This article was submitted to Gastrointestinal Cancers: Hepato Pancreatic Biliary Cancers, a section of the journal Frontiers in Oncology

Received: *06 October 2021*
Accepted: *20 December 2021*
Published: *14 January 2022*

Citation:
Zhang Z, Zhou N, Guo X, Li N, Zhu H and Yang Z (2022) Pretherapeutic Assessment of Pancreatic Cancer: Comparison of FDG PET/CT Plus Delayed PET/MR and Contrast-Enhanced CT/MR. Front. Oncol. 11:790462. doi: 10.3389/fonc.2021.790462

Purpose: This study aims to determine the diagnostic performance of whole-body FDG PET/CT plus delayed abdomen PET/MR imaging in the pretherapeutic assessment of pancreatic cancer in comparison with that of contrast-enhanced (CE)-CT/MR imaging.

Materials and Methods: Forty patients with pancreatic cancer underwent nonenhanced whole-body FDG PET/CT, delayed abdomen PET/MR imaging, and CE-CT/MR imaging. Two nuclear medicine physicians independently reviewed these images and discussed to reach a consensus, determining tumor resectability according to a 5-point scale, N stage (N0 or N positive), and M stage (M0 or M1). With use of clinical-surgical-pathologic findings as the reference standard, diagnostic performances of the two imaging sets were compared by using the McNemar test.

Results: The diagnostic performance of FDG PET/CT plus delayed PET/MR imaging was not significantly different from that of CE-CT/MR imaging in the assessment of tumor resectability [area under the receiver operating characteristic curve: 0.927 vs. 0.925 (p = 0.975)], N stage (accuracy: 80% (16 of 20 patients) vs. 55% (11 of 20 patients), p = 0.125), and M stage (accuracy: 100% (40 of 40 patients) vs. 93% (37 of 40 patients), p = 0.250). Moreover, 14 of 40 patients had liver metastases. The number of liver metastases detected by CE-CT/MR imaging, PET/CT, and PET/MR imaging were 33, 18, and 61, respectively. Compared with CE-CT/MR imaging, PET/MR imaging resulted in additional findings of more liver metastases in 9/14 patients, of which 3 patients were upstaged. Compared with PET/CT, PET/MR imaging resulted in additional findings of more liver metastases in 12/14 patients, of which 6 patients were upstaged.

Conclusions: Although FDG PET/CT plus delayed PET/MR imaging showed a diagnostic performance similar to that of CE-CT/MR imaging in the pretherapeutic assessment of the resectability and staging of pancreatic tumors, it still has potential as the more efficient and reasonable work-up approach for the additional value of metastatic information provided by delayed PET/MR imaging.

Keywords: pancreatic cancer, contrast-enhanced CT/MR, FDG, PET/CT, PET/MR

INTRODUCTION

Pancreatic cancer remains a highly lethal malignancy, with a 5-year survival rate of less than 10%, and is the seventh most common cause of cancer death in both men and women worldwide (1–3). The only potential curative treatment for pancreatic cancer is radical surgical resection (4). However, at the time of initial staging work-up, approximately 80%–85% of patients present with either unresectable or metastatic disease owing to lack of early and specific symptoms when the cancer is still localized, and high metastasis rate (1, 3, 4). Given this, imaging examinations are destined to play an irreplaceable role in early diagnosis and accurate staging, which are crucial for choosing appropriate therapy strategy and preventing unnecessary surgery (5, 6).

Various anatomical imaging modalities including contrast-enhanced computed tomography (CE-CT), magnetic resonance (MR) imaging, and endoscopic ultrasonography are routinely used in the initial staging work-up of pancreatic cancer (5, 7), with CE-CT considered the most commonly used and best validated imaging modality (3, 7). In addition to anatomical imaging examinations, another modality that has shown potential is fluorine 18 fluorodeoxyglucose (FDG) positron emission tomography (PET)/CT, which is sensitive for initial TNM staging (8), evaluation of treatment response (9), detection of recurrence (10), and prediction of treatment efficacy and clinical outcome and has been reported to improve the detection of occult metastases, ultimately sparing these patients from unnecessary surgery (11–13). Recently, PET/MR, as an emerging imaging technology, provides both multiparametric functional imaging, including diffusion-weighted imaging (DWI), and metabolic information from PET, with many potential advantages over PET/CT, including inherently lower radiation exposure, higher soft-tissue contrast, and multiparametric imaging capabilities (5, 7, 14–19).

Coincidentally, due to the different advantages of each imaging modality, multiple imaging modalities are being increasingly used in patients with pancreatic cancer, and this multistep examination process probably leads to delayed surgical treatment for resectable diseases (20, 21). Hence, developing the more efficient and reasonable work-up approach is of great clinical significance for patients with pancreatic cancer. Indeed, a previous study has demonstrated a similar diagnostic performance between FDG PET/MR and PET/CT plus CE-CT in the preoperative evaluation of the resectability and staging of pancreatic tumors (7). To our knowledge, however, the comparison of diagnostic performance between nonenhanced whole-body FDG PET/CT plus delayed abdomen PET/MR and CE-CT/MR for tumor staging and resectability of pancreatic tumors has not been reported. Thus, the purpose of this study was to compare the diagnostic performance of nonenhanced whole-body FDG PET/CT plus delayed abdomen PET/MR in evaluating tumor staging and resectability of pancreatic cancer with that of the conventional CE-CT/MR, which would be useful for simplifying the multistep process and even choosing the more efficient and reasonable work-up flow.

MATERIALS AND METHODS

Patients

This study was performed under a single-center prospective imaging protocol and was approved by the Medical Ethics Committee of Peking University Cancer Hospital (ethical approval No. 2018KT110-GZ01). All patients provided signed informed consent before the examinations.

From December 2019 to April 2021, 67 consecutive patients (33 men and 34 women; mean age ± standard deviation, 60.5 years ± 10.9) with histologically confirmed or suspected pancreatic cancer were prospectively and consecutively enrolled in this study. These candidates took a whole-body nonenhanced FDG PET/CT scan first, followed by a delayed abdomen PET/MR scan with a 120–180-min interval. The key eligibility criteria were as follows: (a) confirmatory evidence with either histology or metastases at follow-up imaging; (b) patients have undergone chest CT, abdomen, and pelvis CE-CT/MR, and the interval time between PET and CT/MR was less than 30 days; and (c) no contraindication to PET/MR imaging. Additionally, patients with any of the following conditions were excluded: (a) age <18 or >80 years old and (b) insufficient follow-up to confirm the reference standard.

Image Acquisition

^{18}F-FDG PET/CT

Imaging was performed using a PET/CT scanner (Biograph64, SIEMENS, Erlangen, Germany) operated in 3D Flow Motion (bed entry speed 1 mm/s) from the apex of the skull to the mid-thigh, with a PET axial field of view of 21.6 cm. The PET images were reconstructed by the TrueX + TOF method offered by the vendor. Low-dose CT scans were acquired in CARE Dose4D mode (120 kV, 3.0 mm slice thickness). The patients were instructed to fast for at least 6 h before ^{18}F-FDG injection. In all cases, the serum glucose concentration met our institutional requirement (≤140 mg/dl). The injected activity was 3.7 MBq/kg, and the time from injection to scan was 60 min.

^{18}F-FDG PET/MR Imaging

^{18}F-FDG PET/MR imaging was performed on an integrated 3.0 T time-of-flight PET/MR scanner (uPMR790, UIH, Shanghai, China). The scan started at 120 min (range: 120–180 min) after FDG-administration. Each patient underwent the same protocol as described in the following. Body array coil was placed around the individual and covered the entire liver and pancreas. Respiratory gating was used in MR acquisition whenever possible. PET reconstruction was conducted using a 3D-OSEM (Ordered Subsets Expectation-Maximization) algorithm applied on a 256 × 256 matrix. A four-compartment-model attenuation map (μ-map) automatically generated based on a water-fat-imaging MR sequence was used for PET attenuation correction. The PET images were smoothed by a Gaussian filter with 3 mm full width at half maximum (FWHM). The MR sequences were performed simultaneously with PET acquisition, including T1-weighted imaging (T1WI), T2-weighted imaging (T2WI), fat-suppressed T2WI, and DWI. The mean scan time for PET/MR was 20 ± 6 min.

Image Interpretation

All images were reviewed using our local picture archiving and communication system (PACS). To avoid bias, two experienced nuclear medicine physicians independently analyzed the nonenhanced whole-body FDG PET/CT, delayed abdomen PET/MR images, and CE-CT/MR images, and the results were discussed to reach a consensus (**Figure 1**).

Assessment of Tumor Resectability

The reviewers determined the resectability of pancreatic tumors on the basis of tumor location, tumor–vascular contact, adjacent organ invasion, and metastatic disease based on a 5-point scale, as follows: 5, definitely resectable; 4, probably resectable; 3, equivocal; 2, probably unresectable; and 1, definitely unresectable (7). Unresectable disease was further specified as locally advanced disease (i.e., pancreatic cancer without distant metastasis but with unresectable vascular invasion) or pancreatic cancer with distant metastasis (22, 23).

Determination of N Stage

The maximum standardized uptake value (SUVmax) of the lymph nodes was calculated in the same lesion on both FDG PET/CT and delayed PET/MR images. Regions of interest were drawn around foci with increased uptake in the transaxial slices, and an original SUVmax was automatically obtained. To ensure SUVmax relatively comparable, the original SUVmax was normalized by the following formula (24):

$$\text{Normalized SUV max} = \text{Original SUV max} / \text{SUV}_{\text{bkgd}}$$

SUV_{bkgd} refers to average SUV of the descending aorta.

Positive lymph nodes were determined on the basis of their size and quantitative assessment of PET images. If the largest regional lymph node was at least 8 mm in its shortest diameter (7) or the uptake greater than the blood pool (normalized SUVmax >1) at quantitative assessment of early or delayed PET scans (25), the patient would be considered node positive, but otherwise as negative.

Determination of M Stage

At PET/MR imaging, the lesions were rated as metastases when at least two of the three following criteria were met: (a) abnormal signal intensity on T2WI, (b) diffusion restriction on DWI with *b* values of 800 s/mm^2, and (c) positivity on PET scans at visual assessment. At PET/CT imaging, the lesions were defined as metastases when PET had positive uptake foci with abnormal density on CT. At CE-CT/MR imaging, the lesions were determined as metastases when they had abnormal density/signal intensity with abnormal enhancement.

Reference Standard

The reference standard for tumor resectability was based on surgical records, pathological findings, and imaging-based decisions. In patients who underwent surgery, tumor resectability was assessed in light of surgical records and pathologic reports, as follows: R0 resection (complete tumor resection with a negative resection margin) was defined as resectable and R1 resection (uncomplete tumor resection with a microscopically positive resection margin) and R2 resection (uncomplete tumor resection with a macroscopically positive resection margin) as no resection of the pancreatic mass due to

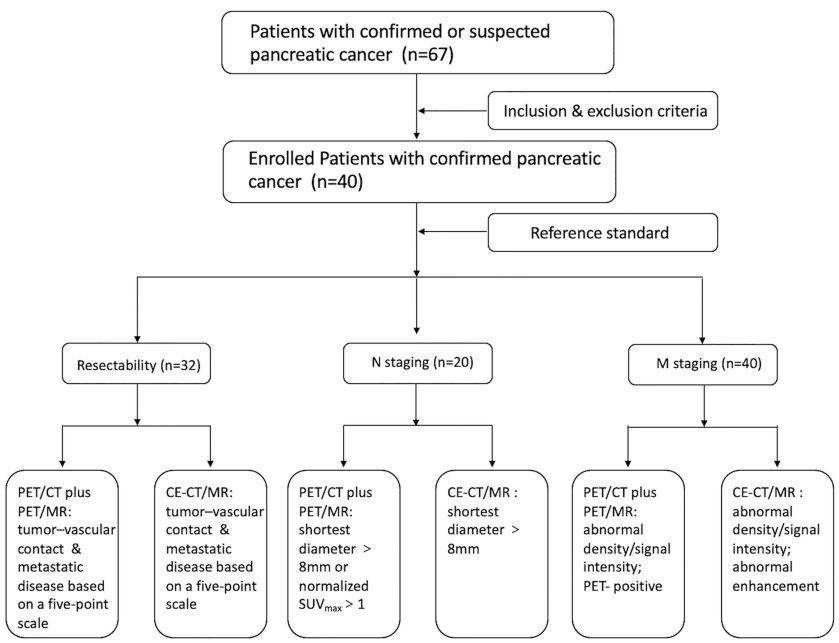

FIGURE 1 | The flow chart of the study.

unresectability confirmed during surgery, and presence of pathologically confirmed distant metastasis were defined as unresectable (7). Additionally, if a patient had distant metastases and/or locally unresectable tumor at preoperative imaging and did not undergo surgery based on a multidisciplinary conference, the patient was also considered unresectable (7). For N staging, the reference standard was determined by the pathologic findings in patients who underwent regional lymph node dissection (7). For M staging, the reference standard of M0 was determined with histopathologic findings or follow-up images, whereas that of M1 was determined with histopathologic results or imaging-based decisions made by means of a multidisciplinary conference (7).

Statistical Analysis

Diagnostic performances for per-patient resectability, N staging, and M staging were evaluated in patients by using standards of reference. Tumor resectability was evaluated with empirical receiver operating characteristic curve analysis based on a 5-point confidence scale. The area under the receiver operating characteristic curve (AUC) was regarded as an indicator of diagnostic performance, and areas under the receiver operating characteristic curve values of PET/CT plus delayed PET/MR imaging and CE-CT/MR imaging were compared by using the *z*-test. Furthermore, the examinations given scores of 4 or 5 (probably or definitely resectable) were defined as resectable. For tumor resectability, N stage and M stage, sensitivity, specificity, and accuracy were compared between PET/CT plus delayed PET/MR imaging and CE-CT/MR imaging by using the McNemar test. Moreover, for per-lesion analysis, the numbers of liver metastases detected by PET/CT plus PET/MR imaging were compared with only PET/CT or CE-CT/MR imaging. All statistical analyses were performed using MedCalc, version 20.0.4 (MedCalc Software, Mariakerke, Belgium). Two-tailed $p < 0.05$ was considered to indicate a significant difference.

RESULTS

Patient Characteristics

On the basis of the inclusion and exclusion criteria, 40 patients (23 men and 17 women; mean age ± standard deviation, 58.9 years ± 9.1) were enrolled finally, of which 24 patients underwent CE-CT scan, and the remaining 16 patients underwent CE-MR scan. Among the 40 patients, the tumor resectability was confirmed in 32 patients (resectable, $n = 17$; unresectable, $n = 15$) based on surgery and distant metastases. Tumor resectability could not be confirmed in 8 patients, which were lost to follow-up. N stage was confirmed with histopathologic findings in 20 patients who underwent surgical resection for pancreatic cancer (node negative, $n = 7$; node positive, $n = 13$), and M stage was confirmed in 40 patients (M0, $n = 23$; M1, $n = 17$) by means of histopathologic reports (M0, $n = 19$; M1, $n = 5$) or imaging-based diagnosis (M0, $n = 4$; M1, $n = 12$). The M1 stage results include 14 patients with hepatic metastases confirmed with surgery ($n = 1$), biopsy ($n = 3$) and imaging-based diagnosis ($n = 10$), 5 patients with peritoneal seeding metastases found with biopsy ($n = 1$) and imaging-based diagnosis ($n = 4$), and three patients with an imaging-based diagnosis of pulmonary metastases. None of them underwent neoadjuvant chemo/chemoradiotherapy before these imaging examinations. The remaining basic characteristics, like tumor size, tumor location, and tumor SUVmax, are presented in **Table 1**.

Assessment of Tumor Resectability and N and M Staging

Tumor Resectability ($n = 32$)

For the evaluation of per-patient tumor resectability, there were no significant differences in the AUC between PET/CT plus delayed PET/MR imaging and CE-CT/MR imaging [0.927 vs. 0.925 ($p = 0.975$)] (**Table 2**). When scores of 4 and 5 (i.e., probably or definitely resectable) were categorized as indicating an imaging diagnosis of tumor resectability, PET/CT plus delayed PET/MR imaging and CE-CT/MR imaging showed the same accuracies of 88% (28 of 32 patients) versus 88% (28 of 32 patients), without a significant difference ($p = 1.000$) (**Table 2**; **Figure 2**). Moreover, PET/CT plus delayed PET/MR imaging showed the same sensitivity and specificity as CE-CT/MR imaging (82% (14 of 17 patients) vs. 82% (14 of 17 patients), and 93% (14 of 15 patients) vs. 93% (14 of 15 patients), respectively), although there were no statistically significant differences (**Table 2**).

N Staging ($n = 20$)

For N staging, diagnostic accuracies were not significantly different between the two image sets (80% (16 of 20 patients) with PET/CT plus delayed PET/MR imaging vs. 55% (11 of 20 patients) with CE-CT/MR imaging ($p = 0.125$) (**Table 3**). In the depiction of any regional lymph node metastasis per patient, PET/CT plus delayed PET/MR imaging showed higher sensitivity [92% (12 of 13 patients) vs. 46% (6 of 13 patients)], with a statistically significant difference ($p = 0.031$) and lower specificity [57% (4 of 7 patients) vs. 71% (5 of 7 patients)] than CE-CT/MR imaging, without a statistically significant difference ($p = 1.000$) (**Table 3**).

M Staging ($n = 40$)

For M staging, PET/CT plus delayed PET/MR imaging and CE-CT/MR imaging demonstrated sensitivities of 100% (17 of 17 patients) and 82% (14 of 17 patients), without a statistically significant difference ($p = 0.250$) (**Table 3**). Both imaging sets showed high specificity [100% (23 of 23 patients)] for M staging. In addition, diagnostic accuracies were not significantly different between the two image sets (100% (40 of 40 patients) with PET/CT plus delayed PET/MR imaging vs. 93% (37 of 40 patients) with CE-CT/MR imaging ($p = 0.250$) (**Table 3**).

Additional Value of PET/MR in Patients With Liver Metastases ($n = 14$)

Of the 40 patients, 14 patients had liver metastases (see **Table 4**; **Figures 3**, **4**). For the lesion-based analysis, the number of liver

TABLE 1 | Basic information of the 40 patients with pancreatic cancer.

Characteristic	Value
Age (years)	58.9 ± 9.1 (40–75)
Gender (M/F)	23/17
Tumor number (*n*)	40
Maximum lesion diameter in axial section (cm)	3.5 + 2.2 (0.9–13.7)
Location	
Head	20 (50)
Neck	3 (7.5)
Body	10 (25)
Tail	7 (17.5)
Tumor SUVmax	
PET/CT	6.2 ± 2.6 (0.9–12.2)
PET/MR	4.9 ± 2.3 (0.9–9.3)
Tumor resectability (*n*)	32
Resectable	17 (53.1)
Unresectable	15 (46.9)
N stage (*n*)	20
Positive	13 (65)
Negative	7 (35)
M stage (*n*)	40
M0	23 (57.5)
M1	17 (42.5)

The data presented are means ± standard deviation (range) or number (percentage) of patients.

metastases detected by CE-CT/MR imaging, PET/CT and PET/MR imaging were 33, 18, and 61, respectively. For the patient-based analysis, compared with CE-CT/MR imaging, PET/MR imaging resulted in additional findings of more metastases in 9/14 patients. Specifically, 3/14 patients with liver metastases were upstaged. Compared with PET/CT, PET/MR imaging resulted in additional findings of more metastases in 12/14 patients, of which 6 patients were upstaged.

DISCUSSION

In this prospective study, we demonstrated that nonenhanced whole-body FDG PET/CT plus delayed abdomen PET/MR imaging showed similar diagnostic performance without a statistically significant difference in the assessment of the tumor resectability and M stage of pancreatic tumors compared with the widely used CE-CT/MR imaging. Excitedly, based on the combination of size and normalized SUVmax of lymph nodes, PET/CT plus delayed PET/MR imaging showed higher sensitivity than CE-CT/MR imaging, with a statistically significant difference. What is more, the number of total liver metastases detected by delayed PET/MR imaging was nearly twice of that of CE-CT/MR imaging. Although this study is only exploratory, with a small number of patients, to our knowledge, the findings are the first to suggest that the combination of nonenhanced whole-body FDG PET/CT and delayed abdomen PET/MR imaging may be a more reasonable examining approach for the preoperative evaluation of pancreatic cancer, hopefully substituting for the widely used CE-CT and leading to improvement in creating a more efficient work-up flow. Indeed, Raman et al. (26) have reported that the accuracy of multidetector CT in excluding distant metastatic disease in patients with pancreatic cancer significantly depreciates over time because the tumor can metastasize during the interval between multidetector CT and surgery. Therefore, FDG PET/CT plus delayed PET/MR imaging may play a valuable role in simplifying the work-up flow and shortening the work-up period of pancreatic tumors, avoiding conversion from resectable status to unresectable status due to the rapidly progressive characteristic of pancreatic tumors.

Patients with pancreatic cancer could benefit from upfront pancreatic resection when achieving a curative resection with negative margins; thus, precise preoperative assessment of tumor resectability is vital (27). Pancreatic cancer resectability is determined primarily by the degree of tumor–vascular contact and distant metastasis (22, 23). In our study, no significant differences of evaluating tumor resectability were observed between PET/CT plus delayed PET/MR imaging and CE-CT/MR imaging. For the evaluation of the presence and/or extent of vascular involvement, CE-CT, with its superior spatial resolution and ability to perform multiplanar and 3D reconstructions to depict vascular involvement, has been regarded as the best method to determine surgical resectability (3, 28). However, in our study, based on the blood flowing void effect at 4 mm-slice T2WI, nonenhanced PET/MR imaging and CE-CT/MR imaging had equivalent diagnostic performance in terms of vascular invasion. Considering that most of our patients with resectable or borderline resectable pancreatic tumors, our study performance may actually have been overestimated. Admittedly, for the evaluation of distant metastasis, PET/MR imaging combines the excellent soft-tissue contrast of MR imaging with the high sensitivity of PET, enabling the depiction of subtle metastatic lesions, which can directly upstage patients from potentially resectable status to metastatic unresectable status. Thus, we considered that nonenhanced PET/CT plus delayed PET/MR imaging has potential as a substitute for CE-CT/MR imaging in assessment of resectability, certainly, which still remains a large sample of research.

TABLE 2 | Diagnostic performance of PET/CT plus delayed PET/MR imaging and CE-CT/MR imaging in the assessment of tumor resectability.

Modality	A_z^a	Sensitivity (%)[b]	Specificity (%)[b]	Accuracy (%)[b]
PET/CT plus PET/MR	0.927 (0.778, 0.989)	82 (14/17)	93 (14/15)	88 (28/32)
CE-CT/MR	0.925 (0.775, 0.988)	82 (14/17)	93 (14/15)	88 (28/32)
p-value	0.975	NA	1.000	1.000

NA, not assessable; A_z, area under the receiver operating characteristic curve.
[a]Data were calculated with the z-test. Numbers in parentheses are 95% CIs.
[b]Calculated with the McNemar's test. Numbers in parentheses are numbers of patients.

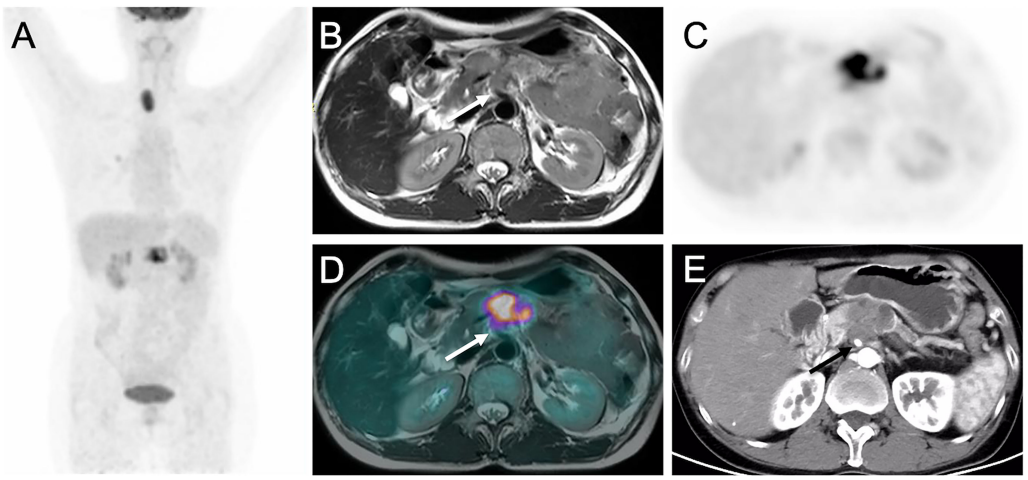

FIGURE 2 | Images of pancreatic ductal adenocarcinoma in 52-year-old woman with vascular invasion. **(A)** MIP from PET/CT showing increased uptake in pancreas. **(B)** T2WI, **(C)** Delayed PET image, **(D)** Corresponding PET/MR imaging fusion image and **(E)** Arterial phase CT image show the mass in the body of pancreas encasing superior mesenteric artery (arrows).

TABLE 3 | Diagnostic performance of PET/CT plus delayed PET/MR imaging and CE-CT/MR imaging in the assessment of N and M stages.

Modality	N staging (%)			M staging (%)		
	Sensitivity	Specificity	Accuracy	Sensitivity	Specificity	Accuracy
PET/CT plus PET/MR	92 (12/13)	57 (4/7)	80 (16/20)	100 (17/17)	100 (23/23)	100 (40/40)
CE-CT/MR	46 (6/13)	71 (5/7)	55 (11/20)	82 (14/17)	100 (23/23)	93 (37/40)
p-value	0.031	1.000	0.125	0.250	NA	0.250

NA, not assessable.

p-values were calculated by using the McNemar's test. Data in parentheses are numbers of patients used to calculate percentages.

Accurate assessment of lymph node metastases in patients with pancreatic cancer plays an important role in the prediction of a patient's prognosis (29). In our study, which used imaging criteria of size (shortest diameter >8 mm) and PET positivity (normalized SUVmax >1) for N staging, PET/CT plus delayed PET/MR imaging showed higher sensitivities than common CE-CT/MR imaging with a statistically significant difference. The result suggests that PET/CT plus delayed PET/MR imaging, which provides both anatomic and metabolic information, can be useful in the detection and characterization of metastatic lymph nodes. However, our preliminary study failed to demonstrate a significant difference between PET/CT plus delayed PET/MR imaging and CE-CT/MR imaging in the specificity and accuracy. This can be attributed to the limitation of size-based assessment that reactive lymph nodes can be enlarged and small lymph nodes can have micrometastases (30). In addition, PET also had limited performance in the detection of lymph node metastases because PET positivity can also be found in the inflammatory and anthracosilicostic nodes (31). Notably, we are the first to select the either parameter of normalized SUVmax from PET/CT or delayed PET/MR imaging to evaluate lymph node metastases, with a good result in the higher sensitivities. Thus, PET/CT plus delayed PET/MR imaging has potential as a valuable tool for N staging and future studies with a larger population are warranted.

As for M staging, most commonly, metastatic disease from pancreatic cancer is observed in the liver (32). Thus, liver metastases in patients with pancreatic cancer should raise suspicion of M1 disease and then, the change from M0 to M1 can directly result in a change from resectability to unresectability. In our study, although diagnostic performance did not significantly differ between PET/CT plus delayed PET/MR imaging and CE-CT/MR imaging in our study, the number of liver metastases detected by delayed PET/MR imaging was nearly twice that of CE-CT/MR imaging and three times that of PET/CT. Although PET/CT was considered as an ideal imaging modality to detect distant metastases that may be missed using other modalities, the study by Fröhlich et al. (33) indicated that PET/CT has high sensitivity (97%) in detecting metastases larger than 1 cm in diameter, sensitivity falls to 43% for smaller lesions, which may be the reason for the less liver metastases detected by PET/CT than PET/MR imaging and CE-CT/MR imaging. However, in the light of the fact that noncontrast MR imaging has far superior soft tissue discrimination compared with noncontrast CT and has also been found to be superior to CT

TABLE 4 | Diagnostic performance of PET/CT plus delayed PET/MR imaging and CE-CT/MR imaging in the detection of liver metastases.

Patients	CE-CT/MR		PET/CT		PET/MR		CE-CT/MR vs PET/MR		PET/CT vs PET/MR	
	M stage	Number	M stage	Number	M stage	Number	Additional finding in PET/MR	Staging change	Additional finding in PET/MR	Staging change
1	1	3	1	3	1	3	None	None	None	None
2	1	6	1	3	1	12	More metastases	None	More metastases	None
3	1	2	0	0	1	2	None	None	More metastases	Up
4	1	5	1	1	1	5	None	None	More metastases	None
5	1	1	0	0	1	2	More metastases	None	More metastases	Up
6	1	1	0	0	1	3	More metastases	None	More metastases	Up
7	1	4	1	2	1	5	More metastases	None	More metastases	None
8	0	0	0	0	1	6	More metastases	Up	More metastases	Up
9	0	0	0	0	1	2	More metastases	Up	More metastases	Up
10	1	4	1	2	1	6	More metastases	None	More metastases	None
11	1	1	0	0	1	1	None	None	More metastases	Up
12	1	2	1	1	1	3	More metastases	None	More metastases	None
13	0	0	1	2	1	7	More metastases	Up	More metastases	None
14	1	4	1	4	1	4	None	None	None	None
Sum	11	33	8	18	13	61	9	3	12	6

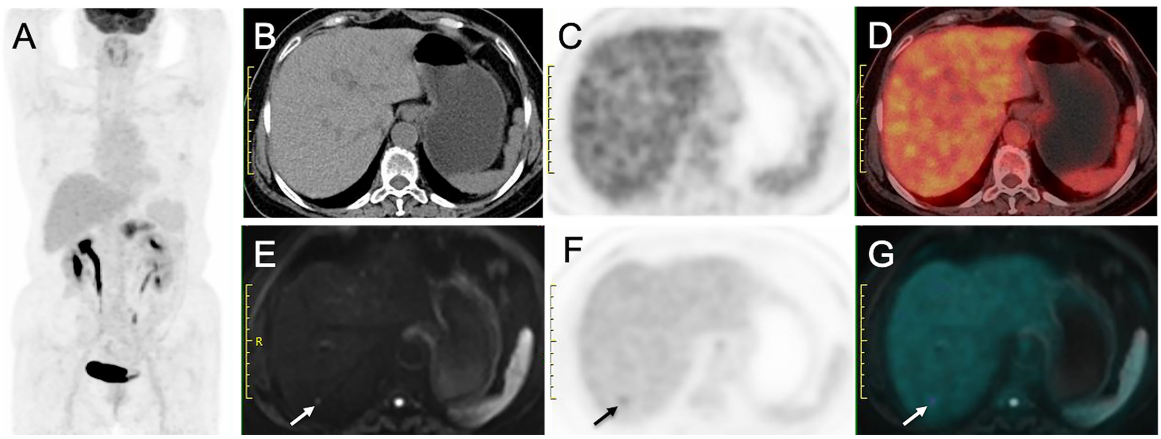

FIGURE 3 | Liver metastasis detected on PET/MRI but not on PET/CT. **(A)** MIP from PET/CT showing increased uptake in pancreas. **(B)** Nonenhanced CT image, **(C)** Early PET image and **(D)** PET/CT fusion image show no hypoattenuating or hypermetabolic lesion in liver. **(E)** DW image (b = 800 sec/mm2) shows a nodule with restricted diffusion (arrow). **(F)** Delayed PET image shows a hypermetabolic lesion in liver. **(G)** Corresponding PET/MR imaging fusion image shows the nodule with both hyperintense and hypermetabolism. This patient was diagnosed as having stage M1 disease on PET/MR imaging but stage M0 disease on PET/CT.

in the detection of liver metastases with a sensitivity of 90%–93% (34), we believed that PET/MR imaging can make up for the disadvantage of PET/CT. Notably, the PET imaging performance of delayed PET/MR is also better than that of PET/CT, which is different from the previous results that the PET imaging performance of PET/MR imaging would be similar to that of PET/CT (7, 35, 36). This may be the foremost reason for that delayed PET/MR imaging had the largest number of liver metastases of the three imaging systems. Our result demonstrated delayed PET/MR imaging has a potential as the most valuable imaging modality for the detection of liver metastases on the basis of the good performance of both delayed PET and MR imaging, especially for the delayed PET imaging performance, which can be conducive to accurate M staging.

This study had several limitations. First, the number of patients in this prospective study is relatively small, so these first results have to be considered preliminary and need further confirmation. Second, we could not match the imaging-based diagnosis of vascular involvement and/or lymph node status with the corresponding pathological results, so we assessed the resectability and staging of pancreatic tumors on a patient-by-patient basis rather than on a lesion-by-lesion basis. Third, given that the imaging features of pancreatic tumor reported by numerous studies, we did not evaluate the size, conspicuity and PET-related parameters of pancreatic tumor, and did not compare PET-related parameters at PET/CT and delayed PET/MR imaging.

In conclusion, nonenhanced whole-body FDG PET/CT plus delayed abdomen PET/MR imaging showed comparable diagnostic performance with CE-CT/MR imaging in the

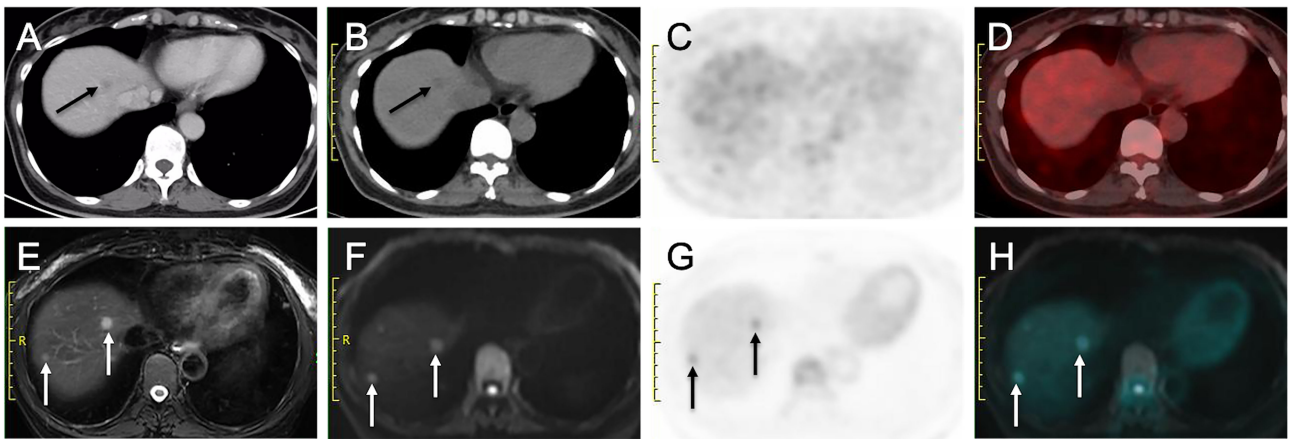

FIGURE 4 | More liver metastases detected on delayed PET/MRI than on CE-CT and early PET/CT. **(A)** Venous phase CT image shows a hypo-enhanced nodule in liver (arrow). **(B)** Nonenhanced CT image shows a hypoattenuating nodule in liver (arrow), **(C)** Early PET image and **(D)** Corresponding PET/CT fusion image show that the nodule does not show obvious hypermetabolism. **(E)** Fat-suppressed T2WI shows two hyperintense nodules in liver (arrows). **(F)** DW image (b = 800 sec/mm2) shows two nodules with restricted diffusion (arrows). **(G)** Delayed PET image shows two hypermetabolic nodules in liver (arrows). **(H)** Corresponding PET and DW fusion image shows the two nodules with both hyperintense and hypermetabolism (arrows).

evaluation of the resectability and staging of pancreatic cancers; furthermore, it provided additional value of detecting liver metastases, which still has potential as the more efficient and reasonable work-up approach.

DATA AVAILABILITY STATEMENT

The original contributions presented in the study are included in the article/supplementary material. Further inquiries can be directed to the corresponding author.

ETHICS STATEMENT

This study was approved by the 76 Medical Ethics Committee of Peking University Cancer Hospital (ethical approval No. 2018KT110-77 GZ01). All patients provided signed informed consent before the examinations.

AUTHOR CONTRIBUTIONS

ZZ and NZ substantially contributed to designing the study and drafting the manuscript. XG and HZ contributed to the acquisition, analysis, or interpretation of the data. NL and ZY revised it critically for important intellectual content. ZY finally approved the version to be published and agreed to be accountable for all aspects of the work in ensuring that questions related to the accuracy or integrity of any part of the work are appropriately investigated and resolved. All authors contributed to the article and approved the submitted version.

FUNDING

The current research was financially supported by the Science Foundation of Peking University Cancer Hospital (No. 2021-4) and Beijing Municipal Administration of Hospitals, Yangfan Project (ZYLX201816).

REFERENCES

1. Siegel RL, Miller KD, Jemal A. Cancer Statistics, 2020. *CA: Cancer J Clin* (2020) 70(1):7–30. doi: 10.3322/caac.21590
2. Bray F, Ferlay J, Soerjomataram I, Siegel RL, Torre LA, Jemal A. Global Cancer Statistics 2018: GLOBOCAN Estimates of Incidence and Mortality Worldwide for 36 Cancers in 185 Countries. *CA: Cancer J Clin* (2018) 68 (6):394–424. doi: 10.3322/caac.21492
3. Mizrahi JD, Surana R, Valle JW, Shroff RT. Pancreatic Cancer. *Lancet* (2020) 395(10242):2008–20. doi: 10.1016/s0140-6736(20)30974-0
4. Lau SC, Cheung WY. Evolving Treatment Landscape for Early and Advanced Pancreatic Cancer. *World J Gastrointest Oncol* (2017) 9(7):281–92. doi: 10.4251/wjgo.v9.i7.281
5. Lee JW, JH O, Choi M, Choi JY. Impact of F-18 Fluorodeoxyglucose PET/CT and PET/MRI on Initial Staging and Changes in Management of Pancreatic Ductal Adenocarcinoma: A Systemic Review and Meta-Analysis. *Diagnostics (Basel Switzerl)* (2020) 10(11):952. doi: 10.3390/diagnostics10110952
6. Wang Z, Chen JQ, Liu JL, Qin XG, Huang Y. FDG-PET in Diagnosis, Staging and Prognosis of Pancreatic Carcinoma: A Meta-Analysis. *World J Gastroenterol* (2013) 19(29):4808–17. doi: 10.3748/wjg.v19.i29.4808
7. Joo I, Lee JM, Lee DH, Lee ES, Paeng JC, Lee SJ, et al. Preoperative Assessment of Pancreatic Cancer With FDG PET/MR Imaging Versus FDG PET/CT Plus Contrast-Enhanced Multidetector CT: A Prospective Preliminary Study. *Radiology* (2017) 282(1):149–59. doi: 10.1148/radiol.2016152798
8. Yeh R, Dercle L, Garg I, Wang ZJ, Hough DM, Goenka AH. The Role of 18F-FDG PET/CT and PET/MRI in Pancreatic Ductal Adenocarcinoma.

Abdominal Radiol (NY) (2018) 43(2):415–34. doi: 10.1007/s00261-017-1374-2
9. Yoshioka M, Sato T, Furuya T, Shibata S, Andoh H, Asanuma Y, et al. Role of Positron Emission Tomography With 2-Deoxy-2-[18F]Fluoro-D-Glucose in Evaluating the Effects of Arterial Infusion Chemotherapy and Radiotherapy on Pancreatic Cancer. *J Gastroenterol* (2004) 39(1):50–5. doi: 10.1007/s00535-003-1244-2
10. Sperti C, Pasquali C, Bissoli S, Chierichetti F, Liessi G, Pedrazzoli S. Tumor Relapse After Pancreatic Cancer Resection is Detected Earlier by 18-FDG PET Than by CT. *J Gastrointest Surg Off J Soc Surg Alimentary Tract* (2010) 14 (1):131–40. doi: 10.1007/s11605-009-1010-8
11. Kim R, Prithviraj G, Kothari N, Springett G, Malafa M, Hodul P, et al. PET/CT Fusion Scan Prevents Futile Laparotomy in Early Stage Pancreatic Cancer. *Clin Nucl Med* (2015) 40(11):e501–5. doi: 10.1097/rlu.0000000000000837
12. Rijkers AP, Valkema R, Duivenvoorden HJ, van Eijck CH. Usefulness of F-18-Fluorodeoxyglucose Positron Emission Tomography to Confirm Suspected Pancreatic Cancer: A Meta-Analysis. *Eur J Surg Oncol J Eur Soc Surg Oncol Br Assoc Surg Oncol* (2014) 40(7):794–804. doi: 10.1016/j.ejso.2014.03.016
13. Farma JM, Santillan AA, Melis M, Walters J, Belinc D, Chen DT, et al. PET/CT Fusion Scan Enhances CT Staging in Patients With Pancreatic Neoplasms. *Ann Surg Oncol* (2008) 15(9):2465–71. doi: 10.1245/s10434-008-9992-0
14. Yoo HJ, Lee JS, Lee JM. Integrated Whole Body MR/PET: Where Are We? *Korean J Radiol* (2015) 16(1):32–49. doi: 10.3348/kjr.2015.16.1.32
15. Furtado FS, Ferrone CR, Lee SI, Vangel M, Rosman DA, Weekes C, et al. Impact of PET/MRI in the Treatment of Pancreatic Adenocarcinoma: A Retrospective Cohort Study. *Mol Imaging Biol* (2021) 23(3):456–66. doi: 10.1007/s11307-020-01569-7
16. Jha P, Bijan B, Melendres G, Shelton DK. Hybrid Imaging for Pancreatic Malignancy: Clinical Applications, Merits, Limitations, and Pitfalls. *Clin Nucl Med* (2015) 40(3):206–13. doi: 10.1097/rlu.0000000000000677
17. Quick HH. Integrated PET/Mr. *J Magn Reson Imaging JMRI* (2014) 39 (2):243–58. doi: 10.1002/jmri.24523
18. Broski SM, Goenka AH, Kemp BJ, Johnson GB. Clinical PET/MRI: 2018 Update. *AJR Am J Roentgenol* (2018) 211(2):295–313. doi: 10.2214/ajr.18.20001
19. Torigian DA, Zaidi H, Kwee TC, Saboury B, Udupa JK, Cho ZH, et al. PET/MR Imaging: Technical Aspects and Potential Clinical Applications. *Radiology* (2013) 267(1):26–44. doi: 10.1148/radiol.13121038
20. Shrikhande SV, Barreto SG, Goel M, Arya S. Multimodality Imaging of Pancreatic Ductal Adenocarcinoma: A Review of the Literature. *HPB Off J Int Hepato Pancreato Biliary Assoc* (2012) 14(10):658–68. doi: 10.1111/j.1477-2574.2012.00508.x
21. Pietryga JA, Morgan DE. Imaging Preoperatively for Pancreatic Adenocarcinoma. *J Gastrointest Oncol* (2015) 6(4):343–57. doi: 10.3978/j.issn.2078-6891.2015.024
22. Hong SB, Lee SS, Kim JH, Kim HJ, Byun JH, Hong SM, et al. Pancreatic Cancer CT: Prediction of Resectability According to NCCN Criteria. *Radiology* (2018) 289(3):710–8. doi: 10.1148/radiol.2018180628
23. Tempero MA, Malafa MP, Al-Hawary M, Asbun H, Bain A, Behrman SW, et al. Pancreatic Adenocarcinoma, Version 2.2017, NCCN Clinical Practice Guidelines in Oncology. *J Natl Compr Cancer Netw JNCCN* (2017) 15 (8):1028–61. doi: 10.6004/jnccn.2017.0131
24. Qin C, Shao F, Gai Y, Liu Q, Ruan W, Liu F, et al. (68)Ga-DOTA-FAPI-04 PET/MR in the Evaluation of Gastric Carcinomas: Comparison With (18)F-FDG PET/Ct. *J Nucl Med Off Publ Soc Nucl Med* (2022) 63(1):81–8. doi: 10.2967/jnumed.120.258467
25. Lee SM, Goo JM, Park CM, Yoon SH, Paeng JC, Cheon GJ, et al. Preoperative Staging of Non-Small Cell Lung Cancer: Prospective Comparison of PET/MR and PET/Ct. *Eur Radiol* (2016) 26(11):3850–7. doi: 10.1007/s00330-016-4255-0
26. Raman SP, Reddy S, Weiss MJ, Manos LL, Cameron JL, Zheng L, et al. Impact of the Time Interval Between MDCT Imaging and Surgery on the Accuracy of Identifying Metastatic Disease in Patients With Pancreatic Cancer. *AJR Am J Roentgenol* (2015) 204(1):W37–42. doi: 10.2214/ajr.13.12439
27. Heestand GM, Murphy JD, Lowy AM. Approach to Patients With Pancreatic Cancer Without Detectable Metastases. *J Clin Oncol Off J Am Soc Clin Oncol* (2015) 33(16):1770–8. doi: 10.1200/jco.2014.59.7930
28. Chu LC, Goggins MG, Fishman EK. Diagnosis and Detection of Pancreatic Cancer. *Cancer J (Sudbury Mass)* (2017) 23(6):333–42. doi: 10.1097/ppo.0000000000000290
29. Sergeant G, Ectors N, Fieuws S, Aerts R, Topal B. Prognostic Relevance of Extracapsular Lymph Node Involvement in Pancreatic Ductal Adenocarcinoma. *Ann Surg Oncol* (2009) 16(11):3070–9. doi: 10.1245/s10434-009-0627-x
30. Padhani AR, Koh DM, Collins DJ. Whole-Body Diffusion-Weighted MR Imaging in Cancer: Current Status and Research Directions. *Radiology* (2011) 261(3):700–18. doi: 10.1148/radiol.11110474
31. Ohno Y, Koyama H, Yoshikawa T, Nishio M, Aoyama N, Onishi Y, et al. N Stage Disease in Patients With non-Small Cell Lung Cancer: Efficacy of Quantitative and Qualitative Assessment With STIR Turbo Spin-Echo Imaging, Diffusion-Weighted MR Imaging, and Fluorodeoxyglucose PET/Ct. *Radiology* (2011) 261(2):605–15. doi: 10.1148/radiol.11110281
32. Nguyen AH, Melstrom LG. Use of Imaging as Staging and Surgical Planning for Pancreatic Surgery. *Hepatobiliary Surg Nutr* (2020) 9(5):603–14. doi: 10.21037/hbsn.2019.05.04
33. Fröhlich A, Diederichs CG, Staib L, Vogel J, Beger HG, Reske SN. Detection of Liver Metastases From Pancreatic Cancer Using FDG PET. *J Nucl Med Off Publ Soc Nucl Med* (1999) 40(2):250–5. doi: 10.1016/j.cireng.2013.10.027
34. Motosugi U, Ichikawa T, Morisaka H, Sou H, Muhi A, Kimura K, et al. Detection of Pancreatic Carcinoma and Liver Metastases With Gadoxetic Acid-Enhanced MR Imaging: Comparison With Contrast-Enhanced Multi-Detector Row CT. *Radiology* (2011) 260(2):446–53. doi: 10.1148/radiol.11103548
35. Rauscher I, Eiber M, Fürst S, Souvatzoglou M, Nekolla SG, Ziegler SI, et al. PET/MR Imaging in the Detection and Characterization of Pulmonary Lesions: Technical and Diagnostic Evaluation in Comparison to PET/Ct. *J Nucl Med Off Publ Soc Nucl Med* (2014) 55(5):724–9. doi: 10.2967/jnumed.113.129247
36. Queiroz MA, Kubik-Huch RA, Hauser N, Freiwald-Chilla B, von Schulthess G, Froehlich JM, et al. PET/MRI and PET/CT in Advanced Gynaecological Tumours: Initial Experience and Comparison. *Eur Radiol* (2015) 25(8):2222–30. doi: 10.1007/s00330-015-3657-8

Conflict of Interest: The authors declare that the research was conducted in the absence of any commercial or financial relationships that could be construed as a potential conflict of interest.

frontiers in Oncology

ORIGINAL RESEARCH
published: 31 March 2022
doi: 10.3389/fonc.2022.789351

Prognostic Effect of Age in Resected Pancreatic Cancer Patients: A Propensity Score Matching Analysis

Yaolin Xu†, Yueming Zhang†, Siyang Han, Dayong Jin, Xuefeng Xu, Tiantao Kuang, Wenchuan Wu, Dansong Wang and Wenhui Lou**

Department of General Surgery, Zhongshan Hospital Fudan University, Shanghai, China

Background: While the elderly population account for an indispensable proportion in pancreatic ductal adenocarcinoma (PDAC), these patients are underrepresented in clinical trials. Whether surgery offered the same benefit for elderly patients as that for younger cohort and which factors affected long-term outcome of elderly population remained unclear.

Aims: This study aims to evaluate long-term prognosis of elderly PDAC patients (≥70 years old) after surgery and to investigate potential prognostic factors.

Methods: This retrospective study included PDAC patients receiving radical resection from January 2012 to July 2019 in Zhongshan Hospital Fudan University. Patients were divided into young (<70) and old groups (≥70). Propensity score matching (PSM) was conducted to eliminate the confounding factors. We investigated potential prognostic factors *via* Cox proportional hazards model and Kaplan–Meier estimator. Nomogram model and forest plot were constructed to illustrate the prognostic value of age.

Results: A total of 552 PDAC patients who received radical resection were included in this research. Elderly patients showed poorer nutritional status and were less likely to received adjuvant treatment. After matching, although age [hazard ratio (HR)=1.025, 95%CI 0.997–1.054; p=0.083] was not statistically significant in the multivariate cox regression analysis, further survival analysis showed that patients in the old group had poorer overall survival (OS) when compared with young group (p=0.039). Furthermore, reception of adjuvant chemotherapy (HR=0.411, 95%CI 0.201-0.837; p=0.014) was the only independent prognostic factor among elderly patients and could significantly improve OS. Subgroup analysis indicated that age had better prognostic value in PDAC patients with good preoperative nutritional status and relative low tumor burden. Finally, a prognostic prediction model contained age, reception of adjuvant chemotherapy, American Joint Committee on Cancer (AJCC) 8th T and N stage was constructed and presented in nomogram, whose Harrell's concordance index was 0.7478 (95%CI, 0.6960–0.7996). The calibration curves at 1 and 3 years indicated an optimal conformity between actual and nomogram-predicted survival probability in the PDAC patient who received surgery.

Conclusion: The elderly PDAC patients were associated with worse OS survival after radical resection, and the noticeable negative effect of age was observed among PDAC

OPEN ACCESS

Edited by:
Kuirong Jiang,
First Affiliated Hospital, Nanjing Medical University, China

Reviewed by:
Chang Moo Kang,
Yonsei University College of Medicine, South Korea
Xiaodong Tian,
Peking University First Hospital, China

****Correspondence:***
Dansong Wang
wang.dansong@zs-hospital.sh.cn
Wenhui Lou
lou.wenhui@zs-hospital.sh.cn

†These authors have contributed equally to this work and share first authorship

Specialty section:
This article was submitted to Gastrointestinal Cancers: Hepato Pancreatic Biliary Cancers, a section of the journal Frontiers in Oncology

Received: *04 October 2021*
Accepted: *04 March 2022*
Published: *31 March 2022*

Citation:
Xu Y, Zhang Y, Han S, Jin D, Xu X, Kuang T, Wu W, Wang D and Lou W (2022) Prognostic Effect of Age in Resected Pancreatic Cancer Patients: A Propensity Score Matching Analysis. Front. Oncol. 12:789351. doi: 10.3389/fonc.2022.789351

patients with better preoperative nutritional status and less aggressive tumor biology. Adjuvant chemotherapy was essential to improve survival outcome of elderly PDAC patients following radical resection.

Keywords: pancreatic ductal adenocarcinoma, the elderly patients, radical resection, adjuvant chemotherapy, prognosis

INTRODUCTION

Pancreatic adenocarcinoma (PDAC) is one of the most malignant solid tumors with poor prognosis. PDAC is strongly age dependent, and increasing population longevity and aging will contribute to the global burden of pancreatic cancer (1). A research derived from the Global Burden of Disease Study showed that incidence rate at ages older than 70 years was three to four times higher than those at ages 50–69 years in 2017, and 20.2% of these were attributable to population aging (2). By 2030, approximately 70% of PDAC will be diagnosed in older adults (3). While the elderly population accounted for an indispensable proportion on PDAC, the older cancer patients were underrepresented in clinical trials (4). A research demonstrated that patients aged 70 years or older accounted for the most of the under-representation among those noted in registration trials for all cancer treatment (5). A research involving of 10,505 PDAC patients based on Surveillance, Epidemiology, and End Results (SEER) database showed that over half of older patients (≥65) with potentially treatable pancreatic cancer did not receive any treatment at all. Only 11% of older patients with locoregional pancreatic cancer received multimodality therapy (6). Thus, the treatment strategies concluded from younger patients may not be implied into the very elderly patients completely. The optimal therapeutic strategy for the elderly patients with PDAC remained to be determined.

Currently, surgery was still the only treatment that could offer a chance to cure pancreatic cancer (7). However, it was uncertain whether surgery will benefit the elderly patients. Some researchers suggested that the prognosis in the elderly was poorer than in the younger patients (8, 9), while others hold the opposed points of view (10–12). What seems clear, though, is that the incidence of postoperative complications is much higher in the elderly patients (13–16). This could be one of the factors that influence the decisions of therapeutic strategies for the elderly patients. As a result, more clinical studies focused on the elderly should be performed to determine the optimal therapeutic strategy.

In the present research, we evaluated the postoperative long-term prognosis of the elderly patients (≥70) with PDAC by comparing with the younger patients. Moreover, we analyzed the prognostic factors for long-term survival in order to explore the optimal therapeutic strategies for the elderly patients.

MATERIALS AND METHODS

Patients and Study Design

The research included PDAC patients receiving radical resection in Zhongshan Hospital Fudan University from January 2012 to July 2019. The inclusion criteria are as follows: (1) with definite pathological diagnosis of pancreatic adenocarcinoma; (2) with definite American Joint Committee on Cancer (AJCC) 8th TNM stage; (3) with complete preoperative blood samples test and all the tests were performed 1 week before surgery; (4) with sufficient follow-up time at least 24 months. The total cohort was divided into two groups included the young group (<70 years) and the old group (≥70 years), according to the age of patients. Overall survival (OS) was calculated from the date of surgery to the date of death or last follow-up. Patients were generally seen in follow-up 4–6 weeks following discharge and every 3–6 months thereafter for physical examination, laboratory test, and imaging to assess for postoperative recovery and cancer recurrence. Besides, telephone interviews every 3 months were performed to supplement follow-up information. Median follow-up time was 40 months. The study outcomes were overall survival (OS) from time of surgery. All the medical information and time of survival were obtained from medical records and telephone interviews.

Clinicopathological Data

Patients' demographic characteristics, pathological results, and blood sample results were extracted from electric medical records. Among the patients who received adjuvant chemotherapy and radiotherapy, only one patient accepted neoadjuvant chemotherapy. The adjuvant chemotherapy regimens were prescribed based on the latest clinical practice guidelines and the clinical evaluation of doctors. The most common chemotherapy regimens were combination regimens, including AS (albumin-bound paclitaxel + S-1), AG (albumin-bound paclitaxel + gemcitabine), GS (gemcitabine + S-1), and FOLFIRINOX. The patients with severe side effects or with negative intentions for chemotherapy mostly received single drug such as gemcitabine or S-1. Second-line treatment mainly depends on the clinical evaluation of doctors. The information of tumor location, AJCC 8th TNM stage, tumor differentiation, microvascular invasion, fatty invasion, and perineural invasion were defined by the pathological results. None of the study population was diagnosed with metastatic tumor. A carbohydrate antigen 19-9 (CA 19-9) cutpoint of 35 U/ml was used to dichotomize patients with normal and elevated values based on a research performed by Aldakkak and colleagues. Elevated CA 19-9 were then further stratified into low (36–200), moderate (201–1,000), and high (>1,000) groups (17). The American Society of Anesthesiologists Physical Status (ASA PS) classification system was performed by the anesthetists before surgery. The ASA classification system contains categories 1–5 and represents increasing levels of patient impairment (18).

Statistical Analysis

Data analyses were performed by R project 3.5.3 for Windows and IBM SPSS Statistics 22.0 version. Normality and homogeneity of variance were tested by Shapiro–Wilk test and Levene's test. Categorical variables were reported as frequencies and percentages. Continuous variables conforming to normal distribution were presented by means and standard error; others were described as medians and interquartile range. The baseline characteristics between different groups were compared using Fisher's precision probability test for categorical variables, using Wilcoxon rank sum test for continuous variables, respectively. Propensity score matching was performed with "MatchIt" packages using R project. A 1:1 ratio propensity score matching study group was created using the nearest neighbor matching method with a 0.6 caliper. Survival curves were drawn with the method of Kaplan–Meier, and log-rank test was used to compare the overall survival of different groups. Cox proportional hazards model was used to estimate the hazard ratio of death. The significant statistical variables ($p<0.1$) in univariate Cox regression analysis were incorporated into the multivariate analysis to identify the independent prognostic factors for survival. Forest plot was performed to show the outcome of subgroup analysis. Forest plot was performed by "forestplot" packages using R project. The survival nomogram was developed starting from Cox model, which allowed to obtain survival probability estimates. The endpoints in building the nomogram model were 1- and 3-year survival. Harrell's concordance index (C-index) was used in the nomogram to evaluate the model performance for predicting outcomes. The nomogram was subjected to 1,000 bootstrap resamples for internal validation of the cohort. Then, calibration curves were used to verify the accuracy between predicted and actual 1- and 3-year survival. All the significance tests in this paper were two-sided tests.

RESULTS

Baseline Characteristics of the Total Cohort

A total of 552 patients diagnosed with PDAC who accepted radical surgery were incorporated in the total cohort. The patients aged 70 years or older were defined as the elderly in this study. The patients' clinicopathological characteristics are listed in **Table 1**. There were 411 patients younger than 70 years old (young group) and 141 patients aged 70 years or older (old group). In the total cohort, the old group was less likely to receive adjuvant chemotherapy and radiotherapy and presented with earlier N stage. Besides, the prealbumin, albumin, white cell count, lymphocyte count, and AFP in the old group were significantly lower than that of the young group. Other factors did not differ significantly between two groups.

The univariate and multivariate Cox regression analysis demonstrated that age was not an independent prognostic factor [hazard ratio (HR)=1.005; 95% confidential index (CI), 0.993–1.018; p=0.416, **Supplementary Table S1**]. Further survival analyses showed no survival difference between two groups among all PDAC patients [old vs. young, median OS (mOS), 29.2 vs. 28.5 months, p=0.82, **Supplementary Figure S1**].

Propensity Score Matching and Survival Analysis

In order to balance confounding factors that might affect survival outcome, propensity score matching (PSM) was performed by a 1:1 ratio. The potentially adjusting variables were based on the results of Cox regression analysis, which included AJCC 8th T stage (p=0.062), N stage (p=0.05), adjuvant chemotherapy (p<0.001), and CA50 (p=0.034). A total of 95 patients younger than 70 years old were matched with 95 patients older than 70 years old in the total cohort. The baseline characteristics between the two groups after PSM are listed in **Table 2**. All adjusting variables were comparable after PSM.

Cox proportional hazards models were constructed to investigate potential prognostic factors in matching cohort (**Table 3**). Univariate Cox regression analysis indicated that age, reception of chemotherapy, AJCC 8th T and N stage, peripancreatic fat invasion, perineural invasion, CA 19-9 level, albumin, and CA50 were independent prognostic factors. These factors were then incorporated into multivariate Cox regression analysis. As shown in **Table 3**, the reception of chemotherapy (HR=0.291; 95%CI, 0.173–0.287; p<0.001) and AJCC 8th T stage (T4, HR=3.706; 95%CI, 1.373–10.002; p=0.01) were independent prognostic factors, although age (HR=1.025; 95%CI, 0.997–1.054; p=0.083) was not statistically significant in the multivariate Cox regression analysis. Further survival analysis showed that patients in the old group had poorer OS when compared with the young group (old vs. young, mOS, 27.5 vs. NA months, p=0.039, **Figure 1A**).

The 1-year survival rate was 87% in the young group and 79% in the old group. The 3-year survival rate was 59% in the young group and 44% in the old group.

We further investigated potential prognostic factors in patients aged 70 and over using Cox regression analysis. As shown in **Table 3**, reception of chemotherapy (HR=0.411; 95%CI, 0.201–0.837; p=0.014) was the only independent prognostic factor in elderly PDAC patients who received surgery. The survival analysis further confirmed that adjuvant chemotherapy significantly improved OS among elderly PDAC patients (no adjuvant chemotherapy vs. receiving adjuvant chemotherapy, mOS, 14.8 vs. 33.8 months, p=0.00062, **Figure 1B**).

Prognostic Nomogram Development and Validation

A prognostic nomogram model was constructed according to the results of multivariate Cox regression analysis (**Figure 2A**). The prediction model incorporated independent prognostic factors in the Cox analysis including age, reception of chemotherapy, and AJCC 8th T and N stage. Each factor could get a point based on their grade from the points scale. The 1- and 3-year survival probability could be predicted according to the total points. The Harrell's concordance index of this model was 0.7478 (95%CI, 0.6960–0.7996). Then, the nomogram model was subjected to 1,000

TABLE 1 | Baseline characteristics of the study population (n=552).

	Total	Age<70 (n=411)	Age≥70 (141)	p-value
Age				
Median (IQR)	64.00 (58.00–70.00)	61.00 (56.00–65.00)	73.00 (72.00–76.00)	**< 0.001**
Sex				
Male	326 (59%)	243 (59%)	83 (59%)	1
Female	226 (41%)	168 (41%)	58 (41%)	
Tumor location				
Head	296 (54%)	227 (55%)	69 (49%)	0.27
Body and tail	243 (44%)	173 (42%)	70 (50%)	
Total pancreas	13 (2%)	11 (3%)	2 (1%)	
CA19-9 level				
<35	147 (27%)	113 (27%)	34 (24%)	0.7
35-200	195 (35%)	145 (35%)	50 (35%)	
>200	210 (38%)	153 (37%)	57 (40%)	
Adjuvant chemotherapy				
No	112 (21%)	69 (17%)	43 (32%)	**<0.001**
Yes	427 (79%)	334 (83%)	93 (68%)	
Adjuvant radiotherapy				
No	424 (77%)	306 (75%)	118 (86%)	**0.009**
Yes	124 (23%)	104 (25%)	20 (14%)	
AJCC 8th T stage				
T1	113 (21%)	84 (20%)	29 (21%)	0.37
T2	306 (56%)	223 (54%)	83 (59%)	
T3	84 (15%)	69 (17%)	15 (11%)	
T4	20 (4%)	16 (4%)	4 (3%)	
Tis	27 (5%)	18 (4%)	9 (6%)	
AJCC 8th N stage				
N0	317 (58%)	223 (55%)	94 (67%)	**0.036**
N1	193 (35%)	152 (37%)	41 (29%)	
N2	39 (7%)	33 (8%)	6 (4%)	
Tumor differentiation				
Well-diff	34 (6%)	23 (6%)	11 (8%)	0.06
Moderately-diff	216 (40%)	150 (37%)	66 (47%)	
Poorly-diff	294 (54%)	231 (57%)	63 (45%)	
MVI				
No	457 (83%)	335 (82%)	122 (87%)	0.2
Yes	95 (17%)	76 (18%)	19 (13%)	
FI				
No	131 (24%)	93 (23%)	38 (27%)	0.3
Yes	421 (76%)	318 (77%)	103 (73%)	
NI				
No	112 (20%)	88 (21%)	24 (17%)	0.28
Yes	440 (80%)	323 (79%)	117 (83%)	
Preglucose				
Median (IQR)	5.80 (5.10–6.90)	5.80 (5.10–6.80)	5.70 (5.10–7.20)	0.89
Albumin				
Median (IQR)	40.00 (38.00–43.00)	41.00 (39.00–43.00)	40.00 (38.00–42.00)	**<0.001**
Prealbumin				
Median (IQR)	0.23 (0.18–0.26)	0.23 (0.19–0.27)	0.21 (0.18–0.25)	**0.012**
Hemoglobin				
Median (IQR)	128.00 (118.50–139.00)	128.00 (120.00–139.00)	126.00 (116.00–136.00)	0.086
WBC				
Median (IQR)	5.34 (4.54–6.39)	5.42 (4.62–6.48)	5.20 (4.46–6.10)	**0.034**
Neutrophil count				
Median (IQR)	3.20 (2.40–3.90)	3.20 (2.50–3.90)	3.00 (2.40–3.90)	0.36
Lymphocyte count				
Median (IQR)	1.50 (1.20–1.90)	1.50 (1.30–1.90)	1.40 (1.10–1.70)	**0.003**
Monocyte count				
Median (IQR)	0.42 (0.34–0.53)	0.42 (0.34–0.52)	0.43 (0.37–0.54)	0.28
ASA				
Grade 1	71 (14.95%)	56 (15.77%)	15 (12.50%)	0.39
Grade 2	391 (82.32%)	291 (81.97%)	100 (83.33%)	
Grade 3	13 (2.74%)	8 (2.25%)	5 (4.17%)	

(Continued)

TABLE 1 | Continued

	Total	Age<70 (n=411)	Age≥70 (141)	p-value
AFP				
Median (IQR)	2.60 (1.90–3.60)	2.70 (2.00–3.70)	2.40 (1.60–3.30)	**0.015**
CEA				
Median (IQR)	3.00 (1.80–4.80)	2.90 (1.75–4.70)	3.30 (2.20–5.20)	0.12
CA242				
Median (IQR)	22.95 (8.88–70.48)	23.30 (8.60–62.70)	22.20(9.65–121.50)	0.49
CA50				
Median (IQR)	68.80 (20.30–180.00)	66.10 (17.45–180.00)	83.80 (29.30–180.00)	0.12
CA125				
Median (IQR)	14.25 (9.40–23.73)	14.50 (9.50–24.00)	13.50 (9.00–22.70)	0.36

IQR, interquartile range; CA, carbohydrate antigen; AJCC, American Joint Committee on Cancer; Tis, tumor in situ; MVI, microvascular invasion; FI, peripancreatic fat invasion; NI, neural invasion; WBC, white blood cell; ASA, American Society of Anesthesiologists; AFP, alpha-fetoprotein; CEA, carcinoembryonic antigen.
The bold values indicates statistically significance.

TABLE 2 | Baseline characteristics of the study population after PSM (n=190).

	Total	Age<70 (n=95)	Age≥70 (n=95)	p-value
Age				
Median (IQR)	69.50 (62.25–73.00)	62.00 (57.50–66.50)	73.00 (72.00–76.00)	**<0.001**
Sex				
Male	113 (59%)	54 (57%)	59 (62%)	0.55
Female	77 (41%)	41 (43%)	36 (38%)	
Tumor location				
Head	87 (46%)	44 (46%)	43 (45%)	0.93
Body and tail	98 (52%)	48 (51%)	50 (53%)	
Total pancreas	5 (3%)	3 (3%)	2 (2%)	
CA19-9				
<35	41 (22%)	20 (21%)	21 (22%)	0.83
35–200	70 (37%)	37 (39%)	33 (35%)	
>200	79 (42%)	38 (40%)	41 (43%)	
Adjuvant chemotherapy				
No	57 (30%)	25 (26%)	32 (34%)	0.34
Yes	133 (70%)	70 (74%)	63 (66%)	
Adjuvant radiotherapy				
No	153 (81%)	71 (75%)	82 (86%)	0.066
Yes	37 (19%)	24 (25%)	13 (14%)	
AJCC 8th T stage				
T1	41 (22%)	22 (23%)	19 (20%)	0.85
T2	107 (56%)	50 (53%)	57 (60%)	
T3	20 (11%)	11 (12%)	9 (9%)	
T4	8 (4%)	5 (5%)	3 (3%)	
Tis	14 (7%)	7 (7%)	7 (7%)	
AJCC 8th N stage				
N0	124 (65%)	62 (65%)	62 (65%)	0.76
N1	60 (32%)	31 (33%)	29 (31%)	
N2	6 (3%)	2 (2%)	4 (4%)	
Tumor differentiation				
Well-diff	15 (8%)	7 (8%)	8 (9%)	0.88
Moderately diff	86 (46%)	41 (45%)	45 (48%)	
Poorly diff	84 (45%)	43 (47%)	41 (44%)	
MVI				
No	159 (84%)	80 (84%)	79 (83%)	1
Yes	31 (16%)	15 (16%)	16 (17%)	
FI				
No	49 (26%)	26 (27%)	23 (24%)	0.74
Yes	141 (74%)	69 (73%)	72 (76%)	
NI				
No	39 (21%)	22 (23%)	17 (18%)	0.47
Yes	151 (79%)	73 (77%)	78 (82%)	
Preglucose				
Median (IQR)	5.80 (5.00–6.80)	5.80 (5.00–6.50)	5.80 (5.00–7.10)	0.82

(Continued)

TABLE 2 | Continued

	Total	Age<70 (n=95)	Age≥70 (n=95)	p-value
Albumin				
Median (IQR)	40.00 (38.00–42.00)	41.00 (39.00–43.00)	40.00 (37.00–42.00)	**<0.001**
Prealbumin				
Median (IQR)	0.22 (0.19–0.25)	0.23 (0.20–0.26)	0.21 (0.18–0.24)	**0.006**
Hb				
Median (IQR)	126.50 (116.00–138.00)	126.00(116.00–139.00)	128.00(115.25–136.75)	0.86
WBC				
Median (IQR)	5.34 (4.48–6.29)	5.52 (4.53–6.42)	5.21 (4.46–6.11)	0.24
Neutrophil count				
Median (IQR)	3.20 (2.50–3.90)	3.25 (2.62–3.80)	3.05 (2.42–3.98)	0.66
Lymphocyte count				
Median (IQR)	1.50 (1.20–1.80)	1.50 (1.30–1.90)	1.40 (1.10–1.70)	0.14
Monocyte count				
Median (IQR)	0.43 (0.35–0.54)	0.43 (0.34–0.54)	0.44 (0.37–0.55)	0.26
ASA				
Grade 1	29 (16%)	16 (18%)	13 (14%)	0.79
Grade 2	143 (80%)	70 (79%)	73 (81%)	
Grade 3	7 (4%)	3 (3%)	4 (4%)	
AFP				
Median (IQR)	2.40 (1.67–3.40)	2.60 (1.80–3.48)	2.35 (1.50–3.18)	0.15
CEA				
Median (IQR)	3.10 (1.90–4.80)	3.00 (1.70–4.70)	3.30 (2.20–5.52)	0.17
CA242				
Median (IQR)	30.00 (11.65–120.90)	33.80 (14.00–86.15)	26.70 (10.30–141.40)	0.58
CA50				
Median (IQR)	84.75 (30.45–180.00)	88.50 (33.25–180.00)	75.20 (29.30–180.00)	0.79
CA125				
Median (IQR)	13.70 (8.95–22.55)	12.80 (8.50–20.50)	14.25 (9.38–24.15)	0.21

IQR, interquartile range; CA, carbohydrate antigen; AJCC, American Joint Committee on Cancer; Tis, tumor in situ; MVI, microvascular invasion; FI, peripancreatic fat invasion; NI, neural invasion; WBC, white blood cell; ASA, American Society of Anesthesiologists; AFP, alpha-fetoprotein; CEA, carcinoembryonic antigen.
The bold values indicates statistically significance.

bootstrap resamples for internal validation of the cohort. The calibration curves at 1 and 3 years indicated an optimal conformity between actual and nomogram-predicted survival probability in the PDAC patient received surgery (**Figures 2B, C**).

Subgroup Analysis of the Cohort After PSM

Further subgroup analyses were conducted to explore whether age remained as a prognostic factor in a certain subgroup. Forest plot (**Figure 3**) showed that the elderly may have poorer prognosis in male (HR=2.333; 95%CI, 1.315–4.136; p=0.00376) patients whose tumor was located at the pancreatic body/tail (HR=2.053; 95%CI, 1.087–3.881; p=0.0267), with N0 stage (HR=1.821; 95%CI, 1.032–3.214; p=0.0385), without perineural invasion (HR=4.702; 95%CI, 1.267–17.46; p=0.0207), albumin higher than 35 g/L (HR=1.604; 95%CI, 1.035–2.485; p=0.0346), hemoglobin higher than 120 g/L (HR=1.788; 95%CI, 1.018–3.141; p=0.0431), white blood cell count between 4 and 10×10^9/L (HR=1.644; 95%CI, 1.012–2.671; p=0.0445), AFP lower than 20 ng/ml (HR=1.584; 95%CI, 1.024–2.450; p=0.0386), CA125 lower than 35 ng/ml (HR=1.701; 95%CI, 1.013–2.855; p=0.0445), CA19-9 lower than 200 U/ml (HR=1.923; 95%CI, 1.036–3.571; p=0.0383), and those patients who did not receive radiotherapy (HR=1.683; 95%CI, 1.019–2.780; p=0.0421). The survival curves between the young and the old group were compared using log-rank method and indicated the prognostic effect of age in these subgroups (**Figure 4**).

DISCUSSION

In the present research, we investigated the prognostic value of age in PDAC patients following radical resection. A total of 552 PDAC patients who received radical resection were included in this research. The elderly showed poorer preoperative nutritional status but earlier N stage and were less likely to receive adjuvant treatment. PSM was then conducted to eliminate the selected bias. After matching, although age (HR=1.025; 95%CI, 0.997–1.054; p=0.083) was not statistically significant in the multivariate Cox regression analysis, further survival analysis showed that patients in the old group had poorer OS when compared with the young group (old vs. young, mOS, 27.5 vs. NA months, p=0.039, **Figure 1A**). Furthermore, we found that reception of adjuvant chemotherapy was the only protective factor in the elderly patients. Subgroup analysis indicated that age had better prognostic value in resected PDAC patients with good preoperative nutritional status and relative low tumor burden.

At present, there is controversy about whether age affected the prognosis of PDAC patients following radical resection. Several studies suggested that age was not an independent prognostic factor, and there were no significant differences in OS between younger and older patients (19–21). On the other hand, some researchers hold the opposed points that the very elderly patients had poorer prognosis after surgery. A research retrospectively included 148,080 periampullary cancer patients, and they

TABLE 3 | Univariate and multivariate Cox regression analysis of the cohort after PSM.

	Total cohort			
	Univariate		Multivariate	
	HR	p-value	HR	p-value
Age (ref=age<70)	1.043(1.017–1.069)	**0.001**	1.025(0.997–1.054)	**0.083**
Gender (ref=male)	0.834(0.539–1.290)	0.414		
Tumor location (ref=pancreatic head)		0.415		
pancreatic body/tail	0.752(0.490–1.155)	0.194		
total pancreas	0.724(0.175–2.987)	0.655		
AJCC 8th T stage (ref=T1)		**0.007**		**0.011**
T2	1.777(0.969–3.259)	0.063	1.425(0.753–2.697)	0.277
T3	2.459(1.117–5.412)	0.025	1.706(0.743–3.920)	0.208
T4	3.534(1.339–9.326)	0.011	3.706(1.373–10.002)	0.01
Tis	0.157(0.020–1.199)	0.074	0.088(0.010–0.801)	0.031
AJCC 8th N stage (ref=N0)		**0.039**		0.182
N1	1.489(0.946–2.343)	0.086	1.292(0.799–2.091)	0.296
N2	2.793(1.105–7.061)	0.03	2.309(0.877–6.081)	0.09
Differentiation (ref=moderately diff)		0.107		
Poorly diff	10.831(1.482–79.135)	0.019		
Moderately diff	12.021(1.653–87.409)	0.014		
Un-diff		0.977		
MVI (ref=no MVI)	1.214(0.682–2.161)	0.51		
FI (ref=no FI)	2.239(1.259–3.980)	**0.006**	1.164(0.619–2.191)	0.637
NI (ref=no NI)	2.193(1.186–4.056)	**0.012**	0.865(0.433–1.728)	0.682
Adjuvant chemotherapy (ref=no-chemo)	0.456(0.294–0.705)	**<0.001**	0.291(0.173–0.487)	**<0.001**
Adjuvant radiotherapy (ref=no-radio)	1.286(0.776–2.129)	0.329		
CA19-9 level (ref=CA19-9<35)		**0.044**		0.683
CA19-9 35-200	1.416(0.738–2.716)	0.295	1.414(0.642–3.114)	0.39
CA19-9>200	2.078(1.117–3.867)	0.021	1.652(0.454–6.012)	0.447
Preglucose (continuous)	1.016(0.914–1.129)	0.768		
Albumin (continuous)	0.945(0.892–1.001)	**0.056**	1.013(0.950–1.080)	0.703
Prealbumin (continuous)	0.064(0.001–3.060)	0.163		
Hemoglobin (continuous)	0.996(0.983–1.009)	0.524		
WBC (continuous)	0.894(0.773–1.035)	0.135		
Lymphocyte count (continuous)	0.759(0.513–1.123)	0.167		
Neutrophil count (continuous)	0.894(0.744–1.075)	0.234		
Monocyte count (continuous)	1.249(0.318–4.905)	0.75		
ASA (ref=grade1)		0.512		
Grade 2	0.811(0.461–1.428)	0.468		
Grade 3	0.443(0.101–1.941)	0.28		
AFP (continuous)	0.886(0.756–1.038)	0.133		
CEA (continuous)	1.009(0.992–1.026)	0.294		
CA242 (continuous)	1.004(0.999–1.008)	0.095		
CA50 (continuous)	1.004(1.001–1.007)	**0.016**	1.001(0.994–1.008)	0.772
CA125 (continuous)	1.003(0.997–1.008)	0.322		

HR, hazard ratio; ref, reference; CA, carbohydrate antigen; AJCC, American Joint Committee on Cancer; Tis, tumor in situ; MVI, microvascular invasion; FI, peripancreatic fat invasion; NI, neural invasion; WBC, white blood cell; ASA, American Society of Anesthesiologists; AFP, alpha-fetoprotein; CEA, carcinoembryonic antigen.
The bold values indicates statistically significance.

demonstrated that age was a factor attenuating the survival of patients with resected periampullary cancers (p<0.001). Besides, their research indicated that octogenarian patients who received radical resection showed superior long-term survival than those who did not undergo surgical treatment (22). Another research that incorporated 1,271 patients who received pancreaticoduodenectomy showed that patients older than 70 years had significantly shorter long-term survival (3-year survival, 0% vs. 29%, p<0.0001) (23). A retrospective multicenter analysis demonstrated that the prognosis of octogenarians was poorer than that of younger patients for both resectable and borderline resectable tumors (median survival time, 16.6 vs. 23.2 months, p=0.006) (24). However, the baseline characteristics between the very elderly and younger patients were unbalanced in most studies. Baseline imbalance in factors that are strongly related to outcome measures could cause bias in effect estimate. Thus, in our research, Cox proportional hazard model was constructed to investigate potential prognostic factors, and PSM was conducted to balance baseline characteristics that related to survival outcome. After matching, although age was not an independent prognostic factor in the multivariate Cox regression analysis, further survival analysis showed that patients in the old group had poorer OS when compared with the young group. While previous researchers hold the view that worse survival outcome in the elderly owed to low proportion of receiving adjuvant chemotherapy and poor preoperative nutritional status, we believed the survival disadvantage may be attribute to biological aging, which could lead to

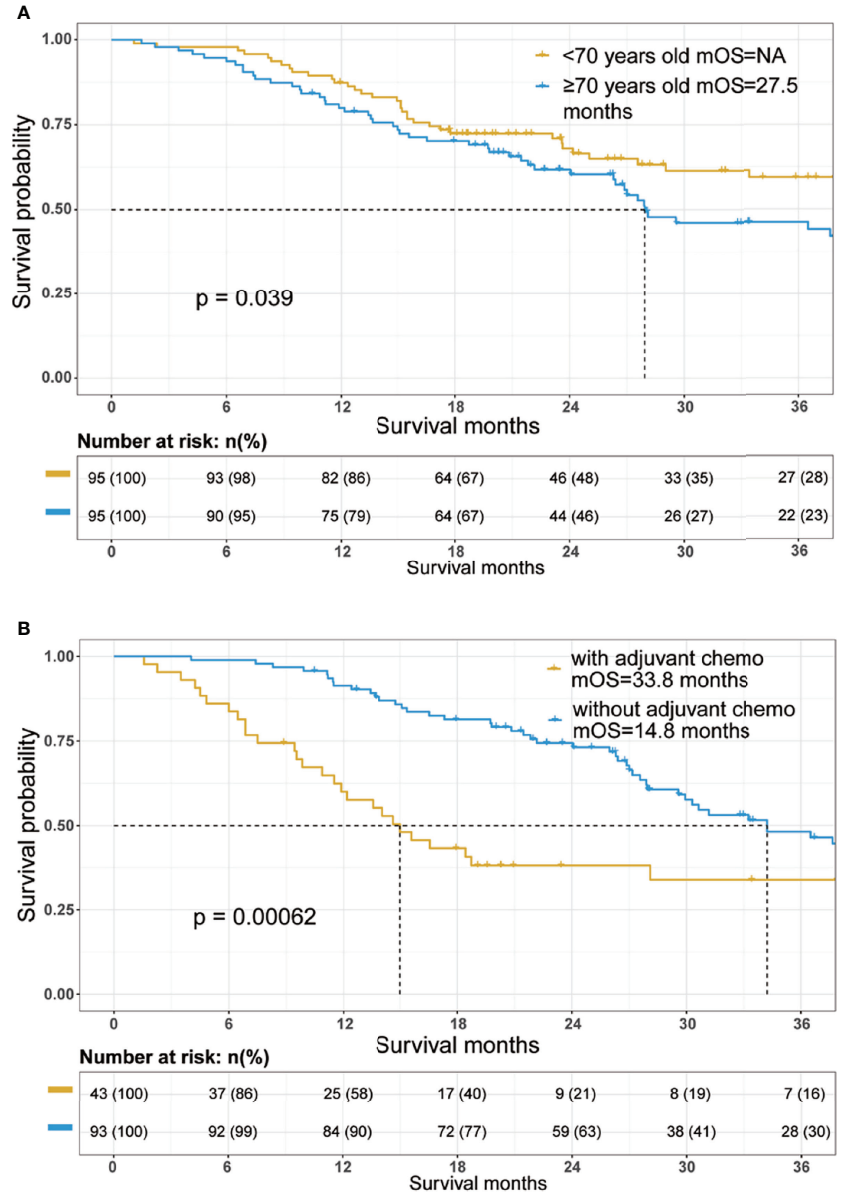

FIGURE 1 | Overall survival Kaplan–Meier survival curves of the cohort. **(A)** Overall survival curves stratified by age in the total cohort after propensity score matching. **(B)** Overall survival curves stratified by the reception of adjuvant chemotherapy in the patients aged 70 years and older. mOS, median overall survival.

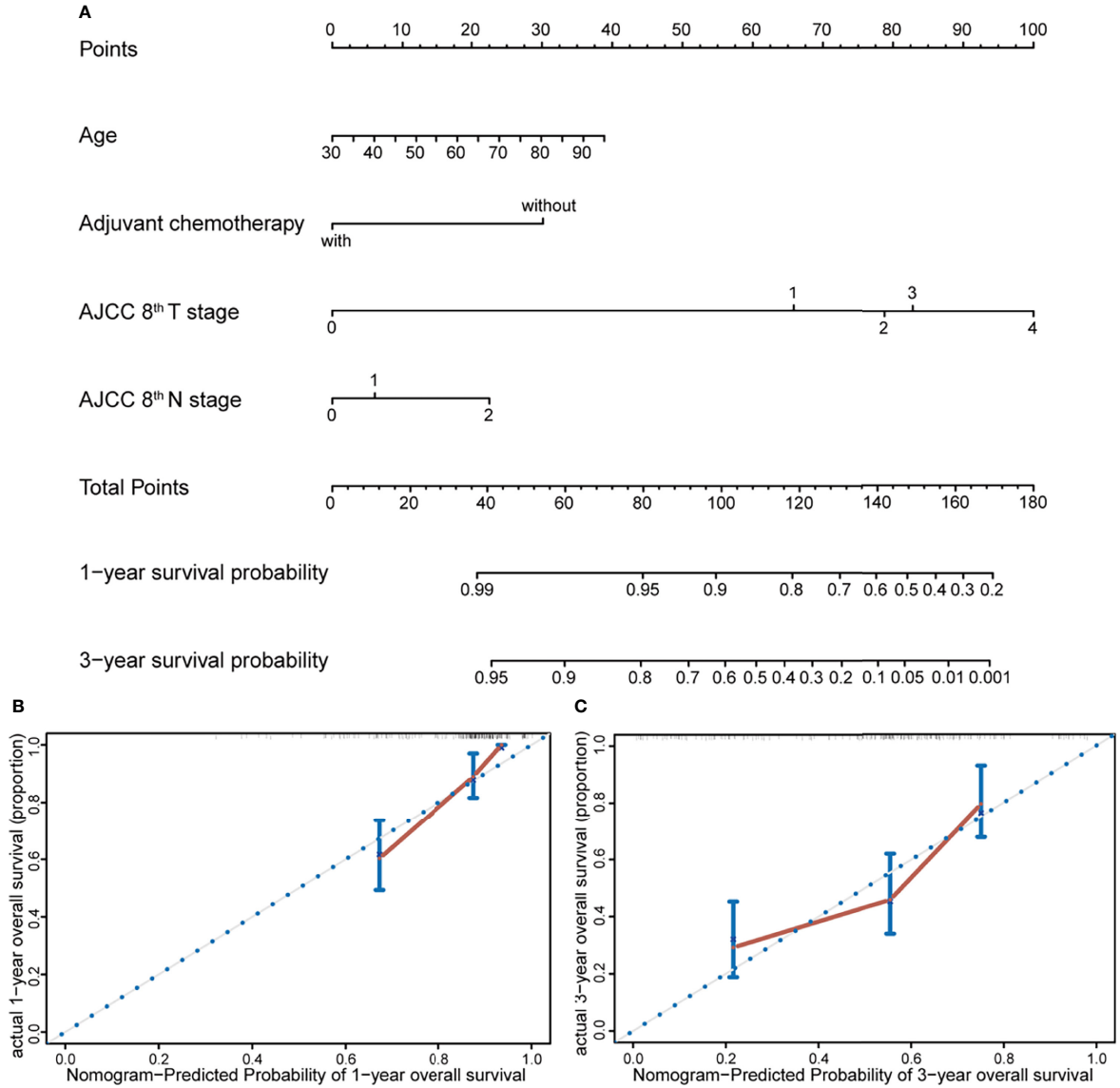

FIGURE 2 | Nomogram and calibration plot for prediction of 1- and 3-year survival. **(A)** Prognostic nomogram for predicting survival probabilities of PDAC patients who received radical resection, constructed by age, reception of adjuvant chemotherapy, and AJCC 8th T and N stage. The 1- and 3-year survival probability could be predicted according to the total points, which were calculated by the summation of each factor's points from the points scale. **(B, C)** Calibration plot of the prognostic nomogram for 1- and 3-year survival, respectively. The nomogram was subjected to 1,000 bootstrap resamples for internal validation of the cohort, and the accuracy of this model could be demonstrated by comparing the actual and predicted probabilities of overall survival.

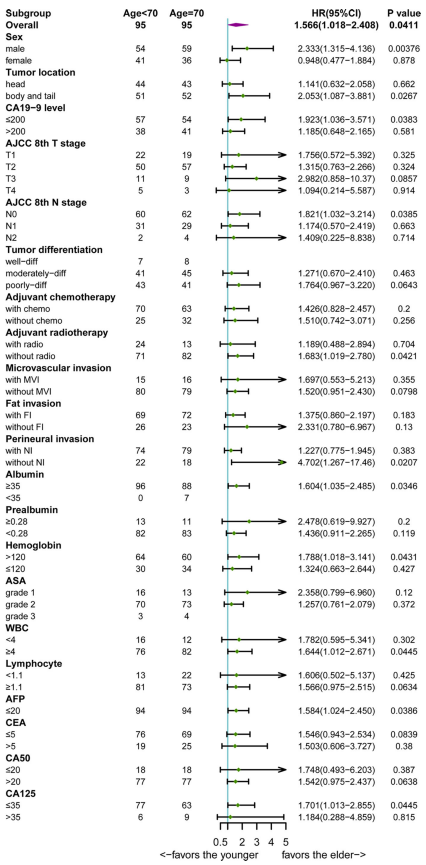

FIGURE 3 | Forest plot of overall survival hazard ratios (HRs) of major subgroups in the cohort after propensity score matching.

vulnerability to cancer and increase risk of cancer death (25). However, additional studies will be needed to investigate the prognostic effect of biological age in oncology research. Besides, a nomogram was constructed as an objective instrument, which could assess the probability of 1- and 3-year survival for PDAC patients after radical surgery. The nomogram model contained four independent prognostic factors including age, reception of adjuvant chemotherapy, and AJCC 8th T and N stage. We first incorporated age into the nomogram model to predict prognosis of resected PDAC patients. The internal validation with the method of bootstrap was performed and showed an optimal conformity between actual and nomogram-predicted survival probability in the PDAC patient who received surgery.

Interestingly, subgroup analyses demonstrated that age remained its prognostic effect in PDAC patients with good nutritional status (normal albumin and hemoglobin) and relative low tumor burden (pancreatic body/tail cancer, N0 stage, without NI, normal AFP, CA125 and CA19-9, and without radiotherapy). These results were not surprising given the fact that among patients with low hemoglobin, albumin, white blood cell count, lymph node metastases, and elevated preoperative tumor marker, the aggressive cancer (26, 27) and poor nutritional status (28–32) would predominantly worsen the survival outcome, whereas the prognostic effect of aging was not apparent.

Our study also showed lower proportion of receiving adjuvant treatment in the elderly group (elderly vs. young, 68% vs. 83%). Meanwhile, adjuvant chemotherapy was the only independent prognostic factor among the elderly (HR=0.411; 95%CI, 0.201–0.837) and significantly improved OS of the elderly patients (mOS, no adjuvant chemotherapy vs. reception of adjuvant chemotherapy, 14.8 vs. 33.8 months). These were consistent with previous published studies. Nagrial et al. demonstrated that older patients (aged ≥70) were less likely to receive adjuvant chemotherapy (51.5% vs. 29.8%; p<0.0001). Older patients who did not receive adjuvant therapy was associated with worse OS (mOS, no adjuvant chemotherapy vs. reception of adjuvant chemotherapy, 13.1 vs. 21.8 months), and adjuvant chemotherapy is the only actionable variable associated with improved survival in older patients (33). The reason of less reception of adjuvant chemotherapy in the elderly patients could be attributed to the worse performance status (34), increased incidence of comorbidities (35), the perception of a less life expectancy, and the longer recovery time following surgery (36).

There were some limitations in our research. First, the study was a retrospective and single-center investigation. Our results require more prospective and multicenter studies for validation. Second, some clinical data such as specific chemotherapy regimens and postoperative complications were not included in this study.

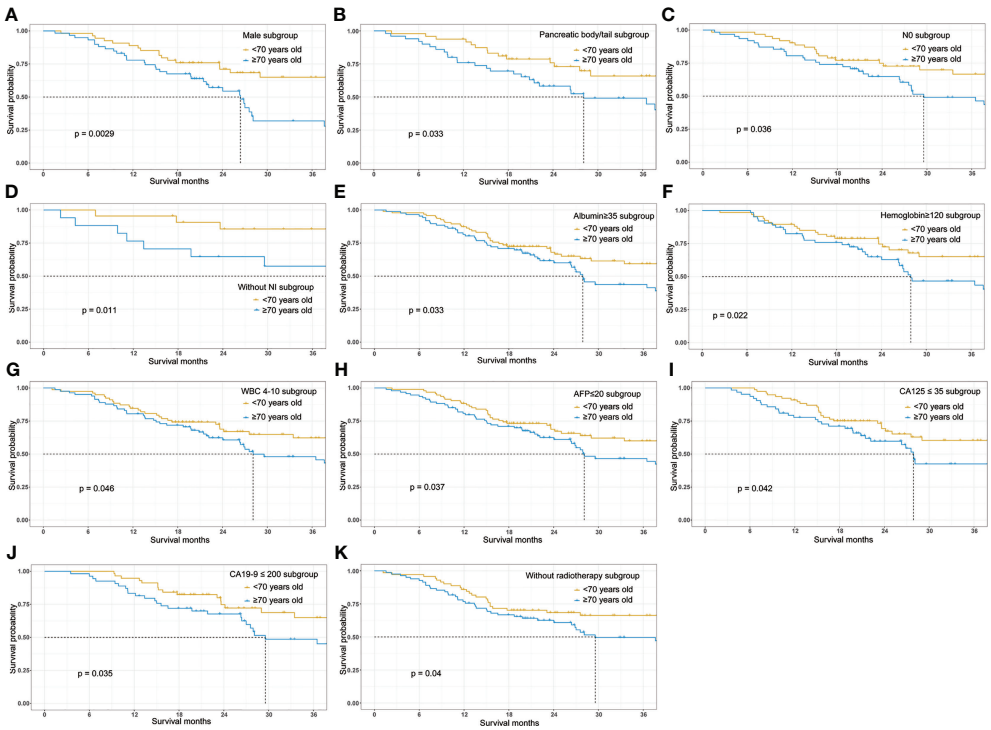

FIGURE 4 | Overall survival Kaplan-Meier survival curves stratified by age (≥70 vs <70) in the major subgroups. **(A)** Survival curve stratified by age in male patients. **(B)** Survival curve stratified by age in patients with pancreatic body/tail cancer. **(C)** Survival curve stratified by age in patients without lymphatic metastasis. **(D)** Survival curve stratified by age in patients without perineural invasion. **(E)** Survival curve stratified by age in patients with serum albumin higher than 35g/L. **(F)** Survival curve stratified by age in patients with hemoglobin higher than 120g/L. **(G)** Survival curve stratified by age in patients with white cell count (WBC) between 4 and 10×109/L. **(H)** Survival curve stratified by age in patients with AFP lower than 20ng/ml. **(I)** Survival curve stratified by age in patients with CA125 lower than 35 ng/ml. **(J)** Survival curve stratified by age in patients with CA19-9 lower than 200U/ml. **(K)** Survival curve stratified by age in patients who didn't receive adjuvant radiotherapy following surgery.

Postoperative complications were an important factor that could affect the decision on subsequent therapies. Taking different chemotherapy regimens could have discrepant prognosis. Then, the follow-up period was not long enough, and the median follow-up time was 40 months. As a result, the survival curves only showed 36-month survival time. Finally, there was only internal validation of the nomogram model. We did not perform external validation because of the low proportion of patients older than 70 years.

Taken together, our research indicated that elderly PDAC patients were associated with worse OS survival after radical resection, and the noticeable negative effect of aging was observed among PDAC patients with better preoperative nutritional status and less aggressive tumor biology. Adjuvant chemotherapy is essential to improve survival outcome of elderly PDAC patients after surgery.

DATA AVAILABILITY STATEMENT

The original contributions presented in the study are included in the article/**Supplementary Material**. Further inquiries can be directed to the corresponding authors.

ETHICS STATEMENT

Written informed consent was obtained from the individual(s) for the publication of any potentially identifiable images or data included in this article.

AUTHOR CONTRIBUTIONS

YL, YM, WH, and DS contributed to conception and design of the study. SY organized the database. YM performed the statistical analysis. YM wrote the first draft of the manuscript. DY, XF, TT, and WC wrote sections of the manuscript. All authors contributed to the article and approved the submitted version.

SUPPLEMENTARY MATERIAL

The Supplementary Material for this article can be found online at: https://www.frontiersin.org/articles/10.3389/fonc.2022.789351/full#supplementary-material

REFERENCES

1. Maisonneuve P. Epidemiology and Burden of Pancreatic Cancer. *Presse Med* (2019) 48(3 Pt 2):e113–23. doi: 10.1016/j.lpm.2019.02.030
2. Chen X, Yi B, Liu Z, Zou H, Zhou J, Zhang Z, et al. Global, Regional and National Burden of Pancreatic Cancer 1990 to 2017: Results From the Global Burden of Disease Study 2017. *Pancreatology* (2020) 20(3):462–9. doi: 10.1016/j.pan.2020.02.011
3. Smith BD, Smith GL, Hurria A, Hortobagyi GN, Buchholz TA. Future of Cancer Incidence in the United States: Burdens Upon an Aging, Changing Nation. *J Clin Oncol* (2009) 27(17):2758–65. doi: 10.1200/JCO.2008.20.8983
4. Hutchins LF, Unger JM, Crowley JJ, Coltman CAJr., Albain KS. Underrepresentation of Patients 65 Years of Age or Older in Cancer-Treatment Trials. *N Engl J Med* (1999) 341(27):2061–7. doi: 10.1056/NEJM199912303412706
5. Talarico L, Chen G, Pazdur R. Enrollment of Elderly Patients in Clinical Trials for Cancer Drug Registration: A 7-Year Experience by the US Food and Drug Administration. *J Clin Oncol* (2004) 22(22):4626–31. doi: 10.1200/JCO.2004.02.175
6. Parmar AD, Vargas GM, Tamirisa NP, Sheffield KM, Riall TS. Trajectory of Care and Use of Multimodality Therapy in Older Patients With Pancreatic Adenocarcinoma. *Surgery* (2014) 156(2):280–9. doi: 10.1016/j.surg.2014.03.001
7. Paulson AS, Tran Cao HS, Tempero MA, Lowy AM. Therapeutic Advances in Pancreatic Cancer. *Gastroenterology* (2013) 144(6):1316–26. doi: 10.1053/j.gastro.2013.01.078
8. Bathe OF, Levi D, Caldera H, Franceschi D, Raez L, Patel A, et al. Radical Resection of Periampullary Tumors in the Elderly: Evaluation of Long-Term Results. *World J Surg* (2000) 24(3):353–8. doi: 10.1007/s002689910056
9. Oguro S, Shimada K, Kishi Y, Nara S, Esaki M, Kosuge T. Perioperative and Long-Term Outcomes After Pancreaticoduodenectomy in Elderly Patients 80 Years of Age and Older. *Langenbecks Arch Surg* (2013) 398(4):531–8. doi: 10.1007/s00423-013-1072-7
10. Tani M, Kawai M, Hirono S, Ina S, Miyazawa M, Nishioka R, et al. A Pancreaticoduodenectomy is Acceptable for Periampullary Tumors in the Elderly, Even in Patients Over 80 Years of Age. *J Hepatobiliary Pancreat Surg* (2009) 16(5):675–80. doi: 10.1007/s00534-009-0106-6
11. de Franco V, Frampas E, Wong M, Meurette G, Charvin M, Leborgne J, et al. Safety and Feasibility of Pancreaticoduodenectomy in the Elderly: A Matched Study. *Pancreas* (2011) 40(6):920–4. doi: 10.1097/MPA.0b013e31821fd70b
12. Lu L, Zhang X, Tang G, Shang Y, Liu P, Wei Y, et al. Pancreaticoduodenectomy is Justified in a Subset of Elderly Patients With Pancreatic Ductal Adenocarcinoma: A Population-Based Retrospective Cohort Study of 4,283 Patients. *Int J Surg* (2018) 53:262–8. doi: 10.1016/j.ijsu.2018.03.054
13. Hodul P, Tansey J, Golts E, Oh D, Pickleman J, Aranha GV. Age is Not a Contraindication to Pancreaticoduodenectomy. *Am Surg* (2001) 67(3):270–275; discussion 275-276. doi: 10.1016/s0016-5085(00)81967-8
14. Finlayson E, Fan Z, Birkmeyer JD. Outcomes in Octogenarians Undergoing High-Risk Cancer Operation: A National Study. *J Am Coll Surg* (2007) 205(6):729–34. doi: 10.1016/j.jamcollsurg.2007.06.307
15. Ito Y, Kenmochi T, Irino T, Egawa T, Hayashi S, Nagashima A, et al. The Impact of Surgical Outcome After Pancreaticoduodenectomy in Elderly Patients. *World J Surg Oncol* (2011) 9:102. doi: 10.1186/1477-7819-9-102
16. Riall TS, Sheffield KM, Kuo YF, Townsend CMJr., Goodwin JS. Resection Benefits Older Adults With Locoregional Pancreatic Cancer Despite Greater Short-Term Morbidity and Mortality. *J Am Geriatr Soc* (2011) 59(4):647–54. doi: 10.1111/j.1532-5415.2011.03353.x
17. Aldakkak M, Christians KK, Krepline AN, George B, Ritch PS, Erickson BA, et al. Pre-Treatment Carbohydrate Antigen 19-9 Does Not Predict the Response to Neoadjuvant Therapy in Patients With Localized Pancreatic Cancer. *HPB (Oxford)* (2015) 17(10):942–52. doi: 10.1111/hpb.12448
18. Doyle DJ, Goyal A, Bansal P, Garmon EH. American Society of Anesthesiologists Classification. In: *StatPearls*. Treasure Island (FL): StatPearls Publishing (2021).
19. Khan S, Sclabas G, Lombardo KR, Sarr MG, Nagorney D, Kendrick ML, et al. Pancreatoduodenectomy for Ductal Adenocarcinoma in the Very Elderly; is it Safe and Justified? *J Gastrointest Surg* (2010) 14(11):1826–31. doi: 10.1007/s11605-010-1294-8
20. Melis M, Marcon F, Masi A, Pinna A, Sarpel U, Miller G, et al. The Safety of a Pancreaticoduodenectomy in Patients Older Than 80 Years: Risk vs. Benefits. *HPB (Oxford)* (2012) 14(9):583–8. doi: 10.1111/j.1477-2574.2012.00484.x
21. Turrini O, Paye F, Bachellier P, Sauvanet A, Sa Cunha A, Le Treut YP, et al. Pancreatectomy for Adenocarcinoma in Elderly Patients: Postoperative Outcomes and Long Term Results: A Study of the French Surgical Association. *Eur J Surg Oncol* (2013) 39(2):171–8. doi: 10.1016/j.ejso.2012.08.017
22. Kang CM, Lee JH, Choi JK, Hwang HK, Chung JU, Lee WJ, et al. Can We Recommend Surgical Treatment to the Octogenarian With Periampullary Cancer?: National Database Analysis in South Korea. *Eur J Cancer* (2021) 144:81–90. doi: 10.1016/j.ejca.2020.10.039
23. Parray A, Bhandare MS, Pandrowala S, Chaudhari VA, Shrikhande SV. Peri-Operative, Long-Term, and Quality of Life Outcomes After Pancreaticoduodenectomy in the Elderly: Greater Justification for Periampullary Cancer Compared to Pancreatic Head Cancer. *HPB (Oxford)* (2020) 23(5):777–84. doi: 10.1016/j.hpb.2020.09.016
24. Sho M, Murakami Y, Kawai M, Motoi F, Satoi S, Matsumoto I, et al. Prognosis After Surgical Treatment for Pancreatic Cancer in Patients Aged 80 Years or Older: A Multicenter Study. *J Hepatobiliary Pancreat Sci* (2016) 23(3):188–97. doi: 10.1002/jhbp.320
25. Mandelblatt JS, Ahles TA, Lippman ME, Isaacs C, Adams-Campbell L, Saykin AJ, et al. Applying a Life Course Biological Age Framework to Improving the Care of Individuals With Adult Cancers: Review and Research Recommendations. *JAMA Oncol* (2021) 7(11):1692–99. doi: 10.1001/jamaoncol.2021.1160
26. Hartwig W, Hackert T, Hinz U, Gluth A, Bergmann F, Strobel O, et al. Pancreatic Cancer Surgery in the New Millennium: Better Prediction of Outcome. *Ann Surg* (2011) 254(2):311–9. doi: 10.1097/SLA.0b013e31821fd334
27. Liu L, Xu HX, Wang WQ, Wu CT, Xiang JF, Liu C, et al. Serum CA125 is a Novel Predictive Marker for Pancreatic Cancer Metastasis and Correlates With the Metastasis-Associated Burden. *Oncotarget* (2016) 7(5):5943–56. doi: 10.18632/oncotarget.6819
28. Kawai H, Ota H. Low Perioperative Serum Prealbumin Predicts Early Recurrence After Curative Pulmonary Resection for non-Small-Cell Lung Cancer. *World J Surg* (2012) 36(12):2853–7. doi: 10.1007/s00268-012-1766-y
29. Bhindi B, Hermanns T, Wei Y, Yu J, Richard PO, Wettstein MS, et al. Identification of the Best Complete Blood Count-Based Predictors for Bladder Cancer Outcomes in Patients Undergoing Radical Cystectomy. *Br J Cancer* (2016) 114(2):207–12. doi: 10.1038/bjc.2015.432
30. Cai W, Kong W, Dong B, Zhang J, Chen Y, Xue W, et al. Pretreatment Serum Prealbumin as an Independent Prognostic Indicator in Patients With Metastatic Renal Cell Carcinoma Using Tyrosine Kinase Inhibitors as First-Line Target Therapy. *Clin Genitourin Cancer* (2017) 15(3):e437–46. doi: 10.1016/j.clgc.2017.01.008
31. McGrane JM, Humes DJ, Acheson AG, Minear F, Wheeler JMD, Walter CJ. Significance of Anemia in Outcomes After Neoadjuvant Chemoradiotherapy for Locally Advanced Rectal Cancer. *Clin Colorectal Cancer* (2017) 16(4):381–5. doi: 10.1016/j.clcc.2017.03.016
32. Loftus TJ, Brown MP, Slish JH, Rosenthal MD. Serum Levels of Prealbumin and Albumin for Preoperative Risk Stratification. *Nutr Clin Pract* (2019) 34(3):340–8. doi: 10.1002/ncp.10271
33. Nagrial AM, Chang DK, Nguyen NQ, Johns AL, Chantrill LA, Humphris JL, et al. Adjuvant Chemotherapy in Elderly Patients With Pancreatic Cancer. *Br J Cancer* (2014) 110(2):313–9. doi: 10.1038/bjc.2013.722
34. Townsley CA, Selby R, Siu LL. Systematic Review of Barriers to the Recruitment of Older Patients With Cancer Onto Clinical Trials. *J Clin Oncol* (2005) 23(13):3112–24. doi: 10.1200/JCO.2005.00.141
35. Yancik R, Wesley MN, Ries LA, Havlik RJ, Edwards BK, Yates JW. Effect of Age and Comorbidity in Postmenopausal Breast Cancer Patients Aged 55 Years and Older. *JAMA* (2001) 285(7):885–92. doi: 10.1001/jama.285.7.885
36. Puts MT, Tapscott B, Fitch M, Howell D, Monette J, Wan-Chow-Wah D, et al. A Systematic Review of Factors Influencing Older Adults' Decision to Accept or Decline Cancer Treatment. *Cancer Treat Rev* (2015) 41(2):197–215. doi: 10.1016/j.ctrv.2014.12.010

Conflict of Interest: The authors declare that the research was conducted in the absence of any commercial or financial relationships that could be construed as a potential conflict of interest.

this article, or claim that may be made by its manufacturer, is not guaranteed or endorsed by the publisher.

Advantages of publishing in Frontiers

OPEN ACCESS
Articles are free to read for greatest visibility and readership

FAST PUBLICATION
Around 90 days from submission to decision

HIGH QUALITY PEER-REVIEW
Rigorous, collaborative, and constructive peer-review

TRANSPARENT PEER-REVIEW
Editors and reviewers acknowledged by name on published articles

Frontiers
Avenue du Tribunal-Fédéral 34
1005 Lausanne | Switzerland

Visit us: www.frontiersin.org
Contact us: frontiersin.org/about/contact

REPRODUCIBILITY OF RESEARCH
Support open data and methods to enhance research reproducibility

DIGITAL PUBLISHING
Articles designed for optimal readership across devices

FOLLOW US
@frontiersin

IMPACT METRICS
Advanced article metrics track visibility across digital media

EXTENSIVE PROMOTION
Marketing and promotion of impactful research

LOOP RESEARCH NETWORK
Our network increases your article's readership